UNIVERSITY of SOPRON

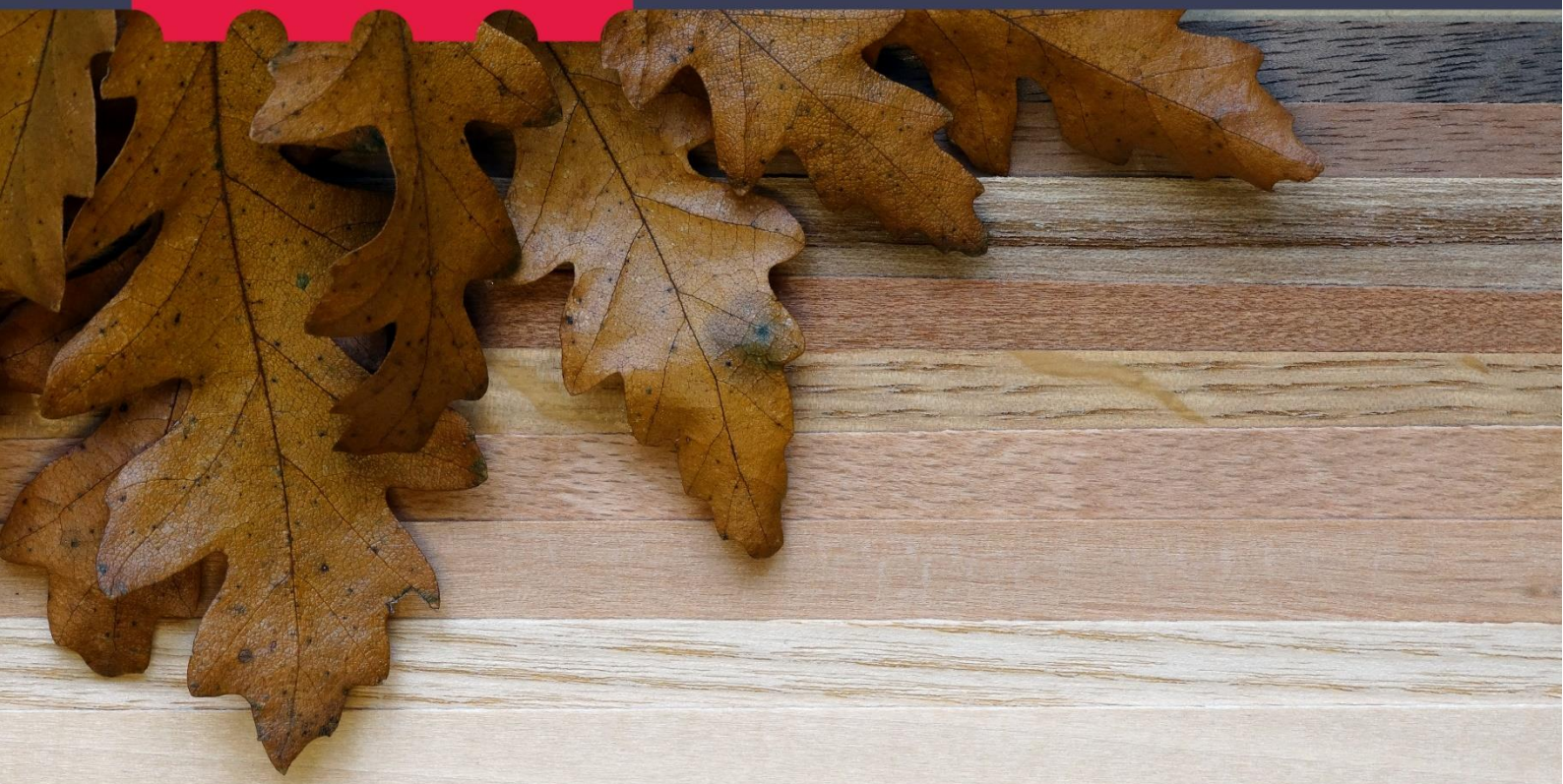

12th Hardwood Conference

18-19 June 2026
Sopron, Hungary

12TH HARDWOOD CONFERENCE PROCEEDINGS

Róbert Németh, Christian Hansmann, Holger Militz, Miklós Bak, Mátyás Báder

12TH HARDWOOD CONFERENCE PROCEEDINGS

Sopron, Hungary, 18-19 June 2026

Editors: Róbert Németh, Christian Hansmann, Holger Militz, Miklós Bak, Mátyás Báder

UNIVERSITY OF SOPRON PRESS

SOPRON, 2026

12TH HARDWOOD CONFERENCE PROCEEDINGS

Sopron, Hungary, 18-19 June 2026

Editorial board

Prof. Dr. Róbert Németh	University of Sopron – Hungary FATE - Scientific Association for Wood Industry – Hungary
Dr. Christian Hansmann	Wood K Plus – Austria
Prof. Dr. Holger Militz	Georg-August University of Göttingen – Germany
Dr. Miklós Bak	University of Sopron – Hungary
Dr. Mátyás Báder	University of Sopron – Hungary FATE - Scientific Association for Wood Industry – Hungary

Scientific committee

Prof. Dr. Joris Van Acker	Ghent University – Belgium
Prof. Dr. Dimitar Angelski	University of Forestry – Bulgaria
Prof. Dr. Milan Gaff	Mendel University Brno – Czech Republic
Dr. Galina Gorbacheva	Bauman Moscow State Technical University – Russian Federation
Prof. Dr. Johannes Konnerth	BOKU University – Austria
Dr. Rastislav Lagana	TU Zvolen – Slovak Republic
Dr. Charalampos Lykidis	Aristotle University of Thessaloniki – Greece
Prof. Dr. Bartłomiej Mazela	Poznań University of Life Sciences – Poland
Prof. Dr. Sergej Medved	University of Ljubljana – Slovenia
Prof. Dr. Goran Milić	University of Belgrade – Serbia
Prof. Dr. Dr. h.c. Peter Niemz	ETH Zürich – Switzerland / Luleå University of Technology – Sweden
Dr. Lê Xuân Phương	Vietnam National University of Forestry – Vietnam
Dr. Emilia-Adela Salca	"Transilvania" University of Brasov – Romania
Prof. Dr. Ali Temiz	Karadeniz Technical University – Turkey
Dr. Katrin Zimmer	NIBIO – Norwegian Institute of Bioeconomy Research – Norway
Dr. Vjekoslav Živković	University of Zagreb – Croatia

Cover design

Dr. Mátyás Báder — University of Sopron – Hungary

Webservices

12th Hardwood Conference official website

Dr. Miklós Bak — University of Sopron – Hungary

ISBN 978-963-334-587-0 (pdf)
DOI https://doi.org/10.35511/978-963-334-587-0
ISSN 2631-004X (Hardwood Conference Proceedings)

Constant Serial Editors: Prof. Dr. Róbert Németh, Dr. Miklós Bak
Cover image based on the photograph of Dr. Miklós Bak, 2026
The manuscripts have been peer-reviewed by the editors and have not been subjected to linguistic revision.
In the articles, corresponding authors are marked with an asterisk (*) sign.

University of Sopron Press, 2026 (Bajcsy-Zsilinszky 4, 9400 Sopron, Hungary)
Responsible for publication: Prof. Dr. Attila Fábián, rector of the University of Sopron

Creative Commons license: CC BY-NC-SA 4.0 DEED

Nevezd meg! - Ne add el! - Így add tovább! 4.0 Nemzetközi
Attribution-NonCommercial-ShareAlike 4.0 International

Sponsors: University of Sopron, Hungary; Wood K Plus, Austria; Georg-August University of Göttingen, Germany; Scientific Association for Wood Industry, Hungary

Content

PLENARY SESSION OF THE 12TH HARDWOOD CONFERENCE

Hardwood Products from Fast-Growing Trees
Joris Van Acker, Jan Van den Bulcke 10

SESSION I
SILVICULTURAL ASPECTS AND FOREST MANAGEMENT OF HARDWOODS

Sustainable High-Quality Wood Production in a Climate Change Context: Enhancing Poplar Resilience through Biotechnology and Digital Twins
Flor Álvarez-Taboada, Carlos Álvarez Cuevas, Jaime Olaizola, Ignacio Arroyo Marcos, Fernando Castedo Dorado, Erika García-Lima 13

Effects of Black Walnut (*Juglans nigra* L.) on the Forest Soil – Case Study
Vilém Podrázský, Ivo Kupka, Otakar Holuša 23

Replacing Norway Spruce Plantations with Birch in Sweden: Climate Effects in a Life Cycle Perspective
Aureo Aparecido Abreu Junior, Maximilian Schulte, Petra Sieber, Ragnar Jonsson, Per-Anders Hansson 31

Volume Production and Stem Quality in Birch Stands of Eastern Norway
Katrin Zimmer, Christian Kuehne, Irena Fundova 33

Resources of Selected Broadleaved Tree Species in Norway
Katrin Zimmer, Oliver Moen Snoksrud 39

Condition Monitoring of Standing Trees based on Dendro-Acoustic Emissions
Frank Schubert, Frank Duckhorn, Michael Reinhold, Clemens Zange, Carsten Hennig, Mario Hopfner, Antje Wilhelms, Maxi Binder, Richard Georgi, Claudia Scharff , Wolfram Scharff 48

Hardwood Afforestation on Extreme Sites in the Czech Republic: Growth Performance and Resistance of Selected Species
Zdeněk Vacek, Stanislav Vacek 50

POSTER SESSION

Application of Microwaves at a Frequency of 5.8 GHz for Hardwood Modification
Grigory Torgovnikov, Alexandra Leshchinskaia 58

Tensile Strength Analysis of Grey Poplar
Fanni Szőke, Antal Kánnár 63

Integrated Multidomain Characterization of Date Palm Trunk Wood (*Phoenix dactylifera* L.)
Firas Naji Al Hachami, Tamas Hofmann, Miklos Bak 68

Finite Element Analysis of a Montessori Climbing Arch Made from Underutilized Hardwoods
László János Dékány, József Garab 73

Natural Durability of Turkey Oak from Various Hungarian Sites Against *Daedalea quercina* (L.)
Máté Nagy, Norbert Horváth 80

Impact of False Heartwood on Compressive Strength in Thermally Treated Beech Wood
Aleš Zeidler, Vlastimil Borůvka, Adam Sikora 85

Finite element analysis of a bedframe made from underutilized hardwood species
Ádám Plangár, Sára Horváth, József Garab 90

Comparative Fractographic Analysis of Wood Surfaces Subjected to Static and Dynamic Tensile Loading Using Reflected Light Microscopy
Gábor Orbán, Antal Kánnár 95

Clone-Specific Intra-Annual Growth Responses of Poplars Under Contrasting Water Conditions in Spain
Flor Álvarez-Taboada, Carlos Álvarez Cuevas, Fernando Castedo Dorado 100

A GIS Model for Hardwood Biomass Availability and Operational Accessibility in the Southern Gulf Coastal Plain of the United States
Michael K. Crosby 105

Research on the Energy Efficiency of Briquettes and Pellets Made from Hardwood Species
Spirchez Cosmin, Lunguleasa Aurel 109

Silvicultural Aspects of *Salix* spp. and Opportunities for Capitalization. A Short Review
George Mușat, Emilia-Adela Manea Salca 114

Dynamics of Viscoelastic Properties of Some Hardwood Species from Romania Subjected to Thermal Variation
Robert Rebrișorean, Sara Trucza, Mariana Domnica Stanciu, Adriana Savin, Florin Dinulică 119

Static Bending Strength of Northern Red Oak (*Quercus rubra* L.) from Southern Poland – A Case Study
Radosław Wąsik, Krzysztof Michalec, Monika Gach, Joanna Kralka-Frycz 124

Enzymatic Strategies of Two *Armillaria* Species in Wood Cell Wall Degradation
Boris Indic, Simang Champramary, Nóra Tünde Lange-Enyedi, Omar Languar, György Sipos 129

Hardwood as a Sustainable Design Trend
Daniel Bodorkós, József Zalavári, Péter György Horváth 134

Stakeholder Perspectives on Swedish Hardwood Solid Wood Value Chains: A Delphi–Based SWOT Analysis
Victor Grubîi, Jimmy Johansson, Sebastian Svensson Meulmann 139

Redesign of a Chair Prototype – A Case Study
Mihnea Molnar-Varlam, Emilia-Adela Manea Salca, Alin M. Olărescu, Laurentiu Safta 146

Exploring Structural Applications of Hardwood Roundwood
Daniel F. Llana, Eva Hermoso, Carlos Osuna-Sequera, Emilio A. Luengo, David Lorenzo 152

Application of Computed Tomography for Assessing Defects in Sawn Beech Timber
Branislav Priadka, Rastislav Lagaňa, Barbora Herdová, Radovan Gracovský. Tomáš Gergeľ 156

Assessment of Stiffness-Based Grading for Thermally Modified Beech Timber in Structural Applications
Filip Valko, Jarmila Schmidtová, Tomáš Ándor, Barbora Herdová, Rastislav Lagaňa 161

Investigation of the Bacterial Communities of *Juglans regia* in Hungarian Plantations
Nóra T. Lange-Enyedi, Boris Indic, Simang Champramary, Aleksandr Pnev, Orsolya Kedves, Attila Szűcs, Annamária Tüh, Árpád Bányi, Younes R. Danesh, Omar Languar, Csaba Vágvölgyi, László Kredics, György Sipos 165

SNS Network VALUE:BIRCH – Valorization from the Forest and Beyond
Katrin Zimmer, Ulf Lemke, Irena Fundova, Henrik Heräjärvi, Mateusz Liziniewicz, Marlene Cramer, Stefanie Wieland, Lukas Emmerich, Thomas Uibel, Anti Rohumaa, Heikki Korpunen, Grace Jones, Ekaterina Nikolskaya, Tom Jansen, Anneli Adler, Tom Mortelmans, Ian Short, Vincent Defays, Karol Tomczak 170

Assessing the Quality of Wood in Beech Trees After a Forest Fire
Ioan-Aurelian Mitrofan, Victor-Mihai Ciomag, Elena-Camelia Musat 175

Cross-Laminated Timber in Romania: Insights from a Stakeholder Survey and Future Development Opportunities
Petruț Fola, Aurel Lunguleasa, Alin Olărescu 180

Study on the Natural Durability of *Quercus pyrenaica* Willd.
Sara M. Santos, Saúl Gutiérrez, María Teresa de Troya, Lee Robertson, Gonzalo Caballé, José Luis Villanueva 185

Visual and Machine Strength Grading of Structural Beech (*Fagus sylvatica* L.) Timber from Spain: Yield Comparison and Characteristic Values
Mario Azaña, Gonzalo Caballe, Silvia Gomez, Guillermo Íñiguez-González 190

The Influence of Forest Roads on the Dimensional Characteristics of Nearby Trees – Case Study for Deciduous and Mixed Forests
Diana-Elena Dumitru, George-Iulian Stanciulescu, Elena-Camelia Musat 196

Relationship Between Preservative Retention and Penetration in Norway Spruce and Pannonia Poplar
Luca Buga-Kovács, Norbert Horváth 201

Plant Residues as Possible Forest Fuels in Deciduous Forests
George Mușat, Daniel Costache, Elena-Camelia Mușat, Emilia-Adela Manea Salca 206

Mechanical Performance of a Longitudinal Joint for Round Spruce Poles Reinforced with an Oak Dowel (Preliminary Investigation)
Nagy Bence, Nadežda Langová, Igor Sršeň, Rastislav Lagaňa 211

Color Changes of Invasive Wood Species Under Heat Treatment
Szabolcs Komán, Benjámin Olivér Kulcsár, Péter Farkas 216

Dynamic Density Tests of New Black Locust (*Robinia pseudoacacia* L.) Clones
Tamás Ábri, Mátyás Báder 221

Eliminating Reading Errors and Automating the Brinell-Mörath Hardness Test
Anett Sütő, Róbert Németh, Mátyás Báder 228

The Use of Adhesives Designed for Conifers on Oak
Dénes Horváth, Sándor Fehér 233

Method of Juvenile and Mature Wood Demarcation with Annual Growth Analysis
Péter Farkas, Szabolcs Komán 239

Exploring the Acoustic Properties of Different Hardwood Species
Antonius Androne, Maria Violeta Guiman, Mariana Domnica Stanciu, Camelia Coșereanu 246

Chemical and Macromolecular Changes in Poplar Wood (*Populus tremula* L.)
Viera Kučerová 251

Differences in the Resistance of Two Longitudinal Beech Wood Joints Under Bending Loads
Tomislav Gržan[1], Goran Mihulja, Josip Miklečić, Tara Crnković, Martin Kašnar, Tomislav Sedlar 256

Concept for Utilisation of Beech False Heartwood Based on the Correlation Between Colour and Hardness
Miroslava Mamoňová, Peter Truban, Tatiana Hýrošová 258

Evaluating the Impact of Adhesive Selection on Bonding Strength in Multi-Layered Floor Elements (GRIpod)
Tomislav Sedlar, Vjekoslav Živković, Goran Mihulja, Mihael Gazilj, Andrija Novosel 261

A Collaborative Robotic System for Automated Measurement of Wood Sorption Isotherms and Associated Shrinkage and Swelling
Edit Földvári-Nagy, Jakub Sandak 262

Prediction of Durability Based on Wood Color
Szabolcs Komán, Zalán Mátyás Balogh, Tamás Hofmann 267

Grey Poplar (*Populus* × *canescens*) in Hungary: Introductory Remarks on Its Underutilization
Hasan Celik, Csilla Csiha, Endre Magoss 268

The Effect of Ageing and Finishing Type on the Service Properties of Lacquer Coatings on Oak Wood (*Quercus robur*)
Tomasz Krystofiak, Ahmet Can, Dimitar Angelski, Barbara Lis 273

Natural Regeneration of European Ash Under Severe Ash Dieback Pressure in Fjugstad Nature Reserve, Norway
Nina Elisabeth Nagy, Mari Mette Tollefsrud, Ane Vollsnes, Volkmar Timmermann, Isabella Børja, Ari Hietala 274

Hardwood's Role in Sustainable Construction: A Multidimensional Analysis
Konstantin Schneider, Sascha Bicke 276

Birch Plywood in Connections of Timber Structures
Roberto Crocetti, Tianxiang Wang, Lars Blomqvist, Dániel Honfi *278*

Integrating Genomics and Transcriptomics to Explore Wood Properties and Stress Responses in Poplar Species
Zoltán Attila Köbölkuti, Klára Cseke, Botond Boldizsár Lados, Katalin Bereczki, Roland Takács, Valter Toldi, Attila Benke *279*

Characterization of UV-Assisted Lignin-Modified Beech Veneer as an Initial Step Towards Transparent Wood Preparation
Dávid Takács, Miklós Bak *280*

SESSION II
HARDWOOD STRUCTURE AND PROPERTIES

Correlations Among Select Properties and Anatomical Parameters of *Simarouba Amara* Wood
Clara Gaspar Fossi de Souza, André Luis Christoforo, Francisco Antonio Rocco Lahr *287*

Comparative Analysis of Chemical Composition, Anatomical Features and FTIR Spectra in Maple Wood: Implications for Musical Instrument Quality
Mariana Domnica Stanciu, Olga A. Shapchenkova, Maria A. Plyashechnik, Marina A. Sheller, Antonina A. Aniskina, Florin Dinulică *296*

Strength Grading of Lesser Used Hardwood Assortments – Examples for Birch and Beech
Philipp Schlotzhauer, Tom Jansen, Florian Gonzalo Fleer, Hieronymus Bischoff, Susanne Bollmus, Thomas Uibel, Holger Militz *305*

Circular Economy in Structural Timber
Daniel F. Llana, Guillermo Íñiguez-González, Mônica Ruy, Katarzyna Ostapska *315*

Static and Dynamic Investigation of the Bending Strength and Modulus of Elasticity of Oak Timber
Mikael Perstorper, Joan W. Gikonyo *322*

State-of-Art NIRS Technology for Wood Products
Satoru Tsuchikawa *324*

Mechanical Characterisation of *Milicia excelsa* (Iroko) from Angola: Experimental Basis for the Structural Valorisation of a Tropical Hardwood
Jorge M. Branco, Wander B. João *326*

The Potential of Grey Poplar as Load-Bearing Material
Laszlo Bejo, Ruben Acs, Zoltan Hantos *336*

The Impact of *Hymenoscyphus fraxineus* and Associated Fungal Pathogens on the Material Structure and Chemical Composition of Common Ash (*Fraxinus excelsior*)
Anett Sütő, Róbert Németh *344*

Acoustic Emission Monitoring of Moisture Uptake in Beech
Alexander Schneider, Mehieddine Derbas, Martin Riegler *351*

Physical and Mechanical Properties of Hardwood from Invasive Species in an Urban Forest in the City of Rio de Janeiro, Brazil
Alexandre Monteiro de Carvalho, Carolina Nogueira Xavier, Andrea Vanini *358*

Comparison of Radial Growth and Mechanical Properties of Sessile and Downy Oaks Grown in a Mixed Forest Stand
Dimitrios Tsalagkas, Sergei Mikhailov, Marko Stojanović, Lenka Foltýnová, Petr Horáček, Kyriaki Giagli, Vladimír Gryc, Hanuš Vavrčík, Luka Krajnc *368*

SESSION III
SURFACE COATING AND BONDING CHARACTERISTICS OF HARDWOODS

Surface Bonding Performance of Birch and Birch-Based Hybrid Combinations for Structural Applications: A Preliminary Study
Maik Slabohm, Philipp Schlotzhauer, Holger Militz 371

Comparative Analysis of Accelerated Weathering and Protective Coating Efficacy on Six Wood Species
M. Pilar Giraldo, Alina Avellaneda, Laia Haurie, Ana M. Lacasta, Vicente Guallart, Marcel Vilches-Casals 375

Hardwood Lignin for Phenolic Resins: More Reactive Than its Reputation
Peter Bliem, Hendrikus W. G. van Herwijnen 383

The Feasibility of Black Locust Wood (*Robinia Pseudoacacia* L.) for Use in Load-Bearing Construction
Dominique Streib, Gerhard Dill-Langer, Max Lutz, Rupert Nieberle, Philippe Grönquist 392

Water Vapor Transport Through Adhesive Layers on Eucalyptus (Eucalyptus Camaldulensis) Wood: Pre-Steady and Steady-State Behavior
Omar Saber Zinad, Csilla Csiha 398

Interactions on Steamed Beech Wood-Epoxy Resin Phase Boundary During Wood Moisture Content Changes
Barbora Slováčková 399

SESSION IV
HARDWOOD PROCESSING AND MODIFICATION TECHNOLOGIES

Effect of Anhydrides Modification on the Properties of Plantation Rubber (*Hevea brasiliensis*), Acacia (*Acacia* spp.), and Oil Palm (*Tinnera* spp.) Trees Grown in Peninsular Malaysia
Norul Hisham Hamid, Mohd. Afiq Mokhtar, Ummi Hani Bin Abdullah, Paiman Bawon 410

Simulating the Sawing of Beech and Birch Logs
Urs Buehlmann, R. Edward Thomas 420

Optimization of Beech Wood Cutting with Circular Saw Blades Using ANN and RSM
Mihai Ispas, Bogdan Bedelean, Sergiu Răcășan, Ana - Maria Angelescu 421

Investigation of Surface Properties of Poplar Wood Impregnated with Lauryl Alcohol After Densification
Ahmet Can, Tomasz Krystofiak, Barbara Lis 422

Combined Wood Modification Using Bark Extractive Impregnation and Ammonia Fuming
Miklós Bak, Fanni Fodor, Zsolt Kajli, Tamás Hofmann 429

SESSION V
HARDWOODS IN COMPOSITES AND ENGINEERED MATERIALS

LVL from Hungarian Under-Utilized Hardwood Species
Tibor L. Alpár, Szili-Török György, György Péter Horváth, László Bejó, József Garab 432

From ABES to Panels: Wood-Species Effects on Adhesive Curing and Mechanical Performance in Strand-Based Composites
Andrej Fašalek, Lukas Malzl, Maximilian Pramreiter, Hendrikus van Herwijnen, Jan Stroobants, Johann Moser, Wolfgang Kantner, Johannes Konnerth 434

Enhanced Thermal Mass of Mycelium-Based Biocomposites for Timber Constructions: A Comparative Study
Benjamín Petržela, Tadeáš Zachara, Miroslav Jozífek, Miloš Pavelek, Štěpán Hýsek 441

Birch Becomes Structural: Valorizing Small-Diameter Silver Birch (*Betula pendula Roth.)* Into Innovative Glue Laminated Beams for Sustainable Construction
Tom Mortelmans, Tom De Mil, Thierry Descamps 442

Pretreatment of Beech Chips with Compression for Accelerated Maceration and Pulp Production
Richard Hrčka, Viera Kučerová, Rastislav Lagaňa, Oľga Mišíková 444

SMADBatt Sustainable Materials and Design for Electric Vehicle Batteries
Stefan Pinkl, Peter Bliem, Kevin Vitzthum, Thomas Krenke 445

Preface to the 12TH HARDWOOD CONFERENCE

Róbert Németh

For the 12th time, we are pleased to organize the Hardwood Conference in Sopron. Over more than two decades, this conference series has become an important international forum for hardwood research, bringing together scientists, forestry experts, and industrial professionals from many countries.

The challenges facing hardwood resources continue to grow. Climate change, emerging pests and diseases, changing forest ecosystems, and increasing demand for renewable materials require innovative scientific solutions and closer cooperation between forestry, wood science, and industry. The contributions presented at this conference clearly demonstrate the strength and diversity of the international hardwood research community.

The program highlights several key research directions. Sustainable forest management, climate adaptation, biodiversity, and plantation forestry are represented alongside studies on wood structure and properties, wood modification, bonding technologies, coatings, engineered wood products, and composite materials. Particular attention is devoted to the utilization of under-utilized hardwood species, value-added products, and the role of hardwoods in sustainable construction and the circular bioeconomy.

The conference also reflects the growing importance of interdisciplinary research. Experts from forestry, biology, chemistry, materials science, engineering, and design contribute to a common goal: increasing the value and utilization potential of hardwood resources while ensuring their long-term sustainability.

One of the greatest strengths of the Hardwood Conference remains the active participation of young researchers and students. Their enthusiasm and scientific achievements give us confidence in the future of hardwood research.

I would like to express my sincere gratitude to all authors, reviewers, keynote speakers, session chairs, and participants whose contributions have made the 12th Hardwood Conference possible. Special thanks are due to the University of Sopron (HU), the Ligneum Visitor Centre (HU), the Scientific Association for Wood Industry (HU), the Wood K plus (AT), and the Georg-August University Göttingen (DE) for their commitment, cooperation, and contribution to the successful organization of the 12th Hardwood Conference.

I hope that the conference will provide valuable scientific discussions, new collaborations, and inspiration for future research.

Sopron, June 2026
Róbert Németh

Plenary Session of the 12TH HARDWOOD CONFERENCE

Hardwood Products from Fast-Growing Trees

Joris Van Acker[1], Jan Van den Bulcke[1]

[1] Ghent University, UGent-Woodlab - Laboratory of Wood Technology, Coupure Links 653, 9000 Ghent, Belgium.

E-mail: Joris.VanAcker@UGent.be; Jan.VandenBulcke@UGent.be

Keywords: fast-growing trees (FGTs), hardwood, wood products.

ABSTRACT

Over the past decades planted forests and more specifically plantations have become a major tool to increase the production of woody biomass and bio-materials. Fast-Growing Trees (FGTs) are considered key in this perspective and, besides softwood resources, the hardwood potential linked to temperate and tropical broadleaved trees is eminent. A considerable set of tree species can be considered as FGTs. Some are well known in temperate regions like poplar (*Populus*) and willow (*Salix*). Others like kiri (*Pauwlonia*), the tulip tree (*Liriodendron*) and alder species (*Alnus*) share similar potential. In tropical regions, many broadleaved tree species also show strong promise for plantation development. Industrial plantations exist for eucalypts (*Eucalyptus*), teak (*Tectona*), and wattles (*Acacia*), but also species important for local livelihoods are relevant, such as yemane (*Gmelina*), batai (*Falcataria*, formerly *Paraserianthes*), she-oak (*Casuarina*), mesquite (*Prosopis*), and neem (*Azadirachta*).

All these species could be used for Engineered Wood Products (EWPs) ranging from structural applications up to the full range of multiple end-uses linked to bio-based materials. This resource will inevitably have an impact on the bioeconomy the coming decades. Although hybrid poplar trees can be considered paving the way, domestication together with selection and breeding tools may be useful also for other hardwoods, as is already the case for eucalypts, acacia and paulownia hybrids. Similarly, as with hybrid poplar, other fast growing tropical hardwoods are likely to be very useful. Some are important related to their indigenous origin with commercial relevance like okoumé (*Aucoumea klaineana*), ayous – obeché (*Triplochiton scleroxylon*), limba (*Terminalia superba*) and balsa (*Ochroma pyramidale*), while others could provide extra domestication option related to their vegetative or clonal regeneration (paulownia, yemane), or focus on other ecosystem services like supporting livelihoods (batai, neem) and underpinning phytoremediation (mesquite).

The IPC, the International Commission on Poplars and Other Fast-Growing Trees Sustaining People and the Environment, is one of the oldest statutory bodies within the framework of the Food and Agriculture Organization of the United Nations (FAO) as it was founded in 1947. The reform of the IPC Convention, adopted in 2019, expanded the Commission's scope beyond poplars and willows to include other fast-growing tree species. This broader mandate reflects the global importance of fast-growing trees for: sustainable wood supply, climate change mitigation, ecosystem services and rural development.

Although wood from fast-growing broadleaved species like hybrid poplars have been used as timber alongside oak for historical construction in many European countries, the use of local and imported softwood timber is considered key for timber-frame structures. The development of newer Engineered Wood Products like CLT, LVL, I-joists and LSL alongside more traditional ones like glulam and plywood enhances the option of using more hardwoods. Since such mechanical transformation (sawing, peeling) of trees hardly can provide a yield considerably higher than 50%, the residuals also need to be valued. Alongside paper and bioenergy, the potential for such resource to be used a bio-material in the building sector are good alternatives for polymer-based insulation materials.

The topic of including lesser used resources for green building is the main objective of the EU funded project WoodStock in developing climate-smart solutions to increase the use of underutilised wood in the European construction sector. This EU Horizon project (ID: 101181021) is focussing on hardwoods but also on lower quality wood, recovered wood to empower climate-smart, circular, and zero-waste use of underutilized wood from the forest and building stock in the construction sector to support the New European Bauhaus.

Complementing the current softwood-based resource for green building with a range of hardwood products based on fast-growing trees both in the temperate and tropical regions, will enable the extra renewable material for the future needs of the forestry wood chain.

Session I
-
Silvicultural Aspects and Forest Management of Hardwoods

Sustainable High-Quality Wood Production in a Climate Change Context: Enhancing Poplar Resilience through Biotechnology and Digital Twins

Flor Álvarez-Taboada[1*], Carlos Álvarez Cuevas[2], Jaime Olaizola[3], Ignacio Arroyo Marcos[4], Fernando Castedo Dorado[1], Erika García-Lima[1]

[1] Universidad de León, DRACONES Research Group, Campus de Ponferrada, 24401, Ponferrada, León, Spain
[2] Garnica Valencia de Don Juan, Valencia de Don Juan, León, 24200, Spain.
[3] ID Forest, Palencia, 34004, Spain
[4] Sociedad Pública de Infraestructuras y Medio Ambiente de Castilla y León, Junta de Castilla y León, Valladolid, 47008, Spain.

E-Mail: flor.alvarez@unileon.es; carlos.alvarez@garnica.one; jaime@idforest.ews; nacho.arroyo@somacyl.es; fcasd@unileon.es; egarl@unileon.es

Keywords: bio-inoculation; water stress; resilience; poplar; wood production; sap flow; IoT; digital twin; *Pisolithus* spp.; *Pseudomonas* sp.

ABSTRACT

Sustainable wood production is increasingly threatened by climate change, particularly through heightened water stress and biotic damage that reduce growth and might increase mortality in poplar plantations. The "Smart Poplar" project addresses these challenges by integrating biotechnology, digital twins, and artificial intelligence in a multi-pronged approach to plantation resilience. This study pursues two complementary objectives: (i) it evaluates the effectiveness of mycorrhizal and bacterial bio-inoculation treatments—consisting of *Pisolithus* spp. and *Pseudomonas* sp.—in enhancing the resilience of two commercially important clonal poplar varieties ('Raspalje' and 'I-214'); and (ii) it employs time-series analyses of sap flow and solar radiation data from IoT-connected Tree Talker sensors to identify early physiological signals associated with water stress. The study was conducted in a 10-year-old poplar plantation in Fresno de la Vega, León, Spain, where 40 trees experienced varying degrees of water stress. Weekly monitoring of diameter at breast height (DBH) growth, visual health assessments, and hourly ecophysiological sensor data were collected from June to August 2024, with bio-inoculation follow-up in 2024 and 2025. Sap flow trend analysis revealed statistically significant negative trends in stressed trees ($p < 0.001$), providing early, near-real-time indicators of water deficit prior to visible crown symptoms. Solar radiation under the canopy increased significantly in stressed trees as leaf cover declined, offering a complementary but less sensitive signal. Optical root analysis confirmed mycorrhization rates exceeding 60% for *Pisolithus tinctorius* in inoculated trees. ANCOVA results for 2025 demonstrated a statistically significant positive effect of bio-inoculation on DBH growth during the critical summer stress period exclusively in previously non-stressed trees ($p = 0.013$), suggesting that preventive application of bio-treatments to not too stressed trees maximises their protective effect. These findings offer a promising pathway for sustainable, zero-residue forest management integrating ecophysiological monitoring (digital twins) and biotechnology.

INTRODUCTION

Poplar (*Populus* spp.) plantations represent a cornerstone of European wood production, providing raw material for the pulp and paper industry, plywood manufacturing, and biomass energy, while simultaneously contributing to landscape connectivity and carbon sequestration. In Spain, hybrid poplar clones such as 'Raspalje' (*Populus* × *generosa*) and 'I-214' (*Populus* × *canadensis*) are among the most widely cultivated for high-quality timber production. However, increasing climate variability—characterised by prolonged drought episodes, higher temperatures, and irregular precipitation—and lower water table depth are exerting growing pressure on plantation productivity and long-term viability (Hicke and Zeppel 2013; Lintao et al. 2024).

Water stress is one of the primary abiotic factors limiting growth and survival in poplar plantations. Under water deficit conditions, trees reduce stomatal conductance to limit transpiration, which simultaneously limits carbon assimilation and, consequently, wood formation. Early detection of these physiological responses is critical for enabling timely adaptive management decisions, such as supplemental irrigation, adjusted cutting cycles, or targeted interventions to improve soil water retention. Traditional methods of stress assessment—based on periodic field surveys or destructive sampling—are insufficient for capturing the rapid, dynamic nature of plant water relations during drought episodes (Mee et al. 2017).

In recent years, ecophysiological sensors coupled with Internet of Things (IoT) networks have emerged as powerful tools for continuous, near-real-time monitoring of tree water status. Sap flow density, in particular, has been demonstrated to be a reliable proxy for stomatal conductance and transpiration, providing integrated, tree-level information that is directly linked to water availability (Hernandez-Santana et al. 2016; Ortuño et al. 2005). Similarly, under-canopy solar radiation provides a non-invasive indicator of canopy structural changes associated with leaf yellowing and defoliation under stress (Matasov et al. 2020). The integration of these sensors with IoT data transmission platforms enables near-real-time data streaming and remote monitoring, opening new possibilities for precision silviculture (Grisales-Sanchez et al. 2023) and a crucial part of digital twins for trees.

In parallel, biotechnological approaches are emerging as promising tools to increase tree resilience. Beneficial fungi and bacteria can improve nutrient acquisition, water-use efficiency and stress tolerance while reducing dependence on chemical inputs. Such approaches align with current European strategies promoting sustainable and environmentally friendly forestry. However, the efficacy of these treatments under field conditions, and particularly their interaction with pre-existing water stress levels, remains insufficiently characterised.

The "Smart Poplar" project, carried out within the DRACONES Research Group at the Universidad de León, in collaboration with private forestry and industrial partner, addresses this knowledge gap through an integrated approach combining ecophysiological monitoring, biotechnology, and geoinformatics. This paper presents the results from two key components of the project: (i) the near-real-time detection and monitoring of water stress using sap flow sensors, IoT technology, and time-series analysis; and (ii) the evaluation of bio-inoculation treatments as a preventive resilience strategy in clonal poplar plantations.

MATERIALS AND METHODS

Study Site and Plant Material

The study was conducted in a 10-year-old clonal poplar plantation located in Fresno de la Vega (42°8'N, 5°25'W; 795 m a.s.l.), León, Spain (Figure 1). This site is characterised by a semi-arid continental climate with hot, dry summers and cold winters. Since its establishment, the plantation has experienced varying degrees of water stress due to progressive fluctuations in the water table. Forty trees were selected for the study: 20 individuals of the 'Raspalje' cultivar (*Populus* × *generosa* A. Henry ex Rehder) and 20 of the 'I-214' cultivar (*Populus* × *canadensis* Moench), representing two of the most commercially important hybrid clones cultivated in Spain. Tree selection was stratified to ensure a representative distribution of initial water stress levels across both clones.

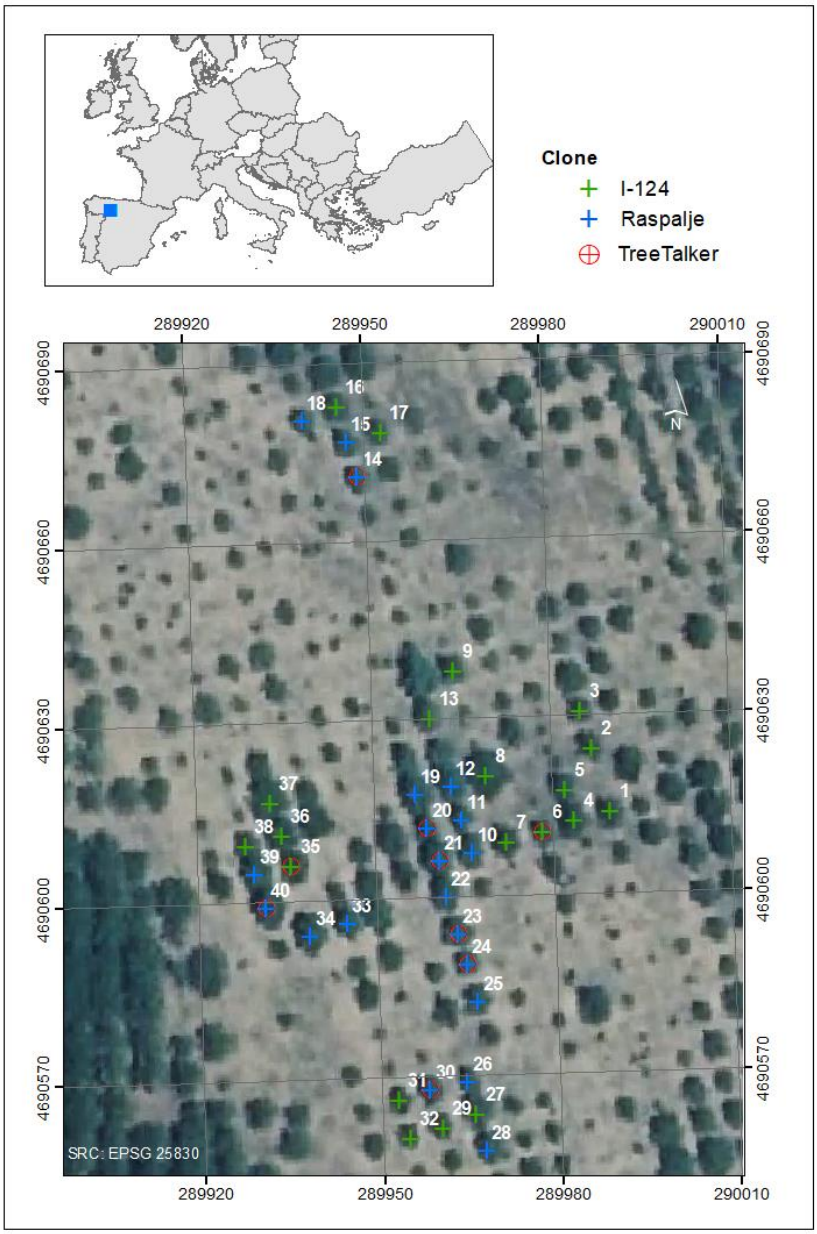

Figure 1: Location of the field plot and distribution of the monitored trees

Water Stress Monitoring

Water stress was assessed through a combination of dendrometric and visual health measurements. Diameter at breast height (DBH) was measured weekly from 26 June to 31 August 2024 using permanent tapes fitted with vernier scales offering a measurement resolution of 0.1 mm. Health status was assessed on a weekly basis using visual scoring of the percentage of yellow leaves and the percentage of defoliation for each tree. At the initial assessment (26 June 2024), none of the monitored trees exhibited crown symptoms of water stress.

Nine eco-physiological Tree Talker (TT) sensors were deployed on nine of the selected trees: six TreeTalker+ version 3.3 (TT+) and three TTcyber units (Nature 4.0 Company) (Table 1). These devices measured (i) sap flow density and (ii) under-canopy solar radiation in multiple spectral bands, recording data at hourly intervals. Data transmission was achieved via GSM/GPRS technology (TT+ units) and NB-IoT (TTcyber units), enabling near-real-time access through the Nature 4.0 online server (Matasov et al. 2020). Sap flow density (SF, l dm^{-2} h^{-1}) was computed hourly, but only values recorded between 12:00 and 16:00 local time were retained for analysis, as this window corresponds to peak stomatal activity and the period of maximum vulnerability to stomatal closure under water deficit conditions (Hernandez-Santana et al. 2016).

Table 1: Characteristics of the ecophysiological sensor network. Clone: R: Raspalje, I: I-214; SN: serial number; YL: yellow leaves; LL: leaf loss

Clone	SN	Model	TT Installation	Health status assessment (31/07/2024)	Health status assessment (28/08/2024)
R	621B0397	TT+	25/06/2024	No symptoms	No symptoms
R	71229005	TT+	25/06/2024	No symptoms	No symptoms
R	71229003	TT+	25/06/2024	No symptoms	No symptoms
R	71229002	TT+	25/06/2024	50% YL; 15% LL	70% LL
R	71229006	TT+	25/06/2024	60% YL; 20% LL	70% LL
R	71229008	TT+	25/06/2024	YL (basal)	YL (basal)
I	8123A077	TTCyber	27/06/2024	50% YL; 50% LL	75% LL
I	8123A081	TTCyber	15/07/2024	Some YL; 5% LL	20% YL; 35% LL
R	8123A075	TTCyber	15/07/2024	No symptoms	No symptoms

Bio-inoculation Treatments

Bio-inoculation treatments were applied to 20 of the 40 trees (10 per clone), while the remaining 20 trees served as untreated controls. The inoculum consisted of a combination of the ectomycorrhizal fungus *Pisolithus tinctorius* and the plant growth-promoting rhizobacterium *Pseudomonas* sp. Initial inoculation was performed in July 2024, and a re-inoculation was carried out in March 2025 on the same trees to reinforce mycorrhizal establishment. Mycorrhizal colonisation was confirmed through optical root tip analysis. Roots from inoculated and control trees were excavated, washed, and examined under a stereomicroscope to determine the proportion of root tips exhibiting characteristic mycorrhizal morphology.

Prior to the treatment analysis, the 40 trees were classified into three levels of initial water stress (StressINI) based on two complementary criteria: (a) retrospective annual diameter increment derived from increment core ring-width measurements, and (b) visual health assessment (percentage of yellow leaves) conducted in July: Class 0 (no initial stress), Class 0.5 (intermediate stress), and Class 1 (severe stress). DBH measurements confirmed that this classification captured significant differences in tree vigour (Class 0 > Class 0.5 > Class 1, Kruskal-Wallis test, $p < 0.05$), while no significant differences between clones were detected, permitting the analysis to focus on the interaction between initial stress class and bio-inoculation.

Statistical Analysis

To demonstrate that sap flows and solar radiation under the canopy of trees under water stress follow a different trend than those of non-stressed trees, time series trend analyses were performed (Zuur et al. 2009). We analysed the July and August time series for (i) sap flow, calculated as averages between noon and 4 pm, and (ii) daily total solar radiation (wavelength of 550 nm (±20 nm)). Two types of analyses were performed, as follows. For the ecophysiological monitoring component, time-series trend analyses were conducted on July and August sap flow records and on daily total under-canopy solar radiation (550 nm ± 20 nm). Individual trend models were fitted using ordinary least squares linear regression showed in Equation 1.

$$Sap\ flow\ or\ Radiation = a + (\beta \times time) \quad (1)$$

where β represents the slope of the linear trend. For sap flow, the null hypothesis stipulated that β would be significantly negative for stressed trees, reflecting progressive stomatal closure and reduced transpiration, whereas no significant trend was expected for non-stressed individuals. Significance of β was assessed using the t-statistic ($p < 0.05$).

Comparison of trends between stressed and non-stressed groups was performed by combining a linear regression analysis and a t-test, creating a categorical variable indicating whether a tree was under water stress or not ('stressed' and 'non-stressed') and fitting a linear regression model for the dependent variables (sap flow or solar radiation) and, as independent variables, the time variable, the grouping variable and the interaction term (time × group). If the interaction term was significant ($p < 0.05$), the trends (slopes) differed significantly between the groups (Zuur et al. 2009). The t and p statistics were calculated for β to test its significance.

The 9 monitored trees were classified as 'stressed' or 'non-stressed' based on two criteria: (a) water stress symptoms on the crown/leaves (yellow leaves/leaf loss) and (b) weekly DBH growth significantly smaller than the average for the other 39 trees in the plot and. Until July 11th 2024 (inclusive) none of the trees showed water stress symptoms in the crown/leaves. By the end of July (Table 1) the three of them showed severe symptoms, which increased during August. Those three trees had a weekly DBH growth close to 0.00 cm. We used a one-sample t-test to compare each one of these individual growth values with the average of the other 39 values (Ruxton 2006). The null hypothesis was that the individual value was not significantly different from the mean of the other values.

For the bio-inoculation component, the effect of bio-treatment on DBH growth during the critical water stress period (July to September) was evaluated using analysis of covariance (ANCOVA) models fitted separately for each initial stress class. The model included the binary bio-inoculation factor (TratBIO: inoculated vs. control) as the fixed effect, with initial DBH as a covariate to control for pre-existing differences in tree vigour. Mean comparisons were conducted using Tukey's range test at the 95% confidence level. Analyses were performed in R and SPSS.

RESULTS AND DISCUSSION

Near-Real-Time Detection of Water Stress Using Sap Flow

Individual sap flow trend analysis for July revealed statistically significant negative trends (standardised $\beta < 0$; $p < 0.001$) for the three trees classified as stressed (SN: 71229002, 71229006, 8123A077), indicating a progressive reduction in transpiration flux during the monitoring period (Table 2). For non-stressed trees, no significant trend was detected ($p > 0.05$) during July, confirming their maintenance of hydraulic function throughout the early summer period. Tree 8123A081, which only developed visible crown symptoms at the end of August, showed no significant sap flow trend in July ($p = 0.34$), consistent with its classification as a late-stressed individual. These results agree with the daily sap flow average values between noon and 4 pm (Figure 2) and align with findings by Grisales-Sanchez et al. (2023), who demonstrated using the same sensor platform that sap flow reductions precede visible foliar symptoms in poplar plantations under drought, and with the broader literature demonstrating that sap flow density tracks stomatal conductance dynamics under water stress (Hernandez-Santana et al. 2016; Ortuño et al. 2005). The negative trend in stressed trees is consistent with progressive stomatal closure in response to declining soil water potential, a well-documented physiological response in *Populus* species (Lintao et al. 2024).

The trend comparison analysis confirmed that the interaction term 'time × stress group' was highly significant for sap flow ($\beta = 0.36$, $t = 8.5$, $p < 0.001$), demonstrating that the sap flow trajectories of stressed and non-stressed trees diverged significantly during the monitoring period. This divergence was robust when using both the three July-stressed trees and when the late-stressed tree (8123A081) was included in the analysis, suggesting the approach can successfully capture early-onset and progressive stress responses within the same monitoring framework.

The practical implications are significant: sap flow sensors connected to IoT networks can provide plantation managers with actionable alerts when individual trees begin exhibiting hydraulic stress, enabling precision interventions such as targeted irrigation before irreversible damage occurs.

Table 2: Results of the trend analysis for sap flow in July (SFJ) and August (SFA), and daily 550 nm solar radiation (SR) for the combined July–August period. β: standardised slope; p: significance; n: number of observations

Variable	71229002 *Stressed*	71229006 *Stressed*	8123A077 *Stressed*	8123A081 *Late*	71229005 *Non-str.*	71229003 *Non-str.*	621B0397 *Non-str.*	71229008 *Non-str.*	8123A075 *Non-str.*
SFJ β	-0.63	-0.94	-0.89	-0.23	-0.13	-0.01	0.27	0.07	-0.16
SFJ p	<0.001	<0.001	<0.001	0.34	0.49	0.97	0.01	0.68	0.53
SFJ n	31	31	16	17	30	31	31	31	17
SFA β	0.64	-0.5	–	-0.53	-0.82	-0.71	0.14	-0.61	-0.5
SFA p	0.12	0.25	–	0.22	0.02	0.07	0.98	0.14	0.24
SR β	0.80	0.77	0.70	-0.26	-0.81	0.40	-0.57	0.39	-0.81
SR p	<.001	<.001	<.001	0.079	<.001	0.002	<.001	0.002	<.001
SR n	60	60	47	47	61	61	53	61	61

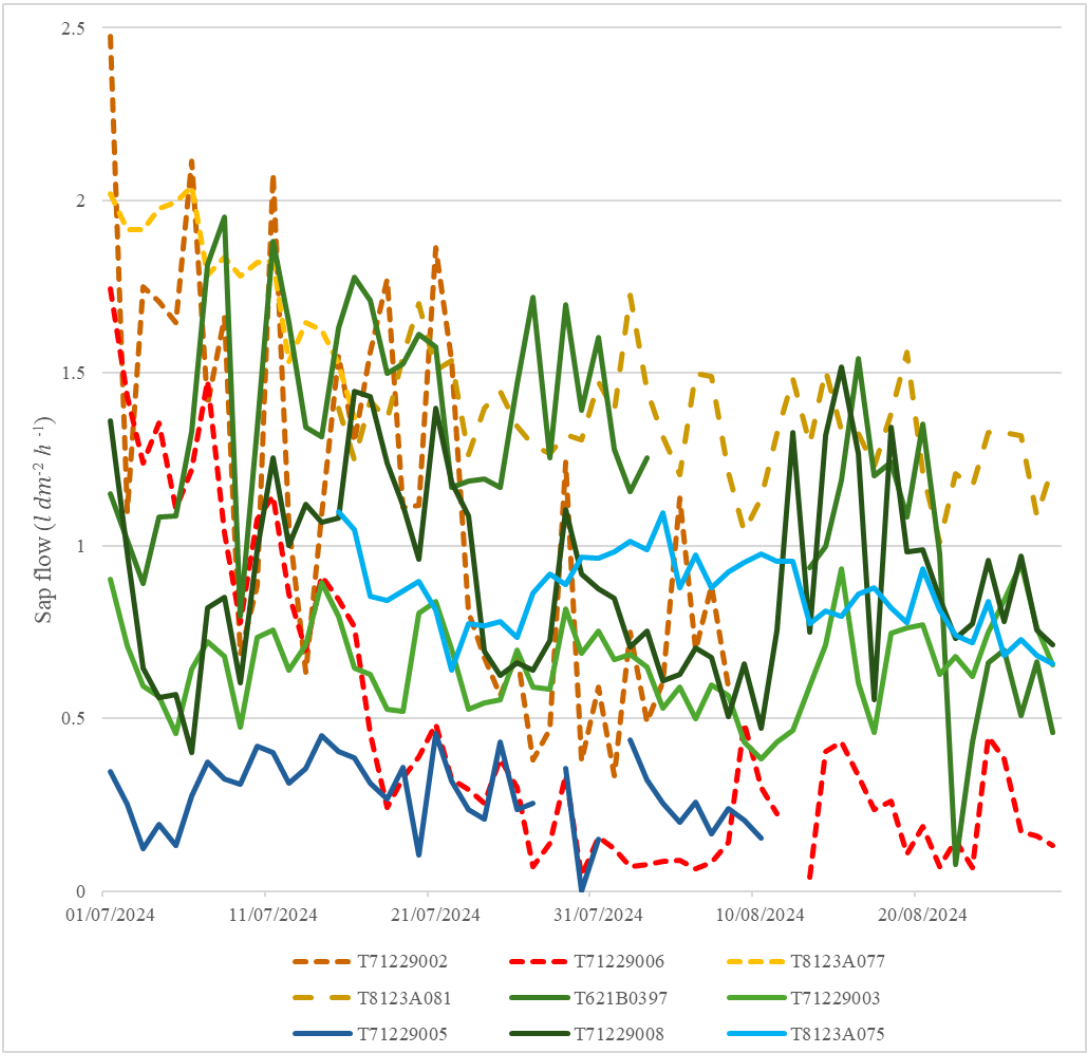

Figure 2: Daily sap flow averages between noon and 4 pm for each tree. Dashed lines correspond to trees classified as "stressed" due to their significantly lower DBH growth or visual assessment

Under-Canopy Solar Radiation as a Complementary Stress Indicator

Time-series analysis of daily 550 nm solar radiation beneath the canopy revealed significant positive trends for all trees that developed visual symptoms of water stress ($\beta > 0.70$; $p < 0.001$ for the three

July-stressed trees), reflecting increasing light penetration through a canopy progressively thinned by leaf yellowing and defoliation (Table 2). For most non-stressed trees, either no significant trend or a significant negative trend was detected, consistent with continued canopy development and increasing shading through the growing season.

The interaction term 'time × stress' for the solar radiation model was highly significant ($\beta = 0.67$, $t = 21.15$, $p < 0.001$; $n = 506$ observations), confirming statistically that the under-canopy radiation dynamics of stressed and non-stressed trees were distinctly different. However, comparing the temporal patterns of sap flow and solar radiation responses, it is apparent that the solar radiation signal becomes prominent only after substantial canopy change has occurred—i.e., at a more advanced stage of water stress—whereas sap flow declines were detectable before visible foliar symptoms appeared. This is consistent with findings by Hölscher et al. (2005), who noted that canopy structural responses to drought lag behind hydraulic responses in broadleaved trees Recent studies have similarly demonstrated that sap flow responds rapidly to declining soil water availability and may provide a more sensitive indicator of drought stress than other tree water-status metrics, supporting its application as an early-warning tool in precision forestry and irrigation management (Fernández et al., 2001; Donfack et al., 2024; Bárek et al., 2025; Uni et al., 2025).

These findings confirm that combining sap flow and solar radiation sensors provides complementary information across different stages of water stress development: sap flow is more sensitive to early hydraulic stress, while solar radiation captures later-stage canopy structural change. Previous studies have shown that radiation-related variables strongly influence transpiration dynamics during drought periods and interact with tree hydraulic status, although optical signals generally reflect canopy-level responses that emerge after physiological regulation has already begun (Donfack et al., 2024; Zhao & Fan, 2024)

Bio-inoculation: Mycorrhizal Establishment and Initial Response

Optical root tip analysis confirmed successful mycorrhizal colonisation in all inoculated trees, with *Pisolithus tinctorius* mycorrhization rates exceeding 60% of examined root tips. This rate is considered indicative of highly productive mycorrhizal symbiosis. No mycorrhizal structures were detected in control trees, validating the experimental design and confirming the specificity of the inoculation. This high colonisation rate is particularly notable given that the trees were already 10 years old at the time of treatment, suggesting that *Pisolithus tinctorius* can establish functional symbiosis even in mature plantation poplars where a native soil microbiome is already present.

Results from the 2024 growing season revealed an irregular treatment response. The irregularity was attributed primarily to the inoculation establishment phase and the presence of high variance (outliers) within the intermediate-stress group (Class 0.5), which limited statistical power. These factors are consistent with the expected lag phase following the introduction of a new fungal symbiont into an existing root system, and with the documented variability of bio-inoculation responses in field settings during the first post-treatment season.

Bio-inoculation Effect on DBH Growth Under Water Stress

The 2025 growing season provided decisive evidence of the bio-inoculation effect during the period of maximum water stress (July–September). ANCOVA analysis of DBH growth during this critical window revealed a statistically significant positive effect of bio-inoculation (TratBIO) exclusively in the Class 0 (no initial stress) trees ($F = 12.116$, $p = 0.013$), after controlling for initial DBH as a covariate (Table 3). The initial DBH covariate was also highly significant in this group ($F = 19.245$, $p = 0.005$), confirming the importance of baseline tree vigour in mediating the treatment response.

In contrast, no significant effect of bio-inoculation was detected in trees with prior intermediate (Class 0.5) or severe (Class 1) water stress. Similarly, no significant treatment effects were observed on accumulated pre-summer growth (January–June) or total annual growth in 2025, suggesting that the bio-inoculation benefit was specifically expressed during the physiologically critical drought period rather than throughout the growing season.

Table 3: ANCOVA results for diametric growth (July–September 2025) according to the level of initial water stress (StressINI). df: degrees of freedom

StressINI (Level)	Source of Variation	df	F	Significance (p)
0 (No initial stress)	TratBIO	1	12.116	0.013*
	Initial DBH (covariate)	1	19.245	0.005
1 (Severe stress)	TratBIO	1	0.414	0.53
	Initial DBH (covariate)	1	0.105	0.75
0.5 (Intermediate stress)	TratBIO	1	1.891	0.19
	Initial DBH (covariate)	1	2.674	0.13

** Statistically significant at the 95% confidence level ($p < 0.05$).*

These results are ecologically coherent and carry important management implications. The fact that bio-inoculation is effective only in vigorous, unstressed trees suggests a facilitative rather than a remedial mechanism. : the mycorrhizal network enhances the hydraulic and nutritional buffering capacity of trees that still possess functional root systems and adequate carbon reserves to support symbiosis, enabling them to sustain growth rates that decline in untreated controls under summer drought. Similar facilitative responses have been reported for ectomycorrhizal inoculation under water deficit conditions, where inoculated plants exhibited improved growth, water relations, photosynthetic performance and drought tolerance relative to uninoculated controls (Sebastiana et al., 2018; Lorente et al., 2021; Li et al., 2023; Xu et al., 2024). In contrast, trees already experiencing severe stress may lack the photosynthetic resources necessary to support active mycorrhizal symbiosis, rendering the treatment ineffective as a remedial measure. Comparable patterns have also been observed in hybrid poplar, where microbial inoculation enhanced drought tolerance primarily through improved physiological functioning and protection against oxidative stress rather than through recovery of already damaged trees (Khan et al., 2016).

This interpretation is consistent with the broader mycorrhizal ecology literature, which identifies ectomycorrhizal fungi as significant carbon sinks dependent on host-derived photosynthates. Recent evidence indicates that carbon allocation to ectomycorrhizal partners varies according to host species, physiological status and fungal community composition, suggesting that drought-stressed trees with reduced photosynthetic capacity may be unable to maintain effective symbiotic functioning (Zak et al., 2019; Xie et al., 2024).

Integration of Monitoring and Biotechnology: Towards Smart Plantation Management

The combination of near-real-time ecophysiological monitoring with preventive biotechnological treatments represents a novel and complementary approach to building resilience in poplar plantations under climate change. The IoT sensor network provides continuous, spatially resolved information on individual tree water status, enabling early triage of trees approaching critical stress thresholds. Bio-inoculation, applied preventively to vigorous trees, reinforces their hydraulic and nutritional resilience, extending the period during which they can maintain positive carbon balance under drought. Together, these tools constitute the core of a digital-twin approach in which continuous monitoring data inform predictive growth models and adaptive management decisions in near-real time. The integration of sap-flow sensing into automated decision-support systems has already been proposed for precision irrigation and water-management applications, demonstrating the potential of continuous physiological monitoring to support data-driven management under increasing climatic variability (Fernández et al., 2001; Bárek et al., 2025; Zhao & Fan, 2024).

The use of *Pisolithus tinctorius* and *Pseudomonas* sp. as bio-inoculants also offers advantages from a sustainability and certification perspective. As biologically-based soil amendments with no synthetic chemical residues, they are compatible with "zero-residue" management frameworks and increasingly stringent sustainability certification schemes for commercial timber. The incorporation of this approach

into precision forestry workflows—where sensor-derived stress maps guide targeted application of bio-treatments—could significantly reduce the cost and environmental footprint of maintaining plantation productivity under climate uncertainty.

CONCLUSIONS

This study demonstrates that near-real-time monitoring of sap flow using IoT-connected Tree Talker sensors provides an effective and early method for detecting water stress in hybrid poplar plantations, with statistically significant signal detection preceding the appearance of visible foliar symptoms. Under-canopy solar radiation offers a complementary but less sensitive indicator, becoming informative only at more advanced stages of stress when canopy structural changes are already underway.

Regarding bio-inoculation with *Pisolithus tinctorius* and *Pseudomonas* sp., field results from the 2025 season confirm a statistically significant positive effect on DBH growth during the critical drought period (July–September), but exclusively in trees without pre-existing water stress (Class 0). This finding underscores the preventive nature of this biotechnological strategy: its efficacy depends on application to vigorous trees capable of sustaining the carbon allocation required for active mycorrhizal symbiosis. Trees already experiencing intermediate or severe stress do not benefit from treatment under the current experimental conditions.

The integration of near-real-time ecophysiological monitoring with preventive biotechnological treatments—embedded within a digital twin framework—offers a promising and scalable approach to sustainable, high-quality wood production under increasing climate uncertainty. Future work should extend this approach to additional clones, sites, and stress regimes, and explore the potential of machine-learning algorithms applied to continuous sensor streams to further advance early warning capabilities in precision forestry.

ACKNOWLEDGEMENTS

This research has been funded by the Ministry of Universities, within the framework of Royal Decree 1059/2021, of November 30, which regulates the direct granting of various subsidies to universities participating in the European Commission's "European Universities" project, and by the European Education and Culture Executive Agency, within Project 101004049 — EURECA- PRO — EAC-A02-2019 / EAC-A02-2019-1.

REFERENCES

Bárek V, Mezey J, Igaz D, Obročník O, Kišš V (2025) Potential of sap flow for identifying stress in horticultural crops. SGEM Int Multidiscip Sci GeoConf Expo Proc. https://doi.org/10.5593/sgem2025/3.1/s11.23

Donfack LS, Mund M, Koebsch F, Schall P, Heidenreich MG, Seidel D, Ammer C, Werner C et al (2024) Linking sap flow and tree water deficit in an unmanaged, mixed beech forest during the summer drought 2022. Plant Biol 28:747–761. https://doi.org/10.1111/plb.13754

Fernández JE, Palomo MJ, Diaz-Espejo A, Clothier BE, Green SR, Girón IF, Moreno F (2001) Heat-pulse measurements of sap flow in olives for automating irrigation: tests, root flow and diagnostics of water stress. Agric Water Manage 51:99–123. https://doi.org/10.1016/S0378-3774(01)00119-6

Grisales-Sanchez I, Arthus-Bacovich R, Castedo-Dorado F, Garnica López J, Alvarez-Taboada F (2023) Near-Real Time Forest Health Monitoring Using Ecophysiological Sensors and the Internet of Things (IoT). A Study Case for Water Stress in Sustainable Poplar Plantations, pp 358–366. https://doi.org/10.1007/978-3-031-25840-4_41

Hernandez-Santana V, Fernández JE, Rodriguez-Dominguez CM, Romero R, Diaz-Espejo A (2016) The dynamics of radial sap flux density reflects changes in stomatal conductance in response to soil and air water deficit. Agric For Meteorol 218–219:92–101. https://doi.org/10.1016/j.agrformet.2015.11.013

Hicke JA, Zeppel MJB (2013) Climate-driven tree mortality: insights from the pinon pine die-off in the United States. New Phytol 200:301–303. http://www.jstor.org/stable/newphytologist.200.2.301

Hölscher D, Koch O, Korn S, Leuschner Ch (2005) Sap flux of five co-occurring tree species in a temperate broad-leaved forest during seasonal soil drought. Trees 19:628–637. https://doi.org/10.1007/s00468-005-0426-3

Khan Z, Rho H, Firrincieli A, Hung SH, Luna V, Masciarelli O, Kim SH, Doty SL (2016) Growth enhancement and drought tolerance of hybrid poplar upon inoculation with endophyte consortia. Curr Plant Biol 6:38–47. https://doi.org/10.1016/j.cpb.2016.08.001

Li M, Wang H, Zhao X, Feng W, Ding G, Quan W (2023) Effect of ectomycorrhizal fungi on the drought resistance of Pinus massoniana seedlings. J Fungi 9:471. https://doi.org/10.3390/jof9040471

Lintao T, Cao P, Zhang S, Liu X, Ge X, Tang L (2024) Two Male Poplar Clones (*Populus* × *euramericana* 'Siyang-1' and *Populus deltoides* 'Nanlin 3804') Exhibit Distinctly Different Physiological Responses to Soil Water Deficit. Forests 15:1142. https://doi.org/10.3390/f15071142

Lorente B, Zugasti I, Sánchez-Blanco MJ, Nicolás E, Ortuño MF (2021) Effect of Pisolithus tinctorius on physiological and hormonal traits in Cistus plants under water deficit: relationships among water status, photosynthetic activity and plant quality. Plants 10:976. https://doi.org/10.3390/plants10050976

Matasov V, Belelli Marchesini L, Yaroslavtsev A, Sala G, Fareeva O, Ivan S, Castaldi S, Vasenev V, Valentini R (2020) IoT Monitoring of Urban Tree Ecosystem Services: Possibilities and Challenges. Forests 11:775. https://doi.org/10.3390/f11070775

Mee C, Balasundram S, Hanif AH (2017) Detecting and Monitoring Plant Nutrient Stress Using Remote Sensing Approaches: A Review. Asian J Plant Sci 16:1–8. https://doi.org/10.3923/ajps.2017.1.8

Nature 4.0 (2020) TT+ User Manual. TreeTalker version TT+, suggested firmware TT3_2_plus.5_0h. Nature 4.0 Company.

Ortuño MF, Alarcón JJ, Nicolás E, Torrecillas A (2005) Sap flow and trunk diameter fluctuations of young lemon trees under water stress and rewatering. Environ Exp Bot 54:155–162. https://doi.org/10.1016/j.envexpbot.2004.06.009

Ruxton GD (2006) The unequal variance t-test is an underused alternative to Student's t-test and the Mann-Whitney U test. Behav Ecol 17:688–690. https://doi.org/10.1093/beheco/ark016

Sebastiana M, Da Silva AB, Matos A, Alcântara A, Silvestre S, Malhó R (2018) Ectomycorrhizal inoculation with Pisolithus tinctorius reduces stress induced by drought in cork oak. Mycorrhiza 28:247–258. https://doi.org/10.1007/s00572-018-0823-2

Uni D, Scott RL, Javadian M, Biederman JA, Dannenberg MP, Smith WK (2025) Drought response in three conifer species detected by sap flow and proximal thermal remote sensing. J Geophys Res Biogeosci 130:e2025JG009127. https://doi.org/10.1029/2025JG009127

Xie L, Lin G, Wang QW, Yin C (2024) Tree species-specific differences in carbon allocation to ectomycorrhizal symbionts tightly relate to ectomycorrhizal fungal community composition. For Ecol Manage 565:121935. https://doi.org/10.1016/j.foreco.2024.121935

Xu L, He J, Meng Y, Zheng Y, Lu B, Zhang J, Zhou Y (2024) Enhancing drought resistance in Pinus tabuliformis seedlings through root symbiotic fungi inoculation. Front Plant Sci 15:1446437. https://doi.org/10.3389/fpls.2024.1446437

Zak DR, Pellitier PT, Argiroff WA, Castillo BT, James TY, Nave LE, Averill C, Beidler KV et al (2019) Exploring the role of ectomycorrhizal fungi in soil carbon dynamics. New Phytol 223:33–39. https://doi.org/10.1111/nph.15679

Zhao X, Fan J (2024) Response of tree sap flow rate to soil water and atmospheric environment, and adaptability to drought in the Loess Plateau region of China. For Ecol Manage 563:122007. https://doi.org/10.1016/j.foreco.2024.122007

Zuur AF, Ieno EN, Walker N, Saveliev AA, Smith GM (2009) Mixed Effects Models and Extensions in Ecology with R. Springer Science & Business Media, New York.

Effects of Black Walnut (*Juglans nigra* L.) on the Forest Soil – Case Study

Vilém Podrázský[1*], Ivo Kupka[1], Otakar Holuša[2]

[1]Czech University of Life Sciences Prague, Faculty of Forest and Wood Sciences, Kamýcká 126, CZ 165 20, Czech Republic
[2]Mendel University Brno, Faculty of Regional Development and International studies, Tř. Gen. Píky 7, CZ 613 00, Czech Republic.

Emails: podrazsky@fld.czu.cz; kupka@fld.czu.cz; holusao@email.cz

Keywords: introduced species; noble hardwoods; forest soils; soil chemistry.

ABSTRACT

Black walnut (*Juglans nigra* L.) represents an example of very successful introduction in Central European conditions. It is appreciated for fast growth, stability and production of highly valuable timber. Due to its environmental demands the cultivation is restricted to lower altitudes and fertile soils. In the past, it was used in floodplain forests, but its silvicultural range is much broader: 1st – 4th Forest Altitudinal Zones and rich to medium sites. The study presented evaluates the effects of black walnut on forest soils, compared to native oak species. The compared sites are located in South Moravia at the locality characterized by Forest Type Group 2H and 2D – medium rich site, the age was 55 and 85 (black walnut) and 115 and 110 (pedunculate and English oak) years. Because of lack of surface humus, soil samples were taken from the depth 0-10 and 10-20 cm respectively in 4 replications in each stand and horizon. Soil chemistry analyses were provided in accredited laboratory. Results confirmed more favorable soil chemical characteristics for black walnut in the whole profile studied: pH, bases content, base saturation, higher plant available K, Ca, Mg contents. The total nitrogen and carbon (humus) content was comparable. Plant available P content was higher under oak due to higher soil acidity. Conclusion: Besides high production potential and timber quality, black walnut does not represent threat to soil fertility and its cultivation in mixtures with native broad-leaves does not represent environmental risk.

INTRODUCTION

Although introduced tree species represent only a minor proportion of European forests (Wohlgemuth et al. 2022), among them, black walnut occupies a prominent position (Nicolescu et al. 2020). The black walnut tree (ORC – *Juglans nigra* L.) is a very important introduced tree species from the warmer regions of the temperate deciduous forest biome of the eastern part of North America. It grows from the East Coast through the Appalachian Mountains to the Great Plains, primarily in river valleys. Like most introduced tree species in Europe, it was first planted in parks and gardens, later, in the Czech lands, sporadically from the end of the 18th century and to a greater extent from the middle of the 19th century, also in forest stands, where its significant production potential soon became evident. In the areas of origin, it is one of the highly valued and often cultivated tree species. Although the history of this tree species in the forests of the Czech lands, especially in the stands of south-eastern Moravia, is older than 200 years and its production potential is quite high, especially in terms of valuable and high-quality assortments, the scientific attention to black walnut has remained limited. It was introduced to Europe in 1629 (Herman 1987) and appeared in Bohemia in 1823 (Mráček 1925), although there are records from Moravia and from an earlier period. In forest stands, it is used significantly in the Czech Republic, practically only within one natural forest area (PLO), namely in PLO 35 – South Moravian Valleys. The first stands of black walnut in Moravia was then established in the Ždanský Forest on the Bučovice estate (Pokorný 1952; Mráček 1925), i.e. in another natural forest area, but today the maximum distribution of this tree in the whole Czech Republic is practically only in the South Moravian valleys, where 94% of the area of this tree species in the whole Czech Republic occurs (Hrib 2005). The first mention of ORC in South Moravia dates back to 1799, when suitable nurseries for the cultivation of North American exotics were established on Liechtenstein estates (Nožička 1956).

At present, the use of black walnut is limited by nature protection bodies as an exotic, non-native species. Despite this situation, the research on the production, vitality, and stability of particular species is vital in spite of climate change, climatic extremes and the necessity to assure sustainable care for forest ecosystems. Besides growth, health state and stability, the evaluation of environmental effects is of high importance. The aim of this pilot study is therefore to assess the influence of black walnut on forest soil properties under specific site conditions in South Moravia.

MATERIAL AND METHODS

The investigation was carried out at two sites in south Moravia, Forest Enterprise Židlochovice, belonging to Forest Site Groups 2H and 2D (Viewegh 2003), middle rich and fresh sites. Symbol H means loamy, nutrient rich, symbol D deluvial loamy, figure 2 indicates 2nd vegetation altitudinal zone – oak-beech stands. In the first case, the stands 48B6 – a stand dominated by black walnut and 45A12 – a neighboring stand dominated by pedunculate oak (according to the valid Forest Management Plan 1.1.2017-31.12.2026, habitat conditions – a set of forest types 2H, altitude 222 m a.s.l., age of walnut - 55, age of oak 115) were selected, in the second case, stands 46B9 – a stand dominated by black walnut and 47B11 – a neighboring stand dominated by pedunculated and English oak, (habitat conditions – a set of forest types 2D, altitude 185 m a.s.l., age walnut – 85, age oaks 110 years) were surveyed. A stand with a clear dominance of oaks and with the dominance of black walnut was always compared, where it was possible to assume a clear and dominant influence of one tree species/genus. In each stand group under each tree species, samples were taken from a depth of 0-10 and 10-20 cm, overlying humus was found only in oak stands, so it was omitted in this case. Four replicates were obtained for each stand and horizon.

The determination of soil chemistry characteristics was carried out by the VÚMOP laboratory using standard methods. The following analyses were performed for individual types of substrates:

- active (H_2O) and potential (1 N KCl) soil reactions, potentiometrically,
- exchangeable acidity, exchangeable hydrogen and aluminum content,
- basic characteristics of the soil sorption complex according to Kappen (1929) (BC – base content, BS – saturation of the sorption complex with bases / base saturation, H – hydrolytic acidity, CEC – cation exchange capacity),
- carbon and organic matter content (Springer-Klee method, e.g. Ciavatta et al. 1989),
- total nitrogen content (Kjeldahl method, e.g. Kirk 1950),
- the content of plant available/exchangeable nutrients in the leachate (Mehlich 1984).

For pedobiological characteristics – decomposition of cellulose – a mixed sample was created in the spring of 2024 from the same samples: ORC-2H, DB-2H, ORC-2D, DB-2D (ORC – black walnut, DB – oaks, H,D – sites), from horizons 0-10 and 10-20 cm as a mixed sample from the given 4 sampling sites. 2 sections of substrate were taken from each mixed sample, spread on the bottom of plastic boxes in a layer of 2 cm and their surface was leveled.

Ten strips of filter paper (80 g/m^2), divided into 1 cm sections, were placed on the surface in each box. In several continuous terms, the color changes and total decomposition were evaluated in the filter paper, indicating:

- the infestation of the paper by cellulolytic organisms,
- and gradual complete decomposition of the filter paper, i.e. its absence.

The samples were incubated in laboratory-room comparable conditions: temperatures of about 20 – 23 °C, the closure of the boxes allows the assumption of 100% air humidity. The arrangement of the experiment is demonstrated in Figure 1. The method used documents the relative potential of decomposition activities in a relatively simple way, but the method is still used as a standard. The experiment was established on 2.3.2024, the samples were evaluated on the dates/terms - T: T1 - 23.3., T2 - 12.4., T3 - 4.5., T4 - 26.5., T5 - 14.6., T6 - 5.7., T7 - 26.7.

Figure 1: Establishing of the experiment with celulose decomposition

RESULTS

The results are documented in Table 1 and Table 2. In the uppermost layer of soil (0-10 and 10-20 cm deep), a significantly higher soil reaction is evident under the black walnut stand in both monitored horizons. The differences exceeded the values of 2 pH levels. Higher acidity is documented at the 2D site, the results are statistically significant, especially in deeper horizons. On the other hand, the differences between the two horizons are not significant. This corresponds to significantly lower values of base content (BC value) and saturation of the sorption complex with bases (BS value) under oak stands. The cation exchange capacity (CEC value) did not differ significantly between horizons and tree species on SLT 2H, it was lower at the site characterized as 2D. On the other hand, hydrolytic acidity (H value) was higher under oak and at site 2D, the differences between the horizons were again not significant.

The total carbon content was slightly lower in the deeper horizon, at the 2H site it did not differ between tree species, at the 2D site it was lower both compared to the second site condition and in the case of oak. The total nitrogen content appeared to be lower in the case of 2D and in the case of oak. Significant tendencies in the case of the C/N ratio were not evident; the values were generally very favorable and indicate good humification under the stands of both tree species.

The content of plant available/exchangeable calcium also did not differ significantly between the two horizons, on the contrary, the content was significantly higher under walnut and in the 2H stand. On the contrary, the content of exchangeable potassium was higher under oak (2H) and decreased with the depth of the horizon. The content of exchangeable magnesium did not change with depth; it was also very significantly lower under the oak and in the lower horizon on 2D site. The content of exchangeable phosphorus was very significantly higher under oak, which is related to the higher acidity of the soil environment under this tree (Binkley 1989). The differences were especially noticeable in the lower horizon of the 2D site.

The process of color changes and decomposition of cellulose strips is documented in Tables 3 and 4 and Figures 2 and 3. Color changes generally occurred faster in the case of substrates under oak growth. Since the 4th term of the evaluation, the full coloring of all the samples is documented, with some exceptions.

Table 1: Basic soil chemical characteristics of soil horizons under stand groups of black walnuts and oak in depth 0-10 cm

Horizon 0-10 Characteristics	ORC – 2H	DB – 2H	ORC – 2D	DB – 2D
pH H_2O	6.86 a	5.85 b	6.52 a	4.53 c
pH KCl	6.33 a	5.04 b	5.96 a	3.66 c
BC mmol/100 g	28.0 a	18.6 b	25.3 a	7.8 c
CEC mmol/100 g	32.08 a	27.94 a	28.12 a	20.92 b
H mmol/100 g	4.08 a	9.34 b	2.82 a	13.12 b
BS %	87.5 a	66.3 b	89.8 a	37.3 c
N tot %	0.29 a	0.34 a	0.28 a	0.20 b
C tot %	3.42 a	3.32 a	2.85 ab	2.29 b
C/N	11.7	9.8	10.2	11.5
Ca ex. mg/kg	40001.3 a	2664.3 b	2789.8 b	1091.8 c
Kex. mg/kg	163.2 a	134.0 b	183.0 c	188.5 c
Mg ex. mg/kg	692.8 a	521.0 b	622.2 ab	199.0 c
P ex. mg/kg	13.3 a	17.8 a	13.8 a	54.3 b

Note: ORC – black walnut, DB – oak, ex. – exchangeable form of nutrients.

Table 2: Basic soil chemical characteristics of soil horizons under stand groups of black walnuts and oak in depth 10-20 cm

Horizon 10-20 Characteristics	ORC – 2H	DB – 2H	ORC – 2D	DB – 2D
pH H2O	6.88 a	5.86 b	6.58 a	4.55 c
pH KCl	6.25 a	4.97 b	5.98 a	3.61 c
BC mmol/100 g	26.7 a	17.3 b	23.3 a	7.8 c
CEC mmol/100 g	30.22 a	27.47 a	25.96 b	20.32 c
H mmol/100 g	3.52a	10.17b	2.66a	12.52b
BS %	88.5 a	63.9 b	89.8 a	38.5 c
N tot %	0.37 a	0.28 b	0.24 b	0.17 c
C tot %	3.03 a	2.71 a	2.46 b	1.88 c
C/N	8.2	9.7	10.2	11.1
Ca ex. mg/kg	3800.5 a	2679.5 b	2731.0 b	903.7 c
K ex. mg/kg	120.0 a	111.5 a	149.3 a	149.3 a
Mg ex. mg/kg	646.5 a	540.8 a	621.5 a	191.8 b
P ex. mg/kg	10.5 a	14.0 a	13.0 a	43.0 b

Note: ORC – black walnut, DB – oak, ex. – exchangeable form of nutrients.

Table 3: Color change in cellulose samples on substrates from oak and walnut stands in two monitored horizons at both sites (% of strips area)

Site	Species	Horizon	T1	T2	T3	T4	T5	T6	T7
H	ORC	1	0.0 a	17.4 a	39.2 a	100.0 a	100.0 a	100.0 a	100.0 a
H	ORC	2	0.0 a	7.3 a	41.0 a	***54.5 b***	***59.5 b***	***70.5 b***	100.0 a
H	DB	1	0.0 a	4.5 a	40.0 a	***63.0 b***	***78.0 b***	91.0 a	100.0 a
H	DB	2	7.5 a	18.5 a	***74.0 b***	100.0 a	100.0 a	100.0 a	100.0 a
D	ORC	1	0.0 a	23.0 a	38.5 a	100.0 a	100.0 a	100.0 a	100.0 a
D	ORC	2	11.5 a	25.8 a	42.5 a	100.0 a	100.0 a	100.0 a	100.0 a
D	DB	1	1.0 a	***55.5 b***	***85.0 c***	100.0 a	100.0 a	100.0 a	100.0 a
D	DB	2	9.5 a	***81.5 c***	***100.0 d***	100.0 a	100.0 a	100.0 a	100.0 a

Notes: Species: ORC – black walnut, DB – oak, T – term of measurement. The same letters and bold letters indicate statistically homogeneous groups.

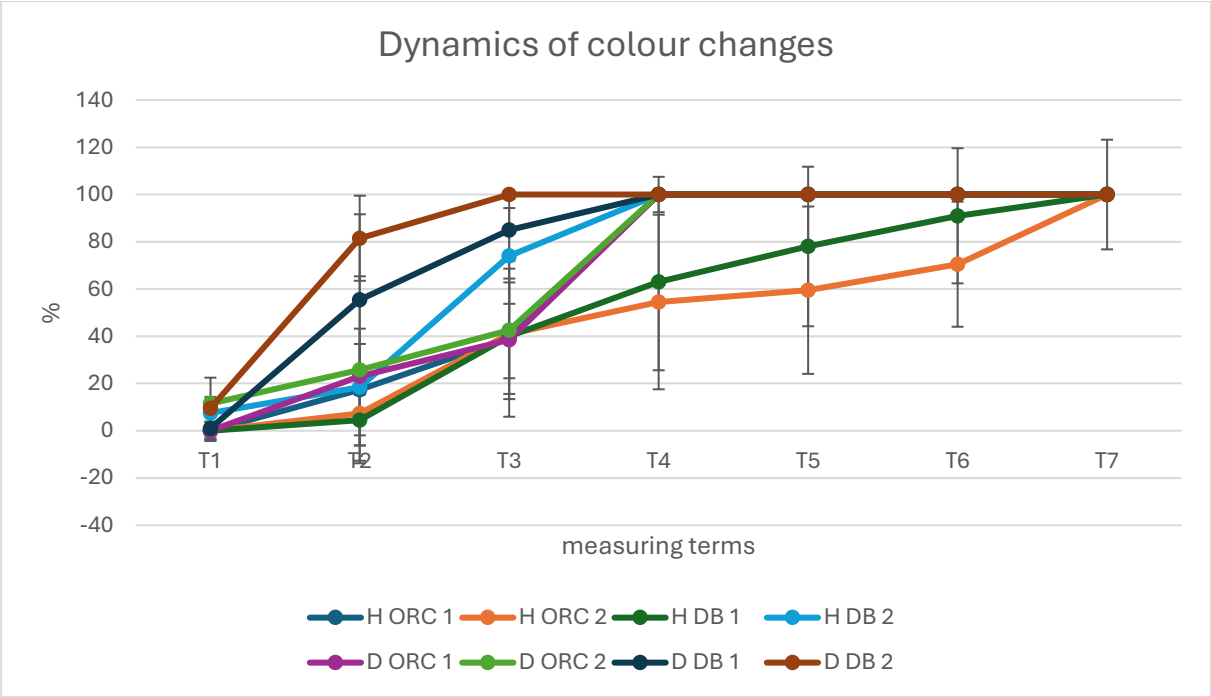

Figure 2: Color changes in samples of cellulose in substrates from soils of stands of oak and black walnut at two sites in two horizons

The colonization of the monitored samples by microbial organisms thus progressed significantly faster in the case of substrates from oak stands. However, within a short period of time, there was a dynamic increase in the activity of decomposition elements and, with some exceptions, the intensity of the coloration of the monitored samples was equalized. The coloring process was faster in the case of the SLT 2D site, with soil chemical characteristics indicating higher acidification of the environment (Table 3, Figure 2).

The total decomposition progressed significantly fastest in the case of a horizon of 0-10 cm in the walnut stand at site H, in the deeper horizon of 10-20 cm, on the other hand, it was significantly slowest here. Other substrates did not differ significantly in their cellulolytic potential with individual exceptions (Table 4, Figure 3). By the end of the investigation period, within a few months, almost complete decomposition occurred in all cases, which indicates a good decomposition potential of both tree litters.

Table 4: Decomposition dynamics of samples of cellulose at substrates from horizons od soil under walnut and oak (% of strips area)

Site	Species	Horizon	T1	T2	T3	T4	T5	T6	T7
D	DB	1	0.0 a	2.0 a	28.0 a	40.7 a	62.0 a	82.0 ab	98.0 ab
D	DB	2	0.25 a	***28.0 b***	42.5 a	63.5 a	87.5 a	92.5 a	100 a
D	ORC	1	0.25 a	0.33 a	***11.0 b***	37.5 a	84.0 a	100 a	100 a
D	ORC	2	4.0 a	2.5 a	24.8 a	53.0 a	***91.0 b***	100 a	100 a
H	DB	1	0.0 a	3.5 a	20.0 a	32.5 a	50.0 a	***58.0 b***	100 a
H	DB	2	0.0 a	2.0 a	30.5 a	48.0 a	62.7 a	73.0 a	***90.0 b***
H	ORC	1	0.5 a	***13.2 c***	***81.0 c***	***96.5 c***	***100 c***	100 a	100 a
H	ORC	2	0.0 a	0.0 a	***1.0 d***	***7.9 d***	***42.5 d***	***58.5 d***	***81.5 d***

Notes: Species: ORC – black walnut, DB – oak, T – term of measurement. The same letters and bold letters indicate statistically homogeneous groups.

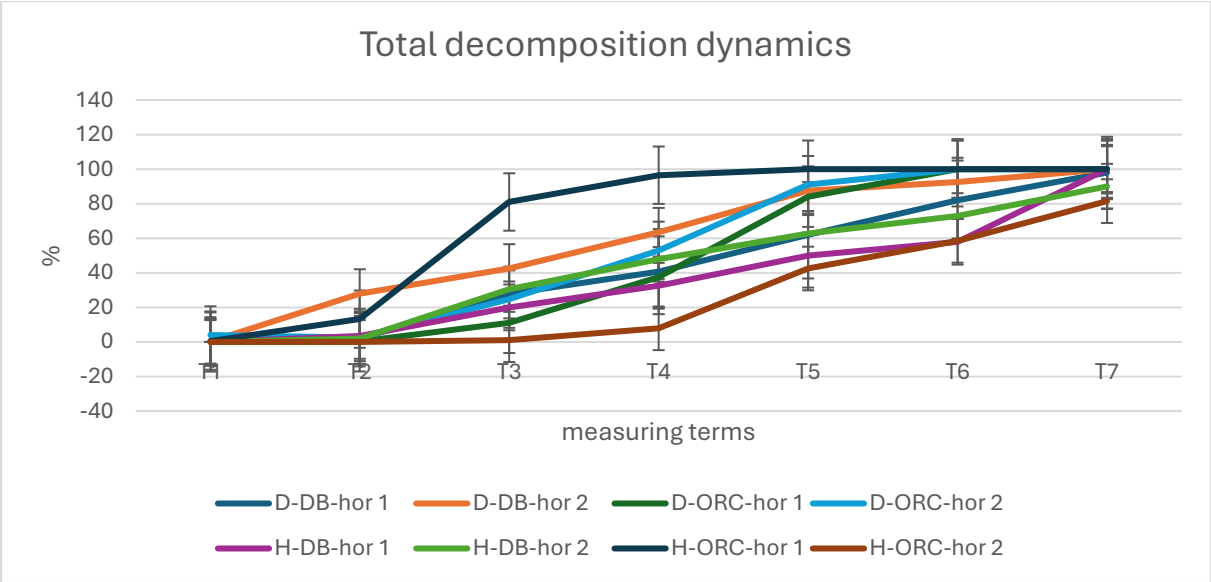

Figure 3: Decomposition of cellulose in samples of substrates from soils of stands of oak and black walnut at two sites in two horizons

DISCUSSION

The results of the research, although preliminary, demonstrate a favorable state of soil chemistry in black walnut stands and provide no indication of soil degradation. In terms of forest soil, walnut fits well into the set of forest tree species suitable for the given habitats (2nd and 3rd Vegetation Altitudinal Zone, ecological series S, H, D, etc. – Viewegh et al. 2003), which is also supported by the research carried out (Holuša et al. 2023, Nicolescu et al. 2020). Higher acidity under oak stands promotes increased phosphorus availability (Binkley 1989). This is also evident in the state of overlying humus, which is almost absent in walnut stands, it was not determinable, while in oak stands the horizons L+F+H formed a layer about 2 cm thick. Negative effects on the biodiversity of ground vegetation have not yet been proven (Hrib et al. 2017, Maděra, Hrib 2002). This tree does not pose a threat to forest ecosystems in terms of forest soils and biodiversity. This is further enhanced by the requirement to grow black walnut as an admixture in forest stands, which combines the requirement of minimal ecological threat and an increase in the volume and, above all, value production of forest stands. The importance of these determinations is growing with the simultaneous extinction of ash as another important tree species of floodplain habitats.

A somewhat different procedure of biologically conditioned decomposition processes is also documented in Fig. 4. In the case of oak, it is more about the application of the activities of soil bacteria and fungi, which first color and then decompose strips of cellulose. In the case of the walnut tree litter, the color changes are not so progressive, so probably a larger fauna comes in, which directly decomposes parts of the cellulose. Differences in the application of individual groups of soil organisms are conditioned by different soil chemistry, where the more acidic soil environment under the oak favors mainly soil fungi, which participate in the decomposition of cellulose (Binkley 1986). Thanks to its relatively weak natural regeneration, the walnut tree is not a species with pronounced invasive potential, on the contrary, it is a tree that significantly increases the quality and quantity of production (Holuša et al. 2023). Thus, black walnut does not pose a threat to existing forest stands and ecological links in ecosystems and can be used to benefit in the cultivation of productive, stable and sustainable forests (Nicolescu et al. 2020, Podrázský et al. 2023, Šálek 2012).

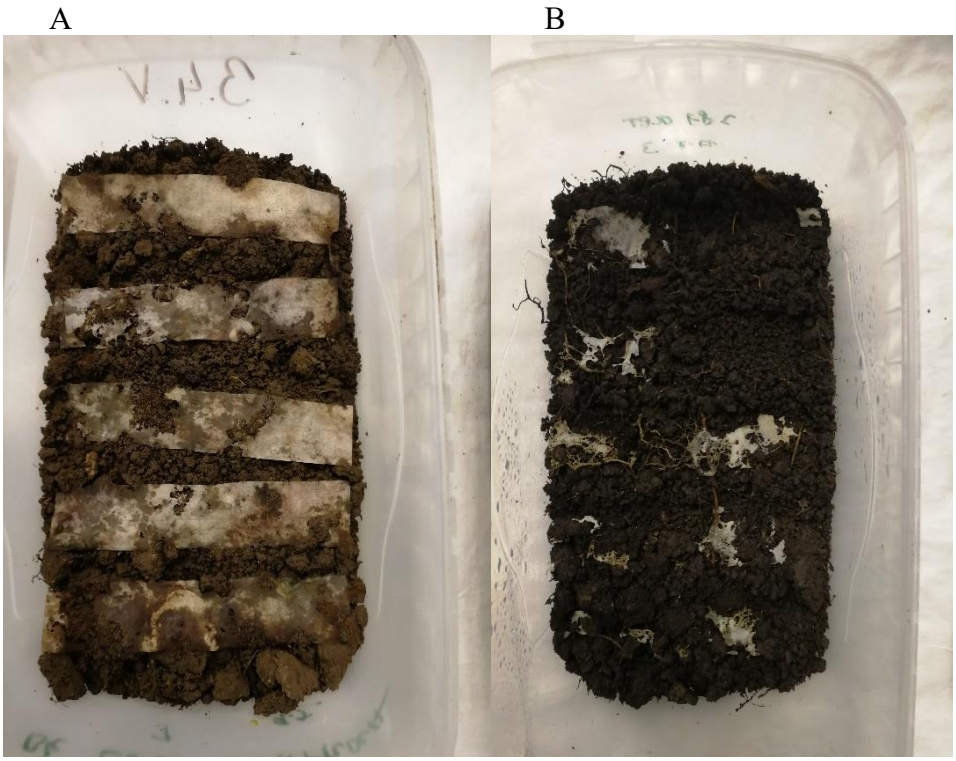

Figure 4: Different progress of decomposition process in the samples of substrates from stand parts dominated by oak (A) and black walnut (B) – horizon 0-10 cm

CONCLUSIONS

Based on the research results so far, it can be assumed that the cultivation of black walnut does not pose a threat to the diversity, stability and production value of forest stands with appropriate cultivation practices. On the contrary, it is possible to count on the preservation of soil fertility, diversity of at least ground vegetation, and above all on the increase in volume and value production of forest stands. Ecosystem services are thus minimally affected, but rather significantly increased. The use of this tree species in mixed and diversified stands can thus contribute very significantly to their production and stability in the context of climate change and sustainable forest management.

ACKNOWLEDGEMENT

Paper originated as a part of research project NAZV: QL26010446 Využití vybraných listnatých geograficky nepůvodních druhů dřevin jako adaptační opatření lesnického hospodaření s ohledem na klimatickou změnu.

REFERENCES

Binkley D (1986) Forest Nutrition Management. New York, J. Wiley, 289 pp

Ciavatta C, Vittori Antisari L. SEQUI P (1989) Determination of organic carbon in soils and fertilizers. Communications in Soil Science and Plant Analysis, 20:759-773

Herman RK (1987) North American Tree Species in Europe. Journal of Forestry, 85:27–32

Holuša O, Holušová K, Gol J, Doležal R (2023) Návrh uplatnění ořešáku černého (*Juglans nigra* L.) při obnově lesních porostů v podmínkách LS Luhačovice na základě analýzy přírodních podmínek a hodnoty produkce. Průběžná zpráva projektu GS LČR. Research report. Brno, Moravský lesnický institut. 98 pp. (in Czech)

Hrib M (2005) Pěstování ořešáku černého (*Juglans nigra* L.) v lesích jižní Moravy. Sborník prací institucionálního výzkumu, MZLU Brno, 2:1–78. (in Czech)

Hrib M, Podrázský V, Matějka K, Viewegh J (2017) Effect of black walnut (*Juglans nigra*) on the understorey vegetation – a case study of South Moravian forests (Czech Republic). Journal of Forest Science, 63:136–148

Kappen H **(**1929) Die Bodenazidität. Springer, Berlin, Germany: 363 pp

Kirk PL (1950) Kjeldahl method for total nitrogen. Analytical Chemistry, 22:354-358

Maděra P, Hrib M (2002) Srovnání synuzie podrostu porostů *Juglans nigra* a *Quercus robur* na LZ Židlochovice v aluviu dolních toků řek Svratky a Jihlavy. In: Viewegh J. (ed.): Problematika lesnické typologie IV. Sborník příspěvků ze semináře v Kostelci nad Černými lesy 30. a 31. 1., 2002: pp 35–37. (in Czech)

Mehlich A (1984) Mehlich 3 soil test extractant: A modification of Mehlich 2 extractant. Communications in Soil Science and Plant Analysis, 15:1409-1416

Mráček J (1925) Ořešák černý (*Juglans nigra* L.). Lesnická práce, Praha: pp 209–217. (in Czech)

Nicolescu VN, Rédei K, Vor T, Bastien JCh, Brus R, Benčať T, Dodan M, Cvjetkovic B, Andrašev S, La Porta N, Lavnyy V, Petkova K, Peric S, Bartlett D, Hernea C, Pástor M, Mataruga M, Podrázský V, Sfecia V, Štefančík I, (2020) A review of black walnut (*Juglans nigra* L.) ecology and management in Europe. Trees, 34, s. 1087–1112.

Nožička J (1956) Z minulosti jihomoravských luhů. Práce výzkumných ústavů lesnických, 10:169–199. (in Czech)

Podrázský V, Holuša O, Šálek L, Resnerová K, Zeidler A, Borůvka V, Prknová H, Bažant V, D'Andrea G (2023) Potenciál pěstování ořešáku černého (*Juglans nigra*) v ČR. In: Využití a pěstování cenných listnáčů v podmínkách České republiky. Praha 16. května 2023, Praha, ČLS 2023, pp 11-22. (in Czech)

Pokorný J (1952) Ořešáky. Praha, Brázda: 83. (in Czech)

Šálek L (2012) Hospodářská úprava porostů ořešáku černého (*Juglans nigra* L.). Dissertation thesis. Praha, Česká zemědělská univerzita v Praze: 98 pp (in Czech)

Viewegh J, Kusbach A, Mikeska M (2003) Czech forest ecosystem classification. Journal of Forest Science, 49:74–82

Wohlgemuth T, Gossner MM, Campagnaro T, Marchante H, van Loo M, Vacchiano G, Castro-Diez P, Dobrowolska D, Gazda A, Keren S, Keseru Z, Koprowski M, La Porta N, Marozas V, Nygaard PH, Podrázský V, Puchalka R., Reisman-Berman O, Straigyte L, Ylioja T, Potzelsberger E, Silva JS (2022) Impact of non-native tree species in Europe on soil properties and biodiversity: a review. NeoBiota, 78:45–69.

Replacing Norway Spruce Plantations with Birch in Sweden: Climate Effects in a Life Cycle Perspective

Aureo Aparecido Abreu Junior[1*], Maximilian Schulte[2], Petra Sieber[3], Ragnar Jonsson[1], Per-Anders Hansson[1]

[1] Swedish University of Agricultural Sciences – SLU, Campus Uppsala, Department of Energy and Technology, Lennart Hjelms väg 9, 75651 Uppsala, Sweden
[2] Swiss Federal Institute of Technology in Zurich – ETH, Rämistrasse 101, 8092 Zürich, Switzerland
[3] Wageningen University & Research – WUR, Droevendaalsesteeg 3, 6708 PB Wageningen, The Netherlands.

E-mail: aureo.abreu.jr@slu.se; maximilian.schulte@wur.nl; petra.sieber@env.ethz.ch; ragnar.jonsson@slu.se; per-anders.hansson@slu.se

Keywords: life cycle assessment; biogenic carbon; potential substitution effects; hardwood; broadleaves.

ABSTRACT

Norway spruce (*Picea abies*) forests have high productivity, and their harvested wood products (HWPs) have an established market in Sweden, but this production system has been constantly threatened by a changing climate. In the last years, frequent heatwaves across Europe have led to severe drought periods, including Southern Sweden. Those affected regions, mainly dominated by spruce vegetation, had been prone to bark beetle outbreaks, and consequently, increased tree mortality and carbon release to the atmosphere. To face those issues, risk mitigation strategies, either by species adaptation (shortening rotations) or species replacement, e.g. increasing the share of broadleaves, could be used considering those challenging scenarios.

However, the climate effects of those strategies are still poorly understood, specially taking in consideration the whole forest system, since seedling planting until the end-use of the HWPs, especially by considering potential uses of broadleaved HWPs and its substitution effects. Thereby, the aim of this work was to investigate whether spruce replacement by birch (*Betula sp*.) genotypes (non-improved and improved) in equivalent site indexes (SIs) could bring climate benefits in Swedish forestry. Also, assessing whether shortening spruce rotations could be climate beneficial when the results from spruce replaced by birch were similar.

Three equivalent SIs were used to compare the scenarios: low, medium, and high SI. For each scenario comparison, spruce was set as the reference scenario (business as usual HWPs portfolio), considering the end-uses of HWPs of birch (*Betula sp.)* for both, current use of non-improved HWPs (pulpwood and fuelwood) and potential HWPs uses (considering the increasing share of sawnwood products for furniture, flooring and packaging) of improved birch genotypes in Sweden. In each scenario, a different rotation age per specie/genotype was set due to economical harvesting rotation (optimal rotation age). A holistic system perspective was applied considering the biogenic (living biomass, soil organic carbon and HWPs) and anthropogenic carbon (value chain emissions), and potential substitution effects from avoided emissions. We used CO2FIX for biogenic carbon modelling, proceeded by a life cycle assessment considering the greenhouse gas emission from each process based on the EcoInvent database inventory (3.11 version). Results were expressed in absolute global temperature change potential (AGTP) considering a period of 140 years.

Results suggest that at low SIs equivalences, the replacement of spruce by improved birch, aiming long-lived wood products or the current use of non-improved birch (pulpwood/fuelwood) for one rotation, could outcome in a climate cooling effect in the atmosphere, being the first alternative (improved birch) the most climate beneficial choice. Whereas shortening spruce rotations at low SI could imply in a slight climate warming effect, representing a not climate smart choice. At medium SIs, the climate cooling

effect is just expected when considering the period of less than one rotation of improved birch. Finally, at high SIs, neither of the risk mitigations strategies were indicated for those sites due to increasing warming effects in the atmosphere (Figure 1).

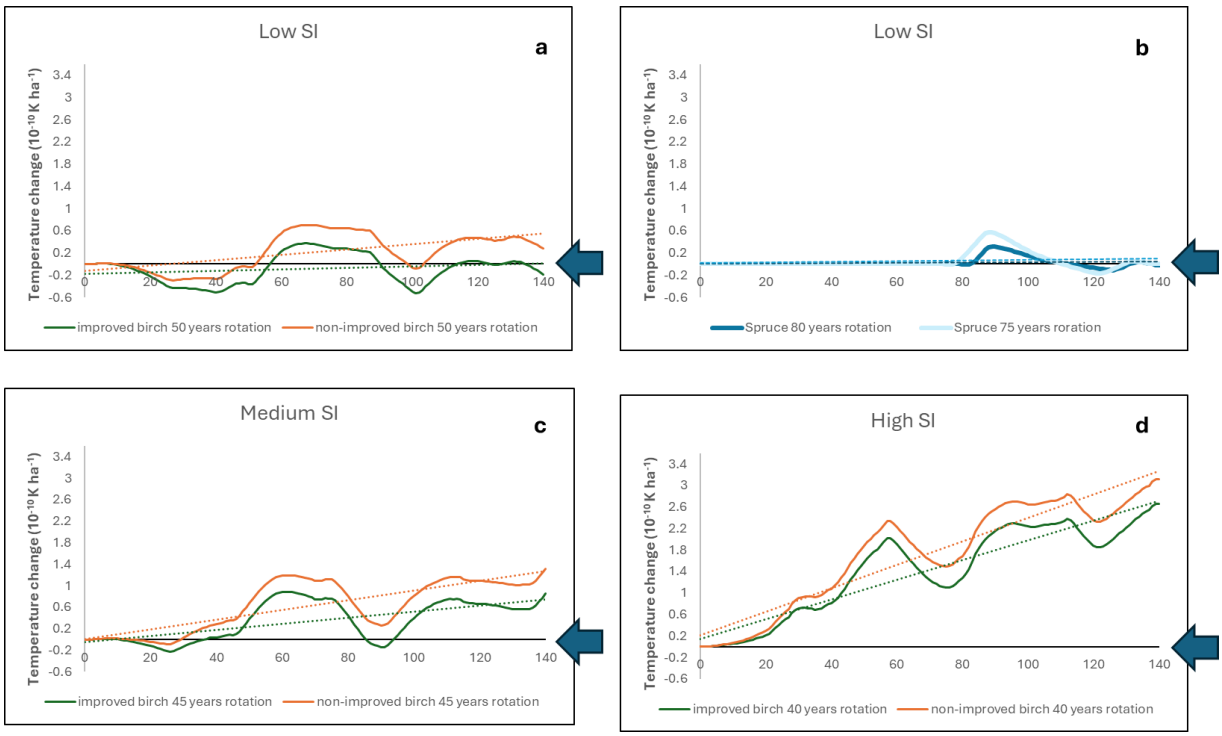

Figure 1: Absolute global temperature change potential (AGTP) difference between the reference (spruce) with respective risk mitigation strategy and site index equivalence. The arrows indicate the reference rotation age considered in the respective scenario: a and b (80 years rotation), c (73 years rotation), and d (55 years rotation). Dashed lines indicate the trend of their respective continuous lines. Positive values (ATPG) represent the climate warming effect in the atmosphere

Overall, the replacement of spruce by birch was just climate beneficial at low SIs. Shortening spruce rotations at low SIs and the replacement of spruce by birch at medium and high SIs could not represent a climate smart choice due to the climate warming effect in the atmosphere. Considering a holistic perspective of the forest system production, the results provide guidance for forest planning specially by recommending better risk mitigation strategies for specific Swedish sites. However, caution should be used to avoid generalization due to specific assumptions used for forest management strategies and assortments of HPWs in each comparison.

The final version of this abstract and the full scientific article are scheduled to be published in the Special Issue "12th Hardwood Conference—Sopron" of the journal MDPI Forests, available at the following link:

MDPI Forests Special Issue: 12th Hardwood Conference—Sopron

Volume Production and Stem Quality in Birch Stands of Eastern Norway

Katrin Zimmer[1*], Christian Kuehne[1], Irena Fundova[1]

[1]Norwegian Institute of Bioeconomy Research, PB 115, NO-1431 Ås, Norway.

E-mail: katrin.zimmer@nibio.no; christian.kuehne@nibio.no; irena.fundova@nibio.no

Keywords: *Betula pendula*, *Betula pubescens*, sawlogs, standing volume, timber grading.

ABSTRACT

There is growing interest in expanding the use of birch in Norwegian forestry, partly to increase broadleaf share and tree-species diversity under climate change. However, timber yield and quality assortments from Norwegian birch stands remain largely unknown. We established temporary sample plots in planted and naturally regenerated birch stands on high-quality sites in Eastern Norway and carried out tree measurements to quantify stand-level production. In addition, the first 6 m of each standing tree were subjected to a detailed timber-quality assessment and subsequently graded accordingly. Volume production in the investigated stands was frequently higher than values reported in birch yield tables from the 1970s and did not differ between planted and naturally regenerated stands. Volume production in the studied birch stands was similar to or higher than for Norway spruce on comparable high-quality sites up to a stand age of about 40 years. Despite the lack of quality-oriented management in most stands, nearly all produced sawlogs and many contained higher-quality assortments. Stand-level sawlog proportion increased with mean tree diameter. While planting and thinning showed no clear relationship with stand-level sawlog proportion, artificial pruning increased the share of higher-quality sawlogs. Overall, productive birch stands in Norway can deliver high yields and meaningful volumes of quality sawlogs.

INTRODUCTION

Birch (*Betula pendula*, *B. pubescens*) is the third most abundant tree species, and, by volume, the most important broadleaved tree species in Norway (Mahnert et al. 2026). It has regained interest within the last few years (Zimmer et al. 2023). One argument for increasing the share of birch and other broadleaved species in Norwegian forests is the ongoing climate change. Greater tree-species diversity in forests and an increased proportion of broadleaved trees in the landscape can reduce the risk of climate-related forest damage (Søgaard et al. 2023). Moreover, existing yield tables for birch developed in the 1960s and 1970s (Braastad 1967, 1977) do not reflect current growth conditions and their potential production.

Depending on forest type and stand development stage, actively managed stands of silver birch in Finland produce 30–70% timber of sawlog quality (Heräjärvi and Verkasalo 2002), and a veneer-log share of 5–10%. Comparable figures are unknown for Norway. This lack of information on timber volume production potential and quality assortments from Norwegian birch stands poses uncertainty among forest owners and the processing industry, potentially hindering future investments in birch.

Therefore, this study aimed to quantify and compare standing volume and sawlog proportions of different qualities in planted and naturally regenerated birch stands growing on highly productive sites.

MATERIALS AND METHODS

Between June and October 2024, field measurements were conducted on 28 temporary field plots across 26 birch stands in the Mjøs region, near Kongsvinger and Ås (Figure 1). In each stand, at least one representative sample plot with a radius of 8.92 m (250 m²) was established. Available information for each studied stand was derived from forest management plans, with the site index H40 (dominant height at 40 years of breast height age in meters) for all stands being 20 or 23, indicating high site productivity for birch (Braastad 1967). Thirteen stands had been planted and eleven had undergone artificial pruning (Table 1).

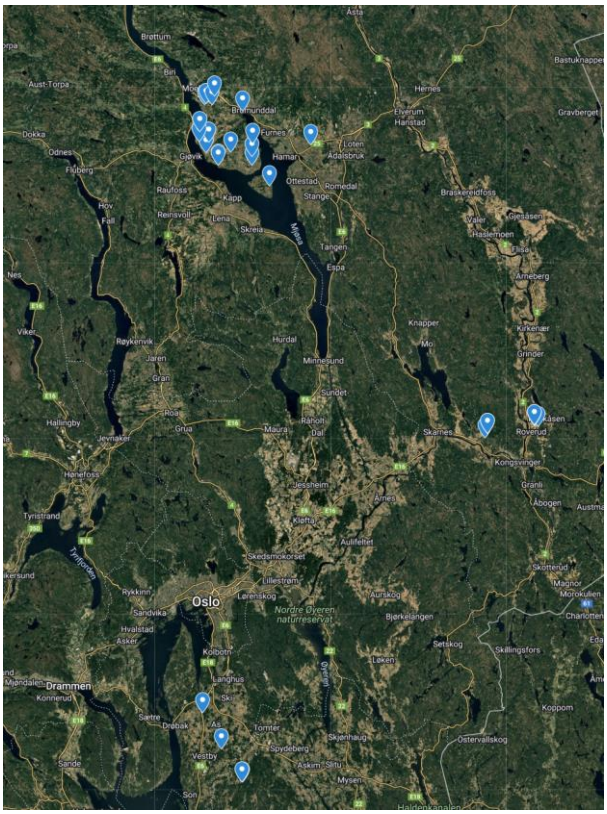

Figure 1: Overview of the location of the evaluated stands

Tree height and diameter at breast height (DBH) were measured for all trees with a DBH ≥ 10 cm in a plot. The first 6 m of the lower stem of all birch trees (n = 548) were evaluated to determine whether they met the minimum requirements for sawlogs (Vanhälls björksåg 2025). Log defects such as crooks, sweep of more than 8% of log length, leaning with more than 20 cm deviation from the vertical (for 3 m) and number of branches (>5 live and dead) concentrated within 1.5 m, were considered exclusion criteria for further sawlog evaluation. Logs exhibiting a butt sweep were assessed based solely on the section above the sweep. The number of branches, live and dead, as well as all other log features were recorded. In addition, the number of large branch scars with a height greater than one-quarter of the stem diameter at the scar position was counted per log (cf. Kuehne et al. 2024).
For the final quality classification of the logs, the grading regulations of an operating birch sawmill in Sweden, Vanhälls björksåg (2025), were used based on a minimum log length of 3 m. The Vanhälls björksåg grading regulations define three sawlog quality classes, A (best), B, and C, which, among other criteria, specify different maximum numbers of permitted live (green) and dead or rotten branches, while sharing a common requirement of a minimum top diameter of 18 cm. Based on Kuehne et al. (2024), large branch scars were also considered, with the combined total number of branches and large branch scars accounted for in the final evaluation.

Individual-tree and log volume were calculated using the taper functions from Hansen et al. (2023) and then accumulated at the stand level. Stand-level summary statistics including dominant height and basal area were compared with values from existing birch yield tables for Norway published in the 1970s (Braastad 1977). Volume production in the studied birch stands was further compared with productivity in spruce stands based on recently updated yield tables for the conifer species in Norway (Kühne et al. 2023).

Table 1: Stand information on the 17 plots that fulfilled the diameter requirements for sawlogs

Stand ID	elevation (a.s.l, m)	trees/ha	Birch trees /ha	HKl*	age	Regeneration
1	282	474	342	5	66	natural
3	253	560	400	5	66	natural
8	312	520	520	5	56	planted
10	146	680	680	4	33	planted
11	203	760	760	4	30	natural
16	301	760	760	4	40	planted
20	140	520	520	4	40	natural
26	196	1120	760	5	45	natural
34	213	1120	960	5	55	natural
38	210	520	400	5	50	natural
39/01	258	1280	840	5	50	natural
39/02	255	720	440	5	50	natural
41	167	480	240	5	55	natural
42	173	480	480	5	73	planted
43/01	168	600	360	5	80	planted
43/02	171	440	360	5	80	planted
65	46	600	600	4	35	planted

**HKl = Harvesting class describes the forest's development stage in five different classes, from HKL 1 – regeneration to HKL 5 - harvest-ready forest (Tomter et al. 2025).*

RESULTS

Age of the studied birch stands ranged from 28 to 80 years (mean 46 years), and the basal-area-weighted mean diameter of birch trees ranged from 14 to 39 cm (mean 24 cm).

Production potentials

Dominant height, basal area, and standing volume for the stands evaluated in this study were generally higher than the values reported for similar site indices in the existing birch yield tables for Norway. We found no difference in volume production between planted and naturally regenerated birch stands when accounting for stand age and density.

Compared with the development in spruce stands, birch stands often showed similar or higher volume production up to a stand age of about 40 years (Figure 2).

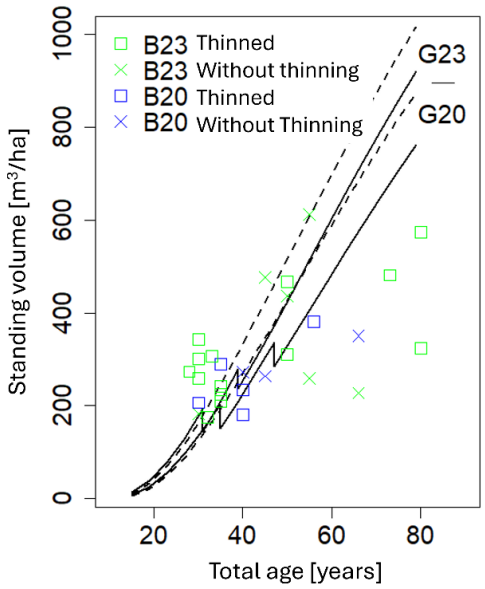

Figure 2: Standing volume for the birch stands in this study (site index classes B20 and B23) compared with the spruce stand development for the site index classes G20 and G23 with solid and dashed lines representing thinned and unthinned stands, respectively

Quality potentials

The majority of the examined 28 sample plots contained sawlogs (n = 27) while many also had sawlogs of the highest quality class A (n = 13). In 11 plots the majority of the examined birch trees did not meet the minimum top-diameter requirement of 18 cm given their development stage. Consequently, no or very few sawlogs were registered.

Most often, sweep (lateral and reverse) and the number of dead branches along the first 6 m of the stem were the reasons why logs meeting the minimum top-diameter requirement were either not further evaluated as sawlogs or downgraded in quality.

In the 17 stands with an average top diameter above 18 cm for the first 6 m of the stem, the lower 6 m stem section accounted for a mean stand-level volume of 160 m^3 ha^{-1} (85–252 m^3 ha^{-1}). Within these stands, the mean volume of sawlogs was 71 m^3 ha^{-1} (0–146 m^3 ha^{-1}; Figure 3). Of this, an average of 16 m^3 ha^{-1} (4–74 m^3 ha^{-1}) met the criteria for quality class A (Figure 3).

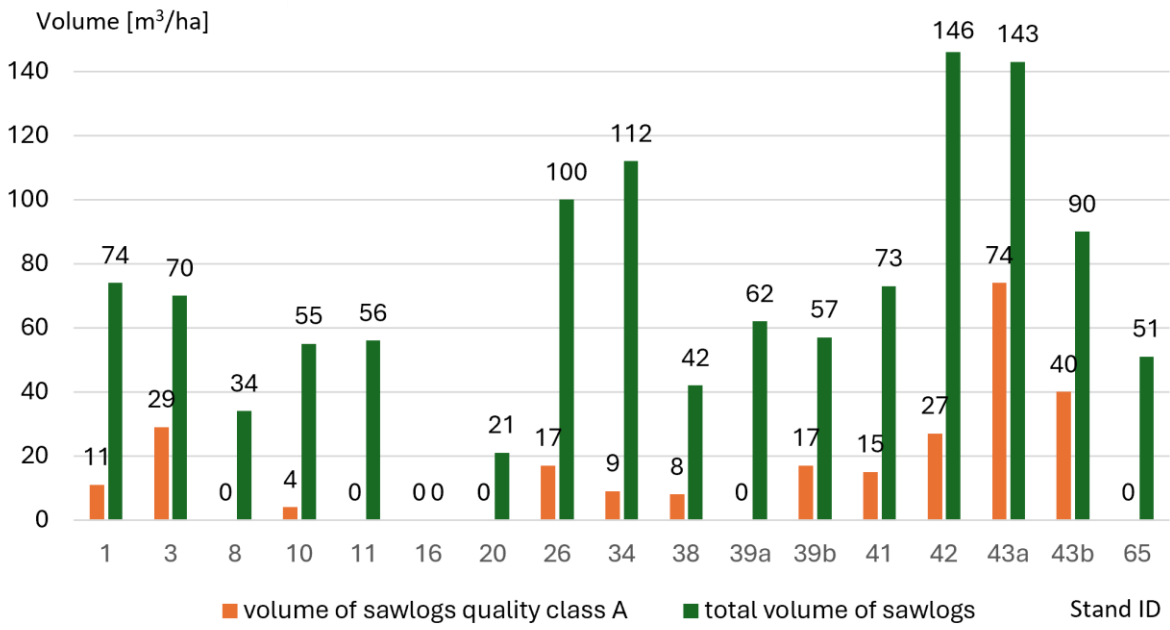

Figure 3: Total volume of sawlogs (green, m^3 ha^{-1}) and volume of sawlogs in quality class A (orange, m^3 ha^{-1}) for stands with an average top diameter above 18 cm for the first 6 m of the stem, classified according to Vanhälls Björksåg (2025)

Data analysis showed no significant relationship between the proportion of sawlogs at the stand level and planting or thinning, while the share of sawlogs increased with increasing mean diameter. In contrast, artificial pruning had a significantly positive effect on the share of sawlogs, but only for the higher grading classes A and B.

DISCUSSION

The vast majority of the birch stands examined in this work were not managed with the aim of producing quality timber within short rotations. At the same time, a conservative grading scheme was used to evaluate and determine stem quality. Most significantly, the original scheme (Vanhälls Björksåg 2025) was extended to include large branch scars. However, the findings are based only on external stem characteristics, i.e. did not account for potential internal timber defects.

The study results showed that most evaluated birch stands produced sawlogs, and that many stands contained some trees with logs that fulfilled the requirements for highest sawlog quality. We found that, in plots meeting the minimum top-diameter requirement, an average of 9.8% of the volume in the first 6 m of the sampled birch trees was classified as the best sawlog quality. This is comparable to findings

from a Finnish study, where 5–10% of the timber was classified into the highest quality classes (Heräjärvi and Verkasalo 2002).

There was no statistically significant difference in quality-timber potential between planted and naturally regenerated birch stands - something also found by Niemistö (1996). Natural birch stands often consist of a mixture of silver and downy birch, with the latter characterised by somewhat lower growth and production (Johansson 1996, Hytönen et al. 2014). Despite a relatively small number of evaluated stands, our results suggest that artificial pruning yields higher sawlog proportions, particularly in the higher grading classes. In addition, the proportion of sawlogs increased with increasing stand-level mean diameter, regardless of whether a stand was pruned or not. Without pruning, however, quality development takes longer, and the total amount of sawlogs at the end of the rotation will likely be reduced (Stener et al. 2017).

Although the primary purpose of management in the studied stands was most often not to produce sawlogs within a short time, the data from the evaluated stands suggest that a 6 m log with a top diameter of 18 cm (DBH approx. 21 cm) can be produced within about 35 years. This is less than half of the rotation length for a spruce rotation on site classes G20 and G23 (Kühne et al. 2023). At the same time, volume production in the studied stands was similar to or somewhat higher than in spruce stands (G20 and G23) up to a stand age of about 40 years, something previously described for both Norwegian (Hanssen & Kuehne 2022) and Finnish growth conditions (Oikarinen 1983). The lack of difference in volume production between planted and naturally regenerated stands found in this study has previously been described for Finnish conditions (Oikarinen 1983). At the same time, it suggests that the planted stands were not established with improved material. The use of newer, genetically improved planting material can be expected to provide both faster growth and higher production (Skrøppa and Kohmann 2018). In addition, studies show that improved material can simultaneously yield higher stem quality (Liebner 2023, Haapanen 2024).

CONCLUSION

In summary, the study shows that both planted and naturally regenerated Norwegian birch stands on high-quality sites have considerable potential for producing sawlogs. The share of sawlogs increases with tree size and is positively influenced by artificial pruning, although unpruned stands can also produce quality sawlogs over time. Given that birch combines high volume production at young and intermediate ages with a shorter rotation than spruce, quality-oriented birch management appears to be a relevant option for enhancing management diversity in Norwegian forestry.

REFERENCES

Braastad H. 1967. Produksjonstabeller for bjørk. Meddelelser fra det Norske Skogforsøksvesen 22: 265–365.

Braastad H. 1977. Tilvekstmodellprogram for bjørk. Norsk Institutt for Skogforskning Rapport 1/77.

Haapanen M. 2024. Realised genetic gains from past Finnish silver birch seed orchards. Silva Fennica 58(1): 23072.

Hansen E, Rahlf J, Astrup R, Gobakken T, 2023. Taper, volume, and bark thickness models for spruce, pine, and birch in Norway. Scandinavian Journal of Forest Research 38(6): 413-428.

Hanssen KH, Kuehne C. 2022. Gran og bjørk i blanding - hvordan går det egentlig? Magasinet Skog 2022(4): 44-46.

Heräjärvi H, Verkasalo E. 2002. Timber grade distribution and relative stumpage value of mature Finnish Betula pendula and B. pubescens when applying different bucking principles. Forest Products Journal 52(7/8): 40-52.

Hytönen J, Saramäki J, Niemistö P. 2014. Growth, stem quality and nutritional status of Betula pendula and Betula pubescens in pure stands and mixtures. Scandinavian Journal of Forest Research 29(1): 1-11.

Johansson T. 1996. Management of birch forest. Norwegian Journal of Agricultural Science Supplement 24: 7-20.

Kühne C, McLean JP, Hanssen KH. 2023. Oppdaterte produksjonstabeller og bonitetskurver for gran og furu i Norge, NIBIO Rapport 9: 109.

Kuehne C, Zimmer K, Smith A. 2024. The relationship between branch scar attributes and knot features in birch (Betula pendula and B. pubescens). Wood Science and Technology 58(3): 907-921.

Liebner H. 2023. Growth and quality of silver birch with different improvement levels. Masteroppgave. Swedish University of Agricultural Sciences.

Mahnert KC, Zimmer K, Snoksrud OM. (2026). Ressursene av utvalgte lauvtreslag i Norge. Treteknisk Rapport 92. https://www.treteknisk.no/publikasjoner/rapport/92-ressursene-av-utvalgte-lauvtreslag-i-norge.

Niemistö P. 1996. Yield and quality of planted silver birch (Betula pendula) in Finland - preliminary review. Norwegian Journal of Agricultural Science Supplement 24: 55-64.

Oikarinen M. 1983. Etelä-Suomen viljeltyjen rauduskoivikoiden kasvatusmallit. Communicationes Instituti Forestalis Fenniae 113.

Skrøppa T, Kohmann K. 2018. Genetisk variasjon mellom og innen norske populasjoner av hengebjørk (Betula pendula). NIBIO Rapport 4/3/2018.

Stener L-G, Rytter L, Jansson G. 2017. Effects of pruning on wood properties of planted silver birch in southern Sweden. Silva Fennica 51(2): 1713.

Søgaard G, Bright R, Clarke N, Fløistad IS, Granhus A, Hagenbo A, Hanssen KH, Hietala A, Kjønaas OJ, Kühne C, Rolstad J, Solberg S, Steffenrem A, Stokland J, Storaunet KO. 2023.

Tomter S, Svensson A, Snoksrud OM.(2025) Skog og skogbruk i Norge – Alder og utviklingstrinn. https://www.skogbruk.nibio.no/alder-og-utviklingstrinn.

Vanhälls Björksåg. 2025. Apteringsinstruks. https://vanhallssag.se/ws/medialibrary/b7a91f2bca8d430eb4c789c3a714fd29/apteringsinstruktion2020.pdf.

Zimmer K, Hylen G, Kühne C, Hanssen KH, Fløistad I, Smith A. 2023. Bjørk i Norge. NIBIO Rapport 9/63/2023.

Resources of Selected Broadleaved Tree Species in Norway

Katrin Zimmer[1*], Oliver Moen Snoksrud[1]

[1] Norwegian Institute of Bioeconomy Research, Høgskoleveien 8, 1431 Ås, Norway.

E-mail: katrin.zimmer@nibio.no, oliver.snoksrud@nibio.no

Keywords: birch, oak, ash, alder, aspen, standing volume, annual volume increment.

ABSTRACT

Broadleaved tree species from Norwegian forests are a valuable raw material if this resource can be utilized effectively. Broadleaved tree species make for approximately one fourth of the total standing volume in Norway today, but in statistics on the resource, it is usually referred to as Broadleaved tree species, instead of giving a detailed description on the different species present. This paper provides detailed data on standing volume and annual volume increment of ash (*Fraxinus excelsior)*, oak *Quercus robur* og *Q. petrea*), silver birch (*Betula pendula*), downy birch (*Betula pubescens*), aspen (*Populus tremula*), grey alder (*Alnus incana*), and black alder (*Alnus glutinosa*) in Norway, and give their distribution across the regions of Eastern Norway, Southern Norway, Western Norway, Trøndelag, and Northern Norway. Information on stand age, site quality, and diameter distribution will be provided.

INTRODUCTION

Broadleaf trees from Norwegian forests are a valuable raw material if this resource can be utilized effectively. Broadleaf trees make for approximately 1/4th of the standing volume in Norway. In the Norwegian National Forest Inventory reports, data on broadleaves are reported only as a cumulative sum. The total volume of broadleaves, in Norway, however, is made up from a variety of wood species. These species are, for example, birch, oak, beech, ash, aspen, alder, elder, cherry, maple, rowan, willow, and many more. While some of these species only occur in smaller volumes and admixtures in the stands, have other species, such as ash, oak, silver birch, downy birch, aspen, grey alder and black alder significant standing volumes and regional importance. Detailed data on species availability, structure and accessibility is only available on request.

Therefore, it is the aim of this paper to improve knowledge about how much of the selected broadleaf species ash (*Fraxinus excelsior*), oak (*Quercus robur* and *Q. petraea*), silver birch (*Betula pendula*), downy birch (*Betula pubescens*), aspen (*Populus tremula*), grey alder (*Alnus incana*) and black alder (*Alnus glutinosa*) is available in Norway and in the different regions, and to give more detailed information on the resource structure and accessibility. This will give us a better idea of how much wood from broadleaved species could possibly be transferred into industrial value chains.

MATERIAL AND METHOD

The study is based on unpublished data from Norway's National Forest Inventory (NFI), which has been gathering forest inventory information since 1919 (Breidenbach et al. 2020). Detailed data is provided on standing volume and annual increment of ash (*Fraxinus excelsior)*, oak *Quercus robur* and *Q. petrea*), silver birch (*Betula pendula*), downy birch (*Betula pubescens*), aspen (*Populus tremula*), grey alder (*Alnus incana)* and black alder (*Alnus glutinosa*) in Norway, and gives their distribution across the regions of Eastern Norway (Østlandet), Southern Norway (Sørlandet), Western Norway (Vestlandet), Trøndelag, and Northern Norway (Nord-Norge) (Figure 1).

The numbers for broadleaf species given are from the NFI data for the period 2018–2022 with reference year 2020 (unpublished). The standing volume stated is defined as the volume of the entire stem from the stump cut to the top of the tree and is expressed without bark (ub). According to data from the NFI, Norway has 223 304 390 m^3 ub of broadleaves — ash, oak, downy birch, grey alder, silver birch, aspen and black alder. The standard errors (SE) for the volume figures by species and region are, in some cases, very high. Despite the high uncertainty (SE) of some numbers in table 1 and 2, we chose to also display those with high uncertainty above 35% to provide an overview of the resource in standing

volume and annual volume increment. Tables 3 to 8 report sawlog volume without bark (ub) on productive forest excluding protected areas. Estimates with a relative standard error (SE) above 35% were not included in these tables. To calculate estimates of usable sawlog volume, the forest volume, i.e. standing volume, must be reduced by 6% for Norway spruce and Scots pine and by 10% for the broadleaf species. It is assumed that the tops of the trees are left on the harvest site after felling. The percentages are based on established empirical figures from the National Forest Inventory on how much coarse material remains on harvest sites (Hylen in Zimmer et al. 2023)

Figure 1: Norway and the 5 regions described

RESULTS

Norway has, in total, approximately 1 billion m^3 of roundwood standing on productive and unproductive forest land across all land uses (Svensson et al. 2021), of which conifers account for 734 million m^3 and the collected broadleaves 264 million m^3 (Snoksrud and Svensson and 2026).

Forest volume and annual volume increment

Productive forest is forest that, on average, can produce at least 1 m^3 of wood including bark per ha per year. This is in contrast to unproductive forest, where wood production is between 0.1 and 1 m^3 per ha per year. Increment is the volume of wood mass a stand or a tree increases by over one year (Svensson et al. 2021). These figures are important because they show how much volume is standing in the forest in different regions by species (Table 1) and how much the wood volume increases over one year (Table 2). This gives us information on how much timber from different species can theoretically be harvested sustainably per region.

Table 1: Standing volume under bark (ub) [1000 m^3 ub] and standard error (SE), for wood species and region, reference year 2020

	Standing volume under bark (ub) [1000 m^3 ub]										
	Eastern N.*		Southern N.*		Western N.*		Trøndelag		Northern N.*		*total*
	volume	SE	volume	SE	volume	SE	volume	SE	volume	SE	volume
Ash	657	47	1 053	25	1 360	27	15	100			*3 085*
Oak	168	49	7 735	10	1 201	25					*9 104*
Silver birch	6 581	10	3 718	12	1 223	20	48	91	5	100	*11 575*
Downy birch	44 219	3	19 116	5	31 544	4	18 550	4	48 104	4	*161 533*
Aspen	4 398	13	7 562	9	2 710	16	965	30	1 827	20	*17 461*
Grey alder	5 547	15	791	26	5 123	11	3 906	15	2 662	13	*18 029*
Black alder	603	31	717	32	1 174	30	22	100			*2 517*
Total	*62 172*		*40 692*		*44 336*		*23 507*		*52 597*		*223 304*

**N = Norway*

According to data from the NFI (reference year 2020), Norway has 223 304 390 m^3 ub of broadleaves — ash, oak, downy birch, grey alder, silver birch, aspen and black alder. Across all regions, downy birch represents the largest volume, from 18.6 million m^3 ub in Trøndelag up to 48 million m^3 ub in Northern Norway. In Northern Norway and Trøndelag, downy birch, aspen and grey alder account for most of the volume. In Western Norway, Eastern Norway, and Southern Norway, the species mix is more varied than in the north. In Southern Norway there are large volumes of oak and aspen (7.7 million m^3 ub and 7.6 million m3 ub) in addition to silver birch (3.7 million m3 ub), downy birch (19 million m3 ub) and ash (1 million m^3 ub). In Western Norway there are about 5 million m^3 ub grey alder plus 2.7 million m^3 ub aspen. Eastern Norway has nearly 4.4 million m^3 ub aspen in addition to 6.6 million m^3 ub silver birch and 5.5 million m^3 ub grey alder (Table 1).

Table 2: Annual volume increment [1000 m^3] and standard error (SE), for wood species and region, reference year 2020

	Volume increment [1000 m^3]										
	Eastern N.*		Southern N.*		Western N.*		Trøndelag		Northern N.*		*total*
	volume	SE	volume	SE	volume	SE	volume	SE	volume	SE	volume
Ash	14	42	26	24	45	34					85
Oak	3,5	46	158	10	32	25					193,5
Silver birch	214	12	99	13	26	21					339
Downy birch	903	4	323	5	571	5	402	5	831	4	3030
Aspen	108	16	164	9	59	16	20	29	43	21	394
Grey alder	222	14	28	26	209	12	175	14	109	15	743
Black alder	17	29	19	35	30	29	1	100			67
Total	1482		817		970		601		984		4854

**N = Norway*

The selected broadleaved species have a total increment of about 5 million m^3, with the highest increment in Eastern Norway at 1.5 million m^3, followed by Northern Norway and Western Norway at about 1 million m^3, each. Downy birch accounts for 3 million m^3 of the total ~5 million m^3 increment. Next largest increments are grey alder (0.7 million m^3) and aspen (0.4 million m^3). Oak has a total increment of 0.2 million m^3 ub, of which 75% is in Southern Norway (Table 2).

Diameter and age

For quality sawlog broadleaf timber, trees with a diameter over 20 cm are of particular interest, as top-diameter sizing is one of the quality criteria (Landbruksdepartementet 1956). High-quality broadleaf sawlog and sawn timber is characterised by knot-free wood and is often cut with a band saw or frame saw, frequently from the outside in to obtain as much knot-free wood as possible. For some species (such as grey alder), smaller diameters are also relevant for sawing. Oak in Southern Norway has a total sawlog volume of 2.3 million m^3 ub in the 30+ cm diameter class. In addition, just under 200000 m^3 ub stands in the next lower diameter class (20–29.9 cm) and will grow into the larger class in the coming decades (Table 3). Silver birch has a total sawlog volume of 3.1 million m^3 ub in the 30+ cm diameter class, with the largest share in Eastern Norway, followed by Southern and Western Norway. Although the largest volumes of downy birch in all regions are in the 5–19.9 cm diameter class, there are 1.3–2.9 million m^3 ub in the 30+ cm class in Southern, Eastern, and Western Norway, while there are 0.4 million m^3 ub in Trøndelag and 0.8 million m^3 ub in Northern Norway. In the 20–29.9 cm class the stock of downy birch is even larger, with 2.6–6.3 million m^3 ub in each of the regions. The largest volume of aspen is in the 30+ cm diameter class, with all regions except Trøndelag having standing volumes between 0.6 and 2.3 million m^3 ub. Neither grey alder, black alder nor ash have standing volume in the 30+ cm diameter class, but there are 0.3 million m^3 ub ash in Southern Norway in the 20–29.9 cm class. In the same diameter class grey alder has 1 million m^3 ub in both Eastern and Western Norway.

Table 3: Sawlog volume without bark and SE, per diameter class [cm], wood species and region

		Sawlog volume without bark (ub) [1000 m³] and standard error (SE)									
		Eastern N.*		Southern N.*		Western N.*		Trøndelag		Northern N.*	
	Diameter class	volume	SE	volume	SE	volume	SE	volume	SE	volume	SE
Ash	≥30										
	20-29.9			322	28						
	5-19.9			344	25	227	24				
Oak	≥30			2276	19						
	20-29.9			1851	12						
	5-19.9	54	34	1908	11	239	31				
Silver birch	≥30	1699	22	992	21	383	29				
	20-29.9	1971	18	1168	14	352	27				
	5-19.9	1931	18	925	14	187	28				
Downy birch	≥30	2366	18	1358	18	2940	12	440	28	789	17
	20-29.9	6169	8	3361	8	6094	7	2578	8	6285	6
	5-19.9	24559	4	9482	5	13302	5	10191	5	26755	5
Aspen	≥30	1781	23	2268	15	1012	12			609	33
	20-29.9	1068	20	2169	12	920	19	254	31	427	27
	5-19.9	683	20	1820	11	321	21	89	26	424	33
Grey alder	≥30										
	20-29.9	1067	33			1080	17	579	28	472	23
	5-19.9	2845	17	368	33	2781	12	2553	14	1672	13
Black alder	≥30										
	20-29.9										
	5-19.9	206	34	200	33	318	29				

**N = Norway*

Table 4: Sawlog volume without bark [1000 m³] and SE, per age class, wood species and region

		Sawlog volume without bark (ub) [1000 m³] and standard error (SE)									
		Eastern N.*		Southern N.*		Western N.*		Trøndelag		Northern N.*	
	Age class	volume	SE	volume	SE	volume	SE	volume	SE	volume	SE
Ash	< 50										
	50 - 99			716	30						
	100 - 149										
	≥ 150										
Oak	< 50			749	19						
	50 - 99			2312	16						
	100 - 149			2779	19						
	≥ 150										
Silver birch	< 50	2447	21	1230	19						
	50 - 99	2527	21	1021	21	587	26				
	100 - 149	386	25	677	28						
	≥ 150										
Downy birch	< 50	7622	9	2504	9	2242	11	2979	9	3207	10
	50 - 99	15830	7	5951	8	12050	7	5138	8	17002	7
	100 - 149	7981	9	4954	9	7381	8	4106	8	12740	8
	≥ 150	1537	16	767	16	622	26	955	13	789	22
Aspen	< 50	441	30	926	18						
	50 - 99	1053	26	2884	14	1118	24			1016	29
	100 - 149	591	28	2110	16	964	25			399	30
	≥ 150										
Grey alder	< 50	2475	29	324	33	1409	21	1688	20	517	29
	50 - 99	2163	32			2260	16	1446	26	1418	18
	100 - 149					434	26	158	26	337	22
	≥ 150										
Black alder	< 50										
	50 - 99			284	33						
	100 - 149										
	≥ 150										

For most of the species, the 50–99-year age class is most relevant for harvesting, except for oak. Old trees may be subject to harvesting restrictions due to environmental certification requirements (Luostarinen and Verkasalo 2000). Looking at the age-class distribution across species, only downy birch has a larger volume in the 150-year-and-older age class. In this class, there are about 4.7 million m3 ub, of which 1.5 million m3 ub stands in Eastern Norway and just under 1 million m3 ub in Trøndelag (Table 4). In Southern Norway, there are 2.8 million m3 ub of oak in the 100–149-year age class.

Site quality (site index, elevation)

In forestry, the term site index is used to classify growing sites with respect to the forest's growth potential for trees. A higher site index is associated with better height growth and higher production. Forests have greater annual increment (diameter and height) and reach harvest maturity earlier on the highest site indices. In Norway, the site index is related to the species spruce, pine and birch. Site index (H40) is defined as the dominant height (average height of the 10 largest trees per hectare) in metres at breast-height age (the tree's age at breast height, i.e. 1.3 m) 40 years and is given in classes, for example G17 (species spruce, 17 m at 40 years), F20 (species pine, 20 m at 40 years) or B23 (species birch, 23 m at 40 years) (Svensson et al. 2021).

In Eastern Norway about 4 million m3 ub of silver birch grows on high site index; additionally, there are 9 million m3 ub of downy birch, 1 million m3 ub of aspen, and 4 million m3 ub of grey alder. Southern Norway has large resources of ash (0.8 million m3 ub), silver birch (1.6 million m3 ub), downy birch (2.8 million m3 ub), oak (1.8 million m3 ub) and aspen (1.6 million m3 ub) growing on high site index (Table 5). In Western Norway, only downy birch and grey alder occur on high site indices, with 1.5 and 1.2 million m3 ub respectively.

Table 5: Sawlog volume without bark (ub) [1000 m³] and standard error (SE), per site index, wood species and region

		Sawlog volume without bark (ub) [1000 m³] and standard error (SE)									
		Eastern N.*		Southern N.*		Western N.*		Trøndelag		Northern N.*	
	Site index	volume	SE	volume	SE	volume	SE	volume	SE	volume	SE
	Low (6-8)										
Ash	Middle (11-14)					325	35				
	High (+17)			755	29						
	Low (6-8)			1159	21						
Oak	Middle (11-14)			3078	15	616	34				
	High (+17)			1798	22						
	Low (6-8)	229	28	324	22						
Silver birch	Middle (11-14)	1368	25	1139	17	631	27				
	High (+17)	3936	17	1623	19						
	Low (6-8)	12648	7	5002	8	8482	9	5473	7	23120	6
Downy birch	Middle (11-14)	11167	8	6334	7	12320	6	6288	7	10364	8
	High (+17)	9281	10	2863	12	1534	14	1448	13	345	24
	Low (6-8)	197	32	993	19					562	26
Aspen	Middle (11-14)	1225	22	3670	12	1545	20			898	32
	High (+17)	1059	27	1593	20						
	Low (6-8)					529	26	135	32	872	23
Grey alder	Middle (11-14)	683	27	50	35	2449	15	1492	18	1352	17
	High (+17)	4025	24	512	25	1153	24	1714	24		
	Low (6-8)										
Black alder	Middle (11-14)			228	35						
	High (+17)										

**N = Norway*

Elevation

The altitude (in meters above sea level (a.s.l.)) of a stand affects growth conditions for trees and other plants. Growth conditions decline with increasing elevation because average temperature decreases with height, reducing height and diameter growth (Kollmann and Côté 1968), up to the treeline where forests can no longer establish. Several factors influence treeline altitude. In the Northern Hemisphere treeline mainly lowers with increasing latitude, but it also varies along a coast–inland gradient and is lower near the coast than inland in Norway. Therefore, we consider timber volume in the lowest elevation class (0–300 m a.s.l.) as a prerequisite for good increment.

Oak, ash and black alder grow only in the lowest elevation class: oak and ash in Southern and Western Norway, and black alder in Western Norway. Silver birch also largely occurs within the lowest elevation class, but in Eastern Norway one third of the volume lies above 300 m a.s.l. Aspen and grey alder occur in all regions in the lowest elevation class (0.7–3.8 million m3 ub for aspen and 0.4–3.7 million m3 ub for grey alder), with larger aspen volumes on Eastern, Western and Southern Norway (0.7, 0.8 and 2 million m3 ub, respectively). Only in Southern Norway does aspen grow in the highest elevation class (0.5 million m3 ub). For downy birch, half the volume is within the lowest elevation class and half above 300 m a.s.l. Very large volumes of downy birch also grow in the highest elevation class: 14 million m3 ub in Eastern, 3.1 million m3 ub in Southern, 1.8 million m3 ub in Western Norway and 2.4 million m3 ub in Trøndelag (Table 6).

Table 6: Sawlog volume without bark (ub) [1000 m3] and standard error (SE), per elevation [m], wood species and region

		Sawlog volume without bark (ub) [1000 m^3] and standard error (SE)									
		Eastern N.*		Southern N.*		Western N.*		Trøndelag		Northern N.*	
	Elevation	volume	SE	volume	SE	volume	SE	volume	SE	volume	SE
Ash	0-300			881	26	824	32				
	301-600										
	>600										
Oak	0-300			5875	11	878	29				
	301-600										
	>600										
Silver birch	0-300	3890	16	2571	13	853	23				
	301-600	1651	24	511	28						
	>600										
Downy birch	0-300	9519	9	5600	8	12005	6	5834	6	26121	5
	301-600	9782	8	5469	8	8566	9	5010	7	7380	10
	>600	13793	7	3131	11	1764	21	2365	14		
Aspen	0-300	1755	19	3784	11	1472	20	711	34	1460	22
	301-600	716	27	2008	17	780	28				
	>600			465	34						
Grey alder	0-300	3684	26	437	14	2854	15	2883	17	2109	14
	301-600	923	24			1199	18	405	24		
	>600										
Black alder	0-300	473	33	583	34	924	32				
	301-600										
	>600										

**N = Norway*

Accessibility

Easy accessibility is a prerequisite for cost-effective harvesting. Harvesting class describes the forest's development stage in five different classes, and takes into account the quality of the land, i.e. the ability to produce wood, in addition to the age of the stand (Tomter et al. 2025). The classification ranges from establishment of the forest to harvest-ready forest and depends on site index, resulting in different lower age limits for different productivities.

In Norway, five harvesting classes (HKL) are used in forest planning (Svensson et al. 2021):

- HKL 1 – regeneration,
- HKL 2 – regeneration and young forest,
- HKL 3 – younger production forest,
- HKL 4 – older production forest approaching harvest maturity. Thinning is often applicable,
- HKL 5 – harvest-ready forest. Increment stagnates and harvesting of the stand is relevant.

Throughout Norway, 91 million m3 ub of broadleaves of the selected species stand in HKL 5, of which 1.3 million m3 ub is ash, 4 million m3 ub silver birch, 59 million m3 ub downy birch, 4.5 million m3 ub oak, 3.4 million m3 ub grey alder, and 8.6 million m3 ub aspen (Table 7). In Eastern Norway about 2 million m3 ub silver birch, 14.5 million m3 ub downy birch, and 1.5 million m3 ub aspen are harvest-ready in HKL 5. Southern Norway has 4.5 million m3 ub harvest-ready oak, and large harvest-ready resources of birch (silver birch 1.3 million m3 ub, downy birch 8.1 million m3 ub), aspen (3.9 million m3 ub) and ash (0.7 million m3 ub). Northern Norway has large volumes of harvest-ready downy birch (25 million m3 ub) and grey alder (1 million m3 ub).

Table 7: Sawlog volume without bark (ub) [1000 m^3] and standard error (SE), per maturity class, wood species and region

		Sawlog volume without bark (ub) [1000 m^3] and standard error (SE)									
		Eastern N.*		Southern N.*		Western N.*		Trøndelag		Northern N.*	
	Maturity class	volume	SE	volume	SE	volume	SE	volume	SE	volume	SE
Ash	1+2										
	3										
	4										
	5			744	29	514	30				
Oak	1+2										
	3			575	21						
	4			825	20						
	5			4509	14						
Silver birch	1+2	138	31								
	3	1502	25	813	20						
	4	1214	21	757	23						
	5	2173	23	1302	21	538	28				
Downy birch	1+2	1644	14	488	16	291	20	377	15	976	15
	3	6559	9	2343	9	1553	13	3263	9	2740	12
	4	10415	9	3247	11	6078	10	2637	11	4907	13
	5	14478	7	8123	7	14414	6	6932	7	25206	5
Aspen	1+2										
	3			527	19						
	4	324	35	1580	18	185	33				
	5	1495	21	3892	12	2018	18			1235	24
Grey alder	1+2	146	31					38	31		
	3	734	30			640	30	1305	19	267	35
	4	1455	26			1982	18	1041	27	874	24
	5					1449	18	957	34	969	19
Black alder	1+2										
	3										
	4										
	5										

**N = Norway*

Skidroad distance, or distance to road, is one of the factors that significantly affects harvesting costs and denotes the distance the timber must be transported from the harvest site to a public road, where a shorter distance to road indicates better accessibility (Svensson et al. 2021).

In Eastern Norway, a total of 32 million m³ ub of broadleaves — silver birch (4.6 million m³ ub), downy birch (20.6 million m³ ub), aspen (2.7 million m³ ub) and grey alder (4.2 million m³ ub) — stand at short distance to road (0–500 m). This represents 70% of the volume of the selected broadleaf species in Eastern Norway (Table 8). In Southern Norway, the proportion of stands with short skidroad distance is 59%, and 18 million m³ ub of the selected broadleaf species stand in the nearest-to-road category (ash 0.8 million m³ ub, oak 4.2 million m³ ub, silver birch 2.3 million m³ ub, downy birch 7.3 million m³ ub, aspen 3.2 million m³ ub, grey alder 0.4 million m³ ub). In Western Norway, only 51%, i.e. 15 million m³ ub of the selected broadleaf species, are within a short distance of the road. Ash (0.9 million m³ ub), oak (0.6 million m³ ub) and silver birch (0.7 million m³ ub) occur exclusively near the road (0–500 m), while downy birch (9.3 million m³ ub), aspen (1.1 million m³ ub) and grey alder (2.8 million m³ ub) have larger volumes totalling 15 million m³ ub located farther from roads. In Trøndelag 61% of downy birch (6.9 million m³ ub), aspen (0.6 million m³ ub) and grey alder (2.9 million m³ ub) stand 0–500 m from road. In Northern Norway only 41% of the same species (downy birch 12.7 million m³ ub, aspen 1 million m³ ub, grey alder 1.5 million m³ ub) are that close to roads.

Table 8: Sawlog volume without bark (ub) [1000 m³] and standard error (SE), per distance to road, wood species and region

		Sawlog volume without bark (ub) [1000 m³] and standard error (SE)									
		Eastern N.*		Southern N.*		Western N.*		Trøndelag		Northern N.*	
	Distance to road	volume	SE	volume	SE	volume	SE	volume	SE	volume	SE
Ash	0-500			842	27	858	32				
	501-1000										
	>1000										
Oak	0-500			4168	14	616	33				
	501-1000			1484	20						
	>1000			383	27						
Silver birch	0-500	4615	16	2251	14	672	25				
	501-1000	572	25	398	30						
	>1000	195	35	436	10						
Downy birch	0-500	20599	6	7328	7	9333	7	6909	7	12712	7
	501-1000	6257	11	3 160	10	5055	10	2092	11	7555	11
	>1000	6239	11	3712	10	7948	10	4207	9	13563	7
Aspen	0-500	2675	24	3191	12	1136	7	574	30	964	29
	501-1000	444	28	1529	19						
	>1000			1536	20	723	29				
Grey alder	0-500	4186	22	445	26	2792	15	2939	17	1516	18
	501-1000					844	21	165	32	487	27
	>1000					495	29	237	31	273	29
Black alder	0-500										
	501-1000										
	>1000										

**N = Norway*

CONCLUSIONS

This paper provides detailed data on standing volume and annual volume increment of ash (*Fraxinus excelsior)*, oak *Quercus robur* and *Q. petrea*), silver birch (*Betula pendula*), downy birch (*Betula pubescens*), aspen (*Populus tremula*), grey alder (*Alnus incana*), and black alder (*Alnus glutinosa*) in Norway, and give their distribution across the regions of Eastern Norway, Southern Norway, Western Norway, Trøndelag, and Northern Norway. In Northern Norway and Trøndelag, mostly downy birch, grey alder and aspen are of relevance, while Southern Norway has the largest variety in broadleaved tree species available. Large volumes of different broadleaved tree species are mature and ready for harvesting in all regions. Large volumes of the different broadleaved tree species grow on high site indexes and produce diameters that are interesting also for saw timber production. Oak, ash and silver birch grow almost exclusively with short distances to roads. Everything indicates that there is capacity for industrial use and value creation of the broadleaved tree resources in Norway.

ACKNOWLOGEMENTS
This article is based on the report "Ressursene av utvalgte lauvtreslag i Norge" (Mahnert et al. 2026) prepared as a collaboration between Treteknisk and NIBIO, funded by SynForest (Research Council of Norway project no. 336381), HUB:NODE (Innovation Norway 2023/381170) and the Research Council of Norway (project no. 342631) and presents a selection of the results of Chapter 3 on the availability of broadleaved tree species in Norway.

REFERENCES

Breidenbach J, Granhus A, Hylen G, Eriksen R, Astrup R. 2020. A century of National Forest Inventory in Norway – informing past, present, and future decisions. For Ecosyst. 7(1):46. doi:10.1186/s40663-020-00261-0.

Kollmann, F.F.P., and Côté, W.A. 1968. Principles of wood science and technology. Springer, Berlin – Heidelberg, Germany.

Landbruksdepartement (1956). Regler for måling og levering av skur- og spesialtømmer av lauvtre. https://lovdata.no/dokument/SFO/forskrift/1956-01-19-1 (in Norwegian)

Luostarinen K. and Verkasalo E. (2000). Birch as sawn timber and in mechanical further processing in Finland. A literature study. Silva Fennica Monographs 1. 40 p. ISBN 951-40-1745-5.

Mahnert K, Zimmer K, Snoksrud OM. (2026). Ressursene av utvalgte lauvtreslag i Norge. Treteknisk Rapport 92. https://www.treteknisk.no/publikasjoner/rapport/92-ressursene-av-utvalgte-lauvtreslag-i-norge.

Solberg, S., Merlin, M., & Eriksen, R. (2025). Periodic site index and climatic stress for Norway spruce in Norway. *Scandinavian Journal of Forest Research*, *40*(7–8), 371–383. https://doi.org/10.1080/02827581.2025.2551924

Svensson A, Eriksen R, Hylen G, Granhus A. (2021). Skogen i Norge - Statistikk over skogforhold og skogressurser i Norge for perioden 2015-2019. NIBIO RAPPORT 7/142/2021. (in Norwegian)

Snoksrud OM. and Svensson A. (Red) 2026. Skog og skogbruk i Norge. Norwegian Institute for Bioeconomy Research. https://www.skogbruk.nibio.no/skogen-i-norge/. (in Norwegian)

Tomter S, Svensson A, Snoksrud OM.(2025) Skog og skogbruk i Norge – Alder og utviklingstrinn. https://www.skogbruk.nibio.no/alder-og-utviklingstrinn.

Zimmer K, Hylen G, Kuehne C, Hanssen KH, Fløistad I, Smith A. (2023). Bjørk i Norge. NIBIO Rapport 9/63/2023.(in Norwegian)

Condition Monitoring of Standing Trees based on Dendro-Acoustic Emissions

Frank Schubert[1*], Frank Duckhorn[1], Michael Reinhold[1], Clemens Zange[2], Carsten Hennig[2], Mario Hopfner[3], Antje Wilhelms[3], Maxi Binder[4], Richard Georgi[4], Claudia Scharff[5], Wolfram Scharff[5]

[1] Fraunhofer IKTS, Maria-Reiche-Str. 2, 01109 Dresden, Germany
[2] Teletronic Rossendorf GmbH, Dresden, Germany
[3] IfU GmbH Privates Institut für Umweltanalysen, Lichtenau, Germany
[4] OGF Forest Innovations GmbH, Wilsdruff, Germany
[5] Früchteverarbeitung Sohra GmbH, Sohra, Germany.

E-mail: frank.schubert@ikts.fraunhofer.de; frank.duckhorn@ikts.fraunhofer.de; michael.reinhold@ikts.fraunhofer.de; clemens.zange@teletronic.net; carsten.hennig@teletronic.net; mho@ifu.de; awi@ifu.de; maxi.binder@ogf.de; richard.georgi@ogf.de; csc@fruechte-sohra.de; wsc@ifu.de

Keywords: dendro-acoustics, acoustic emission, standing trees, condition monitoring, structure-borne sound, autonomous sensor node, vitality assessment.

ABSTRACT

In the areas of road safety, fruit growing and forestry, there is an increased need for assessing the vitality of standing trees. Various micro-acoustic sound emissions potentially allow conclusions to be drawn about the vitality of the trees and various diseases and pest infestations. They can be separated into at least four different event categories:

- Fibre breakage events due to mechanical and thermo-mechanical loads
- Drought stress events based on capillary collapse and crack initiation
- Sap flow events based on trunk diameter changes ("tree breathing")
- Beetle and mouse events based on feeding noises

All types of events produce structure-borne sound inside the tree and can be automatically measured and evaluated by a piezoelectric sensor node attached to the tree trunk. The events are characterized by short, broadband crackling signals. Depending on the type of event, these differ in their number, strength and acoustic centre frequency (up to 60 kHz) and can be separated from various types of background noise (such as traffic, wind, rain, etc.).

In the frame of a German collaborative research project (TreeMon), an autonomous sensor prototype for long- and short-term monitoring based on LoRaWAN technology was developed and successfully tested in the field. We present results of various test and field measurements at different trees, including several hardwood species like beech, birch and fruit trees.

We compare temporal acoustic emission profiles of single trees with simultaneously recorded weather and dendrometer data as well as with drone-based spectral analyses and vegetation indices. From these evaluations we can learn if and how dendro-acoustic emissions are correlated with the vitality of trees and various diseases and pest infestations. Current challenges are the further suppression of external noise and the development of an energy self-sufficient and cost-effective system for a wide variety of applications in road safety, fruit growing and forestry.

Figure 1: Acoustic measurement technology and instrumentation for field measurements

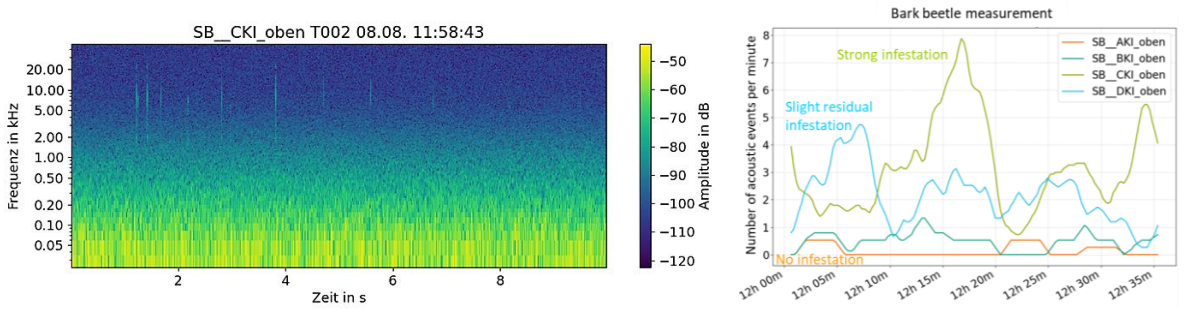

Figure 2: Acoustic data evaluation based on spectrogram classification and temporal event statistics

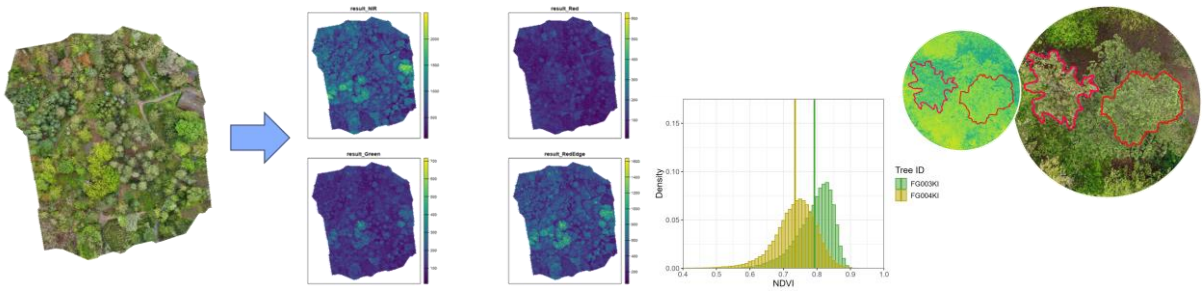

Figure 3: Drone-based visual inspection and vitality assessment for correlation with acoustic data

The final version of this abstract and the full scientific article are scheduled to be published in the Special Issue "12th Hardwood Conference—Sopron" of the journal MDPI Forests, available at the following link:
MDPI Forests Special Issue: 12th Hardwood Conference—Sopron

Hardwood Afforestation on Extreme Sites in the Czech Republic: Growth Performance and Resistance of Selected Species

Zdeněk Vacek[1*], Stanislav Vacek[1]

[1] Faculty of Forestry and Wood Sciences, Czech University of Life Sciences Prague, Kamýcká 129, CZ 165 00 Prague 6–Suchdol, Czech Republic.

E-mail: vacekz@fld.czu.cz, vacekstanislav@fld.czu.cz

Keywords: site stress, climate change, seedling mortality, species suitability, forest restoration.

ABSTRACT

Global climate change is increasingly affecting the vitality, productivity, and resistance of native tree species in Central Europe, while the suitability of introduced species for forest restoration is gaining attention. Rising temperatures, frequent droughts, and increasing climatic variability complicate successful afforestation, particularly on environmentally extreme sites. This study evaluated mortality, health status, and growth potential of 13 native and 9 introduced tree species planted on an extremely unfavorable site in the Czech Republic. The experimental plantation was established on a former forest nursery area (459–481 m a.s.l.) characterized by compacted sandy soils and unfavorable chemical properties. After three years, the highest height increment among native species was recorded for *Ulmus minor* and *Sorbus domestica*, while among introduced species the best growth was observed for *Ulmus pumila* and *Quercus pyrenaica*. The lowest mortality among introduced species was found for *Quercus rubra* and *Q. pyrenaica*, whereas among native species the best survival rates were recorded for *Fagus sylvatica* and *Quercus petraea*. In contrast, *Morus nigra*, *Ginkgo biloba*, and *Aesculus hippocastanum* showed poor adaptation and are not recommended for afforestation of extreme sites in the Czech Republic. Introduced tree species exhibited, on average, 48.7% higher mortality and a 36.2% lower growth increment compared to native species. The results indicate that several especially native hardwood species can maintain satisfactory growth and survival even under highly unfavorable conditions. From a silvicultural perspective, mixed plantations combining tolerant species appear to represent a more stable strategy than monocultures. Future afforestation efforts should emphasize species diversity, suitable plant material, and careful provenance selection to enhance resilience and long-term forest stability under ongoing climate change.

INTRODUCTION

In the context of global climate change (IPCC 2019), it is essential to understand how forest ecosystems will respond to ongoing environmental changes under different site and stand conditions in the Czech Republic. With increasing average temperatures, more frequent and severe occurrences of extreme climatic events, particularly heat waves and drought periods, are expected, significantly affecting the growth, development, and ecological stability of forest ecosystems (Seidl et al. 2017; Vacek et al. 2023). This is closely associated with the increasing vulnerability of forests to warm drought periods, raising concerns about the adaptive capacity of forest stands to ongoing climate change (Šimůnek et al. 2023; Vacek et al. 2023), especially during post-disturbance forest regeneration (Poleno et al. 2009; Leugner et al. 2025).

Forest stands also play a crucial role in providing ecosystem services (Brockerhoff et al. 2017). They produce timber, fuel, fibre, and fodder, while significantly contributing to climate regulation through carbon sequestration, as well as to soil formation and stabilization and the cycling of water and nutrients (MacDicken 2015; MacDicken et al. 2015). Forest ecosystems affected by disturbances therefore require targeted and effective restoration measures (Vacek et al. 2023; Leugner et al. 2025). Although forests are essential for mitigating the impacts of climate change, they are themselves strongly affected by extreme weather events, which may reduce both their stability and the ecosystem services they provide across the European distribution range of tree species (Buras, Menzel 2019; Montagnoli et al. 2022).

For these reasons, it is necessary under Central European conditions to verify the adaptability of promising tree species suitable for the restoration of disturbed and degraded sites under ongoing climate

change (Vacek et al. 2023). Overall, in Central Europe, it is projected that approximately 75% of currently established tree species may occur outside their climatic niche by the end of the century under moderate climate change scenarios (Potterf et al. 2026). One possible approach is the use of introduced tree species to support forest adaptation to changing environmental conditions (Novotný et al. 2023; Tomczak et al. 2025). These species may provide useful traits such as higher drought tolerance or better growth performance, which can improve stand resilience on challenging sites (Vacek et al. 2021; Podrázský et al. 2020). The aim of this contribution was to evaluate the performance of plantations (mortality and growth potential) of not only native but also potentially suitable introduced hardwood tree species on extreme soils with low water retention capacity in the former forest nursery area of Budišov in the Czech Republic.

MATERIALS AND METHODS

Study area

The former forest nursery Budišov is located in the Vysočina Region, Czech Republic, under the management of Lesy České republiky (GPS: 49°14'55"N, 16°0'9"E). The nursery area lies at an elevation of 459–481 m a.s.l. The terrain is flat, with an average slope of 2.1°, and a general westward inclination. The geological bedrock consists of granites to quartz-bearing syenites of Carboniferous age. The soil type is classified as modal Cambisols, characterized by high infiltration and permeability, low water retention capacity, and low plant-available water capacity due to compaction and long-term sand deposition (Trojan et al. 2025). According to data from the Velké Meziříčí meteorological station for the period 1960–2025, the mean annual air temperature is approximately 7.8 °C, and the mean annual precipitation is 581 mm. From a climatic perspective, the year 2023, when most of the plantings were established, can be considered relatively extreme compared to the period 1961–2022. Mean monthly temperatures were higher in all months by 0.5 to 4.3 °C. Monthly precipitation totals were also highly variable and characterized by pronounced extremes (especially long-term droughts).

On the area of the former forest nursery, experimental plantations were established in blocks divided into 20 × 20 m plots with five replicates for native broadleaved species, and 15 × 15 m plots with 2–6 replicates for introduced species. The planting material consisted mainly of seedlings in the 26–35 cm height class. In total, 13 native broadleaved species were planted: *Fagus sylvatica*, *Acer pseudoplatanus*, *Quercus petraea*, *Tilia cordata*, *Alnus glutinosa*, *Ulmus minor*, *Ulmus glabra*, *Juglans regia*, *Sorbus torminalis*, *Sorbus domestica*, *Prunus avium*, *Pyrus pyraster*, and *Malus sylvestris*. In addition, 9 introduced broadleaved species were planted: *Aesculus hippocastanum*, *Castanea sativa*, *Celtis australis*, *Corylus colurna*, *Ginkgo biloba*, *Morus nigra*, *Quercus pyrenaica*, *Quercus rubra*, and *Ulmus pumila*.

Data collection and analyses

In autumn 2025, an assessment of the plantations was carried out. Data were collected using a folding measuring tape and digital calipers. Total height and height increment over the last growing season were measured with an accuracy of 1 cm. Root collar diameter was measured with an accuracy of 0.1 mm. Mortality and tree vitality were also evaluated. Vitality assessment was divided into four categories based on foliage condition and other characteristics (1 – most vital, 2 – vital, 3 – declining, 4 – dead; Trojan et al. 2025).

In Excel, histograms of mean dendrometric parameters (height increment) and health status (mortality) were prepared. In the graphs, mean values are indicated by an interrupted line, while error bars represent data variability. Statistical analyses were performed using basic descriptive and inferential methods (normality and homogeneity of variance testing → ANOVA vs. Kruskal–Wallis test) in the software Statistica 14 (TIBCO). Principal component analysis (PCA) was performed using CANOCO 5 (Ter Braak, Šmilauer, 2012) to evaluate the relationships among growth parameters, health status, and individual tree species. Prior to the analysis, the data were log-transformed and standardized. The results of the multivariate PCA analysis were visualized in the form of an ordination diagram.

RESULTS

Mortality

In terms of mortality, a significant ($p < 0.001$) difference among tree species was detected within the evaluated experimental plots (Fig. 1). Among native broadleaved species, the lowest overall mortality was recorded for *Fagus sylvatica* (14.4%), *Quercus petraea* (20.3%), *Ulmus minor* (21.2%), and *Acer pseudoplatanus* (21.5%). In contrast, the highest mortality rates were documented for *Prunus avium* (67.1%) and *Alnus glutinosa* (65.3%). Regarding introduced broadleaved species, the lowest mortality was observed in *Quercus rubra* (59.5%), *Quercus pyrenaica* (68.4%), and *Castanea sativa* (70.4%). The highest mortality (100%) was recorded for *Ginkgo biloba* and *Morus nigra*. Overall mortality across all native species reached 34.4%, whereas geographically non-native species exhibited a substantially higher mortality of 83.1%.

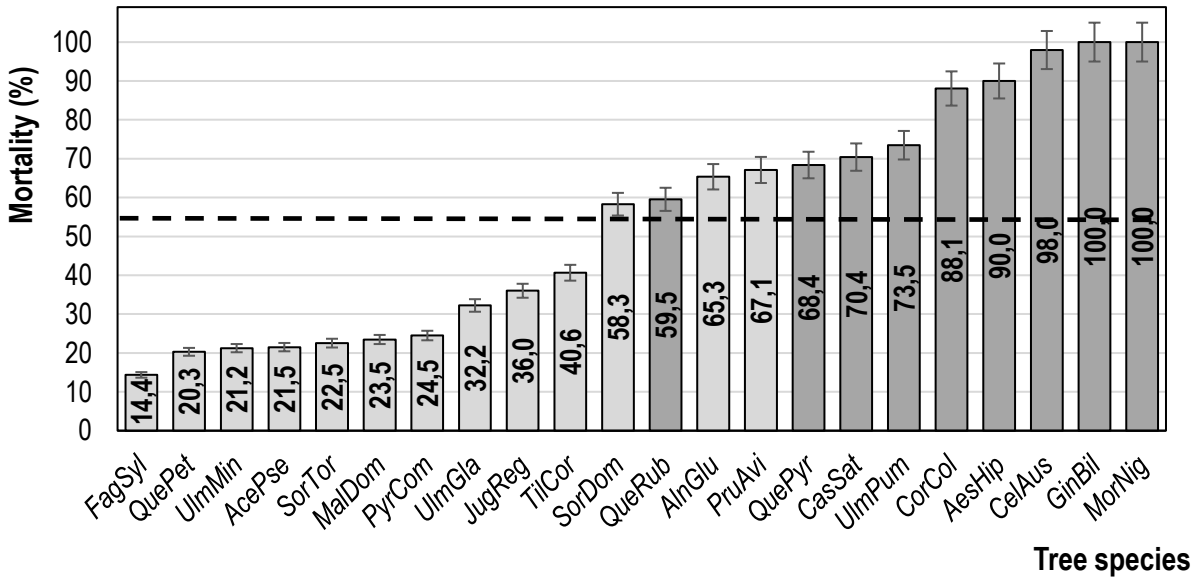

Figure 1: Mortality of native (light) and introduced (dark) hardwood tree species; species descriptions are derived from abbreviations of Latin names

Growth potential

The evaluation of annual mean height increment revealed also a significant ($p < 0.001$) difference among tree species (Fig. 2). The three native broadleaved species with the highest height increment exceeding 20 cm were *Ulmus minor* (27.5 cm), *Sorbus domestica* (25.0 cm), and *Prunus avium* (22.7 cm). In contrast, the lowest height increment was recorded for *Fagus sylvatica* (5.8 cm) and *Quercus petraea* (7.5 cm). Among the introduced broadleaved species, the highest height increment was observed in *Ulmus pumila* (25.0 cm) and *Quercus pyrenaica* (11.6 cm). Compared to native species (16.3 cm), introduced species exhibited a 36.2% lower mean annual height increment (10.4 cm).

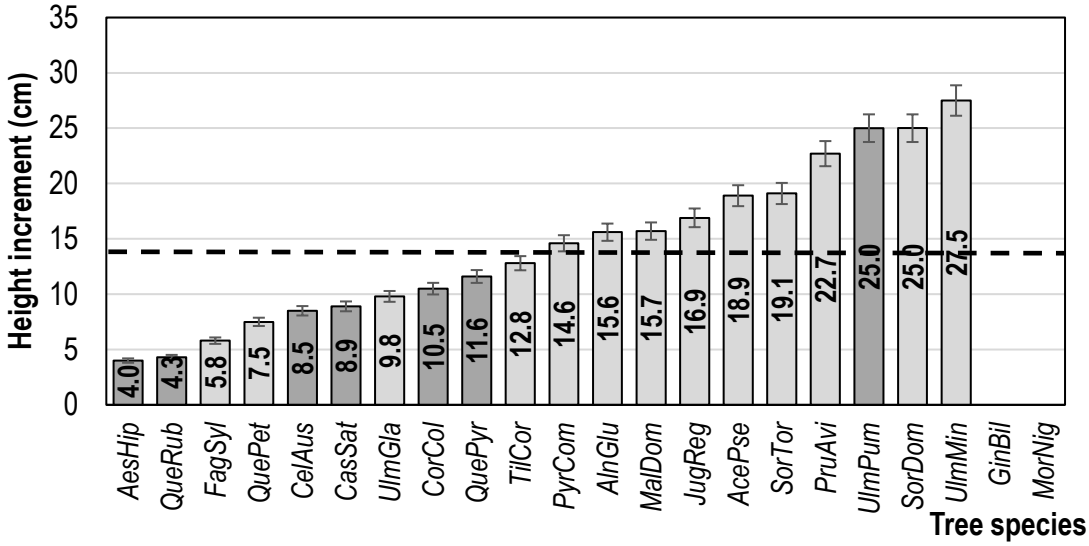

Figure 2: Mean annual height increment of native (light) and introduced (dark) hardwood tree species; species descriptions are derived from abbreviations of Latin names

Interaction between growth parameters, vitality and tree species

The PCA results express the relationship between the seedlings parameters, health status and tree species in Budišov and are presented in the form of an ordination diagram in Fig. 3. The first ordination axis presents 60.7%, the first two axes 79.3% and the four axes together explain 99.1% of the data variability. The x-axis represents seedlings height. Root collar diameter was positively correlated with seedling height, while both parameters were negatively correlated with mortality rate. Mean annual height increment was negatively correlated with vitality classes. The diagram indicates that native tree species exhibited higher growth increments and lower mortality rates compared to introduced species. In general, *Ulmus minor*, *Sorbus torminalis*, and *Acer pseudoplatanus* were identified as the most suitable species for afforestation of extreme sites, being characterized by high growth performance and low mortality.

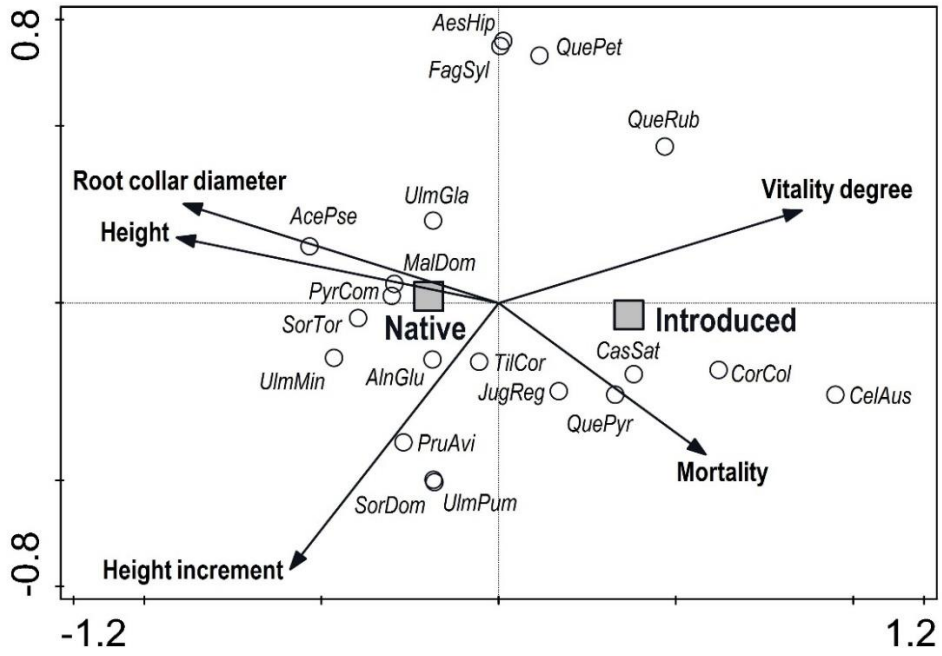

Figure 3: Ordination diagrams showing the results of PCA interaction between seedlings parameters (Height, Root collar diameter, Height increment), health status (Vitality degree, Mortality) and tree species (abbreviations of Latin names) in 2025; symbols indicate ●tree species, ■ native vs. introduced tree species

DISCUSSION

Global climate change is altering forest regeneration concepts, particularly on extreme sites (Vacek et al. 2009, 2021), including areas of the former Budišov nursery. These conditions are driven not only by pronounced warming trends and uneven precipitation distribution, increased solar radiation, and wind exposure, but also by highly restrictive soil conditions with low water retention capacity, where precipitation rapidly drains from the site (Trojan et al. 2025). Forest regeneration on such extreme sites differs substantially from traditional silvicultural approaches, as planning and implementation must consider not only species suitability and ecological characteristics under given site and stand conditions, but also the specific constraints imposed by climatic and edaphic extremity as well as a range of additional microsite factors affecting plantation performance (Brancalion et al. 2019; Masarei et al. 2021). If these site-specific constraints are insufficiently understood, they may result in negative impacts on both regeneration success and overall forest ecosystem functioning (Castro et al. 2021). The ultimate objective is to increase regeneration efficiency and reduce both environmental and economic costs.

In our study conducted in the former Budišov nursery, we present preliminary results of afforestation using both native and introduced hardwood tree species. Comparable studies on formerly agricultural or nursery soils remain scarce; for example, Gallo et al. (2022) and Tama et al. (2025) report related findings. However, these studies were conducted on fertile agricultural soils in Central Bohemia under less extreme climatic conditions, where for example the introduced *Corylus colurna* achieved exceptionally high growth rates. Experimental plantings on forest soils have been addressed, for example, by Šrámek et al. (2025), where among hardwood species the highest growth increments were recorded in *Quercus rubra* and *Quercus cerris*. In our case, elm species—both introduced *Ulmus pumila* and native *Ulmus minor*—achieved the highest growth increments. Nevertheless, comparable studies focusing on plantations established in former nursery sites such as Budišov are still lacking. For this reason, long-term monitoring of these experimental plantations is essential to obtain sufficient knowledge for successful restoration of such extreme sites (Trojan et al. 2025).

The results of health status and mortality assessment of native tree species in the former Budišov nursery reveal substantial interspecific differences. Mortality rate ranged widely from 14.4% in *Fagus sylvatica* to 100% in *Morus nigra* and *Ginkgo biloba*, confirming that survival of young plantations is strongly species-dependent and simultaneously highly influenced by site conditions and weather variability during the initial establishment phase. In another study conducted in the Czech Republic, similarly high mortality rates (>50%) were reported for *Quercus cerris* and *Quercus frainetto* (Šrámek et al. 2025). The early developmental stage of forest plantations represents one of the most sensitive periods in terms of mortality, as young seedlings are exposed to a combination of stress factors such as water deficit, high solar radiation, and competition from herbaceous vegetation (Jandl et al. 2019; Repáč, Belko 2020). For establishing new forest stands under difficult site conditions, a range of approaches can be used, including both native and introduced tree species as well as different types of planting material (Gallo et al. 2022; Novotný et al. 2023).

CONCLUSIONS

The obtained results indicate that several of the tested tree species exhibit considerable growth potential and high resilience, which makes them suitable candidates for forest restoration on extreme sites and post-disturbance clearcuts. These findings suggest that certain species are capable of maintaining satisfactory performance even under highly limiting soil and climatic conditions, and may therefore contribute to increasing the stability and adaptability of future forest stands. From the perspective of practical silvicultural application of native broadleaved species, the following taxa can currently be recommended: *Acer pseudoplatanus*, *Malus sylvestris*, *Pyrus pyraster*, *Sorbus torminalis*, and *Ulmus minor*. Among introduced broadleaved species, particularly *Quercus rubra*, *Quercus pyrenaica*, and *Ulmus pumila* showed promising results in terms of growth and survival under the studied extreme conditions. For obtaining robust and long-term applicable conclusions, it is therefore essential to continue systematic monitoring of the established experimental plots at least until the pole stage development. In the context of ongoing climate change, particular emphasis should be placed on mixed-species plantations rather than monocultures, as species mixtures are generally expected to enhance stand stability, ecological resilience, and functional diversity under increasing environmental variability.

ACKNOWLEDGEMENTS

This contribution was supported by the Grant Service of Lesy České republiky within the project "Experimental approaches to forest restoration using native and introduced tree species under climate change conditions" (No. 125).

REFERENCES

Brancalion PHS, Meli P, Tymus JRC, Lenti FEB, Benini RM, Silva APM, Isernhagen I, Holl KD (2019) What makes ecosystem restoration expensive? A systematic cost assessment of projects in Brazil. Biol Conserv 240:108274. https://doi.org/10.1016/j.biocon.2019.108274

Brockerhoff EG, Barbaro L, Castagneyrol B, Forrester DI, Gardiner B, González-Olabarria JR, Lyver POB, Meurisse N, Oxbrough A, Taki H, Thompson ID, van der Plas F, Jactel H (2017) Forest biodiversity, ecosystem functioning and the provision of ecosystem services. Biodivers Conserv 26:3005–3035. https://doi.org/10.1007/s10531-017-1453-2

Buras A, Menzel A (2019) Projecting tree species composition changes of european forests for 2061–2090 under RCP 4.5 and RCP 8.5 scenarios. Front Plant Sci 9:1986. https://doi.org/10.3389/fpls.2018.01986

Castro J, Morales-Rueda F, Navarro FB, Löf M, Vacchiano G, Alcaraz-Segura D (2021) Precision restoration: a necessary approach to foster forest recovery in the 21st century. Restor Ecol 29: e13421. https://doi.org/10.1111/rec.13421

Gallo J, Záruba J, Baláš M, Podrázský V (2022) Výzkumná plocha Doubek – introdukované dřeviny na zemědělské půdě. In: Nové poznatky ve výzkumu introdukovaných dřevin. Sborník příspěvků. Zámek, nám. Smiřických 1, Kostelec nad Černými lesy, 28. 6. 2022, Česká lesnická společnost, z. s., Praha, pp 45-52. (in Czech)

IPCC (2019) Climate Change and Land. An IPCC Special Report on climate change, desertification, land degradation, sustainable land management, food security, and greenhouse gas fluxes in terrestrial ecosystems. Edited by Valérie Masson-Delmotte, World Meteorological Organization.

Jandl R, Spathelf P, Bolte A, Prescott CE (2019) Forest adaptation to climate change—is non-management an option? Ann For Sci 76:48. https://doi.org/10.1007/s13595-019-0827-x

Leugner J, Bureš P, Černý J (2025) Vyhodnocení různých postupů obnovy lesa na kalamitních holinách. Zpr lesn výzk 70:195–204. https://doi.org/10.59269/zlv/2025/4/773

MacDicken KG (2015) Global Forest Resources Assessment 2015: What, why and how? For Ecol Manage 352**:**3–8. https://doi.org/10.1016/j.foreco.2015.02.006

MacDicken K, Jonsson O, Pin˜a L, Maulo S, Adikari Y, Garzuglia M, Lindquist E, Reams G, D'Annunzio R (2015) Global Forest Resources Assessment 2015: How have the World's Forests Changed? FAO, Rome.

Masarei MI, Erickson TE, Merritt DJ, Hobbs RJ, Guzzomi AL (2021) Engineering restoration for the future. Ecol Eng 159: 106103. https://doi.org/10.1016/j.ecoleng.2020.106103

Montagnoli A, Chiatante D, Godbold DL, Koike T, Rewald B., Dumroese RK (2022): Editorial: Modulation of Growth and Development of Tree Roots in Forest Ecosystems. Front Plant Sci 13:850163. https://doi.org/10.3389/fpls.2022.850163

Novotný S, Gallo J, Baláš M, Kuneš I, Fuchs Z, Brabec P (2023) Silvicultural potential of the main introduced tree species in the Czech Republic–review. Cent Eur For J 69:188-200. https://doi.org/10.2478/forj-2023-0014

Potterf M, Schattenberg C, Krüger K, Hochholzer K, Rammer W, Grünig M, Braziunas KH, Dollinger C, Erhardt A, Gégout JC, Geres L, Greiner S, Hlásny T, Huber A, Kerber J, Lecina-Diaz J, Mandl L, Modlinger R, Mohr JS, Müller J, Mazón MM, Pinto PE, Richter T, Seibold S, Senf C, Serra-Diaz JM, Stritih A, Thom D, Viana-Soto A, Zou J, Seidl R (2026) Tree regeneration after unprecedented forest disturbances in Central Europe is robust but maladapted to future climate change. Glob Chang Biol 32:e70734. https://doi.org/10.1111/gcb.70734

Podrázský V, Vacek Z, Vacek S, Vítámvás J, Gallo J, Prokůpková A, D'Andrea G (2020) Production potential and structural variability of pine stands in the Czech Republic: Scots pine (*Pinus sylvestris* L.) vs. introduced pines–case study and problem review. J For Sci 66:197-207. https://doi.org/10.17221/42/2020-JFS

Poleno Z, Vacek S, Podrázský V, Remeš J, Štefančík I et al. (2009) Pěstování lesů III. Praktické postupy pěstování lesů. Kostelec nad Černými lesy, Lesnická práce, s.r.o. (in Czech)

Repáč I, Belko M (2020) Vývoj lesnej kultury smreka obyčejného a buka lesného po aplikácii hnojiva a hydrogelu na kalamitnej ploche v pohorí Javorie, Stredné Slovensko. Zpr lesn výzk 65:232–241.

Seidl R, Thom D, Kautz M, Martin-Benito D, Peltoniemi M, Vacchiano G, Wild J, Ascoli D, Petr M, Honkaniemi J, Lexer MJ, Trotsiuk V, Mairota P, Svoboda M, Fabrika M, Nagel TA, Reyer CPO (2017) Forest disturbances under climate change. Nat Clim Change 7:395–402. https://doi.org/10.1038/nclimate3303

Šimůnek V, Stejskal J, Čepl J, Korecký J, Vacek Z, Vacek S, Bílek L, Švanda M (2023) Different adaptive potential of Norway spruce ecotypes in response to climate change in Czech long-term lowland experiment. Forests 14:1922. https://doi.org/10.3390/f14091922

Šrámek M, Šenfeldr M, Jelínek B, Horák P, Vitásek R, Martínek P, Úradníček L (2022) Odrůstání výsadeb introdukovaných dřevin na LS Vítkov 4 roky po výsadbě. In: Aspekty související s využíváním introdukovaných dřevin v lesnictví, krajinářství a okrasném zahradnictví. VÚLHM, Strnady. (in Czech)

Trojan V, Moravec J, Vacek Z, Vacek S, Cukor J, Škrleta M (2025) Odrůstání sazenic vybraných introdukovaných jehličnatých dřevin na suchem ohroženém stanovišti ve vztahu k jejich adaptačnímu potenciálu. In: Hušková K. (ed.), Sborník vědeckých prací příspěvků pěstování lesů ve střední Evropě 2025: Adaptační opatření v lesnictví z 25. mezinárodního setkání pěstitelů lesů. Křtiny, 1.–3. 9. 2025, Mendelova univerzita v Brně, Lesnická a dřevařská fakulta, Ústav zakládání a pěstění lesů, pp. 181–188. (in Czech)

Vacek S, Simon J, Podrázský V, Baláš M, Slávik M et al. (2009) Zakládání a stabilizace lesních porostů na bývalých zemědělských a degradovaných půdách. Kostelec nad Černými lesy, Lesnická práce, s.r.o. (in Czech)

Vacek Z, Cukor J., Vacek S, Linda R, Prokůpková A, Podrázský V, Gallo J, Vacek O, Šimůnek V, Drábek O, Hájek V, Spasic M, Brichta J (2021) Production potential, biodiversity and soil properties of forest reclamations: Opportunities or risk of introduced coniferous tree species under climate change?. Eur. J. For. Res 140:1243-1266. https://doi.org/10.1007/s10342-021-01392-x

Vacek Z, Vacek S, Cukor J (2023) European forests under global climate change: review of tree growth processes, crises and management strategies. J Environ Manage 332:117353. https://doi.org/10.1016/j.jenvman.2023.117353

Tama AY, Manourova A, Mohammad RK, Podrázský V (2025) Afforestation of Abandoned Agricultural Land: Growth of Non-Native Tree Species and Soil Response in the Czech Republic. Forests 16:1113. https://doi.org/10.3390/f16071113

Ter Braak CJF, Šmilauer P (2012) Canoco 5, Windows release (5.00). Software for mutivariate data exploration, testing, and summarization. Biometris, Plant Research International: Wageningen, Germany.

Tomczak K, Vacek Z, Cukor J, Vacek S, Bažant V, Zeidler A, Trojan V, Gallo J, Černý J (2025) Unlocking *Pinus ponderosa* (Douglas ex C. Lawson) potential: a comprehensive review of results from native and introduced areas. Front For Glob Change 8:1585253. https://doi.org/10.3389/ffgc.2025.1585253

Poster Session

Application of Microwaves at a Frequency of 5.8 GHz for Hardwood Modification

Grigory Torgovnikov[1*], Alexandra Leshchinskaia[2]

[1]University of Melbourne, School of Agriculture, Food and Ecosystem Sciences.
4 Water St., Creswick, Victoria 3363, Australia
[2] Plekhanov Russian University of Economics, Department of Financial Management
36 Stremyannyy Pereulok, 115093 Moscow, Russia

E-mail: grigori@unimelb.edu.au; alixfl@mail.ru

Keywords: frequency; hardwood; microwave modification: MW power; ray cell; wood structure.

ABSTRACT
A number of hardwood species have a very low permeability, causing problems during timber processing. These include very long drying times, large material losses after drying, expensive drying processes, and difficult impregnation with preservatives and resins. Microwave (MW) wood modification can dramatically increase wood permeability, solving many wood processing problems.
In previous studies, two frequencies 0.922 and 2.45 GHz were used for MW wood structure modification. At these frequencies, MW penetrate deep into the wood and allow modification of large cross-section timber. In some applications, it is required to increase the permeability of timber surfaces areas only (for example, for preservative treatment or resin impregnation). Microwaves at a frequency 5.8 GHz cannot penetrate deep into the moist wood and decay in the surface layers. Therefore, they can be used for the modification of shallow areas of timber.
The study of wood sample treatment was carried out in an experimental MW plant with a maximum power of 550 W (f= 5.8 GHz) with two special MW applicators. MW treatment of three hardwood species showed that energy application to the moist wood in the range between 180 and 320 kWh/m3 produces significant changes in the structure and dramatically increases the permeability of surface layers required for preservative treatment at a depth 5-8 mm. MW timber modification for preservative treatment and resin impregnation to a depth of 5-8 mm requires MW energy consumption, depending on hardwood moisture content and density, in the range of 11-26 kWh/m2 of wood surface.

INTRODUCTION

Some wood species have a very low permeability, causing problems during timber processing. These include very long drying times, large material losses after drying, expensive drying processes and difficult impregnation with preservatives and resins. Furthermore, growth stresses in wood and collapse often lead to drying defects and high material losses in the recovery of sawn timber. MW wood modification can provide an increase in wood permeability, which solves many wood processing problems.
Intensive MW power applied to green wood generates steam pressure within the wood cells. Under high internal pressure, the pit membranes in cell walls, tyloses in vessels and weak ray cells are ruptured to form pathways for easy transportation of liquids and vapors. An increase in the intensity of the microwave energy increases the internal pressure, resulting in the formation of narrow voids in the radial-longitudinal planes. The number of cavities, their dimensions, and distribution are controlled by the intensity of microwave energy supplied. A several thousand-fold increase in wood permeability in the radial and longitudinal directions can be achieved in species previously found to be impermeable to liquids and gases. Other physical properties and technological attributes are also changed. Structural changes in wood after MW modification, their effect on wood properties, and process parameters required for different degrees of wood modification are described in the literature (Torgovnikov and Vinden 2009, Vinden et al. 2003).
In previous studies, two frequencies 0.922 (0.915) and 2.45 GHz, from a range of frequencies allowed for industrial applications, were used for MW wood structure modification. MW at frequencies 0.922 and 2.45 GHz penetrates rather deep to the wood and allow to modify large cross-section timber (at

0.922 GHz logs up to 450 mm and at 2.45 GHz sawn timber up to 120 x 120 mm). But in some applications, it is required to increase the permeability of timber surface areas only (for example, for preservative treatment or impregnations by resins). This impossible to do at frequencies 0.922 and 2.45 GHz.
Microwaves at 5.8 GHz cannot penetrate deep into the moist wood and decay in the surface layers. Therefore they can be used for the modification of shallow areas of timber. It is interesting from scientific and practical points of view to know what kind of structure changes can be done in the wood by microwaves at this frequency and estimate the MW process parameters required for timber surface permeability increase.

MATERIAL AND METHODS

Three species were used for experiments: Sugar gum (*Eucalyptus cladocalyx*), Red Ironbark (*E. sideroxylon),* and Blue gum (plantation) (*E. globulus*). Wood samples measured 8x8x600 mm and 22x48x600 mm had the following properties:

	Oven dry density (kg/m^3)	Moisture content (%)
Sugar gum	1040	34
Red Ironbark	1050	27
Blue gum	710	84

MW experimental plant at frequency 5.8 GHz consists of: MW generator with max power 550 W, waveguide system with autotuner, MW applicators (1 and 2) and water load, air heater and fan for removing steam from the applicator, variable speed electric drive for moving the sample via Applicators 1 (Figure 1) and Applicator 2 (Figure 2).

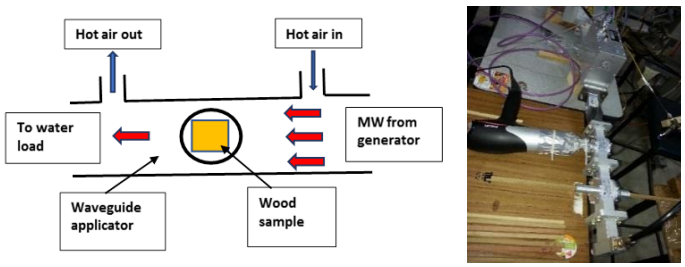

Figure 1: Scheme of wood sample processing in the waveguide Applicator 1

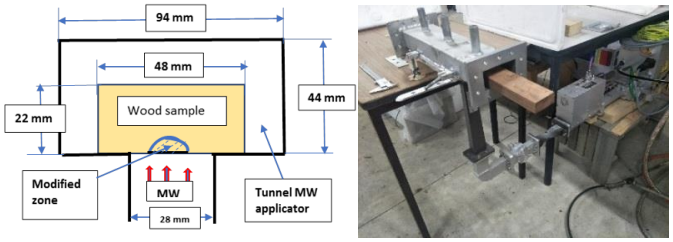

Figure 2: Scheme of wood sample processing in Applicator 2

The plant works in the following way. When the MW generator starts working at the required power, the electric drive connected by cotton with the sample moves it via applicators at the required speed. Microwaves heat wood in applicators, and steam in wood cells ruptures some element of wood structure, increasing wood permeability. MW energy applied to the wood can be changed by the generated power and the transportation speed. Steam released from wood during MW modification is removed by air flow from the fan.
During experiments, MW power was changed in the range 240 to 500 W, and the speed of the sample was changed in the range 2.5 – 5.0 mm/sec.

Generated and reflected power were measured by an autotuner. MW power P absorbed by the sample was calculated by the formula Pabs = P generated – P reflected – P passed. MW energy passed via the wood was measured in water load by the calorimetric method.
Applicator 2 (cross-section 44x94 mm) was used to treat the sample surface and determine the depth of modified zones as a function of applied power.
In both applicators, the electric field strength vector E was oriented parallel to the wood grains to maximize energy release in the surface layers, because dielectric losses in wood are significantly higher at parallel vector E orientation than at perpendicular vector E orientation.

RESULTS AND DISCUSSION

In experiments with Applicator 1, at applied (generated) MW power from 240 to 500 W and sample speed 5 mm/sec, the tuner provided good matching with practically no reflected power. MW energy absorbed by the samples is shown in Table 1.

Table 1: MW energy absorbed by wood samples in Applicator 1

Applied power, [W]	MW energy absorbed by samples, [MJ/m3]		
	Sugar gum	Red Ironbark	Blue gum
240	630	550	720
320	800	750	930
400	890	930	1170
500	1120	1040	1280

Experiments showed that an increase in specific applied MW power from 63 to 130 W/cm3 leads to a proportional increase in energy wood absorption by 1.8-1.9 times. After MW modification, a wood moisture content reduction for Sugar gum is from 34% to 10 -19%, for Red Ironbark - from 27 to 10-19%, for Blue gum - from 84 to 28-43%.
Application of MW energy to wood in the range of specific power from 80 to 130 W/cm3 provides a high degree of wood modification, rupturing some elements of the wood structure. Rupturing of rays (ray cells) in wood is the most indicative factor for the assessment of wood permeability increase. Microscope photos of sample cross sections after MW modification (Figures 3 and 4) demonstrate changes in wood structure.
Sugar Gum sample cross-cut photos are in Figure 3. Wider white lines are ruptured rays. Applied MW energy increases provide an increase in the size of cavities based on ruptured rays.

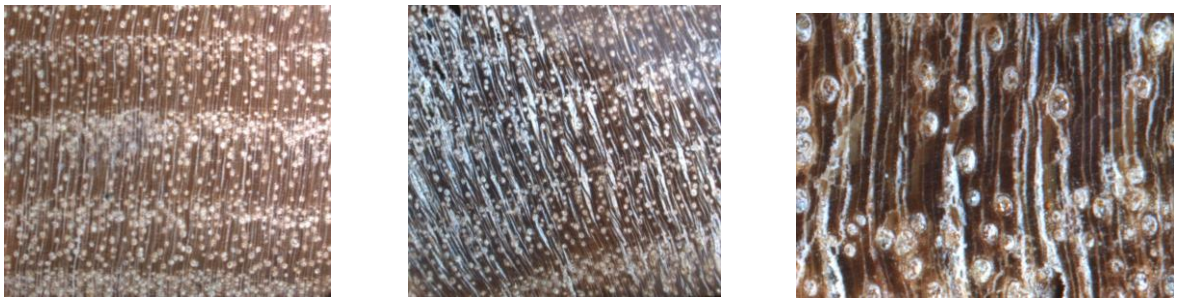

Before MW treatment (magn. +16) After MW treatment (magn. +16 and +50)

Figure 3: Sugar gum sample crosscut after MW modification (magnification +16 and +50). Applied power 400 W, absorbed MW energy 890 MJ/m3. Wider white lines are ruptured rays

Red Ironbark sample cross-cut photos after MW modification are in Figure 4. Wider white lines are ruptured rays.

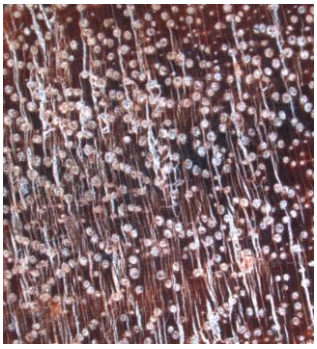

Sample 11a. MW power 400 W, magnification +16

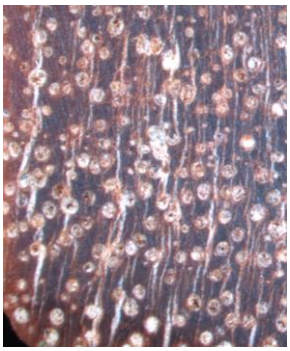

Sample 12b. MW power 500 W, magnification +50

Figure 4: Red Ironbark samples after MW treatment (magnification +16 and +50). Applied power 400 and 500 W, absorbed MW energy 930 MJ/m3 and 1040 MJ/m3. Wider white lines are ruptured rays

Blue Gum sample crosscut photos are shown after MW modification in Figure 5.

Sample 11b. Power 400 W, speed 5 mm/sec, magnification +16

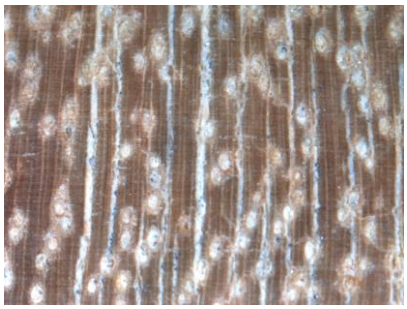

Sample 3a. MW power 400 W, speed 3.4 mm/sec, magnification +50

Figure 5: Blue gum (plantation) samples after MW treatment. Applied power 400 W. Absorbed MW energy 1170 MJ/m3 and 1280 MJ/m3. Wider white lines are ruptured rays

At frequency 5.8 GHz MW energy application to the moist wood in the range 650 to 1200 MJ/m3 produces significant structural changes. Magnified pictures of sample cross sections after MW modification showed destroyed ray cells and widening ray cell areas in tangential and longitudinal directions. Ray destruction leads to an increase in wood permeability, mainly in radial and longitudinal directions. Visual subjective comparison of ray destruction in wood showed that at frequency 5.8 GHz, cavities in wood on the basis of rays have smaller sizes compared to cavities formed by MW treatment at frequencies 0.922 and 2.45 GHz. Other changes in wood structure were not assessed in this study. This requires special study. Experiments with samples 22x48x600 mm in Applicator 2 were carried out to determine the modification zone when the wood surface was irradiated by microwaves, as shown in Figure 2. Experiments showed that the MW irradiation density of 86-143W/cm2 provides a modification depth of 5-8 mm without surface burning. This treatment requires MW energy consumption of 800-1170 MJ/m3. MW timber treatment parameters for easy preservative solution penetration to a depth of 5-8 mm are displayed in Table 2.

Table 2: MW timber treatment parameters for wood modification to the depth 5-8 mm

Wood species	Owen dry density, [kg/m^3]	Moisture content, [%]	Depth of wood modification, [mm]	MW energy consump tion, [MJ/m^3]	MW energy consumption for treatment of 1m^2 of the surface, [kWh/m^2]
Sugar gum	1040	34	5	800	11
			8	890	17
Red Ironbark	1050	27	5	750	10.5
			8	930	21
Blue gum	710	84	5	930	13
			8	1170	26

Experiments showed that an increase in specific applied MW power from 63 to 130 W/cm3 leads to a proportional increase in MW energy wood absorption by 1.8-1.9 times. After MW modification, a wood moisture content reduction for Sugar gum was from 34% to 10 -19%, for Red Ironbark - from 27 to 10-19%, for Blue gum - from 84 to 28-43%.

Microwaves at a frequency of 5.8 GHz can be generated by magnetron and klystron generators. The maximum magnetron power at frequency 5.8 GHz is not more than 1000 W, and the generator efficiency is about 62%. Klystron generators have power up to 100 kW and more, with an efficiency of about 42%. These generators are expensive, and efficiency is rather low; therefore, microwave surface modification can be expensive, and usage will be limited.

A practical application of frequency 5.8 GHz for wood surface treatment is limited because magnetron and klystron generators for this frequency are very expensive, and the efficiency of electric energy transformation to microwaves is only 42-62%.

CONCLUSIONS

An experimental study of MW hardwood modification at frequency 5.8 GHz showed that energy application to the moist wood in the range 180 to 320 kWh/m3 produces significant changes in the structure. MW treatment destroys ray cells and widens ray cell areas in the tangential and longitudinal directions. Ray destruction leads to a dramatic increase in wood permeability, mainly in radial and longitudinal directions. Visual subjective comparison of ray destruction in wood showed that at frequency 5.8 GHz, cavities in wood on the basis of rays have smaller sizes compared to cavities formed by MW treatment at frequencies 0.922 and 2.45 GHz. It is possible to use MW frequency 5.8 GHz to increase wood permeability to a depth of 5-8 mm required for preservative treatment and resin impregnation. MW energy consumption depending on hardwood moisture content and density is in the range 11-26 kWh/m2 of wood surface. A practical application of frequency 5.8 GHz for wood surface treatment can be limited because the MW energy consumption 8000-12000 MJ/m3 is very high, magnetron and klystron generators for this frequency are very expensive, and the efficiency of electric energy transformation to microwaves is only 42-62%.

REFERENSES

Torgovnikov G. Vinden P (2009) High intensity microwave wood modification for increasing permeability. Forest Product Journal 59(4), pp. 84-92.

Vinden P, Romero J, Torgovnikov G (2003) A method for increasing the permeability of wood. US Patent No 6,596,975.

Tensile Strength Analysis of Grey Poplar

Fanni Szőke[1*], Antal Kánnár[1]

[1] University of Sopron, Faculty of Wood Engineering and Creative Industries. Bajcsy-Zs. Str. 4, Sopron, Hungary, 9400.

E-mail: szoke.fanni@phd.uni-sopron.hu; kannar.antal@uni-sopron.hu

Keywords: structural strength; grey poplar; tensile strength; strength surface; anisotropy.

ABSTRACT

Forestry research has shown that the survival of sensitive tree species is threatened by rising average annual temperatures and declining precipitation. The grey poplar (*Populus* × *canescens*) is native to Hungary and is a fast-growing tree species that currently plays a significant role in the economy. All this makes it a potential candidate for structural use, eventually replacing pine species. Further studies are needed to determine the strength values of grey poplar for structural use. To determine the strength properties resulting from anisotropic properties, longitudinal (L), radial (R), and tangential (T) directions and planes were defined for the test specimens, with fibre orientations of 0°, 45°, and 90°, depending on the direction. The 45° grain orientation allows for the experimental determination of shear strength, which is detailed in Askenazi's anisotropic strength theory and practical experience. During the tensile strength measurements, 30-30 sapwood and heartwood specimens were measured in each direction ((LR0°, LR45°, LR90°, LT45°, LT90°, RT45°), for a total of approximately 400 test specimens. Based on these figures, the strength values can be determined with an accuracy of 0.2 MPa. The measurements were performed in accordance with ISO 13061-06. The separate and combined examination of the individual parts – sapwood and heartwood – allows for classification into strength classes, considering the lower 5% quantile. Classification can be carried out using Eurocode 5, a guide currently used for structural design, for practical classification.

INTRODUCTION

One of the most pressing issues of our time is climate change, which is causing average precipitation levels to decline and temperatures to rise. The tree's water requirements are increasing, but since they cannot access enough, this can lead to desiccation and reduced resistance to insects (Hicke – Zeppel 2013, Jaime et al. 2019). The grey poplar (Populus × canescens) is a tree species native to Hungary with a significant domestic population, which can serve as a good alternative to replace declining tree species. It grows quickly and is easy to cultivate. Annually, 1.3 - 1.5 m3 of timber is marketed, accounting for 23-25% of total annual timber harvest (Molnár – Farkas 2024). Its current uses primarily include the production of crates, pallets, coasters, particleboard, and fibreboard. Further studies are needed for its structural applications and practical use.

MATERIALS AND METHODS

The strength properties of grey poplar depend significantly on the grain direction, as well as on whether the sapwood or heartwood predominates in the test specimen. Sapwood accounts for 30-40% of the specimen and has a higher moisture content than the heartwood. According to the literature, the behaviour of these parts depends on the tree species under study. Some studies on oak have shown that the properties of sapwood and heartwood do not differ significantly, and that heartwood did not exhibit greater strength than sapwood (Merela – Čufar 2013). For this tree species, structural designability was not influenced by these parameters, whereas in studies of particularly fast-growing tree species, significant differences were observed among most parameters (Bektas et al. 2020). To enable species-specific testing, the sapwood and heartwood sections were separated during sample preparation so that the strengths measured for each section could be distinguished from one another. During the tensile strength tests, we examined the material's behaviour in three main anatomical directions. In doing so, we distinguished between longitudinal (L), radial (R) and tangential (T) directions and their planes, where test specimens at 0°, 45° and 90° were prepared depending on the direction. Askenazi's anisotropic strength theory and practical experience allow for the experimental determination of shear

strength in the case of a 45° fibre orientation. In this case, the distribution of shear stress is uniform across the shear cross-section (Askenazi 1978). During the tests, tensile strength measurements were performed on 30 sapwood sections and 30 heartwood per directions as shown in Figure 1 – LR0°, LR45°, LR90°, LT45°, LT90°, RT45° – for a total of approximately 400 test specimens.

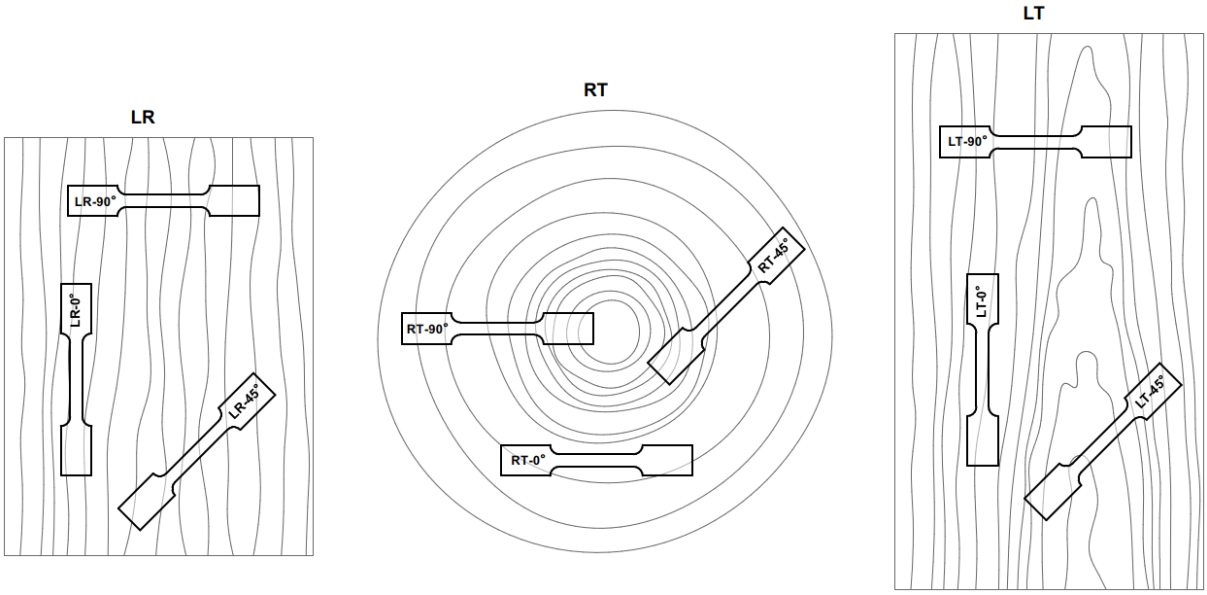

Figure 1: Test specimens designed with anatomical orientations and planes in mind

An Instron 5985 universal testing machine was used for the tests. The test was conducted in accordance with ISO 13061-06 until the test specimens failed (Part 16 2014). We optimized the moisture content of the test specimens of various designs by storing them in a climate-controlled room (temperature 20 °C, humidity 65%), thereby eliminating any differences that might arise from this factor. To account for anatomical orientations and planes, longitudinal limitations arose during the preparation of the test specimens; therefore, we conducted a supplementary test. In this test, the 300 mm-long test specimens specified in the standard were compared with the results of the 150 mm specimens used, which had a higher number of measurements (Figure 2).

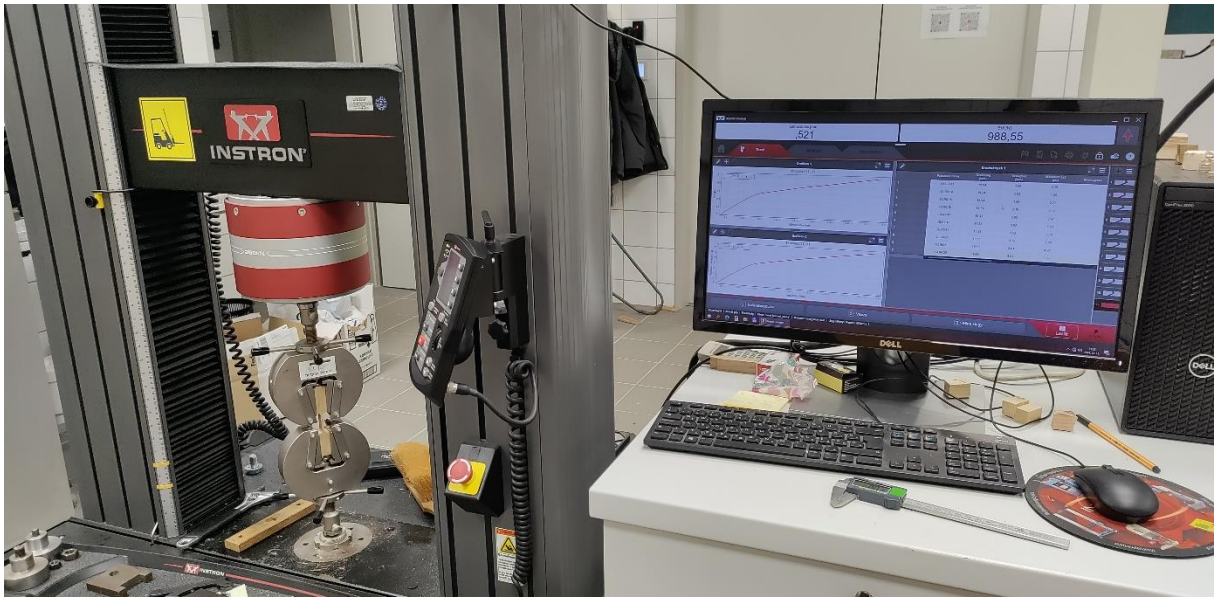

Figure 2: Tensile strength testing using a materials testing machine

Before conducting the tests, the cross-sectional dimensions were recorded. During the tests, the testing machine recorded the maximum tensile force, from which the tensile strength can be calculated using the Equation 1.

$$\sigma_{12} = \frac{F}{A} \quad (1)$$

In the formula, "σ_{12}" is the tensile strength value in the air-dried state, measured in N/mm^2, "F" is the tensile force, measured in N, "A" is the cross-sectional area in mm^2. For comparison with the standard, we considered the lower 5% quantile value, denoted by $f_{t.k}$, which is the direction-dependent characteristic value of tensile strength. This value is the quantile corresponding to the lower 5% probability of occurrence for a given property, which can be considered when calculating load-bearing capacity for stiffness properties. With this, the values can be classified into the Eurocode 5 strength classes.

RESULTS AND DISCUSSION

We verified the reliability of the test specimens resulting from their reduced length by comparing 300 mm – long test specimens with 150 mm-long specimens oriented in the same direction. The results are presented in Table 1. We denote the sapwood with an "S" and the heartwood with an "H".

Table 1: Results of the test – Difference in length

Specimen	σ_{12} [N/mm^2]	$f_{t.k}$ [N/mm^2]	EuroCode5 Strength classification
300 S	60.45	40.53	C50
300 H	31.13	21.00	C35
LR0 S	52.87	34.36	C50
LR0 H	42.07	17.62	C27

The differences between the individual sections are minimal, and that the smaller samples exhibited lower strength in both types. Therefore, the reduction in strength can be considered conservative, as it is done in the interest of safety, and thus the modified-size design can be used with confidence.
The second table presents the results of the measurements taken in various directions, as well as the strength classifications, broken down by sapwood and heartwood sections. Determined in this way, the tensile strength of the wood in different directions not only reached the lower limit of structural strength, but in many cases reached a higher category, as shown in Table 2. Test specimens with a 45° design cannot be classified (N/C) on their own, in such cases, additional methods must be used, so this publication does not go into detail on this matter.

Table 2: Results of the tensile strength analysis and strength classifications

Specimen	σ_{12} [N/mm^2]	$f_{t.k}$ [N/mm^2]	EuroCode5 Strength classification
LR0 S	52.87	34.36	C50
LR0 H	42.07	17.62	C27
LR45 S	8.18	4.64	N/C
LR45 H	6.89	1.76	N/C
LR90 S	3.63	2.93	C50
LR90 H	4.10	1.99	C50
LT45 S	8.32	5.97	N/C
LT45 H	7.03	2.93	N/C
LT90 S	2.71	1.88	C50
LT90 H	1.97	1.00	C50
RT45 S	3.10	2.55	C50
RT45 H	3.06	1.37	C35

A significant difference was observed between the sapwood and the heartwood during the measurements. The sapwood exhibited elastic-ductile behaviour in some areas. The fibres slipped past one another, revealing a fibrous fracture pattern. In contrast, the heartwood's fracture was characterized by brittle behaviour, and failure occurred more rapidly. Based on the data determined during the strength

measurements, the sapwood generally exhibited more elastic behaviour alongside higher strength values, being able to withstand greater deformation, while the heartwood, due to its more brittle behaviour, was less reliable with greater variability and sudden fracture. In terms of their strength classification, the results met the minimum structural requirements in all cases and even achieved higher values. Figure 3 shows the typical fracture patterns for samples of various designs, which is also an important feature.

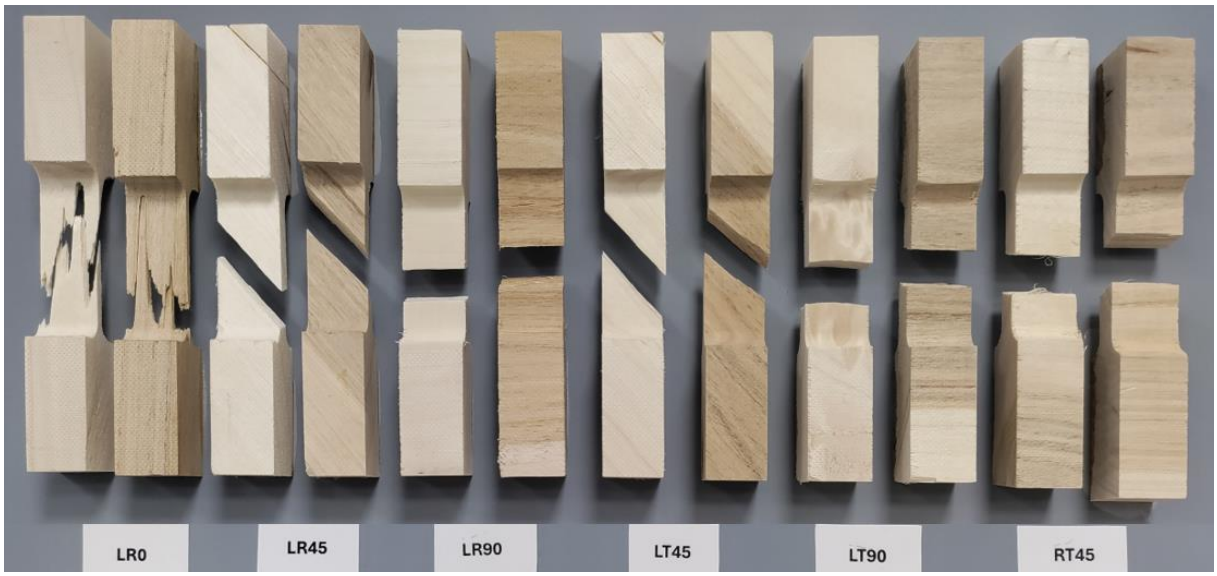

Figure 3: Typical fracture patterns observed during the test

The fracture patterns shown in the figure are characteristic of the modes described in the literature. When tension is applied parallel to the grain, tear fractures, combined tensile and shear fractures, shearing, and brittle fractures are typical. When tension is applied perpendicular to the grain, fractures along the early sapwood, shearing along the growth rings, and fractures along the medullary rays are typical (Bodig J - Jayne B. A 1965, 1982).

CONCLUSIONS

The tensile strength results clearly demonstrate the orthogonally anisotropic properties of wood. By covering all planes and directions, it became possible to map not only the measured values but also the fracture patterns and behaviour of the individual test specimens. Different sections of the wood behave differently under load, which is an important factor to consider when applying the material in practical structural solutions. Since it is not feasible to separate the sections during production and manufacturing, a representative limit value must be determined to establish a reliable basis for structural calculations. Overall, it can be said that the strength of grey poplar meets the strength requirements for structural timber, and based on the results so far, it can be recommended as a substitute for imported pine. The measurements make it possible to map the strength surface of the wood, and the large number of test results provide reliable, predictable values, which is extremely important from a structural design perspective.

ACKNOWLEDGEMENTS

Project no. 2025-2.1.2-EKÖP-KDP-2025-00002 has been implemented with the support provided by the Ministry of Culture and Innovation of Hungary from the National Research, Development and Innovation Fund, financed under the EKÖP-KDP funding scheme.

REFERENCES

Askenazi E. K (1978) Anizotropia dreveszinü i drevesznüh materialov (Anisotropy of wood and wood-based materials). 1st ed. Lesznaja Promüslennoszty, Moscow. pp 97-99 (in Russian)

Bektas İ, Tutuş A, Gültekin G (2020) The effect of sapwood and heartwood differences on mechanical properties of fast-growing tree species. Drvna Industrija, Vol. 71 No. 3. pp 261-269 https://doi.org/10.5552/drvind.2020.1940

Bodig J (1965) The effect of Anatomy on the Initial Stress-Strain Relationship. In: Forest Products Journal 15/5. pp. 197-202.

Bodig J, Jayne B. A (1982) Mechanics of Wood and Wood Composites. New York. Van Nostrand Reinhold. pp. 297-305

EN ISO 13061-06 (2014) Physical and Mechanical Properties of Wood – Test Methods for Small Clear Wood Specimens-. Part 16: Determination of Ultimate Tensile Stress Parallel to Grain.

Hicke J. A, Zeppel B. J. B (2013) Climate-driven tree mortality: Insights from the pinon pine die-off in the United States. New Pyhtologist, 200. pp 301-303

Jaime L, Batllori E, Margalef-Marrase J, Navarro M. Á. P, Lloret F (2019) Scots pine (Pinus sylvestris L.) mortality is explained by the climatic suitability of both host tree and bark beetle populations. In: Forest Ecology and Management, Vol. 448., pp 119-129 https://doi.org/10.1016/j.foreco.2019.05.070

Merela M, Čufar K (2013) Mechanical properties of sapwood versus heartwood in three different oak species. Drvna Industrija, Vol. 64 No. 4. pp 323-334 https://doi.org/10.5552/drind.2013.1325

Molnár S, Farkas P (2024) Nyár (nyár fajok) – Populus spp. In: Földünk ipari fái, 2nd ed. Eds. Molnár S, Farkas P, Börcsök Z, Zoltán Gy, Photog. Richter H. G, Szeles P. Faipari Tudományos Egyesület, Sopron, ISBN 978-963-12-5239-2. pp 97-99 (in Hungarian)

Integrated Multidomain Characterization of Date Palm Trunk Wood (*Phoenix dactylifera* L.)

Firas Naji Al Hachami[1*], Tamas Hofmann[2], Miklos Bak[1]

[1] University of Sopron, Faculty of Wood Engineering and Creative Industries. Bajcsy-Zs. Str. 4, Sopron, Hungary, 9400
[2] University of Sopron, Faculty of Forestry. Bajcsy-Zs. Str. 4, Sopron, Hungary, 9400.

E-mail: al-hachfinaob24@student.uni-sopron.hu; hofmann.tamas@uni-sopron.hu; bak.miklos@uni-sopron.hu

Keywords: date palm wood; monocot lignocellulosic system; hardwood positioning; mechanical characterization; permeability; biological resistance.

ABSTRACT

Date palm (*Phoenix dactylifera* L.) trunk material represents a structurally unique monocotyledonous lignocellulosic system whose engineering behaviour remains insufficiently documented within hardwood engineering research frameworks. Unlike conventional hardwoods and softwoods, date palm trunks exhibit a vascular bundle–parenchyma architecture that generates pronounced structural heterogeneity along the longitudinal axis. A comprehensive, multidomain evaluation is therefore required to understand its true material potential.

This study presents an integrated mechanical, physical, chemical, and biological characterization of mature date palm trunks collected from Wasit Province (Kut City), Iraq. Three independent trunks were selected, and standardized small clear specimens were prepared from three longitudinal regions: top, middle, and bottom. All mechanical tests were conducted according to standardized small clear specimen procedures. The middle region was defined at 1 m above ground level to ensure consistent anatomical positioning across trunks. This sampling strategy enabled assessment of both inter-tree variability and intra-trunk structural gradients.

Mechanical performance was evaluated using static bending (MOR and MOE), impact bending, compression parallel to grain, and Brinell surface hardness testing. Physical behaviour was investigated through density determination, moisture related dimensional stability (swelling and shrinkage), and intrinsic longitudinal permeability measured under steady-state flow conditions. Chemical characterization included determination of structural carbohydrate fractions and lignin balance to interpret compositional tendencies. Biological durability was assessed by exposing specimens to both brown-rot and white-rot fungi to evaluate decay-response patterns across anatomical regions.

The observations indicate in material behaviour associated with vascular bundle distribution and density transitions along trunk height. Mechanical responses demonstrate position-dependent trends reflecting structural organization rather than uniform woody tissue behaviour. Permeability analysis indicates pronounced axial fluid transport capacity, while dimensional stability exhibits anisotropic deformation dominated by transverse shrinkage with negligible longitudinal change. Compositional assessment suggests a carbohydrate-dominant structural profile, and biological resistance patterns further confirm the heterogeneous nature of the material across regions.

Collectively, the findings demonstrate that date palm trunk wood should be interpreted as a structurally graded lignocellulosic system rather than a homogeneous timber analogue. Its engineering behaviour results from the interaction between anatomical architecture, compositional balance, and moisture dependent mechanisms. The present multidomain evaluation establishes a structured performance baseline and provides a scientific foundation for future modification strategies, permeability-driven treatments, durability enhancement, and sustainable valorisation pathways within hardwood-oriented material research.

INTRODUCTION

The increasing global demand for sustainable lignocellulosic resources has intensified scientific interest in underutilized biomass materials and non-conventional wood systems. Date palm (*Phoenix dactylifera* L.) is one of the most important agricultural species in arid and semi-arid regions, particularly throughout the Middle East and North Africa (Alhachami and Bak 2025). Large quantities of date palm trunk biomass become available annually through agricultural maintenance and plantation renewal; however, the engineering utilization of this material remains limited (Zaid and de Wet 2002).

Unlike hardwoods and softwoods, date palm belongs to monocotyledonous plants and exhibits a fundamentally different anatomical organization. Conventional woody tissues are replaced by a vascular bundle–parenchyma architecture lacking annual growth rings and secondary radial growth (Tomlinson 1990). This structural organization produces pronounced heterogeneity within the trunk and strongly influences its physical and mechanical behaviour.

Previous investigations on date palm trunks mainly focused on isolated physical or mechanical properties (Fathi 2014; Jonoobi et al. 2019). Nevertheless, comprehensive multidomain evaluations integrating mechanical behaviour, dimensional stability, biological resistance, and chemical composition remain relatively limited. Furthermore, the influence of longitudinal structural gradients on engineering performance has not yet been sufficiently interpreted within wood engineering frameworks.

The present study aims to establish an integrated characterization framework for mature date palm trunk wood collected from Iraq. Mechanical, physical, biological, chemical, and anatomical properties were evaluated using standardized small clear specimens obtained from different trunk regions. The study seeks to improve scientific understanding of date palm trunk behaviour and provide a foundation for future modification technologies and sustainable utilization strategies.

MATERIALS AND METHODS

Raw Material and Sampling Strategy

Mature date palm trunks (*Phoenix dactylifera* L.) were collected from Wasit Province (Kut City), Iraq. Three independent trunks were selected for investigation. Samples were obtained from three longitudinal trunk regions defined as top (T), middle (M), and bottom (B). The middle section was standardized at approximately 1 m above ground level to ensure consistent anatomical positioning and minimize the influence of soil-related degradation.

The investigated specimen categories included T1M, T2B, T2M, T2T, and T3M. This sampling strategy enabled the evaluation of both inter-trunk variability and intra-trunk structural gradients.

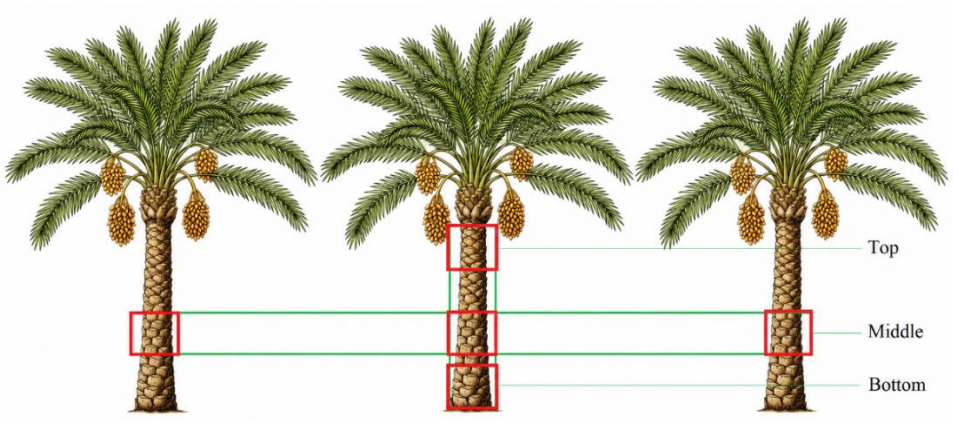

Figure 1: Schematic illustration of the sampling strategy used for date palm trunk specimen selection from three independent palm trunks and five longitudinal regions, according to the distribution presented in the figure. The original conceptual sketch was manually drafted by the author and subsequently digitally refined for visualization purposes

Mechanical Characterization

Mechanical testing was conducted at the Faculty Materials Testing Laboratory I (FMTL I), University of Sopron. Standardized small clear specimen procedures were applied throughout the experimental program.

Static bending and modulus of elasticity (MOE) tests were performed using specimens measuring 20 × 20 × 300 mm. Fifteen specimens were prepared for each category. Impact bending tests were conducted using the same specimen dimensions with a Charpy pendulum impact system.

Compression parallel to grain was evaluated using specimens measuring 20 × 20 × 30 mm. Surface hardness was determined according to the Brinell–Mörath method using 20 × 20 × 30 mm specimens prepared from bending test residues when possible (ISO 13061-2 2014; ISO 13061-4 2017).

Universal testing systems, including Instron and Tinius Olsen equipment, were used for mechanical loading and deformation measurements.

Physical Properties

Density, moisture-related dimensional stability, swelling, and shrinkage behaviour were evaluated using 20 × 20 × 30 mm specimens. Physical measurements included oven-dry conditioning and water-related dimensional response analysis. Dimensional measurements were performed using a digital specimen dimensioning station equipped with Mitutoyo precision gauges (ISO 13061-2 2014; ISO 13061-4 2017).

Biological Durability

Biological resistance was evaluated using fungal decay testing with two representative wood-destroying fungi: *Coriolus versicolor* (white-rot fungus) and *Coniophora puteana* (brown-rot fungus). Specimens measuring 15 × 25 × 50 mm were prepared, and five specimens were tested for each fungal category (European Committee for Standardization (CEN) 2020).

Anatomical and Chemical Characterization

Microscopic investigations were conducted using small cubic specimens measuring approximately 5 × 5 × 5 mm. The observations focused on vascular bundle distribution and structural heterogeneity.

Chemical analyses were performed using residual material obtained from specimen preparation. Structural carbohydrate fractions and lignin-related compositional tendencies were investigated to support interpretation of engineering behaviour.

OBSERVED ENGINEERING TENDENCIES AND STRUCTURAL INTERPRETATION

The present conference contribution focuses primarily on establishing the integrated characterization framework and the observed multidomain tendencies, while the complete quantitative dataset and advanced statistical analyses will be reported in a subsequent full journal publication

Mechanical Behaviour

The investigated date palm trunk material exhibited strong position-dependent mechanical behaviour associated with longitudinal structural gradients. The middle trunk regions generally demonstrated improved mechanical performance compared with upper trunk sections. This tendency can be associated with variations in vascular bundle concentration and density distribution.

Static bending and compression behaviour reflected the highly heterogeneous internal architecture of the material. Unlike conventional hardwoods, the engineering response of date palm cannot be interpreted as a homogeneous wood system. Instead, the observed behaviour corresponds to a structurally graded lignocellulosic material.

Impact bending tests further demonstrated the sensitivity of date palm structure to anatomical organization. The energy absorption behaviour varied considerably between trunk regions, indicating that local bundle distribution strongly affects dynamic mechanical response.

Surface hardness testing showed noticeable differences between cross-sectional and side-sectional measurements, further confirming the anisotropic nature of the material.

Physical Properties and Dimensional Stability

Density-related behaviour exhibited clear longitudinal gradients within the investigated trunks. Variations in density strongly influenced mechanical response and dimensional stability.

Swelling and shrinkage behaviour were dominated by transverse deformation, while longitudinal dimensional changes remained comparatively limited. This behaviour differs from conventional ring-structured timber and reflects the unique monocotyledonous anatomy of date palm.

The material also demonstrated considerable axial transport capability, which can be associated with the orientation and continuity of vascular bundles. Such permeability-related behaviour may provide advantages for future impregnation and modification technologies.

Biological Durability

Fungal decay exposure revealed heterogeneous biological resistance behaviour between trunk regions. The responses to white-rot and brown-rot fungi indicated that anatomical variability and moisture transport mechanisms significantly influence degradation patterns.

The observed biological behaviour further supports the interpretation of date palm trunk material as a structurally heterogeneous lignocellulosic system rather than a uniform timber analogue.

Anatomical and Chemical Interpretation

Microscopic observations confirmed the highly heterogeneous vascular bundle–parenchyma architecture of the material. Bundle concentration and spatial distribution varied considerably between trunk regions.

Chemical analysis suggested a carbohydrate-dominant structural profile consistent with monocotyledonous lignocellulosic systems reported in previous studies. The interaction between anatomical organization, compositional balance, and moisture-related mechanisms appears to govern the overall engineering behaviour of date palm trunks.

CONCLUSIONS

This study presented an integrated multidomain characterization framework for date palm trunk wood (*Phoenix dactylifera* L.) collected from Iraq. Mechanical, physical, anatomical, biological, and chemical investigations demonstrated that the material exhibits pronounced longitudinal heterogeneity associated with vascular bundle distribution and density gradients.

The present observations indicate that date palm trunk material should not be interpreted as a homogeneous timber analogue. Instead, it behaves as a structurally graded monocotyledonous lignocellulosic system with highly position-dependent engineering properties.

The high axial transport potential and the observed multidomain interactions suggest promising opportunities for future permeability-driven treatments, chemical modification technologies, and sustainable valorisation pathways. The present study establishes a scientific foundation for future advanced investigations on date palm utilization within wood engineering and biomaterial research.

ACKNOWLEDGEMENT

This article was made in frame of the project TKP2021-NKTA-43 which has been implemented with the support provided by the Ministry of Culture and Innovation of Hungary from the National Research, Development and Innovation Fund, financed under the TKP2021-NKTA funding scheme.

REFERENCES

Alhachami F, Bak M (2025) Physical and Indentation Properties of Date Palm Wood from the Middle Stem Section under Standard Conditions. In: WOOD 4 SUSTAINABILITY: Processing, Construction, Products and Design 2025. University of Sopron Press, Sopron, Hungary, pp 104–110

European Committee for Standardization (CEN) (2020) EN 113-2:2020 Durability of wood and wood-based products — Test method against wood destroying basidiomycetes

Fathi L (2014) Structural and mechanical properties of the wood from coconut palms, oil palms and date palms. PhD Thesis, Staats-und Universitätsbibliothek Hamburg Carl von Ossietzky

ISO 13061-2 (2014) Physical and mechanical properties of wood—test methods for small clear wood specimens—Part 2: determination of density for physical and mechanical tests

ISO 13061-4 (2017) Physical and mechanical properties of wood–test methods for small clear wood specimens. Part 4: Determination of modulus of elasticity in static bending.

Jonoobi M, Shafie M, Shirmohammadli Y, et al (2019) A review on date palm tree: Properties, characterization and its potential applications. Journal of renewable materials 7:1055–1075

Tomlinson PB (1990) The structural biology of palms. Oxford University Press

Zaid A, de Wet PF (2002) Date Palm Cultivation. FAO Plant Production and Protection Paper 156 Rev. 1. Food and Agricultural Organization of the United Nations

Finite Element Analysis of a Montessori Climbing Arch Made from Underutilized Hardwoods

László János Dékány[1], József Garab[1*]

[1] University of Sopron, Faculty of Wood Engineering and Creative Industries. Bajcsy-Zs. Str. 4, Sopron, Hungary, 9400.

E-mail: DekanyLJ21@student.uni-sopron.hu; garab.jozsef@uni-sopron.hu

Keywords: Montessori furniture; multi-functional furniture; linear static structural analysis; grey poplar, Turkey oak.

ABSTRACT

The structural performance of children's furniture is a critical design consideration due to the diverse and often unpredictable loading conditions encountered during use. At the same time, increasing the utilization of underexploited hardwood species may contribute to a more sustainable and balanced use of forest resources. This study investigates numerically the structural behavior of a multifunctional Montessori climbing arch manufactured from grey poplar (*Populus* × *canescens*) and Turkey oak (*Quercus cerris*), using Norway spruce (*Picea abies*) as a reference material. A three-dimensional finite element model was developed and evaluated under three representative load cases corresponding to climbing, table, and rocking functions. Orthotropic material behavior was assigned to the wooden rungs, while isotropic material properties were applied to the side panels. Structural performance was assessed in terms of maximum displacement, stress distribution, and bending utilization. The results showed that all investigated material configurations satisfied the structural requirements of the considered load cases. The highest bending utilization was obtained for grey poplar under the rocking load case (76.31%), while Norway spruce and Turkey oak reached 59.25% and 11.62%, respectively. Although the utilization values were derived using different sources of strength data for the investigated species, the results indicate that Turkey oak exhibited the most favorable structural performance and may provide improved stability due to its higher density. The results further suggest that grey poplar may also be suitable for this application, although design modifications or hybrid material solutions may be advantageous in highly loaded regions.

INTRODUCTION

Ensuring the structural safety and reliability of children's furniture is a critical engineering task, as such products are subjected to highly variable and often unpredictable loading conditions during use. Furniture designed according to the Montessori principle is characterized by multifunctionality and active interaction (Dobrowolska et al., 2021; D'Elia et al, 2025). These diverse use scenarios introduce complex load cases that must be considered already in the design phase to prevent excessive deformation or structural failure. These diverse scenarios may be supported by modern methods and tools (Horváth and Kovács 2011, Antal and Nagy 2023)

At the same time, increasing attention is being directed toward the use of underutilized wood species to improve the sustainability and resource efficiency of the wood industry. In Hungary, several hardwood species, such as grey poplar (*Populus* × *canescens*) and Turkey oak (*Quercus cerris*), remain relatively underexploited despite their availability and potential mechanical applicability (Borovics et al. 2023, Govina et al. 2023). Their integration into value-added products, including furniture, could contribute to a more balanced utilization of forest resources. However, the structural performance of such species in demanding applications is not yet sufficiently documented, particularly in comparison with widely used materials such as the traditional wood species, the Norway spruce (*Picea abies*).

Finite element analysis (FEA) has become a widely applied tool in engineering design, enabling the evaluation of stress distribution and deformation behavior prior to physical prototyping (Makhlouf et al., 2016). In the context of furniture engineering, FEA supports the concept of virtual prototyping, allowing designers to assess structural performance under representative load cases, optimize geometry, and reduce the need for costly experimental iterations (Kasal et al. 2016, Hu et al. 2019). Despite its

advantages, the application of FEA in the design of wood-based furniture, especially involving alternative hardwood species, remains relatively limited in the literature.
The present study addresses this gap by performing a finite element-based structural assessment of a multi-functional Montessori climbing arch manufactured from underutilized hardwood species. The climbing arch is designed to support the development of motor skills from infancy. The furniture can be used in climbing, table, and rocking configurations, supporting the progressive development of children's motor skills. Furthermore, before movement, the children can lie below the arch and play with figures hanging from the rungs. The climbing arch is designed to evolve with the child, from a baby gym to a functional desk. Based on the Montessori principle of "freedom of movement", encouraging independent motor skill development in a safe environment (Montessori 2011).

MATERIALS AND METHODS

The CAD model of the Montessori climbing arch was designed by shapr3D® CAD software. The finite element analysis was performed by Ansys® Academic Research Mechanical, Release 25 R2 computational software package. The geometry of the designed product is presented in the Figure 1.

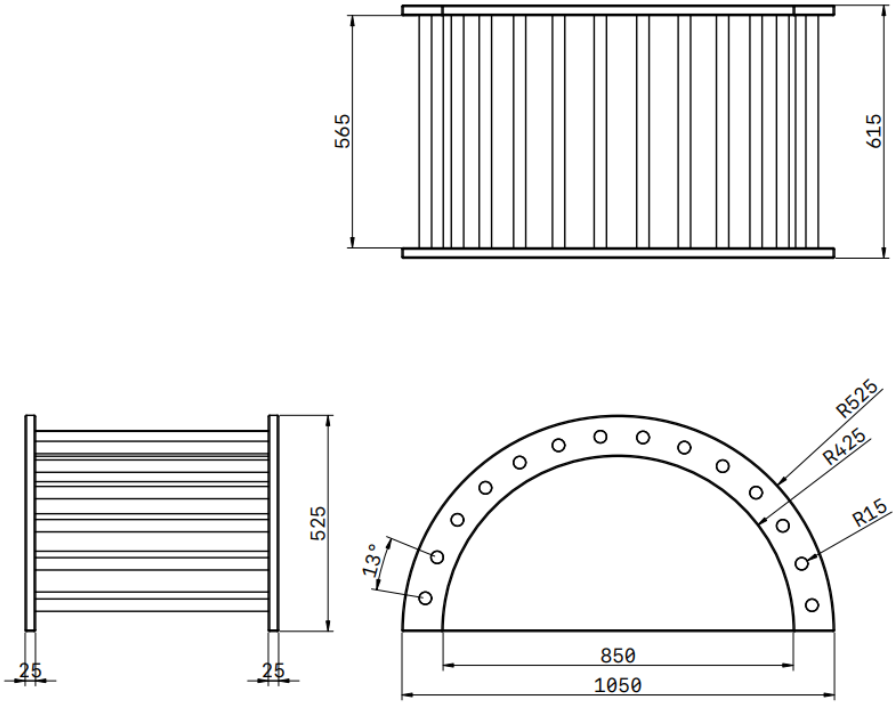

Figure 1: Dimensions of the Montessori climbing arch

Static structural analysis was performed in the Workbench module after geometry import. Orthotropic material model was applied to the wooden rungs (cylindrical dowels) according to the anatomical main directions with the length directions aligned to the anatomical longitudinal direction of wood. Isotropic material model was applied to the side panels forming the primary load bearing frame. Table 1 summarizes the material properties taken from literature. Depending on the case, grey poplar or Turkey oak was used, with Norway spruce (*Picea abies*) serving as the traditional control wood material. Hence the full set of orthotropic elastic constants are not determined yet for grey poplar and Turkey oak, the full set of orthotropic elastic constants were derived from MOE parallel to the grain (E_0) and from the shear modulus for planes parallel to grain (G_0) according to Patlakas et al. (Patlakas et al., 2019). The MOE perpendicular to grain E_{90} was considered instead as a constant fraction of E_0 (E_0/E_{90}=30) and the rolling shear modulus G_{90} as a constant fraction of G_0 (G_0/G_{90}=10). The three Poisson's ratios were considered equal to 0.35. The engineering constants were applied based from the works of the researchers of the University of Sopron (Altaher Omer Ahmed et al. 2023, Govina 2025, Fabrice 2026). The joints were not modelled because the global structural response was the goal of the study. The

contacts were modeled as bonded contacts. The mesh consisted of 67660 quad dominated quadratic elements with 8 mm of the element size.

Table 1: Material properties used in the finite element analysis

Wood Species	Density [g/cm^3]	E_L [MPa]	E_R [MPa]	E_T [MPa]	G_{LR} [MPa]	G_{LT} [MPa]	G_{RT} [MPa]	ν_{LR} [-]	ν_{LT} [-]	ν_{RT} [-]	Bending Strength [MPa]
Norway spruce (C24[a])	0.35	11 000	367	367	690	690	69	0.35	0.35	0.35	24
Grey poplar (C16[a])	0.31	8000	267	267	500	500	50	0.35	0.35	0.35	16
Turkey oak[b]	0.65	8929	298	298	500	500	50	0.35	0.35	0.35	104

[a] Corresponding strength grades according to MSZ EN 338 based on NDT measurements (Altaher Omer Ahmed et al. 2023; Fabrice 2026); [b] The bending strength value corresponds to the minimum value obtained from the experimental measurements reported by Govina (2025). Other engineering constants values are according to the nearest lower strength grade based on E_0 according to MSZ EN 338

The applied loads were approximated based on the expected functional use by children and, in some cases, by an adult. A total load of 1200 N was applied. Three load cases were considered. Load case 1 (LC1) represented climbing, where children were assumed to climb on the top of the arch (Figure 2). Load case 2 (LC2) represented table use, where the arch was assumed to be used as a table (Figure 3). Load case 3 (LC3) represented rocking (Figure 4). Although rocking involves dynamic behavior, it was modelled as a static structural problem. In this case, the child was assumed to stand with one leg on the 3rd rung and the other leg on the 8th rung. To account for the dynamic nature of the loading, twice the child's body weight was applied.

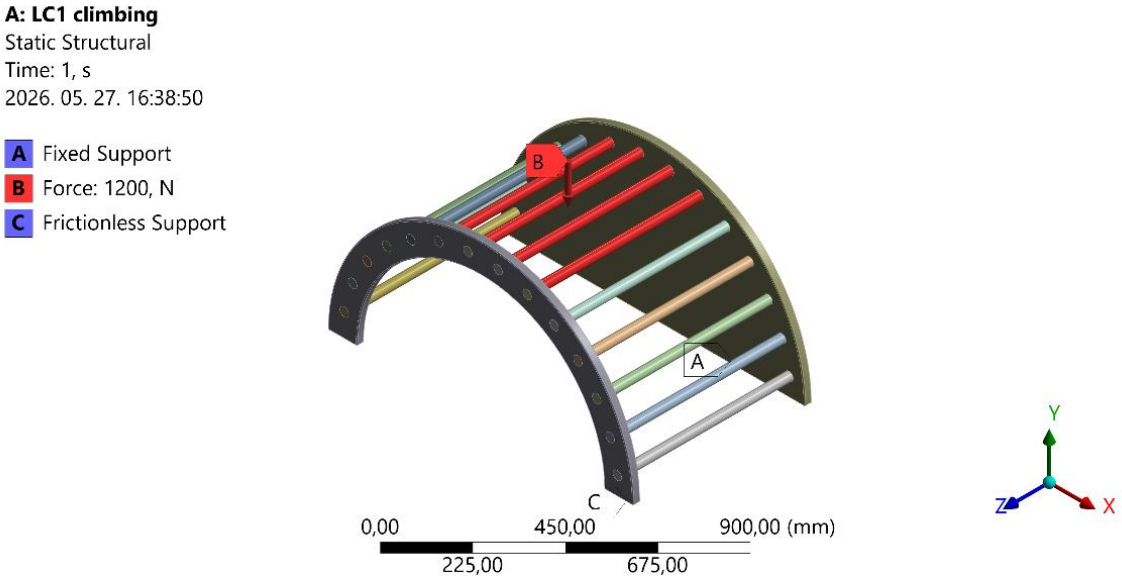

Figure 2: FE model for the climbing function (LC1)

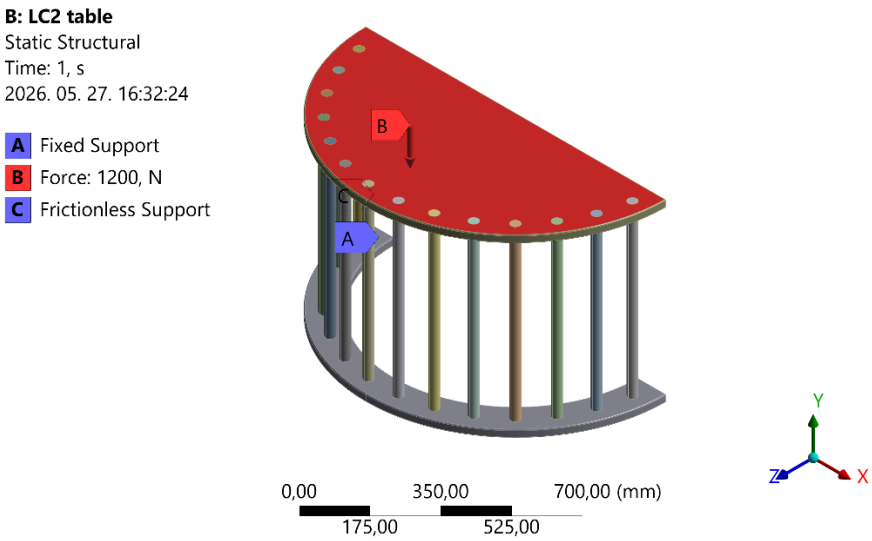

Figure 3: FE model for the table function (LC2)

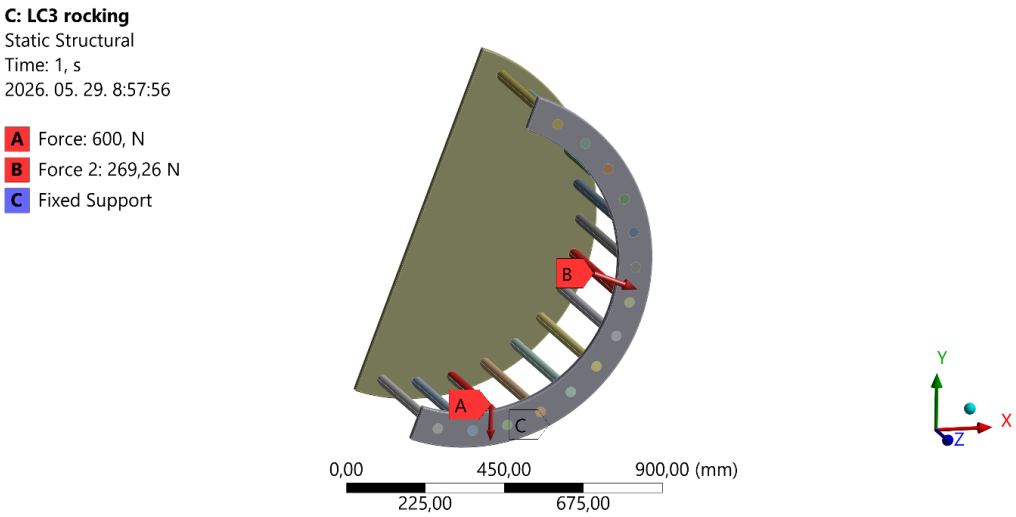

Figure 4: FE model for the rocking function (LC3)

RESULTS AND DISCUSSIONS

The main interest was the global response of the structure according to the 3 load cases. Figures 5-7 show the deflection results according to the load cases and the material was from Turkey oak. Turkey oak was selected due to its relatively high density, which provides favourable mass-related characteristics for the furniture. As a result, the climbing arch is sufficiently heavy, reducing the likelihood of unintended sliding during use by children. Furthermore, the bending utilization was calculated as the ratio of the maximum longitudinal normal stress to the bending strength of the material ($|\sigma_L_{max}|/f_m$) which was presented in percentage (Table 2). The predicted deflections were low for all investigated configurations, indicating adequate global stiffness. Similarly, the calculated stress levels remained below the bending strength of the materials in all cases. However, grey poplar exhibited the highest utilization values, reaching 76.31% in the most demanding loading scenario (LC3), whereas Norway spruce reached 59.25% and Turkey oak only 11.62%. The findings indicate that grey poplar can be considered a viable material for the investigated application, provided that appropriate design modifications, such as increased cross-sectional dimensions, reduced span lengths, or additional supports, are implemented to accommodate severe loading scenarios (e.g. LC3). Turkey oak, however, demonstrates favourable structural performance and low utilization values under all investigated load

cases. In the case of grey poplar, design modifications could be required to achieve comparable structural performance. Consequently, a hybrid material approach may represent a more balanced solution. In such a design, the side frames could be manufactured from grey poplar, while the rungs could be produced from Norway spruce or Turkey oak to achieve higher strength and stiffness without increasing the rung dimensions. Alternatively, the entire furniture piece could be manufactured from Turkey oak, which would provide the highest structural safety reserve while also increasing the overall mass and stability of the product.

However, it should be noted that the bending utilization values are based on different sources of strength data. For Norway spruce and grey poplar, characteristic bending strength values according to MSZ EN 338 were used, whereas the bending strength of Turkey oak was taken from experimental measurements reported by Govina (2025). Consequently, the calculated utilization values are not strictly comparable among the investigated species and should be interpreted as indicative rather than absolute measures of relative structural performance. The characteristic bending strength of Turkey oak may differ from the experimentally measured value applied in this study. Nevertheless, the results demonstrate that Turkey oak provides sufficient strength and stiffness for the investigated furniture application and represents a promising material for children's furniture manufacturing.

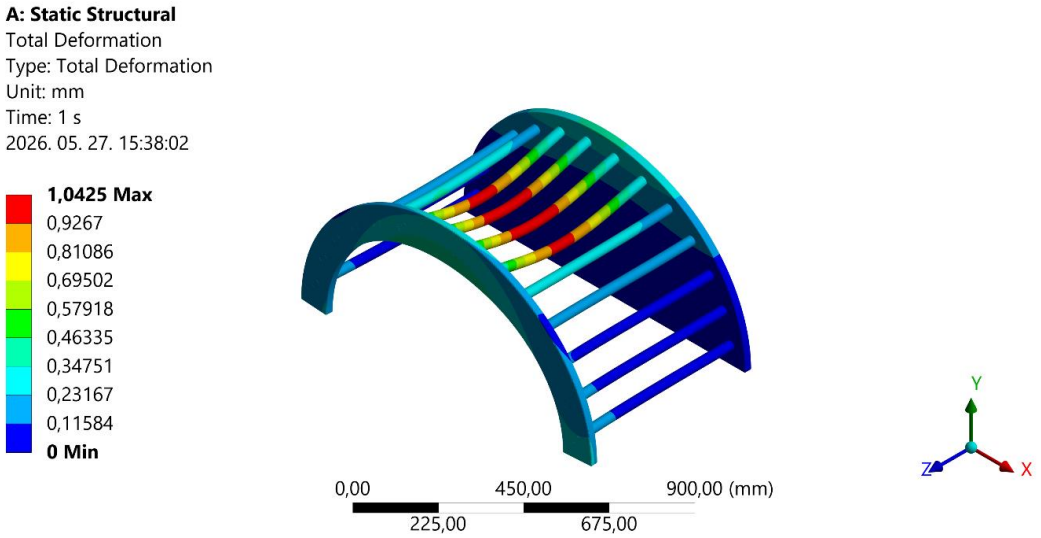

Figure 5: Total deformation for the climbing function (LC1) in case of Turkey oak

Table 2: Results of the numerical simulation

Wood Species	Load case	Maximum displacement [mm]	Maximum longitudinal stress [MPa]	Bending utilization [%]
Grey poplar	LC1	1.15	5.54	34.63
Grey poplar	LC2	1.45	3.77	23.56
Grey poplar	LC3	1.27	12.21	76.31
Turkey oak	LC1	1.04	5.59	5.38
Turkey oak	LC2	1.30	3.79	3.64
Turkey oak	LC3	1.16	12.08	11.62
Norway spruce	LC1	0.84	5.54	23.08
Norway spruce	LC2	1.06	3.77	15.71
Norway spruce	LC3	1.50	14.22	59.25

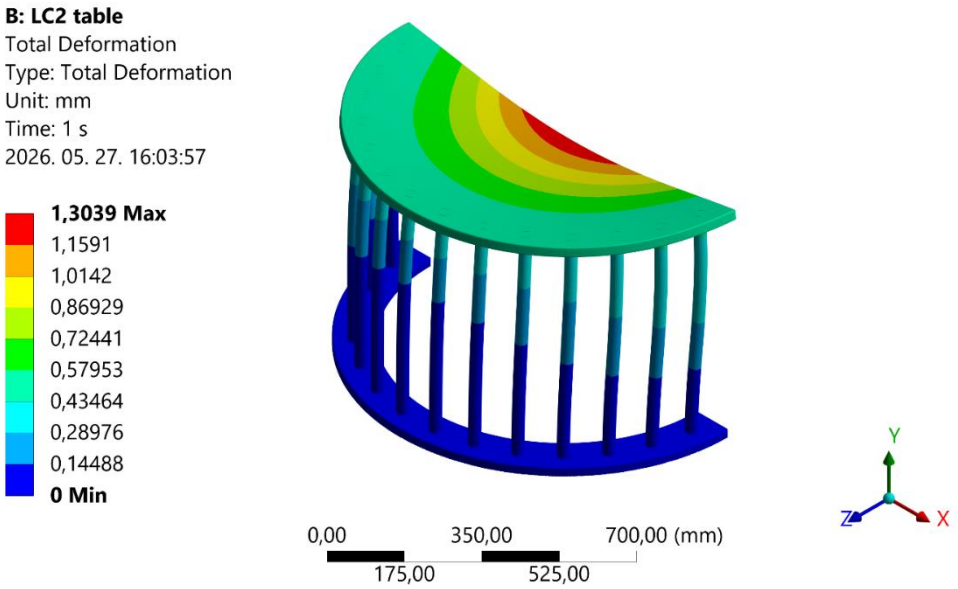

Figure 6: Total deformation for the table function (LC2) in case of Turkey oak

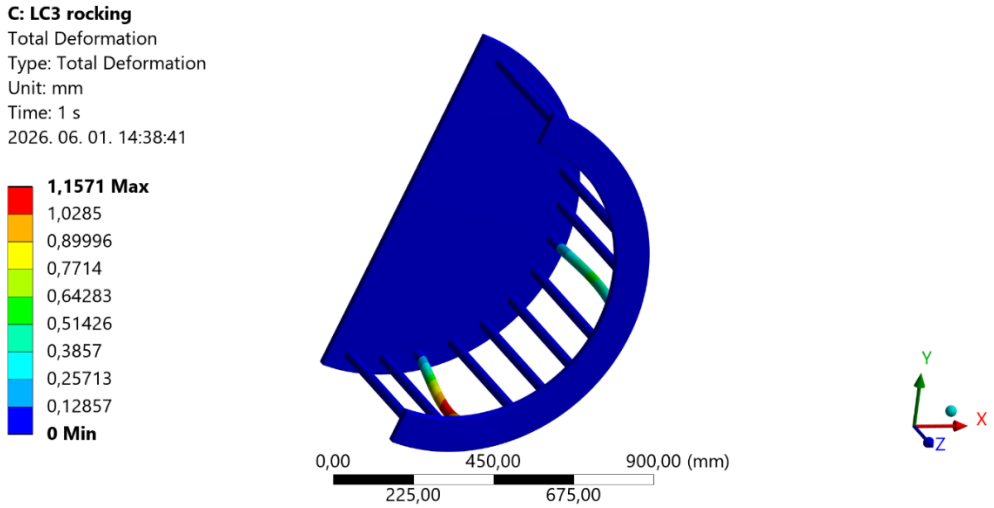

Figure 7: Total deformation for the rocking function (LC3) in case of Turkey oak

CONCLUSIONS

The finite element analysis performed on the Montessori climbing arch demonstrated that all investigated wood species provided adequate structural performance under the considered climbing, table, and rocking load cases. The predicted deflections were low in all configurations, indicating sufficient global stiffness of the structure.

Among the investigated materials, Turkey oak exhibited the lowest bending utilization values, reaching a maximum utilization of 11.62% under the most demanding load case. Norway spruce showed moderate utilization levels, while grey poplar exhibited the highest utilization, reaching 76.31% during the rocking load case. However, it should be noted that the utilization values were calculated using different sources of strength data and therefore should be interpreted as indicative rather than strictly comparable measures of structural performance.

The results suggest that Turkey oak is a highly suitable material for the investigated application, providing excellent structural performance and potentially improved stability due to its higher density. Grey poplar may also be considered a viable alternative; however, additional design modifications may be required in highly stressed regions. Since increasing the dimensions of the rungs may compromise ergonomic requirements, hybrid material solutions appear particularly promising. The use of stronger

materials for the rungs combined with grey poplar side frames could improve structural efficiency while maintaining user comfort and reducing material consumption.

Overall, the study confirms the potential of underutilized Hungarian hardwood species for the manufacture of children's furniture and demonstrates the effectiveness of finite element analysis as a design-support and virtual prototyping tool. Future work should include experimental validation of the numerical results and the investigation of joint behavior and dynamic loading effects.

REFERENCES

Altaher Omer Ahmed, A., Garab, J., Horváth-Szováti, E., Kozelka, J., & Bejó, L. (2023). The bending properties of hybrid cross-laminated timber (CLT) using various species combinations. *Materials*, *16*(22), 7153.

Antal, R. M., & Nagy, V. (2023). Augmented and virtual reality technologies as the future sales' channel in the furniture industry. *Journal of Applied Technical and Educational Sciences*, *13*(1), 341-341.

Borovics, A., Mertl, T., Király, É., & Kottek, P. (2023). Estimation of the overmature wood stock and the projection of the maximum wood mobilization potential up to 2100 in Hungary. *Forests*, *14*(8), 1516.

Dobrowolska, E., Błaszczak, I., Mielnik, A., & Lisiecka, E. (2021). A systemic model of furniture meant for stimulating development of a child based on educational aids from M. Montessori. *Annals of Warsaw University of Life Sciences-SGGW. Forestry and Wood Technology*, (113), 13-20.

D'Elia, L., Belhaj, S., Muscolo, S., & Imbesi, L. (2025). DESIGN-LED CIRCULARITY FOR FURNITURE MANUFACTURING. AN APPLICATION ON MONTESSORI KINDERGARTEN. In *Cumulus conference: Design Across Borders-United in Creativity* (Vol. 13, pp. 1462-1490). Cumulus the Global Association of Art and Design Education and Research.

Govina, J. K., Nemeth, R., Bak, M., & Bader, M. (2023). Effect of variable growth conditions on selected anatomical properties of Hungarian Turkey oak wood. Bulletin of the Transilvania University of Brasov. Series II: Forestry• Wood Industry• Agricultural Food Engineering, 83-98.

Horváth, P. G., & Kovács, Z. (2011). The role of dimensioning in furniture and indoor design. In Innovations in Forest Industry and Engineering Design: Third Scientific and Technical Conference (pp. 202–205).

Hu, W., Wan, H., & Guan, H. (2019). Size effect on the elastic mechanical properties of beech and its application in finite element analysis of wood structures. *Forests*, *10*(9), 783.

Kasal, A., Smardzewski, J., Kuşkun, T., and Erdil, Y. Z. (2016). "Numerical analyses of various sizes of mortise and tenon furniture joints," *BioRes.* 11(3), 6836-6853.

Makhlouf, H., Chevalier, L., Favier, E., & Launay, E. (2016). A stochastic approach for the evaluation of the reliability of wood furniture in an industrial context: managing virtual standardization tests. *Mechanics & Industry*, *17*(5), 503.

Montessori, M. (2011). *The absorbent mind*. Lulu.com.

Patlakas, P., Brunetti, M., Christovasilis, I., Nocetti, M.,& Pizzo, B. (2019). Structural performance of a novel Interlocking Glued Solid Timber system. Materials and Structures/Materiaux et Constructions, 52(1). https://doi.org/10.1617/s11527-019-1324-2

Natural Durability of Turkey Oak from Various Hungarian Sites Against *Daedalea quercina* (L.)

Máté Nagy[1*], Norbert Horváth[1]

[1] University of Sopron, Bajcsy-Zsilinszky u. 4, 9400 Sopron, Hungary.

E-mail: okoskologus@gmail.com, horvath.norbert@uni-sopron.hu

Keywords: Turkey oak; natural durability; site variability; *Daedalea quercina* (L.); EN 113; mass loss; sustainable wood use.

ABSTRACT

This study evaluates the site-dependent natural durability and physical properties of Turkey oak (Quercus cerris L.) juvenile wood against the brown-rot fungus *Daedalea quercina* (L.). Standardized specimens originating from three Hungarian forest stands representing different macroclimates (Hetvehely, Piliscsév, Nagycenk) were tested for oven-dry density, CIELab colour parameters, and mass loss according to EN 113 after a 16-week laboratory incubation. The results revealed a macroclimatic trend: the tree adapted to drier conditions (Nagycenk) produced denser, darker (lower L*), and descriptively more decay-resistant timber compared to the one growing in a humid, high-precipitation environment (Hetvehely). Conversely, chromatic coordinates (a* and b*) displayed no clear correlation with fungal degradation patterns. These findings suggest that macroclimatic conditions indirectly influence juvenile wood durability, emphasizing the importance of site-specific evaluation to support the climate-adaptive and sustainable industrial utilization of Turkey oak.

INTRODUCTION

Global climate change and growing-season droughts are fundamentally altering the composition of domestic forest stands, necessitating a thorough reconsideration of tree species selection strategies (Führer 2018). Within this context, Turkey oak (Quercus cerris L.) is emerging as a key species for climate-adaptive forestry due to its excellent drought tolerance, currently accounting for 11.6% of the Hungarian forest area (Németh et al. 2025). Although its timber was historically often categorized as secondary due to its moderate natural durability (Molnár 1999), precise knowledge of its technical properties is essential for higher value-added industrial utilization. Since growing site conditions can significantly modify wood density and appearance (Németh et al. 2025), this study aims to evaluate the site-dependent properties of Turkey oak wood to better understand its technical performance and support its future climate-adaptive utilization.

MATERIALS AND METHODS

The wood material of Turkey oak (Quercus cerris L.) was harvested from three distinct Hungarian forest stands representing different macroclimatic conditions: Hetvehely (beech climate, 700–720 mm annual precipitation), Piliscsév (hornbeam-oak climate, 650–700 mm annual precipitation), and Nagycenk (Turkey oak-sessile oak climate, 630–660 mm annual precipitation). Due to the exploratory nature of this study the sampling was restricted to one representative log per growing site (Dövényi 2010; NÉBIH 2024).

The specimen preparation was based on the radial zoning principles described by Eichhorn et al. (2017). However, for the final evaluation, the sample pool was strictly limited to the inner, clearly defined juvenile wood zone (specifically the regions corresponding to the 4th, 12th, and 16th annual rings). This strict selection provided highly homogenized and topologically unambiguous tissue zones, eliminating the physiological and color-boundary uncertainties often present in mature heartwood and transition zones.

Standardized specimens (15 × 25 × 50 mm) were prepared, and their oven-dry density (ρ_0) and CIELab colour parameters (L*, a*, b*) were determined prior to fungal inoculation. The laboratory decay test was executed in full accordance with the EN 113 standard, using the brown-rot fungus *Daedalea quercina* (L.) over a 16-week incubation period under controlled conditions (22 °C, 70% RH). Statistical

analyses (one-way ANOVA and Post Hoc Tukey tests) were performed via Jamovi (v2.6) on the dataset, evaluating all treatment effects at a significance level of 5%.

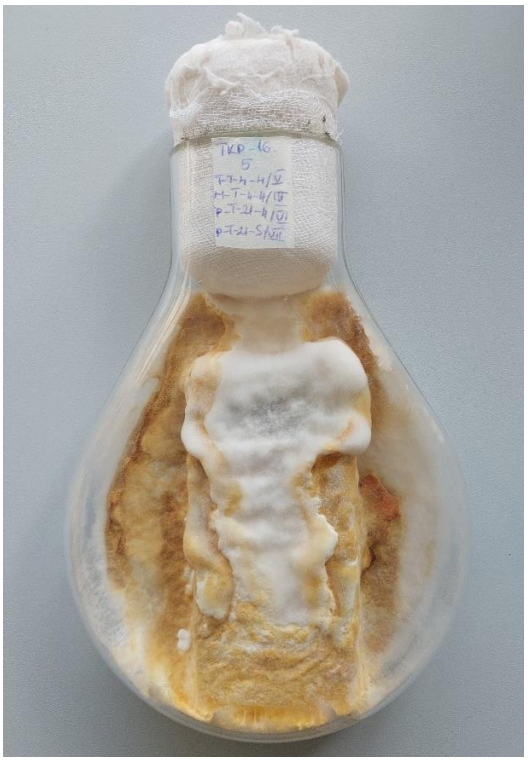

Figure 1: Turkey oak specimens during incubation with Daedalea quercina (L.)

RESULTS

Oven-dry density

The oven-dry density (ρ_0) exhibited prominent variations among the three investigated sites. The highest average density was recorded for the Nagycenk site (0.798 ± 0.016 g/cm³), followed by Hetvehely (0.778 ± 0.015 g/cm³), while the lowest mean value was measured in the specimens from Piliscsév (0.733 ± 0.015 g/cm³). The one-way ANOVA confirmed that these site-dependent differences in juvenile wood density were statistically highly significant ($F(2, 42) = 70.8$, $p < 0.001$). The Post Hoc test revealed that all pairwise comparisons were statistically significant, indicating clear differences between Nagycenk–Piliscsév ($p < 0.05$), Nagycenk–Hetvehely ($p = 0.003$), and Piliscsév–Hetvehely ($p < 0.05$).

CIELab colour parameters

The lightness (L*) analysis revealed a significant effect of the growing site ($F(2, 42) = 9.59$, $p < 0.05$). The juvenile wood from Hetvehely was the brightest (55.7 ± 1.73), followed by Piliscsév (53.8 ± 3.83), while Nagycenk provided the darkest wood structure (51.3 ± 2.35). The Post Hoc test confirmed that the lightness of the Nagycenk samples was significantly lower than both Hetvehely ($p < 0.05$) and Piliscsév ($p = 0.042$), while no significant difference was found between Piliscsév and Hetvehely ($p = 0.164$).

The redness (a*) parameter was significantly influenced by the site conditions ($F(2, 42) = 13.7$, $p < 0.05$). Specimens from Hetvehely exhibited the most intense red hue (10.0 ± 0.36), followed by Piliscsév (9.32 ± 0.90) and Nagycenk (8.66 ± 0.74). The Post Hoc test verified that all pairwise site comparisons differed significantly from each other: Nagycenk–Piliscsév ($p = 0.038$), Nagycenk–Hetvehely ($p < 0.05$), and Piliscsév–Hetvehely ($p = 0.027$).

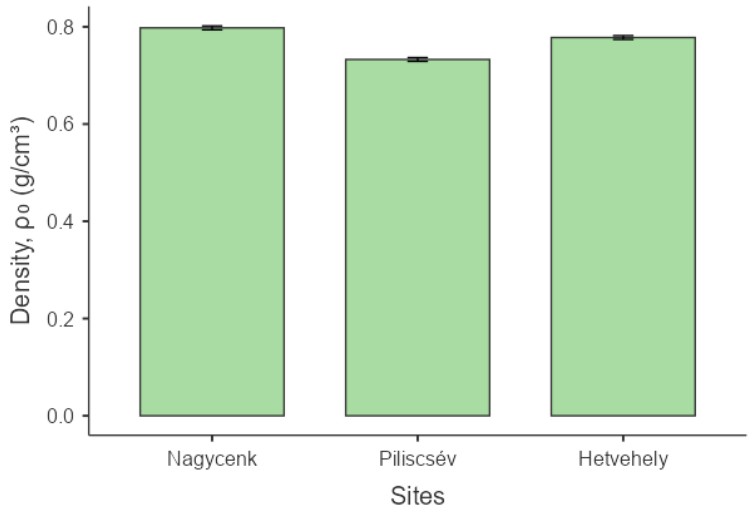

Figure 2: Oven-dry density across the investigated sites

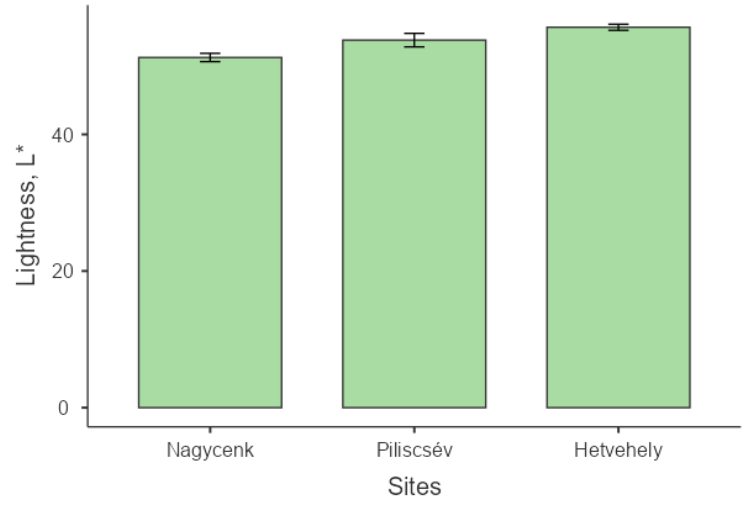

Figure 3: Lightness across the investigated sites

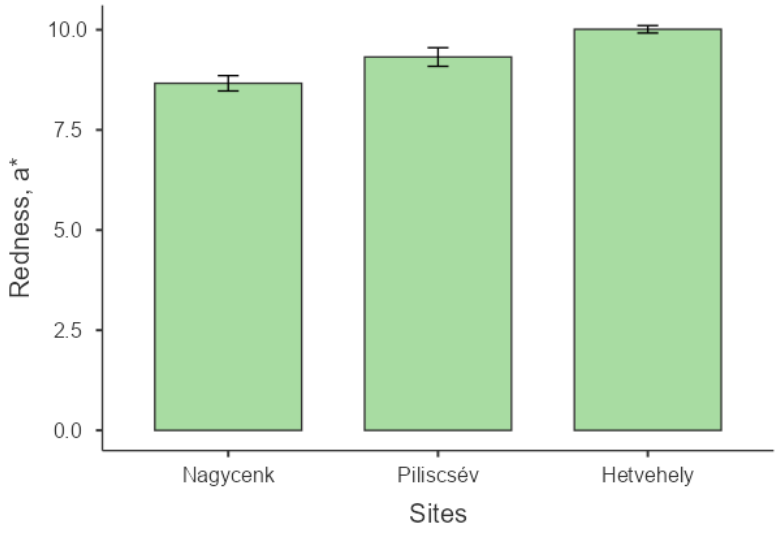

Figure 4: Redness across the investigated sites

Similarly, the yellowness (b*) parameter demonstrated strong site dependency ($F(2, 42) = 17.4$, $p < 0.05$). The highest b* value was found in the Hetvehely group (23.9 ± 0.63), which differed significantly from Nagycenk (22.5 ± 1.04, $p < 0.05$) and Piliscsév (22.1 ± 0.89, $p < 0.05$). The descriptive difference between Nagycenk and Piliscsév did not reach the threshold of statistical significance ($p = 0.376$).

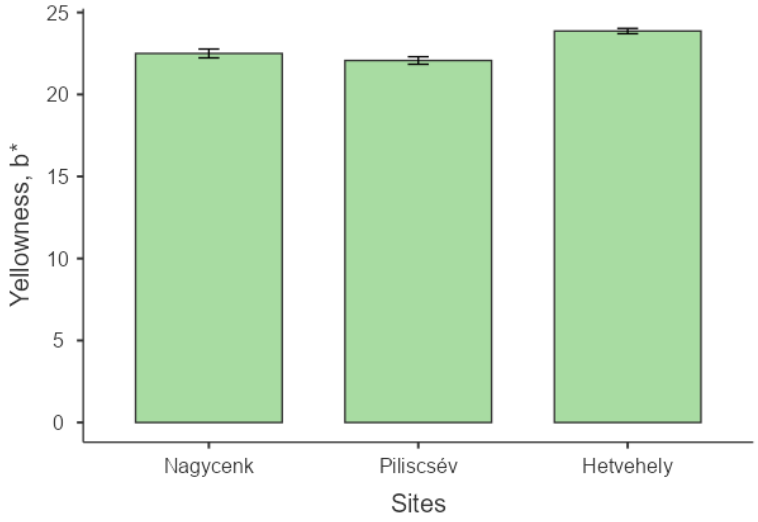

Figure 5: Yellowness across the investigated sites

Natural durability and mass loss

The lowest average mass loss, reflecting the highest relative resistance, was observed in the Nagycenk juvenile wood group (5.77% ± 1.72%). Piliscsév occupied an intermediate position with a mean mass loss of 10.51% ± 6.57%, while the most intense fungal degradation was measured in the specimens originating from Hetvehely (15.37% ± 10.11%). However, the one-way ANOVA indicated that the effect of the growing site on the relative mass loss was not statistically significant ($F(2, 21) = 1.91$, $p = 0.172$).

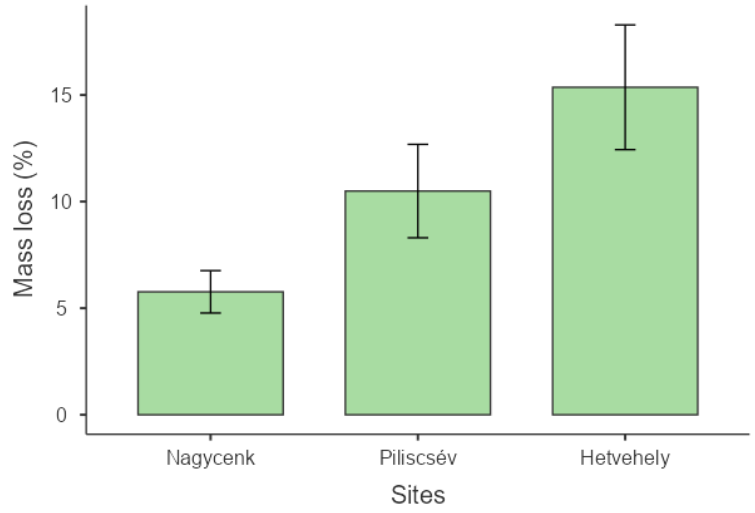

Figure 6: Relative mass loss across the investigated sites

DISCUSSION AND CONCLUSIONS

Despite the lack of statistical significance, the visible descriptive hierarchy of relative mass loss may reflect a correlation with the macroclimatic conditions of the original forest stands. The tree adapted to drier conditions (Nagycenk) produced timber with higher relative biological resistance compared to the one growing in a humid, high-precipitation environment (Hetvehely). The lack of statistical significance in the mass loss analytical model might be attributed to the limited final sample size (N=3 valid data points remaining for the Nagycenk juvenile cohort due to a high exclusion rate of specimens exhibiting a mass loss below the 3% threshold).

The natural durability of Turkey oak (Quercus cerris L.) juvenile wood displays a noticeable variation depending on the macroclimatic characteristics of the growing site. A clear trend was identified, where the tree adapted to drier conditions (Nagycenk) produced denser, darker (lower L*), and descriptively more decay-resistant timber compared to the one growing in a humid, high-precipitation environment (Hetvehely). Conversely, the chromatic coordinates (a* and b*) did not display a clear correlation with the fungal degradation patterns.

To universally validate this environmental relationship for Turkey oak, further investigations with an expanded sample pool are recommended. Consequently, future work incorporating chemical extractive analyses alongside physical testing could provide a deeper understanding of these site-dependent durability variations.

ACKNOWLEDGEMENTS

This work was supported by the National Research, Development and Innovation Office of Hungary under project no. TKP2021-NKTA-43. The authors would also like to thank Luca Buga-Kovács for her valuable guidance, as well as the laboratory and workshop personnel for their technical support and assistance during the study.

REFERENCES

Dövényi Z (2010) Magyarország kistájainak katasztere I-II. MTA Földrajztudományi Kutatóintézet, Budapest

Eichhorn S, Erfurt S, Hofmann T, Seegmüller S, Németh R, Hapla F (2017) Determination of the phenolic extractive content in sweet chestnut (Castanea sativa Mill.) wood. Wood Res 62(2):181–196

Führer E (2018) A klímaértékelés erdészeti vonatkozásai. Erdészettud Közl 8(1):27–42. https://doi.org/10.17164/EK.2018.002

Molnár S (1999) Faanyagtan. Szaktudás Kiadó Ház, Budapest

NÉBIH (2024) Erdőtérkép. Nemzeti Élelmiszerlánc-biztonsági Hivatal. https://erdoterkep.nebih.gov.hu/ Accessed 15 May 2026

Németh R, Tolvaj L, Báder M (2025) Color Variations of Turkey Oak (Quercus cerris L.) Wood from Different Types of Growing Sites. Forests 16(11):1681. https://doi.org/10.3390/f16111681

The jamovi project (2024) jamovi (Version 2.6). https://www.jamovi.org

Impact of False Heartwood on Compressive Strength in Thermally Treated Beech Wood

Aleš Zeidler[1*], Vlastimil Borůvka[1], Adam Sikora[1]

[1] Faculty of Forestry and Wood Sciences, Czech University of Life Sciences Prague;
Kamycka 129, 165 00, Prague, Czech Republic.

E-mail: zeidler@fld.czu.cz; boruvkav@fld.czu.cz; sikoraa@fld.czu.cz

Keywords: *Fagus sylvatica*; red heart; heat modification; density; mechanical properties.

ABSTRACT

European beech is an increasingly important tree species in Central Europe, particularly in the context of anticipated shifts in forest composition due to climate change. Despite its favourable mechanical properties, its broader utilization is limited by defects such as false heartwood and its relatively low natural durability. Thermal modification has been widely applied to enhance wood performance, yet the interaction between heat treatment and structural defects like false heartwood remains insufficiently understood. This study investigates the influence of false heartwood and thermal modification on selected physical and mechanical properties of beech wood. Test specimens were prepared from boards containing false heartwood as well as the reference material free of the heartwood zone. Samples were divided into three groups: untreated reference, thermally treated samples at 160 °C and at 210 °C using Finnish technology of thermal treatment. Wood density and compressive strength were the tested properties to evaluate the effect of the heartwood occurrence and the modification. Results indicate that specimens containing false heartwood exhibited higher density compared to those without it. Thermal modification led to a decrease in density across all samples, with more pronounced reductions at higher temperatures. Compressive strength showed only minor differences between samples with and without false heartwood, and heat treatment resulted in a slight decrease in strength. Equilibrium moisture content decreased significantly with increasing treatment temperature. Overall, false heartwood did not demonstrate a substantial impact on the evaluated properties, and its interaction with thermal modification was negligible. These findings suggest that false heartwood primarily represents an aesthetic limitation rather than a structural one, and its presence should not preclude the use of beech wood in applications where visual appearance is not critical.

INTRODUCTION

European beech (*Fagus sylvatica* L.) is a key deciduous tree species for Central European and plays an increasingly important role in forest management and wood processing industry. Although its current proportion in forest stands is relatively modest, future changes in species composition, particularly the expected decline of spruce due to climate-related stress, are likely to lead to a gradual increase in the share of beech. This shift will further enhance the importance of beech wood as a raw material and intensify the need for its efficient utilization.

Despite its favourable mechanical properties and wide applicability, the utilization of beech wood is limited by several inherent drawbacks. One of the most significant defects is the occurrence of false heartwood, which negatively affects both the aesthetic and technological quality of the material and is frequently encountered in mature beech trees. The presence of false heartwood often reduces the suitability of beech wood for high-value products and represents a major challenge for the wood-processing industry. In addition, beech wood exhibits relatively low natural durability and limited resistance to weathering and biotic degradation, which further restricts its use, especially in exterior applications (Račko and Čunderlík 2006).

Thermal modification has emerged as an effective method for improving selected properties of wood, particularly its dimensional stability and resistance to biological agents, without the use of chemical preservatives. Heat treatment alters the chemical composition of wood, leading to changes in its physical and mechanical properties (Esteves and Pereira 2009, ITA 2003, Sandberg et al. 2017, Gašparík et al. 2024). However, these changes may be influenced by wood structure and defects, such as false

heartwood, which can modify the response of wood to thermal treatment. A comprehensive understanding of how false heartwood interacts with thermal modification is therefore essential for optimizing the use of beech wood in practice (Hansmann et al. 2009).

The issue of false heartwood in beech remains topical, as demonstrated by Goncz et al. (2018) or Dzurenda et al. (2023). In this study we deal with an effect of thermal modification on mechanical properties, namely compressive strength, on physical properties, namely wood density, and of course, an impact of such treatment on moisture content of beech wood.

MATERIALS AND METHODS

Beech (*Fagus sylvatica* L.) boards containing false heartwood were used for the preparation of test specimens. From these boards, clear specimens with dimensions of 20 mm × 20 mm × 30 mm (radial × tangential × longitudinal directions) were carefully machined. In addition, specimens free of false heartwood were prepared from sound sapwood to enable comparison.

The prepared specimens were divided into three experimental groups. The first group served as the untreated reference (control) and was not subjected to thermal modification. The second group was thermally treated at a temperature of 160 °C, while the third group was exposed to a higher treatment temperature of 210 °C (Figure 1). The thermal modification process was carried out according to the principles of Finnish thermo-wood technology (Viitaniemi et al. 1995).

Prior to mechanical and physical testing, all specimens were conditioned in a climate chamber at a temperature of 20 ± 2 °C and a relative air humidity of 65 ± 5% until they reached equilibrium moisture content (EMC). This conditioning ensured consistent moisture levels across all samples and allowed for a reliable evaluation of the effects of thermal treatment.

The physical and mechanical properties of the wood were subsequently determined. Compressive strength parallel to the grain, wood density, and moisture content were measured in accordance with relevant Czech national standards (ČSN 490103, ČSN 490108, ČSN 49 0110). Density was calculated based on the weight of mass for obtained EMC and corresponding volume, while moisture content was determined using the standard gravimetric method. These measurements enabled the assessment of the influence of thermal treatment on the structural performance and physical characteristics of beech wood, particularly in relation to the presence of false heartwood.

Figure 1: The thermally treated test specimens of beech wood with false heartwood (from the left to the right – reference, 160 °C, 210 °C)

RESULTS AND DISCUSSION

The results for wood density, with respect to the false heartwood occurrence and the degree of heat treatment, are presented in Table 1. The specimens with false heartwood reached significantly higher density, in contrast to the samples free of heartwood. Thermal modification decreased the value of wood density for samples featuring occurrence of false heartwood. This is in accordance with results obtained for wood density of birch (*Betula pendula*) wood in study of Borůvka et al. (2019). For the samples without heartwood, there was not statistically significant difference between the reference samples and 1st degree of thermal modification. However, the last degree of the treatment also led to the decrease in density (Figure 2). The samples exhibited relatively low density variability.

Table 1: Basic statistics for density (kg/m^3) of heat-treated wood with and without false heartwood

Heartwood	Treatment	Mean	Min.	Max.	SD	CV
Present	REF	711	650	764	28	3.9
	160 ºC	693	609	789	35	5.0
	210 ºC	654	573	728	34	5.1
Absent	REF	662	590	735	35	5.3
	160 ºC	663	597	770	38	5.7
	210 ºC	621	532	715	46	7.4

SD – standard deviation, CV – coefficient of variation

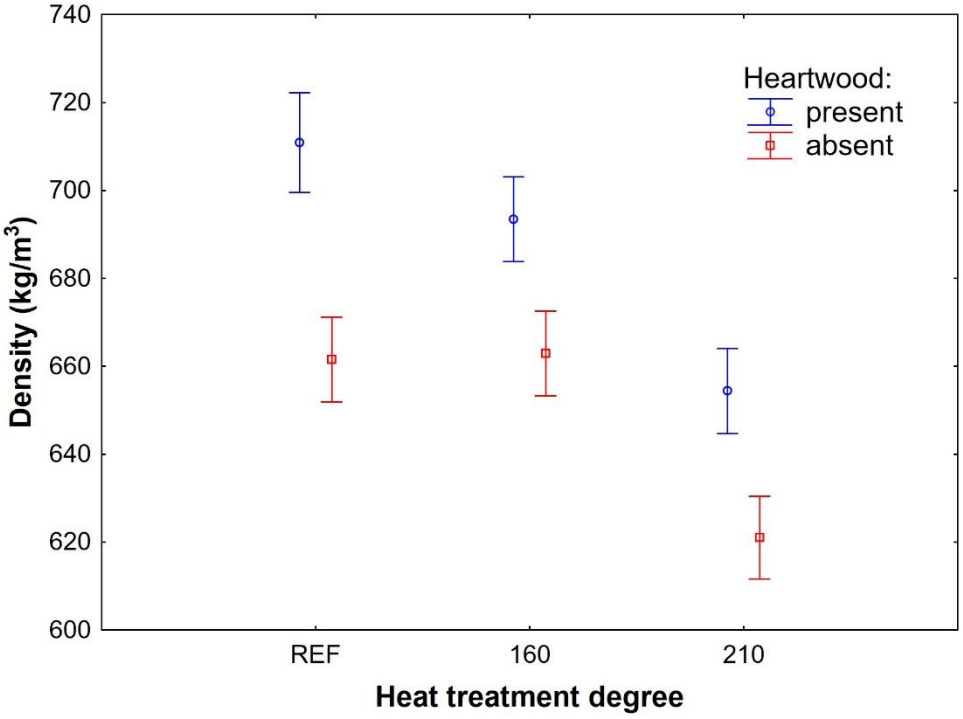

Figure 2: Wood density comparison of heat-treated beech wood with and without false heartwood

In the case of compressive strength, there is almost no difference between specimens with- and without false heartwood. The heat treatment resulted only in slight decrease in strength for both groups (Table 2 and Figure 3) and the samples are so comparable in terms of this property. The impact of higher temperatures is particularly evident, as the positive effect of lower EMC cannot overcome the destructive changes of the key chemical components in the cell walls (Borůvka et al. 2018, Sandberg et al. 2017, Esteves and Pereira 2009, ITA 2003).

Table 2: Basic statistics for compressive strength (MPa) of heat-treated wood with and without false heartwood

Heartwood	Treatment	Mean	Min.	Max.	SD	CV
Present	REF	57.3	47.4	66.9	4.8	8.4
	160	54.9	43.9	65.1	5.1	9.2
	210	53.3	31.1	64.2	6.9	12.9
Absent	REF	54.3	38.1	65.2	5.4	9.9
	160	55.2	38.4	64.0	5.6	10.2
	210	52.6	23.8	64.5	7.4	14.0

SD – standard deviation, CV – coefficient of variation

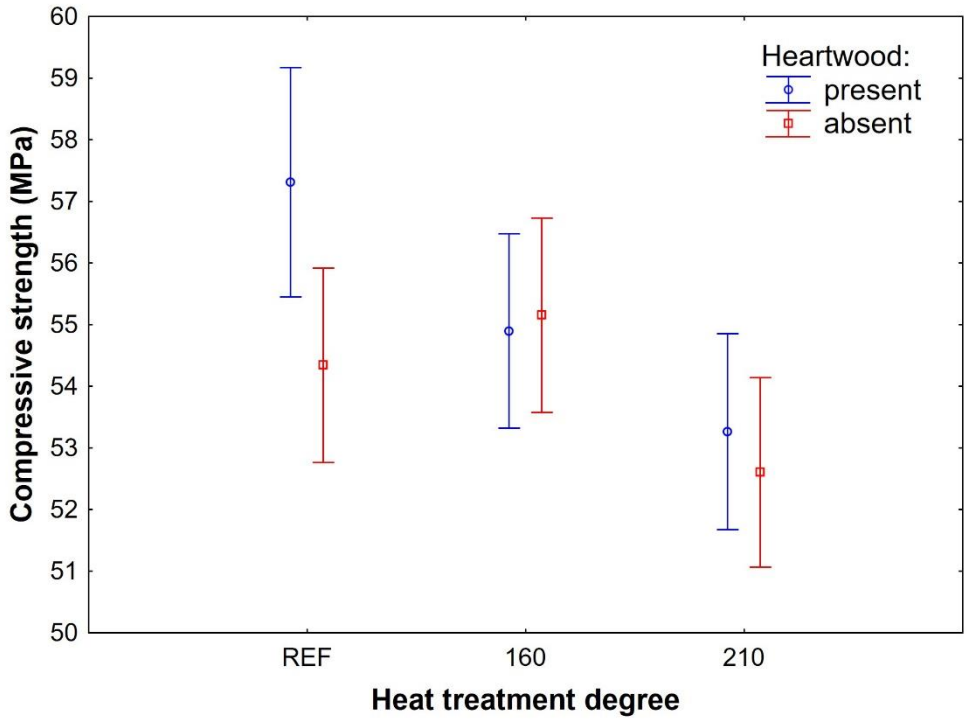

Figure 3: Compressive strength comparison of heat-treated beech wood with and without false heartwood

In terms of moisture content, especially the second degree of the thermal modification caused decrease in EMC. Thermal modification undoubtedly affects hygroscopic nature of wood, as reported by many authors (Borůvka et al. 2019, ITA 2003). As for the false heartwood presence, no clear effect on this characteristic has been confirmed. Heat treatment also led to a reduction in equilibrium moisture content. The first stage of treatment reduced the equilibrium moisture content in heartwood samples by 36.4% and in samples without heartwood by 31.4% compared to the reference samples. The second stage of treatment resulted in a reduction in equilibrium moisture content of 58.2% for samples with heartwood and 54% for samples without heartwood compared to the reference samples. Similar trend, in decreasing equilibrium moisture content with increasing temperature of the treatment, was reported for beech wood by Borůvka et al. (2018).

CONCLUSIONS

Based on the results, we can conclude that false heartwood does not have any serious impact on wood properties, and also the effect of the thermal modification is similar for both groups. With the increasing temperature the tested properties decreased. The occurrence of false heartwood is so more aesthetical issue, and there is no reason to exclude such wood from applications where the surface appearance is not critical.

REFERENCES

Borůvka V, Dudík R, Zeidler A, Holeček T (2019). Influence of site conditions and quality of birch wood on its properties and utilization after heat treatment. Part I—Elastic and strength properties, relationship to water and dimensional stability. Forests, 10(2), 189. https://doi.org/10.3390/f10020189

Borůvka V, Zeidler A, Holeček T, Dudík R (2018). Elastic and strength properties of heat-treated beech and birch wood. Forests, 9(4), 197. https://doi.org/10.3390/f9040197

ČSN 490110 (1980) Drevo. Medza pevnosti v tlaku v smere vlákien. Vydavatelství úřadu pro normalizaci a měření: Prague, Czech Republic. (In Czech)

ČSN 490103 (1979) Drevo. Zisťovanie vlhkosti pri fyzikálnych a mechanických skúškach. Vydavatelství úřadu pro normalizaci a měření: Prague, Czech Republic. (In Czech)

ČSN 490108 (1993) Drevo. Zisťovanie hustoty. Český normalizační institut: Prague, Czech Republic. (In Czech)

Dzurenda L, Dudiak M, Kučerová V (2023) Differences in Some Physical and Chemical Properties of Beechwood with False Heartwood, Mature Wood and Sapwood. Forests, 14, 1123. https://doi.org/10.3390/f14061123

Esteves B M, Pereira H M (2009) Wood modification by heat treatment: a review. BioRes. 4(1), 370-404.

Gašparík M, Zeidler A, Výbohová E, Kačíková D, Kačík F (2024). Chemical changes of polysaccharides in heat-treated European beech wood. J Wood Sci, 70(1), 38. https://doi.org/10.1186/s10086-024-02151-3

Goncz B, Divos F, Bejo L (2018) Detecting the presence of red heart in beech (Fagus sylvatica) using electrical voltage and resistance measurements. Eur J Wood Prod 76, 679–686. https://doi.org/10.1007/s00107-017-1225-4

Hansmann C, Stingl R, Teischinger A (2009). Inquiry in beech wood processing industry concerning red heartwood. Wood Res, 54(3), 1-12.

ITA (2003) Thermowood Handbook, International Thermowood Association, Helsinki, Finland.

Račko V, Čunderlík I (2006) Qualitative and quantitative evaluation of false heartwood in beech logs of various age and qualitative structure. Wood Res, 51(3), 1-10.

Sandberg D, Kutnar A, Mantanis G (2017). Wood modification technologies-a review. Iforest, 10(6), 895. https://doi.org/10.3832/ifor2380-010

Viitaniemi P, Ranta-Maunus A, Jämsä S, Ek P (1995) Method for Processing of Wood at Elevated Temperatures. Patent EP-0759137 VTT, 11 May 1995.

Finite element analysis of a bedframe made from underutilized hardwood species

Ádám Plangár[1], Sára Horváth[1], József Garab[1*]

[1] University of Sopron, Faculty of Wood Engineering and Creative Industries. Bajcsy-Zs. Str. 4, Sopron, Hungary, 9400.

E-mail: LTNEVU@uni-sopron.hu; HorvatSara25@student.uni-sopron.hu;garab.jozsef@uni-sopron.hu

Keywords: furniture; bed; bedframe; linear static structural analysis; grey poplar, Turkey oak.

ABSTRACT

The efficient usage of underutilized hardwood species is an important challenge in the Hungarian wood industry. Species such as grey poplar (*Populus* × *canescens*) and Turkey oak (*Quercus cerris*) are widely available but remain insufficiently explored in structural furniture applications. The aim of this study is to evaluate the mechanical behaviour of a wooden bedframe manufactured from these species using finite element analysis. A three-dimensional CAD model of a single bedframe was developed and analysed under representative service loading conditions based on MSZ EN 1725:2023. Two load cases were considered: distributed loading on the lying surface and localized edge loading. The evaluation focused on maximum deformation, longitudinal stress distribution, and the maximum longitudinal stresses compared to the bending strength. The results show that all materials provide adequate performance under distributed loading conditions. However, under edge loading, significant differences were observed. Grey poplar approaches its bending strength limit, indicating a higher risk of failure. Norway spruce (*Picea abies*) shows moderate utilization, while Turkey oak demonstrates excellent performance. The study confirms that finite element analysis is an effective tool for preliminary material evaluation and supports the engineering application of underutilized hardwood species in furniture design.

INTRODUCTION

The efficient utilization of less-used hardwood species has become an increasingly important issue in European forestry and wood processing. Several locally available hardwoods possess acceptable physical and mechanical properties. However, their industrial use is often limited to low value-added applications (Borovics et al. 2023). In furniture manufacturing, commonly established commercial species still dominate the material selection process, while less-used species such as grey poplar (*Populus* × *canescens*) and Turkey oak (*Quercus cerris*) remain insufficiently explored from an engineering point of view. In many cases, the restricted application of these materials is not caused by the complete lack of structural potential, but rather by the limited amount of available design-oriented performance data.

Furniture products are required to withstand repeated service loads during everyday use, therefore adequate stiffness, load-bearing capacity and structural safety are essential design criteria. Among common wooden furniture structures, bedframes represent a particularly sensitive category because the applied human body load is transferred through relatively slender longitudinal members, cross slats and localized corner connections (Majewski 2019). Consequently, the mechanical suitability of a newly proposed wood species cannot be judged solely on the basis of appearance, density or manufacturability, but requires preliminary structural verification.

Full-scale experimental testing of furniture prototypes is often costly and time-consuming, especially in the early stages of product development. For this reason, finite element analysis has become a widely used engineering tool in furniture research and virtual prototyping. Numerical modelling makes it possible to estimate the global deformation behaviour of the structure, identify local stress concentration zones and reveal potentially critical construction details before manufacturing physical specimens (Koç et al. 2011, Réh et al. 2019, Uysal et al. 2025). This approach offers an efficient way to compare the expected structural performance of alternative material solutions under identical loading conditions.

The aim of the present study is to evaluate the structural behaviour of a wooden bedframe manufactured from underutilized hardwood species by means of linear static finite element analysis. A CAD-based virtual model of the furniture frame was developed and subjected to representative service loading conditions corresponding to normal use. The numerical investigation focuses on total deformation, normal stress distribution in the longitudinal direction, and comparison the maximum longitudinal stresses to the bending strength of the wood species. The investigations support to assess the engineering applicability of the selected hardwood materials in bedframe construction.

MATERIALS AND METHODS

The CAD model of the bed frame under study was designed and analyzed by the finite element method by using Ansys software package (licensed product is Ansys® Academic Research Mechanical, Release 25 R2). The height, width, and thickness of the single bedframe is 1900 mm, 800mm, 70 mm respectively.

Static structural analysis was performed in the Workbench module after the geometry creation in the Discovery module. Orthotropic material models were applied for the slats, therefore local coordinate systems were implemented according to the anatomical directions of the wood. To simplify the model, the frame was modelled as an isotropic material. The engineering constants were corresponding to the longitudinal direction of the wood.

Table 1 summarizes the material properties taken from literature. Depending on the case, grey poplar or Turkey oak was used, with Norway spruce (*Picea abies*) serving as the traditional control wood material. Hence the full set of orthotropic elastic constants are not determined yet for grey poplar and Turkey oak, the full set of orthotropic elastic constants were derived from MOE parallel to the grain grain (E_0) and from the shear modulus for planes parallel to grain (G_0) according to Patlakas et al. (2019). The MOE perpendicular to grain E_{90} was considered instead as a constant fraction of E_0 (E_0/E_{90}=30) and the rolling shear modulus G_{90} as a constant fraction of G_0 (G_0/G_{90}=10). The tree Poisson's ratios were considered equal to 0.35. The engineering constants were applied based from the works of the researchers of the University of Sopron (Altaher Omer Ahmed et al. 2023, Govina 2025, Fabrice 2026).

Table 1: Material properties used in the finite element analysis

Wood Species	Density [g/cm^3]	E_L [MPa]	E_R [MPa]	E_T [MPa]	G_{LR} [MPa]	G_{LT} [MPa]	G_{RT} [MPa]	ν_{LR} [-]	ν_{LT} [-]	ν_{RT} [-]	Bending Strength [MPa]
Norway spruce (C24[a])	0.35	11 000	367	367	690	690	69	0.35	0.35	0.35	24
Grey poplar (C16[a])	0.31	8000	267	267	500	500	50	0.35	0.35	0.35	16
Turkey oak[b]	0.65	8929	298	298	500	500	50	0.35	0.35	0.35	104

[a] Corresponding strength grades according to MSZ EN 338 based on NDT measurements (Altaher Omer Ahmed et al. 2023; Fabrice 2026); [b] measured values (Govina 2025). The minimum value is applied from the measurements. Other engineering constants values are according to the nearest lower strength grade based on E_0 according to MSZ EN 338

The geometry of the bedframe was simplified. The joints were not modelled because the global structural response was the goal of the study. The contacts were modeled as bonded contacts. The mesh consisted of 84947 quad dominated quadratic elements with 10 mm of the element size. The loads were taken from the MSZ EN 1725:2023. The first load case (LC 1) was to investigate the lying area. Hence a static testing is done by 200 diameter cylindrical plate, the 1400 N load was applied on four bed slats for simulate the load distribution (Figure 1a). The second load case (LC 2) was to investigate the edge load. Although the load should be applied on the edge of the siderail according to the standard, the siderail or the edge of the bed was not modelled. Therefore, for comparison purposes one of the longer bedframe components was investigated. Two 1200 N force loads were applied to the one side of the bedframe in the middle of the side frame. The distance between the two load vectors is 600 mm according to the standard (Figure 1b).

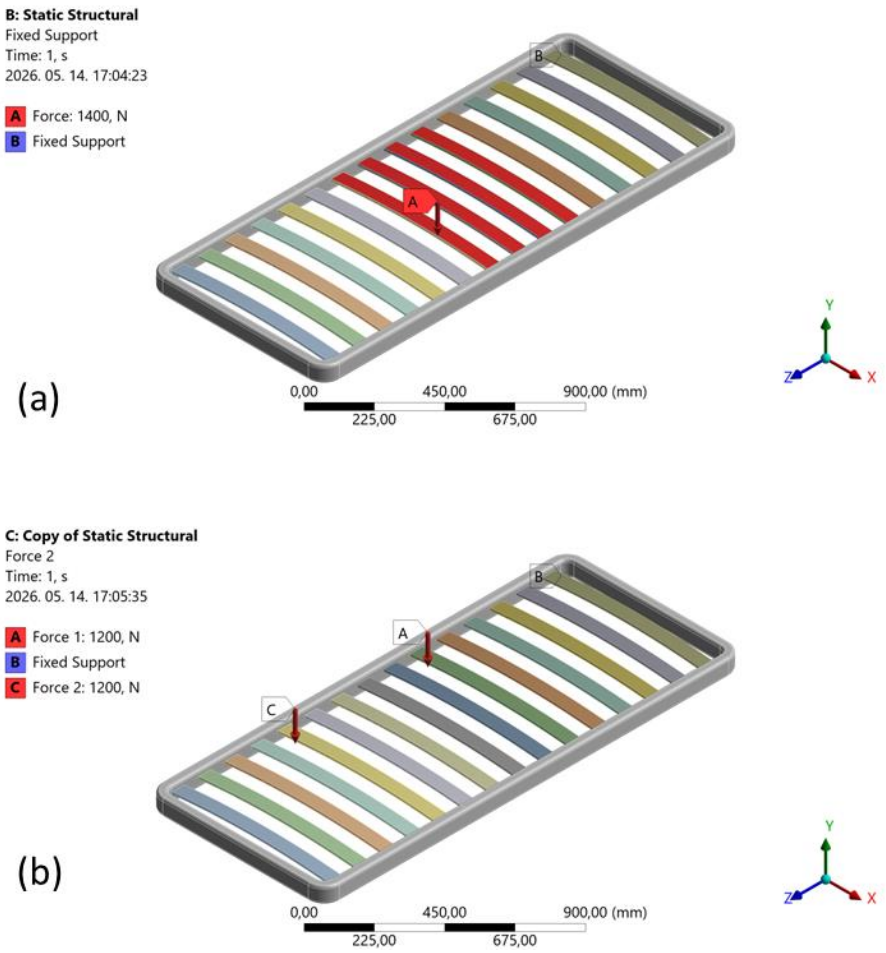

Figure 1: FE model of the load cases: (a) LC1: vertical load on the lying area; (b) LC2: vertical load on the edge

RESULTS AND DISCUSSION

The main interests of this study were the deflection of the slats (LC1 load case) and the edge (LC2 load case). The maximum displacement and the maximum longitudinal stresses are presented. The deflection of the bedframe made from grey poplar is presented on the Figure 2. Furthermore, the bending utilization was calculated as the ratio of the maximum longitudinal normal stress to the bending strength of the material ($|\sigma_L_{max}|/f_m$) which was presented in percentage (Table 2). Under LC1, all investigated materials exhibit low stress levels and moderate deflections, indicating sufficient stiffness for typical service conditions. In contrast, LC2 represents a more critical loading scenario, where significantly higher stress and deformation values are observed. However, it should be noted that the LC2 scenario is only a theoretical load case because the load should be applied onto the side rail of the bed. Nevertheless, for material response comparison reason was useful to perform the virtual testing.

Grey poplar approaches the bending strength limit under edge loading, reaching a utilization of 93%, which indicates a high risk of failure. Norway spruce shows moderate utilization, while Turkey oak remains significantly below critical levels. The outcome suggest that grey poplar may be suitable for applications with design modifications (e.g.: increased cross section, or reduced span, application of supports) when severe load case is simulated, while Turkey oak provides a robust alternative with a hight safety. For comparison reasons it should be noted that the bending strength values were taken from MSZ EN 338 standard, which are the characteristics values. But the bending strength values of the Turkey oak were taken from the experimental measurements (Govina 2025). Therefore, the characteristics bending strength of Turkey may be different. Furthermore, in design point of view, the density of the Turkey oak could influence another issue with the weight of the furniture structure made by Turkey oak. Which should be considered during the design process.

Table 2: Results of the numerical simulation

Wood Species	Load case	Maximum dispacement [mm]	Maximum longitudinal stress [MPa]	Bending utilization [%]
Grey poplar	LC1	2.25	4.79	29.94
Grey poplar	LC2	7.18	14.92	93.25
Turkey oak	LC1	2.03	4.80	4.61
Turkey oak	LC2	6.43	14.93	14.36
Norway spruce	LC1	1.63	4.78	19.92
Norway spruce	LC2	5.21	14.92	62.16

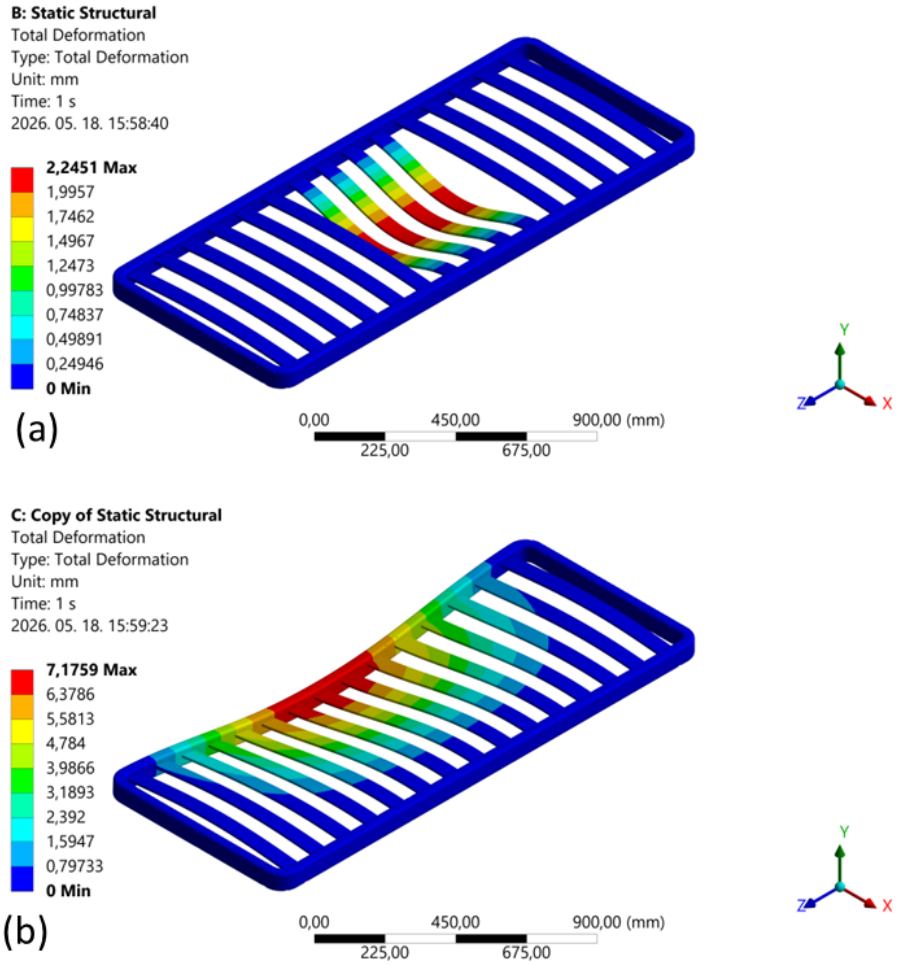

Figure 2: Deflection results for the bedframe made of grey poplar: (a) LC1: vertical load on the lying area; (b) LC2: vertical load on the edge

CONCLUSIONS

The study demonstrates that finite element analysis is an effective tool for the preliminary evaluation of alternative wood species in furniture design. The application of standardized loading conditions provides a consistent framework for virtual testing and comparison of different material solutions. The performance of the bedframe structure made by grey poplar and Turkey oak is comparable to the performance of the structure made by Norway spruce according to the simulation of load cases based on MSZ EN 1785:2023. Especially the distributed loading conditions (LC1) show promising results. For complete analysis, the siderails should have been incorporated into the FE model, therefore the results of LC2 are only for comparative reasons. The results confirms that underutilized hardwood species have potential for furniture applications. While grey poplar requires careful structural design adjustments, Turkey oak appears to be a promising alternative material comparing to Norway spruce. The findings support the use of finite element analysis as a decision-support tool in the early stages of furniture development.

REFERENCES

Altaher Omer Ahmed, A., Garab, J., Horváth-Szováti, E., Kozelka, J., & Bejó, L. (2023). The bending properties of hybrid cross-laminated timber (CLT) using various species combinations. *Materials*, *16*(22), 7153.

Borovics, A., Mertl, T., Király, É., & Kottek, P. (2023). Estimation of the overmature wood stock and the projection of the maximum wood mobilization potential up to 2100 in Hungary. *Forests*, *14*(8), 1516. https://doi.org/10.3390/f14081516

Fabrice, S. (2026). CLT made of Hungarian indigenous poplar material (Master's thesis, University of Sopron).

Govina, J. K. (2025). Comparative study of wood properties for *Quercus cerris* L. (Turkey oak) from different sites in Hungary (Doctoral dissertation, University of Sopron).

Koç, K. H., Kizilkaya, K., Erdinler, E. S., & Korkut, D. S. (2011). The use of finite element method in the furniture industry. *African Journal of Business Management*, *5*(3), 855. https://doi.org/10.5897/AJBM10.551

Majewski, A. (2019). Furniture use safety at early design stage. *Annals of Warsaw University of Life Sciences-SGGW. Forestry and Wood Technology*, *108*. https://doi.org/10.5604/01.3001.0013.7686

Hitka, M., Lagaňa, R., Naď, M., Klement, I., & Sydor, M. (2024). Analysis of the lamella dimensions of the bed slat for the bariatric respondent: a modelling approach. *Wood Material Science & Engineering*, *19*(1), 19-26.

Patlakas, P., Brunetti, M., Christovasilis, I., Nocetti, M.,& Pizzo, B. (2019). Structural performance of a novel Interlocking Glued Solid Timber system. Materials and Structures/Materiaux et Constructions, 52(1). https://doi.org/10.1617/s11527-019-1324-2

Réh, R., Krišťák, Ľ., Hitka, M., Langová, N., Joščák, P., & Čambál, M. (2019). Analysis to improve the strength of beds due to the excess weight of users in Slovakia. *Sustainability*, *11*(3), 624. https://doi.org/10.3390/su11030624

Uysal, M., Kuskun, T., Smardzewski, J., Kasal, A., & Haviarova, E. (2025). Use of lower tolerance limits for designing chair frames with round-end mortise and tenon joints. *Wood Material Science & Engineering*, *20*(2), 427-438. https://doi.org/10.1080/17480272.2024.2352801

Comparative Fractographic Analysis of Wood Surfaces Subjected to Static and Dynamic Tensile Loading Using Reflected Light Microscopy

Gábor Orbán[1], Antal Kánnár[1]

[1] University of Sopron, Institute of Wood Architecture Bajcsy-Zs. Str. 4, Sopron, Hungary, 9400.

E-mail: orbangabor@phd.uni-sopron.hu; kannar.antal@uni-sopron.hu

Keywords: reflected light microscopy, dynamic- and static tensile.

ABSTRACT

This research investigates the fracture mechanisms of wood under longitudinal tensile stress, focusing on the microstructural differences between static and dynamic loading conditions. The primary objective is to determine how the rate of loading influences the failure of the wood's anisotropic structure at the cellular level. Using a Nikon Eclipse 80i research microscope equipped with epi-fluorescence and reflected light illumination, we analyze the morphological features of fracture surfaces and the specific characteristics of crack propagation. To overcome the limitations of the shallow depth of field at high magnifications, Extended Depth of Field (EDF) processing via Z-stacking was employed to generate high-resolution, all-in-focus images of the complex fracture topography. The working hypothesis suggests that under static loading, viscoelastic relaxation allows for gradual delamination of the cell wall layers and significant longitudinal microfibril pull-out, leading to a more fibrous and heterogeneous fracture appearance. Conversely, dynamic impacts are expected to trigger a brittle response, where rapid stress accumulation causes the crack to propagate in a transcrystalline manner with minimal plastic deformation. This study aims to clarify the role of interfacial cohesion between the cellulose framework and the lignin matrix in energy dissipation processes. The findings are expected to provide essential data for the accurate numerical modeling of wood-based structures under various dynamic influences, ultimately facilitating more reliable engineering design for extreme mechanical impacts.

INTRODUCTION

Wood has complex and varied mechanical properties. Geoffrey (2016) summarized that light and electron microscopy play key roles in understanding wood's structure and biodegradation. Light microscopy is mainly used for analyzing wood's cellular structure and chemistry, while electron microscopy provides detailed information at higher resolution across various levels.

Sakagami et al (2009) examined microcracks in Acacia hybrid (*Acacia mangium* × *Acacia auriculiformis*) and *Melia azedarach* using confocal laser scanning microscopy. In the Acacia hybrid, many microcracks developed between wood fibers and ray parenchyma, extending toward the pith and bark, and some closed during drying. In Melia azedarach, few microcracks formed, which also closed later. These findings indicate differences in wood structure create weak points vulnerable to checking.

Bariska (1996) observed two types of fractures in parallel tensile tests:

Transverse fractures run parallel to the cell axis, following intercellular bonds and appearing randomly. These fractures grow and converge together, forming a fracture line and zones of high stress. Micro-cracks only develop where stress exceeds local strength, spreading stress peaks and causing higher loads on remaining tissues, leading to random initial failures in the specimen.

Tensile failure starts with separation between cells and then fractures the cell wall. The occurrence of these fractures varies by wood species and specific gravity. Acacia (*Robinia Pseudoacacia*), having lower density, exhibits a brittle fracture, while Rapanea (*Rapanea melanophloeos*), with higher density, shows a fibrous fracture.

Kánnár (2014) found that low-density rubberwood (*Hevea brasiliensis*) fractures primarily occur through thin cell walls, especially at the S1/S2 interface. Higher density species like red oak (Quercus rubra) break with a less sharp fracture in tension, showing protruding fibers from the surface. Untwisting behavior is observed in hickory (Carya) specimens loaded in tension along the grain. Very little cell wall elongation was found in red oak.

The fracture properties of wood are greatly affected by its uneven microstructure. Understanding how structure relates to function in terms of damage and fracture requires detailed examination.
Divos and Tanaka (2005) measured static and dynamic modulus of elasticity (MOE) of spruce (P*icea abies*) lumber under various conditions. The characteristic time, as a typical MOE determination time, was introduced. Shorter times led to higher MOE values. They found evidence of creep on a short timescale.
Stanzl-Tschegg et al. (2005) experimented with spruce (*Picea abies*) and beech (*Fagus sylvatica*) wood using micro-wedge splitting specimens in an Environmental Scanning Electron Microscope (ESEM) chamber. This setup enabled stable crack growth and simultaneous observation of crack progression while recording load-displacement curves. The experiments showed that specific fracture energies are not a straightforward addition of shear and tensile components, but an interaction between the two modes.
Ümit (2017) studied how loading rates influence the micro-mechanical properties of oak wood (*Quercus petraea*). Tests measured bending strength, modulus of elasticity in bending, compression strength parallel to the grain, and tensile strength parallel to the grain using small samples. Three loading rates were tested, showing that loading rates significantly affected the modulus of elasticity, tensile strength, and compression strength, but not bending strength.
Kucera and Bariska (1982) studied structural changes in spruce (*Picea abies*) and aspen wood (*Popolus tremula*) under axial compression using a scanning electron microscope. Macroscopic model experiments with paper tube-shaped samples were also conducted to represent fibriform xylem cells. The findings reveal common fracture patterns typical of wood and specific patterns for each species. General wood characteristics appear at the cellular level, while species-specific features are seen in the growth rings, influenced by tissue composition and arrangement. The model experiments indicate that cell geometry partly explains the failure patterns of xylem cells.

MATERIALS AND METHODS

Microstructural Analysis

The morphological evaluation of the fracture surfaces was performed using a Nikon Eclipse 80i advanced research microscope (Nikon Instruments Inc., Tokyo, Japan). To capture the complex, three-dimensional topography of the wood splinters, the system was configured with a 100W halogen lamp, for optimized surface visualization. Observations were conducted using Nikon CFI60 infinity optical system objectives, specifically a Plan Fluor 4x (N.A. 0.13, W.D. 17.1 mm), which provided a suitable balance between field of view and resolution for structural analysis.

Image Acquisition and EDF Reconstruction

Due to the significant vertical irregularities of the fracture surfaces (exceeding the native depth of field of the optics), an Extended Depth of Field (EDF) technique was employed. Image acquisition was performed using a Nikon Digital Sight DS-Fi3 digital camera controlled by NIS-Elements software. For each representative area, a Z-stack of 200-500 individual frames was acquired with a step size of 2-5 µm along the optical axis. The final all-in-focus micrographs were reconstructed using the standard EDF module of the imaging software, ensuring that both the protruding fiber bundles and the deeper crack initiation sites remained sharp for qualitative fractographic analysis

Tested tree species and their anatomical characteristics

Ring-porous hardwood species: Pedunculate oak (*Quercus robur*), Black locust (*Robinia pseudoacacia*), Flowering ash (*Fraxinus ornus*).
Diffuse-porous hardwood species: Common hornbeam (*Carpinus betulus*), White poplar (*Populus alba*).
The specimens were optimized for tensile loading in the grain direction. Before fracture surface analysis, the specimens were conditioned (e.g. 20°C, 65% relative humidity) to ensure comparable moisture content, avoiding brittle or ductile fracture modifications caused by moisture.

RESULTS AND DISCUSSION

The ring-porous structure and high density of black locust (*Robinia pseudoacacia*) resulted in specific forms of failure.

Figure 1 shows a massive, continuous, whitish zone of destruction. Here, the fibers have not simply separated, but the cell walls have suddenly ruptured. In the large bright area on the left, a strong fibrillation can be observed. Due to the breakdown of the cell walls into layers, the surface becomes "cotton-like", which is direct evidence of high-speed energy absorption (Figure 1).

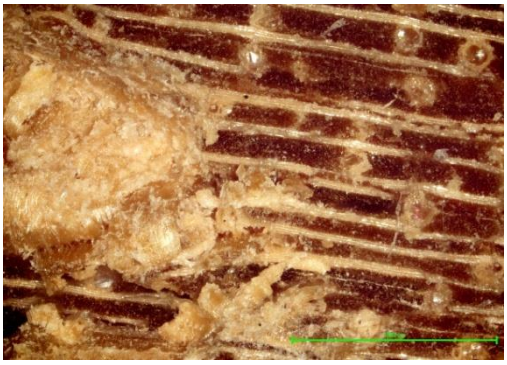

Figure 1: Colored light microscopic picture of Robinia pseudoacacia dynamic fracture surface

Figure 2: Colored light microscopic picture of Robinia pseudoacacia static fracture surface

In Figure 2 the fracture line follows the fibers. The failure is characterized by brittle shear fracture parallel to the fibers, and in some places, peeling of the secondary cell wall can be observed. The outlines of the large earlywood vessels (pores) and the outline of the surrounding tissue structure remains relatively sharp. The fracture often follows these vessels, but does not completely crush them (Figure 2).

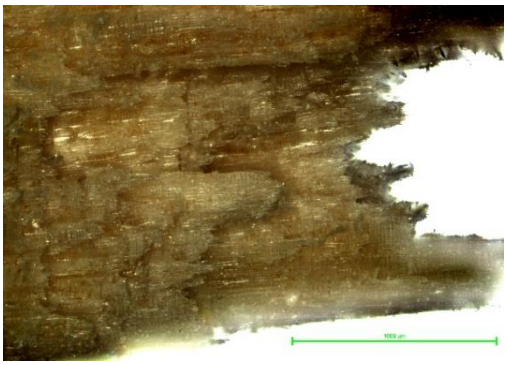

Figure 3: Colored light microscopic picture of Carpinus betulus dynamic fracture surface

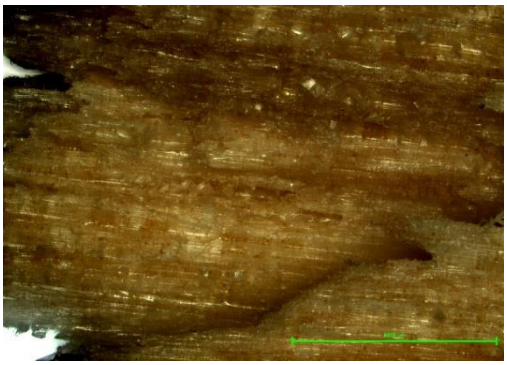

Figure 4: Colored light microscopic picture of Carpinus betulus static fracture surface

Despite the high density of the hornbeam, under dynamic loading, the tissue elements shatter because the sudden burst of energy cannot be distributed evenly along the fibers. In Figure. 3. the fracture surface is more fleecy, indicating that the cell walls themselves have been damaged (intracellular fracture), not just slipped past each other (Figure 3).

Figure. 4. shows that the fracture occurred along relatively large, continuous fiber blocks. The failure is of a brittle shear nature. The slow loading allowed the dense tissue of hornbeam to separate in a controlled manner. There is little microscopic debris on the surface; the fibers did not crumble, but rather broke away from the surrounding tissue leaving a clean surface (Figure 4).

Under dynamic loading, the tension difference between the large vessels characteristic of ash and the dense fiber tissue is suddenly released. In Figure 5. white, cottony, heavily damaged zones dominate. This is a sign of high-speed energy absorption: the fibers do not only separate, but also break down into layers of cell walls (delamination), resulting in a fleecy texture with a high specific surface area. The

surroundings of the large earlywood vessels (the dark, wide cavities) almost “exploded”. The fracture line did not bypass them, but the sudden tension caused the vessel walls and surrounding parenchyma cells to shatter into fragments (Figure 5).

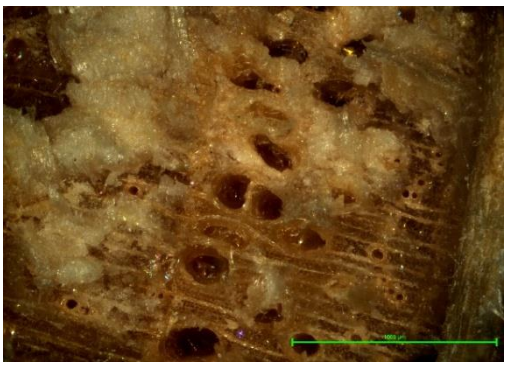

Figure 5: Colored light microscopic picture of Fraxinus ornus dynamic fracture surface

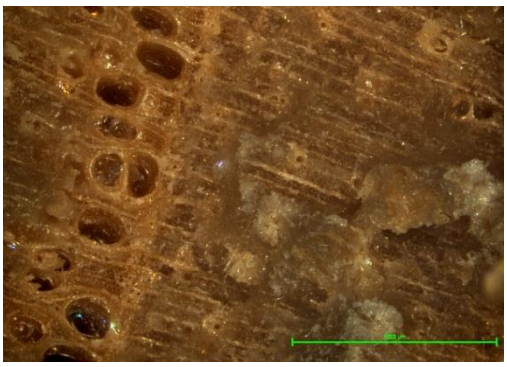

Figure 6: Colored light microscopic picture of Fraxinus ornus static fracture surface

In Figure 6, longitudinal, orderly separation of the fibers is visible. The surface is less fleecy, showing a cleaner, grooved morphology. The fibers stuck together in bundles, the rupture occurred mainly along the intercellular space.

Figure 7: Colored light microscopic picture of Quercus robur dynamic fracture surface

Figure 8: Colored light microscopic picture of Quercus robur static fracture surface

Despite the high density of oak, the cell walls separate under the dynamic impact, resulting in the yellowish-whitish, fuzzy surface seen in Figure 7. The large vessels of the earlywood (the darker cavities at the edges) not only separated, but also disintegrated along with the surrounding tissue. The sudden transfer of energy also shattered the walls of the vessels (Figure 7).
In Figure. 8. the walls of the vessels on the left remain sharp. The static fracture line runs along these, but does not crush their internal structure. The failure process is characterized by brittle fracture through the cell wall and secondary cell wall separation. The destruction is localized, the fracture planes are well defined, and the usually ubiquitous microscopic debris is more-or-less absent.
Figure 9 exhibits complete and widespread destruction. The entire field is covered with raised fibers and cell wall fragments. There are no intact areas; the sudden high energy almost shattered the tissue structure. Strong micro-fibrillation is visible. Not only have the fibers separated from each other, but the cell walls themselves have also separated longitudinally and transversely, creating a fleecy, cotton-like texture. This is a sign of high-speed energy absorption (Figure 9).
Figure 10 shows a more localized fracture. A distinct, continuous group of fibers, which has separated, is clearly visible, almost forming a single block. In the background, the tissue structure (pores) remains relatively intact and recognizable; brittle shear fracture is observed here. It is characterized by longer, more fragmented fiber slippages. The fibers have had time to separate at the weaker connections (midplate) (Figure 10).

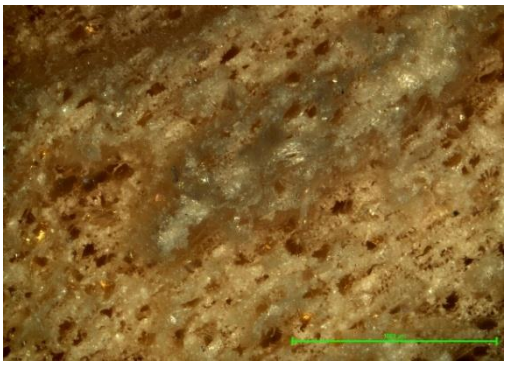

Figure 9: Colored light microscopic picture of Populus alba dynamic fracture surface

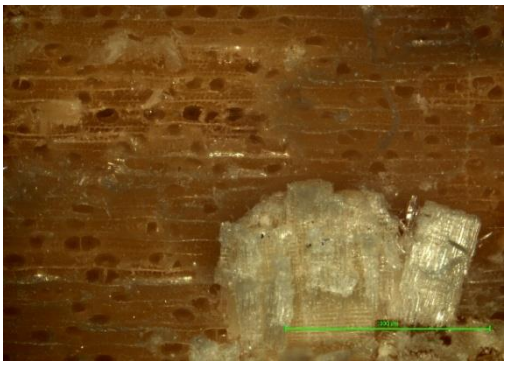

Figure 10: Colored light microscopic picture of Populus alba static fracture surface

CONCLUSIONS

Under dynamic loading, the material is unable to dissipate the stress along the natural tissue boundaries due to the sudden burst of energy. This leads to extreme fibrillation (fibrosis). The cell walls are destroyed, which results in a cotton-like, light, fleecy surface on the images. This process consumes a lot of surface energy. Under static conditions, the slow loading allows the fibers to slide. The fracture surface is more orderly, more fibrous, and the fiber bundles often pull out intact (fiber pull-out), leaving less microscopic debris behind.

Tissue integrity and the role of pores in ring-porous species (robinia, ash, oak), the wide vessels of the earlywood are critical points. In the dynamic case, these almost tend to explode, while in the static case, the crack often only touches or avoids them. In diffuse-porous species (poplar, hornbeam), due to the more homogeneous structure, the static fracture line is straighter, while the dynamic effect is more chaotic, causing widespread destruction throughout the entire tissue. In case of dynamic failure, some wood parts partially failed with brittle shear fracture, while the delamination of the secondary cell wall or fiber pullout was observed in other places on the fracture surface.

REFERENCES

Bariska, M. (1996). Fracture mechanics and wood anatomy. New Zealand Forest Research Institute, 429 p.

Divos, F., Tanaka, T. (2005). Relation Between Static and Dynamic Modulus of Elasticity of Wood. Acta Silvatica & Lignaria Hungarica. 1. 105-110. https://doi.org/10.37045/aslh-2005-0009

Geoffrey, D. (2016). Chapter 15 - Microscope Techniques for Understanding Wood Cell Structure and Biodegradation. Secondary Xylem Biology, Origins, Functions, and Applications 309-343 https://doi.org/10.1016/B978-0-12-802185-9.00015-2

Kánnár A. (2014). A faanyag mikro- és makro- tönkremeneteli folyamatai. Szerzői kiadás 2014. 30-36

Kučera, L.J., Bariska, M. (1982). On the fracture morphology in wood. *Wood Sci. Technol.* **16**, 241–259 https://doi.org/10.1007/BF00353147

Sakagami, H., Matsumura, J. & Oda, K. In situ visualization of hardwood microcracks occurring during drying. J Wood Sci 55, 323–328 (2009). https://doi.org/10.1007/s10086-009-1041-5

Stanzl-Tschegg, S. & Frühmann, K. & Tschegg, Elmar. (2005). Fracture and microstructure of wood. 11th International Conference on Fracture 2005, ICF11. 8. 6263-6268.

Ümit, B. (2017). Effect of loading rate on mechanical properties of micro-sized oak wood. Maderas, Cienc. tecnol. vol.19 no.2 Concepción (2017). http://dx.doi.org/10.4067/S0718-221X2017005000014

Clone-Specific Intra-Annual Growth Responses of Poplars Under Contrasting Water Conditions in Spain

Flor Álvarez-Taboada[1*], Carlos Álvarez Cuevas[2], Fernando Castedo Dorado[1]

[1] Universidad de León, DRACONES Research Group, Campus de Ponferrada, 24401, Ponferrada, León, Spain
[2] Garnica Valencia de Don Juan, Valencia de Don Juan, León, 24200, Spain.

E-mail: flor.alvarez@unileon.es; carlos.alvarez@garnica.one; fcasd@unileon.es

Keywords: poplar; growth; water stress; resilience; relative growth reduction index.

ABSTRACT

Understanding how different poplar clones adjust their intra-annual growth to water availability is crucial for optimizing clone selection and plantation management under Mediterranean climate conditions. We analyzed stem diameter growth of four poplar clones ('I-214', 'AF8', 'Beaupré', and 'Raspalje') established in four plantations across the province of León (Spain). One of the sites experiences recurrent water stress, due to a decrease in the water table level and drought conditions. Weekly diameter increments recorded during 2023–2025 were grouped into two growth periods: before and after July 1. The Relative Growth Reduction Index (RGRI)was to quantify the proportion of summer growth relative to early-season growth, and it was used to assess drought sensitivity. Results revealed marked clone- and site-dependent differences in intra-annual growth dynamics. Across non-stressed sites, post-July growth typically represented 80–100% of pre-July increment, indicating sustained summer growth. Clone AF8 was the most sensitive, with RGRI values as low as 3% in 2025, while I-214 maintained higher resilience. Two-way ANOVA and mixed-effects modeling confirmed significant effects of clone ($p < 0.001$), site ($p < 0.001$), year ($p < 0.01$), and their interactions on post-July growth ratios. Post-hoc Tukey and Bonferroni tests identified significant differences between clones and sites, especially under drought stress. These findings demonstrate that genetic variation among clones substantially modulates their intra-annual growth response to hydric stress. Selecting clones with higher mid-season resilience—such as 'I-214' and 'Raspalje'—could improve yield stability of poplar plantations under increasingly dry summer conditions in southern Europe.

INTRODUCTION

Poplar plantations (*Populus spp*.) constitute a fundamental socioeconomic and ecological resource in the temperate and Mediterranean regions of Europe, providing high-quality timber while acting as efficient carbon sinks. However, poplars are characterized by high transpiration rates and marked sensitivity to water availability, making them highly vulnerable to global climate change scenarios. In the Mediterranean Basin, and particularly in areas of the Iberian Peninsula such as the province of León (Spain), the viability of commercial short-rotation coppice (SRC) plantations is strongly constrained by the severity of summer droughts (Cañellas et al. 2012; Oliveira et al. 2020).

Traditionally, the criteria for genetic material selection have been based on evaluations of cumulative annual yield or productivity at the end of the rotation cycle, an approach that obscures the ecophysiological and intra-annual mechanisms that trees deploy to cope with acute water deficits occurring at specific stages of the growing season. Previous research suggests that poplar genotypes exhibit a strong trade-off between potential productivity and drought/water stress tolerance: clones that are exceptionally productive under optimal conditions often experience the most severe declines under water stress (Monclus et al. 2006; Rosso et al. 2023). This differential tolerance is closely linked to underlying physiological and anatomical traits, such as xylem cavitation resistance, stomatal regulation strategy (isohydric versus anisohydric behavior), cellular osmotic adjustment, and water-use efficiency (WUE) (Guo et al. 2010; Viger et al. 2016; Chen et al. 2022; Kojima et al. 2024). Recent genomic association studies have confirmed that traits such as stem diameter under drought conditions are regulated by complex molecular networks and specific transcription factors (such as PtobZIP18) that

coordinate structural growth and hydraulic safety (Jin et al. 2025). Likewise, in response to soil water deficits, contrasting clones adjust biomass allocation (prioritizing root development), induce early stomatal closure, and activate antioxidant defense systems (Tang et al. 2024).

To capture these dynamic responses under field conditions, high-temporal-resolution monitoring through weekly stem diameter measurements provides a direct diagnostic window into cambial kinetics and the phenology of xylogenesis (Michelot et al. 2012; Qian et al. 2024). In seasonally dry environments, fluctuations in intra-annual growth and the precise timing of cambial activity cessation or deceleration accurately reflect pulses of environmental stress (Tamudo et al. 2025). July 1st marks a critical climatic transition in northern Spain, where the coupling of rising temperatures and the depletion of soil water reserves commonly induces severe water stress compared with the wetter spring season.

The main objective of this study was to evaluate the stability of intra-annual growth and water stress resilience of four widely cultivated commercial poplar clones ('I-214', 'AF8', 'Beaupré', and 'Raspalje') grown across an environmental and water-management gradient in León, Spain. Through the formulation of the Relative Growth Reduction Index (RGRI) and the application of advanced linear mixed-effects modeling, this work aims to provide quantitative and operational criteria to improve forest management planning and clonal selection under scenarios of increasing aridity in southern Europe.

MATERIALS AND METHODS

Study Sites and Materials

The research was conducted across four distinct commercial poplar plantations located in the province of León, Spain: Turcia (established in 2014), Villasabariego (2012), Villoria de Órbigo (2015), and Villamañán (2011). The latter experiences recurrent summer water stress related to changes in the water table depth.

Four representative poplar cultivars were monitored within each plantation: 'I-214', 'AF8', 'Beaupré', and 'Raspalje'. High-resolution monitoring was executed from 2023 to 2025 by performing weekly stem diameter increment measurements on representative individuals. To capture structural shifts in intra-annual vegetative kinetics, the raw weekly increments were aggregated into two separate seasonal growth periods: (i) Early-Season Growth: Increments recorded from the onset of spring vegetative activity up to June 30, and (ii) Late-Season (Summer) Growth: Increments accumulated from July 1 onwards until autumn growth cessation.

Data Analysis

The Relative Growth Reduction Index (RGRI) (Equation 1) was proposed and calculated to quantify the proportion of summer growth relative to early-season growth, and it was used to assess drought sensitivity. Lower values generated by this index denote a sharp reduction in late-season growth, functioning as a proxy for high hydric stress sensitivity. Lower values generated by this index denote a sharp reduction in late-season growth, functioning as a proxy for high hydric stress sensitivity.

$$RGRI = \left(\frac{\Delta D_{post\text{-}July}}{\Delta D_{pre\text{-}July}}\right) \times 100 \quad (1)$$

Where $D_{\text{post-July}}$ corresponds to the absolute increase in diameter recorded after July 1st, and $\Delta D_{\text{pre-July}}$ is equivalent to the increase obtained before that date. Values close to or greater than 100% indicate sustained summer growth comparable to that of spring, while drastically reduced values denote a cessation or collapse of growth induced by stressors, primarily water deficit.

The statistical significance of clonal, spatial, and temporal variations was tested via a Two-way ANOVA and post-hoc Tukey HSD and Bonferroni tests ($p < 0.05$). To account for the longitudinal nature of the dataset and the hierarchical structure of trees nested within sites across years, a Mixed Linear Model Regression (MixedLM) was deployed using Restricted Maximum Likelihood (REML) estimation. The model used 384 total observations, evaluating the continuous parameter "growth ratio" against fixed effects of Period, Clone, Site, Year, and their multi-way interactions.

RESULTS AND DISCUSSION

Site and Clonal Macro-Trends in RGRI

The experimental results unveiled highly significant differences driven by both site conditions and genetic variations. At the non-stressed control sites (Turcia, Villasabariego, and Villoria de Órbigo), poplars maintained stable vegetative development after July 1, with RGRI values stabilizing between 80% and 100%, demonstrating sustained structural carbon synthesis.

In contrast, the water stressed site at Villamañán triggered a comprehensive collapse in post-July growth kinetics across almost all evaluated clones and study years, with RGRI values dropping below 40%. Clone AF8 was the most sensitive, with RGRI values as low as 3% in 2025, while I-214 maintained higher resilience. Beaupré and Raspalje showed intermediate responses, with RGRI values ranging from 15–35% under water stress conditions.

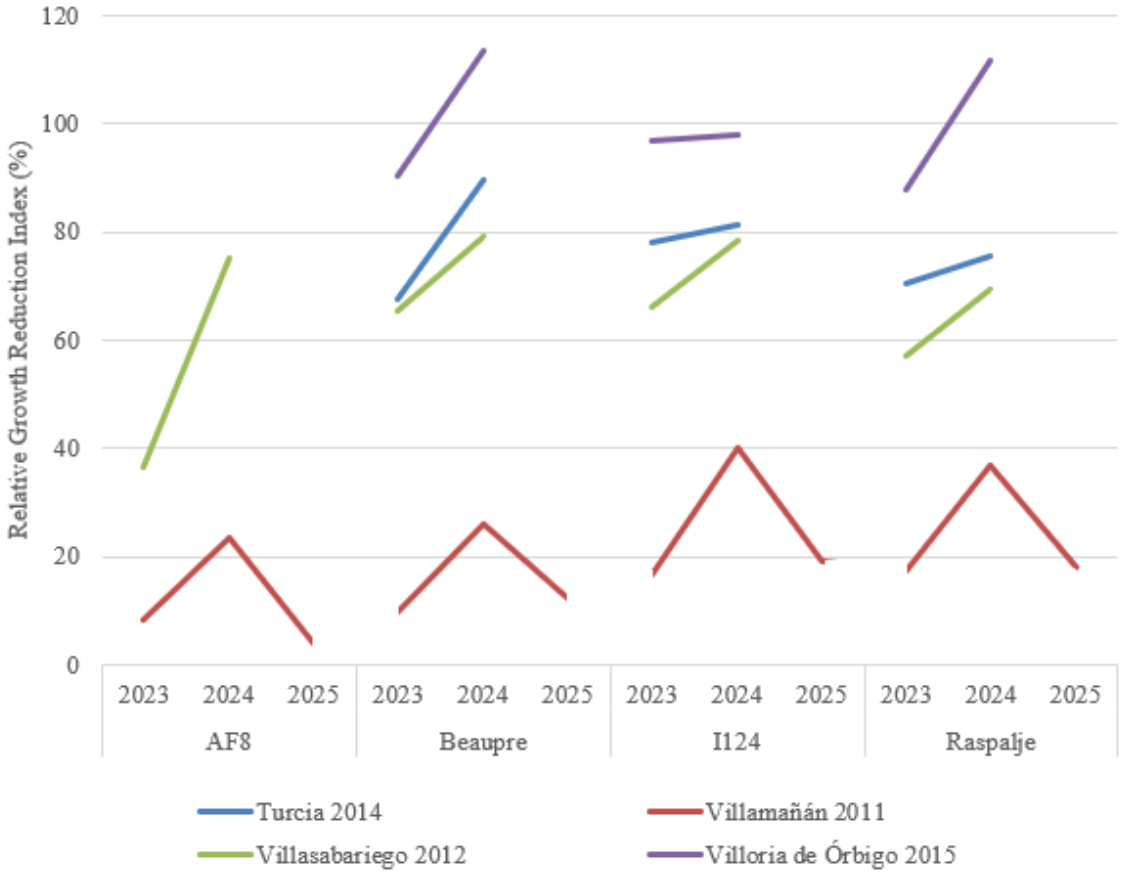

Figure 1: Temporal evolution of Relative Growth Reduction Index (RGRI) by clone and site

Mixed Linear Model Analysis

The Mixed Linear Model fitted via REML provided a deep numerical validation of these structural trends. The global model converged successfully with a Log-Likelihood of 88.36 and a residual scale of 0.0243. The estimated fixed-effects parameters are systematically detailed in Table 1.

The baseline negative coefficient for *Period [Post-July]* ($\beta = -0.215$, $p < 0.001$) confirms a significant global reduction in growth velocity during the summer months. The structural impact of drought is explicitly captured by the main effect of *Site [Villamañán]* ($\beta = -0.249$, $p < 0.001$) and, critically, by its interaction term with the post-July period , which exhibits a severe negative drop ($\beta = -0.327$, $p < 0.001$). This statistically confirms the localized post-July growth collapse under water stress. Conversely, optimized sites like Villoria de Órbigo exhibited highly positive growth parameters ($\beta = 0.348$ for main effect; $\beta = 0.198$ for post-July interaction, both $p < 0.001$), supporting the macro-trends of sustained summer growth under high water availability. The highly significant negative *Year* coefficient ($\beta = -0.302$, $p < 0.001$) directly highlights the worsening limitations over the 2023–2025 window.

Table 1: Mixed Linear Model Regression results for intra-annual poplar growth parameters

Predictor/Variable	β Coefficient	Std. Error	z	P > |z|
Intercept	611.323	32.205	18.982	0.000
Period [Post-July]	-0.215	0.039	-5.452	0.000
Clone [I-124]	0.051	0.040	1.278	0.201
Clone [Raspalje]	0.066	0.040	1.660	0.097
Site [Villamañán]	-0.249	0.045	-5.514	0.000
Site [Villasabariego]	0.112	0.045	2.485	0.013
Site [Villoria de Órbigo]	0.348	0.045	7.675	0.000
Period [Post July] : Clone [I-124]	0.000	0.040	0.005	0.996
Period [Post July] : Clone [T.Raspalje]	-0.038	0.040	-0.956	0.339
Period [Post July] : Site [Villamañán]	-0.327	0.045	-7.259	0.000
Period [Post July] : Site [Villasabariego]	-0.110	0.045	-2.453	0.014
Period [Post July] : Site [Villoria de Órbigo]	0.198	0.045	4.383	0.000
Year	-0.302	0.016	-18.95	0.000
Group Variance (Random Effect)	0.012	0.020	—	—

Post-Hoc Structural Interpretations

Post-hoc pairwise tests (Tukey HSD and Bonferroni) isolated multiple significant differences across clone and site configurations. Multiple post-hoc comparisons made using Tukey HSD tests and Bonferroni conservative correction allowed us to clearly identify significant differences between genotypes and plots. At the clonal level, strong statistical asymmetries were detected in the average summer growth. The mean difference was highly significant when comparing the sensitive clone ‘AF8’ against its counterparts ‘I-214’ (difference = 0.3832, p = 0.0007) and ‘Raspalje’ (difference = 0.415, p = 0.0002), confirming that this last pair maintains a significantly higher exchange rate competence under resource restriction scenarios. The conservative Bonferroni correction validated these clonal differences, reinforcing that specific genotypes retain significantly better wood-accumulation capacity under stress. In the plot analysis, post-hoc tests confirmed that the implantation site introduces a determinant variation in the genetic expression of the chop. The biggest differences in averages were evident when contrasting the restrictive environment of Villamañán against Villoria de Órbigo and Villasabariego, demonstrating that the local edaphic properties, the microclimate and the management history drastically modulate the productivity levels and the intra-annual resilience of the plantation. These spatial differences highlight that while genetic selection is paramount, the matching of specific clones to precise site typologies is critical for maximizing resilience.

From an ecophysiological perspective, the resilient behavior of ‘I-214’ coincides with the literature documenting greater resistance to catastrophic cavitation and balanced stomatal control in stable hybrids of *Populus* × *euramericana* (Monclus et al. 2006, Kojima et al. 2024). On the contrary, the sensitivity of 'AF8' ratifies the existence of a macrostructural compromise: genotypes selected for their outstanding speed of cell elongation in the presence of water suffer an abrupt physiological block (total stomatal shutdown or embolism) when the water potential of the soil drops critically in summer (Rosso et al. 2023, Tang et al. 2024). These findings demonstrate the operational utility of the RGRI index to discriminate early and precisely the ecological vulnerability of commercial clones.

CONCLUSIONS

This study confirms that genetic variation among poplar clones substantially modulates their intra-annual growth response and structural resilience when subjected to seasonal hydric stress. While favorable, well-watered sites enable uniform growth expression across all genotypes, acute summer water deficit triggers highly distinct survival and growth preservation strategies among clones. The severe post-July growth collapse observed in sensitive genotypes like 'AF8' highlights the high risks associated with poor clonal selection in arid or semi-arid zones. Conversely, selecting and deploying poplar clones that exhibit high mid-season resilience—most notably 'I-214' and 'Raspalje'—offers a concrete pathway to stabilize commercial biomass yields. Integrating high-resolution intra-annual growth tracking into forest breeding and management programs is highly recommended to secure the long-term ecological and economic viability of poplar plantations under the increasingly dry summer conditions of southern Europe.

REFERENCES

Cañellas I, Huelin P, Hernández M, Ciria P, Calvo R, Gea-Izquierdo G, Sixto H (2012) The effect of density on short rotation Populus sp. plantations in the Mediterranean area. Biomass Bioenerg 46:645–652. https://doi.org/10.1016/j.biombioe.2012.06.032

Chen Y, Rademacher T, Fonti P, Eckes-Shephard A, LeMoine J, Fonti M, Richardson A, Friend A (2022) Inter-annual and inter-species tree growth explained by phenology of xylogenesis. New Phytol 235:939–952. https://doi.org/10.1111/nph.18195

Guo X, Zhang X, Huang Z (2010) Drought tolerance in three hybrid poplar clones submitted to different watering regimes. J Plant Ecol 3:79–87. https://doi.org/10.1093/jpe/rtq007

Jin Z, Li P, Huang R, Li L, Zhang M, Zhang D, Yuan M, Du J, Zhou J, Zhang W, Du L, Ji L, Quan M, Zhang D, Liu L, Du Q (2025) Natural variation in PtobZIP18 confers the trade-off between stem growth and drought tolerance in Populus. Plant Biotechnol J 23:4633–4649. https://doi.org/10.1111/pbi.70261

Kojima E, González C, Mundo I, Guevara A, Giordano C (2024) Mechanisms of drought resistance in Populus deltoides and P. × canadensis clones to possible situations of water restriction in irrigated systems in drylands. Trees 38:1267–1281. https://doi.org/10.1007/s00468-024-02551-4

Michelot A, Simard S, Rathgeber C, Dufrene E, Damesin C (2012) Comparing the intra-annual wood formation of three European species (Fagus sylvatica, Quercus petraea and Pinus sylvestris) as related to leaf phenology and non-structural carbohydrate dynamics. Tree Physiol 32:1033–1045. https://doi.org/10.1093/treephys/tps052

Monclus R, Dreyer E, Villar M, Delmotte F, Delay D, Petit J, Barbaroux C, Thiec L, Bréchet C, Brignolas F (2006) Impact of drought on productivity and water use efficiency in 29 genotypes of Populus deltoides x Populus nigra. New Phytol 169:765–777. https://doi.org/10.1111/j.1469-8137.2005.01630.x

Oliveira N, Pérez-Cruzado C, Cañellas I, Rodríguez-Soalleiro R, Sixto H (2020) Poplar Short Rotation Coppice Plantations under Mediterranean Conditions: The Case of Spain. Forests 11:1213. https://doi.org/10.3390/f11121352

Rosso L, Cantamessa S, Bergante S, Biselli C, Fricano A, Chiarabaglio P, Gennaro M, Nervo G, Secchi F, Carra A (2023) Responses to Drought Stress in Poplar: What Do We Know and What Can We Learn? Life 13:533. https://doi.org/10.3390/life13020533

Tamudo E, Gazol A, De Andrés E, Valeriano C, Camarero J (2025) Climatic drivers of growth and intra-annual wood density fluctuations in juniper species from seasonally dry environments. Dendrochronologia 89:126437. https://doi.org/10.1016/j.dendro.2025.126437

Tang L, Cao P, Zhang S, Liu X, Ge X, Tang L (2024) Two Male Poplar Clones (Populus × euramericana 'Siyang-1' and Populus deltoides 'Nanlin 3804') Exhibit Distinctly Different Physiological Responses to Soil Water Deficit. Forests 15:1142. https://doi.org/10.3390/f15071142

A GIS Model for Hardwood Biomass Availability and Operational Accessibility in the Southern Gulf Coastal Plain of the United States

Michael K. Crosby[1*]

[1] School of Agricultural Sciences and Forestry, Louisiana Tech University. P.O. Box 10138, Ruston, LA, USA.

E-mail: mcrosby@latech.edu

Keywords: harvest feasibility; biomass availability; GIS decision models.

ABSTRACT

The southeastern United States is widely regarded as one of the world's wood-baskets. Much of the forest in this area is managed pine plantation but there is also a considerable amount of hardwood forest. Recently, pellets have become an important export market utilizing hardwood biomass. Much of the hardwood is found in bottomland areas and consequently have saturated soils for much of the year. This study seeks to use data from the U.S. Forest Service Forest Inventory Analysis (FIA) program, the U.S. Soil Survey (SSURGO), and a layer of all roadways on which timber can be transported. A 75 km buffer was placed around each inventory plot, estimating average haul distances from a source, and volumes in 10 m pixels. Distance to the nearest road was then determine for each forested pixel and soil drainage class utilized as a proxy for forest operations after calculated an index of drainage class ranging from 0-1. The data were masked so that only hardwood forested pixels are considered for two states in the southeastern United States (Mississippi and Louisiana). The values for volume, soil drainage class, and distance to roads, were normalized to scale from 0-1 and the three values were combined to create a multiplicative model that has a 0-1 score for each hardwood pixel in the region for volume and harvestability potential, representing areas where hardwood timber and harvest are most likely to be successful.

INTRODUCTION

Timber harvesting is a vital part of the economy of the southeastern United States. Specifically, in Louisiana and Mississippi, forestry is a multi-billion-dollar industry (USD) and provides tens of thousands of jobs in each state. Over 50 percent of the land area of each state is forested, providing ample opportunity for forest growth and harvest. In terms of volume harvested, each state annually produces approximately 20-30 million tonnes of timber. Of the volume harvested each year, approximately 85 percent is comprised of pine species (*Pinus* spp.), primarily from pine plantations throughout the region. However, a significant portion of the forested area in these states is hardwood (Oswalt, 2019; Oswalt, 2025) and regionally, hardwood growth is increasing (Oswalt et al., 2026).

Given the focus on pine species, there is a potential market opportunity for hardwood forest. There are few production facilities that accept hardwood timber in these states. Much of the hardwood available in Louisiana is found in bottomland areas, which is difficult to access (Oswalt, 2025) and much of the timber is not desirable of preferred appearance-grade quality. Other factors, outside of market concerns favoring pine production, include difficulty accessing standing timber and a variable tree for making it difficult to move timber. The area is also dominated by private ownership and generally partial harvests that impacts quality, e.g., epicormic branching (Kellison and Young, 1997). Understanding where the majority of hardwood volume is located and its accessibility is critical to helping these private landowners understand their timber's standing value. The objectives of this study are to identify the spatial distribution of hardwood forests in these two states and develop a model that identifies availability and harvestability.

MATERIALS AND METHODS

Two states in the southeastern United States, Mississippi and Louisiana (Figure 1), were selected for analysis. These states were selected for the dominance of pine biomass harvested each year given the widespread prevalence of hardwood forest composition. This region has a long growing season due to ample rainfall and a warm climate. Forests in both states have some hardwood harvest each year; however, there is much more hardwood biomass available, which the model developed will show along with its accessibility.

Figure 1: The location of the area assessed, Louisiana (LA) and Mississippi (MS), in the southeastern United States

The datasets chosen for model development are publicly available and commonly utilized in large-scale biomass studies. Forest inventory data was obtained from the Forest Inventory Analysis (FIA) program (FIA, 2024) collected by the United States Forest Service on an incremental basis. The other datasets were obtained from the United States Geological Survey for the soil drainage data (NRCS, 2026) and from OpenStreetMap for the roads data (OSM, 2026). The FIA plot locations were used to generate 75 km^2 grids and volume estimates expanded to that area, with volume estimates being normalized from 0-1. The soil drainage classes were divided into seven classes scaled 0-1 to indicate drainage and equipment usage feasibility for harvest. Distance to roads from each volume polygon to the nearest road was determined and all values normalized so that values ranged from 0-1. The National Land Cover Dataset was utilized to extract values for each variable using areas with hardwood forest cover.

The 0-1 values for drainage, road distance, and volume were then combined in a multiplicative model to indicate both volume availability combined with harvest feasibility based on soil drainage class and distance to the nearest road. This provides a 0-1 indication of where the greatest volume estimates are available, harvest operability is maximized (i.e., soil impacts from harvesting activities will be minimized), and access to a road network for transport to a processing facility is minimized.

RESULTS AND DISCUSSION

The model results show approximately 6 million ha of forest containing hardwood species in the two-state area, with approximately 131 million tonnes of standing timber volume. The distribution matches what is expected of the mixed forest types in the region and the volume distribution follows what is expected with greater volumes being found in bottomland areas in Louisiana and upland species found in the loess/Brown Loam Bluff areas in southwestern parts of Mississippi (Oswalt, 2019; Oswalt, 2025). The model results (Figure 2) are enhanced by the areas where the greatest volumes and accessibility occurs.

Northern portions of Louisiana and areas in southwestern and northern Mississippi exhibit the greatest index values approaching 0.1. The overall values not exceeding 0.1 is a result of at least one low normalized variable value. For example, an area could have high volume availability, a high harvestability in terms of adequate soil drainage, and a low normalized value by being nearer to a roadway. Conversely, low values for volume, drainage, and distance to roads could produce a similarly small value. The index indicates where adequate target locations for hardwood harvest but additional details would be required to determine if the right conditions are met for harvest (e.g., adequate volume availability). The likely limit on harvestability will be soil drainage, particularly in areas with greater composition of clay soils which impacts the available harvest days for equipment operation (Pote et al., 2000).

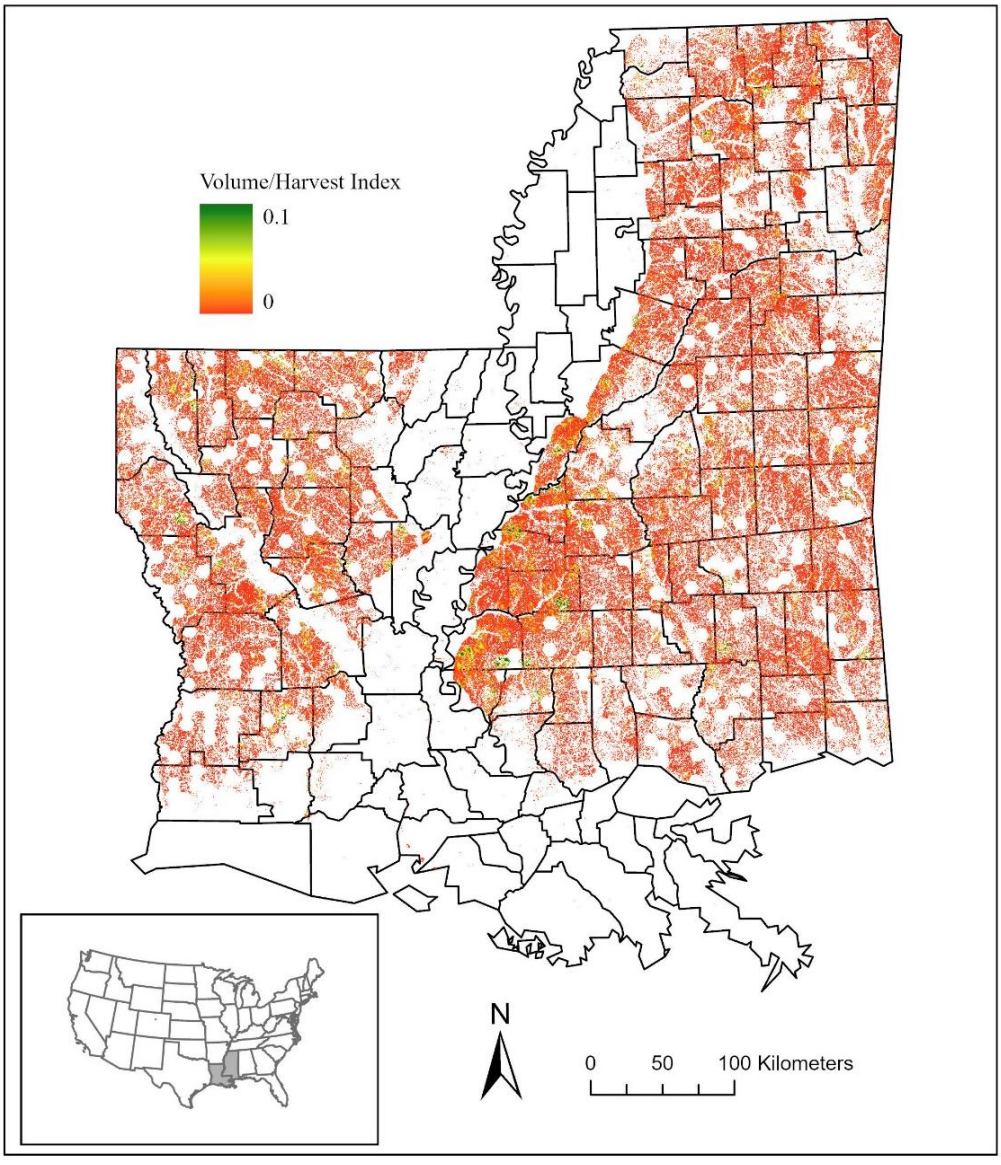

Figure 2: Result of the timber availability and harvestability index for Mississippi and Louisiana

An understanding of the location of harvestable volume provides an opportunity to utilize hardwood forests in the study area. It is worth noting that this model only considers volume presence and has no indication of species composition or wood quality that warrants consideration, particularly in bottomland areas (Kellison and Young, 1997). This model could be utilized to site the optimal location for hardwood processing facilities if volumes were incorporated so that mill demands and transportation networks could be more thoroughly evaluated.

CONCLUSION

The primary goal of this study was to produce an index that provides insights into where the greatest amount of biomass is available in areas that optimizes harvestability. This work could be expanded, provided a location of a processing facility, to determine optimal transport routes given the road networks in this region. Future research should also consider expanding the methodology into the rest of the southeastern region, although topography in the Piedmont and southern Appalachia will need to be considered. This model provides a "first look" at where to focus additional efforts on those interested in harvesting hardwood species.

ACKNOWLEDGEMENTS

This work was supported by funding from the McIntire-Stennis Program (Project# LAX-437626). The author thanks Dr. Eric McConnell at Mississippi State University for his constructive review of this paper.

REFERENCES

Forest Inventory and Analysis Database (FIA). 2024. US Department of Agriculture, Forest Service, Northern Research Station. St. Paul, MN. https://apps.fs.usda.gov/fia/datamart/datamart.html.

Kellison, R.C. and M.J. Young. 1997. The bottomland hardwood forest of the southern United States. Forest Ecol. Managem. 90:101–115. https://doi.org/10.1016/S0378-1127(96)03905-9.

NRCS. 2026. Soil Survey Staff, Natural Resources Conservation Service, United States Department of Agriculture. Soil Survey Geographic (SSURGO) Database for Louisiana and Mississippi. Available online, https://www.nrcs.usda.gov/resources/data-and-reports/soil-survey-geographic-database-ssurgo. Accessed 26 February 2026.

OpenStreetMap contributors (OSM). 2026. Road data for Mississippi and Louisiana. www.openstreetmap.org. Data accessed 17 February 2026.

Oswalt, S.N. 2019. Mississippi's forests, 2017. Resour. Bull. SRS–226. Asheville, NC: U.S. Department of Agriculture Forest Service, Southern Research Station. 68 p. https://doi.org/10.2737/SRS-RB-226.

Oswalt, S.N. 2025. Louisiana's Forests, 2017. Resour. Bull. SRS-247. Asheville, NC: U.S. Department of Agriculture, Forest Service, Southern Research Station. 94 p. https://doi.org/10.2737/SRS-RB-247.

Oswalt, S.N., R. Bush, L.T. Murray, and D. Walker, coords. 2026. Forest resources of the United States, 2022: a technical document supporting the Forest Service 2020 RPA Assessment. General Technical Report WO-107. Washington, DC: U.S. Department of Agriculture, Forest Service, Washington Office. 230 p. https://doi.org/10.2737/WO-GTR-107.

Pote, J., C.L. Wax, and B.L. Karr. 2000. Effects of climate and soil type interactions on probably work days with harvest equipment in Mississippi and Alabama. South. J. Appl. For. 24(4):312-218. https://doi.org/10.1093/sjaf/24.4.213.

U.S. Geological Survey (USGS), 2024, Annual NLCD Collection 1 Science Products: U.S. Geological Survey data release, https://doi.org/10.5066/P94UXNTS.

Research on the Energy Efficiency of Briquettes and Pellets Made from Hardwood Species

Spirchez Cosmin[1*], Lunguleasa Aurel[1]

[1] Transilvania University of Brasov, Faculty of Furniture Design and Wood Engineering, Str.Universitatii, Nr.1, Brașov, Romania, 500068.

E-mail: cosmin.spirchez@unitbv.ro; lunga@unitbv.ro

Keywords: biomass; briquettes; pellets; calorific power; energy efficiency.

ABSTRACT

Approximately 50.1% of the European Union's total area of 4303401 km^2 is used, with 1041423 km^2 used for agriculture and 309844 km^2 for forestry.

The quantities of wood waste are valued by producing briquettes and pellets. Through combustion, wood waste can be recovered, dried and processed for burning in thermal power plants. High performance power plants that use biomass offer maximum efficiency (85%-90%). Biomass resources play an important role in the global energy. This research addresses a tipical issue in the field of renewable energy production, assessing the energy potential of biomass by increasing its calorific value.

The importance of using wood biomass lies in the fact it is renewable resource and is found in large quantities in nature in various form.

Biomass participates in the annual carbon cycle through the use of carbon dioxide. Carbon dioxide is involved both in the process of photosynthesis during plant growth as the component that enables complete combustion during wood biomass. Through the elementary process that occur during photosynthesis, approximately 1% of the energy received from the sun is converted into chemical energy by plants during their growth.

INTRODUCTION

Biomass can be used in combustion processes and, in most cases, does not require very large investments compared to hydropower, solar, wind or geothermal energy. Biomass contributes about 12% to global primary energy production, and in developing countries it accounts for approximately 50% of the energy supply. The use of renewable combustible materials, such as forest residues, for the production of biofuels increases the potential and availability of biomass on the energy market. In the European Union, in 2020, 430 million m³ of roundwood were harvested. Considering that forest exploitation residues represent about 15% of the harvested material, it results that a total of approximately 45,180.14 thousand m³ of waste was generated (Gavrilescu 2008). This material can be valorized through the production of briquettes and pellets, or other biofuel materials. By drying and processing sawdust, briquettes and pellets can be obtained, which reduce environmental pollution compared to the use of current fossil fuels. The use of wood as an energy source has increased significantly in recent decades in all developing countries (Gaur 1998). The potential of biomass could be tripled by recovering organic waste (household, agricultural, forestry, industrial). Romania is a country with high potential in the field of renewable energy sources, particularly in the production of energy from biomass (Lunguleasa 2007).

The total biomass potential available for harvesting for energy production ranges between 240,000 and 290,000 tons of dry matter per year, and in its fresh state this amount can be doubled. According to specialized literature, the energy potential of biomass is estimated to reach 1,500 EJ/year by 2050 (1 EJ = 10^{18} J). Romania has a biomass potential estimated at 3.3 PJ (7,594 thousand toe) per year, representing 19% of the total primary resource consumption at the level of 2024. The production of bioenergy raw materials can create additional sources of income and help stabilize prices for agricultural and forestry products, creating new opportunities for farmers to invest in more efficient production, which will lead to related socio-economic benefits for rural communities.

A solid policy framework will be essential to minimize potential negative aspects and to maximize the social, environmental, and economic benefits of bioenergy production (Lunguleasa 2008). Only then can bioenergy contribute to meeting energy demand and reducing greenhouse gas emissions in a

sustainable way. Most of these considerations apply to developing countries in Asia and Africa, where the traditional use of biomass in stoves remains the main source of energy in the residential sector. Traditional biomass, including wood, charcoal, agricultural residues, and animal manure, is mainly used for cooking and water heating; in colder climates, biomass-based stoves are also used for space heating. In addition, biomass often comes from unmanaged sources, leading to deforestation and soil degradation, which highlights the importance of investments in biomass energy production as a way to reduce excessive forest exploitation (Teuch et al. 2004). Heat generated from biomass can also be a cost-competitive option today, depending on the raw material, the scale of operation, and the fuel source. It is generally accepted that the amount of carbon stored in biomass is approximately 50% of its weight (Lunguleasa 2010), and through thermal treatment processes, the carbon content increases while the mineral substance content decreases.

The processing and drying of wood material under proper conditions are established according to the European standards CEN/TS 14961 and STAS 9279-89. According to these standards, the optimal moisture content for storing wood chips is 30%, while for use in thermal plants it should not exceed 20% (Walkowiak and Bartkowiak 2012).

The physical characteristics as well as the chemical composition of biomass influence the quality of wood material used as a solid fuel. Biomass characteristics vary from one species used as fuel to another (Moya and Tenorio 2011). For example, the moisture content may vary between 20–55% of the dry mass for firewood, or drop below 10% for pellets and briquettes. For these reasons, fuel quality can be improved through pre-treatment technologies of the wood material (torrefaction processes). This treatment can have several beneficial effects for use in heating systems with thermal plants (as increasing the lower heating value, reducing the content of volatile substances, increasing the carbon C - content, and decreasing the influence of moisture on the torrefied material) (Rahmann and Masood 2013). Their efficiency compared to fireplaces is considerably higher: fireplaces may even have a negative efficiency over the course of a year (due to heat losses through the chimney), while modern internal heating systems can achieve efficiencies of 70–90% with reduced emissions. The application of such systems is particularly observed in countries such as Scandinavia, Austria and Germany. In Sweden, advanced biomass pellet heating systems have been developed, where pellets are burned in automated combustion systems (Uslu et al.2011).

MATERIALS AND METHODS

The determination of the calorific value for wood and wood-based or lignocellulosic materials is largely similar to that for coal (as a solid fuel), with only minor differences compared to liquid fuels (gasoline, diesel) or gaseous fuels (natural gas, LPG, biogas, etc.). In general, the method for determining calorific value is carried out separately for solid fuels (ASTM D3286-96) and for liquid and gaseous fuels.

The number of tests required by standards and other researchers is 5, 8, or 10 experimentally analyzed samples (ASTM D3286-96; DIN 51900-1:2000). In this study, experiments were performed on 5 samples (DIN 51900-1:2000) for each species or type of material analyzed and the validated study value was taken as their average, provided it had a probability of over 95%. For determining the calorific value of bark, the Pre-Control method with strict limits was used, in which case only 3 specimens were tested and their average value was considered.

The equipment used to determine the calorific value of woody biomass was an XRY-1C oxygen bomb calorimeter, manufactured by Shanghai Changji Geological Instrument Co., China (Figure 1).

The test consists of three distinct periods (Figure 2), namely:

Initial period ("fore"), which aims to determine the temperature variations of the water in the calorimetric vessel due to heat exchange with the surroundings before combustion. During this period, usually lasting 5 minutes, the temperature is displayed and recorded minute by minute using a precision thermocouple. The last temperature in the initial period actually represents the first temperature of the main period. The temperature values recorded during this stage are generally six.

After recording the 6th value, the ignition of the sample takes place and this moment is displayed in the menu bar (“Burning time”).

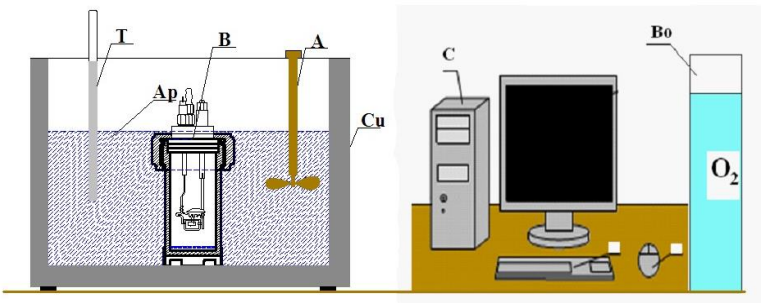

Figure 1: Installation for determining the calorific value of woody biomass using a bomb calorimeter with dedicated software

Main period ("main"), which begins with the ignition of the sample and results in an increase in the temperature of the water in the calorimetric vessel due to the combustion of the wood particle and the release of heat. For determining the final temperature, the temperature is displayed minute by minute. The final temperature is given by the maximum temperature value, since once it starts to decrease, it indicates that the calorimetric vessel no longer receives heat from the bomb. The number of recorded values during this period depends on the combustion duration of the sample in the calorimetric bomb, typically ranging between 19 and 42 temperature readings.
Final period ("after"), which aims to determine the average variation of the water temperature in the calorimetric vessel due to heat exchange with the surroundings after combustion. As in the initial stage, the temperature is recorded every 30 seconds for about 4–5 minutes, resulting in an average of 8–10 recorded temperature values.

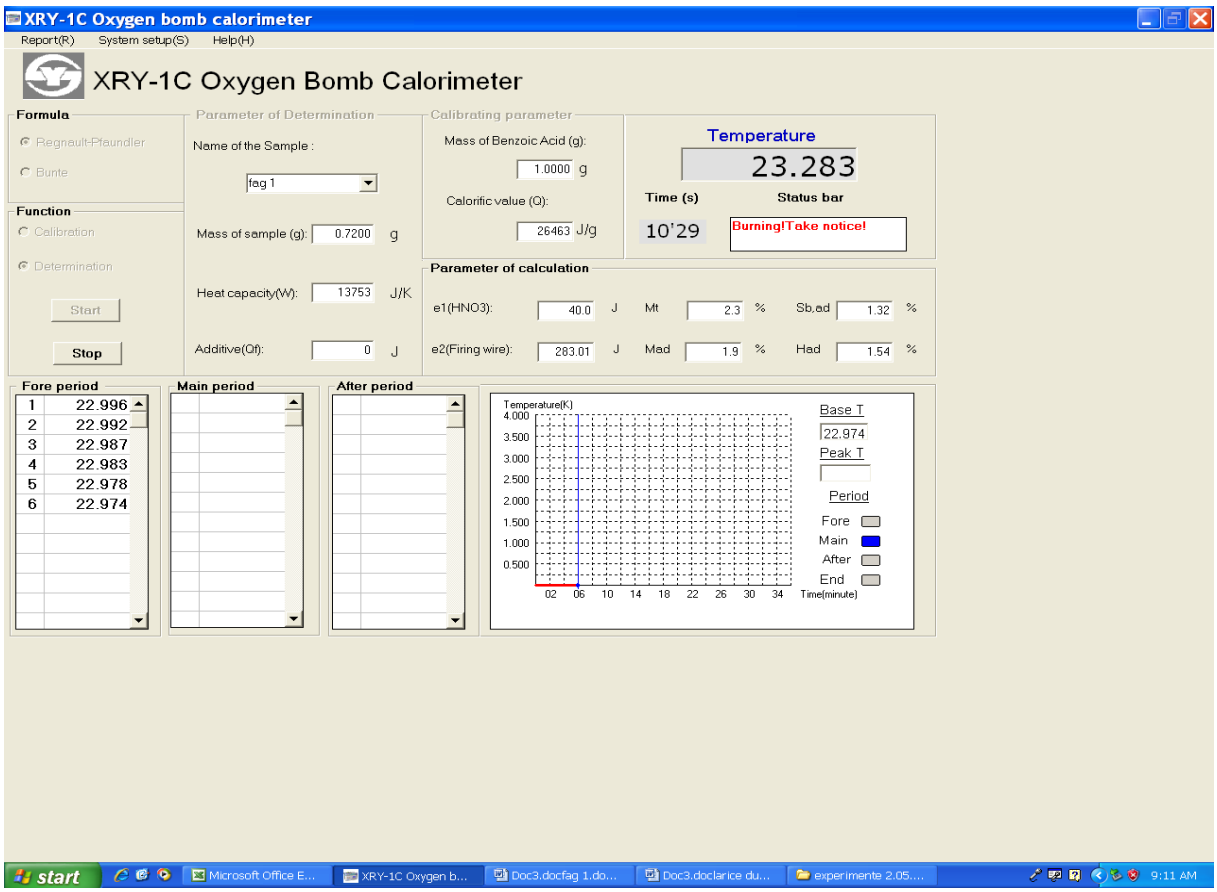

Figure 2: Determination of the calorific value

RESULTS AND DISCUSSION

One of the possibilities for using woody biomass as fuel is in the form of briquettes and pellets. Briquettes and pellets made from woody biomass are superior products obtained from shredded wood, produced by compression without additional additives. Their importance compared to traditional firewood lies in the fact that these products are dried to a moisture content of about 10% and maintain this constant moisture until use, due to the polyethylene packaging in which they are stored. For this reason, their calorific value is higher. By adding natural additives (starch, sugar, sodium lye, lime, gypsum, molasses) (Stelte et al., 2012), the surface consistency of briquettes is improved, while thermal treatments or lignin activation further enhance the quality of these products (Sjostrom, 2006). Additionally, mixing biomass with coal or enriching biomass powder with carbon are other methods to improve the performance of this type of fuel, namely compacted products such as briquettes and pellets (Uslu et al.,2011).

$$E_Y = \{(M_I * PCI_I)/(M_U * PCI_U)\} * 100\ [\%] \quad (1)$$

where:
E_y- energy efficiency of the fuel material (%);
M_i-dry mass of the fuel material, g;
PCI_i- lower heating value of the dry fuel material, kJ/kg;
M_U- mass of the wet fuel material, g;
PCI_u-lower heaiing value of the wet fuel material, kJ/kg.

For oak pellets, m_i = 0.6900 g, at U =0%, higher calorific power (PCS) = 18800 kJ/kg, lower caloriifc power (PCI) = 18421 kJ/kg, sample density = 0.625 g/cm^3, for m_1= 0.8500 g, at U = 10%, higher calorific power (PCS) = 16700 kJ/kg, lower caloriifc power (PCI) = 16101 kJ/kg, sample density = 0.771 g/cm^3, energy efficiency = 94%, for m_1 = 0.7200 g, at U = 20%, higher calorific power (PCS) = 15300 kJ/kg, lower calorific power (PCI) = 13120 kJ/kg, sample density = 0.719 g/cm^3, energy efficiency = 89%, for m_i = 0.8250 g, at U = 50%, higher calorific power (PCS) = 9800 kJ/kg, lower caloriifc power (PCI) = 6101 kJ/kg, sample density = 0.746 g/cm^3, energy efficiency = 63 %.

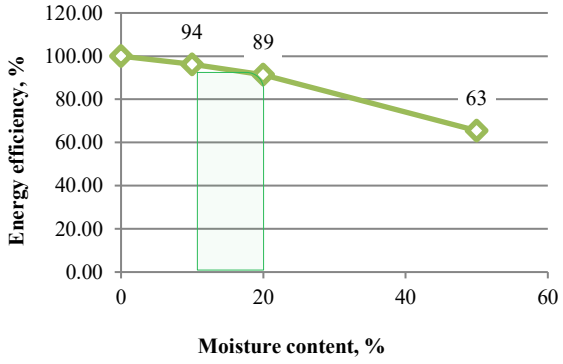

Figure 3: Influence of moisture content on the energy efficiency of oak pellets

For oak briquettes, m_i = 0.7200 g, at U =0% higher calorific power (PCS) = 18700 kJ/kg, lower caloriifc power (PCI) = 18144 kJ/kg, sample density = 0.750 g/cm^3, for m_1= 0.5700 g, at U = 10%, higher calorific power (PCS) = 17300 kJ/kg, lower caloriifc power (PCI) = 16101 kJ/kg, sample density = 0.446 g/cm^3, energy efficiency = 97%, for m_1 = 0.3100 g, at U = 20%, higher calorific power (PCS) = 15920 kJ/kg, lower calorific power (PCI) = 13790 kJ/kg, sample density = 0.321 g/cm^3, energy efficency = 89%, for m_i= 0.4150 g, at U = 50%, higher calorific power (PCS) = 10260 kJ/kg, lower calorific power (PCI) = 4901 kJ/kg, sample density = 0.390 g/cm^3, energy efficiency = 51%.

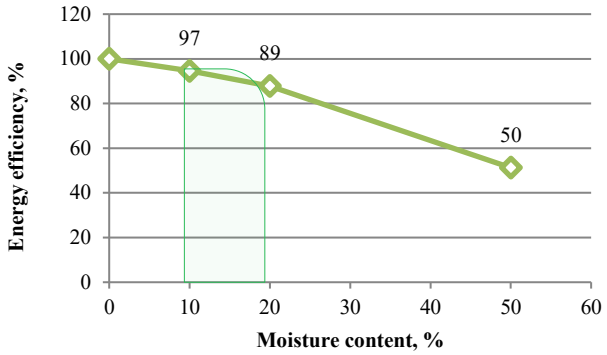

Figure 4: Influence of moisture content on the energy efficiency of oak briquettes

CONCLUSIONS

Energy is the foundation of all human activities, and its development cannot be interrupted. Combustion is one of the most important thermochemical processes for energy production. It should not be overlooked that combustion processes are only possible in the presence of oxygen, which is usually introduced into the combustion chamber through combustion air.

At present, all countries are directing their investments toward energy production from alternative sources, which, according to forecasts, were estimated to reach around 20% of total energy consumption at the European level by 2030. Biomass holds the greatest potential for energy production (47%), followed by hydropower (45%) at the European level. Therefore, it is necessary to understand the energy released during the combustion of different forms of biomass.

Data from the specialized literature are not centralized, making it difficult to compare different types of biomass available on the market. Furthermore, there is no consistency in the way calorific value and measurement units are expressed. As a result, these ambiguities and shortcomings must be systematically studied and analyzed.

REFERENCES

Gavrilescu D (2008) Energy from biomass in pulp and paper,Environmental Engineering and Management Journal, 7(5), pp.537-546, https://doi.org/10.30638/eemj.2008.077

Gaur S, Reed TB (1998) Thermal data for natural and synthetic materials, Marcel Dekker, New York

Lunguleaasa A, Patachia S, Costiuc L, Ciobanu, V (2007) Ecological combustion wood biomass, Transilvania University of Brasov Press

Lunguleasa A (2008) Quality management wood biomass, Transilvania University of Brasov Press.

Lunguleasa A (2010) The compressive strength of wooden briquettes used as renewable fuel, Environmental Enginnering and Management Journal, 9(7), pp.977-981

Moya R, Tenorio C (2011) Fuelwood characteristics and its relation with extractives and chemical properties of ten fast-growth species in Costa Rica, Biomass and Bioenergy, vol.56, pp.14-21

Rahmann A, Masood M A (2013) Influence of size and shape in the strength by briquettes, Fuel Process Technology, vol.22, pp.125-145

Sjostrom E (2006) Wood chemistry, Academic Press, Helsinki

Stelte W, Dahl J, Nielsen NPK, Hansen HO (2012) Densification concepts for torrefied wood based materials carbonised in a nitrogen atmosphere, 20th European Biomass Conference and exhibition, June 21, 2012, Milan, Italy

Teuch O, Hofeanuer A, Troger F, Fom J (2004) Basic properties of specific wood based materials carbonised in a nitrogen atmosphere, Wood Science and Technology, vol.38(3), pp.467-455

Uslu A, Faaji APC, Bergman PCA (2011) Pre-treatment technologies and their effect on international bioenergy supply chain logistics. Techno-economic evaluation of torrefaction, fast pyrolysis and palletisation, Energy, vol.33(8), pp.1206-1223

Walkowiak M, Bartkowiak M (2012) The kinetics of the thermal decomposition of the willow wood (Salix Viminalis L.) exposed to the torrefaction process, Drewno, vol.55(187), pp.37-50

Silvicultural Aspects of *Salix* spp. and Opportunities for Capitalization. A Short Review

George Mușat[1*], Emilia-Adela Manea Salca[1]

[1] Transilvania University of Brasov, Faculty of Furniture Design and Wood Engineering, University street no. 1, 500068, Brasov, Romania.

E-mail: george.musat@unitbv.ro; emilia.salca@unitbv.ro

Keywords: *Salix alba*; *Salix caprea*; wood superior uses; anti-erosion functions; medicinal uses.

ABSTRACT

The growing demand for wood and wood products worldwide has necessitated the use of wood from species that, until now, have not had high industrial importance. For this reason, the purpose of the paper is to highlight the biological characteristics and the possibilities of superior uses of willow wood in the context of species diversification in the wood industry. The genus *Salix* comprises over 350 species with a wide distribution, from warm-climate regions to beyond the Arctic Circle. The species are characterized by diverse morphologies and dimensions, ranging from dwarf forms to shrubby and even arborescent forms. Willow species are found across diverse climatic and pedological conditions, from floodplains (*Salix alba* L.) to the upper forest limit in the high alpine zone (*Salix caprea* L.). The wide spread of these species has made the areas of use very diverse, so that some uses target the ecological peculiarities of *Salix* sp. – through anti-erosion actions, water filtration, land decontamination, afforestation of degraded lands (pioneer species) and protection of communication routes through protective curtains – others uses involve the salicin acid from bark and leaves (pharmaceutical field), some refer to the use of young shoots for handicrafts, others involve the construction of fascines for land stabilization (construction), and some to the use of wood for furniture. In the current context, considerable emphasis has been placed on short-rotation crops for biomass production, used for chipboard, the paper industry, and energy purposes. Willow wood, in turn, has various uses because it is generally a light, soft wood. Instead, it is not very durable in the natural environment, which limits its uses to the pulp and boards industry, matches, or firewood. It can also be used for lightweight packaging, cricket bats, tool handles, racks, small furniture, and handicrafts produced from various curved or twisted plant parts. Willow wood has low mechanical strength but high flexibility, which makes it suitable for applications such as basketry and weaving; these characteristics can be further improved by steaming. Continued research and sustainable management may further expand their applications in industry and traditional practices.

INTRODUCTION

The genus *Salix*, belonging to the Salicaceae family, comprises over 350 species of trees and shrubs, distributed predominantly in the temperate and cold regions of the Northern Hemisphere (Șofletea and Curtu 2007). In the Romanian flora, the genus is well represented, found especially in humid areas, along watercourses, and in floodplains, where it plays an important ecological role. Due to its high ecological plasticity, *Salix* species adapt to a wide range of environmental conditions, especially on alluvial and hydromorphic soils (Achim et al. 2025).

GENUS *SALIX* – DESCRIPTION, BIOLOGICAL CHARACTERISTICS AND AREAL

Morphologically (Table 1), willow species are characterized by rapid growth, flexible stems, and a well-developed root system, adapted to high humidity conditions. The leaves are generally lanceolate, and the flowers are unisexual, arranged in aments, pollination being carried out both entomophilously and anemophilously (Șofletea and Curtu 2007). The high capacity for vegetative regeneration, including by cuttings, is an essential characteristic of the genus, frequently exploited in forestry and in ecological reconstruction works (Achim et al. 2025).

Table 1: Distribution, biological characteristics, and description of the main willow species in Romania (Şofletea and Curtu 2007)

Species	Distribution and biological characteristics	Species description
Salix alba L.	 • native species, with a very wide range, from the Mediterranean region to below the Arctic Circle; • in Romania, it can be found from the Danube floodplain to the hilly regions; • early maturity; • it can be propagated via cuttings; • growths are very active in youth; • it is highly resilient to major and repeated flooding.	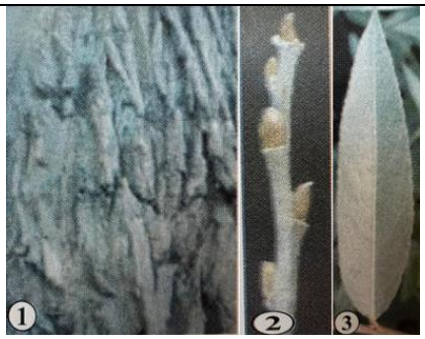 1) rhytidome; 2) twig; 3) leaf (abaxial surface) • arborescent species (10-15 m in height); • sinuous stem; • greyish-green bark; • brownish-gray outer bark; • irregular, globose, and sparse crown; • slender, flexible twigs, greenish-yellow or brown; • small, elongated buds, appressed to the twig, yellowish or reddish; • lanceolate leaves, 4–10 cm long and 1–2 cm wide.
Salix fragilis L.	 • native species, with a very wide range, from the Mediterranean region to below the Arctic Circle (extending further into northern regions than the white willow); • in Romania, it occurs less frequently in the Danube Floodplain and the Danube Delta; • it is more shade-tolerant than the white willow; • a species tolerant of heavy and acidic soils; • adapted to climates with less summer heat.	 1) twig; 2) leaf • arborescent species (can reach up to 20 m in height) • sinuous stem; • rhytidome formed at an early stage; • twigs more vigorous than those of ***S. alba***, shiny, green or brownish-green, which break easily at the point of insertion on the branch; • buds blackish towards the tip, obtuse or nearly acute, appressed to the twig; • oblong-lanceolate leaves, 6–16 cm long and 1.5–3 cm wide.

Salix caprea L.	 • a wider distribution than the white willow and the crack willow, surpassing them in northern regions and crossing the Arctic Circle; • in Romania, it is found in hilly and mountainous areas; • pioneer species, extremely hardy, adapted to various site conditions; • active growth in youth; • short longevity, rarely exceeding 50 years.	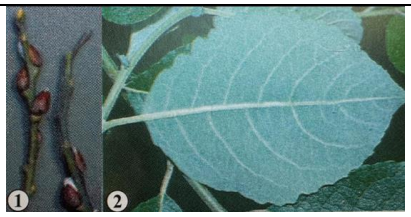 1) twig; 2) leaf • shrub or tree (reaching heights of up to 9–10 m); • crooked stem; • bark smooth in youth, greyish-green; • rhytidome formed late, thin, and irregularly fissured; • twigs brownish-red or greenish-yellow, greyish-hairy when young, then globous and shiny; • ovo-conical buds, globous, yellowish-reddish; • broadly elliptical to oblong leaves, 4–8 (11) cm long.
Salix viminalis L.	 • indigenous species; • Eurasian range; • in Romania, it occurs sporadically in the plains and hills, within river floodplains; • it thrives on humus-rich, moist-to-wet soils, including heavy, loamy, or clay-loam soils; • active growth from the very first years after establishment.	 1) twigs; 2) leaves • shrub, rarely a tree (4–8 m in height); • long, erect branches; long twigs, greenish-gray or brownish-yellow, greyish-pubescent when young, then globous; unequal buds, at least twice as long as wide, whitish-hairy, appressed to the twigs, velvety; • lanceolate or linear-lanceolate leaves, 8–15 cm long and 0.5–1.5 cm wide.
Salix purpurea L.	 • native species, with a Eurasian distribution; • in Romania, it is widespread from the plains to the mountain regions, occurring on river gravel, in riparian forests, as well as in marshy areas or on rocky outcrops near watercourses; • it prefers sandy-clay soils, moist to wet, but withstands well on shallow soils with a relatively high degree of dryness.	 1) twig; 2) twigs and leaves; 3) leaves • shrub up to 4 m in height, bushy; • slender and elastic twigs, globous, reddish-purple or yellow, with yellow-olive inner bark; • elongated buds, reddish-brown to yellowish; • obovate-lanceolate leaves, 4–7 (11) cm long.

PHYSICAL-MECHANICAL PROPERTIES OF WILLOW WOOD AND POSSIBLE USES

Although the fields of use of *Salix* species are extremely varied, the use of wood in the furniture industry is conditioned by its physico-mechanical properties (Żabowski et al. 2024). The most important of these refer to Janka hardness, modulus of rupture, modulus of elasticity, compression strength, and shrinkage (radial, tangential, and volumetric). Some data on the physico-mechanical properties of willow wood, for the species *Salix alba* and *Salix fragilis*, are given in Table 2, together with the degree of workability and brief possible uses.

Table 2: Physical-mechanical properties of willow wood and possible uses

<table>
<tr><th colspan="3">Salix alba L.
(https://www.wood-database.com/white-willow/)</th><th colspan="3">Salix fragilis L.
(https://www.wood-database.com/crack-willow/)</th></tr>
<tr><td colspan="6">A. Physical-mechanical properties</td></tr>
<tr><td colspan="3"> </td><td colspan="3"> </td></tr>
<tr><td colspan="2">Density</td><td>400 kg/m^3</td><td colspan="2">Density</td><td>430 kg/m^3</td></tr>
<tr><td colspan="2">Janka Hardness</td><td>2.530 N</td><td colspan="2">Janka Hardness</td><td>2.830 N</td></tr>
<tr><td colspan="2">Modulus of Rupture</td><td>56,2 MPa</td><td colspan="2">Modulus of Rupture</td><td>64,9 MPa</td></tr>
<tr><td colspan="2">Modulus of Elasticity</td><td>7,76 GPa</td><td colspan="2">Modulus of Elasticity</td><td>7,95 GPa</td></tr>
<tr><td colspan="2">Compression strength</td><td>26,9 MPa</td><td colspan="2">Compression strength</td><td>24,4 MPa</td></tr>
<tr><td rowspan="4">Shrinkage</td><td>Radial</td><td>4,2%</td><td rowspan="4">Shrinkage</td><td>Radial</td><td>N/A</td></tr>
<tr><td>Tangential</td><td>7,2%</td><td>Tangential</td><td>N/A</td></tr>
<tr><td>Volumetric</td><td>11,5%</td><td>Volumetric</td><td>N/A</td></tr>
<tr><td>T/R Ratio</td><td>1,7</td><td>T/R Ratio</td><td>N/A</td></tr>
<tr><td colspan="6">B. Workability</td></tr>
<tr><td colspan="6">• low density, which leads to poor workability, often resulting in fuzzy surfaces;
• develops numerous defects during drying
• it glues and finishes well.</td></tr>
<tr><td colspan="6">C. Uses</td></tr>
<tr><td colspan="6">baskets, utility wood, crates, furniture, cricket bats, carvings, and other small specialty wood items</td></tr>
</table>

Most willow species have soft, light wood, which is not very durable in the open, but becomes more durable when used in sheltered areas. In addition, for higher processing, it has been found that the low density can lead to poor processing characteristics, and shrinkage influences the behavior after drying, with numerous defects being encountered, but the wood is easily finished (Żabowski et al. 2024).
On the other hand, some physical and mechanical properties of willow wood can be compared to those of some poplar species, such as *Populus alba, Populus tremula, Populus nigra* – to which it closely resembles, but also to lime wood – *Tilia europaea* – or alder – *Alnus glutinosa*. However, there are also some differences, so that, although linden wood is soft and easy to process, it is not as elastic as willow, while alder wood is slightly harder and more resistant in conditions of high humidity.

USES OF WILLOW WOOD

Willow wood (*Salix* spp.) is a lignocellulosic resource characterized by low density, elasticity, and rapid growth rate, being exploited in a wide range of fields, such as:

- **Manufacturing, crafts, and furniture** – used in the form of wicker for weaving (baskets, decorative elements) and for making lightweight furniture; its properties of flexibility and workability favour both traditional production and contemporary design;
- **Wood industry and specialized applications** – raw material for particleboard, veneer, and pulp for paper; in addition, certain species (e.g., white willow) are used in the

manufacture of cricket bats, due to the optimal combination of elasticity and mechanical strength (Żabowski et al. 2024);

- **Pharmaceutical industry** – the bark contains salicin, a compound with analgesic and anti-inflammatory properties, used as a precursor in the development of modern drugs (Mahdi 2010);
- **Energy industry** – utilized as biomass in short rotation plantations, including for the production of pellets and briquettes, contributing to renewable energy and reducing carbon emissions (Baker et al. 2022; Zastocki et al. 2024);
- **Ecological reconstruction and natural engineering** – used for soil stabilization, erosion control, and restoration of degraded lands (Scriba et al. 2017; Achim et al. 2025); willow twig fascines are frequently used in hydrotechnical and bank protection works.

CONCLUSIONS

Willow wood stands out as a multifunctional resource, integrated into both traditional practices and modern industrial and ecological applications.

From an ecological perspective, *Salix* species contribute significantly to soil stabilization, erosion reduction, and streambank protection, being used in bioengineering and land reclamation works. At the same time, they support biodiversity, providing habitat and resources for numerous species.

From an economic point of view, willow is of particular importance due to its rapid growth rate and adaptability, being used in energy plantations, in the wood industry, and in various traditional and modern applications.

Some *Salix* species lend themselves very well to short crop cycles, which leads to obtaining significant amounts of biomass that can be used for energy purposes.

Some parts of the plants can be successfully used in the pharmaceutical field due to the significant amounts of salicin, which, in addition, also contributes to the preservation of the pulp and the protection of crops against animals.

Willow wood is soft, light, and in terms of physical and mechanical properties, it is most similar to poplar.

Although the uses of Salix species are multiple, the wood has a limited range of superior uses, often being used for handicrafts and small furniture.

REFERENCES

Achim F, Dinca L, Chira D, Raducu R, Chirca A, Murariu G (2025) Sustainable management of willow forest landscapes: A review of ecosystem functions and conservation strategies. Land 14:1593. https://doi.org/10.3390/land14081593

Baker P, Charlton A, Johnston C, Leahy JJ, Lindegaard K, Pisano I, Prendergast J, Preskett D, Skinner C (2022) A review of willow (*Salix* spp.) as an integrated biorefinery feedstock. Ind. Crop. Prod. 189:115823. https://doi.org/10.1016/j.indcrop.2022.115823

https://www.wood-database.com/ accessed on April 21, 2026.

Mahdi JG (2010) Medicinal potential of willow: A chemical perspective of aspirin discovery. J. Saudi Chem. Soc. 14(3):317-322. https://doi.org/10.1016/j.jscs.2010.04.010

Scriba C, Mușat EC, Salca EA, Ciobanu VD (2017). Influence of energy willow crops on soil features in the case of contaminated land. J. Environ. Prot. Ecol. 18(4):1403-1410.

Șofletea N, Curtu L (2007) Dendrologie. Transilvania University Publishing House, 418 p.

Żabowski B, Wronka A, Kowaluk G (2024) Selected physical and mechanical properties of particleboards manufactured from plantation willow and poplar wood. Materials 17(16):4069. https://doi.org/10.3390/ma17164069

Zastocki D, Staniszewski P, Bijak S, Fortuna W, Kopec S (2024) Selected features of willow *Salix* spp. biomass affecting plantation productivity. Sylwan 168(11):822-834. https://doi.org/10.26202/sylwan.2024048

Dynamics of Viscoelastic Properties of Some Hardwood Species from Romania Subjected to Thermal Variation

Robert Rebrișorean[1], Sara Trucza[1], Mariana Domnica Stanciu[2], Adriana Savin[3], Florin Dinulică[4]

[1] Faculty of Furniture Design and Wood Engineering, Transilvania University of Brasov, B-dul Eroilor 29, 500036, Brasov, Romania
[2] Faculty of Mechanical Engineering, Transilvania University of Brașov, B-dul Eroilor 29, 500036 Romania
[3]Institute of Research and Development for Technical Physics, B-dul Mangeron 47, 700050, Iași, România
[4] Faculty of Silviculture and Forest Engineering, Transilvania University of Brasov, Str. Sirul Beethoven, nr. 1, 500123, Brasov, Romania.

E-mail: robert.rebrisorean@student.unitbv.ro; sara.trucza@student.unitbv.ro; mariana.stanciu@unitbv.ro; asavin@phys-iasi.ro, dinulica@unitbv.ro

Keywords: viscoelastic properties; thermal variation; alder, cherry, beech, maple.

ABSTRACT

The viscoelastic properties of wood are an important factor in the medium and long-term behaviour of wood, being closely related to the chemical composition of the wood, the moisture content, the environmental conditions of use and the variations produced by the loads. The objective of the work is to study the dynamics of changes in the viscoelastic properties of four deciduous species from Romania subjected to cyclic loading, both under isothermal conditions and with temperature variations. The cherry, alder, beech and maple samples were subjected to 3-point bending, using DMA 242C Netzsch equipment. As a result of the different architecture of the anatomical structure, the different proportions of lignin, cellulose and hemicelluloses, the four species under study react differently with increasing temperature. If the conservation modulus (denoted E') shows a similar trend for all species, with different values, the viscous modulus (denoted E") and damping (denoted tan d) evolve differently depending on the structural particularities of the species. Based on dynamic mechanical analysis (DMA), the behaviour of each wood species subjected to simultaneous loading and thermal degradation at a mild temperature regime can be predicted.

INTRODUCTION

Wood's increasing utility as a performance material from its complex rheological and anisotropic nature, with properties varying significantly across its longitudinal, radial, and tangential planes. Accurately modeling its time-dependent behavior is crucial for structural integrity. Wood creep typically progresses through primary, secondary, and tertiary stages (Curtu &Ghelmeziu 1984, Bucur 2006). In engineering applications, wood is often represented by elasto-viscos plastic models that incorporate moisture effects and mechanical loads. Wood is studied as a viscoelastic material due to its chemical composition based on natural polymers - cellulose, hemicellulose and lignin, the proportion of these substances depending on the wood species. Kaboorani et al 2013 showed through investigations carried out on wood cut in radial and tangential directions that the application of the dynamic mechanical analysis (DMA) method can detect the effects of moisture content on wood flow, affecting both viscoelastic and plastic deformation, at different stress levels (Menard (2008), Ranta-Maunus (1990), Ranta-Maunus A (1993)). Applying dynamic mechanical thermal analysis (DMTA), Kelley et al. (1987) showed that the main softening of wood occurs at temperatures of 50°C and 100°C, corresponding to the glass transition of lignin. Secondary relaxations corresponding to softening of other carbohydrates (amorphous cellulose and hemicelluloses) occur at lower temperatures (Pang (2001), Rice et al (1990)). Placet et al 2008 studied the mechanical response of wood across the grain affected by a severe hygrothermal treatment, under water-saturated conditions below 135 C, observing that the temperature level acts as an activator of viscoelastic properties but also as a degradation factor between the softened samples, the differences between radial and tangential samples being insignificant (Stanciu et al 2013, 2018, 2020). In previous

studies, the Gall et al 2024 analysed the viscoelastic behaviour of wood varnished with different types of varnishes, applied in different thicknesses, on spruce and maple wood.
The aim this study is to analyse the viscoelastic thermal behaviour of different hardwood species as cherry, alder, beech and maple, subjected to dynamic mechanical stresses. The results obtained are useful both for predicting the behaviour of wood under long-term stress, evaluating changes in the viscos-elastic properties of wood under extreme climatic conditions (high environmental temperatures), identifying the optimal softening temperature to bend beech or cherry without breaking the fibres; analysing the efficiency of thermal modification to make wood more resistant to moisture and rot, predicting how vibrations (dynamic stress) are damped by the wood structure.

MATERIALS AND METHODS

Sample preparation

To evaluate the viscoelastic properties, samples with dimensions of 50x10x3 mm^3 were prepared from alder, beech, maple and cherry wood, cut in the longitudinal direction, 6 of each species. Table 1 summarizes the physical characteristics of the samples.

Table 1: Features of wood samples

Species	Length [m]	Width [m]	Height [m]	Moisture content [%]	Density [g/cm^3]
Alder	50	10	4	10.4%	0.500
Beech	50	10	4	10.2%	0.733
Maple	50	10	4	8.5%	0.555
Cherry	50	10	4	9.8%	0.563

Experimental set-up

The viscoelastic properties of the wood samples were determined by the method of mechanical analysis in dynamic mode, using the DMA242 C Netzsch analyzer – Germany (Figure 1). The test consisted of applying the samples to dynamic bending loads in three points, as presented in Figure 1. The dynamic test consisted of two stages:
Stage I - determination of the complex modulus of elasticity E*, with its two components (conservation modulus E' and loss modulus E") and the damping factor tanδ, under isothermal (T=30 °C) and isochronous (t = 30 minutes) conditions and loading frequency of 1 Hz with 6 N intensity.
Stage II - variation of temperature conditions in the range 30 °C... 120 °C, with a rate of 2°C/min.

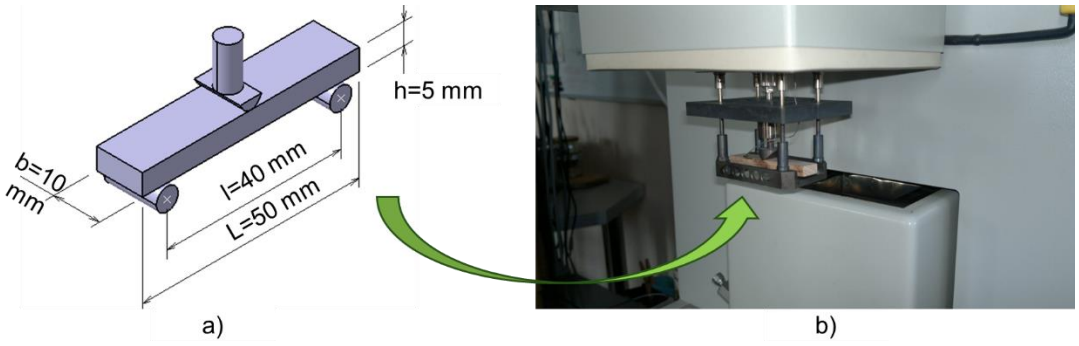

Figure 1: Sample geometry (a) and experimental set-up (b)

RESULTS AND DISCUSSION

Visco-elastic properties depending on the loading frequency

For all four types of wood, a similar behaviour over time is observed. Regarding the evolution of storage Modulus (E') which represents the stiffness of the material, it can be noticed that this increases constantly in all samples, suggesting that the wood becomes stiffer as time passes (Figure 2). Damping (tand) which represents the material's ability to dissipate energy, this decreases constantly, indicating that the material becomes more elastic and less "viscous". The beech wood samples show the highest values for storage modulus (between 8400 and 8600 MPa) (Figure 2b), less stiff is alder wood which recorded the lowest values for E' (7150–7350 MPa) (Figure 2a). The graph for cherry wood shows the highest fluctuations (data noise) for the damping factor, also having the lowest coefficient of determination (R^2 = 0.6282) (Figure 2d). The values of the coefficient of determination R^2 close to 1 (as is the case for the storage modulus of maple wood, (R^2= 0.992, Figure 2c) indicate that the chosen polynomial models describe the evolution of stiffness almost perfectly. The decrease in damping generally follows a logarithmic or downward polynomial curve. During the experiment, the wood samples undergo a process of structural consolidation, becoming stiffer and more efficient at storing elastic energy.

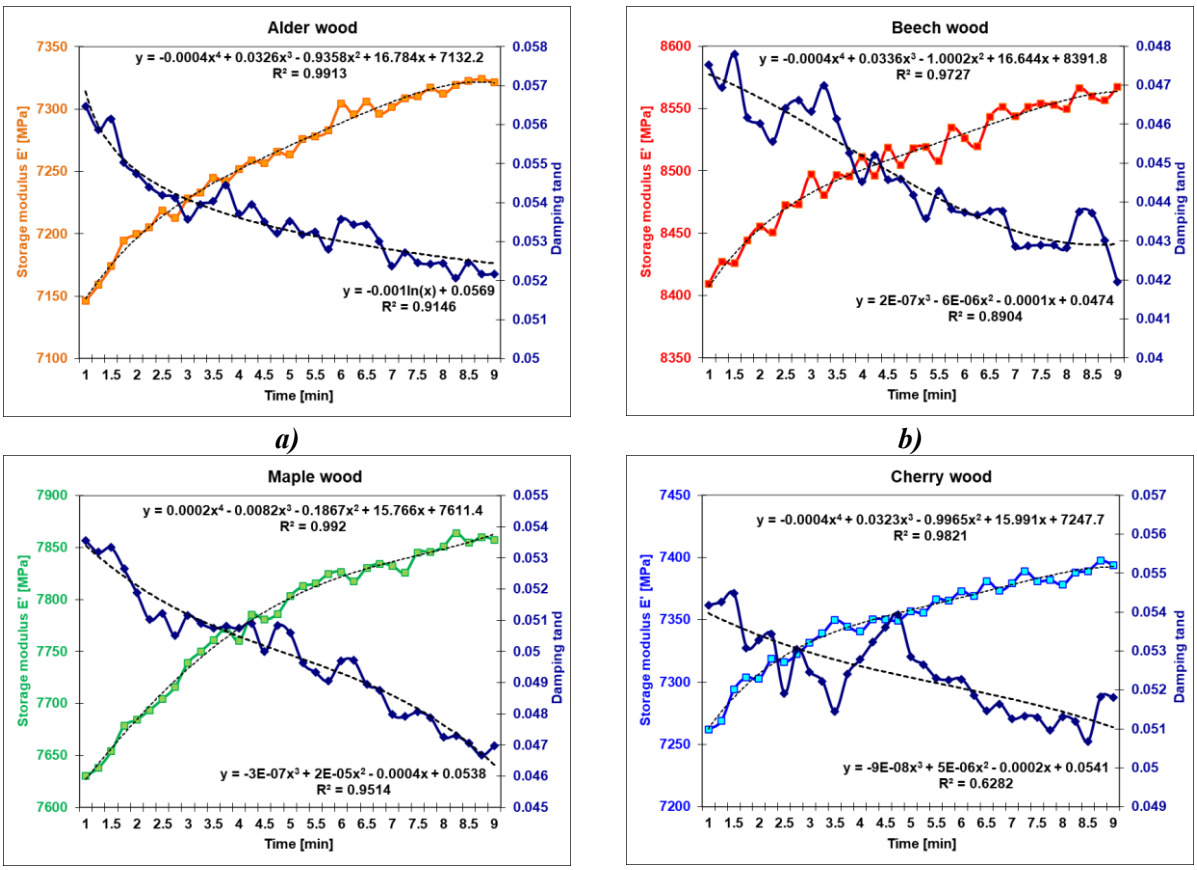

Figure 2: Variation of viscos-elastic properties in isothermal condition: a) alder; b) beech; c) maple; d) cherry

Table 2 summarizes the percentage changes in viscoelastic quantities produced during dynamic loading.

Table 2: Quantitative variation of viscoelastic properties during dynamic loading

Species	Storage modulus E' %	Loss modulus E" %	Damping tand %
Alder	2.49↑	4.89↓	6.71↓
Beech	2.72↑	8.21↓	9.71↓
Maple	2.37↑	7.12↓	5.94↓
Cherry	2.16↑	3.49↓	4.38↓

The effect of thermal degradation

The variation of viscoelastic characteristics with increasing temperature can be observed in Figure 3. For all species, E' decreases as temperature rises, a trend attributed to the wood's polymeric composition (lignin and hemicellulose), which is susceptible to degradation in the presence of heat, making the material less rigid. Comparative analysis shows that beech wood (Figure 3b) is the stiffest, while cherry wood (Figure 3d) is at the opposite end of the spectrum. As temperature increases, damping tends to rise, often exhibiting peaks (as observed in the case of alder samples around 65°C) (Figure 3a). The increase in damping indicates that the wood becomes more "viscous" and better able to absorb vibrations as it heats up and approaches a transition state. Another component characterizing the viscoelastic behavior of wood is the loss modulus (E") – which measures the energy dissipated as heat. Generally, E" increases with temperature. This shows that as the wood structure undergoes thermal relaxation, internal friction between molecules increases, dissipating more mechanical energy (Shen et al (2009), Shapchenkova et al (2022)).

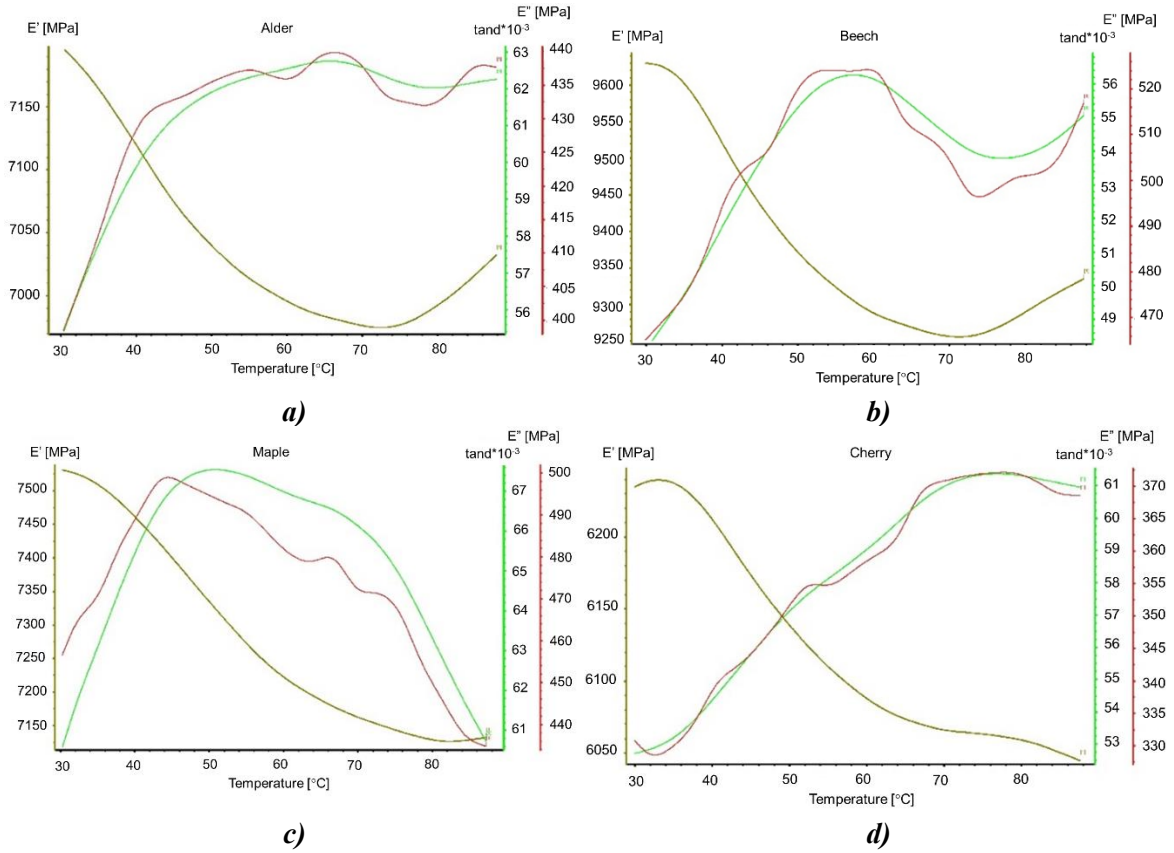

Figure 3: Variation of viscos-elastic properties due to temperature variation: a) alder; b) beech; c) maple; d) cherry

CONCLUSION

The work aimed to analyse the viscoelastic behaviour of four deciduous species with different anatomical structures. The following aspects resulted from the dynamic mechanical analysis:

- Beech wood: It has the greatest structural stability at high temperatures, maintaining high stiffness values.
- Alder and Maple wood: It presents similar stiffness evolutions (in the range of 7000-7500 MPa), but Alder has more pronounced fluctuations in the damping factor at high temperatures.
- Cherry: Although it is the least rigid, it has a very clear damping curve (tand), indicating a linear structural transition under the influence of heat.

REFERENCES

Bucur V (2006) Acoustics of Wood. Springer Verlag, Berlin, Germany.

Curtu I, Ghelmeziu N (1984) Mecanica lemnului si a materialelor pe baza de lemn. Editura Tehnica, Bucuresti (in Romanian)

Gall R, Savin A, Stanciu MD, Campean M, Gliga VGh (2024) The influence of the type of varnish on the viscous-elastic properties of maple wood used for musical instruments, 11th Hardwood conference, Sopron, Hungary, 30-31 May 2024, p. 426 - 434

Kaboorani A, Blanchet P, Laghdir A (2013) A rapid method to assess viscoelastic and mechanosorptive creep in wood, Wood and Fiber Science 45(4):370-382

Kelley S, Rials T, Glasser W (1987) Relaxation behaviour of the amorphous components of wood, J. Mater. Sci. 22:617-624.

Menard H (2008) Dynamic Mechanical Analysis – a practical introduction. Second Edition, CRC Press, New York, ISBN 978-1-4200-5312-8

Moutee M (2006) Modeling The Mechanical Behaviour Of Wood In Drying/Modélisation Du Comportement Mécanique du Bois au Cours du Séchage, Phd Theses Département Des Sciences Du Bois Et De La Forêt, Faculté De Foresterie Et Géomatique, Université Laval, Québec

Pang S (2001) Modelling of stresses and deformation of radiate pine lumber during drying. Proc. 7th International IUFRO Wood Drying Conference, Tsukuba, Japan, pag. 238-245

Placet V, Passard J, Perre P (2008) Viscoelastic properties of wood across the grain measured under water-saturated conditions up to 135°C: evidence of thermal degradation. J. Mater. Sci. 43:3210–3217

Rice RW, Youngs RL (1990) The mechanism and development of creep during drying of red oak. Holz als Roh und Werkstoff 48:73-79

Ranta-Maunus A (1990) Impact of mechano-sorptive creep to the long-term strength timber. Holz als Roh und Werkstoff. 48:67-71

Ranta-Maunus A (1993) Rheological behaviour of wood in directions perpendicular to the grain. Materials and Structures. 26:362-369.

Shen DK, Gua S, Luo KH, Bridgwater AV, Fang MX (2009). Kinetic study on thermal decomposition of woods in oxidative environment. Fuel 88(6):1024

Shapchenkova O, Loskutov S, Aniskina A et al. (2022) Thermal characterization of wood of nine European tree species: thermogravimetry and differential scanning calorimetry in an air atmosphere. Eur. J. Wood Prod. 80:409–417

Stanciu MD, Curtu I, Grimberg R, Savin A (2013) Research Regarding the Complex Modulus Determined with Dynamic Mechanical Analysis (DMA) in Case of Beech (Fagus Sylvatica L.) and Alder (Alnus Glutinosa Gaertn) PRO LIGNO 9(4): 587-593

Stanciu MD, Bucur V, Valcea CS, Savin A, Sturm R (2018) Oak particles size effects on viscous-elastic properties of wood polyester resin composite submitted to ultraviolet radiation, Wood Sci Technol 52 (2): 365-382

Stanciu MD, Șova D, Savin A, Iliaș N, Gorbacheva G (2020) Physical and Mechanical Properties of Ammonia- Treated Black Locust Wood, Polymers,12:377

Static Bending Strength of Northern Red Oak (*Quercus rubra* L.) from Southern Poland – A Case Study

Radosław Wąsik[1*], Krzysztof Michalec[1], Monika Gach[1], Joanna Kralka-Frycz[2]

[1] University of Agriculture in Krakow, Forestry Faculty, Department of Forest Utilization and Forest Technic. Aleja Mickiewicza 21, 31-120 Kraków
[2] Tilia – Edukacja Przyrodnicza; ul. Ułanów 46/84, 31-455 Kraków.

E-mail: radoslaw.wasik@urk.edu.pl; krzysztof.michalec@urk.edu.pl; monika.gach@urk.edyu.pl; tilia.przyroda@gmail.com

Keywords: modulus of rupture; wood; northern red oak; southern Poland.

ABSTRACT

Currently, the annual harvest of northern red oak wood in Poland is minimal, but considering various scenarios of changes in tree species composition due to climate change, as well as the invasiveness of this species, an increase in the harvest of this wood seems to be a matter of time. The small number of publications on the mechanical properties of the northern red oak wood motivated the authors to undertake such research. The wood for the study came from a fresh mixed coniferous forest in southern Poland. The diameters at breast height (DBH) of all red oaks in the stand were measured and the average was calculated. Then, three trees with an average DBH (range 20-22 cm) were selected for felling. A zone approximately 50 cm long was marked on the trunks of the selected trees, with a height of 1.3 m in the centre, and the north direction was marked. The trees were then felled and the marked 0.5 m long logs were cut off. Radial boards were cut from the logs in the N, S, E and W directions. The boards were cut into 30 cm long beams, marking their relative distance from the bark (section 1 – closest to the bark, section 2, section 3, core). Bending strength tests (Modulus of Rupture – MOR) were carried out in accordance with Polish (PN-77/D-04103) and international (ISO 13061-3:2014) standards. A total of 36 beams were tested. No significant differences in MOR were found between the tested trees, compass directions and sections. The average value obtained, 136.9 MPa, is slightly higher than the average values reported for red oaks growing in North America and also higher than the averages for native European oaks.

INTRODUCTION

There are almost fifty non-native tree species in Poland's forests, but they are found on only around 5% of the country's total forested area, with the northern red oak (Quercus rubra L.) occupying the largest area. In 2017, it was recorded in the species composition of stands covering a total area of almost 300,000 ha in areas administered by the Polish State Forests (LP). In the same year, the volume of its timber in stands within the LP area was estimated at over 46,000 m³, (Gazda et al. 2017). Red oak timber is used to a limited extent in Poland. It is primarily used in interior finishing, mainly for flooring, stairs, panelling and furniture. Following prior impregnation, it can be used to construct garden features such as gazebos or terraces. Given the analyses of scenarios for changes in forest species composition under the influence of climate change, which predict an increase in the proportion of red oak in European forests (Dyderski et al. 2017) and the invasiveness of this species (Tokarska-Guzik et al. 2012), it seems that in the near future we should expect an increase in the volume of red oak, as well as in the harvesting and utilisation of its timber. To the authors' knowledge, no studies have yet been conducted in Poland on the mechanical properties of red oak wood of native origin. The aim of the present study was to determine the static bending strength, also known as the modulus of rupture (MOR), of wood from this species.

MATERIALS AND METHODS

The study was conducted in the Regional Directorate of State Forests in Katowice, Olkusz Forest District, in the Żurada Forest Division. The species composition of the stand is: 50% *Quercus robur*, 20% *Betula pendula*, 20% *Pinus sylvestris* and 10% *Larix decidua*. The stand is located in a fresh coniferous forest habitat, and the soil in this area is a podzolised arenosol on loose sand. The average age of the northern red oak in this area was 45 years. The DBH of all northern red oak trees in the stand was measured in two directions: N-S and E-W. The average DBH was calculated and found to be 21 cm, three trees with diameters closest to the average were then selected. The DBH and the direction of north were marked on the trees with paint. The trees were then felled, and from each trunk, rollers about 40 cm long were taken, i.e. 20 cm above and below the DBH. From each roller, one radial board was first cut in the N-S direction, followed by two radial boards in the E and W directions. The thickness of the radial boards was about 2.5 cm. The boards were planed on both sides to a thickness of 20 mm, then, starting from the bark towards the pith, they were cut into sections approximately 2.5 cm wide. The section closest to the bark was marked with the number 1, and the next sections were marked with consecutive numbers. The sections were planed on both sides to a width of 20 mm, then cut into 30 cm long beams. Each beam was marked with the tree number, the compass direction and the section number. Immediately before the strength test, the height and width of each beam were measured with a calliper to an accuracy of 0.1 mm. Static bending strength was tested on an EDZ20 testing machine connected to a computer recording the test procedure. The machine's support spacing was 240 mm. The MOR was calculated using the following formula (Eq 1) (PN-77/D-04103, ISO 13061-3:2014 (E)):

$$\sigma_{w\%} = \frac{3 \cdot Pmax \cdot 240}{2 \cdot b \cdot h^2} \quad (1)$$

$\sigma_{w\%}$ -
MOR at wood moisture content W% [MPa]
Pmax -
breaking force [N]
b -
beam width [mm]
h -
beam height belki [mm]

The moisture content of the wood beam at the time of testing was determined using the oven-drying and weighing method in accordance with the Polish standard (PN-77-D-04100). The MOR for 12% wood moisture content was calculated using the following formula (Eq 2) (PN-77/D-04103):

$$\sigma_{12\%} = \sigma_{w\%}[1+\alpha(W-12)] \quad (2)$$

$\sigma_{12\%}$ -
MOR at 12% wood moisture content [MPa]
α -
conversion factor = 0,04
W -
moisture content of the wood at the time of testing [%]

The results obtained were compiled, and means and coefficients of variation (V) were calculated for the trees, directions and sections, as well as for the whole of the material studied. The following procedures were used in the statistical analyses (TIBCO Software 2017):
- the normality of the distributions of the data was assessed using the Shapiro-Wilk test,
- the significance of the differences was tested using the Kruskal-Wallis test (K-W test)
- an assessment of which factors are responsible for rejecting the null hypothesis of no significant differences was carried out using a multiple comparison test (M-C test)
- a significance level of p=0.05 was used in statistical analyses.

RESULTS

A total of 36 beams were tested: 13 were taken from tree no. 1, 11 from tree no. 2 and 12 from tree no. 3. The average MOR for the entire tested material was 136.9 MPa; the averages for individual trees ranged from 133.1 to 140.8 MPa (Table 1). Variation in this property between the tested trees was small, with a coefficient of variation of 2.8%. Greater variability was observed within trees, where the coefficients ranged from 8.3% to 18.3% (Table 1). No significant differences in MOR were found between the trees studied (K-W test: p=0.5556) and compass directions (K-W test: p=0.3042). However, although the result of the K-W test (p=0.0431) indicates significant differences in MOR between sections, the M-C test did not indicate between which sections such differences occur (Table 2).

Table 1: Results of MOR

Tree No	Type of statistics	MOR [MPa]
1	min	112.2
	mean	140.8
	max	162.2
	V [%]	13.4
2	min	115.1
	mean	133.1
	max	148.0
	V [%]	8.3
3	min	88.4
	mean	136.9
	max	175.9
	V [%]	18.3
TOTAL	min	88.4
	mean	136.9
	max	175.9
	V [%]	2.8

V – coefficient of variation [%]

Table 2: Values of "p" of M-C test

Section	1	2
2	0.0800	
3	1.0000	0.1167

Figure 1 shows that slightly higher MOR values were observed in section 2, which includes wood located in the central zone of the trunk's cross-sectional radius.

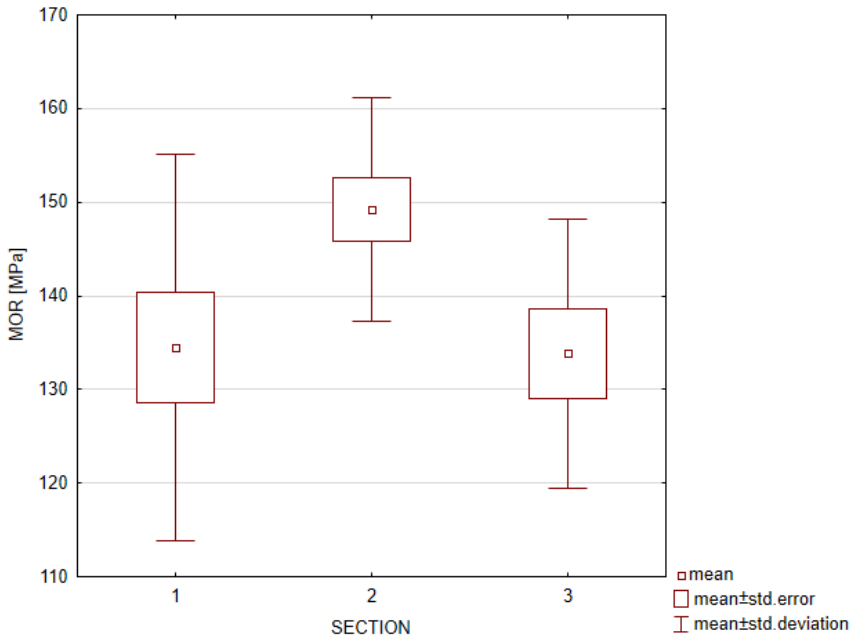

Figure 1: MOR in sections

DISCUSSION

The average MOR value obtained in this study was 136.9 MPa. This is slightly higher than the MOR values for northern red oaks growing in North America, for which average values of around 100 MPa are reported (Ross 2010, Meier 2021). For Europe, MOR values are reported within a rather wide range: 80–141 MPa (Galewski and Korzeniowski 1958, Wagenführ and Scheiber 1989, Kozakiewicz and Wiktorski 2006], so the averages obtained in this study for individual trees and the average for the whole sample are close to the upper limit of the given range. No significant differences in MOR were found between the trees studied, what indicates that this feature does not show significant variation between individual trees. This is also confirmed by the low coefficient of variation. No significant differences in MOR were found between geographical directions. However, significant differences were found between sections along the radius of the trunk cross-section. Although the M-C test did not reveal between which sections such differences occur, analysis of the graph showing the variation of the feature across the stem cross-section suggests that wood from the central parts of the radius has a higher MOR compared to the pith and circumferential (near-bark) regions. It seems that the reasons for this result should be found in the variation in the macrostructural characteristics of the wood under study, particularly the proportion of latewood. However, these characteristics were not the subject of the analyses. Compared to native oak species, namely English oak (*Quercus robur* L.) and sessile oak (*Quercus petraea* (Matt.) Liebl.), for which MOR values in the range of 74–117 MPa are reported (Galewski and Korzeniowski 1958, Krzysik 1974), northern red oak showed a higher MOR. This confirms the results of trials using northern red oak as structural timber, in which this species demonstrated better strength properties than European oaks (Orlikowska 2020). It is therefore to be expected that interest in this raw material from the timber industry in Europe will increase in the near future.

CONCLUSIONS

Based on the results of static bending strength tests carried out on northern red oak wood from southern Poland, the following observations and conclusions can be drawn:

- The average MOR value obtained, amounting to 136.9 MPa, is slightly higher than that of North American oaks
- No significant differences in MOR were found between the trees tested, indicating little variation in this property
- The highest MOR values were observed in the central parts of the cross-sectional radius of the stem

- The MOR values obtained for northern red oaks were higher than those for native oak wood, which confirms the results of previous observations and indicates the potential for using native red oak as structural timber.

REFERENCES

Dyderski MK, Paź S, Frelich LE, Jagodziński AM (2017) How much does climate change threaten European forest tree species distributions? Glob Change Biol, 24(3):1150–1163. https://doi.org/10.1111/gcb.13925

Galewski W, Korzeniowski A. (1958). Atlas Najważniejszych Gatunków Drewna. PWRiL, Warszawa, Poland (in Polish)

Gazda A, Miścicki S, Wąsik R, Goczał J, Kędra K. (2017) Poland–Country report. In: Hasenauer H, Gazda A, Konnert M, Lapin K, Mohren F, Spiecker H, van Loo M, Pötzelsberger E, Non-Native Tree Species for European Forests: Experiences, Risks and Opportunities. University of Natural Resources and Life Sciences, Vienna, Austria, pp 284–297.

ISO 13061-3 (2014) Physical and mechanical properties of wood - Test methods for small clear wood specimens - Part 3: Determination of ultimate strength in static bending. International Organization for Standardization, Geneva, Switzerland

Kozakiewicz P, Wiktorski T, (2006) Dąb czerwony [Quercus rubra L.] - drewno egzotyczne z Ameryki Północnej. Przemysł Drzewny, 57(11):19–22 (in Polish)

Krzysik F, (1974) Nauka o drewnie. PWN, Warszawa, Poland (in Polish)

Meier E. 2021. Northern red oak (Quercus rubra L.) In: The Wood Dictionary - from acacia to ziricote, a guide to the world's wood. Amazon Fulfillment, Wrocław, Poland

Orlikowska K, (2020) Rynek europejski najbardziej perspektywiczny dla drewna amerykańskiego. Gazeta Przemysłu Drzewnego, 278 (3):18–19 (in Polish).

PN-77-D-04100 (1978) Drewno – Oznaczanie wilgotności. Wydawnictwa Normalizacyjne (in Polish)

PN-77/D-04103 (1978) Drewno – Oznaczanie wytrzymałości na zginanie statyczne. Wydawnictwa Normalizacyjne (in Polish)

Ross RJ (2010) Wood handbook: wood as an engineering material USDA Forest Service, Forest Products Laboratory, General Technical Report FPL-GTR-190, Madison, USA

TIBCO Software Inc. Statistica (Data Analysis Software System), Version 13; TIBCO Software Inc.: Palo Alto, CA, USA

Tokarska-Guzik B, Dajdok Z, Zając M, Zając A, Urbisz A, Danielewicz W, Hołodyński C. (2012) Rośliny obcego pochodzenia w Polsce ze szczególnym uwzględnieniem gatunków inwazyjnych. Generalna Dyrekcja Ochrony Środowiska. Warszawa, Poland (in Polish).

Wagenführ R, Scheiber C. (1989) Holzatlas, VEB Fachbuchverlag Leipzig 2. 3rd ed, Leipzig, Germany (in German)

Enzymatic Strategies of Two *Armillaria* Species in Wood Cell Wall Degradation

Boris Indic[1*], Simang Champramary[1], Nóra Tünde Lange-Enyedi[1], Omar Languar[1,2], György Sipos[1]

[1] University of Sopron, Functional Genomics and Bioinformatics Group, Bajcsy-Zsilinszky 4, 9400 Sopron, Hungary
[2] University of Szeged, Department of Biotechnology and Microbiology, Közép fasor 52, 6726 Szeged, Hungary.

E-mail: indic.boris@uni-sopron.hu; simang5c@gmail.com; lange-enyedi.nora@uni-sopron.hu; o.languar@gmail.com; sipos.gyorgy@uni-sopron.hu

Keywords: *Armillaria*; wood decay; lignocellulose degradation; CAZymes; hardwood durability.

ABSTRACT

Fungi of the *Armillaria* genus are important pathogens and saprotrophs in forest ecosystems, capable of colonizing and degrading woody tissues, leading to root rot and structural damage in trees. As white-rot fungi, they possess enzymatic systems that enable the breakdown of lignin as well as other major components of plant cell walls, including cellulose and hemicellulose.

This study focuses on the predicted enzymatic systems involved in wood cell wall degradation in *Armillaria ostoyae* and *Armillaria borealis*. An *in vitro* stem invasion assay using wood segments was applied to simulate fungal colonization. High- and low-virulence isolates were inoculated onto autoclaved stem segments representing fully dead wood to focus on degradation-related processes. Subcortical mycelial samples were collected and analyzed using RNA sequencing and differential gene expression analysis. Particular attention was given to carbohydrate-active enzymes (CAZymes) associated with lignocellulose degradation.

The results indicate that both species possess diverse enzymatic systems targeting the main structural components of wood. While several enzyme groups were shared, differences in enzyme composition and expression patterns were observed between species and isolates, suggesting variation in degradation strategies. These findings contribute to a better understanding of fungal wood degradation mechanisms and may support further research on wood durability, forest health and the management of fungal diseases in forest ecosystems.

INTRODUCTION

Wood degradation is a fundamental biological process in forest ecosystems, contributing to nutrient cycling and carbon turnover. At the same time, it significantly affects forest health, timber quality and the structural integrity of wood products (Goodell et al., 2020). Among wood-decaying organisms, white-rot fungi are recognized as the most efficient degraders of lignocellulosic biomass due to their ability to decompose all major plant cell wall components, including cellulose, hemicellulose, pectin and lignin (Sánchez, 2009; Li et al., 2022). This capability is mediated by a complex enzymatic system composed primarily of carbohydrate-active enzymes (CAZymes) and oxidative enzymes involved in lignin mineralization (Floudas et al., 2012; Sipos et al., 2017).

The plant cell wall forms the primary structural and defensive barrier of woody tissues. It is composed of cellulose microfibrils embedded in a matrix of hemicellulose and pectin, all reinforced by lignin (Showalter, 1993). White-rot fungi achieve coordinated degradation of these polymers through the secretion of cellulases, hemicellulases, pectinases and lignin-modifying enzymes such as laccases and peroxidases (Goodell et al., 2008). The degradation of lignin is particularly important, as this aromatic polymer limits access to structural polysaccharides within the cell wall.

Species of the genus *Armillaria* are among the most ecologically and economically important white-rot fungi affecting forest ecosystems. These fungi function both as saprotrophs decomposing dead wood and as necrotrophic pathogens causing root rot diseases in living trees (Baumgartner et al., 2011; Heinzelmann et al., 2019; Kedves et al., 2021). Their capacity to degrade woody tissues is directly linked to an extensive repertoire of plant cell wall degrading enzymes (PCWDEs), enabling efficient

colonization of both living and dead wood substrates (Sipos et al., 2017; Sahu et al., 2023). Among European species, *Armillaria ostoyae* is considered a highly virulent pathogen primarily associated with coniferous hosts, whereas *Armillaria borealis* generally exhibits weaker pathogenicity and broader ecological behavior (Heinzelmann et al., 2019; Kedves et al., 2021).

Recent advances in transcriptomics have enabled detailed investigation of fungal wood degradation mechanisms at the molecular level. Comparative analyses of gene expression provide valuable insights into the enzymatic systems activated during host colonization and lignocellulose decomposition. In particular, the study of fungal secretomes and CAZyme repertoires has become essential for understanding fungal adaptation to different ecological niches and degradation strategies (Girard et al., 2013).

Carbohydrate-active enzymes are categorized into several functional families, including glycoside hydrolases (GHs), carbohydrate esterases (CEs), auxiliary activity enzymes (AAs), glycosyltransferases (GTs) and carbohydrate-binding modules (CBMs) (Zhang et al., 2014). Previous genomic studies demonstrated that *Armillaria* species possess expanded repertoires of CAZymes associated with cellulose, hemicellulose, pectin and lignin degradation, highlighting their strong wood-decaying capabilities (Sipos et al., 2017; Sahu et al., 2023). However, differences in enzymatic composition and regulation between species with contrasting lifestyles remain insufficiently understood.

The present study focuses on the comparative analysis of wood degradation-related enzymes in *A. ostoyae* and *A. borealis*. Using transcriptomic analysis of fungal colonization in Norway spruce stem segments, the study investigates candidate genes associated with lignocellulose degradation, with particular emphasis on CAZyme families involved in the decomposition of cellulose, hemicellulose, lignin and pectin. The results aim to improve understanding of fungal wood degradation strategies and contribute to broader knowledge of forest pathology, wood durability and fungal ecology.

MATERIALS AND METHODS

Norway spruce (*Picea abies*) stem segments obtained from two recently felled trees were used for fungal colonization experiments. Trunks were cut into 10 cm segments and only undamaged sections were selected. Autoclaved stem segments were sterilized at 121 °C and 15 psi for 15 min to eliminate microbial activity and host defense responses, thereby enabling analysis focused specifically on wood degradation mechanisms.

High- and low-virulence isolates of *Armillaria ostoyae* and *Armillaria borealis* originating from Switzerland were used in the study (Heinzelmann et al., 2017). Fungal cultures were maintained on Roth and Shaw (RS) medium (Shaw and Roth, 1976) and incubated in darkness at 24 °C. Prior to the experiments, fresh cultures were established and grown for approximately three weeks.

Wood colonization was performed using an in vitro stem invasion assay adapted from Sipos et al. (2017). Developing mycelial fans were collected aseptically from infected stem segments, immediately frozen in liquid nitrogen and stored at -80 °C. Total RNA was extracted using the RNeasy Plant Midi Kit (Qiagen Inc.) following the manufacturer's protocol. RNA quality and quantity were assessed using Qubit fluorometric analysis.

Transcriptome libraries were prepared using the NEBNext Ultra II Directional RNA Library Prep Kit for Illumina following rRNA depletion with RiboCop kits (Lexogen). Sequencing was performed on an Illumina NovaSeq 6000 platform using paired-end 2 × 151 bp reads.

Raw reads were quality filtered using FastQC and Trimmomatic before alignment to the reference genomes of *A. ostoyae* and *A. borealis* using STAR. Gene expression levels were estimated with RSEM and normalized using the TMM method implemented in edgeR. Differential expression analysis was conducted using Limma-Voom with a significance threshold of $|\log2FC| \geq 2$ and FDR ≤ 0.05.

Functional annotation focused on genes associated with plant cell wall degradation. Carbohydrate-active enzymes (CAZymes) were identified using dbCAN2, while additional annotations were obtained using InterProScan, PANZERR and KofamScan. Candidate wood degradation genes were selected based on differential expression, predicted secretion signals and functional association with lignocellulose degradation.

RESULTS AND DISCUSSION

Both high- and low-virulence isolates of *Armillaria ostoyae* and *Armillaria borealis* successfully colonized autoclaved *Picea abies* stem segments.

RNA sequencing generated between 20.7 and 88.3 million reads per sample, with average mapping rates of 71% for *A. ostoyae* and 74% for *A. borealis*. Multidimensional scaling analysis revealed clear clustering according to species, virulence level and treatment, confirming distinct transcriptomic responses associated with wood colonization.

Differential expression analysis identified numerous genes related to wood degradation. Highly degrading isolates of *A. ostoyae* exhibited a greater number of constitutively upregulated genes and secreted proteins than *A. borealis*, suggesting a broader degradation strategy. Secretome analysis revealed extensive representation of carbohydrate-active enzymes (CAZymes) involved in degradation of cellulose, hemicellulose, lignin and pectin.

The results (Figure 1) demonstrate that both *A. ostoyae* and *A. borealis* possess diverse enzymatic systems capable of degrading major structural components of the plant cell wall. Shared cellulase families (GH1, GH3, GH6, GH7 and GH12) indicate coordinated cellulose degradation through synergistic endoglucanase and cellobiohydrolase activities, consistent with mechanisms previously described in white-rot fungi (Nagy et al., 2016; Hage and Rosso, 2021). Species-specific differences were also observed. *A. ostoyae* expressed AA16 enzymes potentially involved in disrupting cellulose crystallinity, while *A. borealis* showed inducible AA9 lytic polysaccharide monooxygenases, suggesting a more adaptive cellulose degradation strategy.

Both species also possessed a broad hemicellulose-degrading repertoire, including CE16, GH10, GH31, GH35 and GH51 families targeting xylan and related polymers. Unique enzymes such as GH29 in *A. ostoyae* and GH93 in *A. borealis* may reflect species-specific substrate preferences and ecological adaptations.

Lignin degradation represented one of the most pronounced differences between species. Both fungi expressed AA1_1, AA2 and AA3_2 lignin-modifying enzymes; however, *A. ostoyae* showed substantially higher abundance of laccases and aryl-alcohol oxidases associated with oxidative lignin breakdown. Additionally, constitutive expression of AA5_1 glyoxal oxidase in *A. ostoyae* suggests enhanced hydrogen peroxide generation supporting peroxidase activity and more efficient lignin mineralization (Floudas et al., 2012; Andberg et al., 2017).

Pectin degradation enzymes were also highly represented. While both species expressed CE8, CE12, GH28, GH78 and GH88 families, *A. ostoyae* possessed a substantially broader constitutive pectinolytic repertoire, including CBM67, GH53, GH105, PL1_7 and PL26 enzymes. The presence of inducible PL14_4 exclusively in *A. ostoyae* further suggests adaptation for efficient degradation of complex pectin structures. Expansion of pectinolytic CAZyme families in *Armillaria* species has previously been associated with necrotrophic pathogenicity and aggressive wood decay (Sipos et al., 2017; Champramary et al., 2022; Sahu et al., 2023).

CONCLUSIONS

Overall, the findings indicate that although both species utilize common white-rot degradation mechanisms, *A. ostoyae* possesses a broader and more constitutively expressed enzymatic repertoire, particularly for lignin and pectin degradation. In contrast, *A. borealis* appears to rely on a narrower and more inducible set of enzymes. These differences likely reflect distinct ecological strategies and substrate utilization patterns during wood colonization.

This work provides a molecular framework for understanding wood decay strategies in *Armillaria* and establishes candidate gene sets for future functional validation and potential applications in forest pathology management and fungal biotechnology.

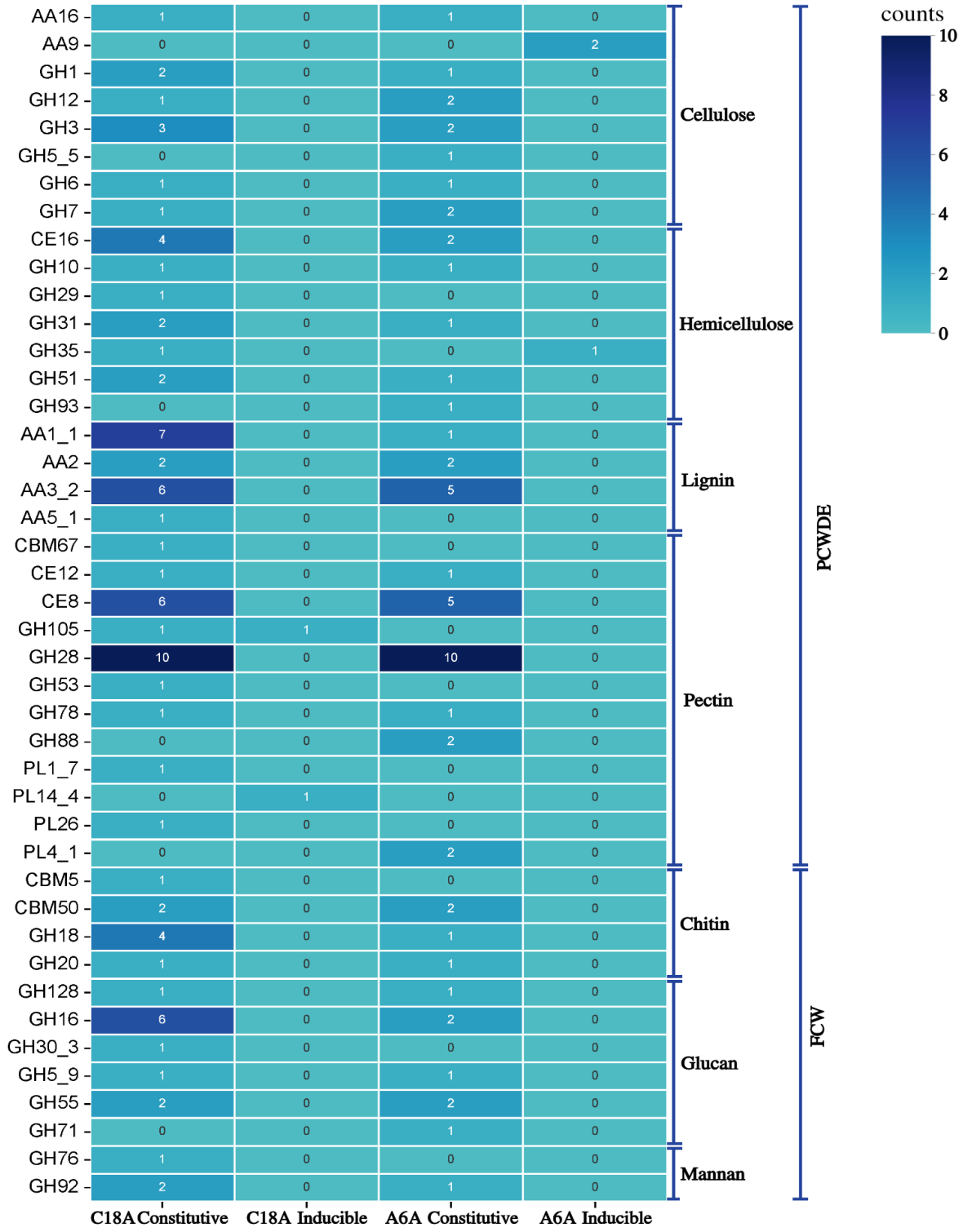

Figure 1: Distribution and abundance of CAZyme families in A. ostoyae (C18A) and A. borealis (A6A) incubated in autoclaved stems

REFERENCES

Andberg, M., Mollerup, F., Parikka, K., Koutaniemi, S., Boer, H., Juvonen, M., Master, E., Tenkanen, M., and Kruus, K. (2017). A novel *Colletotrichum graminicola* raffinose oxidase in the AA5 family. *Appl. Environ. Microbiol.*, 83(20), e01383-17. https://doi.org/10.1128/AEM.01383-17

Baumgartner, K., Coetzee, M. P., and Hoffmeister, D. (2011). Secrets of the subterranean pathosystem of *Armillaria*. *Mol. Plant Pathol.*, 12(6), 515–534. https://doi.org/10.1111/j.1364-3703.2010.00693.x

Champramary, S., Indic, B., Kredics, L., and Sipos, G. (2022). A comparison of the wood decay abilities of common white-rot fungi from the Carpathian Basin.

Floudas, D., Binder, M., Riley, R., Barry, K., Blanchette, R. A., Henrissat, B., et al. (2012). The Paleozoic origin of enzymatic lignin decomposition reconstructed from 31 fungal genomes. *Science*, 336(6089), 1715–1719. https://doi.org/10.1126/science.1221748

Girard, V., Dieryckx, C., Job, C., and Job, D. (2013). Secretomes: the fungal strike force. *Proteomics*, 13(3–4), 597–608. https://doi.org/10.1002/pmic.201200282

Goodell, B., Qian, Y., and Jellison, J. (2008). Fungal decay of wood: soft rot—brown rot—white rot. In *Development of Commercial Wood Preservatives*. ACS Symposium Series, 982, 9–31. https://doi.org/10.1021/bk-2008-0982.ch002

Goodell, B., Winandy, J. E., and Morrell, J. J. (2020). Fungal degradation of wood: Emerging data, new insights and changing perceptions. *Coatings*, 10(12), 1210. https://doi.org/10.3390/coatings10121210

Hage, H., and Rosso, M. N. (2021). Evolution of fungal carbohydrate-active enzyme portfolios and adaptation to plant cell-wall polymers. *J. Fungi*, 7(3), 185. https://doi.org/10.3390/jof7030185

Heinzelmann, R., Dutech, C., Tsykun, T., Labbé, F., Soularue, J. P., and Prospero, S. (2019). Latest advances and future perspectives in *Armillaria* research. *Can. J. Plant Pathol.*, 41(1), 1–23. https://doi.org/10.1080/07060661.2018.1558284

Heinzelmann, R., Prospero, S., and Rigling, D. (2017). Virulence and stump colonization ability of *Armillaria borealis* on Norway spruce seedlings in comparison to sympatric *Armillaria* species. *Plant Dis.*, 101(3), 470–479. https://doi.org/10.1094/PDIS-06-16-0933-RE

Kedves, O., Shahab, D., Champramary, S., Chen, L., Indic, B., Bóka, B., et al. (2021). Epidemiology, biotic interactions and biological control of armillarioids in the Northern Hemisphere. *Pathogens*, 10(1), 76. https://doi.org/10.3390/pathogens10010076

Li, T., Cui, L., Song, X., Cui, X., Wei, Y., Tang, L., Mu, Y., and Xu, Z. (2022). Wood decay fungi: An analysis of worldwide research. *J. Soils Sediments*, 22(6), 1688–1702. https://doi.org/10.1007/s11368-022-03225-9

Nagy, L. G., Riley, R., Tritt, A., Adam, C., Daum, C., Floudas, D., et al. (2016). Comparative genomics of early-diverging mushroom-forming fungi provides insights into the origins of lignocellulose decay capabilities. *Mol. Biol. Evol.*, 33(4), 959–970. https://doi.org/10.1093/molbev/msv337

Sahu, N., Indic, B., Wong-Bajracharya, J., Merényi, Z., Ke, H.-M., Ahrendt, S., et al. (2023). Vertical and horizontal gene transfer shaped plant colonization and biomass degradation in the fungal genus *Armillaria*. *Nat. Microbiol.*, 8, 1687–1703. https://doi.org/10.1038/s41564-023-01448-1

Sánchez, C. (2009). Lignocellulosic residues: biodegradation and bioconversion by fungi. *Biotechnol. Adv.*, 27(2), 185–194. https://doi.org/10.1016/j.biotechadv.2008.11.001

Showalter, A. M. (1993). Structure and function of plant cell wall proteins. *Plant Cell*, 5(1), 9–23. https://doi.org/10.1105/tpc.5.1.9

Sipos, G., Prasanna, A. N., Walter, M. C., O'Connor, E., Bálint, B., Krizsán, K., et al. (2017). Genome expansion and lineage-specific genetic innovations in the forest pathogenic fungi *Armillaria*. *Nat. Ecol. Evol.*, 1(12), 1931–1941. https://doi.org/10.1038/s41559-017-0347-8

Zhang, J., Bruton, B. D., and Biles, C. L. (2014). Cell wall-degrading enzymes of *Didymella bryoniae* in relation to fungal growth and virulence in cantaloupe fruit. *Eur. J. Plant Pathol.*, 139, 749–761. https://doi.org/10.1007/s10658-014-0429-2

Hardwood as a Sustainable Design Trend

Daniel Bodorkós[1*], József Zalavári[1], Péter György Horváth[1]

[1] University of Sopron, Institute of Creative Industries, Sopron, Hungary, 9400 Bajcsy-Zs. Str. 4.

E-mail: bodorkos.daniel@phd.uni-sopron.hu; zalavari.jozsef@uni-sopron.hu; horvath.peter.gyorgy@uni-sopron.hu

Keywords: design, interior design, sustainability, furniture.

ABSTRACT

In contemporary society, sustainable design extends beyond the boundaries of an aesthetic or ethical position and has emerged as a significant conceptual framework for interpreting objects, patterns of consumption, and the broader implications of everyday decision-making. In a cultural context increasingly shaped by rapidly changing trends, digitally mediated visibility, and identity-based self-representation, material culture has become both accelerated and hyper-visible. Within this environment, sustainable design assumes a critical role in counterbalancing the logic of "fast novelty" by foregrounding durability, reparability, and long-term value. In this sense, design should be understood not only as the creation of objects, but also as a practice that constructs meanings, shapes behavioural patterns, and mediates relationships between raw materials, production, use, and the intergenerational transmission of artefacts.

Against this background, hardwood products occupy a particularly important position in the fields of design and interior architecture, both as newly manufactured objects and as items recirculating through second-hand markets. The material characteristics of hardwood—such as its density, mechanical durability, and versatility in surface treatment—not only support extended product lifespans, but also embody aesthetic and tactile qualities closely aligned with the principles of slow design.

This study examines the criteria and foundational principles of sustainable interior architecture through the experiences and perspectives of professionals actively working in the field. The findings indicate that the integration of these principles into the design process can contribute to a coherent and ecologically conscious design methodology. Accordingly, such considerations should be treated as essential design criteria within the disciplines of design, interior architecture, and furniture design.

INTRODUCTION

Based on proposals for defining the concept of the contemporary, something may be considered contemporary if, from the perspective of the present, it reaches back roughly 40-50 years. In connection with this view, Vance Packard already described in accessible terms in his 1960 book The Waste Makers that consumer society increasingly produces objects with short lifespans, intended for rapid replacement (The Waste Makers 1960). Victor Papanek's 1971 work Design for the Real World, which became one of the best-known critiques of consumer design and irresponsible object design, and Rachel Carson's Silent Spring (1962) are similarly significant; these works can be regarded as early foundational texts of sustainable design and ecological thinking. The social significance of design lies in the fact that it shapes not only objects, services, and interfaces, but also people's everyday lives, behaviour, and possibilities. While it makes our environment more comfortable, more understandable, and safer, it also communicates values concerning what a society considers important: functionality, beauty, rapid consumption, or sustainability. For this reason, design has a responsibility to create solutions that are durable, repairable, reusable, and associated with a lower environmental burden. Social media platforms such as Instagram, TikTok, and Pinterest, together with affordably available interior design products, further accelerate trend cycles and consumption; these phenomena can be classified under the category of fast fashion furniture and decoration, which are characterised by short product lifespans and usage cycles (Furmston et al. 2025).

Hardwood in the Practice of Design and Interior Architecture

On the basis of the physical and strength properties of wood, a distinction can be made between coniferous woods, soft hardwoods, and hard hardwoods (Fehér 2017). Our research focuses on hardwood products, particularly in the fields of design and interior architecture, where these materials fulfil both visual and functional roles, primarily in the form of coverings and furniture. Although the outdoor application of hardwood also has considerable potential due to its durability and mechanical properties, our investigation is limited exclusively to solutions used in interior spaces.

Figure 1: Illustration based on Philip STARCK – Adela Rex Oak Chair

The oak chair shown in Figure 1 was designed by the French star designer Philip Starck for Andreu World. In the design of the chair, a tradition can be observed that refers back to the morphology of armchairs through a contemporary interpretation. The bent elements, the backrest, and the armrests lend the chair a soft, flowing character, which is counterbalanced by the legs constructed from more defined lines. The chair named Adela Rex supports our thesis that natural wood occupies a prominent position in contemporary interior architectural applications.

RESEARCH EXPERIENCE AND PROFESSIONAL PERSPECTIVES

The relevance of the research lies in the fact that while sustainability has become one of the fundamental considerations in design and interior architecture, consumer culture continues to be characterised by rapidly changing trends and products with short lifecycles. This tension is particularly important in the case of furniture, as furniture carries not only functional and aesthetic meanings, but also economic, cultural, and environmental ones. The research seeks to answer how respondents interpret sustainability, value-based design, and timelessness in relation to furniture, with particular attention to hardwood furniture as a possible sustainable alternative.

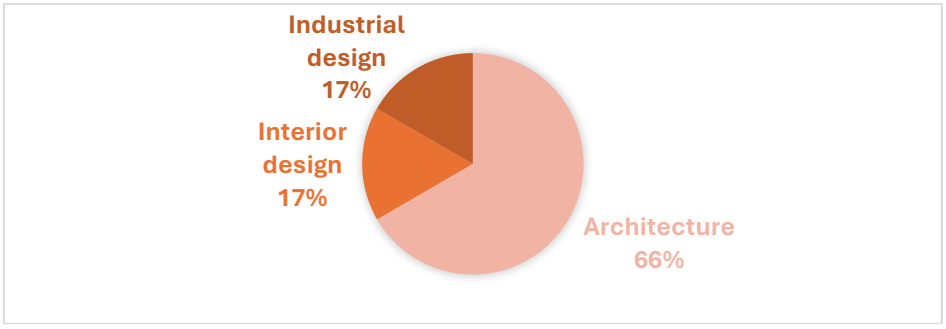

Figure 2: Distribution of professional fields

Taking these factors into account, the data shown in Figure 2 illustrate the proportional distribution of the professionals and professional actors who participated in the research. The respondents included university students who were already working in the creative industries and design professions, as well as students with active student status. The figure shows that a larger proportion of measurable and

analysable data came from the fields of architecture and architectural art. Architecture accounted for 66%, interior architecture for 17%, and product design for 17%. During the questionnaire-based survey, special attention was paid to sustainability and to the integration of this designer identity within the fields of product design, design, interior architecture, and architectural art.
The majority of respondents considered sustainability and timelessness to be particularly important: 50% of the participants in the pilot interview rated the importance of integrating sustainability into the design process as 4, while 41.7% rated it as 5, and 8.3% gave a value of 2. In relation to hardwood interior elements, especially oak and beech, the use of natural raw materials proved to be the most decisive factor (91.7%), followed by durability and repairability (83.3%). At the same time, only a smaller proportion of respondents, 25%, considered local production and the role of local actors to be decisive, which suggests that, for them, the concept of sustainability is primarily associated with long-term usability, durability, and timelessness.
Among respondents with an interior architectural background, the conscious application of value-based design principles is more frequent than among other professional groups. This suggests that training in interior architecture more strongly supports an approach based on the coordination of functionality, aesthetics, and user needs, as well as the recognition of long-term value creation. This relationship also highlights that professional background and professional socialisation play a significant role in the extent to which these principles appear consciously in design thinking.

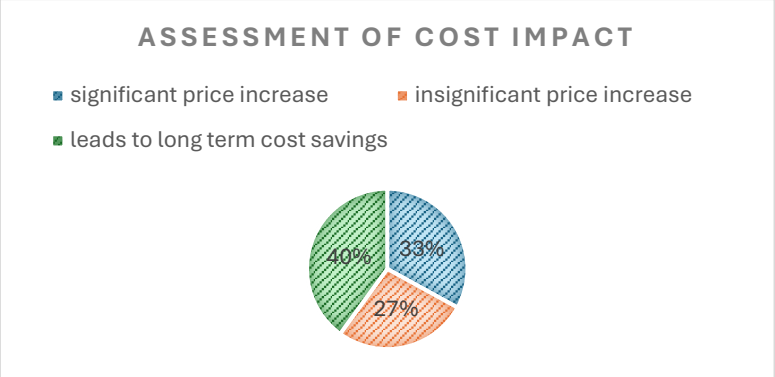

Figure 3: (Perceived cost impact x Price as a barrier)

Figure 3 shows that respondents who believe sustainable solutions significantly increase project costs generally also identified price as a barrier. The production and sale of sustainable solutions and products tend to result in products positioned in a higher price category. A certain percentage of consumers can "afford" this, meaning that purchasing a sustainable product does not represent a significant additional expense for them.

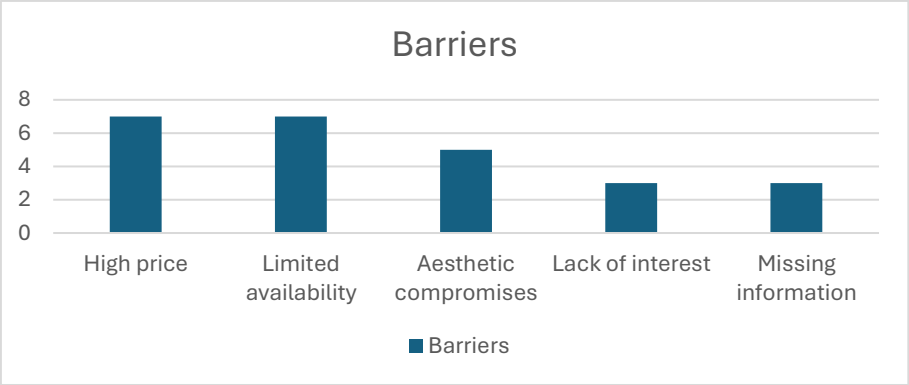

Figure 4: Barriers

The data presented in Figure 4 are intended to show the factors that hinder the application of interior architectural elements. Based on the data obtained from the pilot interview, it can be seen that high price and limited availability are the most frequent factors associated with interior architectural elements and furniture made from sustainable sources and raw materials.

CONCLUSION

In our present meta-society, the integration of sustainable raw materials into product design is a pivotal issue. The complex systems of criteria that determine sustainable product positioning constitute an extremely important step for environmentally conscious product design, architecture, and interior architecture. The physical and mechanical properties of hardwood form a synergy with its aesthetic value and quality, which are expressed in the texture and structure of its surfaces. Throughout the mutual history of hardwood and humankind, numerous examples demonstrate that it is a sustainable material that fits perfectly into the circular economy. In our pilot questionnaire, we examined the thinking of professional actors in relation to this topic. Based on the responses received, the balance clearly tilted in a positive direction, toward the application of sustainability in design. In light of the pilot nature and experiences of this questionnaire, we plan to repeat the study in the future with additional aspects and questions, using a broader sample and involving more actors in the research.

REFERENCES

Azemeraw Tadesse Mengistu, Marcos Dieste, Roberto Panizzolo, Stefano Biazzo (2024): Sustainable product design factors: A comprehensive analysis, https://doi.org/10.1016/j.jclepro.2024.142260

Bednárik Éva and Pakainé Kováts Judit (2011): Consumer Behaviour in the Furniture Market, University of West Hungary Press, ISBN 978-963-9883-78-9

BM Certification (2023): EUDR and FSC/PEFC compliance. Accessed: 2026.01.03. https://hu.bmcertification.com/az-europai-unio-erdoirtasmentes-termekekrol-szolo-rendelete-eudr-megfelel-az-fsc-es-a-pefc-felugyeleti-lanc-rendszerenek/

Dr. Fehér Sándor (2017): Technical Knowledge course, university lecture notes, NYME FMK Institute of Wood Science, 2017, Sopron.

Ecodesign, Environmental Regulations (2022): Guide To Sustainable Product Design (2024 Update), https://ecochain.com/blog/guide-to-sustainable-product-design/

Ellen MacArthur Foundation (EMF). (2019): *Completing the Picture: How the Circular Economy Tackles Climate Change*. Cowes: Ellen MacArthur Foundation. https://circulareconomy.europa.eu/platform/sites/default/files/emf_completing_the_picture.pdf

European Parliamentary Research Service EPRS (2024): Ecodesign for sustainable products https://www.europarl.europa.eu/RegData/etudes/BRIE/2022/733524/EPRS_BRI(2022)733524_EN.pdf#:~:text=Further%20steps%20were%20detailed%20in%20the%20new,many%20are%20made%20for%20single%20use%20only'.

Födémes Zoltán (2025): The Circular Economy and Sustainable Fashion, University of Pannonia Faculty of Business and Economics, Zalaegerszeg, https://perepo-dolgozat.uni-pannon.hu/id/eprint/26432/1/f%C3%B6demes_zolt%C3%A1n_2025jan_publikus.pdf

Furmston, K. & Braithwaite, N. (2025): How “Fast” is Fast Furniture?; Proceedings of the 6th PLATE Conference – Product Lifetimes and the Environment 2025, Aalborg, Denmark, 2–4 July 2025. Aalborg University, Aalborg

Herman Miller (2024): Sustainability Report FY24. Accessed: 2026.01.03. [https://www.hermanmiller.com]

Horváth Balázs (2019): The Sick Planet - A Cultural History of Unsustainability and Disease. Typotex Publishing House. ISBN 9789634930617

IKEA 2024 Sustainability Report, Inter IKEA Systems B.V., 2025. Accessed: 2026.01.01. https://www.ikea.com/hu/hu/files/pdf/46/26/46265c83/ikea_hu_25.pdf

ISO 14040. (2006): Life Cycle Assessment - Principles and Framework. https://www.cscses.com/uploads/2016328/20160328110518251825.pdf [Last downloaded: 2025.11.13.]https://www.cscses.com/uploads/2016328/20160328110518251825.pdf

Jem Bendell and Rupert Read 2021, Hungarian translation by Stumpf-Bíró Balázs (2023): Deep Adaptation: Navigating the Realities of Climate Chaos, L’Harmattan Publishing House, Budapest, ISBN 9789636460181, ISSN 3004-0574 [2025.12.05.]

Kalina Prelikj (2025): Fast Furniture and Micro-Trends: How Consumer Culture Is Destroying Good Design https://architizer.com/blog/inspiration/stories/fast-furniture-micro-trends-consumer-culture-destroying-good-design

Katryn Furmston, Naomi Braithwaite (2025): How "Fast" is Fast Furniture? Research paper, Nottingham Trent University, Nottingham, UK, 6th PLATE, Product Lifetime And The Environment 2025 Conference Aalborg, Denmark, 2-4 July 2025

Paola Bertola (2024): Designing Sustainability Today: An Analytical Framework for Sustainable Design (MDPI Sustainability, 2024). https://doi.org/10.3390/su16083240

Papanek, V. (1971): Design for the Real World. Pantheon Books. ISBN: 9780500295335

Pogátsa Zoltán (2023): Sustainable Economy or Social Collapse. Kossuth Publishing House, Budapest. ISBN: 9789635449804

Rachel Caron (2025): What is sustainable design, https://blogs.sw.siemens.com/digital-transformation/sustainable-design/

Rachel Louise Carson (1962): Silent Spring, Hungarian translation: 2007, Katalizátor Publishing House, ISBN: 9789638639646

Reményi, A. (2022): The Relationship Between Sustainability and Design in Hungarian Furniture Manufacturing. Gazdaság & Társadalom / Journal of Economy & Society 15 (33) (2022) 4, 21-46. DOI: https://doi.org/10.21637/GT.2022.4.02

Retail Insider: How Young Shoppers Are Currently Revolutionizing The Home Décor Marketplace https://retail-insider.com/articles/2026/03/how-young-shoppers-are-currently-revolutionizing-the-home-decor-marketplace

Shamraiz Ahmad [a b], Kuan Yew Wong [a], Ming Lang Tseng [c], Wai Peng Wong [d] (2018): Sustainable product design and development: A review of tools, applications and research prospects, https://doi.org/10.1016/j.resconrec.2018.01.020

Steelcase (2024): Cradle-to-Cradle Certification Report. Accessed: 2026.01.03. [https://www.steelcase.com]

Sustainable product design https://www.upm.com/solutions-and-innovations/product-development/product-stewardship/sustainable-product-design/

Vance Packard (1960): The Waste Makers, Printed in Great Britain by Lowe & Brydone (Printers) Ltd., London, N.W.10

Vantia (2026): What 2025 Taught Us About Hardwood Flooring Trends — and What to Expect in 2026 https://www.vantiahardwoods.com/hardwood-flooring-blog/what-2025-taught-us-about-hardwood-flooring-trends-and-what-to-expect-in-2026/

Vitra (2024): Sustainability Report 2024. Accessed: 2026.01.03. https://static.vitra.com/static/external/vitra-bhag/assets/Vitra-Sustainability-Report-2024-EN.8afcd3c6.pdf

Zalavári József (2008): Designing Form - Design Ecology, Scolar Publishing House, ISBN 9789632440446.

Stakeholder Perspectives on Swedish Hardwood Solid Wood Value Chains: A Delphi–Based SWOT Analysis

Victor Grubîi[1*], Jimmy Johansson[1], Sebastian Svensson Meulmann[1]

[1] Department of Forestry and Wood Technology, Faculty of Technology, Linnaeus University, Växjö SE 35195, Sweden
E-mail: victor.grubii@lnu.se jimmy.johansson@lnu.se sebastian.svenssonmeulmann@lnu.se

Keywords: birch (*Betula* spp.); Delphi; hardwood; sawmill processing; SWOT analysis; wood value chains.

ABSTRACT

The processing of solid hardwood timber in Sweden has steadily declined since its peak in the mid-1990s. At the same time, the standing volume of hardwood species has steadily increased and now represents approximately 20% of the total standing volume, with birch species (*Betula spp.)* constituting the majority. Despite the growing availability of hardwoods, their predominant use in pulp, paper, and energy applications reflects a relatively low–value utilization. Consequently, hardwood solid wood processing value chains require strategic adaptation to evolving market conditions to enhance their competitiveness. Therefore, this study aims to assess the current competitiveness of Swedish hardwood solid wood processing value chains and to identify strategic development areas needed to strengthen and advance them.

To address this aim, the study examined the internal and external factors shaping hardwood value chains in Sweden by applying a SWOT analysis. The method involved a combined literature–based and panel–based SWOT analysis using a Delphi method. Two Delphi rounds were conducted to evaluate a literature–based SWOT matrix together with identification of additional factors impacting the hardwoods solid wood processing value chains in Sweden. The Delphi method of the SWOT analysis was based on online surveys distributed to a panel of specialists within various stakeholder groups, i.e., forestry and forest management, the processing industry, markets and distribution, academia and governmental organisations.

The identified main challenge was the lack of sawmills, which reduces interest in hardwood forestry and contributes to insufficient forest management. The steadily increasing demand for wood products was ranked as the greatest strength of the hardwood value chain. The panel identified the main opportunity the innovation and new knowledge in product development and processing in order to strengthen the competitiveness of the wood products industry. The greatest threat was identified as competition for raw materials from other industries, namely pulp and paper, and bioenergy.

The paper further provides insight into how perceptions of hardwood value chains in Sweden differ among stakeholder groups, emphasising the need for coordinated planning to align future raw-material supply with competitive and resilient value chains.

INTRODUCTION

Climate change and the increasing competition for softwood raw material are expected to put pressure on softwood supply chains; thus, hardwoods are likely to play an increasing role in the future forest value chains. A notable change in hardwoods survivability and extension of their endemic habitats is predicted in hemi-boreal and boreal forests (Mauri et al. 2022). In these forests, hardwoods already represent a significant standing volume, e.g., in Sweden ca. 630 $\times 10^6$ m^3 or 20% of the total standing volume (Skogsdata 2024), approximately 513 $\times 10^6$ m^3 or ca. 20% in Finland (Natural Resources Institute Finland 2025), 257 $\times 10^6$ m^3 or 25% in Norway (Statistisk sentralbyrå 2025). The most common hardwoods are silver and downy birch (*Betula pendula* Roth and *Betula pubescens* Ehrh.), European aspen (*Populus tremula* L.), alder (*Alnus spp*.), oak (*Quercus spp*). Other hardwoods that may be endemic to the hemi-boreal forests but have limited availability and/or quality for industrial utilisation include beech, ash, willow, cherry, and elm.

The utilization of hardwoods is dominated by pulp and paper production; for example, in Sweden, 6.5 $\times 10^6$ m^3 of pulp production is based on hardwoods, representing 17.9% of produced pulp (Björklund et

al. 2024). The use of hardwood for energy production is estimated at 3.5 – 6 $\times 10^6$ m^3 (Johansson 2008). In comparison, the use of hardwoods for timber production is only 0.17 $\times 10^6$ m^3 (Björklund et al. 2024), of which the majority originates from oak sawmilling. Hardwood production peaked in mid–1990s, when about 0.4 $\times 10^6$ m^3 logs were processed annually (Nylinder et al. 2006).

The reduction in hardwood consumption can be partly attributed to the change in product construction i.e. the substitution of solid wood with fibreboards in the furniture production (Luostarinen and Verkasalo 2000), as well as global competition and economic recessions (Karlsson et al. 2011). Hardwoods such as birch and beech have been shown to possess advantageous properties in engineered structures and at timber level (Jeitler et al. 2016; Glavinic et al. 2020; Lemke et al. 2023). Despite the technical potential, their use remains limited, which suggests that the true barriers could be insufficient standardisation, certification, and market acceptance for load-bearing applications.

To understand the potential competitiveness of the hardwood solid wood processing (HSWP) value chains and the regional specifics it is critical to map the existing state and determine its main challenges and opportunities. The competitiveness is defined hereby as the capacity of HSWP value chains to create and capture value both sustainably and economically favourable to alternative value chains and land-use options. The objective of the study was to identify key challenges and opportunities in the HSWP value chains particular to Sweden.

MATERIAL AND METHODS

To address the study objectives, a hybrid SWOT analysis was conducted using a Delphi method implementation, referred to in the literature as the hybrid SWOT–Delphi method (Auer and Rauch 2021). In this approach, the initial SWOT framework is developed based on literature review and authors' interpretation of existing evidence and is subsequently refined and validated through iterative consultation with an expert panel.

SWOT analysis is a common tool for assessing the competitiveness of an organisation or an entire sector the (Pesonen et al. 2001). It identifies internal and external factors affecting performance, categorised into strengths, weaknesses, opportunities and threats. Its simplicity and practicality have made it a common tool in business and strategic management. In the forest sector, SWOT has been used to analyse various aspects of the forest products value chains, including the competitiveness of hardwoods value-chains in Sweden (Karlsson et al. 2011) and Germany (Auer and Rauch 2021).

Some drawbacks of the SWOT method are the lack of factor–weighting and a degree of subjectivity due to its often ad-hoc application (Pesonen et al. 2001). To address these shortcomings, SWOT may be extended using analytical hierarchy approaches that allow for the quantification and prioritisation of factors (Pesonen et al. 2001; Auer and Rauch 2021). Nevertheless, the reliability of the SWOT–based methods is dependent on the implementation method and may suffer from subjectivity bias. To compensate that, implementing the SWOT matrix using the Delphi method was suggested by Auer and Rauch (2021) particularly in a broad sector such as HSWP value chains, due to diverse stakeholders stance. The goal with Delphi implementation is to find a weighted solution by finding the consensus among the inquired groups.

The initial SWOT matrix was generated using a non–systematic literature review using knowledge of relevant sources focused on HSWP and a *Web of Science* search. The search included keywords such as *hardwoods*, *birch*, *alder, aspen,* further refined by their relevance to timber production.

Subsequently, a SWOT evaluation was carried out using the Delphi method. Experts representing both existing and potential HSWP value chains in Sweden were invited to assess the identified SWOT factors. This was performed using anonymous sequential online surveys, consistent with Delphi requirements.

The expert panel was structured around five stakeholder groups: forest management, wood products industry, markets and distribution, academia, and governmental organisations (Table 1). The panel of experts from the commercial sectors, i.e., forest management, processing industry, and market and distribution was selected based on recommendations from industry networks and reputational knowledge of active companies in the field. Respondents from academia group were selected based on a Web of Science database inquiry using keyword "hardwoods", limited to Sweden and publications from the past 25 years. Additionally, the respondent list was completed using a web search using keyword *hardwoods*.

The SWOT rounds were conducted using web surveys during April–June 2025. For survey management, the *SR flow* (Artologik, Växjö, Sweden) was used. Round I survey was sent to 42 (out of 103 selected)

respondents that answered positively to participation invitation. The survey included mandatory questions on SWOT factors, graded based on their importance on a 1–5 Likert scale (1=insignificant, 5=very important). In addition, respondents were asked to provide a non–mandatory commentary related to the answer to the question. The literature–based SWOT matrix contained 22 factors (six strengths, seven opportunities, six strengths, and three threats). In round I, respondents were asked to provide one additional factor per category. In round II, respondents were asked to regrade the original SWOT matrix plus the newly identified factors, selected based on the most common occurrence principle. The final SWOT matrix contained 29 factors. To assess whether respondents' evaluations changed between the two Delphi rounds, a paired t–test was conducted in *MATLAB* (MathWorks, Natick, MA, USA). This method was used to determine whether the mean ratings assigned by the same respondents differed significantly between rounds.

Table 1: Number of participants in the two Delphi rounds based on the stakeholder group

Category	No. participants round I	No. participants round II
Forestry (forest management)	6	5
Industry (wood processing and wood products)	8	3
Academia and governmental organisations	7	1
Market and supply chains	3	2
Total	24	11

RESULTS AND DISCUSSION

Results of the literature and Delphi–based SWOT analysis are presented in Table 2. A paired t–test showed no significant variation between the two Delphi rounds ($t(21)= -1.267$, $p=0.22$, 95% CI [-0.15 0.04]). This suggests that respondents' evaluations were consistent across rounds. At the individual level, the change in responses between rounds ranged from 0 to 1.14 points per question. A Delphi effect was also observed based on respondents who answered both rounds who tended to adjust their evaluations towards the Round I mean.

All the literature–based factors were graded as of fair to high importance, indicating potential similarities in the competitiveness of HSWP value chains across regional contexts. More notably, at least one panel-derived factor in each SWOT category was assigned high importance, highlighting the knowledge of the participating panel on HSWP value chains in Sweden.

Weaknesses

The highest scoring weakness factors was identified by the panel and constituted the depart point of this study – *the lack of sawmill and further processing (W7)*. Although this factor has limited strategic base, it reflects a fundamental constraint within the HSWP in Sweden. Another highly–rated weakness was the *lack of proper forest management and other biotic and non-biotic factors (W6)*. This factor reflects both a limited knowledge of quality–oriented hardwood silviculture and the practical difficulty of obtaining high–quality timber due to bordering endemic conditions for hardwoods growth in Sweden. The third highest–ranked weakness was found to be a *lack of knowledge for optimal material processing and handling various material properties (W5)*. Panel comments suggested that hardwoods are often more difficult to process to consistent quality standards, partly because softwood-based production technologies, such as sorting criteria and drying practices, are not always directly transferable.

Opportunities

The panel identified *innovation and new knowledge in product and process development* (O3) as the most important opportunity factor for strengthening HSWP value chains in Sweden. Respondents emphasised the role of innovation and knowledge development in improving hardwood utilisation in finished products with the goal to develop optimal value chains, new product categories and applications, and provide a sustainable raw material utilisation. Another high–rated opportunity was *the development of forest management and plant breeding to improve wood quality (O5)*. This factor received a lower score in Round I compared to Round II, which may reflect differing views among participants regarding whether current hardwood quality and availability are sufficient, or whether

improved silviculture and breeding programmes are necessary to enhance the competitiveness of HSPW value chains. The third highest–ranked opportunity consisted in *supporting biodiversity (O8)* aspect of hardwoods. Participants highlighted species such as birch and aspen as pioneer species with an important ecological role in supporting biodiversity.

Threats

The highest–ranked threat factor was the *raw material competing industries, such as pulp and energy (T2)*. Mölle and Fors (2023) noted that forest owners may sell potentially sawable timber as pulpwood because of sorting practices and high penalisation fees. Competition from bioenergy was also considered important, especially in relation to rising fuel prices. The second highest–rated threat was the *limited interest in hardwoods among both society and industry (T4)*. The panel comments point to a situation in which industrial priorities remain focused on large–scale production systems characteristic of softwood processing. This also appears to be linked to limited product development, weak market positioning, and insufficient innovation in sawmill–based hardwood utilisation (Makkonen 2019).

Strengths

The highest–ranked strength was the *strong demand for wood products (S2)*. The panel viewed the market needs as prerequisite for the development of sustainable HSWP value chains. Several other strengths received similarly high scores in Round II (all rated 4.09, corresponding to "important"), including *raw material availability (S1)*, *good hardwood productivity (S4)*, and *existing knowledge of hardwood forestry (S8)*. Together, these results suggest that the panel recognised a broader shift in Sweden, in which hardwoods, particularly birch, are increasingly seen not as unwanted species but as a potentially viable industrial resource.

Table 2: SWOT factors ranking scores for the 1st and 2nd Delphi rounds (grading scale 1 to 5)

	Factors	Ref.	Round I		Round II	
			Mean	St. dev	Mean	St. dev
W1	Low share of hardwoods in final cuts	(Mölle and Fors 2023)	3.46	1.31	3.36	0.77
W2	Lack of product applications and marketing; niched and fragmented market	(Espinoza and Buehlmann 2018; Makkonen 2019)	3.58	1.21	3.82	0.83
W3	Lower volume production of hardwoods compared to softwoods	(Hynynen et al. 2009)	3.24	0.99	3.27	0.75
W4	Lower processing productivity compared to softwoods, e.g. longer drying time, processing yield, quality issues	(Perre 2007; Hiltunen et al. 2008; Espinoza and Buehlmann 2018; Adhikari 2020)	3.79	1.00	3.55	0.89
W5	Lack of knowledge for optimal material processing and handling various material properties	(Heräjärvi 2002; Bond and Araman 2008; Gazo et al. 2018)	3.88	0.91	3.91	0.51
W6	Lack of proper forest management and other factors, e.g. browsing and climate impacting low quality	(Karlsson et al. 2011; Morin et al. 2016)	3.64	1.16	4.09	0.79
W7*	Lack of sawmill and further processing				4.36	0.77
W8*	Logistics shortcomings in handling low harvest volume				3.36	0.88
O1	Challenges in softwood supply chains and imports of hardwood	(Kogler and Rauch 2023; Björklund et al. 2024)	3.67	0.85	3.55	0.78
O2	Economic feasibility evaluation of products and the scale of product categories	(Verkasalo et al. 2007; Nicholls and Bumgardner 2015; Verkasalo et al. 2017)	3.83	0.76	3.36	0.98
O3	Innovation and new knowledge in product and process development	(Karlsson et al. 2011; Woxblom L. 2025)	4.20	0.75	4.18	0.57
O4	Existence of vertically integrated organisations and cluster associations to increase cooperation and information flow	(Brege et al. 2010; Karlsson et al. 2011)	3.32	1.01	3.36	0.48
O5	Development in forest management and plant breeding to improve wood quality	(Hynynen et al. 2009; Fahlvik et al. 2021; Jones 2022)	3.72	1.15	4.18	0.57

O6	Improved human well-being in the living environment and current design trends towards wood material	(Alapieti et al. 2020)	3.44	0.94	3.64	0.48
O7	Possibility to improve the employment rate in remote areas	(Karlsson et al. 2011)	3.08	1.19	3.00	0.43
O8*	Support biodiversity				3.91	0.67
O9*	Increased forest carbon sequestration				3.64	0.88
T1	Global competition and unstable markets	(Karlsson et al. 2011; Bumgardner et al. 2014)	3.62	0.74	3.64	0.64
T2	Raw material competing industries, i.e., pulp and paper, and bioenergy	(Björklund et al. 2024)	4.19	0.88	4.27	0.75
T3	Hardwood pathogens, e.g. ash dieback, Dutch elm disease	(Norkutė 2018)	3.08	1.02	3.00	0.43
T4*	Lack of interest and engagement from society and industry towards hardwood				4.18	0.72
S1	Raw material availability	(Skogsdata 2024)	4.12	0.75	4.09	0.51
S2	Stable and increasing demand for wood products	(Jonsson et al. 2021)	4.20	0.75	4.36	0.64
S3	Advantageous properties, such as mechanical properties, lack of extractives and appearance	(Palm et al. 2005; Johansson et al. 2013; Jeitler et al. 2016)	3.38	1.15	3.45	0.78
S4	Good productivity and new stand establishment of certain hardwoods, e.g. birch	(Hynynen et al. 2009; Dubois et al. 2020; Fahlvik et al. 2021)	3.85	0.99	4.09	0.67
S5	Improved biodiversity of mixed species forestry	(Liziniewicz 2009; Fahlvik et al. 2021)	3.46	1.28	3.64	0.64
S6	Improved forest resilience through mixed species forestry	(Dubois et al. 2020)	3.65	0.87	3.82	0.83
S7*	Utilising current logistics and supply chains				3.36	0.88
S8*	Good knowledge of hardwood forest management and sawmill production				4.09	0.51

**Panel-identified factors*

CONCLUSIONS

Key challenges and opportunities in the Swedish hardwoods solid wood processing value chains were identified through a combined literature review and SWOT–Delphi analysis. The main challenges identified were the limited sawmilling and downstream processing capacity, the lack of quality–oriented forest management, and insufficient knowledge of optimal material handling. The study also indicated that key opportunities for strengthening Swedish hardwood value chains lie in the development of new products and processes, together with advances in quality–oriented forest management, including plant breeding

ACKNOWLEDGEMENTS

The authors gratefully acknowledge the support from the Knowledge Foundation through the project ‘Competitive timber structures – Resource efficiency and climate benefits along the wood value chain through engineering design’ (grant number 20230005).

REFERENCES

Adhikari S (2020) Assessment of Cross Laminated Timber Markets for Hardwood Lumber. Virginia Polytechnic Institute & State University

Alapieti T, Mikkola R, Pasanen P, Salonen H (2020) The influence of wooden interior materials on indoor environment: a review Eur J Wood Wood Prod 78:617-634

Auer V, Rauch P (2021) Developing and evaluating strategies to increase the material utilisation rate of hardwoods: a hybrid policy Delphi-SWOT analysis Eur J Wood Wood Prod 79:1419-1433 https://doi.org/10.1007/s00107-021-01725-y

Björklund L, Jägbrant S, Persson L (2024) Skogsindustrins virkesförbrukning 2019-2023.

Bond B, Araman P Effect of curve sawing on lumber recovery and warp of short cherry logs containing sweep. In: 16th central hardwoods forest conference, 2008. pp 105–113

Brege S, Nord T, Sjöström R, Stehn L (2010) Value-added strategies and forward integration in the Swedish sawmill industry: positioning and profitability in the high-volume segment Scand J For Res 25:482-493 https://doi.org/10.1080/02827581.2010.496738

Bumgardner M, Johnson S, Luppold W, Maplesden F, Pepke E (2014) Market and Market Forces for Lumber. In: Hansen EP, R.; Vlosky, R., eds. (ed) The global forest sector: changes, practices and prospects. CRC Press, Boca Raton, FL, pp 41-76

Dubois H, Verkasalo E, Claessens H (2020) Potential of Birch (Betula pendula Roth and B. pubescens Ehrh.) for Forestry and Forest-Based Industry Sector within the Changing Climatic and Socio-Economic Context of Western Europe Forests 11:336

Espinoza O, Buehlmann U (2018) Cross-Laminated Timber in the USA: Opportunity for Hardwoods? Current Forestry Reports 4:1-12 https://doi.org/10.1007/s40725-018-0071-x

Fahlvik N et al. (2021) Björkens möjligheter i ett framtida klimatanpassat brukande av skogen. Uppsala

Gazo R, Wells L, Krs V, Benes B (2018) Validation of automated hardwood lumber grading system Comput Electron Agric 155:496-500 https://doi.org/10.1016/j.compag.2018.06.041

Glavinic IU, Boko I, Toric N, Vrankovic JL (2020) Application of hardwood for glued laminated timber in Europe Gradevinar 72:607-616 https://doi.org/10.14256/jce.2741.2019

Heräjärvi H (2002) Properties of birch (Betula pendula, B. pubescens) for sawmilling and further processing in Finland., Forest Research Institute

Hiltunen E, Mononen K, Alvila L, Pakkanen TT (2008) Discolouration of birch wood: analysis of extractives from discoloured surface of vacuum-dried European white birch (Betula pubescens) board Wood Sci Technol 42:103-115 https://doi.org/10.1007/s00226-007-0143-8

Hynynen J, Niemistö P, Viherä-Aarnio A, Brunner A, Hein S, Velling P (2009) Silviculture of birch (Betula pendula Roth and Betula pubescens Ehrh.) in northern Europe Forestry 83:103-119 https://doi.org/10.1093/forestry/cpp035

Jeitler G, Augustin M, Schickhofer G GLT+CLT - Mechanical properties of Glued Laminated Timber and Cross Laminated Timber produced with the wood species birch. In: WCTE 2016 - World Conference on Timber Engineering Article MS1-07:2 Wien, 2016. Technische Universität

Johansson J (2008) The Swedish hardwood sawmill industry: Structure, present status and development potential Wood Mater Sci Eng 3:94-101 https://doi.org/10.1080/17480270902778135

Johansson M, Säll H, Lundqvist S-O (2013) Properties of materials from Birch – Variations and relationships : Part 2. Mechanical and physical properties. Linnaeus University, Växjö

Jones G (2022) Birch Stem and Wood Traits in Genetic and Silviculture Trials in Southern Sweden. Doctoral thesis, comprehensive summary, Linnaeus University Press

Jonsson R, Rinaldi F, Pilli R, Fiorese G, Hurmekoski E, Cazzaniga N, Robert N, Camia A (2021) Boosting the EU forest-based bioeconomy: Market, climate, and employment impacts Technol Forecast Soc Change 163:120478 https://doi.org/10.1016/j.techfore.2020.120478

Karlsson R, Palm J, Woxblom L, Johansson J (2011) Konkurrenskraftig kundanpassad affärsutveckling för lövträ - Metodik för samordnad affärs- och teknikutveckling inom leverantörskedjan för björkämnen. Sveriges lantbruksuniversitet, Institutionen för skogens produkter, Uppsala

Kogler C, Rauch P (2023) Lead time and quality driven transport strategies for the wood supply chain Res Transp Bus Manag 47:100946 https://doi.org/10.1016/j.rtbm.2023.100946

Lemke U, Johansson M, Ziethén R, Briggert A (2023) New Criteria For Visual Strength Grading Of Sawn Timber From Birch Grown In Sweden. https://doi.org/10.52202/069179-0102

Liziniewicz M (2009) The development of beech in monoculture and mixtures. Swedish University of Agricultural Sciences

Luostarinen K, Verkasalo E (2000) Birch as sawn timber and in mechanical further processing in Finland. A literature study Silva Fenn Monogr 1 https://doi.org/10.14214/sf.sfm1

Makkonen M (2019) Renewing the sawmill industry: studies on innovation, customer value and digitalization Dissertationes Forestales 269

Mauri A, Girardello M, Strona G, Beck PSA, Forzieri G, Caudullo G, Manca F, Cescatti A (2022) EU-Trees4F, a dataset on the future distribution of European tree species Scientific Data 9:37 https://doi.org/10.1038/s41597-022-01128-5

Mölle E, Fors O (2023) Björktimmer i svenskt skogsbruk - En studie över björkens potential i timmerproduktion. Bachelor thesis, Sveriges lantbrukuniversitet, SLU

Morin RS, Pugh SA, Steinman J (2016) Mapping the occurrence of tree damage in the forests of the northern United States. U.S. Department of Agriculture, Forest Service, Northern Research Station. https://doi.org/10.2737/nrs-gtr-162

Natural Resources Institute Finland (2025) Growing stock volume on forest land and on poorly productive forest land on mineral soils and peatlands by tree species by inventory, region, principal site class group and tree species. Natural Resources Institute Finland

Nicholls D, Bumgardner M (2015) Low-grade and character-marked hardwoods: A research review and synthesis of solid wood manufacturing and marketing The Forestry Chronicle 91:548-559 https://doi.org/10.5558/tfc2015-094

Norkutė G (2018) Characterization of populations of invasive pathogens–causal agents of three major forest tree diseases: alder decline, Dutch elm disease, and ash dieback., Vilniaus universitetas.

Nylinder M, Woxblom, L., Fryk H, lantbruksuniversitet S (2006) Ädellöv : Virke och förädling (2. uppl.. ed.). Sveriges lantbruksuniversitet, SLU

Palm J, Åhström A, Wijk G, Johansson S (2005) FAKTA OM LÖVTRÄ. Nässjö

Perre P (2007) Fundamentals of wood drying. A.R.BO.LOR & European COST

Pesonen M, Kurttila M, Kangas J, Kajanus M, Heinonen P (2001) Assessing the Priorities Using A'WOT Among Resource Management Strategies at the Finnish Forest and Park Service For Sci 47:534-541 https://doi.org/10.1093/forestscience/47.4.534

Skogsdata (2024) Aktuella uppgifter om de svenska skogarna från SLU Riksskogstaxeringen

Tema: Arter. Institutionen för skoglig resurshushållning, SLU Umeå, Infra service, SLU, Uppsala 2024

Landsskogtakseringen (2025) https://www.ssb.no/en/jord-skog-jakt-og-fiskeri/skogbruk/statistikk/landsskogtakseringen. Accessed 14 April 2026

Verkasalo E, Heräjärvi H, Arponen J, Toppinen A Perspectives of wood resources, industry competitiveness and wood product markets for birch industries in the Baltic Sea area. In: Blanchet Pe (ed) SCHP '07 International Scientific Conference on Hardwood Processing, Quebec City, 2007. FP Innovations, Division Forintek, pp 29-35

Verkasalo E, Heräjärvi H, Möttönen V, Haapala A, Brännström H, Vanhanen H, Miina J Current and Future Products as the Basis for Value Chains of Birch in Finland. In: 6th International Scientific Conference on Hardwood Processing, 2017.

Woxblom L. (2025) Björk som material i byggande - En intervjustudie om attityder och tankar hos aktörer i kedjan från plantförädling till produktion av träbyggsystem. Skogforsk

Redesign of a Chair Prototype – A Case Study

Mihnea Molnar-Varlam[1*], Emilia-Adela Manea Salca[1], Alin M. Olărescu[1], Laurentiu Safta[1]

[1] Transilvania University of Brasov, Faculty of Furniture Design and Wood Engineering, Eroilor 29, 500036, Brasov, Romania.

E-mail: mihnea.molnar@unitbv.ro; emilia.salca@unitbv.ro; a.olarescu@unitbv.ro; safta_laurentiu@yahoo.com

Keywords: redesign, chair prototype, epoxy resin.

ABSTRACT

The challenge in design involves solving a problem that has been discovered, defined, and understood by developing potential solutions in cycles. To do this, methods such as sketching, research, brainstorming, modeling, and prototyping are used to achieve a final solution that works and can be implemented. The subject of this paper is the redesign of a prototype carpentry chair whose legs were made by joining two pieces at an angle, using epoxy resin poured in a layer, which serves a reinforcing and decorative purpose. The chair was made from three types of hardwood, namely sessile oak, black locust, and wild cherry. Compression strength tests were performed on the legs of the chairs made from the three species. The cherry wood components absorbed some of the resin and needed to be filled, while the black locust and sessile oak components did not need to be filled with resin. In order to achieve a contemporary aesthetic while retaining the legs of the prototype, creative redesign interventions were made to the backrest, seat, and component connections, resulting in two chair variants made of oak and walnut. The redesign approaches are closely related to potential users and how they interact with the piece of seating furniture. It was found that the walnut wood chair variants were more aesthetically pleasing. The two variants were validated in the 2024 National Furniture Design Competition and achieved fourth place prize.

INTRODUCTION

The design of furniture and decorative objects has a significant impact on modern interiors, enhancing usability, visual appeal, and functional adaptability. Traditional design methods rely on the designer's experience and ability to create new, optimal results in the form of aesthetic and practical objects, adapting to the latest creative and production technologies (Jing He 2025). "Design creates value and contributes to competitiveness, prosperity, and well-being in Europe" emphasizes that innovation in the design of everyday products can convey a message to an entire community and, alongside socio-cultural aspects, objects gain significance in the eyes of users (Conti et al. 2021).

The main stages of design are complex and involve understanding and identifying a problem, interpreting it, and proposing solutions. The design-oriented process cannot be formalized, and manufacturing companies, as well as small workshops, must maintain close connections with designers and artists in the same way they work with suppliers or other companies in different sectors. The purpose of a design object is to give true meaning to an object (including furniture) for its users and customers (Conti et al. 2021).

Within the context of exploring new techniques for furniture design and production, this paper proposes a detailed redesign of a carpenter's prototype chair whose legs consist of two pieces assembled and reinforced at an angle using a layer of epoxy resin. This solution is not only durable, but also has a striking visual impact. The chair's aesthetics and longevity are further complemented by the use of several local hardwood species, including: sessile oak, black locust, wild cherry, oak, and walnut (Bismialban AA et al. 2025).

The study aims to understand the role of a designer in the redesign of strictly utilitarian products and the process of transforming them into aesthetic objects without a negative impact on functionality. The development of a new object involves various phases of the creative process that are closely interlinked, while the designer plays a key role in conceptualization and the transition to a tangible, functional, safe, and user-friendly product that satisfies the end user, with the potential for large-scale marketing through small, medium, or industrial production series (Conti et al. 2021).

MATERIALS AND METHODS

The carpentry style prototype

The initial prototype is a carpenter's stool made from scrap wood or wood with various defects, joined together using epoxy resin in order to salvage and enhance value of the wood. The name of this seating object is "ECOSEAT" (Figure 1).

Figure 1: The initial prototype of the ECOSEAT chair

Crafted by a carpenter, the primary material used for the components of the chair prototype was painted spruce wood finished with oil and for the seat were used only salvaged oak scraps glued and joined with epoxy resin. The dimensions of the object are in line with the recommendations for seating furniture design, specifically a seat depth of 500 mm, height of 450 mm and a seat angle of 103°. The chair's overall shape is purely geometric, based on standard angles and carpentry techniques, while also presenting an innovative design in the legs area, offering potential for the further exploration of new chair designs.
This prototype was analysed in detail, with tests carried out to assess its resistance to compression, in order to validate the connection of the leg components using epoxy resin. At the same time, new solutions were also sought to transform the product into a more aesthetically balanced, comfortable and easy-to-integrate piece for our contemporary homes.

Testing the joint between the leg components

The leg testing was conducted on April 12, 2023, at the Research and Development Institute of Transilvania University of Brașov using a Zwick Roell testing machine, in accordance with the following standards: Pre-load – 0.1 N/mm², Test Speed – 2 mm/min. The legs are joined at a 145° angle and are 450 mm long, with identical thickness and width (36 mm). The epoxy resin used was poured in a 7 ±0.5 mm thick layer in between the two components of the legs, under conditions of 60 ± 5% of relative air humidity and a temperature of 20 ± 2°C, followed by a drying and curing time of 48 hours. Specimens of cherry, black locust, and sessile oak were tested and anatomical differences in fiber and density among the three wood species were observable during the pouring stage. One hour after casting, it was found that the cherry wood specimens had absorb part of the resin, requiring a supplement, compared to acacia and oak specimens, which did not require additional resin.

The chair redesign

Redesign involves transforming a concept, prototype, or existing product into a new, more efficient version by applying subtle or, in other cases dramatic changes in order to improve productivity, quality and end-user satisfaction, lower production costs (in terms of time, energy and labor) and simplify operations, while maintaining the overall design harmony of the object. Design is a dual process, a continuous dialogue between designer and manufacturer and a balancing formula of both directions and visions to create an authentic, harmonious and useful product. Knowledge of woodworking and the manufacturing of finished products, understandings of the technology and workshop practices of the maker, and the designer's creative, ingenious and conceptual skill sets complement one another in unity (Leinonen T et al. 2014, Abdullah MF et al. 2012).
A well-designed chair can be used anytime and anywhere, for a variety of reasons, and serves as a symbol of the designer's values which are recognized or appreciated differently by each individual, in

various contexts and spaces. The design of a chair involves all aspects of artistry and meticulous craftsmanship and, beyond the work invested in it, it is an essential cultural object around which our daily activities are organised (Alkholy I 2024).
By observing the potential innovative features through the designer's eyes, I believed that this object could gain added value through redesign. As a physical prototype, potential issues related to aesthetics, functionality, and user experience were much easier to analyze and identify (Table 1) and improvements could be made to the new versions (Antal 2016). The main objectives of the prototype redesign were to shift away from traditional woodworking techniques while retaining the shape and innovative technology used to join the legs together at an angle.

Table 1: Characteristics of the carpentry chair prototype

Product Defects	- The lack of rounded edges gives the chair a carpentry-like appearance - The seat is geometric, serving only its utilitarian function - The seat can become uncomfortable after a short period of sitting - The backrest elements do not have a clear aesthetic connection with the rest of the chair - The backrest is too tall and can become uncomfortable as it does not provide any lumbar support - The connections between the chair's components are included simply because "they are necessary" and have no aesthetic value
Product Features	- The innovative, unique method of joining the legs at an angle using resin - The object is both useful and sustainable, making use of recycled materials

RESULTS AND DISCUSSION

Compressive strength test results

The tests registered maximum forces ranging from 3,000 N (for black locust) to 9,500 N (for cherry), equivalent to a user weighing 300–950 kg for just a single leg, demonstrating the strength and feasibility of using this joint in seating furniture. The compressive strength of the chair legs varied by species as follows: Black Locust (*Robinia pseudoacacia* L.) – 2.19 [N/mm²]; Sessile Oak (*Qercus petrea* spp.) – 3.13 [N/mm²]; Cherry (*Prunus avium* L.) – 4.26 [N/mm²] (Figure 2). Furthermore, the study found that the cherry specimen absorbed the highest amount of resin (22 ± 3 ml), while the black locust specimen absorbed the least (12 ± 3 ml).

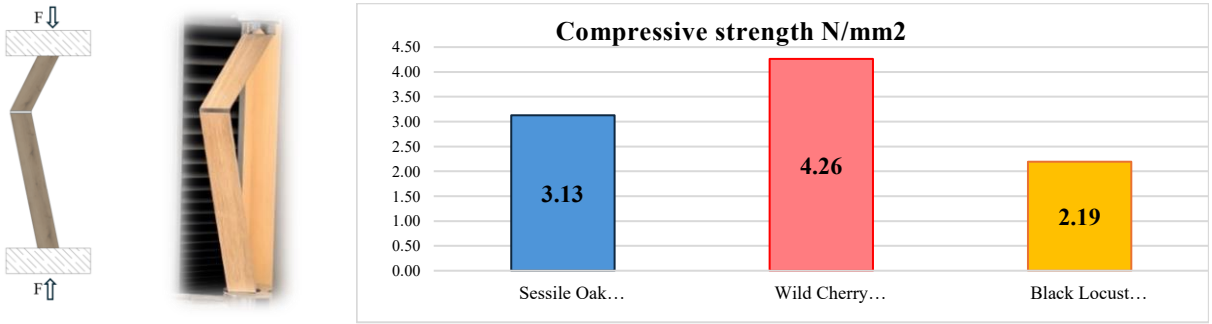

Figure 2: Testing of the legs (455 x 36 x 36 mm) on the Zwick Roell machine and the results of their compressive strength tests for the three wood species

Design variation results

Based on the study, two new seating designs were created, inspired by the ECOSEAT carpentry prototype. These are now known as "ECOSEAT DELUXE" chairs and demonstrate the significant impact that redesigning can have, mainly through changes to the aesthetics and harmonization between the user and the object. ECOSEAT DELUXE aims to shift away from traditional woodworking techniques toward redesigned objects that highlight the importance of collaboration in the applied arts. In this way, local craftsmen will be able to benefit from the creativity of designers, while designers themselves will have the advantage of bringing their creations to life. This process must be comprehended, promoted and implemented among the younger generations by treating design as a form of applied art. To ensure that these ideas do not remain mere concepts (art), it is necessary to transform them into actual products through the efforts of those who work with, understand, and respect the material.

ECOSEAT DELUXE F (Figure 3) is the stylish and feminine version of the series. The tapered leg joints make the chair lighter and also contribute to the harmony between the wooden frame and the seating elements. The backrest and seat are circular, upholstered shapes built over a plywood frame designed to provide softness and enhance user comfort. The assembly of the ECOSEAT DELUXE F chair (Figure 4) is a fixed structure built from the wooden frame plus the seat and backrest upholstered cushions. The wooden frame consists of the front and rear legs (2,5) joined and glued with epoxy resin, as tested in the laboratory. The legs are joined and glued to the connectors (1,3,6,8,9) and form the structural frame of the chair. The upholstered seat cushion is attached to joints 3 and 8 and the backrest cushion is attached on the structural element 6.

Figure 3: The "ECOSEAT DELUXE F" concept

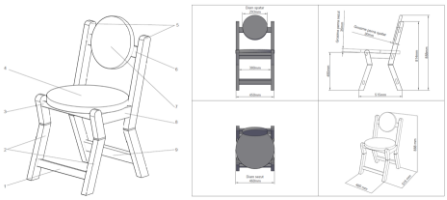

Figure 4: Components of the ECOSEAT DELUXE F chair and dimensions

The ECOSEAT DELUXE M (Figure 5) is the user-friendlier chair option, designed to ensure ease of maintenance. Even though the components retain a slightly primitive geometry, the details that make it stand out are the cushions on the seat and backrest, held in place by leather straps attached to the wooden frame. These emphasize the object's rustic appearance and symbolically yet elegantly illustrate the strong connection between the three types of materials (wood, epoxy resin, and leather). The straps are flexible and can be positioned asymmetrically, adjusted or detached to remove the cushions, making them easier to wash or replace directly by the user. The assembly of the ECOSEAT DELUXE M chair (Figure 6) has a fixed structure, with the only removable elements being the seat and backrest cushions. The wooden frame consists of the legs joined and glued with epoxy resin at the front and back (2,5). These are joined and glued with the connecting pieces (1,8,9), forming the frame of the seating unit. The seat plate (3) is mounted on top of the connectors (8). The backrest (6) and seat (3) are fitted with upholstered cushions (4,7) attached and secured by adjustable leather straps.

Figure 5: The "ECOSEAT DELUXE M" concept

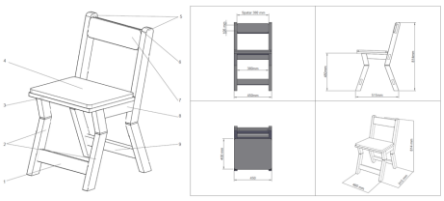

Figure 6: Components of the ECOSEAT DELUXE M chair and dimensions

Both versions of the ECOSEAT DELUXE chairs were produced in a sustainable manner (Figure 7), using reclaimed materials and with the help of a small woodworking workshop in Romania. All parts were precisely machined to their rough shapes using a CNC machine, followed by manual finishing to achieve the final forms. The upholstery was also done at a local upholsterer's workshop.

Figure 7: The production stages of the ECOSEAT DELUXE chairs

The ECOSEAT DELUXE models (Figure 8) are among the winners of the Prototype stage of the 2024 National Furniture Competition, Romania, which took place during the BIFE-SIM 2024 exhibition in Bucharest. The pieces were exhibited to the public and companies attending the event and the jury analysed, scored, and selected the winners at the Awards Ceremony on the main stage.

Figure 8: ECOSEAT DELUXE: a) F Oak; b) F Walnut; c) M Oak; d) M Walnut

CONCLUSIONS

This paper explores the redesign of a carpentry chair prototype by reimagining two seating options adapted to contemporary style and new trends in interior design.

Local manufacturers are experts when it comes to the actual processing of materials, but they need new ideas to keep moving beyond purely functional items. This comes directly from the designer's creative process, along with the experience and solutions needed to bring real products to life. The transition from art objects to design objects is achieved only through close collaboration between creators and craftsmen, aiming to produce objects that are both aesthetically pleasing and useful in everyday life.

The initial prototype of the chair had untapped potential and laboratory tests validated potential areas of uncertainty. Following a design analysis, new aesthetic formulas for the chairs were developed through the two ECOSEAT DELUXE variants. For aesthetic reasons, these objects were made using two types of hardwood: Walnut (Juglans regia) and Oak (Quercus robur).

The ECOSEAT DELUXE F is a model distinguished by its elegance and femininity, featuring a slim, more rounded fixed frame. This model showcases the circular contours of the seat and backrest, designed to harmonize with the frame. This model is also very comfortable.

ECOSEAT DELUXE M offers a more practical design with a slightly rustic look, with removable cushions attached to the wooden frame using leather straps. This model symbolically brings together wood, epoxy resin, and leather, while also allowing user-friendly maintenance.

REFERENCES

Abdullah MFAA, Zahari SESSM, Lamat M (2012) Industrial Design Inovation of Sarawak Contemporary Furniture Design

Alkholy I (2024) Theorizing the Chair: History, Culture and Design

Antal MR, Domljan D, Horváth P G (2016) Functionality and Aesthetics of Furniture – Numerical Expression of Subjective Value https://doi.org/10.5552/drind.2016.1544

Bismialban AA, Hapsari PS, Sumarno (2025) Form transformation of the Shield and the Application of the Throne Concept in the Design of the Shield of Throne Chair with Bohemian Style https://doi.org/10.38035/dijemss.v7i2

Conti E, Chiarini A (2021) Design-driven innovation: exploring new product development in home appliances and furniture industry https://www.emerald.com/insight/1754-2731.htm

Jing He (2025) Interior Design layout Optimization Based on Convolutional Neural Network

Leinonen T, Durall E (2014) Design Thinking and Collaborative Learning http://dx.doi.org/10.3916/C42-2014-10

Exploring Structural Applications of Hardwood Roundwood

Daniel F. Llana[1*], Eva Hermoso[1], Carlos Osuna-Sequera[1], Emilio A. Luengo[2], David Lorenzo[3]

[1] Timber Products Laboratory, ICIFOR-INIA, CSIC, Ctra. La Coruña 7,5, 28040, Madrid, Spain
[2] Escuela de Ingeniería de Fuenlabrada, Universidad Rey Juan Carlos URJC, Fuenlabrada, Spain
[3] AITIM – Wood Industry Association Research, Madrid, Spain.

E-mail: daniel.llana@inia.csic.es; hermoso@inia.csic.es; carlos.osuna@inia.csic.es; emilio.luengo@urjc.es; d.lorenzo@aitim.es

Keywords: *Acacia melanoxylon*; alien invasive species; broadleaves; construction products; *Eucalyptus globulus*; non-destructive testing; THRIVE project.

ABSTRACT
Structural use of timber is growing every year, not only because of its good mechanical properties and low weight, but also due to its potential to mitigate climate change. One of the most sustainable wood products is roundwood. Its low level of processing means low energy consumption and little wood waste generation. Furthermore, roundwood usually has higher strength properties than the sawn timber obtained from it. During the sawing process, wood fibers are cut, which can create stress concentrations around knots. Most structural timber used nowadays consists of softwoods; however, there is currently a growing interest in the use of hardwoods.

This research is part of the "Innovation in Hardwood Timber for Rural Activation and Climate Resilience (THRIVE)" Interreg Sudoe 3-year European project (2025–2028), involving 9 partners from 3 European countries (Portugal, Spain, and France). The project aims to map the hardwood timber sector, promote the economic valorization of timber resources through the qualification of construction-related products, and foster the development and implementation of architectural solutions using hardwood timber.

This research work presents the testing campaign in Spain. Southern blue gum (*Eucalyptus globulus*) proposing alternative structural end-uses beyond pulp and paper. A total of 100 roundwood divided in two batches from different sources will be tested by non-destructive and destructive testing. The results are expected to enhance the market potential of these hardwood species for structural applications.

INTRODUCTION

THRIVE is an Interreg Sudoe project (https://interreg-sudoe.eu/proyecto-interreg/thrive/). The SUDOE area (Andorra, Portugal, Spain and south of France) comprises 22.2 million hectares of forests, including species from the genera *Eucalyptus*, *Quercus*, *Fagus*, *Castanea*, *Fraxinus*, and *Populus*, which have experienced significant expansion over recent decades. In certain areas, this growth has occurred without adequate forest management because of land abandonment driven by population migration toward major urban centers. This issue affects all three territories involved in the THRIVE project (Portugal, Spain and the south of France). Table 1 shows project members.

These forest stands are of particular importance because they can promote the discontinuity of conifer-dominated areas, which in itself represents a valuable factor for climate change mitigation, enhancement of associated biodiversity, and reduction of wildfire risk. Moreover, these species exhibit attractive physical and mechanical properties, enabling their transformation into high-quality products suitable for applications in the construction sector.

THRIVE was conceived with the objective of contributing to the preservation of natural capital through the valorization and dissemination of hardwood species. The project will promote the valorization and dissemination of hardwood species through the implementation of active forest management practices with a direct impact across the entire value chain, aiming to strengthen social cohesion as well as

territorial and demographic balance. Furthermore, it will reduce the risk of wildfires, pests, and diseases, thereby contributing to climate change mitigation and the conservation of natural capital.

THRIVE will ensure the mapping of the hardwood timber sector, the economic valorization of timber resources through the qualification of construction-related products, and the promotion and implementation of architectural solutions based on hardwood timber within the SUDOE area. The project will enhance the resilience of the entire territory to climate change and its consequences through the application and dissemination of sustainable forest management practices. These are critical challenges affecting the whole SUDOE region, and their solutions rely on the transnational cooperation established through this project, benefiting all participating regions equally.

Table 1: THRIVE project members

No.	Member	Country
1	SerQ - Centro de Inovação e Competências da Floresta - Associação	Portugal
2	Universidad Politécnica de Madrid Escuela Técnica Superior de Arquitectura	Spain
3	Universidade de Lisboa Instituto Superior de Agronomia Centro de Estudos Florestais	Portugal
4	Forest Science Institute ICIFOR-INIA, CSIC	Spain
5	Asociación del sector forestal madera de Euskadi BASKEGUR	Spain
6	Asociación de Investigación Técnica de la Industria de la Madera y Corcho AITIM	Spain
7	Município da Sertã	Portugal
8	Association pour la valorisation des bois des Pyrénées	France
9	École nationale supérieure d'architecture et de paysage de Bordeaux	France

The objectives of the project related to timber products included three products: timber (round or sawn), engineering wood products and products modified to increase durability.

In the present study, the testing campaign focus on timber (round or sawn) in Spain carried out by ICIFOR-INIA, CSIC and AITIM is presented.

TESTING CAMPAIGN

In order to develop a testing campaign in Spain, several variables were analyzed:

Species

The hardwood species commonly available on the Spanish market in sawn timber form are southern blue gum (*Eucalyptus globulus*), shining gum (*Eucalyptus nitens*), sweet chestnut (*Castanea sativa*), and European oak (*Quercus robur* and *Quercus petraea*).

Other species that are not commonly processed as sawn timber, but could nevertheless be of interest, include beech (*Fagus sylvatica*) and Pyrenean oak (*Quercus pyrenaica*). In addition, two invasive alien species may also present potential opportunities: silver wattle (*Acacia dealbata*) and Australian blackwood (*Acacia melanoxylon*). Silver wattle, also known as mimosa, is a widespread invasive species in Portugal and northwestern Spain (Suazo-Uribe 2026). However, its trunks are generally not sufficiently straight for structural applications. Australian blackwood is often found mixed with southern blue gum in plantations and is typically processed together with it for pulp and paper production.

Southern blue gum was selected for this study because it is a fast-growing hardwood species currently used in Spain mainly for pulp and paper production. Extensive plantations are located in the northwestern region of Spain, particularly in Galicia and Asturias (Fig. 1). Alternative end uses beyond pulp and paper production will be investigated, with a particular focus on structural applications. If possible, Australian blackwood will also be purchased from the same contractor supplying the southern blue gum, although its availability is not always guaranteed.

Figure 1: Southern blue gum plantation in Galicia, Spain (source: Economía digital Galicia)

Product

Sawn timber of southern blue gum from Spanish source is already well studied; it can be visually graded according to UNE 56546 and strength class assigned according to EN 1912. Some timber structures were built with sawn southern blue gum in Spain (Fig. 2).

Figure 1: Gridshell structure manufactured from Spanish southern blue gum at PEMADE, USC, Lugo, Spain

Southern blue gum roundwood has commonly been used in northwestern Spain over the last 100 years, especially small-diameter roundwood used as rafters. However, no research studies on this application have been found. Moreover, roundwood is considered one of the most sustainable timber products due to its low level of processing and the minimal generation of wood waste. In addition, roundwood generally exhibits higher strength properties than the sawn timber produced from it. Previous studies on softwood roundwood were already carried out by ICIFOR-INIA, CSIC (Fernández-Golfín et al. 2007). Therefore, roundwood was selected as the product to be studied.

Amount of timber and testing procedure

Two batches of 50 southern blue gum roundwood logs, with an average diameter of 150 mm, will be tested: one batch from Galicia and another from Asturias. Furthermore, if available, some Australian blackwood roundwood will also be tested. Non-destructive testing (NDT), including longitudinal vibration and time-of-flight measurements, will be performed on both green and dry logs. For the mechanical tests, four-point bending tests will be carried out according to the EN 14251 standard. Mechanical properties will then be estimated from the NDT results. Llana et al. reported coefficients of determination of 51% when estimating the modulus of elasticity (MOE) from NDT measurements performed on green hardwood logs.

In parallel, since southern blue gum plantations are widespread in Portugal, SerQ plans to test additional roundwood samples and compare the results with the Spanish testing campaign.

CONCLUSIONS

There is a European project called THRIVE, involving partners from Portugal, Spain, and France, focused on promoting the valorization of hardwood species. The project includes mapping the hardwood timber sector, valorizing timber resources through the qualification of construction-related products, and promoting and implementing architectural solutions based on hardwood species. Regarding timber products, three levels will be studied: timber (roundwood or sawn timber), engineered wood products, and the modification of timber products to improve durability.

With regard to timber, alternative end-uses beyond the traditional pulp and paper industry oriented to increase hardwood added value, are being explored for southern blue gum (*Eucalyptus globulus*) in Spain. Sawn timber from this species in Spain has already been well studied, and its strength class has been defined. However, there is still a lack of information about the mechanical properties of Spanish southern blue gum roundwood. The testing campaign consists of two batches of 50 roundwood logs from two different areas. Non-destructive measurements under both green and dry conditions will be performed before mechanical testing.

ACKNOWLEDGEMENTS

The THRIVE Project S2/2.7/P0220 co-financed by the Interreg Sudoe Programme 2021-2027 through the European Regional Development Fund (ERDF).

REFERENCES

European standard EN 1912 (2024) Structural Timber - Strength classes - Assignment of visual grades and species. European Committee of Standardization (CEN) Brussels Belgium.

European standard EN 14251 (2003) Structural round timber - Test methods. European Committee of Standardization (CEN) Brussels Belgium.

Fernández-Golfín JI, Díez-Barra MR, Hermoso E, Mier R (2007) Mechanical characterization of visually classified, small-diameter laricio pine round timber. SJAR 5(3):304-311 https://doi.org/10.5424/sjar/2007053-251

Llana DF, Short I, Harte AM (2020) Use of non-destructive test methods on Irish hardwood standing trees and small-diameter round timber for prediction of mechanical properties. Ann. For. Sci. 77(62):1-13. https://doi.org/10.1007/s13595-020-00957-x

Spanish standard UNE 56546 (2024) Clasificación visual de la madera aserrada para uso estructural. Madera de frondosas. UNE, Madrid, Spain. (in Spanish)

Suazo-Uribe ME (2026) Assessment of Small-Diameter and Minimally Processed Round Logs of the Invasive Species *Acacia dealbata* Link for Structural Applications. Doctoral dissertation. Universidade do Minho. https://repositorium.uminho.pt/entities/publication/a98c431b-5eae-4b85-83f7-98c4cd8eac3c

Application of Computed Tomography for Assessing Defects in Sawn Beech Timber

Branislav Priadka[1*], Rastislav Lagaňa[1], Barbora Herdová[1], Radovan Gracovský[2]. Tomáš Gergeľ[2]

[1] Technical University in Zvolen, Faculty of Wood Sciences and Technology, Department of Wood Science, T. G. Masaryka 24, SK - 960 01 Zvolen, Slovak Republic
[2] National Forest Centre – Forest Research Institute Zvolen, T. G. Masaryka 2175/22, SK – 960 92 Zvolen, Slovak Republic.

E-mail: xpriadka@tuzvo.sk; lagana@tuzvo.sk; xherdova@tuzvo.sk; Radovan.gracovsky@nlcsk.org; tomas.gergel@nlcsk.org

Keywords: automated grading beech timber, computed tomography (CT), timber quality, wood density.

ABSTRACT

This research focuses on the use of computed tomography (CT) to develop, implement and evaluate a method for detecting selected quality parameters of unedged beech timber (*Fagus sylvatica* L.). In response to the increasing demand for hardwoods in load-bearing applications, a methodology was created that allows non-invasive identification of internal defects, including knots, cracks and fibre deviation. CT scanning was proved capable of capturing local variations in density that correspond to the presence of these defects. Calibration performed on seven wood species with different density levels demonstrated a strong linear correlation between CT image intensity and material density (r = 0.998). The findings indicate that CT technology can be effectively used not only for sorting roundwood but also for assessing sawn boards after processing, supporting production optimisation and enhancing the added value of wood products. Density-based detection of defects further opens new possibilities for automated grading supported by machine-learning techniques.

INTRODUCTION

Climate change is reshaping forest species composition. European beech (*Fagus sylvatica* L.), widely distributed across western and central Europe, has been traditionally utilized primarily in furniture manufacturing; however, its application in load bearing structural elements is now receiving increasing attention (Ehrhart et al., 2016, Pramreiter, Grabner, 2023).

Computed tomography (CT) enables detailed visualization of the internal structure of wood, allowing the detection of defects such as knots, cracks, and decay, as well as the assessment of local density and moisture distribution (Davis, Wells, 1992). As positive attributes cannot be directly assigned to wood, its evaluation must rely on negative characteristics, specifically the presence of defects (Gejdoš et al., 2021). The market value of sawn timber is primarily determined by surface-visible defects, particularly knots, notches, and others (Stängle et al. 2015). The application of CT scanning for log analysis and subsequent cutting-plan optimization has been shown to increase yield by up to 20% (Stängle et al., 2015; Rais et al., 2017).

Manufacturers of commercial CT scanners supply calibration procedures, typically based on standardized water-filled samples, which must be performed regularly to ensure that Hounsfield units (HU) are set to HU = 0 for water and HU = −1000 for air, independent of the X-ray energy applied (Davis, Wells, 1992; Parr et al., 2004).

Nevertheless, the assessment of CT-based quality in beech wood remains insufficiently resolved, as the standards for visual strength grading were originally developed for coniferous species and subsequently adopted for hardwoods, where they do not fully reflect their specific characteristics (Plos et al., 2018). Moreover, as highlighted by Frühwald and Schickhofer (2005), the correlation between strength and density in hardwood timber is relatively low, reaching only about 16 %. In contrast, local features that negatively affect the strength performance of timber can be detected through density variations. Consequently, the application of CT scanning is more appropriate for identifying local density heterogeneity rather than for determining the average density of the timber.

The objective of this study was to develop, implement, and evaluate a methodology for assessing selected qualitative characteristics of unedged beech timber. The main contribution of the research lies in the application of CT scanning as a non-contact approach for wood grading aimed at the production of wood products with higher added value.

MATERIALS AND METHODS

A beech log classified as quality class 3.B according to STN 48 0056:2007 was used in the analysis. The log had a length of 5700 mm, with end diameters of 370 mm and 400 mm, respectively. It was felled in September 2023 and scanned after two months of storage in an outdoor log yard.

In January 2024, live sawn timber with a thickness of 55 mm was produced. The live sawing pattern was chosen as it is the most commonly applied method in studies utilizing CT scanning of sawn timber (Chang, Gazo, 2009; Stängle et al., 2015). Nevertheless, several authors have reported lower qualitative and quantitative yields of this cutting method compared to alternative sawing patterns (Vilkovský et al., 2023). Following sawing, the logs were reassembled from individual boards. The moisture content of the boards immediately after sawing ranged from 39% to 45% and was measured using a GMH 3851 (Greisinger) moisture meter for solid materials. The prepared samples were air dried for 21 months under covered and dry conditions while being secured with clamping straps. The ambient temperature in the storage area varied seasonally. Prior to CT scanning, the moisture content of the individual boards was measured, with an average value of 16%. During the reassembly of the logs, each board was marked for identification purposes (Figure 1).

Figure 3: Labelling of sawn timber from a beech log prior to CT scanning

The boards were arranged to approximate the original log geometry and secured using plastic clip strapping. The scanning procedure and methodological framework have been described in detail by Gejdoš et al., (2023). Prior to image analysis, Hounsfield units were converted into an 8-bit intensity scale (digital numbers) ranging from 0 to 255.

Image processing was performed using the open-source software 3D Slicer version 5.6.2 (Fedorov et al., 2012). As an initial step a region of interest (ROI) with dimensions of 200 × 2000 mm, as specified by STN EN 975-1:2009, and with a height exceeding the board thickness, was defined and inserted into the image. For each board, the most favourable position of the ROI was selected. The occurrence of selected defects, namely knots, cracks, and fibre deviation, was then identified within the ROI on both the upper and lower board surfaces in accordance with STN EN 975-1:2009.

To verify the relationship between CT image intensity and material density, device calibration was required. Seven wood species with densities ranging from 300 to 800 $kg \cdot m^{-3}$ were used, all conditioned to a moisture content of 12%. The calibration set included samples of paulownia, willow, aspen, pine, birch, beech, and ash. The samples had dimensions of 700 × 16 × 100 mm (length × thickness × width). Initially, an individual segment was created for each calibration sample, after which the corresponding CT image intensity was determined using the Segment Statistics function.

RESULTS AND DISCUSSION

The relationship between CT image intensity expressed as digital numbers (DN) and wood density exhibited a linear correlation (Figure 2). Using seven wood species with different density levels, a correlation coefficient of 99.8% was achieved (Wei et al., 2011; Wang et al., 2019). The established relationship between density (kg·m⁻³) and CT image intensity, represented by DN values indicating the numerical intensity of the reflected or emitted signal in individual image pixels, is specific to the CT device used in this study. Provided that the scanning conditions remain constant, the derived linear equation can be applied to subsequently estimate the density of unedged timber.

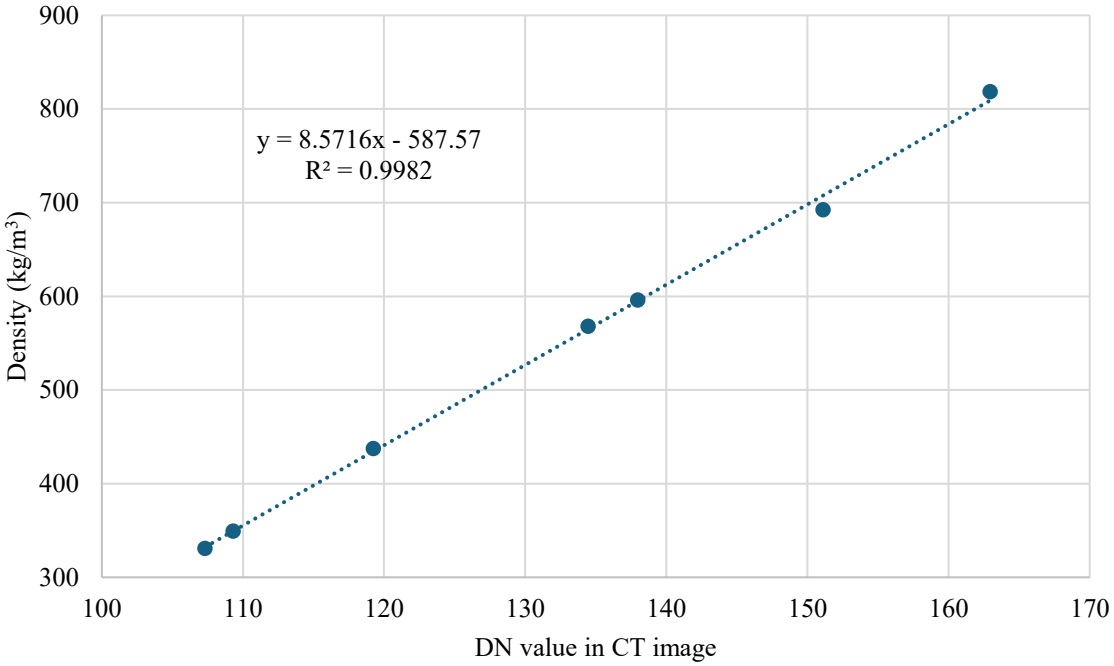

Figure 4: Graph showing the relationship between average segment density and average density of calibration samples

Within the defined ROI, knot identification was straightforward (Figure 3). Defects can be detected not only in sawn timber but also during the cutting preparation stage, where the positioning of knots within the board can be influenced (Gejdoš et al. 2023).

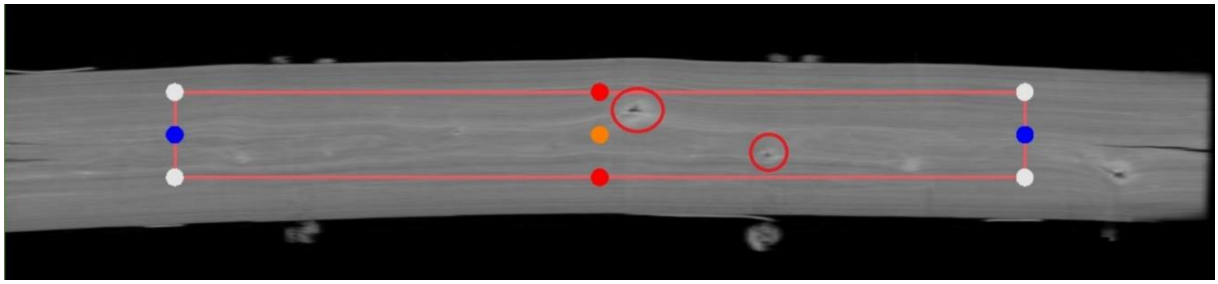

Figure 5: Identified knots on the longitudinal section

When processing dried timber, cracks can be readily identified (Figure 4) and are most commonly located in the vicinity of the sapwood (Wei et al., 2011; Gejdoš et al., 2023). In the case of log-level analysis, a substantially larger number of cross-sections would need to be evaluated to obtain sufficient data for the development of a predictive model capable of forecasting the formation of drying cracks in wood.

Fibre deviation represents the most challenging defect to identify using CT scanning. In the case of beech wood, the assessment of fibre deviation is generally problematic, and visual evaluation methods are considered unreliable. The only dependable approach for determining fibre deviation in beech timber

is the measurement of the fracture angle after destructive testing (Aicher et al., 2001; Frühwald, Schickhofer, 2005; Westermayr et al., 2018). However, when employing a live sawing pattern, it can be assumed that fibre deviation largely corresponds to the natural taper and convergence of the roundwood. An additional influencing factor may be spiral grain around the pith, which varies radially and can currently be resolved by CT technology only at ultra-high imaging resolutions (Hu et al., 2022).

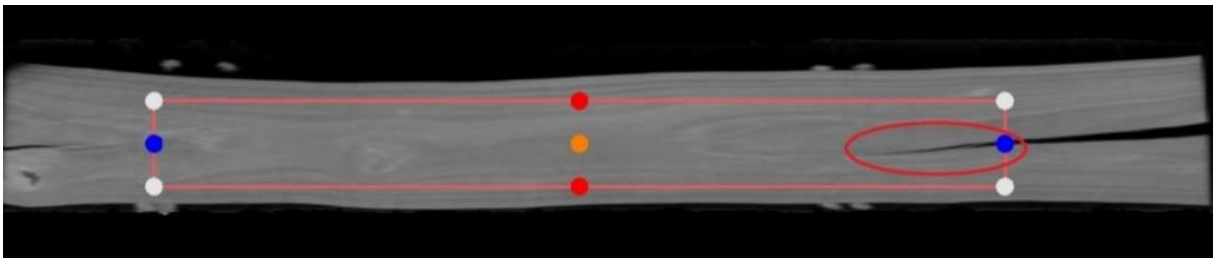

Figure 6: Identified cracks on longitudinal section

The analysis was carried out on 11 boards produced from two sections of a single log. The occurrence of knots and cracks was identified on 4 boards, representing 36 %. Fibre deviation was identified visually on 2 boards, representing 18 %. For this reason, we would classify both cuts as quality class F-S3 according to the STN EN 975-1:2009. The density of individual boards in an air-dry state ranged from 695 to 734 kg/m^3, with an average density of 719 kg/m^3. Our density values are between those reported in the literature, where Lagaňa and Babiak (2012) report a density of 680 kg/m^3 for beech, and Gryc et al. (2008) report values ranging from 736 to 768 kg/m^3.

CONCLUSIONS

Within the framework of the study, a comprehensive methodology was developed and implemented to assess selected qualitative attributes of unedged beech timber through computed tomography (CT). Each methodological stage was examined individually, and its influence on the overall outcome was systematically evaluated. The results confirmed that the use of CT scanning allows for reliable evaluation of the qualitative characteristics of beech timber, both prior to and following the cutting process.

The analysis further revealed a statistically significant linear relationship between CT image intensity and wood density. These findings underscore the potential for broader implementation of CT technology in the assessment of sawn timber, offering prospects for optimizing wood processing workflows and facilitating the production of higher value-added products.

Recent study points to the future research focusing on extending CT-based quality assessment from logs to construction timber, thereby broadening the technology's applicability. Additional efforts will include expanding the calibration dataset and examining the influence of moisture content on CT image intensity.

ACKNOWLEDGEMENTS

This work was funded by VEGA 1/0599/25, IPA Internal project agency of the Technical University in Zvolen, Project no. 5/2026 and by the EU NextGenerationEU through the Recovery and Resilience Plan for Slovakia under the project No. 09I03-03-V05-00016.

(1)

REFERENCES

Aicher, S., Höfflin, L., Behrens, W., 2001. A study on tension strength of finger joints in beech wood laminations. Otto-Graf-Journal 12, 169-186.

Davis, J., Wells, P., 1992. Computed tomography measurements on wood. Industrial Metrology 2, 195-218. https://doi.org/10.1016/0921-5956(92)80004-D

Ehrhart, T., Fink, G., Steiger, R., Frangi, A., 2016. Strength grading of European beech timber for the production of GLT & CLT, in: Proceedings Meeting 49 of International Network on Timber Engineering Research. Graz, pp 29-44. https://doi.org/10.3929/ethz-a-010795316

Fedorov, A., Beichel, R., Kalpathy-Cramer, J., Finet, J., Fillion-Robin, J., Pujol, S., Bauer, Ch., Jennings, D., Fennessy, F., Sonka, M., Buatti, J., Aylward, S., Miller, J.V., Pieper, S., Kikinis, R., 3D Slicer as an Image Computing Platform for the Quantitative Imaging Network. Magnetic Resonance Imaging 30, 1323-1341. https://doi.org/10.1016/j.mri.2012.05.001

Frühwald, K., Schickhofer, G., 2005. Strength grading of hardwoods, in: Proceedings 14th International Symposium on Nondestructive Testing of Wood. Eberswalde, pp 199-210. ISBN 3-8322-3949-9.

Gejdoš, M., Gergeľ, T., Michajlova, K., Bucha, T., Gracovský, R., 2023. The Accuracy of CT Scanning in the Assessment of the Internal and External Qualitative Features of Wood Logs. Sensors 23, 8505. https://doi.org/10.3390/s23208505

Gejdoš, M., Suchomel, J., Danihelová, Z., 2021. Analysis of Qualitative Features of Beech and Oak Trunks as a Determinant of the Quality Assessment. Forests 12, 15. https://doi.org/10.3390/f12010015

Gryc, V., Vavrčík, H., Gomola, Š., 2008. Selected properties of European beech (Fagus sylvatica L.). Journal of Forest Science, 54. 418-425. https://doi.org/10.17221/59/2008-334

Hu, M., Olsson, A., Hall, S., Seifert, T. 2022. Fibre directions at a branch-stem junction in Norway spruce: a microscale investigation using X-ray computed tomography. Wood Science and Technology, 56. 147-169. https://doi.org/10.1007/s00226-021-01353-y

Chang, S., Gazo, R., 2009. Measuring the effect of internal log defect scanning on the value of lumber produced. Forest Products Journal 59, 56-59. https://doi.org/10.13073/0015-7473-59.11.56

Lagaňa, R., Babiak, M., 2012. Quality of Beech Standing Trees Related to Properties of Structural Timber, in: Proceedings 55th International Convention of Society of Wood Science and Technology. Beijing, pp 347-352. ISBN 978-0-9817876-3-3.

Parr, D., Stoel, B., Stolk, J., Nightingale, P.G., Stockley, R.A., 2004. Influence of Calibration on Densitometric Studies of Emphysema Progression Using Computed Tomography. American Journal of Respiratory and Critical Care Medicine 170, 883-890. https://doi.org/10.1164/rccm.200403-326OC

Plos, M., Fortuna, B., Šuligoj, T., Turk, G., 2018. Beech as construction wood, in: Proceedings Common Foundations 2018 - uniSTem: 6th Congress of Young Researchers in the Field of Civil Engineering and Related Sciences. Split, pp 180-185. https://doi.org/10.31534/CO/ZT.2018.25

Pramreiter, M., Grabner, M., 2023. The Utilization of European Beech Wood (Fagus sylvatica L.) in Europe. Forests 14, 1419. https://doi.org/10.3390/f14071419

Rais, A., Ursella, E., Vicario, E., Giudiceandrea, F., 2017. The use of the first industrial X-ray CT scanner increases the lumber recovery value: case study on visually strength-graded Douglas-fir timber. Annals of Forest Science 74, 28. https://doi.org/10.1007/s13595-017-0630-5

Stängle, S.M., Brüchert, F., Heikkila, A., Usenius, T., Usenius, A., Sauter, U.H., 2015. Potentially increased sawmill yield from hardwoods using X-ray computed tomography for knot detection. Annals of Forest Science 72, 57–65. https://doi.org/10.1007/s13595-014-0385-1

STN 48 0056, 2007. Qualitative classification of hardwood round timber. Slovak Office of Standards, Metrology and Testing.

STN EN 975-1, 2009. Sawn Timber. Appereance grading of hardwoods. Part 1: Oak and beech. Slovak Office of Standards, Metrology and Testing.

Vilkovský, P., Klement, I., Vilkovská, T., 2023. The Impact of the Log-Sawing Patterns on the Quantitative and Qualitative Yield of Beech Timber (Fagus sylvatica L.). Applied Sciences 13, 8262. https://doi.org/10.3390/app13148262

Wang, Q., Liu, X., Yang, S., Jiang, M., Cao, J., 2019. Non-destructive detection of density and moisture content of heartwood and sapwood based on X-ray computed tomography (X-CT) technology. European Journal of Wood and Wood Products 77, 1053–1062. https://doi.org/10.1007/s00107-019-01459-y

Wei, Q., Leblon, B., La Rocque, A., 2011. On the use of X-ray computed tomography for determining wood properties: a review. Canadian Journal of Forest Research 41, 2120–2140. https://doi.org/10.1139/x11-111

Westermayr, M., Stapel, P., van de Kuilen, J.W., 2018. Tensile Strength and Stiffness of 380 Low Quality Beech (Fagus Sylvatica) Sawn Timber, in: Proceedings WCTE 2018 World Conference on Timber Engineering. Seoul. https://pure.tudelft.nl/ws/portalfiles/portal/47891668/4.pdf

Assessment of Stiffness-Based Grading for Thermally Modified Beech Timber in Structural Applications

Filip Valko[1], Jarmila Schmidtová[2], Tomáš Ándor[1], Barbora Herdová[1], Rastislav Lagaňa[1*]

[1] Department of Wood Science, Faculty of Wood Sciences and Technology, Technical University in Zvolen, T.G. Masaryka 24, 96001 Zvolen, Slovakia
[2] Department of Mathematics and Descriptive Geometry, Faculty of Wood Sciences and Technology, Technical University in Zvolen, T.G. Masaryka 24, 96001 Zvolen, Slovakia.

E-mail: xvalko@tuzvo.sk; schmidtova@tuzvo.sk; andor@mjbusiness.sk; xherdova@tuzvo.sk; lagana@tuzvo.sk

Keywords: thermally modified wood; European beech; structural timber; bending strength; non-destructive evaluation; strength grading.

ABSTRACT

Thermally modified wood is primarily used in exterior applications due to its improved resistance to biotic degradation. However, its reduced mechanical performance limits broader structural use. This study investigates the structural potential of high-temperature-treated European beech timber (Fagus sylvatica L.) and evaluates its mechanical properties together with grading models applicable to structural design. Timber obtained from 32 beech logs was air-dried and divided into untreated (NoTMW) and thermally modified (TMW) groups. Thermal modification was carried out under commercial conditions in an oxidizing atmosphere at 190 °C. All specimens were visually graded according to DIN 4074-5 and assessed using acoustic non-destructive methods prior to four-point bending tests performed in accordance with EN 408. The modulus of elasticity (MOE), modulus of rupture (MOR), and density were determined, and characteristic values were calculated according to EN 384. On average, TMW showed a 17% reduction in bending strength compared with untreated wood, while neither static nor dynamic MOE was significantly affected. A multiple regression model provided only a slight improvement in the prediction of bending strength compared with a single linear regression based on global modulus, with the coefficient of determination increasing from 17% to 19%. In contrast, the prediction of stiffness in thermally modified beech timber was substantially improved by combining local and acoustic moduli, which explained 76% of the total variation.

INTRODUCTION

European hardwoods are receiving increasing attention in timber construction because softwood resources are under pressure and mixed, climate-resilient forests are promoted across Europe. Beech is therefore an important candidate for higher-value structural use, especially where its naturally high stiffness can be exploited (Pramreiter and Grabner 2023).

Thermal modification improves dimensional stability, reduces equilibrium moisture content and increases resistance to biological degradation by changing the chemical structure of wood. These benefits explain its common use in cladding and other exterior products, but the same process can reduce strength and toughness in a species- and treatment-dependent manner (Hodžić and Bahmani 2023).

For beech, previous work showed that stiffness may be retained relatively well, while bending strength, fracture energy and reliability may decrease substantially after severe treatment. This means that a visually acceptable and stiff member may still be unsafe in strength-controlled design (Widmann et al. 2012; van Blokland 2020; Al-Musawi et al. 2023).

High-resolution scanning of fibre direction has improved strength prediction for thermally modified timber, but practical grading data for structural-size treated beech are still limited (van Blokland et al. 2019). The present study addresses this gap for beech timber thermally modified at 190 °C by comparing treated and untreated boards, determining characteristic values, and evaluating whether stiffness-based non-destructive indicators can provide a practical grading basis.

MATERIALS AND METHODS

Beech stems harvested in the Zvolen district, Slovakia, were sawn into boards, air-dried and paired so that neighbouring boards from the same log could be compared before and after treatment. Industrial thermal modification was carried out in an oxidizing air atmosphere at 190 °C for 3.5 h. Untreated boards are referred to as NoTMW and thermally modified boards as TMW (Figure 1).

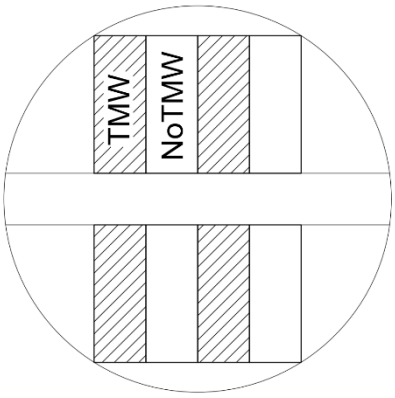

Figure 7: Segmental sawing pattern and adjacent-board pairing for TMW and NoTMW

The boards were visually graded according to DIN 4074-5:2003. Ultrasound and natural-frequency measurements were used to determine dynamic stiffness indicators before destructive testing. Four-point bending tests were then performed according to EN 408:2011 on boards with final dimensions of 50 × 150 × 3100 mm. Moisture content, density, local and global modulus of elasticity, and modulus of rupture were evaluated.

Characteristic values were calculated according to EN 384:2016+A2:2022 and EN 14358:2016. Paired t-tests were used to identify treatment effects. Linear and multiple regression models were then fitted to determine whether strength and stiffness could be predicted from non-destructive stiffness indicators.

RESULTS AND DISCUSSION

The paired comparison confirmed the central weakness of the treated material: thermal modification significantly reduced moisture content, density and bending strength, but did not significantly change the measured elastic moduli. The complete dataset showed the same trend. Mean bending strength decreased from 76.31 MPa in NoTMW to 63.33 MPa in TMW, a reduction of approximately 17%, while local, global and acoustic moduli remained at a similar level (Table 1).

The most important structural consequence was not only the lower mean strength, but also the much higher scatter. The coefficient of variation of bending strength increased from 14% in untreated boards to 45% in TMW. This is the part that makes blind use of standard hardwood grading rules a bad idea: stiffness looks good, but strength reliability does not.

Table 2: Mechanical properties and characteristic values of thermally modified and untreated beech timber

Property (unit)	TMW Mean	TMW CV* (%)	NoTMW Mean	NoTMW CV* (%)	Difference (%)
$f_{m,h150}$ (MPa)	63.33	45%	76.31	14%	−17%
$MOE_{sylv,w}$ (GPa)	20.05	8%	20.01	7%	0%
$MOE_{MTG,w}$ (GPa)	17.91	7%	17.38	9%	3%
$MOE_{l,ref\,w}$ (GPa)	16.00	12%	15.67	10%	2%
$MOE_{g,ref\,w}$ (GPa)	14.92	10%	14.61	8%	2%
$\rho_{408,ref\,w}$ (kg.m^{-3})	663.1	5%	694.5	5%	−5%
MC (%)	6.09	11%	14.93	7%	−59%

***** *Coefficient of variation.*

The characteristic bending strength of TMW reached only 17.27 MPa, which is below the lowest deciduous strength class D18 in EN 338:2016. In practical terms, the treated beech cannot be treated as a normal high-performance hardwood structural material. It may be stiff, but its characteristic strength is too low and too variable for direct assignment to a standard hardwood class.
Regression analysis showed that global MOE was the best single predictor of bending strength, but the relationship remained weak. It explained only about 17% of strength variation. Multiple regression increased this value only to about 19%, so adding further stiffness-related variables did not solve the strength prediction problem (Figure 2).

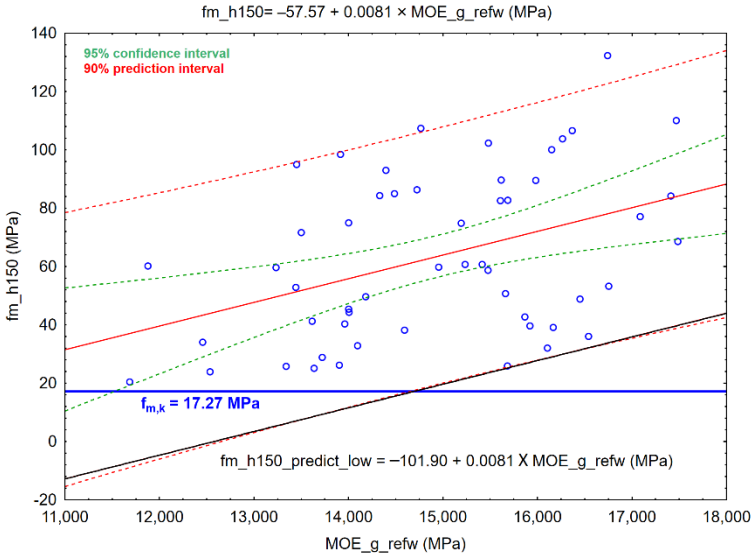

Figure 8: Relationship of characteristic strength with global MOE for heat-treated beech timber. The black line represents the prediction of the fifth percentile boundary; horizontal blue lines represent characteristic values $f_{m,k}$; the solid red line is the regression line

The weakness of strength prediction does not mean that non-destructive testing is useless. It means that stiffness indicators are much better suited for stiffness grading than for safe strength prediction in this material. When local and acoustic moduli were combined, the model explained about 76% of the variation in bending stiffness. This confirms that TMW beech can be characterized reliably in terms of stiffness, but not with the same confidence in terms of bending strength.
The findings agree with earlier studies showing that thermally modified beech often keeps stiffness while losing toughness and strength reliability (Widmann et al. 2012; Hodžić and Bahmani 2023; Al-Musawi et al. 2023). For practice, this points to a narrow but realistic field of use: low-stress, stiffness-controlled elements, facade substructures, selected short members or components where strength demand is limited and quality control is strict. Stronger claims would be overconfident.

CONCLUSIONS

Structural-size European beech timber thermally modified at 190 °C retained static and dynamic stiffness, but lost bending strength and became much more variable. The characteristic bending strength fell below EN 338:2016 class D18, so direct use of conventional hardwood grading rules is unreliable.
Global MOE can serve as a first stiffness-related grading indicator, but it is too weak for robust strength prediction. Multiple regression with additional stiffness indicators improved strength prediction only marginally. Stiffness prediction, however, improved substantially when local and acoustic moduli were combined.
Thermally modified beech should therefore be considered only for conservative, stiffness-controlled structural applications unless improved grading procedures, fibre-orientation data or milder treatment regimes are used.

ACKNOWLEDGMENT

This condensed paper is based on the original article by Schmidtová et al. and preserves its core methodology and findings. The research was funded by the ERDF project LignoPro (ITMS: 313011T720) and the Slovak Research and Development Agency project APVV-21-0015. Data are available in the source article and its supplementary materials. The authors gratefully acknowledge Ondrej Bajza and Alena Rohanová for their cooperation. No conflict of interest was declared in the source publication.

REFERENCES

Al-Musawi H, Manni E, Stadlmann A, Ungerer B, Hassan Vand M, Lahayne O, Nobile R, Baumann G, Feist F, Müller U (2023) Characterisation of thermally treated beech and birch by means of quasi-static tests and ultrasonic waves. Sci Rep 13:6348. https://doi.org/10.1038/s41598-023-33054-w

DIN 4074-5 (2003) Sortierung von Holz nach der Tragfähigkeit - Teil 5: Laubschnittholz. Deutsches Institut für Normung, Berlin, Germany

EN 338 (2016) Structural Timber - Strength Classes. European Committee for Standardization, Brussels, Belgium

EN 384:2016+A2:2022 (2022) Structural Timber - Determination of characteristic values of mechanical properties and density. European Committee for Standardization, Brussels, Belgium

EN 408 (2011) Timber structures - Structural timber and glued laminated timber - Determination of some physical and mechanical properties. European Committee for Standardization, Brussels, Belgium

EN 14358 (2016) Timber structures - Calculation and verification of characteristic values. European Committee for Standardization, Brussels, Belgium

Hodžić A, Bahmani M (2023) Physical and mechanical changes in thermal modified wood: A review. Zastita Materijala 64:314-326. https://doi.org/10.5937/zasmat2303314H

Pramreiter M, Grabner M (2023) The utilization of European beech wood (Fagus sylvatica L.) in Europe. Forests 14:1419. https://doi.org/10.3390/f14071419

van Blokland J (2020) Thermally modified timber: novel aspects of bending behaviour towards grading and structural applications. PhD thesis, Linnaeus University, Växjö, Sweden

van Blokland J, Olsson A, Oscarsson J, Adamopoulos S (2019) Prediction of bending strength of thermally modified timber using high-resolution scanning of fibre direction. Eur J Wood Wood Prod 77:327-340. https://doi.org/10.1007/s00107-019-01388-w

Widmann R, Fernández-Cabo JL, Steiger R (2012) Mechanical properties of thermally modified beech timber for structural purposes. Eur J Wood Wood Prod 70:775-784. https://doi.org/10.1007/s00107-012-0615-x

Investigation of the Bacterial Communities of *Juglans regia* in Hungarian Plantations

Nóra T. Lange-Enyedi[1*], Boris Indic[1], Simang Champramary[1], Aleksandr Pnev[1], Orsolya Kedves[2], Attila Szűcs[3], Annamária Tüh[4], Árpád Bránvi[5], Younes R. Danesh[6], Omar Languar[1], Csaba Vágvölgyi[2], László Kredics[2], György Sipos[1]

[1] Functional Genomics and Bioinformatics Group, Faculty of Forestry, University of Sopron, Bajcsy-Zs. Str. 4, Sopron, Hungary, 9400
[2]Department of Biotechnology and Microbiology, Faculty of Science and Informatics, University of Szeged, Közép fasor 52., Szeged, Hungary, 6726
[3] University of Innsbruck, Innsbruck, Austria
[4] Government Office of Zala County Plant Protection and Soil Conservation Unit, Kinizsi Str. 81, Zalaegerszeg, Hungary, 8900
[5] Pannon-Trade Ltd., Mayer Lajos Str. 69, Győr, Hungary, 9026
[6] Department of Plant Protection, Van Yuzuncu Yil University, Van, Turkey.

E-mail: lange-enyedi.nora@uni-sopron.hu, indic.boris@uni-sopron.hu, simang5c@gmail.com, aleksandr.pnev41@gmail.com, kedvesorsolya91@gmail.com, a.szunyi@gmail.com, tuh.annamaria@gmail.com, info@pannon-trade.com, y.rdanesh@yahoo.com, o.languar@gmail.com, mucor1959@gmail.com, laszlo.kredics@gmail.com, sipos.gyorgy@uni-sopron.hu

Keywords: walnut; walnut husk fly; microbiota; plant pathogens; bacteria.

ABSTRACT

Walnut husk flies (*Rhagoletis completa*) are considered important pests in walnut plantations and may contribute to the spread of associated microorganisms. However, next-generation sequencing data on the composition of their microbial communities remain relatively scarce. In this study, the microbiota of walnut husk flies, non-symptomatic and infected walnut and leaf samples originating from two plantations in Hungary were investigated using whole-genome and amplicon sequencing to assess potential relationships between them. Long-read sequencing was performed on Oxford Nanopore MinION platform. UPGMA clustering and similarities in bacterial composition suggest that flies may contribute to the propagation of potentially plant pathogenic bacteria within infected plantations. *Pseudoxanthomonas* and uncultured *Lysobacteraceae* showed the highest relative abundance in infected walnuts, whereas flies most frequently harboured *Pseudomonas*, *Falsochrobactrum*, *Daeguia*, and uncultured Enterobacteriaceae. The results suggest synergistic plant tissue-decomposing activities of multiple bacteria, including *Erwinia, Pantoea, Samsonia, Enterobacter,* and *Lelliottia*. These findings require further validation through functional transcriptomic analyses.

INTRODUCTION

Common (English or Persian) walnut (*Juglans regia*) production in Europe has declined in the recent years. The trees have multiple agricultural importance from food and nutrition through pharmaceutical components to wood technology. Ensuring the production of walnuts is an essential economic task in Hungary, as the area under production exceeds 9000 hectares (Bujdoso and Cseke 2021). Climate change and drought decrease the systemic stress response of plants and pose a synergistic effect on pathogen invasion. Several bacterial pathogens have emerged in Europe that damage walnut production, such as *Xanthomonas arboricola* pv. *juglandis* (bacterial blight, brown apical necrosis) (Kałużna et al. 2021), *Brenneria nigrifluens* and *B. rubrifaciens* (canker) (Cabello et al. 2016). Insects also play role in the transmission of infections as vector organisms. In recent years, the walnut husk fly (*Rhagoletis completa*), native to North America, has appeared and spread significantly in Europe, including Hungary (Oláh et al. 2014). The primary aim of the study was to observe if there is a connection between the spreading of the pathogens and the walnut husk fly that hatches and develops inside the husk. A further objective of the study was to test the efficiency of the previously used in-house methods for describing the bacterial community of different plant and insect tissues.

MATERIALS AND METHODS

Sampling and DNA extraction

Walnut plantations were visited near Felsőpáhok and Hidegség, Hungary. We have collected non-symptomatic walnuts (F1W1) and leaves (F1L1) as control, infected walnuts with brown discoloration (F1W3, H1W3), and small, brown-spotted leaves (F1L2) from different trees into sterile containers (Figure 1). All samples were kept at 4 °C until processing. Infected walnuts were collected from trees growing in the orchard near Felsőpáhok, then the walnuts were kept on sterile neutral soil to raise flies. Pupae (F1P1) and imagoes (F1I1) were collected for DNA extraction. DNeasy PowerSoil Pro kit (Qiagen) was applied to isolate DNA after grinding of the samples in liquid nitrogen.

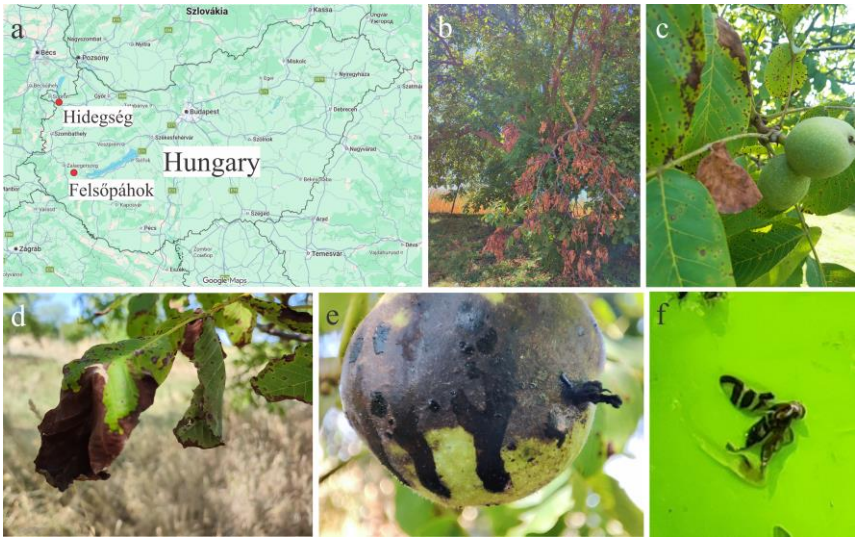

Figure 1: Sampling setup for analysing the microbial communities of Juglans regia: a) sampling points near Hidegség (Győr-Moson-Sopron County) and Felsőpáhok (Zala County) (based on Google Maps). General state of walnut trees: b) dry branches, c-d) brown necrotic spots on leaves, e) walnuts with black infusion caused by the walnut husk fly. f) Walnut husk fly collected near Felsőpáhok

Sequencing

DNA samples of F1P1 and F1I1 were subjected to shotgun metagenome sequencing on the Oxford Nanopore MinION platform (Oxford Nanopore Technologies, Oxford, UK). Raw reads were trimmed with Porechop (https://github.com/rrwick/porechop) and filtered using Filtlong (https://github.com/rrwick/filtlong). Cleaned reads were aligned to the NCBI Nucleotide database using the KMA aligner and CCMetagen (https://github.com/vrmarcelino/CCMetagen).

For metabarcoding, primers 27F and 1492R were used to amplify the 16S rRNA gene sequences (Lane 1991). Library was prepared with Native Barcoding Kit 24 V14 and sequenced on the MinION platform according to the manufacturer's protocol. Raw sequences were processed in R v. 4.4.3 (R Core Team 2026) using the ShortRead (Morgan et al. 2009), dada2 (https://github.com/benjjneb/dada2), and tidyverse (https://tidyverse.tidyverse.org) packages. Taxonomic assignment was conducted using the custom-formatted SILVA reference database (SILVA nr99 v138.2, trimmed to the genus level) (Quast et al. 2013). The dendrogram based on Unweighted Pair Group Method with Arithmetic Mean (UPGMA) of Bray-Curtis similarity distances and the bubble plot were prepared by vegan (Oksanen et al. 2025) and the ggplot2 packages. The diversity indices were calculated with PAleontological STatistics Version 3.14 (Hammer et al. 2001).

RESULTS AND DISCUSSION

The whole-genome metagenomic analysis resulted in 1684 and 4941 reads for F1P1 and F1I1, respectively. These read counts are relatively low for typical microbiome whole-genome sequencing and may impact the depth of coverage, limiting the detection of low-abundance species. Filtering for bacteria in the metagenomes excluded all reads from F1P1. The analysis was restricted to identifying possible members of the microbial communities. Close relatives were only identified to the genus or family level, particularly *Escherichia, Klebsiella, Raoultella, Pantoea* and *Pseudomonas*.

During the amplicon sequencing, a total of 58,541 reads were acquired from the 7 samples varying from relatively low to relatively high sequence numbers (Table 1). The bacterial communities of F1W1 and F1L1 contained only chloroplast sequences amplified by PCR with 16S rRNA gene primers. These products could be excluded by using peptide nucleic acid clamps to block amplification (Hussain et al. 2025). Alternatively, the overall bacterial diversity may have been negligible and therefore underrepresented during PCR amplification. According to the diversity indices, the highest microbial diversity was observed in F1L2. Excluding the potential bias from the low sequence number, F1I1 appeared to harbour the most diverse microbiome.

Table 1: The description of the collected samples and the results of 16S rRNA gene amplicon sequencing and subsequent bioinformatic analysis (n.d. – no data)

Sample	Description	Sequence number	Genus number	Shannon index	Inverse Simpson index
F1P1	walnut husk fly pupae	178	23	1.64	0.573
F1I1	walnut husk fly imagoes	9.596	24	2.57	0.883
F1W1	Felsőpáhok, non-symptomatic walnut	8.750	n.d.	n.d.	n.d.
F1L1	Felsőpáhok, non-symptomatic leaves	10.459	n.d.	n.d.	n.d.
F1W3	Felsőpáhok, infected walnut (2nd stage)	19.875	15	2.41	0.880
F1L2	Felsőpáhok, infected leaves	322	26	2.68	0.893
H1W3	Hidegség, infected walnut (2nd stage)	9.361	5	1.22	0.645

The phylum Pseudomonadota had the highest relative abundance in every sample, predominantly the classes Gammaproteobacteria (44-100%) and Alphaproteobacteria (5-40%). Regarding the genus level affiliation of the insects' microbiota (Figure 2), the most dominant genus was *Pseudomonas* in F1P1. The genus *Pseudomonas* comprises both walnut-pathogenic strains (Kim et al. 2020) and strains associated with plant growth promotion (Ansari et al. 2021). In the case of F1I1, *Falsochrobactrum, Daeguia, Pseudomonas* and uncharacterised Enterobacteriaceae were the most abundant. In the plant-related samples, *Pseudomonas* was also significant in F1L2, accompanied by uncharacterised Enterobacteriaceae and *Raoultella*. *Pseudoxanthomonas* and uncharacterised Lysobacteraceae had the highest relative abundance in F1W3 and H1W3. Close relatives of *Pseudoxanthomonas* spp. were not connected to plant diseases so far, but the family Lysobacteraceae contains plant pathogenic members (Wells et al. 1987). The microbial community of the two walnuts showed variation across different areas. *Stenotrophomonas maltophilia* was proved to be responsible for necrotic lesions and stem bleeding on oak trees in Iran (Ahmadi et al. 2019). Members of the family Enterobacteriaceae are considered the main causal agents of soft rot diseases, such as *Enterobacter* and *Pantoea* (Zhao et al. 2022). The results suggest synergistic plant tissue decomposing activities of multiple low-abundant (<2%) bacteria, including *Erwinia, Pantoea, Samsonia, Enterobacter,* and *Lelliottia*. These preliminary results need further verification by functional transcriptomic analysis.

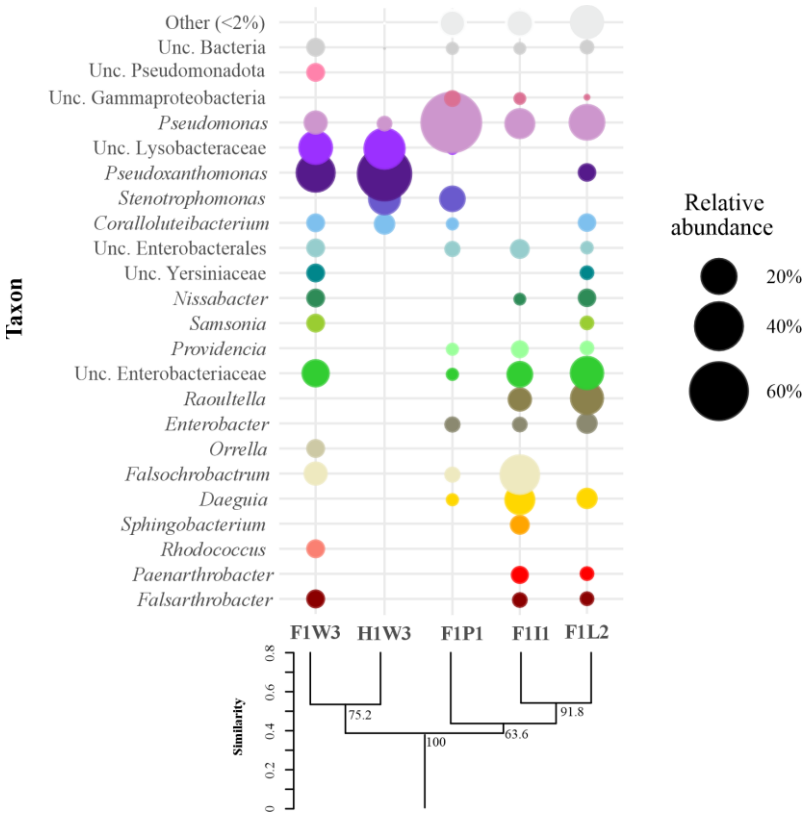

Figure 2: UPGMA dendrogram (based on 500 bootstrap replicates) combined with taxonomic composition of bacterial communities in different developmental stages of the walnut husk fly (pupae – F1P1, imagoes - F1I1), infected leaves (F1L2) and walnuts (F1W3, H1W3) at the genus level. Genera having <2% relative abundance are combined in the "Other" category. Unc: Uncharacterised

Bacteria commonly associated with insect gut communities (Raza et al. 2020), especially in the order Enterobacterales were prominent in F1L2 and F1W3 (Figure 2). Their presence in the leaves suggests a mixture of bacteria persisting within the circulation system of the infected trees. This observation suggests a significant role for the flies in the primary development of symptoms. The F1P1 flies reared on sterile soil were likely to carry bacteria originating from the infected walnuts. This bacterial community may have gradually developed within the imagoes and subsequently been transferred to the walnuts during oviposition. Walnuts provide distinct growth conditions for bacterial communities, while also being more exposed to environmental microorganisms.

CONCLUSIONS

This preliminary study provides a foundation for future investigations. The results indicate that the applied methods require further optimization for the analysis of plant samples, particularly for whole-genome sequencing. Nevertheless, the amplicon sequencing approach provided valuable insights into the potential impact of the walnut husk fly microbiota in walnut plantations.

ACKNOWLEDGEMENTS

We acknowledge the sequencing service of the Hungarian Centre for Genomics and Bioinformatics, Szentágothai Research Centre, University of Pécs. This study was supported by the National Research, Development and Innovation Office (Grants 2022-1.2.6-TÉT-IPARI-TR-2022-00009 and 2020-2.1.1-ED-2024-00313), and the Ministry of Agriculture of Hungary (Grant EGF/388/2025). N.T.L-E. acknowledges the University of Sopron's Postdoctoral Scholarship.

REFERENCES

Ahmadi E, Kowsari M, Azadfar D, Salehi Jouzani G (2019) *Bacillus pumilus* and *Stenotrophomonas maltophilia* as two potentially causative agents involved in Persian oak decline in Zagros forests (Iran). For Pathol 49(5):e12541. https://doi.org/10.1111/efp.12541

Ansari FA, Jabeen M, Ahmad I (2021) *Pseudomonas azotoformans* FAP5, a novel biofilm-forming PGPR strain, alleviates drought stress in wheat plant. Int J Environ Sci Technol 18(12):3855–3870. https://doi.org/10.1007/s13762-020-03045-9

Bujdoso G, Cseke K (2021) The Persian (English) walnut (*Juglans regia* L.) assortment of Hungary: Nut characteristics and origin. Sci Hortic 283:110035. https://doi.org/10.1016/j.scienta.2021.110035

Cabello JA, Valdés RA, Chávez EC, Beache MB, Ortiz JCD, Fuentes YMO (2016) Review of diagnosis techniques for *Brenneria* spp. in walnut (*Juglans regia*). Rev Mex Fitopatol 34(2):158–172. https://doi.org/10.18781/R.MEX.FIT.1601-3

Hammer Ø, Harper DAT, Ryan PD (2001) PAST: paleontological statistics software package for education and data analysis. Palaeontol Electron 4 (1):4, p 9. http://palaeo-electronica.org/2001_1/past/issue1_01.htm

R Core Team (2026) R: A Language and Environment for Statistical Computing. R Foundation for Statistical Computing Vienna, Austria https://doi.org/10.32614/R.manuals

Hussain U, Downie J, Ellison A, Denman S, McDonald J, Cambon MC (2025) Peptide nucleic acid (PNA) clamps reduce amplification of host chloroplast and mitochondria rRNA gene sequences and increase detected diversity in 16S rRNA gene profiling analysis of oak-associated microbiota. Environ Microbiome 20(1):14. https://doi.org/10.1186/s40793-025-00674-w

Kałużna M, Fischer-Le Saux M, Pothier JF, Jacques MA, Obradović A, Tavares F, Stefani E (2021) *Xanthomonas arboricola* pv. *juglandis* and pv. *corylina*: Brothers or distant relatives? Genetic clues, epidemiology, and insights for disease management. Mol Plant Pathol 22(12):1481–1499. https://doi.org/10.1111/mpp.13073

Kim HS, Lee DH, Lee SK, Lee SH, Seo ST (2020) First report of walnut blight canker on walnut tree (*Juglans regia*) by *Pseudomonas flavescens* in South Korea. J Plant Pathol 102(3):943–943. https://doi.org/10.1007/s42161-020-00520-7

Lane DJ (1991) 16S/23S rRNA Sequencing. In: Stackebrandt, E and Goodfellow, M, (eds) Nucleic Acid Techniques in Bacterial Systematics, John Wiley and Sons, New York, USA pp 115–175.

Morgan M, Anders S, Lawrence M, Aboyoun P, Pagès H, Gentleman R (2009) ShortRead: a Bioconductor package for input, quality assessment and exploration of high-throughput sequence data. Bioinform 25:2607–2608. https://doi.org/10.1093/bioinformatics/btp450

Oksanen J, Simpson G, Blanchet F, Kindt R, Legendre P, Minchin P, ... Weedon J (2025) vegan: Community Ecology Package https://doi.org/10.32614/CRAN.package.vegan

Oláh R, Orosz Sz, Vétek G (2014) Diót károsító Diptera fajok elterjedése és életmódja Magyarországon. In: Gál P, Novák R, Pánczél M, Ripka G (eds) Integrált termesztés a kertészeti és szántóföldi kultúrákban (XXXI.). Magyar Növényvédelmi Társaság, Budapest, Hungary pp 36–42. (in Hungarian)

Quast C, Pruesse E, Yilmaz P, Gerken J, Schweer T, Yarza P, Peplies J, Glöckner FO (2013) The SILVA ribosomal RNA gene database project: improved data processing and web-based tools. Nucl Acids Res 41 (D1):D590–D596. https://doi.org/10.1093/nar/gks1219

Raza MF, Yao Z, Bai S, Cai Z, Zhang H (2020) Tephritidae fruit fly gut microbiome diversity, function and potential for applications. Bull Entomol Res 1–15. https://doi.org/10.1017/S0007485319000853

Wells JM, Raju BC, Hung HY, Weisburg WG, Mandelco-Paul L, Brenner DJ (1987) *Xylella fastidiosa* gen. nov., sp. nov: gram-negative, xylem-limited, fastidious plant bacteria related to *Xanthomonas* spp. Int J Syst Evol Microbiol 37(2):136–143. https://doi.org/10.1099/00207713-37-2-136

Zhao X, Tian Y, Yue L, Liu Y, Yan Y, Zhou Q, ... Wang R (2022) Identification and characterization of pathogenicity of *Lelliottia nimipressuralis* causing soft rot of *Codonopsis pilosula* (dangshen) roots in China. Plant Pathol 71(8):1801–1811. https://doi.org/10.1111/ppa.13606

SNS Network VALUE:BIRCH – Valorization from the Forest and Beyond

Katrin Zimmer[1*], Ulf Lemke[2], Irena Fundova[1], Henrik Heräjärvi[3], Mateusz Liziniewicz[4], Marlene Cramer[5,6], Stefanie Wieland[7], Lukas Emmerich[7], Thomas Uibel[8], Anti Rohumaa[9], Heikki Korpunen[1], Grace Jones, Ekaterina Nikolskaya[9], Tom Jansen[7,8], Anneli Adler[10], Tom Mortelmans[11,12], Ian Short[13], Vincent Defays[14], Karol Tomczak[15,16]

[1]Norwegian Institute of Bioeconomy Research, Postboks 115, 1431 Ås, Norway
[2]Research Institutes of Sweden, Brinellgatan 4, Borås, Borås, Sweden
[3]University of Eastern Finland, P.O. Box 111, FI-80101 Joensuu, Finland
[4]Skogforsk, Ekebo 2250, SE-268 90 Svalöv, Sweden
[5]Forest Research, Northern Research Station, Roslin, Midlothian EH25 9SY, UK
[6]Edinburgh Napier University, Sighthill Campus, Sighthill Court, Edinburgh, EH11 4BN, UK
[7]Landesbetrieb Wald und Holz Nordrhein-Westfalen, Centre of Forest and Wood-Based Industries, Team Wood-Based Industries, Carlsauestrasse 91A, D 59939 Olsberg, Germany
[8]Aachen University of Applied Sciences, AZH – Aachener Zentrum für Holzbauforschung, PB 100560, 52005 Aachen, Germany
[9]South-Eastern Finland University of Applied Sciences, Vipusenkatu 9, 57200 Savonlinna, Finland
[10]SLU, Department of Southern Swedish Forest Research Centre, Sundsvägen 3, 234 56 Alnarp, Uppsala, Sweden
[11] Forest is Life, TERRA Teaching and Research Centre, Gembloux Agro-Bio Tech, University of Liège, 5030 Gembloux, Belgium
[12] University of Mons, Place du Parc 20, 7000 Mons, Belgium
[13] Teagasc Forestry Development Department, Ashtown Research Centre, Dublin D15 DY05, Ireland
[14] Filière Bois Wallonie, Zoning du Wex, Rue de la Plaine 9, B-6900 Marche-en-Famenne, Belgium
[15] Poznań University of Life Sciences, ul. Wojska Polskiego 28, 60-637, Poznań, Poland
[16]Łukasiewicz Research Network – Poznań Institute of Technology, 6 Ewarysta Estkowskiego St., 61-755 Poznań, Poland.

E-mail: katrin.zimmer@nibio.no; irena.fundova@nibio.no; ulf.lemke@ri.se; henrik.herajarvi@uef.fi; mateusz.liziniewicz@skogforsk.se; m.cramer@napier.ac.uk; stefanie.wieland@wald-und-holz.nrw.de; lukas.emmerich@wald-und-holz.nrw.de; uibel@fh-aachen.de; anti.rohumaa@xamk.fi; heikki.korpunen@nibio.no ; gracejnomes@gmail.com ; ekaterina.nikolskaya@xamk.fi; tom.jansen@fh-aachen.de; anneli.adler@slu.se ; tmortelmans@uliege.be; ian.short@teagasc.ie; v.defays@filiereboiswallonie.be; karol.tomczak@up.poznan.pl

Keywords:

ABSTRACT
Birch is the third most abundant tree species in northern Europe and the Baltic region, but remains underutilized in several countries despite wood properties that support a broad range of applications, including pulp, veneer, plywood, furniture, flooring, joinery, and potentially structural products. Constraints on higher-value utilization include insufficient logistics for sorting and transport, the lack of standardized grading methods, and limited data infrastructure for systematic quality assessment across supply chains. The Nordic Forest Research (SNS) network VALUE:BIRCH was established to examine these constraints through transnational collaboration among researchers, industry actors, and students across northern Europe. In 2025 and 2026, the network held workshops in Borås, Sweden, and North Rhine-Westphalia, Germany, with emphasis on strength properties, grading, and quality assessment of birch wood. The activities integrated technical presentations, laboratory and field visits, and student contributions, enabling comparison of birch value chains across countries with differing levels of industrial development. The network identified shared technical and organizational bottlenecks related to birch silviculture and management, grading, mobilization, and market formation, while also strengthening inter-institutional co-creation and collaboration. The results indicate that coordinated work on grading systems, quality data, logistics, and market development is essential to support more efficient and value-adapted utilization of birch.

INTRODUCTION

Fennoscandian and Baltic forests are dominated by Norway spruce and Scots pine (*Picea abies* and *Pinus sylvestris* respectively), resulting in industries adapted to the use of those species (Hannerz and Ekström, 2023). Conversely, silver and downy birch (*Betula pendula* and *B. pubescens* respectively), despite ranking third in stem volume, receive less attention, resulting in limited knowledge about optimal planting, management, and logistics. Increasing the planting of or utilizing naturally regenerated broadleaved species (i.e. pioneer tree species), such as birch, is seen as a strategy to mitigate the impacts of climate change and economic losses from biotic and abiotic risks, including bark beetle outbreaks, drought, root rot, and wind damage (Søgaard et al. 2023). Birch's widespread distribution, wood quality, and rapid initial growth make it a promising native option. A major limiting factor of broader planting of birch is the overgrown moose population – unfenced birch seedling stands are subjected to severe browsing damages (e.g., Härkönen et al. 2009)

Birch as an early successional tree species is characterized by rapid initial growth, high genetic variability, and phenotypic plasticity, which benefits biodiversity, soil fertility, and resilience (e.g., Thompson et al. 2009, Dubois et al. 2020). Birch is among the most versatilely used wood species. Its homogeneous, diffuse-porous wood has higher density, stiffness and strength than Norway spruce, making it suitable for products such as pulp, veneers, plywood, furniture, flooring, joinery, and structural timber (Zobel and Van Buijtenen 2012, Alao et al. 2024). In Finland and the Baltic countries, high-quality birch timber is primarily used for veneer and plywood, with limited sawmilling due to the dominance of plywood industries. Lower quality roundwood is used in pulp mills that also allow producing process derivatives for food and chemical industries (Verkasalo et al. 2007, 2017). In Norway and Sweden, birch is often underutilized, mostly as firewood, though efforts are underway to change this (Fridblom et al. 2026). In North Rhine-Westphalia, Germany, birch has only recently been considered for high-value engineered wood products by forest and wood research and some medium-sized wood-processing companies. Increasing interest in alternative species is driven by recent bark beetle damage and the need for diverse, resilient forest structures, with management approaches that mimic natural successional dynamics. In Belgium, birch is currently limited to fuelwood and pulpwood applications, due to the absence of a standardised grading framework and the generally low perceived quality of the available resource. As part of the forest diversification in Scotland, birch is considered as one of the species with potential for wider planting for timber production (Edwards et al. 2025), but to date plays a marginal role as a timber species.

An anticipated higher proportion of birch in Nordic and central European forests brings about a need to explore possibilities for the most efficient utilization of birch wood. Considering its physical and mechanical properties, application in building systems appears to be highly appropriate (Kilde et al. 2006, Collins and Fink 2022**,** Lemke et al. 2023, Duyck et al. 2025**)**. Technically, birch could be used in construction alongside with softwood. Recent work in Ireland (Gil-Moreno et al. 2026) has shown that birch can potentially produce high yields of D18 strength class timber at a relatively young age, potentially exceeding the performance of Sitka spruce (*Picea sitchensis* (Bong.) Carr.). Easy and standardized grading systems for birch have yet to be established, but efforts are ongoing at institutions such as Research Institutes of Sweden, Norwegian Institute of Bioeconomy Research, Edinburgh Napier University, Wald und Holz Nordrhein-Westfalen, FH Aachen University of Applied Sciences, University of Liège, and Poznań University of Life Sciences. A Belgium national grading system is currently being finalised, which will enable the use of birch as a structural timber in the near future (Duyck and Mortelmans, 2025). The current Nordic Timber Grading rules are primarily designed for softwood species and are thus applicable to Norway spruce and Scots pine, but not necessarily to birch. All industrial sawmills in Nordic and Baltic countries follow this guideline in their production, highlighting a significant gap in grading birch wood. Furthermore, Comprehensive knowledge on birch sawlog properties and how they can be predicted with non-destructive measurements is absent, which represents another obstacle to the effective utilization of this resource in sawing. New and undeveloped value chains encounter numerous bottlenecks and barriers that hinder the increased use and value creation of birch (Zimmer et al. 2023). Among these barriers is a lack of systems for logistics, distribution, transportation, and sorting of the timber in many countries (Dubois et al. 2020). These are also the focus areas for the 2025 and 2026 network. Industrial contracts and distribution channels for

hardwood sawlogs are sparse and often fragmented posing challenges for timber harvest, mobilization and transportation logistics (Zimmer et al. 2023).

Sorting timber into various quality assortments can contribute to optimized timber utilization and improved income from forestry activities. In birch processing, as with other tree species, efficient logistics ensure that raw material is quickly delivered to the processing facility. However, these systems often require development to increase the valorization of underutilized wood species, such as birch. Acquiring data for quality assessments and sorting is crucial. One of the key measures is the development of communication solutions to enhance mobilization and information flow on available birch timber.

Another significant barrier is that birch and its qualities are not marketed in some of the participating countries. To increase quality-adapted birch utilization and establishment of long-term viable value chains for the species several actions are necessary. These involve creating a market for birch products beyond firewood, highlighting and marketing birch's features and benefits, and product development for birch and other hardwoods, including medium-quality timber (Dubois et al. 2020) and engineered wood products (Gil-Moreno et al. 2026).

NETWORK RATIONALE AND OBJECTIVES

The VALUE:BIRCH network was established to connect researchers, forest owners, and industrial actors to increase value creation from birch in the Nordic region and beyond. Rather than focusing on a single segment, the network spans the full value chain from forest resources and silviculture to sorting, logistics, processing, and end-use applications, which is also reflected in the working areas of the participating researchers. A central rationale has been that many countries are addressing similar challenges, but often in isolation and at different stages of value-chain development.

NETWORK ACTIVITIES AND OUTCOMES

The network brought together researchers and industry representatives from several European countries, including Norway, Sweden, Finland, Germany, Ireland, the United Kingdom, Belgium, and Poland. The activities showed that birch value chains differ markedly among participating countries, ranging from relatively mature systems to early-stage development, but also reflecting different motivations for their development. Despite these differences, the discussions revealed common technical and organizational barriers, particularly the absence of standardized strength grading for birch timber and the lack of coordinated approaches to data collection, sorting, and mobilization.

Core activities were the network meetings in Borås, Sweden, 2025, and North Rhine-Westphalia, Germany, 2026, which combined technical presentations, laboratory-, field visits, and student contributions. Forest visits fostered discussion around tree breeding and silviculture, as well as challenges around logistics and promotion of the species. The programme focused on grading, strength properties, and quality assessment, while also creating space for exchange between countries with different industrial contexts. The network meetings help connect previously separate initiatives and strengthened the basis for joint research and innovation activities. Tangible outcomes include a discussion platform, the initiation of a manuscript on the European birch resource, the development of a project application with a dedicated work package on birch quality, and stronger links between research institutions and industry actors.

Through the network activities in 2025 and 2026, birch grading was identified as a means to open the market for birch into other standardised product segments, and this became one of the main focus areas for the network.

DISCUSSION AND FUTURE PERSPECTIVES

The network demonstrates that birch has strong potential to contribute to more diversified, resilient, and regionally adapted forest bioeconomy in northern Europe. At the same time, the discussions confirmed that higher-value utilization depends on progress in several connected areas: grading systems, quality databases, logistics, communication between actors, and market development for assortments beyond firewood. By bringing together expertise from countries with different resource bases and industrial traditions, the network creates shared competence and clarified priority topics for future collaboration.

These findings are relevant not only for birch, but also for broader efforts to diversify forest-based bioeconomies and increase the use of local hardwood resources. The VALUE:BIRCH network shows how transnational collaboration can accelerate learning, reveal common bottlenecks, and support the formation of new research and innovation partnerships. Priorities identified for continued work include tailored logistics solutions, improved mobilization of raw material, harmonized quality assessment approaches, grading and targeted product and market development for medium- and high-value birch applications.

CONCLUSIONS

VALUE:BIRCH illustrates how a research and industry network can help identify and unlock the potential of an underutilized hardwood resource by aligning expertise across countries and value-chain links. The VALUE:BIRCH activities produced concrete collaborative outcomes and identified a shared agenda for future work on grading, logistics, mobilization, and market development. As such, the network provides both a practical platform for cooperation and a model for strengthening resilient, knowledge-based forest value chains in Europe.

ACKNOWLEDGEMENTS

We acknowledge Nordic Forest Research (SNS) for funding the VALUE:BIRCH network. We also thank the participating institutes and universities for providing complementary internal support that enabled network activities. Special thanks are extended to Ulf Lemke at RISE, Sweden (2025), and to Stefanie Wieland and Lukas Emmerich at Zentrum HOLZ NRW, Germany (2026), for organizing the network meetings.

REFERENCES

Alao PF, Dembovski KH, Rohumaa A, Ruponen J, Kers, J. (2024). The effect of birch *(Betula pendula* Roth) face veneer thickness on the reaction to fire properties of fire-retardant treated plywood. Constr Build Mater 426:136242. https://doi.org/10.1016/j.conbuildmat.2024.136242.

Collins S, Fink G. (2022). Mechanical behavior of silver birch structural timber under compression loading. Wood Material Sicence and Engineering, 17:2, 121-128. https://doi.org/10.1080/17480272.2020.1801836.

Dubois H, Verkasalo E, Claessens H. Potential of Birch (*Betula pendula* Roth and *B. pubescens* Ehrh.) for Forestry and Forest-Based Industry Sector within the Changing Climatic and Socio-Economic Context of Western Europe. *Forests*. 2020; 11(3):336. https://doi.org/10.3390/f11030336

Dunham R, Cameron AD, Petty JA. (1999). The effect of growth rate on the strength properties of sawn beams of silver birch (*Betula pendula* Roth). *Scand J For Res*, 14(1):18-26. https://doi.org/10.1080/02827589908540805

Duyck A, Mortelmans T. (2025). Technical, Environmental, and Economic Properties of Several Wood Species from Forests of Western Europe. https://doi.org/10.5281/zenodo.15038880.

Duyck A, Mortelmans T, De Mil T, Van Parys L, Descamps T. (2025). Timber selection for sustainable construction: A holistic approach to species assessment and decision support. Constr. Build. Mater. 490, 142483. https://doi.org/10.1016/j.conbuildmat.2025.142483.

Edwards et al., 2025, Future productive species for Scotland, The Research Agency of the Forestry Commission, https://cdn.forestresearch.gov.uk/2025/09/Future-productive-species-for-Scotland.pdf.

Fridblom M, Woxblom L, Hellgren M. (2026). Färdplan för svensk lövträindustri 2026–2040. https://www.svenskttra.se/siteassets/6-om-oss/nyheter/2026/april/kortversion_fardplan-for-svensk-lovtraindustri-2026-2040_final.pdf

Gil-Moreno D, Sheridan O, Harte AM and McGetrick PJ. (2026) Structural properties of Irish-grown birch and use of non-destructive acoustic techniques for timber grading. *Forestry* 99: 1-13. https://doi.org/10.1093/forestry/cpaf047

Hannerz M, Ekström H. (2023). Nordic Forest Statistics 2023, Resources, industry, trade, prices, environment and climate. Nordic Forest Research (SNS) secretary. https://share.google/Ge2ljvuyLs9IhTklb.

Härkönen S, Pulkkinen A, Heräjärvi H. (2009). Wood quality of birch (*Betula* spp.) damaged by moose. Alces 45: 67–72. https://alcesjournal.org/index.php/alces/article/view/15.

Kilde V, Solli KH, Pitzner B, Lind P, Bramming J. (2006). Bjørk i synlige konstruksjoner. Norsk Treteknisk Institutt, Rapport, (67). https://www.treteknisk.no/publikasjoner/rapport/67-bjork-i-synlige-konstruksjoner.

Lemke U, Johansson M, Ziethén R, Briggert A. (2023) New criteria for visual strength grading of sawn timber from birch grown in Sweden. World Conference on Timber Engineering, 19-22 June 2023, Oslo, Norway; 2023. https://www.proceedings.com/content/069/069179-0102open.pdf.

Søgaard G, Bright R, Clarke N, Fløistad IS, Granhus A, Hagenbo A, Hanssen KH, Hietala A, Kjønaas OJ, Kühne C, Rolstad J, Solberg S, Steffenrem A, Stokland J, Storaunet KO. (2023). Oppdatering av kunnskapsgrunnlag for klimatiltak i skog: Gjennomgang av 11 utvalgte tiltak i bestandsskogbruket. NIBIO Rapport 9/22/2023. https://hdl.handle.net/11250/3069701.

Thompson I, Mackey B, McNulty S, Mosseler A. (2009). Forest resilience, biodiversity, and climate change. Secretariat of the Convention on Biological Diversity, Montreal Technical Series no 43 1-67; https://www.cbd.int/doc/publications/cbd-ts-43-en.pdf.

Verkasalo E, Heräjärvi , Möttönen, V, Haapala A, Brännströ H, Vanhanen H, Miina, J. (2017). Current and future products as the basis for value chains of birch in Finland. ISCHP 2017: 6th International Conference on Hardwood Processing. Lahti, Finland, p. 81-96. http://urn.fi/URN:ISBN:978-952-326-509-7

Verkasalo E, Toppinen A, Arponen J, Heräjärvi H. (2007). Perspectives of wood resources, industrial competitiveness and wood product markets for birch industries in the Baltic Sea area. International Scientific Conference on Hardwood Processing, 24–26.09.2007, Quebec City, Canada. Pp. 29–35. (http://www.ischp.ca/pdf/ISCHP_Proceedings.pdf)

Zimmer K, Hylen G, Kuehne C, Hanssen KH, Fløistad I, Smith A. (2023). Bjørk i Norge. NIBIO Rapport 9/63/2023.(in Norwegian). https://hdl.handle.net/11250/3067785.

Zobel BJ, Van Buijtenen JP (2012) Wood variation: its causes and control. Springer Science & Business Media.

Assessing the Quality of Wood in Beech Trees After a Forest Fire

Ioan-Aurelian Mitrofan[1], Victor-Mihai Ciomag[1], Elena-Camelia Musat[1*]

[1] Transilvania University of Brasov, Faculty of Silviculture and Forest Engineering, Sirul Beethoven no. 1, 500123, Brasov, Romania

E-mail: ioan.mitrofan@unitbv.ro; victor.ciomag@yahoo.com; elena.musat@unitbv.ro

Keywords: burned wood; beech trees; tomogram; quality evaluation; forest fires.

ABSTRACT

Wood species play a significant role in the development and behaviour of a forest fire, due to differences in the chemical composition, structure, and characteristics of wood. Unlike softwoods, hardwoods have a low content of volatile oils, which makes their wood less flammable. However, some deciduous species are more resistant to fire than others, with thin bark or an anatomical structure sensitive to high temperatures, such as the beech, which can even suffer from sunstroke during very sunny days in summer. Thus, trees can be affected by forest fires in different ways, in some cases the impact of the fire being so intense that the life of the tree ceases. Trees that survive a fire can continue to exist after it has passed, but their subsequent development is closely linked to the intensity of the fire, which influences the degree of damage suffered by the trees, their capacity for regeneration and their resistance to subsequent stressors. Based on these considerations, the purpose of the work was established, namely to evaluate the impact of a forest fire on the wood quality of the remaining beech trees in the affected area. The research was carried out in the summer of 2025 in the compartment 83 within the Production Unit 8 - Măneciu Forest District, Prahova Forestry Directorate, Romania, in a 110-year-old beech stand, affected by a litter fire in the Autum of 2023. The fieldwork involved visual analyses and investigations with the Arbotom Rinntech sonic tomograph, after which, depending on the results obtained, point determinations were made with the IML F-500 Resi resistograph and the Pressler drill. Following visual analyses of all the trees in the plot affected by the fire, it was found that numerous trees are dry, and those that are still growing are in advanced stages of deterioration. It was also observed that the most affected trees were found in the direction of fire propagation. The results obtained through modern non-invasive techniques indicated significant deterioration of the wood inside the trunk, which was in various stages of decay. Areas where the Arbotom sound tomograph indicated reduced sound transfer velocities through the wood were verified by extracting growth cores, which confirmed the presence of internal rot. In the period from the outbreak of the fire until the date of the investigations, the stand was not cleared of trees affected by the fire, which led to a considerable depreciation of the trees and the quality of the wood, so that they cannot be used solely for firewood.

INTRODUCTION

Forest fires are uncontrolled fires that spread rapidly in wild vegetation, including forests, meadows and other wooded or naturally vegetated areas (Ciobanu and Ioraș 2007). Most often, human negligence causes most vegetation fires. However, the combustible materials in a forest, also known as forest fuels, play a crucial role in the behavior and spread of fires. These materials can vary significantly depending on the type of forest, the composition of the vegetation and local conditions. The large amount of combustible materials, characterized by dense layers of dry leaves, branches and other plant debris, favors the spread of fires (Blanchet and Roudier 2016).

On the other hand, hot weather contributes to the drying of vegetation, increasing the risk of fire, as low humidity combined with dry vegetation creates favorable premises for the onset and rapid development of a fire (Brady et al. 2015). In addition, the terrain configuration, particularly steep slopes and sunny exposure, favors the rapid ascent of fire, as flames tend to uphill faster than downhill, while sun-exposed slopes are drier and more susceptible to wildfires.

Forest fires affect different parts of trees, depending on the intensity and location of the fire (Ciobanu and Ioraș 2007). Trees that survive a fire can continue to exist even after the fire has passed, but their subsequent development is closely linked to the intensity of the fire (Mușat 2024). This influences the

degree of damage suffered by trees, their capacity for regeneration, and their resistance to subsequent stress factors.
To evaluate the impact of forest fires on the remaining trees, both visual analyses and more detailed investigations using modern technology can be performed (Mușat 2024), which allows the assessment of the trees' internal condition without damaging them. Among these methods, the resistograph and the tomograph are the most suitable instruments, being considered near-nondestructive techniques that provide valuable information about the health and structure of the wood inside the trunk (Rinn, 2014). However, for detailed assessments of internal quality, destructive methods such as the Pressler borer are also sometimes used.
Thus, the aim of this study was to evaluate the wood quality of European beech trees (*Fagus sylvatica* L.) remaining after a litter fire, by using a sonic tomograph and a resistograph. The study aimed both to evaluate the transfer velocity of sonic waves through the wood and to analyze the relative drilling resistance, as well as to compare the results obtained through non-destructive techniques with the actual condition of the wood as determined by growth cores.

MATERIALS AND METHODS

The research was conducted in a 110-year-old beech stand originating from natural seed regeneration, with the soil partially covered by litter and herbaceous vegetation of the Asperula-Dentaria type. The forest affected by the fire covers an area of 13.49 ha and is located in the mountainous region of Prahova County, in the Măneciu area, Romania (Figure 1a and 1b). The terrain configuration consists of an undulating slope with a south-western exposure and a steep incline (35 degrees).
The fire broke out in the autumn of 2023 (Figure 1c) and affected a significant part of the management unit. It spread from an area adjacent to the forest, where dry vegetation had been set on fire. The forest fire developed as a litter fire which, due to the accumulation of dry leaves on the ground, eventually affected the base of the trees, with some displaying charring in the root collar zone or the lower part of the trunk. At the time of the field investigations (May, 2025), it was observed that the fire had a specific propagation direction (Figure 1d), which resulted in the greatest damage being concentrated in certain areas, particularly along the path of the fire.

a. b. c. d.

Figure 1: fire location (a.), images during the fire (b.), forest appearance at the time of the investigations (c.) and the direction of fire spread (d.)

The methodology first involved surveying the forest stand to identify the trees for analysis, alongside a visual assessment (Figure 2a) to record the main identified defects. Subsequently, the actual measurements were conducted using the Arbotom Rinntech sonic tomograph (Figure 2b). Based on these results, localized measurements were then carried out using the IML F-500 Resi resistograph and the Pressler increment borer (Figures 2c and 2d). The sonic tomography investigations were performed at two trunk levels, specifically at 50 and 100 cm, measured from the uphill side, as the management unit was located on a steeply sloping terrain (35°).
After completing the data entry phase and verifying the correct connection between the sensors, the actual measurement process was initiated. Thus, each sensor, starting with S1, was successively tapped seven times with the hammer. The number of impacts was chosen based on the ambient noise level in the area, in compliance with literature recommendations (Rinn 2014), which state that between 5 and 10 impacts should be applied to each sensor.

a. b. c. d.

Figure 2: Height measurement for the level at which the investigation is to be performed (a.), placement of sensors on the torso and acquisition of the tomogram (b), conducting resistograph testing (c.) and extracting increment cores using a Pressler borer (d.)

RESULTS

Visual analysis of the stand highlighted the impact of fire on the remaining standing trees, revealing that numerous trees suffered directly or indirectly from the fire (Figure 3). Some of these individuals have died standing, others sustained various structural breakages, while others exhibited visible trunk damage, such as scorched or even charred bark.

a. b. c. d.

Figure 3: Trees dried due to direct fire impact (a.), trees with cracked bark on the trunk (b.), beech trees with partially dieback crowns (c.) and beech trees with fungal fruiting bodies on the trunk (d.)

The results obtained from the investigations will be presented below for two trees: one that is still growing, although under difficult conditions (beech_1), and another that died as a result of the fire (beech_3).

At the level of beech tree number 1—a tree that continues to grow under harsh conditions, exhibiting a partially dieback crown and numerous signs of fire impact at the base of the trunk (Figures 4a and 4b)—a certain difference was observed between the investigated sections. Consequently, the tomogram corresponding to the 100 cm level displays a more extensive area in the central zone of the trunk where propagation velocities are lower, causing the central part of the tomogram to exhibit shades of yellow.

The drilling resistance measurements were performed along the path of sensor S1 at the 100 cm level, and the extraction of the increment core was carried out along the same direction. Based on the cumulative analysis of the sonic tomogram line matrix, the trunk photograph in the investigated area, the resistogram, and the extracted increment core along the same direction (Figure 5), somewhat contradictory aspects were found. Specifically, along the S1-S9 sensor path, the sound propagation velocities through the wood are 1109 m/s (S1 to S9) and 1215 m/s (S9 to S1), respectively, which does not indicate severe wood degradation. This is further supported by the drilling resistance profiles, which display multiple large-amplitude oscillations occurring after the first 3 cm of the sample, where the drilling resistance is close to zero (Figure 5c).

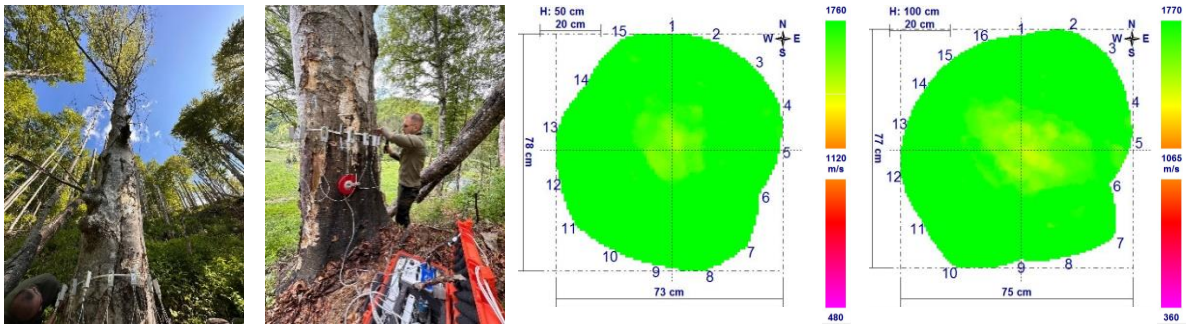

a. b. c.

Figure 4: Beech Tree_1 (a.), tomogram at 50 cm – Beech_1_50 (b.), tomogram at 100 cm – Beech_1_100 (c.)

On the other hand, the increment core also indicates sound wood inside the trunk and a section of degraded and even decayed wood within the first centimeters of the sample (Figure 5c). All these aspects can influence the results provided by the tomograph, in the sense that it calculates the average propagation velocities for the entire distance between the two sensors, across all 7 strikes applied to the emitting sensors (S1 and S9). Consequently, the colors corresponding to the sensor line matrix and the tomogram itself ultimately display values and colors characteristic of sound wood, without significant degradation or internal irregularities.

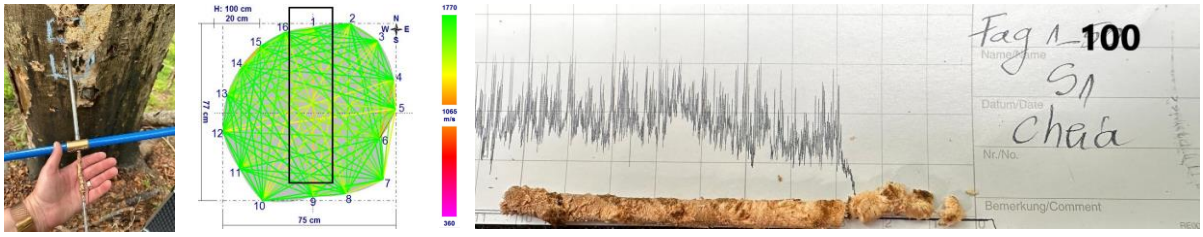

a. b. c.

Figure 5: Extraction of the increment core at Beech_1_100_S1 (a.), sensor line matrix at Beech_1_100 (b.), resistogram and the corresponding increment core for tree Beech_1_100 (c.)

In the case of beech tree number 3 (Beech_3), a peculiar situation arose where high sound propagation velocities through the wood were recorded—reaching up to 2500–3000 m/s (Figures 6b and 6c) across both investigated sections. This aspect is somewhat contradictory to the actual condition of the tree, which is nearly dead and exhibits numerous fruiting bodies on the trunk (Figure 6a). These extreme velocities cause both tomograms to be colored predominantly in shades of yellow and orange, which would normally draw attention.

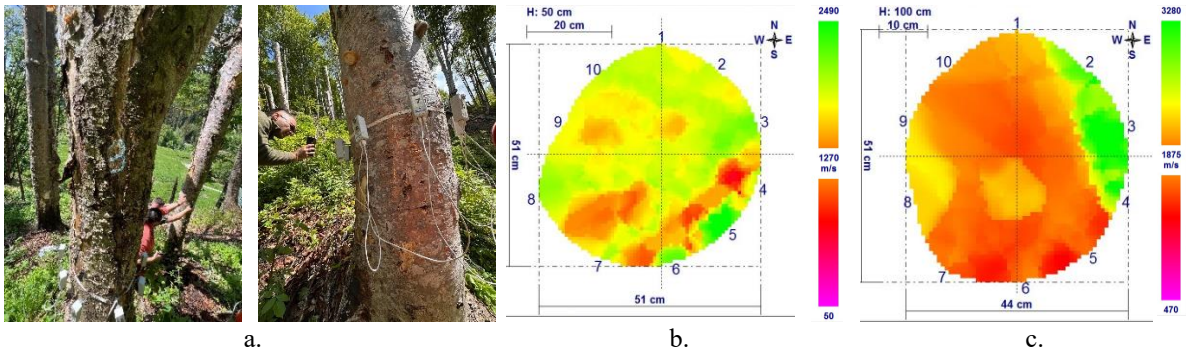

a. b. c.

Figure 6: Beech Tree_3 (a.), tomogram at 50 cm – Beech_3_50 (b.) and tomogram at 100 cm – Beech_3_100 (c.)

The additional investigations conducted with the resistograph and the Pressler borer are highly conclusive for this tree, aligning with the external appearance of the trunk in the analyzed zone, which indicates the presence of decay right from the surface (Figure 7a). Comparing the appearance of the trunk with the results indicated by the tomograph reveals a major discrepancy between them. This is because the sensor line matrix indicates relatively high sound propagation velocities through the wood (1546 and 1594 m/s for the S1–S6 and S6–S1 directions, respectively – Figure 7b), whereas the external appearance of the trunk shows clear signs of severe tissue degradation. On the other hand, comparing the resistogram with the actual condition of the wood for the section of the trunk subjected to measurements (the first 8 cm) reveals a certain similarity. Specifically, as the drill bit advances, frequent large-amplitude oscillations are recorded (Figure 7c); however, these are located at the lower end of the resistogram, indicating the presence of heavy degradation that has not completely destroyed the wood structure, which is much easier to identify on the increment core.

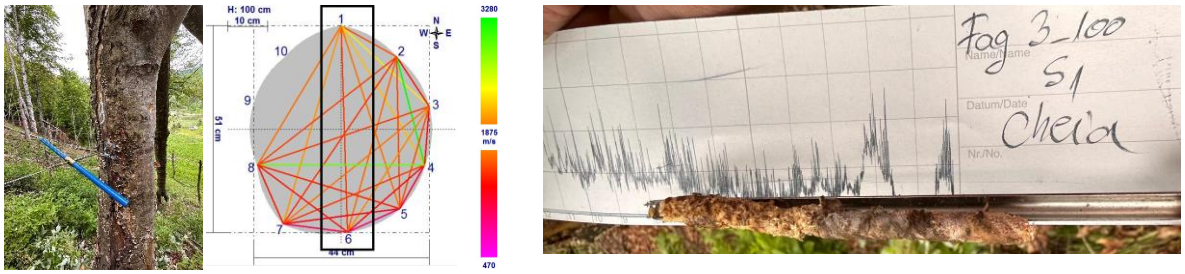

a. b. c.

Figure 7: Extraction of the increment core at Beech_3_100_S1 (a.), sensor line matrix at Beech_3_100 (b.), resistogram and the corresponding increment core for tree Beech_3_100 (c.)

CONCLUSIONS

The direction of fire propagation was highly significant, as it dictated the zone containing the trees most severely affected by the forest fire.

The impact of the fire was directly felt by the trees through the depreciation of wood quality and the death of intensively burnt trees—consequences that affected the individuals within a short period of time.

There were also trees where the impact of the fire, although direct, manifested over a longer period; these individuals continue to grow under precarious conditions, resulting in parts of their crowns being affected by dieback and the presence of fungal fruiting bodies on their trunks.

For the investigated trees, it was found that the predominant velocities provide a certain level of confidence in determining the internal wood quality. However, the coloring of the tomograms is scaled relative to the extreme sound propagation velocities recorded through the wood, which can compromise the accuracy of result interpretation.

Although punctual measurements conducted with the resistograph and the Pressler borer provide more precise information regarding the actual quality of the internal trunk wood, they remain invasive methods to varying degrees, making them unsuitable for widespread application on future crop trees.

REFERENCES

Blanchet, A., Roudier, P., 2016. Ultrasonic testing for wood quality assessment, vol. 33, pp. 29-45.

Brady, M., Hristov, J., Sahrbacher, C., Wilhelmsson, F., 2015 Passivt jordbruk: inlåsning av mark eller bevarande av öppna landskap? Agri. Food Economic Centre, Working paper no. 3, 34 p.

Ciobanu V., Ioraș Fl., 2007. Incendii forestiere. Transilvania University Publishing House, 131 p.

Mușat, E.C., 2024. How well can sound tomograms characterize inner-trunk defects in beech trees from a burned plot? BioRes. 19(4):7530-7565. DOI: https://doi.org/10.15376/biores.19.4.7530-7565

Rinn F., 2014. Central basics of sonic tree tomography, 14(4):8–10. https://ictinternational.com/casestudies/central-basics-of-sonic-tree-tomography/ Accessed 04 October 2024.

Cross-Laminated Timber in Romania: Insights from a Stakeholder Survey and Future Development Opportunities

Petruț Fola[1*], Aurel Lunguleasa[1], Alin Olărescu[1]

[1] Transilvania University of Brasov, Faculty of Furniture Design and Wood Engineering, Universității 1, 50068, Brasov, Romania

E-mail: petrut.fola@unitbv.ro; lunga@unitbv.ro; a.olarescu@unitbv.ro

Keywords: Cross-laminated timber; hardwood and hybrid CLT; mass timber construction; stakeholder survey; hardwood resources; Romania;

ABSTRACT

Cross-laminated timber (CLT) has emerged as one of the most promising engineered wood products for sustainable and low-carbon construction. Over the past decade, CLT has experienced rapid development in Europe and North America, becoming a key component of mass timber construction. While most commercially produced CLT panels are manufactured from softwood species, recent research has increasingly focused on the potential use of hardwood species such as beech, poplar, and birch, which offer higher mechanical performance and opportunities for improved resource utilization.

Despite these global developments, the adoption of CLT in Romania remains limited, and little information is available regarding industry awareness and market readiness. Therefore, this study aims to evaluate the current perception and adoption potential of CLT in Romania while also discussing the possible role of hardwood resources in future CLT production.

A structured survey was conducted among professionals from the construction sector, including architects, structural engineers, researchers, and representatives of the wood industry. The questionnaire investigated the level of awareness of CLT, previous experience with mass timber construction, perceived advantages of CLT systems, and the main barriers to their implementation in Romania.

The results indicate a growing interest in CLT and mass timber construction, although limited technical knowledge, regulatory constraints, and the lack of local production remain significant challenges. At the same time, respondents acknowledged the potential of Romania's hardwood resources as a possible basis for future CLT development.

INTRODUCTION

In the context of growing global concerns regarding climate change and the need to reduce the carbon footprint of the construction sector, sustainable building materials have become a major priority in both research and practice. The construction industry is responsible for a significant share of greenhouse gas emissions, which necessitates the adoption of innovative, energy-efficient solutions based on renewable resources. In this regard, engineered wood products have attracted considerable attention due to their capacity to store carbon and to substitute conventional materials with high environmental impact, such as concrete and steel (Gustavsson & Sathre, 2011; Churkina et al., 2020).

Among these, cross-laminated timber (CLT) has emerged as one of the most promising technologies for modern construction. The rapid development of CLT in Europe and North America has led to the rise of the "mass timber" concept, enabling the construction of large-scale structures, including multi-storey buildings, with high structural performance and durability (Brandner et al., 2016; Karacabeyli & Douglas, 2013). Traditionally, CLT panels are manufactured from softwood species, due to their availability and favorable processing characteristics. However, recent research has increasingly focused on the use of hardwood species, such as beech, poplar, and birch, which can offer superior mechanical properties and more efficient utilization of forest resources (Aicher et al., 2016; Ringhofer et al., 2018).

Despite these international developments, the adoption of CLT in Romania remains limited. The Romanian construction sector is still largely dominated by conventional materials, while the integration of innovative timber-based solutions is influenced by factors such as regulatory frameworks, the level

of technical knowledge, and the availability of local production. At the same time, Romania possesses significant forest resources, including a considerable potential of hardwood species, which could support the development of a domestic CLT industry.

In this context, understanding the perceptions of industry stakeholders becomes essential for assessing the prospects of CLT implementation. An analysis of awareness levels, professional experience, and perceived barriers can provide valuable insights for the development of strategies aimed at promoting and integrating these construction systems. Survey-based approaches are widely used in construction research to capture stakeholder perspectives and support decision-making processes (Creswell, 2014; Fellows & Liu, 2015).

Therefore, the aim of this study is to evaluate the current perception of CLT in Romania and its adoption potential, while also exploring the possible role of hardwood resources in the future development of this sector. To address these objectives, the study is based on a structured survey conducted among professionals from the construction sector and the wood industry, providing insights into the level of awareness, experience, and perceived barriers associated with the use of CLT in the national context.

In addition, the increasing implementation of nearly Zero-Energy Buildings (nZEB) requirements in Romania further supports the relevance of timber-based construction systems such as CLT. Due to their low environmental impact, prefabrication potential, and favorable thermal performance, CLT systems may contribute to achieving national and European sustainability targets for energy-efficient buildings. In this context, the development of local CLT solutions based on domestic timber resources could represent an important opportunity for the Romanian construction sector.

MATERIALS AND METHODS

A structured questionnaire was developed to assess the perception and adoption potential of cross-laminated timber (CLT) in Romania. The survey targeted professionals involved in the construction and wood industry sectors, including architects, structural engineers, researchers, and other stakeholders.

The questionnaire consisted of multiple-choice and Likert-scale questions addressing key aspects such as level of awareness, practical experience, perceived performance, and barriers to the implementation of CLT. In addition, several questions focused on identifying priority areas for improvement and future research directions.

The survey was distributed online using Google Forms, and responses were centralized and processed using Google Sheets. 23 valid responses were collected and analysed. The data were processed using descriptive statistical methods, including frequency distribution and percentage-based analysis, in order to identify trends and patterns in respondents' perceptions.

RESULTS AND DISCUSSION

The survey included 23 Romanian participants with diverse professional backgrounds related to the construction and wood industry sectors. The majority of respondents were design engineers (structures/building services), accounting for 39.1% of the sample, followed by researchers/academic staff (26.1%) and architects (17.4%), (Figure 1). Other categories, including CLT manufacturers, clients/developers, technical controllers, and machinery sales representatives, each represented 4.3% of the respondents. The distribution indicates that the survey primarily reflects technical and research-oriented perspectives, with limited representation from production and market-related stakeholders.

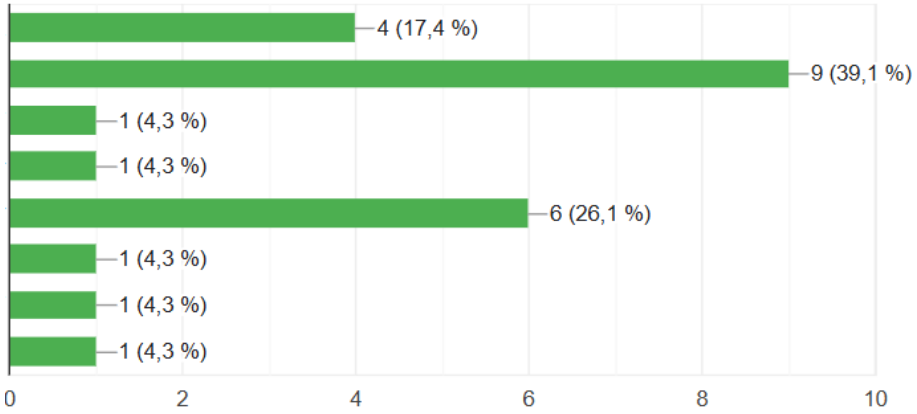

Figure 1: Distribution of respondents according to their primary professional role in relation to cross-laminated timber (CLT)

In terms of experience with CLT, more than half of the respondents (52.2%) reported only theoretical knowledge, while 34.8% had experience in more than three projects (Figure 2). This highlights a limited level of practical implementation despite a relatively high degree of awareness, a pattern also observed in emerging CLT markets (Espinoza et al., 2016). A smaller proportion of respondents reported either limited practical involvement, through analysing proposals/studies (8.7%) or participating in one to two projects (4.3%).

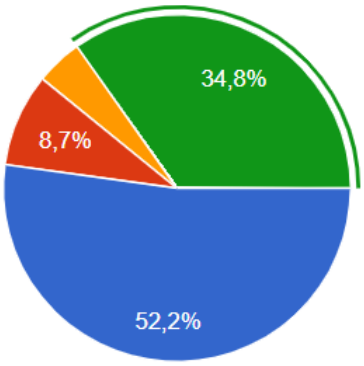

Figure 2: Level of professional experience with cross-laminated timber (CLT) among respondents

These results suggest that, despite a relatively high level of awareness and interest, practical experience with CLT remains limited in the Romanian context, highlighting a gap between knowledge and implementation. Overall, the perception of CLT is positive, with all respondents indicating that they would consider using CLT in a project.

The results indicate that the most significant barriers to CLT adoption are related to economic and informational aspects. Cost was identified as the primary constraint (73.9%), followed by lack of information in the market (69.6%) and limited availability of experienced companies (56.5%). Fire-related concerns (34.8%) and regulatory/approval issues (26.1%) were also mentioned, while seismic performance and standard panel dimensions were not perceived as major barriers.

These findings suggest that the limited adoption of CLT in Romania is influenced more by market maturity and knowledge dissemination than by structural or technical concerns, consistent with trends reported in emerging CLT markets (Espinoza et al., 2016). (Figure 3).

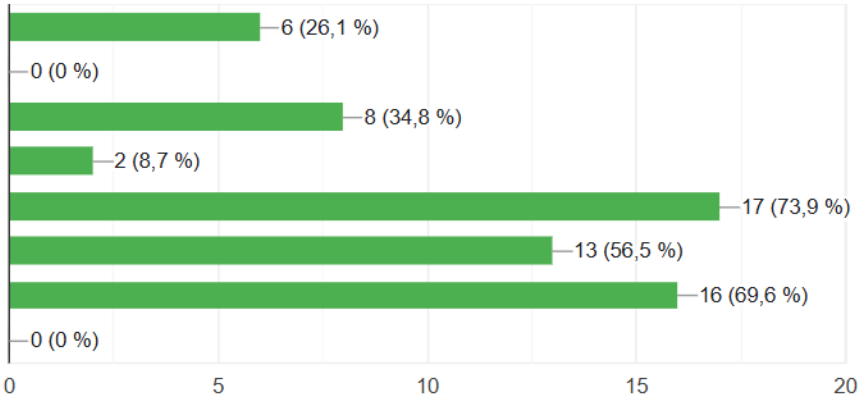

Figure 3: Main barriers to the adoption of cross-laminated timber (CLT) in Romania, as identified by respondents

Respondents identified several key areas for improvement in order to support the wider adoption of CLT in Romania (Figure 4). The most important include cost optimization (65.2%), moisture control and airtightness (60.9%), and the development of local standards and guidelines (56.5%) as the most important priorities for the wider implementation of CLT in Romania.

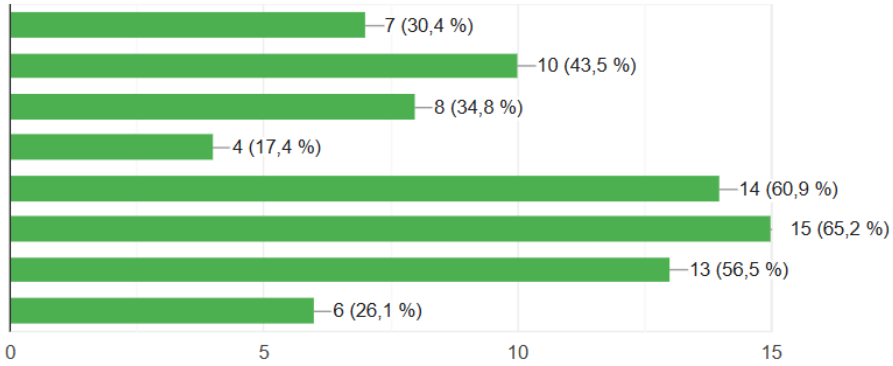

Figure 4: Priority areas for development of CLT in Romania

In addition, fire protection (43.5%) and acoustic/vibration performance (34.8%) were highlighted as important technical aspects requiring further research. These findings are consistent with ongoing research trends focused on improving CLT performance and adapting design approaches to specific conditions (Frangi et al., 2009; EN 1995-1-1).

Furthermore, the interest in improving performance and optimizing resource use suggests a potential for the integration of locally available timber, including hardwood species, in future CLT development (Aicher et al., 2016; Ringhofer et al., 2018).

Regarding realistic product improvements over the next 2–5 years, respondents emphasized the importance of panel standardization for the local market, integrated fire protection solutions, hybrid CLT systems, and improved acoustic performance. In addition, several participants highlighted the need for optimizing bonding technologies and developing more environmentally friendly adhesives.

These findings reflect current international research trends focused on improving CLT performance, sustainability, and adaptability to specific market requirements (Frangi et al., 2009; Aicher et al., 2016)

CONCLUSIONS

The results of this study indicate a generally positive perception of cross-laminated timber (CLT) among professionals in Romania, with a high willingness to adopt this system in future projects. However, the level of practical experience remains limited, highlighting a gap between awareness and implementation, consistent with trends observed in emerging CLT markets (Espinoza et al., 2016).

The main barriers to adoption are primarily economic and informational, particularly cost, lack of market knowledge, and limited availability of experienced companies. These findings suggest that the challenges associated with CLT implementation are strongly related to market maturity rather than purely technical limitations.

From a technical perspective, CLT is recognized for its structural performance and aesthetic qualities (Brandner et al., 2016; Karacabeyli & Douglas, 2013). Nevertheless, aspects such as moisture behavior, vibration performance, and fire resistance remain areas of concern, requiring further research and validation.

Future research should focus on improving the technical performance of CLT systems, especially in relation to fire, acoustics, and environmental durability. In addition, particular attention should be given to the potential use of locally available hardwood species, which may enhance mechanical performance and contribute to a more efficient utilization of Romania's forest resources (Aicher et al., 2016; Ringhofer et al., 2018). At the same time, increasing market awareness, developing local expertise, and improving cost competitiveness are essential for supporting the wider adoption of CLT in Romania.

REFERENCES

Aicher, S., Christian, Z., & Dill-Langer, G. (2016). Hardwood glulams—Emerging timber products of superior mechanical properties. Construction and Building Materials, 102, 989–1002.

Brandner, R., Flatscher, G., Ringhofer, A., Schickhofer, G., & Thiel, A. (2016). Cross laminated timber (CLT): Overview and development. European Journal of Wood and Wood Products, 74(3), 331–351.

Espinoza, O., et al. (2016). Cross-laminated timber: Status and research needs in North America. BioResources, 11(1), 281–295.

Frangi, A., Fontana, M., Hugi, E., & Jöbstl, R. (2009). Experimental analysis of cross-laminated timber panels in fire. Fire Safety Journal, 44(8), 1078–1087.

Churkina, G., Organschi, A., Reyer, C. P. O., Ruff, A., Vinke, K., Liu, Z., Reck, B. K., Graedel, T. E., & Schellnhuber, H. J. (2020). Buildings as a global carbon sink. Nature Sustainability, 3, 269–276.

Creswell, J. W. (2014). Research design: Qualitative, quantitative, and mixed methods approaches (4th ed.). Sage Publications.

Fellows, R., & Liu, A. (2015). Research methods for construction (4th ed.). Wiley-Blackwell.

Gustavsson, L., & Sathre, R. (2011). Energy and carbon balances of wood construction. Energy and Buildings, 42(2), 230–242.

Hameury, S. (2005). Moisture buffering capacity of wood. Building and Environment, 40(10), 1404–1412.

Karacabeyli, E., & Douglas, B. (2013). CLT handbook: Cross-laminated timber. FPInnovations.

Ringhofer, A., Brandner, R., Schickhofer, G., & Thiel, A. (2018). Cross-laminated timber (CLT) made from hardwoods. European Journal of Wood and Wood Products, 76(2), 677–689.

EN 16351 (2015). Timber structures – Cross-laminated timber – Requirements.

EN 1995-1-1 (Eurocode 5). Design of timber structures.

Study on the Natural Durability of *Quercus pyrenaica* Willd.

Sara M. Santos[1], Saúl Gutiérrez[2*], María Teresa de Troya[1], Lee Robertson[1], Gonzalo Caballé[2], José Luis Villanueva[2]

[1] Institute of Forest Sciences (ICIFOR), National Institute of Agrarian and Food Research and Technology (INIA) - Superior Council for Scientific Research (CSIC), Ctra. de La Coruña km. 7, 28040 Madrid, Spain
[2] Center for Forestry and Industry Services of Castilla y León (CESEFOR), Pol. Ind. Las Casas, Calle C Parcela 5, 42005 Soria, Spain.

E-mail: santos@inia.csic.es; saul.gutierrez@cesefor.com; troya@inia.csic.es; robertson.lee@inia.csic.es; gonzalo.caballe@cesefor.com; joseluis.villanueva@cesefor.com

Keywords: natural durability; *Quercus pyrenaica*; xylophages; basidiomycetes; subterranean termites.

ABSTRACT

The European project LIFE+REB, establishes a Climate-Smart Forestry (CSF) framework applied to Quercus pyrenaica forests in Castilla and León, with the aim of improving their climate change mitigation capacity while ensuring forest adaptation through biodiversity conservation. The project develops a systematic decision-making methodology to evaluate the different management options and their transferability to wider areas of the species' range, incorporating the cascading use of wood products as a key mitigation strategy to replace fossil-based materials. A core objective is the creation of new value chains through innovative long-life wood products from sustainable forest management.

Evaluating wood natural durability is essential when establishing the level of protection required depending on the end use to extend its service life. Natural durability is defined as the intrinsic resistance of wood against the attack of destructive organisms. There are standardized methods to estimate a durability value. In Europe, the standard EN 350:2016 is responsible for establishing the basic guidelines, as well as the necessary tests to determine this value. This standard applies to commercial wood, both native and imported, and helps to improve and obtain better construction applications depending on the final use. This work aimed to study the resistance of wood of *Quercus pyrenaica* Wild. to be decayed by Basidiomycetes (*Coniophora puteana* (Schumacher ex Fries) Karsten and *Trametes versicolor* (Linnaeus) Quélet and termites (*Reticulitermes grassei* Clément). The Standards applied were EN 113-2:2021 and EN 117:2023.

Achieving new value chains requires a thorough characterisation of the timber properties of *Q. pyrenaica*, a species not yet included in the European standard EN 350:2016 on natural durability. The study addresses this gap by evaluating, under standardised methods, the natural durability of *Quercus pyrenaica* Willd. against wood decay fungi and subterranean termites.
The conclusions are that the heartwood of the *Quercus pyrenaica* is highly durable against both xylophages basidiomycetes and subterranean termites. The sapwood is highly durable against xylophages fungi, but not against termites, where it is moderately durable, pleacing *Q. pyrenaica* among the most resistant European hardwoods. These results open the door for commercialization of this species, and it is expected to be included in EN 350:2016.

INTRODUCTION

Pyrenean oak (*Quercus pyrenaica* Willd.) occupies approximately 1.1 million hectares in Spain, accounting for 3.9 % of the national forest area and 21 % of its broadleaved woodland (MITECO, 2021). In Castilla y León with 739,642 ha mapped as principal species according to the Spanish Forest Map (Cesefor, 2022). Despite this territorial relevance, the industrial uptake of *Q. pyrenaica* has been historically constrained. Marked growth stresses, the predominance of sprout-origin stands, modest log diameters and a complex drying behaviour have restricted its valorisation to firewood and charcoal production. This pattern is reflected in the regional carbon balance: long-life wood products derived

from rebollo absorb only 1,124 tCO_2 yr^{-1}, whereas emissions from short-life uses exceed 197,000 tCO_2 yr^{-1} (Sánchez Pellicer & Blázquez Casado, 2023).
The LIFE+REB project (LIFE20 CCM/ES/001778) addresses this scenario through the development of a Climate-Smart Forestry (CSF) framework for *Q. pyrenaica* in Castilla y León. The framework integrates sustainable silvicultural management, biodiversity conservation and the cascading use of harvested timber, aimed at maximising the carbon retained in long-life wood products. Twenty demonstration stands distributed across the regional range of the species sustain a systematic decision-making methodology, transferable to wider areas of distribution, and supply the industrial demonstrations of new value chains. Alternative silvicultural itineraries, close-to-nature thinning regimes and the conversion of coppice stands into irregular high forests, have been evaluated within this framework by means of the SIMANFOR decision-support system (Vázquez-Veloso et al., 2025).
The development of these value chains relies on a robust technical characterisation of the material, currently being consolidated in parallel by the project. Previous autecological and xylological studies in north-western Spain (Díaz-Maroto et al., 2006) had already identified the timber potential of the species, and the LIFE+REB physical and mechanical characterisation has determined a mean basic density of 830 kg m^{-3} together with bending properties compatible with structural and high-grade joinery applications. Natural durability, however, remains an unresolved technical gap. In the absence of a recognised classification under EN 350:2016, the assignment of *Q. pyrenaica* to outdoor, ground-contact and biologically exposed structural applications cannot be technically substantiated, precisely the end uses associated with the longest residence time of carbon in the harvested wood product.
Natural durability is defined as the intrinsic resistance of wood to attack by xylophagous organisms. Its determination is essential to establish the level of protection required by each end use and, ultimately, to extend the service life of the material. In Europe, EN 350:2016 establishes the general principles, the test methods and the classification system, and applies to native and imported commercial wood species (CEN, 2016). The present work was conceived within the LIFE+REB project to address this normative gap for *Q. pyrenaica* under standardised laboratory conditions, evaluating its resistance to wood-decay basidiomicetes, *Coniophora puteana* (Schumacher ex Fries) Karsten and *Trametes versicolor* (Linnaeus) Quélet, and to subterranean termites, *Reticulitermes grassei* Clément, in accordance with EN 113-2:2021 (CEN, 2021) and EN 117:2023 (CEN, 2023). *Pinus sylvestris* L. was used as the conifer reference required by both standards, and *Fagus sylvatica* L. was included as a hardwood reference, in accordance with the recommendation of EN 350:2016 for testing broadleaved species.
The objective of this study is to determine, under standardised conditions and following EN 350:2016 protocols, the natural durability of *Q. pyrenaica* sapwood and heartwood against wood-decay basidiomycetes (*C. puteana, T. versicolor*) and subterranean termites (*R. grassei*), with a view to generating the technical evidence required to support the inclusion of the species in EN 350:2016 and to enable its assignment to use classes compatible with high-value, long-life wood products.

MATERIALS AND METHODS

Materials

Heartwood and sapwood specimens of *Q. pyrenaica* were obtained from the LIFE+REB demonstration stands in Castilla y León, where silvicultural interventions had been implemented in accordance with the project's Climate-Smart Forestry framework. The macroscopic distinction between sapwood (A) and heartwood (D) on a freshly sawn board is shown in *P. sylvestris* and *F. sylvatica* were employed as reference species. After drying, the boards were dimensioned into 50 × 25 × 15 mm blocks, selected in the number and orientation prescribed by each test standard EN 113-2:2021 for wood-destroying basidiomycetes and EN 117:2023 for termites. Sapwood and heartwood specimens were identified and tested independently.
The xylophagous organisms employed in the trials were the following:
• Basidiomycete fungi: *Coniophora puteana* (Schumacher ex Fries) Karsten, strain BAM Ebw 15, and *Trametes versicolor* (Linnaeus) Quélet, strain CTBA 863A.
• Subterranean termites: *Reticulitermes grassei* (Clément), the predominant subterranean termite species in the Iberian Peninsula, supplied by the ICIFOR-INIA breeding facility.

Methods

EN 350:2016 (CEN, 2016) sets out the general principles for testing and classifying the natural durability of European wood species and refers to the specific test procedures applicable in each case. The two procedures applied in the present study are described below.

Natural durability against basidiomycete fungi. The test was conducted in accordance with EN 113-2:2021 (CEN, 2021). Pure cultures of *C. puteana* and *T. versicolor* were grown on a malt-agar medium (1.5 % agar, 3 % malt). Once mycelium had colonised the surface of the medium, the wood specimens were placed in contact with each fungus under sterile conditions and incubated for 16 weeks at 22 ± 2 °C and 70 ± 5 % relative humidity. Degradation was quantified as the percentage mass loss under anhydrous conditions, and the ratio between the mass loss of the test specimens and that of the reference wood was used to assign a durability class according to EN 350:2016 (classes 1 to 5).

Natural durability against *Reticulitermes grassei*. The test was conducted in accordance with EN 117:2023 (CEN, 2023). Each test container received remoistened sand and was inoculated with a colony composed of 250 workers and 2-3 soldiers and nymphs; after 2-3 days of acclimation, a wood specimen was introduced. Incubation proceeded for 8 weeks at 28 ± 2 °C and a minimum relative humidity of 80 ± 5 %, under controlled air circulation. At the end of the test, specimens were extracted and visually examined on a 0-4 attack scale (0: no attack; 1: attempted attack; 2: slight attack; 3: average attack; 4: strong attack). Worker survival and the presence of living soldiers or nymphs were recorded. Although not required by the standard, the mass loss of each specimen was also determined as complementary information. Durability classes (D, M, S) were assigned according to EN 350:2016.

RESULTS

Natural durability against B*asidiomycete fungi*

Mass losses caused by both basidiomycete fungi were very low for *Q. pyrenaica* and clearly differentiated from those recorded in the controls (Table 1). Heartwood exhibited negligible degradation — 0.027 % against *C. puteana* and 0.055 % against *T. versicolor* — while sapwood remained well below the 5 % threshold defined by EN 350:2016 (0.254 % and 1.548 %, respectively). Both tissues are therefore assigned to durability class 1 (very durable). The reference species behaved as expected: *P. sylvestris* recorded mass losses of 39.861 % against *C. puteana* and 20.273 % against *T. versicolor*, and *F. sylvatica* reached 35.125 % and 42.455 %, respectively, confirming the validity of the testing conditions.

Natural durability against *Reticulitermes grassei*

Under termite exposure (Table 1), *Q. pyrenaica* heartwood remained intact, with attack grade 0, null worker survival and a mass loss of 1.1 %, corresponding to durability class D (durable). Sapwood recorded an attack grade of 1.9, a worker survival of 73.6 % and a mass loss of 4.76 %, falling within class M (moderately durable). Both reference species were classified as S (susceptible), with mass losses of 12.12 % for *P. sylvestris* and 5.30 % for *F. sylvatica*.

Table 1: Durability of Q. pyrenaica sapwood and heartwood against basidiomycetes

Wood	*C. puteana* (ML, %)	*T. versicolor* (ML, %)	Fungal class	Termite attack	Termite class
Q. pyrenaica sapwood	0.254	1.548	1 – Very durable	1.9	M – Moderately durable
Q. pyrenaica heartwood	0.027	0.055	1 – Very durable	0	D – Durable
P. sylvestris (control)	39.861	20.273	5 – Not durable	4	S – Susceptible
F. sylvatica (control)	35.125	42.455	5 – Not durable	2.7	S – Susceptible

DISCUSSION

The basidiomycete trial places *Q. pyrenaica* among the most resistant European hardwoods. Mass losses against both *C. puteana* and *T. versicolor* are negligible and both tissues remain well below the 5 % threshold, in clear contrast with the *P. sylvestris* and *F. sylvatica* controls. The termite assay revealed a differentiated response: heartwood behaved as a fully durable material, with no attack and no termite survival, whereas sapwood, although moderately durable, still outperformed the susceptible references. This pattern entails a direct industrial implication sapwood must be removed during edging and logs with high heartwood fraction prioritised and has been incorporated into the LIFE+REB sawing protocol at the partner sawmills and validated with value-chain actors during the RebolloLabs co-creation sessions.

When compared with other European hardwoods, the values obtained are highly competitive. *Q. robur* is rated as durable (class 2) under EN 350:2016, but its performance can decrease to classes 4–5 under prolonged ground contact (Brischke et al., 2009); *Castanea sativa* show considerable between-tree variability under soil exposure (Militz et al., 2003); and *F. sylvatica* and *Fraxinus excelsior* are systematically classified as slightly or non-durable. The values determined for *Q. pyrenaica* class 1 for both tissues against fungi and class D for heartwood against termites therefore place the species at the top of the European hardwood durability scale and constitute robust technical evidence supporting its inclusion in EN 350:2016. These durability levels, combined with the project's basic density (830 kg m^{-3}), enable the allocation of *Q. pyrenaica* to long-life value chains (decking, exterior joinery, structural applications, cooperage), with long-term carbon retention of 122, 77 and 27 kg C m^{-3} roundwood in flooring/laminated profiles, glulam and cooperage staves respectively. Sapwood field performance, machinability, dimensional stability and ground-contact verification under EN 350:2016 remain open lines of work within the project.

CONCLUSIONS

The natural durability assays carried out under EN 113-2:2021 and EN 117:2023 demonstrate that *Quercus pyrenaica* ranks among the most durable European hardwoods. Heartwood is classified as very durable (class 1) against the basidiomycetes *C. puteana* and *T. versicolor*, with mass losses below 0.06 %, and as durable (class D) against *R. grassei*, with no attack and null termite survival. Sapwood is also classified as very durable against both fungi (mass losses of 0.254 % and 1.548 %) and as moderately durable (class M) against termites. The reference species *P. sylvestris* and *F. sylvatica* behaved as expected, confirming the validity of the testing conditions.

These results constitute robust technical evidence to support the inclusion of *Q. pyrenaica* in EN 350:2016, which currently does not list the species. This inclusion represents a relevant outcome of the LIFE+REB project, as the formal recognition of its durability class is a prerequisite for its assignment to use classes (EN 335) compatible with biologically exposed end uses. Specifically, the durability levels reported here qualify the heartwood for use class 2 and (covered structures with occasional moisture, exterior applications protected from direct contact with the ground, and ground-contact uses for heartwood-only components), opening the way for the development of new long-life products with high added value structural elements, exterior joinery, decking, cooperage and high-quality flooring, which had hitherto been excluded from the rebollo value chain due to the absence of a recognised durability classification.

The transition from a resource currently dominated by firewood and charcoal towards a portfolio of long-life products would substantially extend the residence time of harvested carbon and reinforce the contribution of the species to climate-change mitigation. The technical evidence generated by this work, integrated within the broader LIFE+REB framework, lays the foundations for that transition and provides the regulatory anchor required for the industrial uptake of *Q. pyrenaica* timber from Castilla y León.

ACKNOWLEDGEMENTS

This research was funded by the European LIFE Programme through the LIFE+REB project (LIFE20 CCM/ES/001778) and conducted at the Wood Protection laboratories of the Forest Products Department of ICIFOR (INIA-CSIC). The authors wish to thank the Junta de Castilla y León, the Universidad de Valladolid and the industrial partners of the project (Maderas García Varona, Gámiz and Tonelería Intona) for the supply of material and their support of the demonstration and RebolloLabs activities.

REFERENCES

Brischke, C., Welzbacher, C. R., Rapp, A. O., Augusta, U., & Brandt, K. (2009). Comparative studies on the in-ground and above-ground durability of European oak heartwood (*Quercus petraea* Liebl. and *Quercus robur* L.). *European Journal of Wood and Wood Products*, 67(3), 329–338. https://doi.org/10.1007/s00107-009-0329-x

CEN (2016, 2021, 2023). *EN 350:2016 Durability of wood and wood-based products – Testing and classification of the durability to biological agents; EN 113-2:2021 Test method against wood-destroying basidiomycetes (Part 2); EN 117:2023 Wood preservatives – Determination of toxic values against Reticulitermes species*.

Cesefor (2022). *Estudio de los impactos en los stocks de carbono de las acciones de gestión y los incendios forestales. Acción A1.1 del proyecto LIFE+REB (LIFE20 CCM/ES/001778)*.

Díaz-Maroto, I. J., Fernández-Parajes, J., & Vila-Lameiro, P. (2006). Autecology of rebollo oak (*Quercus pyrenaica* Willd.) in Galicia (Spain). *Annals of Forest Science*, 63(2), 157–167. https://doi.org/10.1051/forest:2005108

García, I., & Jiménez, P. (2009). 9230 Robledales de *Quercus pyrenaica* y robledales de *Quercus robur* y *Quercus pyrenaica* del Noroeste ibérico. In VV.AA., *Bases ecológicas preliminares para la conservación de los tipos de hábitat de interés comunitario en España* (66 pp.). Ministerio de Medio Ambiente, y Medio Rural y Marino.

Militz, H., Busetto, D., & Hapla, F. (2003). Investigation on natural durability and sorption properties of Italian chestnut (*Castanea sativa* Mill.) from coppice stands. *Holz als Roh- und Werkstoff*, 61(2), 133–141. https://doi.org/10.1007/s00107-002-0357-2

MITECO (2021). *Tercer Inventario Forestal Nacional (IFN3)*. https://www.miteco.gob.es/es/biodiversidad/temas/inventarios-nacionales/inventario-forestal-nacional/

Santos, S. M., de Troya, M. T., Robertson, L., Gutiérrez, S., Caballé, G., & Villanueva, J. L. (2025). Study on the Natural Durability of *Quercus pyrenaica* Willd. to Wood Decay Fungi and Subterranean Termites. Forests, 16(9), 1486. https://doi.org/10.3390/f16091486

Sánchez Pellicer, T., & Blázquez Casado, Á. (2023). *Balance de carbono en los rebollares de Castilla y León: línea base. Acción A1.3 del proyecto LIFE+REB (LIFE20 CCM/ES/001778)*. Fundación CESEFOR.

Vázquez-Veloso, A., Ordóñez, C., & Bravo, F. (2025). Silviculture alternatives evaluation for managing complex *Quercus pyrenaica* Willd. stands. *Forest Systems*, 34(3), 21005. https://doi.org/10.5424/fs/2025343-21005

Visual and Machine Strength Grading of Structural Beech (*Fagus sylvatica* L.) Timber from Spain: Yield Comparison and Characteristic Values

Mario Azaña[1,2], Gonzalo Caballe[1], Silvia Gomez[1], Guillermo Íñiguez-González[2*]

[1] CESEFOR, Centro de Servicios y Promoción Forestal y de su Industria de Castilla y León, C/ Agustín de Betancourt 2, 42004 Soria, Spain
[2] Escuela Técnica Superior de Ingeniería de Montes, Forestal y del Medio Natural, Universidad Politécnica de Madrid (UPM), Av. de la Complutense s/n, 28040 Madrid, Spain.

E-mail: mario.azana@cesefor.com; gonzalo.caballe@cesefor.com; silvia.gomez@cesefor.com; guillermo.iniguez@upm.es

Keywords: beech timber; visual strength grading; machine strength grading; structural timber; *Fagus sylvatica*; strength classes; non-destructive testing.

ABSTRACT

The structural use of European hardwoods has attracted increasing interest in recent years due to the need to diversify timber resources and expand the availability of raw materials for structural applications and engineered wood products. Among these species, European beech (*Fagus sylvatica* L.) shows considerable structural potential because of its relatively high density and favourable mechanical properties. Nevertheless, its use as structural sawn timber remains limited compared with the softwood species traditionally employed in European construction, and grading systems specifically adapted to Spanish-sourced beech have not been available until now.

This study presents a comparative analysis of grading yield and characteristic mechanical properties obtained through visual and machine strength grading of Spanish beech structural timber. A dataset of 538 specimens tested in bending, was assembled from four subsamples representative of the main beech-producing regions in Spain: La Rioja, Basque Country South, Basque Country North and the Pyrenees. Cross-sections ranged from 25 × 70 mm to 45 × 145 mm.

All specimens were visually graded according to the proposed national criteria, and subsequently evaluated by machine grading using longitudinal vibration measurements obtained with a portable device (MTG 960, Brookhuis). From these measurements, the dynamic modulus of elasticity was derived and used as the indicating property. Bending strength, modulus of elasticity and density were determined according to EN 408 and EN 384, and characteristic values were derived following EN 14358. Grading models were then developed for both approaches, and the resulting strength class assignments were compared in terms of structural yield.

The results show that Spanish beech timber exhibits high mechanical performance, allowing the assignment of strength classes ranging from D24 to D50 depending on the grading method applied. These findings provide an experimental basis for the development of grading systems adapted to this species and support its increased use in structural applications and engineered wood products.

INTRODUCTION

In Spain, efforts to develop structural grading tools for sawn timber have traditionally focused on the main domestic softwood species. The standards UNE 56544 and UNE 56546 (AENOR 2022a, b) establish the visual grading criteria for softwoods and hardwoods, and the species, origin and strength class assignments are listed in EN 1912:2024(CEN 2024). Spanish hardwood species are at a markedly lower development level: although they have been included in national visual grading for decades, the corresponding machine grading tools are recent or still unavailable. For softwoods, the settings included in EN 1912:2024 cover the main productive species, *Pinus sylvestris* L., *P. pinaster* Aiton, *P. nigra* J.F. Arnold and *P. radiata* D. Don, with strength classes between C16 and C30 depending on the visual grade (Moltini et al. 2022). Among hardwoods, the only Spanish species with approved settings in EN 1912 are eucalyptus (*Eucalyptus globulus* Labill. in MEF grade assigned to class D40, and *E. nitens* H. Deane & Maiden assigned to class C35) and chestnut (*Castanea sativa* Mill. in MEF and MEF-G grades assigned to D27 and D24) ((Martins et al. 2023)).

Spain is well below its sustainable ecological harvesting capacity: the annual extraction-to-growth ratio is markedly lower than the European average, indicating substantial room to increase timber mobilization without compromising the forest balance (Forest Europe 2025). Similarly, the use of structural timber in construction is limited compared with other European countries, particularly the Nordic and Central European countries where timber construction is significantly more established (Otero et al. 2022; Pramreiter and Grabner 2023). In this context, ensuring availability and diversification of the national forest resource is a strategic priority for strengthening the timber value chain and the resilience of the sector against climate change. Diversifying the species used in construction and incorporating native hardwoods into the structural market are two complementary lines to advance in that direction (Cabrera and Moltini 2022).

Spanish beech forests cover an area of 387 776 ha, equivalent to 2.12 % of the wooded forest area in the country. The resource is concentrated in the northern strip of the Iberian Peninsula, with Navarra (124 195 ha, 32 % of the national beech area), Asturias (68 290 ha, 18 %), Castilla y León (54 178 ha, 14 %), Basque Country (49 641 ha, 13 %), Cantabria (31 759 ha, 8 %), La Rioja (25 555 ha, 7 %), Catalonia (21 533 ha, 6 %) and Aragon (12 201 ha, 3 %) as the autonomous regions with significant presence of the species. The average annual beech harvest between 2005 and 2019 was 154 122 m³, never exceeding 225 000 m³ in any single year, which represents approximately 12 % of the theoretical annual yield potential. The provincial distribution of mobilized volume is markedly asymmetric: Navarra accounts for 79 % of the national volume harvested between 2009 and 2019 (1 524 747 m³ cumulative), followed at a distance by Catalonia (118 916 m³), Castilla y León (107 782 m³), La Rioja (88 660 m³) and the Basque Country (43 541 m³). More than half of the harvested beech is used as firewood or bioenergy, with estimates placing this fraction above 70 % when neighbouring firewood is properly accounted for (MITECO 2021, 2023; FAGUS 2023). The fraction directed to the transformation industry is mainly used for joinery, cabinetmaking and furniture, preferentially exploiting sapwood or the timber not affected by red heartwood, a chromatic defect that penalises commercial value although it does not significantly compromise the mechanical properties of the wood (Pöhler et al. 2006).

In the Central European context, structural grading and mechanical characterisation of beech are well developed, with seminal work in Germany, Switzerland and Austria establishing visual and machine grading criteria mainly oriented to glued laminated timber production (Glos and Lederer 2000; Frühwald and Schickhofer 2005; Westermayr et al. 2018, 2022). However, Spanish-sourced beech timber has received limited research attention so far, beyond the work of Cabrera, Moltini and Baño (2022, 2023) addressing specific load configurations (embedment strength of metallic-dowel connections) or small unclassified batches not conforming to European grading standards, and a recent contribution (Martins et al. 2025). To the best of the authors' knowledge, no previous study has addressed the derivation of visual and machine grading criteria for Spanish beech structural timber according to EN 14081 on a sample representative of the national resource. The incorporation of beech timber into the structural market would allow the revalorisation of resource fractions currently destined to firewood or limited to non-structural uses due to red heartwood, multiplying its use value. This work addresses this gap by deriving and comparing a visual grading system and a machine grading system for Spanish beech structural timber, on a sample of 538 specimens representative of the four main provenances of the national resource. The visual grading developed will be proposed for inclusion in UNE 56546 and in EN 1912:2024, together with the machine grading settings already approved by CEN TC124 WG2 TG1 (Moltini et al. 2024). The results allow Spanish beech to be assigned strength classes within the D series of EN 338 that lie among the highest obtained for Spanish hardwoods included in EN 1912:2024.

MATERIALS AND METHODS

Sample and conditioning

The studied population is European beech (*Fagus sylvatica* L.) of Spanish origin. A total of 538 specimens of rectangular cross-section were collected from four subsamples representative of the main beech-producing regions in Spain: La Rioja (A), Basque Country South (B), Basque Country North (C) and the Pyrenees (D). Nominal cross-sections ranged from 25 × 70 mm to 45 × 145 mm, with a minimum cross-sectional area of 1575 mm². All boards were selected from standing trees and corresponded to the section sizes and qualities currently processed by the Spanish primary transformation industry. Material representativeness was ensured according to EN 384.

After delivery to the testing laboratory, each specimen was identified and conditioned in a climate chamber at (20 ± 2) °C and (65 ± 5) % relative humidity, in accordance with EN 408, until constant mass was reached at a target moisture content close to 12 %.

Visual grading

Each specimen was visually graded prior to destructive testing following the criteria developed for the proposed inclusion of Spanish beech in UNE 56546 and DIN 4074-5 (OENORM 2008). The singularities recorded along the full length of each board comprised single and clustered knots on face and edge (expressed as the d/h and d/b ratios, respectively), growth ring width, slope of grain, shakes (drying, ring, lightning), bark pockets, wane (length and width), pith, biological alterations (decay, insect attack, brown discoloration), reaction wood, mechanical damage and overall distortion (bow, spring, twist, cup). A single visual grade was defined and designated MEF; specimens not meeting all the corresponding thresholds were classified as reject. The main thresholds applied to assign a board to the MEF grade are summarised in Table 1. The possibility of defining two visual grades (MEF-1 and MEF-2) was examined but discarded, as no combination of stricter thresholds produced a second grade compatible.

Table 1: Main thresholds of the proposed MEF visual grade for Spanish beech

Quality criterion	MEF grade
Knot size on face (d/h)	d ≤ 1/3 h
Knot size on edge (d/b)	d ≤ 1/2 b
Drying shakes	Permitted
Ring, lightning or felling shakes	Not permitted
Ring shake / through cracks	Not permitted
Wane length	G ≤ 1/4 L
Wane width or thickness	G ≤ 1/4 b
Pith	Not permitted
Decay	Not permitted
Insect attack	Not permitted
Brown discoloration (red heartwood)	Permitted
Maximum bow	10 mm (per 2 m length)
Maximum spring	8 mm (per 2 m length)
Maximum twist	1 mm (per 25 mm of h)
Cup	No restriction

Machine grading

The 538 specimens tested in bending were also evaluated with the MTG 960 hand-held device (Brookhuis Applied Data Intelligence B.V., Enschede, The Netherlands). The frequency of the first longitudinal vibration mode was obtained from an external hammer blow and recorded by the Timber Grader software. The indicating property, taken as the dynamic modulus of elasticity E_{dyn}, was computed according to Equation 1:

$$E_{dyn} = (2 f_0 L)^2 \rho_{12} \times 10^{-6} \quad (1)$$

where f_0 is the first longitudinal vibration frequency (Hz), L is the total board length (m) and ρ_{12} is the board density corrected to 12 % moisture content (kg/m³). Machine settings were derived for seven strength class combinations and verified against the requirements of clause 6.4.2.2 of EN 14081-2 (CEN 2022). In the present paper, only the reference combination D50/D35/D24 is used for the yield comparison with visual grading, as it shares the upper class with the visual outcome and spans the full D24–D50 range achieved by the species.

Destructive testing and characteristic values

Tests were carried out according to EN 408, and the local modulus of elasticity $E_{m,l}$ was used as the parallel-to-grain modulus of elasticity E_0. Density and moisture content was determined on a defect-free slice cut from each specimen after bending failure.

Characteristic values of bending were derived the mean for modulus of elasticity $E_{0,mean}$, and the 5th percentile for strength $f_{m,k}$ and density ρ_k according to EN 384 and EN 14358. A parametric estimation (log-normal distribution for f_m, normal distribution for ρ) was used when $n < 40$, and a non-parametric estimation otherwise.

RESULTS AND DISCUSSION

Descriptive statistics of the unclassified sample

Table 2 summarises the descriptive statistics of the 538-specimen sample tested in bending, broken down by subsample. Mean bending strength varied between 63.6 N/mm² (C) and 79.6 N/mm² (D), with an overall sample mean of 72.0 N/mm² and a coefficient of variation of 36 %. Mean modulus of elasticity ranged from 13.7 kN/mm² (C) to 15.4 kN/mm² (D), and mean density from 710 kg/m³ (D) to 731 kg/m³ (C), with low coefficients of variation in density (6–7 %) indicating geographical homogeneity of the material in this property. These descriptive figures correspond to the unclassified sample, before application of grading filters and EN 384 adjustments.

Table 2: Summary statistics of the unclassified sample by subsample

Property	La Rioja	Basque Country South	Basque Country North	Pyrenees	All
Number, n	115	130	150	143	538
$f_{m,mean}$ [N/mm²]	70.8	74.6	63.6	79.6	72.0
$f_{m,k}$ [N/mm²]	33.8	27.4	27.8	32.2	30.3
CoV f_m [%]	33	36	37	34	36
$E_{0,12\%,mean}$ [kN/mm²]	15.0	15.1	13.7	15.4	14.8
CoV E_0 [%]	25	27	22	24	25
$\rho_{12,mean}$ [kg/m³]	725	724	731	710	723
$\rho_{12,k}$ [kg/m³]	631	643	650	633	639
CoV ρ_{12} [%]	8	6	7	7	7
$u_{test,mean}$ [%]	11	10	12	11	11

Visual grading outcome and characteristic values

292 (54.3 %) specimens visually inspected, met all the MEF acceptance thresholds and 246 (45.7 %) were classified as reject. The distribution by provenance is summarised in Table 3. Characteristic values were derived for the MEF subsample (n = 292) following EN 384 and EN 14358, applying the corresponding k_n factor for four subsamples. The values obtained are: $f_{m,k}$ = 36.5 N/mm², $E_{0,mean}$ = 17.9 kN/mm² and ρ_k = 620 kg/m³. According to EN 338, the MEF grade is assigned to strength class D35.

Table 3: Visual grading yield by subsample and characteristic values of the MEF grade

Source	*n*	MEF [n]	Reject [n]	MEF [%]	Reject [%]
A: La Rioja	115	70	45	61	39
B: BC South	130	68	62	52	48
C: BC North	150	77	73	51	49
D: Pyrenees	143	77	66	54	46
Total	538	292	246	54	46

Yield comparison: visual vs machine grading

For the reference machine combination D50/D35/D24, the 538 specimens tested in bending are assigned as follows: 16.5 % to class D50, 37.7 % to class D35, 44.8 % to class D24 and 1.0 % to reject. Compared with the single-grade visual outcome (54.3% % MEF assigned to D35 and 45.7 % reject), machine grading recovers 99.0 % of the sample distributed across three strength classes, including a non-negligible fraction (16.5 %) of material reaching D50, the highest D class so far derived for Spanish structural timber. Table 4 summarises the comparison.

Table 4: Yield comparison between visual (MEF) and machine grading (combination D50/D35/D24) over the 538-specimen sample

Strength class	D50 [%]	D35 [%]	D24 [%]	Reject [%]
Visual (MEF)	—	54.3	—	45.7
Machine (D50/D35/D24)	16.5	37.7	44.8	1.0

The single-grade visual approach concentrates the entire accepted volume in D35, with a yield higher than 50 %. The mechanical approach with MTG redistributes nearly the whole sample across three D classes, multiplying the variety of declarable products and minimising rejection. The proportion assigned to D50 confirms the high structural potential of Spanish beech and provides a competitive position against Central European beech sources and other Spanish hardwoods. Density figures support the robustness of the national setting: with $\rho_{12,mean} \approx 723$ kg/m³ and CoV between 6 % and 7 % across all four provenances, no relevant geographic effect is observed in this property, which is the dominant predictor of the dynamic modulus of elasticity used as the indicating property for machine grading.

CONCLUSIONS

A visual grading system and a machine grading system have been derived and compared for Spanish-sourced beech (*Fagus sylvatica* L.) structural timber on a sample of 538 specimens representative of the four main provenances of the national resource. The proposed MEF visual grade, intended for inclusion in UNE 56546 and in EN 1912:2024, assigns Spanish beech to strength class D35 with a yield of approximately 50 % over the inspected sample. Machine grading with the MTG 960 device, on the reference combination D50/D35/D24 already approved by CEN TC124 WG2 TG1, achieves a global yield close to 99 %, with 16.5 % of the sample reaching class D50. These results provide the experimental basis for the certification and CE marking of Spanish beech structural timber and place the species among the Spanish hardwoods with the highest strength classes included in EN 1912. The work also supports the industrial revalorisation of the beech fraction currently directed to firewood or non-structural uses, including timber affected by red heartwood. Further work will address the use of this material in hybrid engineered wood products and the extension of the proposed criteria to additional cross-section ranges and provenances.

ACKNOWLEDGEMENTS

This work has been developed within the framework of the Operational Group GO Fagus (2021–2023) and the LIFE HFH (Hardwood for Hybrids) project (2025–).

REFERENCES

AENOR (2022a) UNE 56544:2022 Clasificación visual de la madera aserrada para uso estructural. Madera de coniferas

AENOR (2022b) UNE 56546:2022 Clasificación visual de la madera aserrada para uso estructural. Madera de frondosas

Cabrera G, Moltini G (2022) Embedment Strength of Low- and Medium-Density Hardwood Species from Spain

CEN (2024) EN 1912:2024 Structural Timber. Strength classes. Assignment of visual grades and species

CEN (2022) EN 14081-2:2019+A1:2022 Timber structures — Strength graded structural timber with rectangular cross section Part 2 : Machine grading ; additional requirements for initial type testing

FAGUS GO (2023) Manual de resultados finales GO Fagus

Forest Europe (2025) State of Europe's Forests 2025

Frühwald A, Schickhofer G (2005) Strength grading of hardwoods. Proceedings of the 14th International Symposium on Nondestructive Testing of Wood, Hanover, Germany

Glos P, Lederer B (2000) Strength grading of beech and oak sawn lumber and determination of characteristic strength and stiffness values. Report No. 98508, Holzforschung München, Munich.

Martins C, Ferreira C, Azaña M, et al (2025) Experimental assessment of glulam beams made by European beech from Spain. Eur J Wood Wood Prod 83:182. https://doi.org/10.1007/s00107-025-02333-w

Martins C, Moltini G, Dias AMPG, Baño V (2023) Machine Grading of High-Density Hardwoods (Southern Blue Gum) from Tensile Testing. 1–13

MITECO (2023) Anuario de estadistiva forestal
MITECO (2021) Mapa Forestal de España a partir de los datos del IFN4 realizado por el Ministerio de Transición Ecologíca y el Reto Demogratico. https://www.miteco.gob.es/es/cartografia-y-sig/ide/descargas/biodiversidad/mfe.html
Moltini G, Azaña M, Villanueva JL (2024) TG1/202404/14 _rev1: Derivation of machine settings for D-classes of European beech from Spain according to EN 14081-2 : 2018
Moltini G, Íñiguez-gonzález G, Cabrera G (2022) Evaluation of Yield Improvements in Machine vs . Visual Strength Grading for Softwood Species
OENORM (2008) DIN 4074-5:2008-12. Sortierung von Holz nach der Tragfähigkeit - Teil 5: Laubschnittholz (Strength grading of wood - Part 5: Sawn hard wood)
Otero, Basterra L-A, Vallelado P, et al (2022) Aplicación y difusión de la innovación para la promoción de la construcción en altura con madera en el espacio SUDOE: Identificación y análisis. Fund Cesefor
Pöhler E, Klingner R, Künniger T (2006) Beech (Fagus sylvatica L .) – Technological properties , adhesion behaviour and colour stability with and without coatings of the red heartwood. 63:129–137. https://doi.org/10.1051/forest
Pramreiter M, Grabner M (2023) The Utilization of European Beech Wood (Fagus sylvatica L.) in Europe. Forests 14:. https://doi.org/10.3390/f14071419
Westermayr M, Stapel P, Van De Kuilen JW (2018) Tensile strength and stiffness of low quality beech (Fagus sylvatica) sawn timber. WCTE 2018 - World Conf Timber Eng
Westermayr M, Zeilhofer M, Rais A, et al (2022) Tensile strength grading of beech (Fagus sylvatica L.) lamellas from multiple origins, cross sections and qualities. Holzforschung 76:397–407. https://doi.org/https://doi.org/10.1515/hf-2021-0029

The Influence of Forest Roads on the Dimensional Characteristics of Nearby Trees – Case Study for Deciduous and Mixed Forests

Diana-Elena Dumitru[1], George-Iulian Stanciulescu[1], Elena-Camelia Musat[1*]

[1] Transilvania University of Brasov, Faculty of Silviculture and Forest Engineering, Sirul Beethoven no. 1, 500123, Brasov, Romania.

E-mail: elena.dumitru@unitbv.ro; george.stanciulescu@unitbv.ro; elena.musat@unitbv.ro

Keywords: deciduous species; mixed forests; impact of forest roads; dimensional characteristics.

ABSTRACT

The forest road network plays an essential role in sustainable forest management, facilitating forestry operations, timber transport and emergency interventions. However, the presence of these access roads can have significant effects on ecosystems, especially on trees in their immediate vicinity. Changes occurring at the microclimatic, edaphic and biological levels can directly influence the development of woody vegetation. On the other hand, stands go through several stages of development, each requiring specific silvicultural operations to ensure healthy and productive tree growth. For this reason, the research aims to evaluate the influence of accessibility on the development of trees in the vicinity of forest roads, in deciduous and mixed stands, tracking their development at various distances within the forest. Field data collection was carried out in state forests, administered by the Domnești Forest District (Argeș Forestry Directorate, Romania), accessible through the Podul lui Ștefan forest road. In total, 6 transects were delimited with a length of 50 m and a width of 3 m, located at a distance of 100 meters from each to other, upstream and downstream of the road. For all the 300 trees studied, there were collected data about the species, the diameter at the breast height, the total height, the pruning height, the crown radii on four cardinal points, and the distance to the road. Following the centralization of the data and the interpretation of the results, it was found that trees located near the road show significant differences compared to those located at greater distances, both in terms of total height and other dimensional characteristics, such as diameter at the breast height, pruning height or crown dimensions. The influences are greater in the area downstream of the road, where weaker tree development was observed. Higher values of average height and average diameter were recorded in the upstream area, suggesting a more favourable development environment. In contrast, downstream, trees showed weaker growth and lower vitality. At the same time, crown dimensions, including surface area, demonstrated balanced development in areas less affected by the road, especially upstream of the road.

INTRODUCTION

Forest roads represent an essential infrastructure for efficient and sustainable forest management (Mușat et al. 2014), being private utility roads intended for timber transport and other activities related to forests management (Brown and Thompson 2020). Forest areas made accessible through forest roads are subject to much more frequent and intense interventions compared to less accessible zones. In forests where access is limited due to the lack of road infrastructure, stand tending and cultural operations are performed less frequently, which can lead to uneven stand development due to tree competition and an increased risk of pests and diseases that can affect trees in the long term (Green and White 2017).

The accessibility of the forest fund via forest roads has a direct impact on the growth of trees in the proximity of the roads. Trees located close to the road benefit from different light and space conditions compared to those inside the forest interior (Vișan et al. 2017). For example, trees next to the road receive more lateral light, which stimulates a more vigorous crown growth. They tend to develop larger and denser crowns at a lower height on the trunk compared to interior trees, which are taller and have narrower crowns located higher up (Brown and Thompson 2020).

In addition to light, trees next to the road can benefit from a different microclimate, as roads can slightly alter air circulation and moisture levels (Vișan et al. 2017). This can lead to differentiated, sometimes faster, growth rates at the roadsides compared to trees inside the forest. However, these changes in

growth and conformation can also introduce vulnerabilities, such as increased wind sensitivity due to larger crowns and reduced mechanical stability (Anderson 2021).
In the context of sustainable forest management, the existence of forest roads plays a crucial role in how forests are managed and maintained; therefore, the aim of this study was to examine the influence of accessibility on the development of trees near forest roads by evaluating growth parameters, namely diameter at the breast height, total height, height to crown base, and crown characteristics.

MATERIALS AND METHODS

The research was conducted in forests made accessible by the *Podul lui Ștefan* forest road (Figure 1b), located at the foothills of the Făgăraș Mountains (Southern Carpathians, Romania), at altitudes ranging from 700 to 800 m. The *Podul lui Ștefan* forest road has a length of 600 m and serves the compartments 104A and 106 (Figure 1a), managed by the Domnești Forest District, Argeș County Forest Administration. The studied area is characterized by a moderate mountain climate with continental influences. The average annual temperature is low, and the thermal regime is influenced by altitude. The precipitation regime is rich, with annual values ranging between 800 and 1000 mm, depending on altitude and exposure. Precipitation is relatively evenly distributed throughout the year, with peaks in May–June and November.
Regarding the vegetation, the research area is situated within the beech zone (*Fagus sylvatica*), transitioning toward the sessile oak zone (*Quercus petraea*) at lower altitudes, and toward Norway spruce (*Picea abies*) at higher elevations. The forests are composed of relatively pure or mixed stands including beech, hornbeam, sessile oak, maple, and lime. In some places, particularly in compartment 106, natural regeneration of pioneer species such as birch and willow occurs. In wetter areas, the understory vegetation is well-developed, and floristic diversity is high, with the presence of indicator species for acidic soils.
A total of six sample plots were established; each of them located at a distance of 100 m from one another (Figure 2a). In each sample plot, trees were selected up to a distance of 50 m from the road, both upslope and downslope, measuring all trees within a 2-meter-wide strip. In total, 300 trees were measured across the sample plots, belonging to the following species: Norway spruce (*Picea abies*), European beech (*Fagus sylvatica*), European alder (*Alnus glutinosa*), Douglas fir (*Pseudotsuga menziesii*), and Scots pine (*Pinus sylvestris*). For each tree, the following data were recorded (Figure 2b): species, diameter at breast height (DBH), total height, height to crown base, crown radii along the four cardinal directions (North, South, East, West), and distance from the road. All trees were numbered from 1 to 300 using blue marking spray.

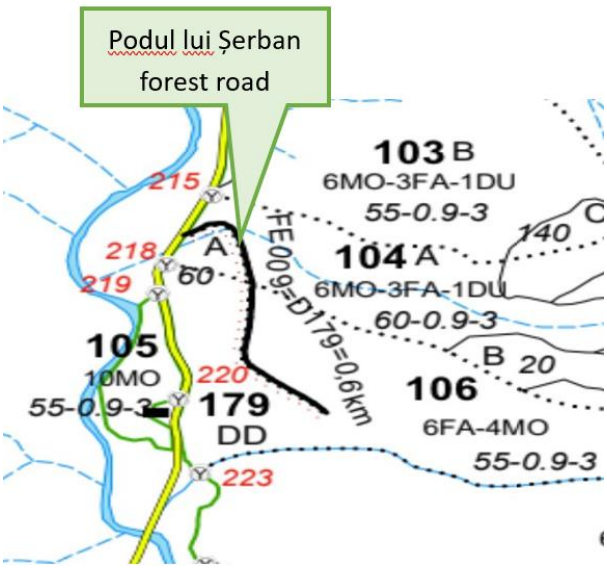

a.

b.

Figure 1: Compartments served by the Podul lui Ștefan forest road (a), and an overview of the Podul lui Ștefan forest road (b)

a. b.

Figure 2: Measuring the distance from the tree to the road (a.), and measuring the diameter at breast height (DBH) using a forest caliper (b.)

RESULTS AND DISCUSSION

The distribution of trees by species shows that European alder (*Alnus glutinosa*) is the most frequent species in the studied stands, accounting for 37% of the total (110 trees) (Figure 3). This species is commonly found in wet areas and contributes to soil improvement. European beech (*Fagus sylvatica*) ranks second, representing 25% (76 trees); it is a widespread deciduous species that prefers fertile soils and shaded areas. Norway spruce (*Picea abies*) accounts for 23% (69 trees), being a characteristic species of mountainous regions. Douglas fir (*Pseudotsuga menziesii*) accounts for 14% (43 trees), representing an exotic species introduced to Romania for timber production due to its rapid growth rate. Scots pine (*Pinus sylvestris*) is underrepresented within the analyzed tree sample, accounting for only 1% (2 trees).

Tree diameter measured at the breast height represents an essential dendrometric parameter, used to evaluate volume, age, vitality, and regeneration potential. Based on the measurements performed, the recorded DBH vary within substantial minimum and maximum values, indicating a structural heterogeneity characteristic of natural forests (Figure 4). Diameters at breast height (DBH) are slightly smaller downslope, indicating lower vigor, while the slenderness coefficient—calculated as the ratio between total height and DBH—presents mean values of 0.69 m/cm, ranging between 0.40 and 1.28 m/cm.

In the literature (Păcurar 2011), for instance in approximately 70-year-old Norway spruce stands, a mean slenderness coefficient of 0.98 m/cm is reported. The lower mean values observed in the present study suggest that the trees are generally more stable, an aspect that may be attributed to a lower stand density or to efficient silvicultural tending operations.

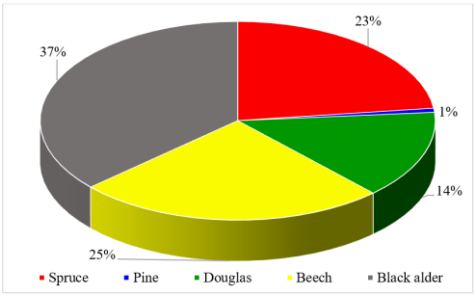

Figure 3: Distribution of trees by species

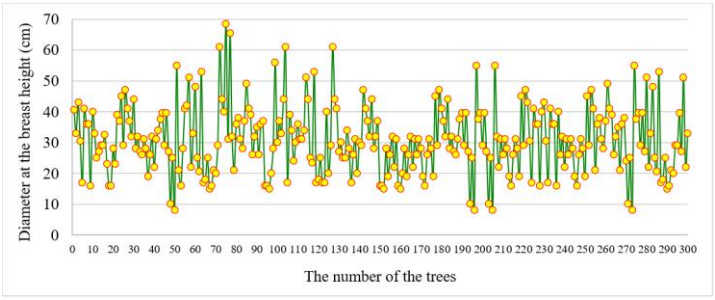

Figure 4: Variation of diameter at breast height (DBH) in the studied trees

To highlight more clearly the influence of positioning relative to the road, the trees were grouped into two categories: those located upslope (Figure 5) and those located downslope (Figure 6) from the permanent transport route. Comparing these two groups provides important information regarding the

potential differential effects of the road on tree development. Visual and statistical analyses reveal that trees in the upslope area tend to achieve higher mean height values compared to those downslopes. Descriptive statistics indicate a mean height of approximately 21.3 m upslope, compared to a mean of 18.7 m downslope. The median is also higher upslope (22 m), while downslope it stands at 19 m. These differences are further supported by the recorded extremes—downslope trees reach lower minimum heights, and the dispersion of values is generally narrower than upslope.

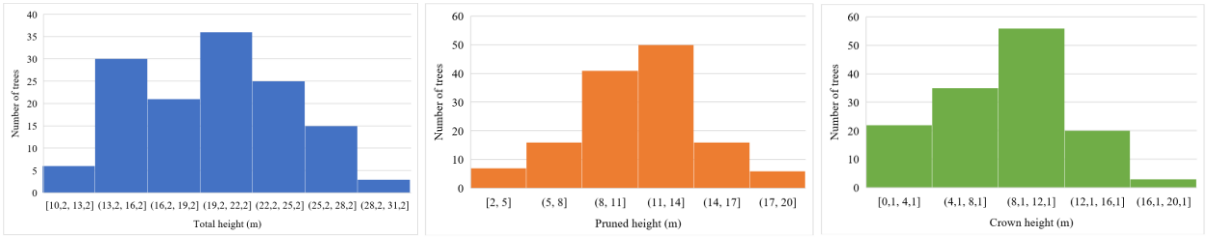

a. b. c.

Figure 5: Classification of upslope trees by height categories: a. total height; b. height to crown base; c. crown height

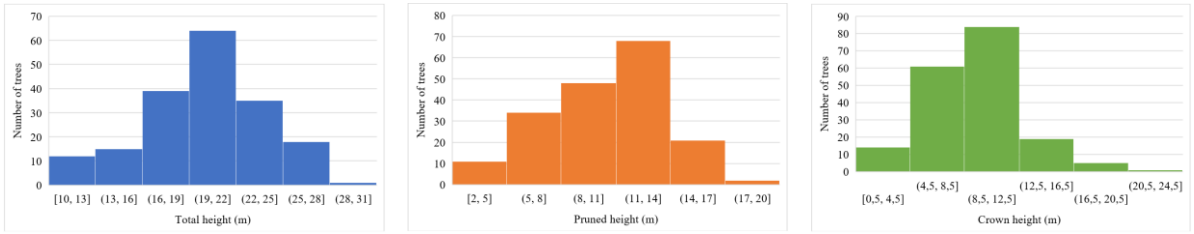

a. b. c.

Figure 6: Classification of downslope trees by height categories: a. total height; b. height to crown base; c. crown height

These findings are clearly consistent with the literature. A conclusive example is the study conducted by Popescu (2018) in a mountainous forest within Suceava County, which observed that trees located downslope from forest roads had, on average, 2.1 meters lower heights compared to those outside the direct influence of the road, particularly on steep, downward-sloping hillsides. Another example is provided by Smith and Johnson (2015), who studied over 600 trees in temperate forests in Sweden. They observed that tree height systematically decreases within the first 20 meters from unpaved forest roads, especially in fill slope zones. In Romania, another example is the study conducted by Vasilescu (2014), who analyzed a Norway spruce stand in the Apuseni Mountains, observing that trees on the downslope hillsides of forest roads exhibited not only lower heights but also a higher frequency of partial windthrow events. The mean height was 1.5–2.5 m lower than in the upslope areas, and the difference was even more pronounced in the case of young trees.

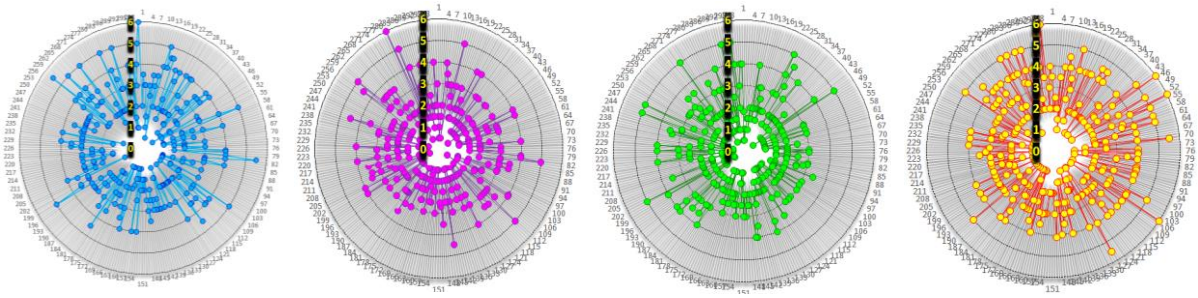

a. b. c. d.

Figure 7: Variability of tree crown radii along the four cardinal directions: a. North; b. East; c. South; d. West

To highlight the influence of the forest road on crown development, four crown radii were measured, one for each cardinal direction. The radial chart representations (Figure 7) allow for a clear visualization of the variability of these radii depending on orientation, providing a comparative perspective on how trees develop their crowns in relation to their spatial positioning.
Overall, a significant variation in the size of the radii across the four directions is observed, suggesting a clear influence of environmental and structural factors on tree morphology.

CONCLUSIONS

It was found that trees located near the road exhibit significant differences compared to those situated at greater distances, both in terms of total height and other dendrometric characteristics such as diameter at breast height (DBH), height to crown base, or crown dimensions. The influences are particularly evident in the downslope area relative to the road, where runoff, soil compaction, and sediment accumulation lead to poorer tree development.
The differences between upslope and downslope trees confirm the initial hypothesis that forest roads affect not only accessibility and silvicultural operations, but also the structure and vitality of adjacent stands.
In the upslope area, higher mean values for height and diameter at breast height (DBH) were recorded, suggesting a more favorable growth environment, possibly due to better water drainage and a more balanced light exposure. In contrast, downslope trees exhibited poorer growth, indicating a direct or indirect negative impact of the road on the edaphic and microclimatic environment.
The slenderness ratio indicates good mechanical stability of the trees, which is a positive sign for the health of the forest structure.
Crown dimensions and the recorded values for crown projection area demonstrated a balanced development in areas less affected by the road's influence, particularly upslope.
The research results are consistent with the literature, which emphasizes that forest roads can create microclimatic changes, affect the hydrologic regime, and significantly influence forest structure and dynamics. Furthermore, the study confirms the observations of other researchers regarding the reduction in tree height and vigor in the areas immediately adjacent to roads, particularly on downslope hillsides.

REFERENCES

Anderson, K., 2021. Dendrometric changes in proximity to forest access roads: A study of edge effects. Ann. For. Sci.78(5):465-480.

Brown, H., Thompson, L., 2020. Forest road influence on tree growth and structure in managed woodland ecosystems. For. Ecol. Manage 126(4):512-526.

Green, S., White, E., 2017. The role of forest roads in promoting sustainable forest management and accessibility. Int. J., For. Res. 52(3):303-321.

Muşat, E.-C., Ciubotaru, A., Ciobanu, V.D., 2014a. The external defects and the particularities of the trees crowns located into the green areas of Braşov. Conference Proceedings of the International Multidsciplinary Scientific Geoconferences (SGEM 2014), 14th GeoConference on Water Resources. Forest, Marine and Oceanic Ecosystems, vol. II, pp. 461-468.

Păcurar, V.D., 2011. Possible climate change impacts on forests in mountain regions. Proceedings of the Biennial International Symposium "Forest and Sustainable Develpment", 15-16 octombrie, 2010, Brasov, Romania, pp. 465-468.

Popescu, I., 2018. Impactul drumurilor forestiere asupra creșterii arborilor în păduri montane din Suceava. Revista de Silvicultură și Cinegetică, vol. 23(2), pp. 45-52.

Vasilescu, M.M., 2014. Studiu privind influența drumurilor forestiere asupra stabilității arborilor în păduri montane. Analele Institutului de Cercetări Silvice, vol. 57(1), pp. 87-96.

Vişan, J., Alexandru, V.M., Ciobanu, D.V., Muşat, E.C., 2017. The impact of forest roads on the environment: A short review. Proceedings of the International Simposyum "Forest and Sustainable Development", Brasov, Romania, pp. 133-138.

Relationship Between Preservative Retention and Penetration in Norway Spruce and Pannonia Poplar

Luca Buga-Kovács[1*], Norbert Horváth[1]

[1]University of Sopron, Faculty of Wood Engineering and Creative Industries. Bajcsy-Zs. Str. 4, Sopron, Hungary, 9400.

E-mail: kovacs.luca@phd.uni-sopron.hu; horvath.norbert@uni-sopron.hu

Keywords: wood impregnation; preservative retention; penetration depth; treatability; Norway spruce; Pannonia poplar.

ABSTRACT

The effectiveness of wood impregnation treatments is commonly evaluated based on preservative uptake (retention). However, previous studies have shown that the anatomical structure of wood plays a decisive role in determining preservative uptake and treatability. Differences in wood structure may therefore lead to substantial variations in the efficiency of impregnation processes. The aim of this study was to investigate relationship between preservative uptake and penetration characteristics in two wood species with different treatability: Norway spruce (*Picea abies*) and Pannonia poplar (*Populus* × *euramericana* cv. Pannonia). Impregnation experiments were carried out using vacuum–atmospheric–vacuum (VAV) and Bethell processes with different pre-vacuum durations. A 5% aqueous copper sulphate solution was used as the impregnating agent. Preservative retention was determined based on mass uptake, while penetration characteristics were evaluated by measuring minimum penetration depth and the proportion of penetrated cross-sectional area using microscopic measurements and image analysis. The results revealed clear differences between the two investigated species. Pannonia poplar showed nearly complete cross-sectional penetration under all treatment schedules despite considerable variation in preservative uptake values. In contrast, Norway spruce exhibited lower penetration levels and greater variability depending on treatment conditions. In spruce samples, increased preservative uptake was generally associated with deeper penetration; however, the relationship between retention and penetration was not strictly linear. These findings indicate that preservative retention alone may not adequately describe the effectiveness of wood impregnation treatments. The combined evaluation of retention and penetration characteristics provides a more comprehensive understanding of wood treatability and the performance of impregnation processes.

INTRODUCTION

Wood is widely used as a structural material due to its favourable mechanical properties, renewable origin, and high strength-to-weight ratio (Ayanleye et al., 2021; Horváth and Csiha, 2022; Panigrahi et al., 2018). However, untreated wood is susceptible to biological degradation caused by fungi, insects, and other organisms, which may significantly reduce its service life, particularly under outdoor conditions (Horváth and Csiha, 2022; Yildiz et al., 2010). To improve durability and extend the service life of wood products, preservative treatments are commonly applied using industrial impregnation processes (Ayanleye et al., 2021; Thaler et al., 2012; Yildiz et al., 2010).

The effectiveness of wood impregnation is typically evaluated based on preservative retention, which describes the amount of preservative absorbed by the wood (Sidorova et al., 2016; Yildiz et al., 2010). Retention is widely used in both research and industrial practice as an indicator of treatment quality, and minimum retention levels are often specified in standards depending on the intended service conditions of the treated wood (Yildiz et al., 2010). In many studies, preservative retention and penetration depth are considered among the principal criteria for evaluating impregnation efficiency (Sint et al., 2011). However, retention alone may not fully describe treatment effectiveness, since penetration depth and preservative distribution may also strongly influence performance (Tarmian et al., 2020).

However, previous investigations have highlighted that retention values alone can be misleading when evaluating wood treatability, as they do not adequately describe the micro-distribution, penetration depth, and uniformity of preservatives within the complex wood structure (Sint et al., 2011; Tarmian et

al., 2020). Penetration is often heterogeneous due to the complex anatomical structure of wood, and local areas with insufficient penetration may remain even when retention values are relatively high (Tarmian et al., 2020; Buschalsky et al., 2025). For instance, in refractory softwood species like Norway spruce, preservative penetration may occur preferentially via specific pathways such as resin canals, leaving large portions of the wood matrix untreated (Civardi et al., 2016). Such untreated or weakly treated zones may increase the susceptibility of wood to biological degradation during service life (Sint et al., 2011). Imaging-based investigations of refractory wood species have also revealed the presence of untreated pockets and difficult-to-treat regions caused by anatomical barriers that limit preservative transport within the wood structure (Civardi et al., 2016; Shirmohammadi et al., 2023).

The treatability of wood is strongly influenced by its anatomical characteristics, including cell structure, permeability, and the presence of extractives (Ayanleye et al., 2021). As a result, different wood species may exhibit significantly different impregnation behaviour due to variations in fluid transport pathways and anatomical barriers within the wood structure (Tarmian et al., 2020). Refractory softwood species such as Norway spruce (*Picea abies*) typically show limited preservative penetration because of the low permeability of the wood structure and the aspiration of bordered pits during drying (Lehringer et al., 2009; Yildiz et al., 2010). In contrast, poplar species generally exhibit higher permeability and more favourable impregnation characteristics, allowing more uniform preservative penetration (Ahmed et al., 2025). Nevertheless, even highly permeable hardwood species may show local heterogeneity in preservative distribution due to anatomical complexity and variations within the wood structure (Buschalsky et al., 2025).

Despite the widespread use of preservative retention as an evaluation parameter, the relationship between preservative retention and penetration characteristics is not yet fully understood. Previous studies have demonstrated that similar retention values may still result in substantially different penetration depths and preservative distribution patterns within the wood structure (Tarmian et al., 2020). Furthermore, retention values alone may not adequately reflect the micro-distribution and uniformity of preservative penetration in different anatomical regions of the wood (Sint et al., 2011). Consequently, it remains unclear whether higher preservative retention necessarily results in deeper or more uniform penetration.

The aim of this study was to investigate the relationship between preservative retention and penetration characteristics in two wood species with markedly different treatability, Norway spruce (*Picea abies*) (Civardi et al., 2016; Lehringer et al., 2009) and Pannonia poplar (*Populus* × *euramericana* cv. *Pannonia*) (Buschalsky et al., 2025; Horváth and Csiha, 2022), using different impregnation processes. Particular attention was given to the relationship between preservative uptake, penetrated cross-sectional area, and minimum penetration depth.

MATERIALS AND METHODS

Norway spruce (*Picea abies*) and Pannonia poplar (*Populus* × *euramericana* cv. *Pannonia*) timber specimens were used for the experiments. The investigated wood species were selected due to their substantially different treatability characteristics. Specimens with cross-sectional dimensions of 30 × 50 mm and a length of 240 mm were prepared from sawn timber. Prior to impregnation, the samples were conditioned under standard climate conditions (20 °C and 65% relative humidity). The average moisture content of the conditioned specimens was approximately 10% for Norway spruce and 8% for Pannonia poplar. Three specimens were used for each treatment schedule.

Impregnation experiments were carried out using vacuum–atmospheric–vacuum (VAV) and Bethell impregnation processes. Different pre-vacuum durations were applied in order to investigate the relationship between preservative uptake and penetration characteristics under varying treatment conditions. A 5% aqueous copper sulphate solution specified in EN 14734 (CEN 2022) was used as the impregnating agent. The impregnation schedules applied in the experiments are summarized in Table 1.

Table 1: Impregnation schedules used in the experiments

Schedule	Pre-vacuum	Pressure	Post-vacuum
VAV15	200 mbar, 15 min.	atmospheric	200 mbar, 30 min.
VAV30	200 mbar, 30 min.	atmospheric	200 mbar, 30 min.
VAV45	200 mbar, 45 min.	atmospheric	200 mbar, 30 min.
VAV60	200 mbar, 60 min.	atmospheric	200 mbar, 30 min.
Bethell15	200 mbar, 15 min.	8 bar, 60 min.	200 mbar, 60 min.
Bethell30	200 mbar, 30 min.	8 bar, 60 min.	200 mbar, 60 min.
Bethell45	200 mbar, 45 min.	8 bar, 60 min.	200 mbar, 60 min.
Bethell60	200 mbar, 60 min.	8 bar, 60 min.	200 mbar, 60 min.

Preservative uptake was determined based on the mass difference of the specimens before and after impregnation. The conditioned specimens were weighed prior to treatment and immediately after impregnation following surface drainage. The absorbed preservative solution was calculated from the difference between the initial and final masses of the specimens according to Equation 1.

$$\Delta m = m_u - m_e \quad (1)$$

where:

- Δm = absorbed preservative solution [g],
- $\boldsymbol{m_u}$= specimen mass after impregnation [g],
- $\boldsymbol{m_e}$= specimen mass before impregnation [g].

Preservative penetration was evaluated using the chromazurol S indicator solution specified in EN 14734 (CEN 2022). Minimum penetration depth was determined microscopically, while the proportion of penetrated cross-sectional area was evaluated using digital image analysis. Detailed penetration evaluation methodology was described previously (Buga-Kovács and Horváth, in press).

RESULTS AND DISCUSSION

The measured preservative uptake and penetration parameters are summarized in Table 2.

Table 2: Preservative uptake and penetration characteristics of Norway spruce and Pannonia poplar under different impregnation schedules, expressed as mean values ± standard deviations

Process	Species	Uptake (g)	Penetrated area (%)	Minimum penetration depth (µm)
VAV15	Spruce	60.11 ± 28.53	55.85 ± 26.78	481 ± 128
VAV15	P. poplar	156.73 ± 5.70	99.98 ± 0.02	n.d.
VAV30	Spruce	57.38 ± 9.19	45.06 ± 17.43	483 ± 151
VAV30	P. poplar	127.62 ± 35.82	95.76 ± 5.74	389 ± 86
VAV45	Spruce	56.64 ± 44.36	45.13 ± 15.21	324 ± 62
VAV45	P. poplar	147.13 ± 13.97	99.99 ± 0.01	n.d.
VAV60	Spruce	162.64 ± 1.96	81.63 ± 11.	775 ± 569
VAV60	P. poplar	141.41 ± 0.11	98.56 ± 1.74	1282 ± 1147
Bethell15	Spruce	160.48 ± 42.26	81.10 ± 14.10	1343 ± 460
Bethell15	P. poplar	221.08 ± 14.97	99.77 ± 0.10	n.d.
Bethell30	Spruce	161.82 ± 37.29	87.77 ± 4.79	1616 ± 679
Bethell30	P. poplar	201.07 ± 6.42	99.60 ± 0.60	n.d.
Bethell45	Spruce	153.65 ± 7.46	82.35 ± 13.24	1336 ± 1050
Bethell45	P. poplar	216.39 ± 0.47	99.99 ± 0.01	n.d.
Bethell60	Spruce	211.81 ± 30.20	85.59 ± 2.86	989 ± 125
Bethell60	P. poplar	204.44 ± 3.48	98.55 ± 0.10	n.d.

n.d. = not determined due to complete cross-sectional penetration.

Pannonia poplar exhibited nearly complete penetration under almost all impregnation schedules, with penetrated area ratios ranging between 95.76 ± 5.74% and 99.99 ± 0.01%, despite considerable variation in preservative uptake values. These results indicate that penetration in poplar was largely independent of uptake. In contrast, Norway spruce showed substantially lower penetrated area ratios and greater

variability depending on the applied treatment conditions. The lowest penetration values were observed in the VAV30 and VAV45 treatments, where penetrated area ratios remained close to 45%, despite preservative uptake values exceeding 56 g. Increasing preservative uptake generally resulted in improved penetration in spruce, particularly in the VAV60 and Bethell treatments, where penetrated area ratios exceeded 80%.

However, the relationship between preservative uptake and penetrated cross-sectional area in Norway spruce was not strictly linear. Similar uptake values occasionally resulted in substantially different penetration characteristics, indicating that preservative distribution within the wood structure was also influenced by anatomical factors and flow path accessibility. The large standard deviations observed in several treatments further suggest heterogeneous preservative distribution within the wood structure. These findings indicate that preservative uptake alone does not necessarily provide sufficient information about penetration characteristics or the uniformity of preservative distribution.

The relationship between preservative uptake and minimum penetration depth also differed substantially between the investigated wood species. In Norway spruce, increased preservative uptake generally resulted in deeper penetration; however, considerable variability was observed among the different impregnation schedules. The lowest minimum penetration depths were observed in the VAV30 and VAV45 treatments, where minimum penetration depths remained below 400 µm despite preservative uptake values exceeding 56 g. In contrast, substantially deeper penetration was achieved in the Bethell treatments, particularly in Bethell15 and Bethell30, where minimum penetration depths exceeded 1300 µm.

However, the relationship between preservative uptake and minimum penetration depth was not strictly proportional. For example, the highest preservative uptake observed in the Bethell60 treatment did not result in the deepest minimum penetration depth. This indicates that preservative uptake alone may not adequately describe local penetration characteristics within the wood structure. Large standard deviations observed for minimum penetration depth in several spruce treatments further suggest substantial local heterogeneity in preservative distribution. In Pannonia poplar, minimum penetration depth could not be determined in most cases due to complete cross-sectional penetration. This indicates that the preservative solution penetrated nearly the entire cross-section regardless of the exact uptake value. Only the VAV30 and VAV60 treatments showed measurable minimum penetration depths, suggesting slight local variability in preservative distribution. The refractory behaviour of Norway spruce can primarily be explained by the low permeability of the wood structure and the aspiration of bordered pits during drying, which significantly restrict fluid flow pathways within the tracheid system (Lehringer et al., 2009; Yildiz et al., 2010). As a result, preservative penetration in spruce often remains heterogeneous even under pressure impregnation conditions. In contrast, Pannonia poplar exhibited nearly complete penetration under most treatment schedules regardless of preservative uptake. This behaviour reflects the generally higher permeability of poplar species associated with the presence of vessel elements and more favourable fluid transport pathways (Ahmed et al., 2025). Nevertheless, measurable minimum penetration depths observed in certain VAV treatments suggest that local heterogeneity in preservative distribution may still occur under less intensive treatment conditions. Overall, the results indicate that preservative retention alone may not fully describe impregnation effectiveness, particularly in refractory wood species. While penetrated cross-sectional area showed a relatively strong relationship with preservative uptake in spruce, minimum penetration depth proved to be more sensitive to local variability within the wood structure.

CONCLUSIONS

The results demonstrated that the relationship between preservative uptake and penetration characteristics strongly depends on wood species and anatomical structure. Norway spruce exhibited substantially lower and more variable penetration compared with Pannonia poplar, reflecting the refractory nature of spruce and the influence of anatomical barriers on preservative transport. A strong positive relationship was observed between preservative uptake and penetrated cross-sectional area in Norway spruce. However, the relationship between uptake and minimum penetration depth was considerably more variable, indicating that preservative uptake alone does not fully describe local penetration characteristics within the wood structure. In several cases, higher preservative uptake did not result in deeper minimum penetration depth.

Pannonia poplar exhibited nearly complete penetration under most impregnation schedules despite considerable variation in preservative uptake. This suggests that in highly permeable species, penetration may become largely independent of uptake after the wood structure approaches saturation. The results also demonstrated that different penetration parameters provide different information regarding treatment effectiveness. While penetrated cross-sectional area proved useful for evaluating overall preservative distribution, minimum penetration depth was more sensitive to local variability and weakly treated regions within the wood structure. Overall, the findings indicate that preservative retention alone may not provide sufficient information for evaluating impregnation effectiveness, particularly in refractory wood species. The combined evaluation of preservative uptake, penetrated cross-sectional area, and minimum penetration depth provides a more comprehensive assessment of wood treatability and preservative distribution.

REFERENCES

Ahmed AAO, Csiha CM, Alpár T, Bejó L (2025) Comparative analysis of wettability of hybrid and indigenous poplar strands. Forests 16:1528. https://doi.org/10.3390/f16101528

Ayanleye S, Udele K, Nasir V, Zhang X, Militz H (2021) A comparative cradle-to-gate life cycle assessment of mid-rise office building construction alternatives / Wood preservation review. (Kézirat/Review)

Buga-Kovács, L., Horváth, N. (in press): Influence of pre-vacuum duration on preservative penetration during Bethell and VAV impregnation of Norway spruce and Pannonia poplar. Acta Silvatica et Lignaria Hungarica.

Buschalsky A, Militz H, Koddenberg T (2025) Anatomical barriers to impregnation in hybrid poplar: a comparative study of pit characteristics in normal and tension wood. Forests 16:1151. https://doi.org/10.3390/f16071151

Civardi C, Van den Bulcke J, Schubert M, Michel E, Butron MI, Boone MN, Dierick M, Van Acker J, Wick P, Schwarze FWMR (2016) Penetration and effectiveness of micronized copper in refractory wood species. PLoS ONE 11:e0163124. https://doi.org/10.1371/journal.pone.0163124

Horváth N, Csiha C (2022) Measurements of the load-bearing structural aspects of Pannónia poplar from sites in Western Transdanubia, Hungary. Acta Silv Lign Hung 18:119–127. https://doi.org/10.37045/aslh-2022-0008

Lehringer C, Richter K, Schwarze FWMR, Militz H (2009) A review on promising approaches for liquid permeability improvement in softwoods. Wood Fiber Sci 41:373–385.

Panigrahi S, Kumar S, Panda S, Borkataki S (2018) Effect of permeability on primary processing of wood. J Pharmacogn Phytochem 7:2593–2598.

Shirmohammadi M, Karbaschi MR, Hassan B, Leggate W (2023) Investigating wood anatomical factors influencing the treatability of refractory southern pine- an imaging approach. In: IRG54 Scientific Conference on Wood Protection. The International Research Group on Wood Protection, Cairns, Australia.

Sidorova E (2016) Combination of heating and preservative impregnation of wood for outdoor exposure. Licentiate thesis, Luleå University of Technology, Luleå, Sweden.

Sint KM, Militz H, Hapla F, Adamopoulos S (2011) Treatability and penetration indices of four lesser-used Myanmar hardwoods. Wood Res 56:13–22.

Tarmian A, Zahedi Tajrishi I, Oladi R, Efhamisisi D (2020) Treatability of wood for pressure treatment processes: a literature review. Eur J Wood Wood Prod 78:635–660. https://doi.org/10.1007/s00107-020-01541-w

Thaler N, Lesar B, Kariz M, Humar M (2012) Bioincising of Norway spruce wood using wood inhabiting fungi. Int Biodeterior Biodegrad 68:51–55.

Yildiz S, Yildiz ÜC, Dizman E, Temiz A, Gezer ED (2010) The effects of pre-acid treatment on preservative retention and compression strength of refractory spruce wood impregnated with CCA and ACQ. Wood Res 55:103–105.

Plant Residues as Possible Forest Fuels in Deciduous Forests

George Mușat[1], Daniel Costache[2], Elena-Camelia Mușat[2*], Emilia-Adela Manea Salca[1]

[1] Transilvania University of Brasov, Faculty of Furniture Design and Wood Engineering, University Dtreet no. 1, 500068, Brasov, Romania
[2] Transilvania University of Brasov, Faculty of Silviculture and Forest Engineering, Sirul Beethoven no. 1, 500123, Brasov, Romania.

E-mail: george.musat@unitbv.ro; daniel.costache@yahoo.com; elena.musat@unitbv.ro; emilia.salca@unitbv.ro

Keywords: forest fires; forest fuels; dry leaves, dry grass; forest fires impact.

ABSTRACT

Forest fires are complex phenomena that cause an ecological imbalance not only in the forest, where they occur, but also outside it, due to negative influences on the environment. Although forest fires can be divided into several categories according to the level at which they occur, the most common are litter fires, which occur at ground level, when all combustible materials are affected, represented by both ground-level vegetation (moss, grasses, bushes, saplings, shrubs and trees) and plant debris. As a result, the research aimed to evaluate and identify the types of forest fuels in deciduous forests in the forest-steppe areas of Romania. The research was conducted within the Ciucurova Forestry District, within the Tulcea Forestry Directorate, in three compartments with 60–80-year-old trees, of the lime, oak, hornbeam and other deciduous species. The choice of the Tulcea Forestry Directorate as the location of the research was based on the climatic particularities of the area, which are characterized by high temperatures and prolonged drought periods, optimal conditions for the development of large-scale forest fires, an assertion also supported by the fact that in 2021, five forest fires occurred in Tulcea county, affecting 5240 ha, i.e. approximately 50% of the area affected by fires in the last 10 years. The working methodology involved the creation of 2 x 2 m experimental plots, in which various types of combustible materials were differentiated and weighed (dry leaves and seeds, branches with a diameter of less than 5 cm, wood with a diameter greater than 5 cm and dry grass). After the centralization of the data, it was observed that most combustible materials are represented by leaves and seeds which are highly flammable in dry conditions. In contrast, fuels in the category of branches with a diameter of less than 5 cm and wood with a diameter greater than 5 cm were encountered in smaller quantities, a fact also justified by the age of the stands in which the field measurements were carried out. On the other hand, the combustible materials identified in the experimental plots are found on the forest floor in significant quantities, in a continuous field and, due to their small size and large specific surface area, can quickly lose moisture, constituting a total combustible material which, in the event of a litter fire, would lead to its rapid development.

INTRODUCTION

Forest fires are complex phenomena that cause an ecological imbalance not only within the forest but also outside it, and can be triggered by a multitude of causes (Mușat 2024), which is why the inventory and evaluation of a fire within the forest fund remains an approximation, as the determining elements are very difficult to establish with precision (Adam 2007). In addition, forests contain a very wide variety of combustible materials that possess the property to ignite, kindle, and burn in the presence of air, a phenomenon that contributes significantly to the increase in the amount of heat generated by the fire (Burlui and Burlui 2018). Thus, in most forests, plant materials are represented by (Ciobanu and Ioraș 2007): litter, ground cover, stand, undergrowth, and logging residues.

The physical and chemical characteristics of fuels determine both the possibility of a fire outbreak and its subsequent behavior and released energy, making it difficult to control (Ciobanu and Ioraș 2007). The amount of combustible material can be determined by the mass of dry fuels found per unit area (kg/m^2 or t/ha). The moisture content of combustible materials is the most important factor in fuel testing, determining the probability of fire occurrence and spread. The calorific value is influenced by fuel density (wood – Burlui 2012) and can be expressed by the heat released from the complete

combustion process of a significant amount of fuel (Lunguleasa et al. 2007), being 13,800 kJ/kg for fir and 19,250 kJ/kg for beech and oak (Ciobanu and Ioraș 2007).
In the case of forest species, coniferous stands are considered to have high combustibility compared to broadleaved ones, due to resins and volatile substances that significantly influence fire development. Thus, according to the specialized literature (Adam 2007; Burlui and Burlui 2018), spruce represents the most flammable species in terms of burning rate and ranks second after the calorific value of pines. Due to the implications that forest fires have on the environment, material assets, and even human life, these phenomena must be researched. Consequently, the study aimed to quantify the types of combustible materials in broadleaved forests located in the steppe and forest-steppe zones of Romania.

MATERIALS AND METHODS

The research was conducted in compartments 72B, 76B, and 78B of the Management Unit number II Ciucurova (Figure 1a), a public state-owned forest fund managed by the Ciucurova Forest District through the Tulcea County Forest Administration. The area where the field work was carried out and from which the data were collected corresponds to mixed forests in the steppe region of Romania. Due to its geographical location and climatic features, Tulcea County is prone to long periods without precipitation, which implies, to some extent, an increased risk of forest fires.

a. b. c.

Figure 1: Location of the compartments within Management Unit number Ciucurova (a.), delineation of the sample plots (b.), and appearance of the plots after the collection of all combustible materials (c.)

The compartments where the field work was conducted exhibit an average terrain slope of 8 degrees, while the forest stands have a canopy density of 0.9, with ages ranging between 60 and 80 years, having undergone the first thinning (72B – Figure 2a) and the second thinning (76 B and 78 B – Figures 2b and 2c).

a. b. c.

Figure 2: Images from the studied compartments: 72B (a.), 76B (b.), and 78B (c.)

The work methodology involved establishing ten sample plots in each compartment, distributed relatively homogeneously across the entire area to encompass all terrain forms and all categories of combustible materials. The dimensions of the sample plots were 2 x 2 m (4 m²), and their delineation was carried out using tape secured with wooden stakes (Figure 1b). In total, 30 sample plots were established, with sorting and weighing of all combustible materials performed in each plot (Figure 1c)

according to the following categories (Figure 3): leaves and seeds, branches with a diameter of less than 5 cm, wood with a diameter of more than 5 cm, and dry grass. All combustible materials located inside the sample plot were taken into account, while materials that were partially inside and partially outside were cut at the boundary line, with only the part corresponding to the sample plot being weighed. The adopted unit of measurement was the kilogram, and the quantities were rounded to two decimal places.

a. b. c. d.

Figure 3: Categories of combustible materials from the sample plots: leaves and seeds (a.), branches with a diameter of less than 5 cm (b.), wood with a diameter of more than 5 cm (c.), and dry grass (d.)

RESULTS AND DISCUSSION

The combustible materials found in the sample plots, by their nature, were dead fuels, represented by (Table 1): seeds and leaves, branches with a diameter of less than 5 cm, wood with a diameter of more than 5 cm, and dry grass. The seeds and leaves, the branches, and wood within the delimited perimeter of the sample plots belonged to the following species: lime, sessile oak, ash, hornbeam, and various other hardwoods. The dry grass found in the sample plots belongs to the species *Lolium perenne*, which is relatively abundant in the area.

The analysis of Table 1 highlights the large quantities of leaves and seeds in all three compartments compared to the other categories of combustible materials, while dry grass shows the lowest quantities. Regarding the homogeneity of the data on the quantities of combustible materials, it is noted that in the case of compartment 78B, the values are relatively close to the average, showing variations of 0.26–0.46 kg, whereas the compartment 72B exhibits the highest data variability, causing all types of combustible materials to vary within relatively wide limits from one sample plot to another (0.61–0.89). Figure 4a illustrates the contribution proportion of each combustible material category across each of the ten sample plots established in compartment 72B, revealing a predominance of leaves and seeds, which represent more than 60% of the total amount of combustible materials in every sample plot. The characteristic situation of the second compartment (76B) indicates, once again, the significant share of leaves and seeds, although some fluctuations occur; this material category represents between 60% and 80% of the total dead fuels identified and weighed in compartment 76B (Figure 4b). Furthermore, it is observed that dry grass is absent in some sample plots, while the percentage of wood with a diameter of more than 5 cm can reach up to 25% of the total amount of combustible materials identified within a sample plot. In the case of compartment 78B, dry grass appears in seven sample plots (Figure 4c), whereas wood with a diameter of more than 5 cm exhibits a more significant share.

Table 1: Descriptive statistical indicators regarding the total quantities of combustible materials identified in the sample plots established within the three management units

Compartment	Descriptive statistical indicator	Leaves and seeds [kg]	Branches d<5 cm [kg]	Wood d>5 cm [kg]	Dry grass [kg]
72B	Mean	5.82	1.34	1.39	0.11
	Median	5.72	1.31	1.16	0.00
	Minimum	4.87	0.23	0.00	0.00
	Maximum	7.27	2.42	2.93	0.33
	Standard deviation	0.71	0.61	0.89	0.14
	Range	2.40	2.19	2.93	0.33
76B	Mean	6.17	1.31	1.33	0.11
	Median	6.05	1.22	1.44	0.00
	Minimum	5.14	0.79	0.00	0.00
	Maximum	7.14	2.24	2.39	0.45
	Standard deviation	0.57	0.38	0.82	0.16
	Range	2.00	1.45	2.39	0.45
78B	Mean	5.61	1.10	1.45	0.17
	Median	5.66	1.13	1.45	0.21
	Minimum	4.75	0.43	1.03	0.00
	Maximum	6.12	1.87	1.85	0.35
	Standard deviation	0.43	0.36	0.26	0.13
	Range	1.37	1.44	0.82	0.35

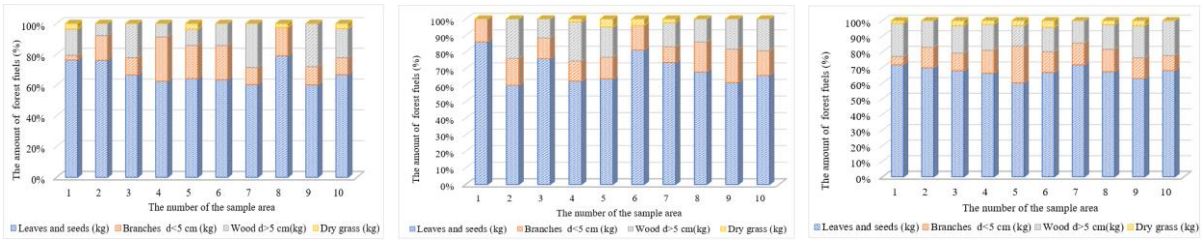

a. b. c.

Figure 4: Contribution proportion of the combustible materials identified in management unit: 72B (a.), 76B (b.), and 78B (c.)

By summing the quantities of combustible materials by category, the total amount of combustibles was obtained for all ten sample plots in each compartment. Thus, in compartment 72B (Figure 5a), it was found that 67% of the combustible materials consist of leaves and seeds, 16% branches with a diameter of less than 5 cm, 16% wood with a diameter of more than 5 cm, and 1% dry grass. According to the graphical representation in Figure 5b, all types of combustible materials are present in compartment 76B, with their shares being approximately 69% leaves and seeds, 15% branches with a diameter of less than 5 cm, 15% wood with a diameter of more than 5 cm, and 1% dry grass. It is noted that, unlike in compartment 72B, the quantity of leaves and seeds slightly increased at the expense of woody materials. On the other hand, in compartment 78B (Figure 5c), the share of leaves and seeds is similar to that in 72B, whereas wood with a diameter of more than 5 cm appears in a higher proportion, and branches with a diameter of less than 5 cm in a lower proportion.

A comparative analysis of the quantities and types of combustible materials found across the 30 sample plots established within the three compartments reveals a significant share of dry leaves and seeds. In the event of a fire outbreak, this could decisively influence its development, especially since—as observed in the field and evidenced by the photographs—these types of materials cover the forest floor uniformly, consequently leading to the rapid, continuous spread of a potential fire.

One of the most important influencing factors in the outbreak and development of forest fires is the moisture content of both the dead and live ground cover. The greatest hazards are posed by dry litter composed of coniferous needles (Burlui and Burlui 2018). Taking into account the results obtained in the studied area, it can be easily observed that the ground-level cover consists largely of combustible materials that can dry out very easily and possess a high specific surface area, which positively influences the potential development of a litter fire.

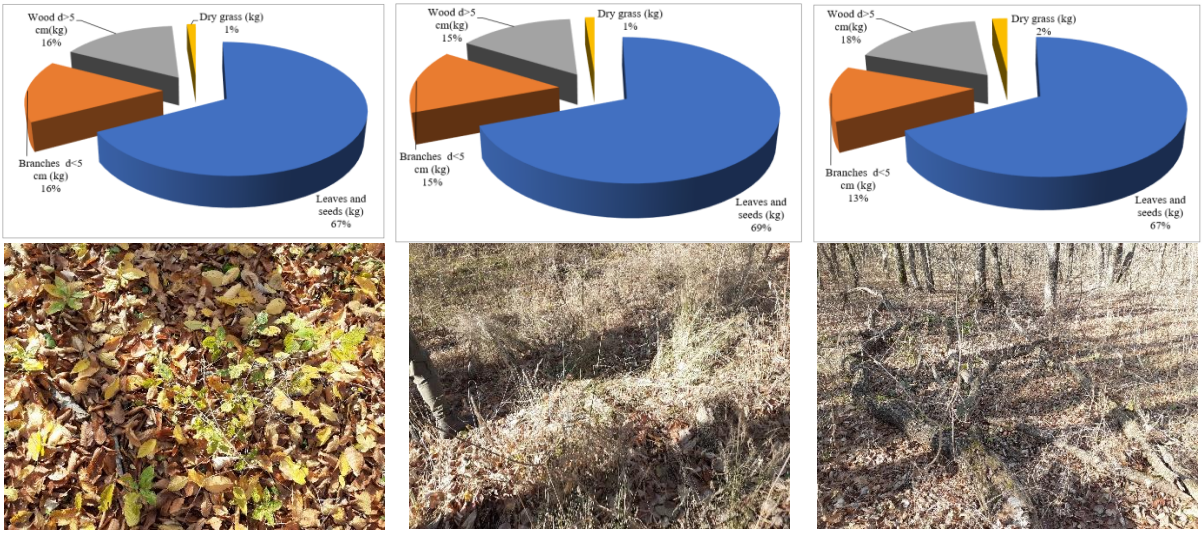

a. b. c.

Figure 5: Fuel proportion per hectare in compartments: 72B (a.), 76B (b.), and 78B (c.)

The packing ratio, defined as the ratio between the fuel quantity and the air volume within a fuel bed (Ciobanu and Ioraș 2007), plays a decisive role in fire development. Thus, a lower packing ratio implies more air within the fuel mass, consequently causing a potential fire to ignite much faster. On the other hand, fuel continuity, viewed as both horizontal and vertical continuity, conditions flame propagation and influences the possibility of fire spreading to the tree crowns (Ciobanu and Ioraș 2007). In the case of the studied stands, it is observed that horizontal continuity is present, which would favor the accelerated development of a potential litter fire.

CONCLUSIONS

The most significant combustible materials identified and weighed were leaves and seeds.

The highest combustibility among the three studied compartments was recorded in 76B, indicating an increased vulnerability to the occurrence of forest fires.

In the Dobrogea region, temperatures are high from early on, and summers are long and dry, causing leaves and seeds to dry out very easily. Within the studied compartments, leaves and seeds exhibit an uninterrupted horizontal continuity. In the event of an outbreak, it will manifest as a litter fire and will spread very easily due to the dryness level and the significant amounts of forest fuels present on the forest floor.

REFERENCES

Adam, I., 2007. Metodă de evaluare a riscului de incendiu în pădurile României. Analele ICAS 50:261-271.

Burlui, I., 2012. The particularities of firefighting in the mountain forests. AAB Bioflux 4(3):131-142.

Burlui, I., Burlui, C., 2018. Incendiile forestiere: elemente caracteristice, factori determinanți și măsuri de gestionare. Bucovina Forestieră 18(2):165-175.

Ciobanu, V., Ioraş, F., 2007. Incendii forestiere [Forest fires]. Transilvania University Publishing House, Brasov, Romania, 131 p.

Lunguleasa A., Pațachia S., Costiuc L., Ciobanu V., 2007. Combustia ecologică a biomasei lemnoase [Ecological combustion of woody biomass]. Transilvania University Publishing House, Brasov, Romania, 124 p.

Mușat, E.C., 2024. Impact of forest fires on the trees and wood quality – A case study for a beech stand. Fire 7(9):325. DOI: https://doi.org/10.3390/fire7090325

Mechanical Performance of a Longitudinal Joint for Round Spruce Poles Reinforced with an Oak Dowel (Preliminary Investigation)

Nagy Bence[1], Nadežda Langová[2], Igor Sršeň[3], Rastislav Lagaňa[1*]

[1] Technical University in Volen, Faculty of Wood Sciences and Technology, Department of Wood Science, T. G. Masaryka 24, 960 01 Zvolen, Slovakia
[2] Technical University in Zvolen, Faculty of Wood Sciences and Technology, Department of Furniture and Wood Products, T. G. Masaryka 24, 960 01 Zvolen, Slovakia
[3] Technical University in Zvolen, Faculty of Wood Sciences and Technology, Department of Wooden Constructions, T. G. Masaryka 24, 960 01 Zvolen, Slovakia.

E-mail: woodworking.nb@gmail.com; langova@tuzvo.sk; igor.srsen@tuzvo.sk; lagana@tuzvo.sk

Keywords: round pole, longitudinal extension, joint, oak dowel, bending, DIC, FEM.

ABSTRACT

This study investigated the mechanical performance of a detachable longitudinal extension joint developed for round spruce poles and designed for CNC-based fabrication. The joint geometry was based on a half-lap configuration and incorporated an oak dowel as the principal shear-transfer element, while external steel clamps were used to improve contact integrity and restrain joint opening. Experimental specimens were prepared from milled spruce roundwood with a nominal diameter of 100 mm. The test program included specimens evaluated in the horizontal orientation, the vertical orientation (10 replicates each), and 18 unjointed reference specimens. Mechanical performance was evaluated under four-point bending and supplemented by density determination, full-field deformation monitoring using ARAMIS 3D digital image correlation, and finite element analysis in ANSYS.

Relative to the reference specimens, the stiffness of the horizontally oriented joint reached 42%, while the vertically oriented joint reached 57%. The corresponding bending strength values were 40% and 46%, respectively. Full-field strain analysis revealed critical stress concentrations in the inner notch region of the joint and in the vicinity of the oak dowel, consistent with the experimentally observed failure pattern and the predictions of the finite element model. The proposed joint shows potential for use in segmented roundwood members for large-span skeletal structures, particularly temporary timber systems such as scout tipis.

INTRODUCTION

Timber structures are currently increasingly assessed not only in terms of structural performance, but also with respect to efficient raw-material use, reduced environmental impact, and the potential reuse of building components. In this context, alongside glued laminated timber, cross-laminated timber, and other engineered wood products, the direct use of roundwood and whole timber members is again receiving attention. This approach may reduce material losses during processing while preserving the natural continuity of wood fibres. However, as noted by Ranta-Maunus (1999) and Bukauskas et al. (2019), the wider use of roundwood in load-bearing structures is associated with several technical limitations, particularly the geometric irregularity of members, taper, eccentricity, and the difficulty of designing reliable connections.

Roundwood members are traditionally used in posts, poles, auxiliary structures, temporary buildings, and lightweight skeletal systems. Their circular cross-section and preserved fiber continuity may be structurally advantageous, particularly when the member is used without major interruption of the material. However, when such members are to be connected into larger or segmented structures, the design of longitudinal extension joints becomes a critical issue. The joint must transfer bending moment and shear forces while limiting slip, rotation, embedment deformation, splitting, and joint opening. This task is more demanding than in prismatic timber members, mainly because roundwood provides less regular bearing surfaces and greater geometric variability. Previous experimental research on roundwood connections has shown that connection parameters and configuration must be verified specifically for the intended structural detail. For example, Dias et al. (2014) investigated connections

for roundwood members using multiple glued-in rods and demonstrated the importance of connection design parameters for the mechanical response of such joints.
Longitudinal half-lap joints represent a simple and technologically feasible solution, particularly when CNC machining is used. Their disadvantage, however, is the local weakening of the cross-section and the formation of stress concentrations around notches and transition zones. Under bending, the behavior of such joints is affected by the shape of the half-lap geometry, the quality of contact between bearing surfaces, wood embedment around the dowel, shear and bending action in the dowel, and the ability of the joint to resist opening. In spruce wood, these factors are further influenced by the natural variability of the material, especially density, fiber direction, knots, moisture content, and local anatomical structure, which are among the principal factors governing the mechanical properties of wood (Kretschmann 2010). In addition, strength relationships in spruce and pine are not always direct or uniform; Gil-Moreno et al. (2022), for example, showed that the relationship between bending and tension strength depends on species and material source. This supports the need to evaluate the tested joint experimentally rather than relying only on general material-property assumptions.
In recent years, wooden dowels have been investigated as a materially compatible and potentially demountable alternative to metal fasteners. Their mechanical action, however, cannot be reduced solely to shear transfer. According to Xu et al. (2022) and Tomasi et al. (2025), the load-carrying capacity of wooden dowels may depend on a combination of several mechanisms, particularly dowel bending, wood embedment, shear failure, compression perpendicular to the grain, and the risk of splitting. From the perspective of mechanical joint design, the principles for testing and evaluating joint deformation and strength specified in EN 26891, as well as the design principles given in EN 1995-1-1, are also relevant.
Detachable connections are of particular importance in structures intended to be temporary, disassembled, or reused. Ottenhaus et al. (2023) emphasized that reversible connections are one of the prerequisites for designing structures for disassembly, repair, and reuse of components. CNC fabrication can contribute to higher precision, repeatability, and control of joint geometry in this regard. At the same time, digitally designed and fabricated wood-to-wood joints must be evaluated not only in terms of manufacturability, but also with respect to assembly, contact efficiency, durability, and fiber orientation relative to load transfer (Larsson et al. 2020, de-los-Aires-Solís and Gonzalez-Quintial 2023).
The available literature indicates that roundwood connections, wooden dowels, and digitally fabricated wood-to-wood joints have mostly been studied separately. However, only limited research has addressed their combination in a single detachable longitudinal joint for small-diameter spruce roundwood. In particular, the effects of joint orientation, wood density variation, and local stress concentrations in the half-lap and dowel regions remain insufficiently clarified.
Therefore, the aim of this study is to experimentally assess the mechanical behavior of a detachable longitudinal extension joint designed for spruce roundwood members and adapted for CNC fabrication. The investigated joint is based on a half-lap geometry, in which an oak dowel serves as the main shear-transfer element and steel clamps limit joint opening. Horizontal and vertical joint orientations were compared with unjointed reference specimens under four-point bending. Stiffness, apparent bending strength, the effect of joint orientation, the influence of density, and the critical zones of stress concentration governing the failure mechanism were evaluated.

MATERIALS AND METHODS

For specimen preparation, milled roundwood members made of spruce wood with dimensions of D = 100 mm and l = 2200 mm were selected. The material contained juvenile wood throughout the entire cross-section. A detachable longitudinal extension joint based on a half-lap configuration was chosen. To increase joint stiffness and simplify production, the dowel dimensions were modified. The dowel hole was shifted by 1 mm towards the inside of the joint in order to create a wedging effect (Figure 1a). To further increase stiffness and strength, the joint was reinforced with a GBS W1 clamp with an adjustable diameter of 98–103 mm (Figure 1b), complying with DIN 3017-2 (2002). The material was conditioned for an extended period at a temperature of 20 °C and a relative humidity of 60%. The moisture content of the specimens was measured using a GANN Hydromette HT 85 T resistance moisture meter. After testing, a 100 mm long sample was cut from each specimen for density and determination.

a) 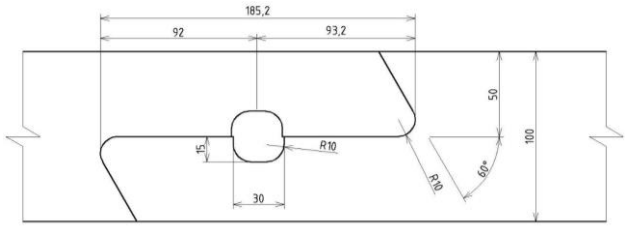

b)

Figure 1: Design of the lap-joint (a) and the final version of CNC processed lap-joint (b)

The strength of the joint was determined by a bending test using a HECKERT FPZ 100/1 universal testing machine equipped with fixtures for four-point bending in accordance with STN EN 408 (2010). The mid-span deflection of the beam was measured using a displacement transducer (AHLBORN, Germany).

The joint stiffness was calculated from the slope of the load–deflection curve according to Eq. (1):

$$k = \frac{l}{6} \cdot \frac{\Delta F}{\Delta y} \tag{1}$$

The joint strength was determined as the apparent bending strength according to Eq. (2):

$$f = \frac{16 \cdot l \cdot F_{max}}{3 \cdot \pi \cdot d^3} \tag{2}$$

where f is the apparent bending strength, l is the span between the supports of the testing machine, Fmax is the maximum load at failure, and d is the diameter of the member.
FEM model of the joint was made using ANSYS and the model was compared to the strain distribution evaluated by ARAMIS 3D system.

RESULTS AND DISCUSSION

The average moisture content of the test specimens was 14.3%, with measured values ranging from 10.9% to 19.3%. This moisture level corresponds to the expected service conditions of the members; therefore, the mechanical properties were not adjusted to the reference moisture content of 12%. The average wood density at 14.3% moisture content was 436 kg·m^{-3}, with values ranging from 353 to 529 kg·m^{-3}. After adjustment to 12% moisture content, the average density was 432.5 kg·m^{-3}. Although the material consisted of juvenile wood, the average density was comparable to typical values reported for spruce. The relatively high density variation was probably associated with differences in the number of annual rings and with the natural variability of wood, which is one of the main factors affecting its mechanical properties (Kretschmann 2010).
The stiffness of the unjointed reference specimens was 126.42 kN·m/m. In the jointed specimens, stiffness was markedly lower. The horizontally oriented joint reached 53.13 kN·m/m, corresponding to 42.02% of the reference value, whereas the vertically oriented joint reached 71.65 kN·m/m, corresponding to 56.67% of the reference value. A one-way ANOVA showed that joint orientation had a statistically significant effect on stiffness ($F(1, 18) = 6.90$, $p = 0.017$), with the vertical configuration exhibiting superior mechanical performance (Figure 2a). This was also confirmed by Duncan's test, which indicated a significant difference between the horizontally and vertically oriented joints ($p = 0.0188$).
A similar trend was observed for apparent bending strength. The reference specimens reached an average strength of 45.57 MPa, whereas the horizontally and vertically oriented joints reached 10.50 MPa and 15.10 MPa, respectively (Figure 2b). These values correspond to 40.25% and 45.84% of the strength of the unjointed members. ANOVA confirmed a significant effect of joint orientation on strength ($F(1, 18) = 35.42$, $p < 0.001$); however, Duncan's test did not indicate a statistically significant difference between the horizontal and vertical joint configurations ($p = 0.0872$). Overall, the results show that the presence of the joint reduced both stiffness and strength by more than one half compared with the unjointed reference specimens.

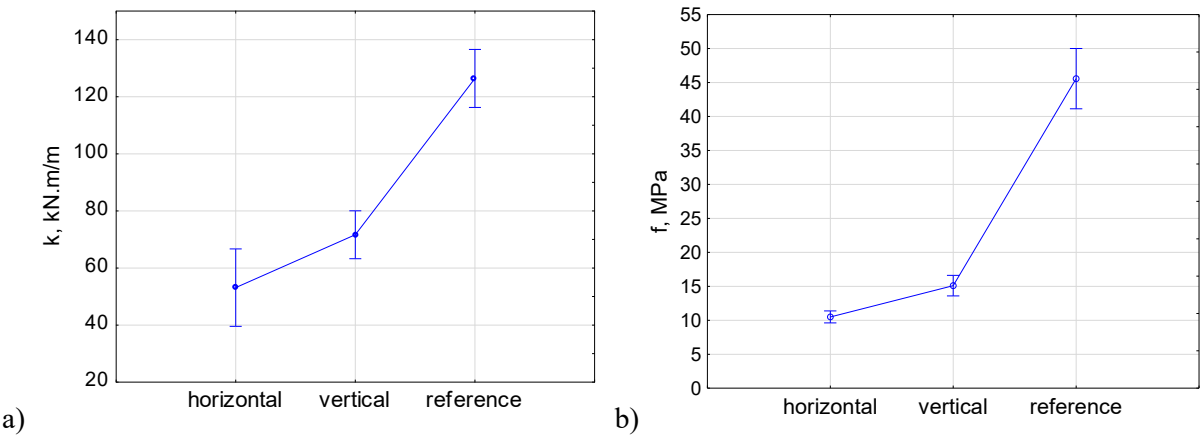

Figure 2: Stiffness (a) and strength (b) of joints tested in the horizontal and vertical orientations

The reduction in mechanical efficiency can be attributed to the weakened cross-section in the half-lap region, stress concentrations around the notch and dowel, and local deformation of the contact surfaces. A similar influence of joint geometry and loading configuration in roundwood members was reported by Dias et al. (2014). The present results are also consistent with Xu et al. (2022), who showed that wooden dowels can act as effective connecting elements, although their load-bearing behavior depends on the combined effects of dowel bending, embedment, shear, and the risk of splitting. The steel clamps probably improved the contact integrity of the joint and restricted joint opening; without this restraint, even lower stiffness and strength values would be expected.

Because the horizontally oriented joints showed lower stiffness and strength, these specimens were selected for detailed deformation analysis. Full-field deformation measurement using the ARAMIS 3D system showed that the highest strain concentrations occurred in the dowel region and at the inner notch tip of the joint (Figure 3a). The analysis focused mainly on shear strains in the xy-plane, which were observed in all monitored specimens. The numerical model developed in ANSYS confirmed the same deformation pattern (Figure 3b). The model also indicated joint opening behind the left clamp and local compression of the joined members near the right clamp. The steel clamps therefore played an important role in maintaining joint integrity, limiting joint opening, and slowing crack propagation in the dowel region and at the notch transitions.

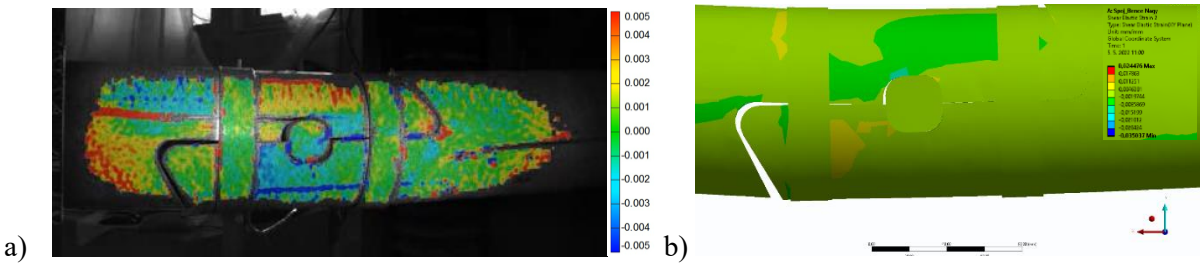

Figure 3: Shear deformation of the joint region, (a) FEM model and (b) measured strain field (b)

CONCLUSIONS

The study demonstrated that the proposed detachable half-lap joint with an oak dowel and external steel clamps can transfer bending loads in segmented round spruce members, although with a substantial reduction in mechanical performance compared with unjointed reference specimens. The jointed members retained approximately 42–57% of the reference stiffness and 40–46% of the reference bending strength, with the vertical joint orientation showing better performance than the horizontal orientation. Full-field deformation analysis and numerical modelling consistently identified the dowel region and the inner notch transition as the critical zones of strain concentration and crack initiation. The steel clamps contributed to maintaining contact integrity and limiting joint opening, indicating their importance for the function of the joint. Further optimization will focus on reducing notch-related stress

concentrations, improving dowel geometry and material properties, and refining manufacturing tolerances to increase the structural efficiency of the joint.

ACKNOWLEDGEMENTS
This study was supported by the Scientific Grant Agency, project VEGA 1/0599/25, project VEGA 1/0450/25 and by the Slovak Research and Development Agency, Project no. APVV-23-0369.

REFERENCES

Bukauskas, A., Mayencourt, P., Shepherd, P., Sharma, B., Mueller, C., Walker, P., and Bregulla, J. 2019. Whole timber construction: A state of the art review. Construction and Building Materials 213: 748–769. https://doi.org/10.1016/j.conbuildmat.2019.03.043

EN 26891:1991. Timber structures — Joints made with mechanical fasteners — General principles for the determination of strength and deformation characteristics. European Committee for Standardization, Brussels.

EN 1995-1-1:2004. Eurocode 5: Design of timber structures — Part 1-1: General — Common rules and rules for buildings. European Committee for Standardization, Brussels.

EN 408:2010+A1:2012. Timber structures — Structural timber and glued laminated timber — Determination of some physical and mechanical properties. European Committee for Standardization, Brussels.

de-los-Aires-Solís, A. J., and Gonzalez-Quintial, F. 2023. A wood-wood joining system suitable for digital fabrication and its application in the design of a "wood-only" spatial module. Frontiers of Architectural Research 12(3): 523–540. https://doi.org/10.1016/j.foar.2022.12.005

Dias, A., Morgado, T., Negrão, J., and Machado, J. S. 2014. Connection for round wood timber members using multiple glued-in rods. In: Proceedings of the World Conference on Timber Engineering, WCTE 2014, Quebec City, Canada.

Gil-Moreno, D., Ridley-Ellis, D., O'Ceallaigh, C., and Harte, A. M. 2022. The relationship between bending and tension strength of Irish and UK spruce and pine. European Journal of Wood and Wood Products 80: 585–596. https://doi.org/10.1007/s00107-022-01787-6

Kretschmann, D. E. 2010. Mechanical properties of wood. In: Wood Handbook — Wood as an Engineering Material. General Technical Report FPL-GTR-190. USDA Forest Service, Forest Products Laboratory, Madison, WI.

Larsson, M., Yoshida, H., Umetani, N., and Igarashi, T. 2020. Tsugite: Interactive design and fabrication of wood joints. In: Proceedings of the 33rd Annual ACM Symposium on User Interface Software and Technology, pp. 317–327. https://doi.org/10.1145/3379337.3415899

Ottenhaus, L. M., Yan, Z., Brandner, R., Leardini, P., Fink, G., and Jockwer, R. 2023. Design for adaptability, disassembly and reuse — A review of reversible timber connection systems. Construction and Building Materials 400: 132823. https://doi.org/10.1016/j.conbuildmat.2023.132823

Ranta-Maunus, A. 1999. Round small-diameter timber for construction: Final report of project FAIR CT 95-0091. VTT Publications 383. Technical Research Centre of Finland, Espoo.

Tomasi, R., De Santis, Y., Aloisio, A., Crocetti, R., Sæby, V. H., and Nyrud, A. Q. 2025. Experimental and analytical investigation on timber connections with beech, birch and laminated densified wooden dowels. Construction and Building Materials 494: 142692. https://doi.org/10.1016/j.conbuildmat.2025.142692

Xu, B.-H., Jiao, S.-Y., Wang, B.-L., and Bouchaïr, A. 2022. Mechanical performance of timber-to-timber joints with densified wood dowels. Journal of Structural Engineering 148(4): 04022023. https://doi.org/10.1061/(ASCE)ST.1943-541X.0003317

Color Changes of Invasive Wood Species Under Heat Treatment

Szabolcs Komán[1*], Benjámin Olivér Kulcsár[1], Péter Farkas[1]

[1]University of Sopron, Faculty of Wood Engineering and Creative Industries. Bajcsy-Zs. Str. 4, Sopron, Hungary, 9400.

E-mail: koman.szabolcs@uni-sopron.hu; GNZ7EV@uni-sopron.hu; farkaspeter@phd.uni-sopron.hu

Keywords: C*eltis occidentalis*, *Acer negundo*, color change, wood aesthetics, heat treatment.

ABSTRACT

Heat treatment is a widely used modification process in the wood industry that improves the dimensional stability and biological durability of wood while also significantly influencing its aesthetic appearance. The aim of this study was to examine the color changes of two hardwood species, hackberry (*Celtis occidentalis*) and boxelder maple (*Acer negundo*), after heat treatment at 180°C and 200°C.

Color measurements were carried out using a Konica Minolta spectrophotometer owned by the University of Sopron, which determines CIE L*a*b* color coordinates by analyzing the spectrum of reflected light. During the measurements, lightness (L*), the red–green coordinate (a*), and the yellow–blue coordinate (b*) were evaluated.

Based on the measured data, ΔL*, Δa*, and Δb* values were calculated, along with chroma difference (ΔC*) and total color difference (ΔE*). The results indicate that heat treatment leads to significant color modification, with the intensity of change increasing at higher temperatures. The ΔE* values exceeded the commonly accepted perceptibility threshold, indicating clearly visible color differences.

INTRODUCTION

Heat treatment is an environmentally friendly wood modification method that improves the physical and biological properties of wood without the use of chemical additives. During the treatment, high temperatures induce chemical transformations in the cell wall components, primarily in hemicelluloses and lignin. These reactions not only enhance dimensional stability and durability but also result in significant changes in the color of the wood.

The color of wood is an important aesthetic parameter in the furniture industry and interior design. The darker and warmer tones produced by heat treatment are often advantageous from a market perspective. Objective evaluation of color changes can be performed using the CIE L*a*b* color system, which quantifies lightness and chromatic coordinates (Figure 1). The aim of this study was to determine the extent and characteristics of color changes in the examined wood species at different heat-treatment temperatures (Hill 2006).

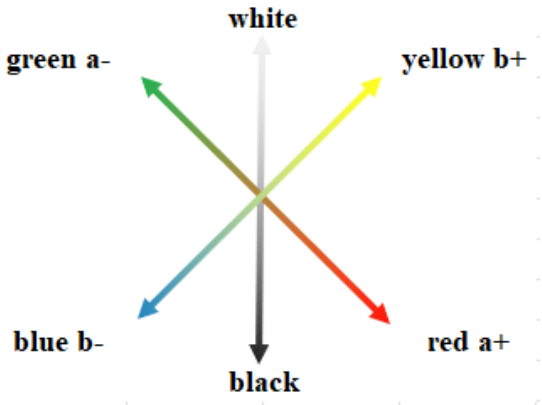

Figure 1: CIE L*a*b* color space diagram (own work)

MATERIALS

Western hackberry (Celtis occidentalis)

The western hackberry is a medium- to large-sized deciduous tree native to the eastern and central regions of North America. It can reach a height of 20–25 meters and a trunk diameter of up to 60–100 cm. It is easily recognizable by its characteristic grayish-brown bark, which is deeply furrowed and corky or warty in texture. Its leaves are ovate with serrated margins and pointed tips, while the underside is slightly hairy. After producing small greenish-yellow flowers, it develops dark brown to black, berry-like drupes.

In Hungary, it has been planted as an ornamental and street tree because it tolerates drought, urban conditions, and air pollution well. However, due to its rapid growth and strong adaptability, it has become invasive in some areas, particularly in lowland and disturbed habitats (Bartha and Csiszár 2008). Its wood is moderately heavy (≈595 kg/m³), with a density of 0.59–0.65 g/cm³. Its mechanical properties are favorable: bending strength is about 76 N/mm², modulus of elasticity is 8.2 GPa, and compressive strength is 37.5 MPa. The wood is easy to work with and flexible, with characteristics similar to elm. It is mainly used in furniture manufacturing, interior paneling, turned objects, and smaller structural elements. Its natural durability is moderate, so surface treatment is recommended for outdoor use (Zoltán and Börcsök 2024).

Boxelder (Acer negundo)

The boxelder is a fast-growing deciduous tree that often develops multiple trunks and can reach a height of 10–25 meters. Its bark is light grayish-brown, and its young shoots often have a greenish tint. Its leaves are typically compound, consisting of 3–7 leaflets, which gives it a distinctive appearance among maples. It flowers in early spring, and its fruit is a winged samara pair that falls in autumn.

Its native range is also North America. It was introduced to Europe as an ornamental tree but is now known as an invasive species. It spreads rapidly, especially in disturbed areas, along riverbanks, and beside roads (Udvardy 2008).

Its wood is relatively light (≈485–536 kg/m³), and its mechanical properties are more moderate: bending strength is about 55 N/mm², modulus of elasticity is 7.24 GPa, and compressive strength is 34 MPa. The wood is light yellowish-white in color, sometimes with reddish figuring. Its natural durability is low, so it is mainly used as raw material for particleboard and wood chips, as well as for small crafts and decorative purposes. It is less suitable for applications requiring significant structural strength (Molnár and Zoltán 2024).

METHODS

Color measurements were carried out using a Konica Minolta spectrophotometer. The instrument analyzes the reflectance spectrum of light directed onto the surface and converts it into CIE Lab* coordinates. The measurement aperture had a diameter of 8 mm, which provided adequate sampling for a balanced assessment of the wood's natural grain (Seiji H 2020).

The following sample numbers were used for each species, and all measurements were made in the same place and under the same conditions:

80 untreated measurement points,

40 measurement points on samples heat-treated at 180 °C for 12 hours

40 measurement points on samples heat-treated at 200 °C for 12 hours

During the measurements, the following parameters were recorded:

L* – lightness,

a* – red–green coordinate,

b* – yellow–blue coordinate.

Changes in chroma and total color difference were calculated using the following formulas:

Eq.1: Chroma change:

$$\Delta C^* = \sqrt{(\Delta a^2) + (\Delta b^2)} \quad (1)$$

Eq.2: Total color difference:

$$\Delta E^* = \sqrt{(\Delta L^*)^2 + (\Delta a^*)^2 + (\Delta b^*)^2} \quad (2)$$

Eq.3: Calculation of delta values:

$$\Delta = untreated - heat\ treated \quad (3)$$

RESULTS

The average L* value of the untreated western hackberry samples was 64.32. The lightness of the samples heat-treated at 180 °C increased to 69.41, indicating a slight lightening (ΔL* = 6,02). In contrast, the L* value of the samples treated at 200 °C decreased to 33.52; resulting in a substantial darkening of 30.80 units (Figure 2).

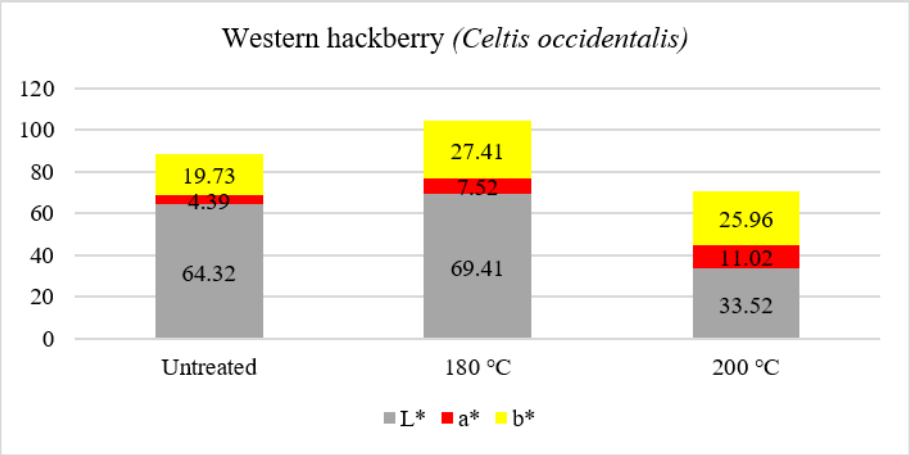

Figure 2: Color composition of western hackberry after different heat treatments

The a* and b* coordinates increased at both temperatures, indicating enhanced reddish and yellowish tones. The rise in ΔC* values confirm the increase in chroma.

The ΔE* values exceeded the generally accepted perceptibility threshold of approximately 10 reported in the literature. The difference between the 180 °C and 200 °C treatments was 21.09; producing a clearly distinct visual appearance. These changes are attributed to the partial decomposition of hemicelluloses and structural alterations of lignin. Higher temperatures promote more intensive chromophore formation, resulting in stronger browning (Figure 3).

For the boxelder, the average L* value of the untreated samples was 77.35. Heat treatment at 180 °C reduced this value to 63.42 (ΔL* = 13.93), while at 200 °C it decreased further to 59.34 (ΔL* = 18.01). The reduction in lightness is clearly correlated with the increase in temperature (Figure 4.).

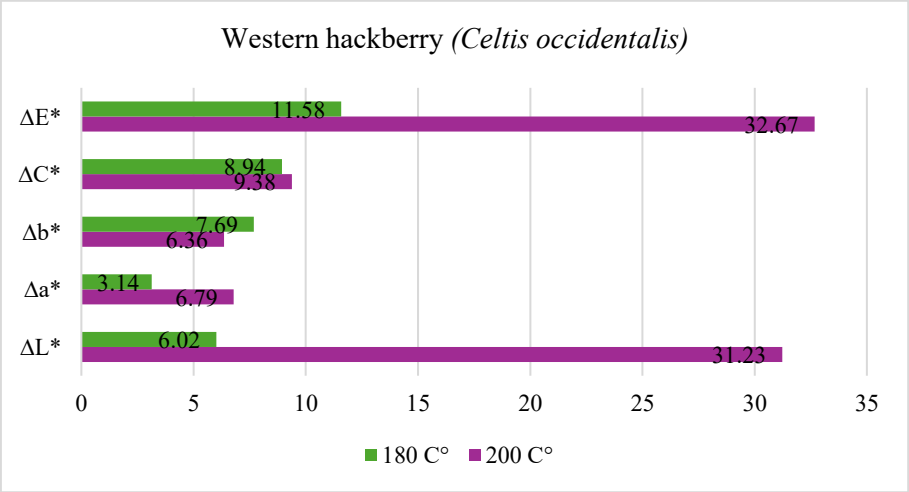

Figure 3: Changes in the color composition of western hackberry broken down by Δ values

For the boxelder, the average L* value of the untreated samples was 77.35. Heat treatment at 180 °C reduced this value to 63.42 (ΔL* = 13.93), while at 200 °C it decreased further to 59.34 (ΔL* = 18.01). The reduction in lightness is clearly correlated with the increase in temperature (Figure 4)

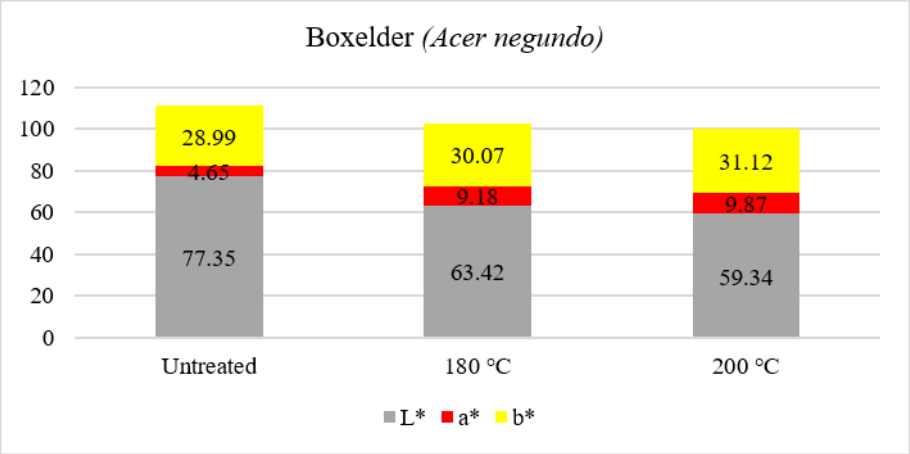

Figure 4: Color composition of boxelder after different heat treatments

The a* and b* coordinates increased at both temperatures, producing a more intense reddish-yellow tone. The ΔC* values were 6.38 at 180 °C and 9.30 at 200 °C, indicating higher chroma at the elevated temperature. The total color difference (ΔE*) was 15.49 and 22.62, respectively, reflecting a clearly visible and pronounced color change. Based on the magnitude of ΔE*, it can be concluded that the heat-treatment temperature of up 200 °C is certainly directly proportional to the intensity of the color change (Figure 5).

Heat treatment caused significant color changes in both wood species, although the extent of the modification differed. At 180 °C, boxelder showed a greater response, with an 18,0% decrease in L* value, while western hackberry exhibited a slight lightening of about 7.9%. At 200 °C, western hackberry underwent the most pronounced change, with its lightness decreasing by approximately 47.9%, indicating intensive darkening. In comparison, boxelder showed a more moderate but continuous reduction in lightness, reaching a total decrease of 23.3%. The increases in a*, b*, and ΔC* values in both species indicate stronger reddish-yellow tones and higher chroma after treatment. Overall, higher treatment temperature intensified chromophore formation and browning, especially in western hackberry.

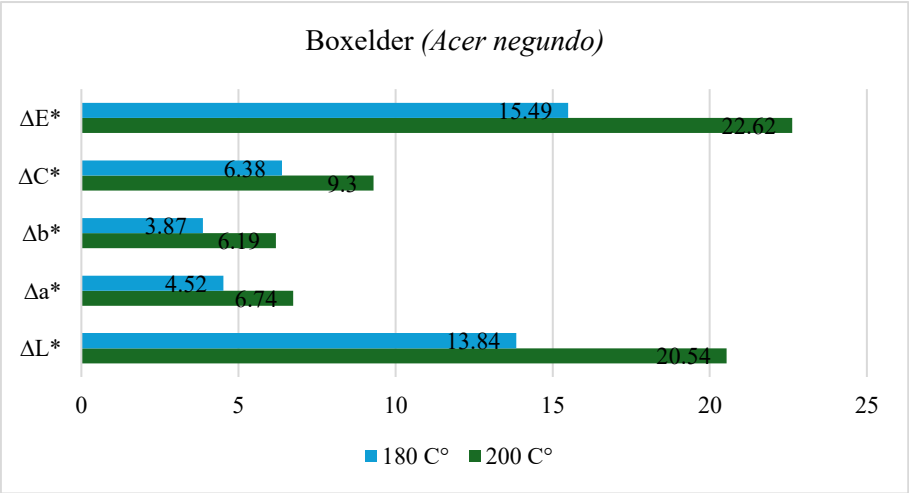

Figure 5: Changes in the color composition of boxelder broken down by Δ values

CONCLUSIONS

Based on the investigations, the following conclusions can be drawn:

1. Heat treatment significantly alters the L*, a*, and b* color coordinates in both wood species.
2. Increasing the temperature generally enhances both darkening and chroma.
3. The ΔE* values exceed the perceptibility threshold in all cases, making the color change visually pronounced.
4. The intensity of the color change is proportional to the treatment temperature.

Thus, the heat treatment not only affects the appearance of the wood, but also causes significant changes in its internal structure and properties. As a result of the treatment at high temperature, the moisture content of the wood decreases, the cell structure changes to a certain extent, and some chemical components are degraded or modified. As a result, the wood becomes more dimensionally stable, its tendency to absorb moisture is reduced, and it can be more resistant to fungi and other biological damage. In addition, the heat treatment also makes the color of the wood darker and more uniform, which can also be favorable from an aesthetic point of view. These physical, chemical and visual changes allow the properties of heat-treated wood to be consciously used in various woodworking applications.

ACKNOWLEDGMENT

The publication was supported by the project no. TKP2021-NKTA-43, which has been implemented with the support provided by the Ministry of Innovation and Technology of Hungary (successor: Ministry of Culture and Innovation of Hungary) from the National Research, Development and Innovation Fund, financed under the TKP2021-NKTA funding scheme.

REFERENCES

Hill C. (2006) Thermal Modification of Wood. In: Callum A. S. Hill: Wood Modification: Chemical, thermal and other processes, John Wiley & Sons, Ltd, pp 99-127

Bartha D, Csiszár Á (2008) Common hackberry (Celtis occidentalis L.). In: The most important invasive plants in Hungary. Institute of Ecology and Botany Hungarian Academy of Sciences, Vácrátót, pp 95–102

Molnár S, Zoltán G (2024) Juhar (juhar fajok) – Acer spp. In: Molnár S, Farkas P, Börcsök Z, Zoltán G (eds) Földünk ipari fái, 2nd edn. Faipari Tudományos Egyesület, Sopron, pp 83–86

Udvardy L (2008) Boxelder (Acer negundo L.). In: The most important invasive plants in Hungary. Institute of Ecology and Botany Hungarian Academy of Sciences, Vácrátót, pp 115–120

Zoltán G, Börcsök Z (2024) Nyugati ostorfa – Celtis occidentalis. In: Molnár S, Farkas P, Börcsök Z, Zoltán G (eds) Földünk ipari fái, 2nd edn. Faipari Tudományos Egyesület, Sopron, pp 177–179

Seiji H, Saori H, Masamitsu O (2020) Konica Minolta and color conversion formula. In: Color measurements according to three sections of wood, Hirata et al. J Wood Sci, pp 1-13

Dynamic Density Tests of New Black Locust (*Robinia pseudoacacia* L.) Clones

Tamás Ábri[1], Mátyás Báder[2*]

[1] University of Sopron, Forest Research Institute, Department of Plantation Forestry. Farkassziget 3, Püspökladány, Hungary, 4150
[2] University of Sopron, Faculty of Wood Engineering and Creative Industries. Bajcsy-Zs. Str. 4, Sopron, Hungary, 9400.

E-mail: abri.tamas@uni-sopron.hu; bader.matyas@uni-sopron.hu

Keywords: clone testing; cultivar; dynamic test; moisture content; Pilodyn; Xylodyn; wood density.

ABSTRACT

Black locust (*Robinia pseudoacacia* L.) is one of the most important tree species in Hungary due to its rapid growth, high nectar production, and durable wood. This study evaluated the physical wood properties of four newly bred black locust clones (NK1, NK2, PL040, and PL251) and the control Üllői cultivar in a five-year-old experimental plantation established near Napkor, Hungary. Green wood density, oven-dry density, and moisture content were determined, while penetration depth was measured using a Xylodyn handheld instrument as a rapid indicator of wood density related properties.

The results revealed significant differences among the investigated clones. The Üllői cultivar exhibited the highest mean oven-dry density (698.4 kg m^{-3}), although it also showed the highest variability (coefficient of variation: 14.8%). According to the statistical test, the oven-dry densities of the Üllői cultivar and NK1 clone did not differ significantly, whereas NK2 and PL251 exhibited the lowest statistically equivalent values. Significant differences were also found in moisture content, which strongly influenced green wood density. The relationship between density and penetration depth varied among clones. While the Üllői cultivar, PL040, and PL251 clones exhibited the expected decrease in penetration depth with increasing density, the NK1 clone showed an unexpected positive relationship, suggesting potential differences in wood anatomy and related physical properties. The findings provide a preliminary assessment of the industrial utilization potential of the tested black locust clones and demonstrate the importance of clone selection for achieving uniform wood quality and reliable raw material performance in future tree plantations.

INTRODUCTION

Black locust (*Robinia pseudoacacia* L.), native to North America, is currently one of the most widespread non-native tree species in Europe (Nicolescu et al. 2020), while in Hungary it represents the most extensively distributed forest tree species (Ministry of Agricultureof the Ministry of Agriculture 2026). Owing to the presence of tyloses, tannins, and robinetin-related compounds, its wood is highly durable and resistant to a wide range of biological degradation agents, making it an excellent raw material for outdoor wood products such as fences, posts, playground structures (Keresztesi 1988; Savill 2019). Its expected service life is 25–40 years in outdoor ground-contact conditions, 80–100 years outdoors above ground, and more than 500 years in dry indoor conditions or under water. Its oven-dry density ranges from 540 to 870 kg m^{-3}, while its fresh density varies between 800 and 950 kg m^{-3}. The moisture content of freshly harvested black locust wood is relatively low, typically only 35–45% (net moisture content). Among the tree species cultivated in Central Europe, black locust exhibits outstanding strength and stiffness properties (Molnár 2008).

One of the main directions of black locust improvement in Hungary is the selection of individuals with superior stem shape and their vegetative propagation using cost-effective techniques. Additional breeding objectives include rapid juvenile growth, increased wood and nectar production, and enhanced resistance to abiotic stress factors, particularly drought and heat stress. As a result of previous breeding and research efforts, numerous officially registered cultivars and clones are currently available (Keresztesi 1988; Rédei et al. 2008; Ábri et al. 2023).

The most recent black locust breeding and research project is being conducted through a consortium-based collaboration. In addition to the Forest Research Institute of the University of Sopron, the cooperation involves the Forestry and Energy Propagation Material Product Council as well as several private forest managers (e.g. Napkori Erdőgazdák private company). The primary objective of the project was the development and deployment of new high-performance black locust cultivars. These cultivars may achieve an industrial roundwood yield of at least 50–55%, thereby increasing the quantity, quality, and value of wood produced per unit area. Successful operational deployment, however, requires an innovative and integrated technical and technological framework; therefore, one of the main objectives of the project is the development and optimization of this framework for practical application. The new cultivars and associated technologies are primarily intended for the establishment of high-quality black locust industrial tree plantations in Hungary. To facilitate their evaluation under operational conditions, experimental field trials have been established at several locations across the country, simultaneously serving as clone comparison experiments (Ábri et al. 2023). One of these trial sites was established near Napkor in 2020, where the performance of the Farkasszigeti (PL040), Laposi (NK1), Napkori (NK2), and Püspökladányi (PL251) clones is being assessed and compared with that of the control Üllői cultivar (Ábri et al. 2022, 2026).

A substantial body of Hungarian and international literature is available on the favourable properties of black locust wood (Molnár 2008; Nicolescu et al. 2020; Younis et al. 2023; Németh et al. 2026). In contrast, comparatively limited information is available concerning the wood properties of cultivars and clones; one notable example is the study of Halupáné (1982). Even that work addressed only a limited number of wood-quality characteristics. This knowledge gap is particularly evident for recently bred clones. In the present study, green and oven-dry density and the winter dormant moisture content of living trees of the aforementioned black locust clones are presented. The analysis investigates whether differences exist among the clones with respect to these parameters and whether density values are related to tree slenderness (*h/d* ratio, where *h* denotes tree height and *d* denotes diameter at breast height). These results may provide a preliminary indication of the suitability of the clones for industrial processing and help identify which clones are the most suitable for such applications.

MATERIALS AND METHODS

In 2025, tree height (*h*) and diameter at breast height (*d*) were measured for 30 individuals of each five-year-old black locust clone (NK1, NK2, PL040, PL251 and Üllői) at the Napkor experimental plantation (Table 1). For wood property investigations, a 120 cm long log section was harvested from the lower stem of each selected tree and was transported to the Central Laboratory of the Faculty of Wood Engineering and Creative Industries, Sopron campus of the University of Sopron.

Table 1: Basic data and main averages of the clones used for the tests (27.01.2025, Napkor, Hungary)

Clone code	Diameter at breast height [cm]	Height [m]
Üllői	9.42	8.2
NK1	10.68	10.0
NK2	11.21	11.1
PL040	10.26	10.3
PL251	11.23	10.3

The *h* and *d* data were used to calculate the slenderness ratio (*h/d*). Tree *h/d* provides important information on stem shape and mechanical stability, both of which are highly relevant during stand development and silvicultural management. From the perspective of industrial utilization, the *h/d* also provides an indication of the dimensions of the logs that can be expected at harvest. Shorter but thicker logs require different processing approaches in the veneer and sawmilling industries than long, slender stems, which are often more suitable for pole production (Pretzsch and Rais 2016, Kang et al. 2021).

At the laboratory, penetration depth measurements were performed on the delivered logs using a German-developed Xylodyn handheld instrument (Figure 1). The spring force of the device was constant, while the pin had a diameter of 2.5 mm and a blunt tip. Penetration depth was recorded on a millimetre scale. During the measurements, the pin showed no signs of wear or deformation. Ten

penetrations were performed on each side of every log, uniformly distributed along its length and positioned opposite one another. The moisture content of the specimens corresponded to the winter dormant period. Taking advantage of these conditions, the measurements were carried out shortly after harvesting and transportation. Penetration was initiated from the bark surface, thereby accounting for the full bark thickness.

Figure 1: Xilodyn device, used to determine penetration depth

Cylindrical specimens with a diameter of 15 mm were extracted using a plug cutter, with the penetration points of the Xylodyn serving as the centres of the specimens (Figure 2). Green wood density was determined from mass and volume measurements. Following oven drying to an absolutely dry condition, oven-dry density and the moisture content of the wood at the time of the penetration measurements were also determined. The relationship between clone specific *h/d* ratios and wood density was analysed using linear regression.

Figure 2: PL251 sample consisting of 20 specimens made by plug cutter

RESULS AND DISCUSSION

The highest oven-dry density was recorded for the Üllői cultivar, reaching 698.4 kg m^{-3}. This value is in close agreement with the data reported by Molnár et al. (1989), who measured an oven-dry density of 706 kg m^{-3}. According to the Games–Howell post hoc test, the oven-dry densities of the Üllői cultivar and NK1 clone did not differ significantly. Similarly, the NK2 and PL251 clones exhibited statistically equivalent oven-dry densities and, at the same time, represented the lowest values among the tested clones.

Climate change is expected to substantially alter precipitation patterns in the future (Mátyás et al. 2018; Móricz et al. 2025). Extreme weather events are increasingly associated with intense rainfall and strong winds, posing a growing risk to forest ecosystems, particularly young plantations. Such an event was observed in year 2025 in the experimental stand included in this study, where NK2 clones suffered considerable stem breakage (Figure 3). Consequently, planting of tree species or clones with greater mechanical stability may be advantageous. Wood density may serve as one potential indicator of such stability. The relationship between average green wood density and average penetration depth was examined for the tested clones (Figure 4).

Figure 3: Storm damage in part of the investigated Napkor plantation planted with black locust clone 'NK2'

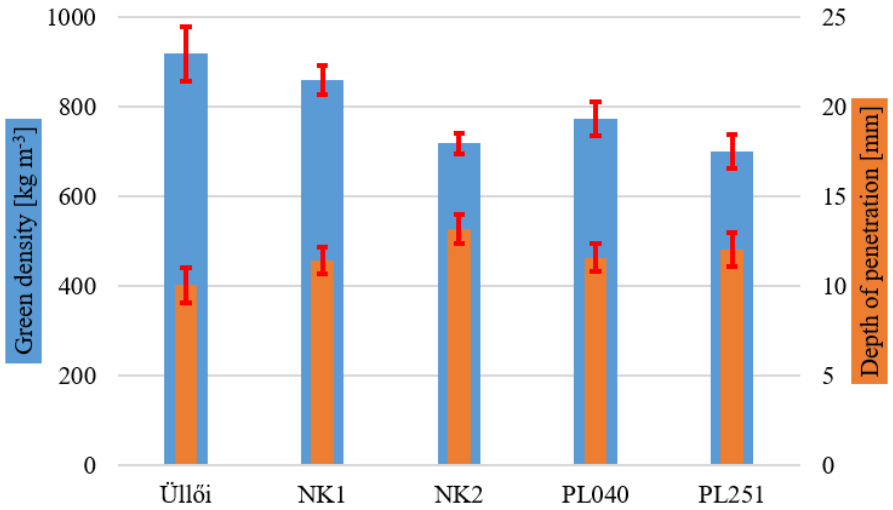

Figure 4: Average green density and average depth of penetration of the black locust clones. Standard deviation is shown by red bars

The results indicate that no consistent relationship can be established between mean green wood density and mean penetration depth values. In several cases, higher density values were associated with greater penetration depths, as observed for the NK1 clone. This corresponds to a relatively low density to penetration depth ratio. The ratios and their standard deviations are presented in Figure 5. For the Üllői cultivar, a comparatively low penetration depth was associated with exceptionally high green wood density, whereas the lowest ratios were observed for the PL251 and NK2 clones. For these three clones, penetration depth exhibited a relatively consistent relationship with wood density.
The Üllői cultivar showed substantially greater variability than the other clones, with a coefficient of variation of 14.8%, resulting in higher measurement uncertainty. It should be noted, however, that a coefficient of variation below 20% is generally not considered high in wood science due to the inherent within-species variability of wood properties. Since the remaining clones exhibited considerably lower coefficient of variation, their wood properties may be regarded as more uniform and therefore potentially more reliable from an industrial perspective.
The relationship between penetration depth and density observed in the PL040 and NK1 clones differed markedly from that of the other three clones. This may be attributed to substantial differences in wood properties among the clones. Their green wood densities differed considerably (Figure 4), suggesting corresponding differences in anatomical structure, wood hardness, and splitting behaviour, all of which may influence the penetration of a foreign object into the wood. Verification of these assumptions will require further investigations using wood obtained from older trees.
Wood density is strongly influenced by moisture content. The mean moisture content of the samples was 49.6%, with a coefficient of variation of 14.2%. As the dataset did not meet the assumption of homogeneity, the Games–Howell test was again applied. The NK1 clone exhibited the highest moisture content (54.9%), differing significantly from all other clones except Üllői cultivar. In contrast, the PL251 clone showed the lowest value (42.9%), which differed significantly from all other clones. The statistical analysis demonstrated that substantial differences exist among the clones with respect to moisture content, which affects green wood density as well as numerous other wood properties.

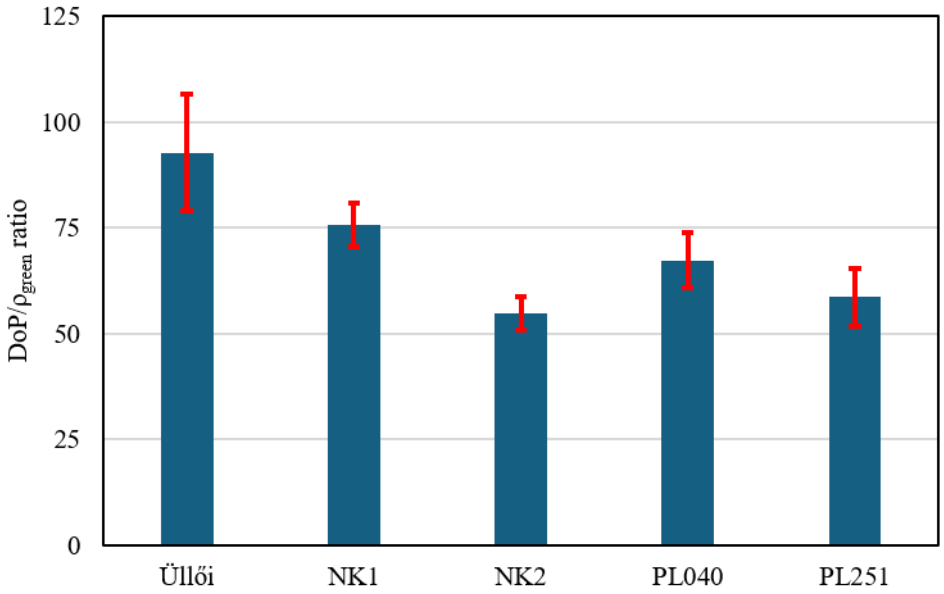

Figure 5: Ratio of the depth of penetration (DoP) and the green density (ρ_{green}) of the black locust clones. Standard deviation is shown by red bars

Based on the currently available data, it appears more appropriate to analyse the relationship between green wood density and penetration depth at the individual measurement level, matching each penetration depth value with its corresponding density (Figure 6).

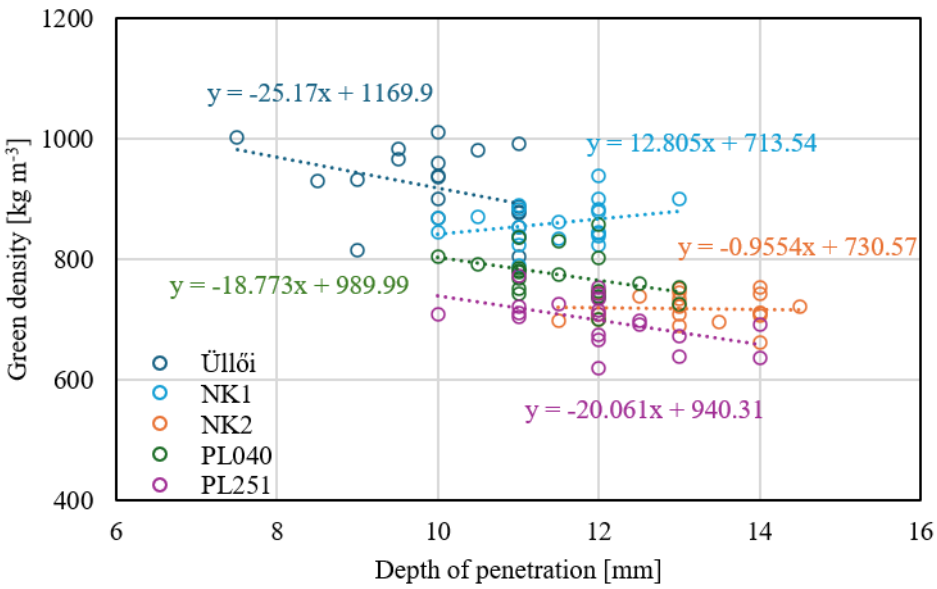

Figure 6: Relationships between green density (n=20) and the depth of penetration (n=20) of each tested black locust clones. The dashed lines and the equations associated with the colours of the lines are linear trend lines

As shown in Figure 6, the NK1 clone exhibited a pronounced positive trend, which contradicts the general assumption that nails penetrate more easily into lower-density wood. No clear trend could be identified for the NK2 clone as density increased. In contrast, the remaining three clones displayed trend lines with remarkably similar negative slopes: penetration depth decreased as density increased. For the Üllői cultivar, PL040, and PL251 clones, wood density appears to be strongly correlated with hardness and other wood characteristics influencing resistance to penetration. No relationship was detected between penetration depth and moisture content above the fibre saturation point.
Although the present results clearly demonstrate differences among the studied clones, these relationships may vary depending on site conditions. It would therefore be advisable to test promising clones across a range of site types and subsequently conduct the same physical and mechanical wood property assessments. Such investigations would allow the identification of clone-specific site requirements and provide valuable information on their wood quality performance and industrial utilization potential under different growing conditions.

CONCLUCIONS

The study revealed significant differences among the investigated black locust (*Robinia pseudoacacia* L.) clones in terms of density, moisture content, and penetration depth of a pin, highlighting the importance of clone selection for industrial wood production. The Üllői cultivar exhibited the highest mean oven-dry density (698.4 kg m^{-3}), although it also showed the greatest variability, with a coefficient of variation of 14.8%. Statistical analysis demonstrated that the oven-dry densities of the Üllői cultivar and the NK1 clone did not differ significantly, while NK2 and PL251 formed the lowest-density group. The average moisture content of the samples was 49.6%, ranging from 42.9% in PL251 to 54.9% in NK1, significantly affecting green wood density. Relationships between density and penetration depth varied considerably among clones. Üllői, PL040, and PL251 showed the expected decrease in penetration depth with increasing density, whereas NK1 exhibited an unusual positive trend, suggesting anatomical differences affecting hardness-related properties. Overall, the results indicate that the examined clones differ not only in density but also in structural behaviour, which may strongly affect their industrial utilization potential and mechanical stability.

REFERENCES

Ábri T, Keserű Z, Borovics A, Rédei K, Csajbók J (2022) Comparison of juvenile, drought tolerant black locust (Robinia pseudoacacia L.) clones with regard to plant physiology and growth characteristics in Eastern Hungary: Early evaluation. Forests 13(2):292. https://doi.org/10.3390/f13020292

Ábri T, Cseke K, Keserű Z, Porcsin A, Szabó FM, Rédei K (2023) Breeding and improvement of black locust (Robinia pseudoacacia L.) with a special focus on Hungary: a review. iForest – Biogeosciences and Forestry 16(5):290–298. https://doi.org/10.3832/ifor4254-016

Ábri T, Csajbók J, Keserű Z, Szabó G, Szabó L (2026) Growth and multispectral analysis of new black locust (Robinia pseudoacacia L.) clones. Forests 17(2):208. https://doi.org/10.3390/f17020208

Halupa L Ms. (1982) A nemesített akácfajták műszaki tulajdonságai. Agrártudományi Közlemények 41(3-4):552–555.

Kang J, Ko C, Lee SJ, Yim JS, Moon GH, Lee SH (2021) Relationship of H/D and crown ratio and tree growth for *Chamaecyparis obtusa* and *Cryptomeria japonica* in Korea. Forest Science and Technology 17(3):101–109. https://doi.org/10.1080/21580103.2021.1904009

Keresztesi B (1988) The Black Locust. Akadémiai Kiadó, Budapest, Magyarország

Mátyás Cs, Berki I, Bidló A, Csóka G, Czimber K, Führer E, Gálos B, Gribovszki Z, Illés G, Hirka A, Somogyi Z. (2018) Sustainability of Forest Cover under Climate Change on the Temperate-Continental Xeric Limits. Forests 9(8):489. https://doi.org/10.3390/f9080489

Ministry of Agriculture, Forest Planning Department, Hungary (2026) https://foldalap.am.gov.hu/Magyarorszag_erdeivel_kapcsolatos_adatok_news_513 Accessed 16 Apr 2026

Molnár S, Babos K, Pápai Lné, Horváth L (1989) Az akác nemesítés néhány faanyagminőségi összefüggése. Faipar 1989(2): 51-57

Molnár S (2008) Az ültetvényszerűen termeszthető fafajok fájának minősége és hasznosítása. In: Führer E, Rédei K, Tóth B (eds) Ültetvényszerű fatermesztés 2., 2nd ed. Agroinform Kiadó és Nyomda Kft., Budapest, Magyarország, pp. 153–190

Móricz N, Mészáros I, Kern Z, Illés GZ, Garamszegi B, Eötvös CB, Berki I Németh TM (2025) Evaluating the drought tolerance of five native broadleaf tree species using dendroecological analysis in East Central Europe. Frontiers in Forests and Global Change 8:1625371. https://doi.org/10.3389/ffgc.2025.1625371

Németh R, Tolvaj L, Govina JK, Seidu H, Younis FAAA, Báder M (2026) Effects of growing sites on the color variations in black locust (Robinia pseudoacacia L.) wood. Forests 17(4):471. https://doi.org/10.3390/f17040471

Nicolescu VN, Rédei K, Mason WL, Vor T, Pöetzelsberger E, Bastien JC, Brus R, Benčať T, Đodan M, Cvjetkovic B, Andrašev S, La Porta N, Lavnyy V, Mandžukovski D, Petkova K, Roženbergar D, Wąsik R, Mohren GMJ, Monteverdi MC, Musch B, Klisz M, Perić S, Keça L, Bartlett D, Hernea C, Pástor M (2020) Ecology, growth and management of black locust (Robinia pseudoacacia L.), a non–native species integrated into European forests. J For Res, 31(4):1081–1101. https://doi.org/10.1007/s11676-020-01116-8

Pretzsch H, Rais A (2016) Wood quality in complex forests versus even-aged monocultures: review and perspectives. Wood Science and Technology 50:845–880. https://doi.org/10.1007/s00226-016-0827-z

Rédei KM, Osváth-Bujtás Z, Veperdi I (2008) Black locust (Robinia pseudoacacia L.) improvement in Hungary: a review. Acta Silvatica et Lignaria Hungarica 4:127–132. https://doi.org/10.37045/aslh-2008-0011

Savill PS (2019) The Silviculture of Trees Used in British Forestry. CABI, Boston, MA, USA

Younis FAA, Govina JK, Seidu H, Németh R (2023) Basic characteristics of black locust (Robinia pseudoacacia L.) wood grown under different site conditions: a review. Acta Silvatica et Lignaria Hungarica 19:21–35. https://doi.org/10.37045/aslh-2023-0002

Eliminating Reading Errors and Automating the Brinell-Mörath Hardness Test

Anett Sütő[1], Róbert Németh[1], Mátyás Báder[1*]

[1] University of Sopron, Faculty of Wood Engineering and Creative Industries. Bajcsy-Zs. Str. 4, Sopron, Hungary, 9400.

E-mail: suto.anett@phd.uni-sopron.hu; nemeth.robert@uni-sopron.hu; bader.matyas@uni-sopron.hu

Keywords: linear regression, ICC, Bland-Altman analysis.

ABSTRACT

This study investigates the comparability of manual and automated Brinell-Mörath hardness measurements for wood and evaluates the potential of replacing traditional optical readings with a sensor-based automated system. Tests were conducted on black locust (*Robinia pseudoacacia*), Turkey oak (*Quercus cerris*), and hornbeam (*Carpinus betulus*) using a 10 mm steel ball under a load of approximately 485 N. Manual hardness values were determined from residual indentation diameters according to EN 1534:2020, while automated values were calculated from maximum indentation depth recorded during loading. The linear regression model showed a strong relationship between the datasets ($R^2 = 0.7575$; Pearson correlation = 0.8125), although the slope of 0.7239 indicated proportional error between the methods. The root mean square error was 16.45 hardness units, corresponding to an average relative error of 11.33%. Statistical analysis confirmed a significant systematic bias between the procedures ($p = 2.82 \times 10^{-30}$). Despite these discrepancies, the intraclass correlation coefficient value of 0.926 demonstrated excellent consistency between the methods. The results indicate that the differences originate primarily from elastic recovery of wood rather than measurement inaccuracy. Consequently, automated hardness testing can reliably replace manual evaluation if elastic deformation effects are incorporated into the calculation model.

INTRODUCTION

The precise determination of the physical and mechanical properties of wood is essential in the timber industry. Among these properties, hardness is one of the most critical, as it shows a strong correlation with density, wear resistance, and machinability (Molnár 2004; Sitkei 1994). One of the standardized procedures in the timber industry is the Brinell-Mörath hardness test, which is a version of the traditional Brinell method used in metallurgy, optimized for wood. During the test, a steel ball with a diameter of 10 mm must be pressed into the wood with a force of 490.33 N. The diameter of the resulting indentation is then read, based on which the hardness value is calculated (MSZ 6786:1982; EN 1534:2020).

Reading the two diameters of the indentation image carries significant uncertainty. Even with surface colouring and the use of a scaled magnifier, the read value remains subjective, and time-consuming manual reading carries potential for error. For greater accuracy and the automation of the measurement, it would be advantageous to calculate the hardness value directly from the data provided by the measuring instrument. However, a fundamental physical difference exists: the manual method measures only the residual (plastic) deformation, while the automated system records the total (elastic and plastic) indentation under load. Due to the anisotropic and viscoelastic nature of wood, this theoretical difference can lead to systematic measurement discrepancies.

The original aim of the research was to verify the reliability of traditional microscopic evaluation (the accuracy of human reading) using data from a modern, sensor-based device. The initial hypothesis (null hypothesis) was that geometric calculations based on the data from the automated equipment would validate the manual readings. However, during the investigations, other relationships and properties must also be considered when comparing the two methods. The aim of the present research is to compare the results of automated and manual measurements on black locust (*Robinia pseudoacacia*), Turkey oak (*Quercus cerris*), and hornbeam (*Carpinus betulus*) species. The objective is to statistically examine whether the automated procedure can replace manual measurement and, if so, what degree of correlation can be achieved.

MATERIALS AND METHODS

The tests were conducted on the transverse (end grain) surfaces of five black locust, three Turkey oak, and four hornbeam samples with a minimum thickness of 40 mm (Table 1). The samples were conditioned at a temperature of 20 °C and 65% relative humidity until mass stability was reached. The investigated surfaces were smooth, sanded, and positioned perpendicular to the axis of the compression head of the Instron 5985 universal testing machine (Instron Corporation, Norwood, Massachusetts, USA).

Table 1: Data of the samples used

Wood species	Provenance	EOV coordinates (east, north)
Black locust	Ófehértó 33/A	877527, 291922
Black locust	Pap 3/C	881955, 321529
Black locust	Baktalórántháza 52/C	875568, 296031
Black locust	Ófehértó 31/B	878676, 290636
Black locust	Kunfehértó 41 G	674622, 114344
Turkey oak	Northern part of the Pilis Mountains	465940, 200738
Turkey oak	Mélykút 28 J	680503, 100633
Turkey oak	Nagycenk 10/F	471701, 251059
Hornbeam	Sopron 106/A	461269, 259553
Hornbeam	Hegyhátszentmárton 5/A	452400, 177726
Hornbeam	Sopron 106/A	461269, 259553
Hornbeam	Tormás 92/D	566556, 92854

In the vicinity of each designated measurement site, three tests were performed, and at least three measurement points were designated on each specimen. Every tested point and its surroundings were free of wood defects. Due to the typically dense annual ring structure of the examined species, each measurement covered multiple growth rings. From the moment of reaching the specimen surface, the ball was pressed into the material for 15 seconds until it reached the specified 490 N load under uniform load increase. The exact value deviated slightly, averaging 485 N (range: 484.8–486 N). This was followed by a constant load for 30 seconds, during which the ball pressed deeper into the wood. Unloading also lasted for 15 seconds.

Manual method: Measurements were performed according to the standard Brinell-Mörath procedure (MSZ 6786:1982; EN 1534:2020), also considering the original specifications of the method's creators (Mörath 1932). Following unloading, after a waiting period of at least 3 minutes, the diameter of the residual indentation (d) on the surface was read using a scaled magnifier with an accuracy of 0.1 mm. Manual hardness ($H_{Bmanual}$) was calculated based on the formula from EN 1534:2020 standard (Equation 1).

$$H_{Bmanual} = \frac{2 \cdot F}{g \cdot \pi \cdot D \cdot (D - \sqrt{D^2 - d^2})} \quad (1)$$

where

g is the acceleration of gravity, in metres per second squared;

π is the "pi" factor (3.14);

F is the maximum load applied force, in newtons;

D is the diameter of the steel ball: 10 mm.

Automated method: During the measurements, the indentation diameter was calculated based on the maximum indentation depth (h) measured by the instrument (thus not accounting for the elastic recovery of the wood). Automatically determined hardness ($H_{Bautomatic}$) was then calculated using the calculated diameter according to the standard formula (Equation 2).

$$H_{Bautomatic} = \frac{2 \cdot F}{D \cdot \pi \cdot h} \quad (2)$$

The datasets generated by the two procedures were evaluated in Excel. The investigation consisted of the following steps:

- A scatterplot was created for visual exploration of the measurement data, supplemented by linear regression.
- Bland-Altman analysis was applied to identify the error structure (constant and proportional errors) between the methods (Bland and Altman 1986).
- The substitutability of the measurement methods was determined by calculating the root mean square error (RMSE), the relative error percentage, and the intraclass correlation coefficient (ICC) (based on a two-way, non-repeated ANOVA model).
- The statistical significance of the systematic bias was checked using a two-sample paired t-test (at a significance level of $p < 0.05$).

RESULTS

During the comparison of manual and automated Brinell-Mörath hardness measurement procedures, the data were evaluated using linear regression, intraclass correlation coefficient (ICC), and Bland-Altman analysis.

Visual Diagnostics and Linear Regression

The relationship between the two measurement methods is illustrated by the scatterplot (Figure 1). The fit of the data was examined relative to the line of identity. The equation for the linear trendline fitted to the point cloud is $y = 0{,}7239 \cdot x + 29859$, and the coefficient of determination is $R^2 = 0.7575$.

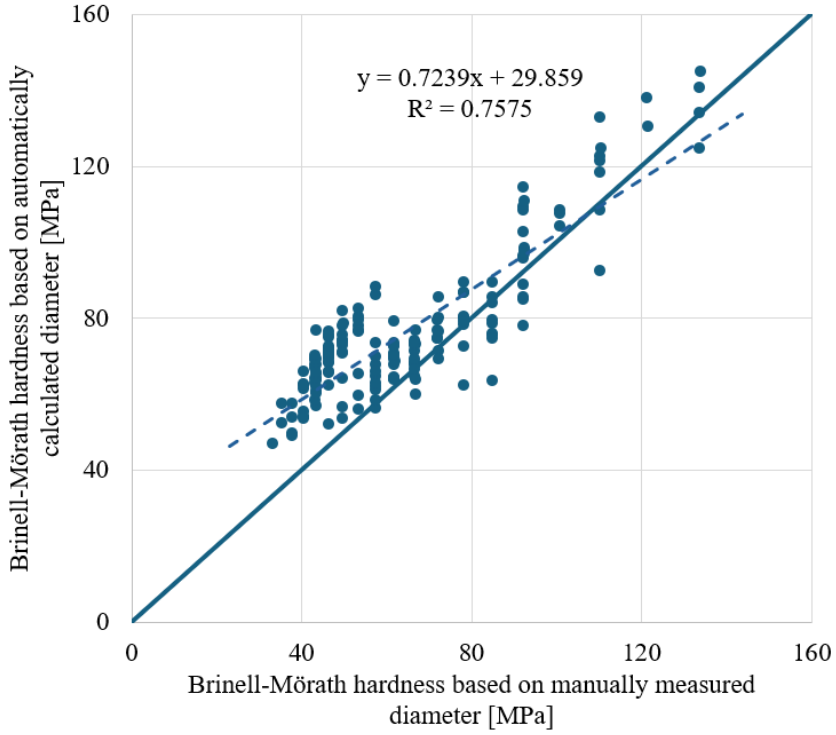

Figure 1: Scatterplot comparing the results of the two measurement methods

The scatterplot reveals two distinct phenomena:

- Difference in resolution: On the horizontal axis (manual measurement), the data points are organized into vertical columns. This proves the resolution limits of the manual optical evaluation and the reading scale, whereas the automated method records continuous values.
- Proportional error: The slope of the trendline (0.7239) significantly deviates from the line of identity and intersects it at a hardness value of 107.5 MPa. This means that in lower hardness ranges, the automated method systematically measures higher values compared to the manual method, while for extremely hard samples, it measures lower values.

Measurement Errors and Limits of Agreement

The Pearson correlation coefficient shows a strong linear relationship (0.8125); however, to assess the interchangeability of the methods, the distribution of differences was also examined. The root mean square error (RMSE) between the two methods was 16.45 units, representing an 11.33% relative error across the entire measurement range. The Bland-Altman plot (Figure 2) visually confirms the proportional error observed in the scatterplot: the point cloud describes a negative slope trend along the increasing average values.

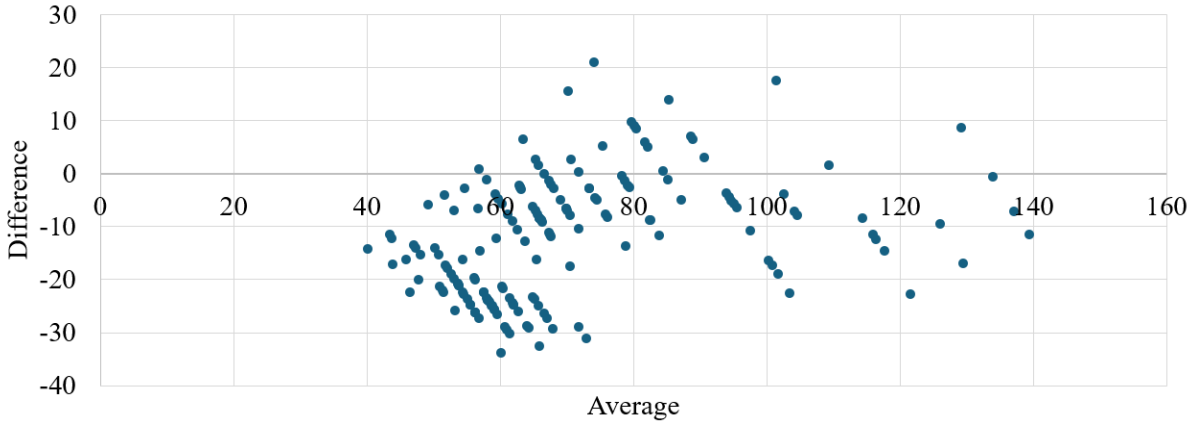

Figure 2: Bland-Altmann diagram to examine differences in averages

Systematic Bias and Consistency

The difference between the two measurement procedures was analysed using a paired t-test. The result $p=2.82\times10^{-30}$) statistically proves that the discrepancy between the methods is not a measurement error but an explicit systematic bias. Although the raw data differ for this reason, the ICC measuring the internal consistency of the two methods is exceptionally high, at 0.926 (Koo and Li 2016). This value highlights that the two datasets move together: despite the systematic bias and proportional error, both procedures detect hardness differences between samples in almost perfectly the same order and proportion.

DISCUSSION AND CONCLUSIONS

Although the original focus of the study was to reveal human measurement error (subjective reading), the results clarified that the significant difference between manual and automated datasets (11.3% average error) in this investigation does not stem from the error of the person reading the data. The manual measurement recorded the physical state prescribed by the standard (residual deformation), while the automated measurement data did not account for this.

The causes of measurement differences can be explained by the following technological and physical factors:

- Effect of elastic recovery: The automated system records indentation data at the peak of the load (including both plastic and elastic deformation), while the manual method measures the residual (plastic) mark after unloading (Oliver and Pharr 1992). The y-intercept of +29.85 units on the scatterplot (Figure 1) proves that the automated measurement starts with a constant over-measurement due to the elastic component.
- Proportional error and material-dependent behaviour: The proportional error observed in the Bland-Altman plot and the 0.72 slope of the regression line suggests that as wood density and hardness increase, the ratio of elastic to plastic deformation changes. For softer materials, the total indentation (automated measurement) is significantly larger than the residual mark (manual measurement), while for harder, more brittle structures, this difference decreases.
- Data resolution and digitalization: The staggered nature of the manual method on the scatterplot highlights the resolution limits of human reading and the optical scale. In contrast, the much more continuous, sensor-based data recording of the automated method allows for finer differentiation between specimens.

- Interchangeability and calibration: The extremely high ICC value (0.926) proves that the automated method is reliable. Since the error stems from physical laws rather than random noise, the two procedures can be made compatible. The degree of elastic deformation must be taken into account, which is influenced by factors such as wood density, structural composition, chemical system, or moisture content.

Based on the comparative analysis of manual and automated Brinell-Mörath hardness measurement procedures, the following main conclusions can be drawn:

- Statistically, the two methods do not provide identical raw data. The automated equipment shows a clear proportional error and systematic bias (averaging 11.3% relative error) compared to the manual reference.
- The difference does not stem from the inaccuracy of the measuring equipment but from the elastic recovery of the wood. Since the automated system records maximum penetration under load and the manual system records the residual state after unloading, the two methods describe different mechanical behaviours of the wood.
- Despite the discrepancies, the internal consistency between the procedures (ICC = 0.926) is outstandingly high. The automated system records wood properties stably, precisely, and free from the optical limitations of human reading.
- The automated method can be successfully validated and is suitable for replacing the manual procedure, provided that elastic deformation is considered alongside plastic deformation.

The direction of future research may involve mathematically accounting for the degree of elastic deformation. Furthermore, extending the current series of tests and the mathematical model to wood species with higher moduli of elasticity (e.g., ash) is necessary, where the degree of proportional error is expected to result in even more marked differences between under-load and residual deformations. The analysis of side hardness, which can be measured with higher error, will also be necessary.

ACKNOWLEDGEMENTS

The publication was made in frame of the project TKP2021-NKTA-43, which has been implemented with the support provided by the Ministry of Culture and Innovation of Hungary from the National Research, Development and Innovation Fund, financed under the TKP2021-NKTA funding scheme.

REFERENCES

EN 1534 (2020) Wood flooring and parquet - Determination of resistance to indentation - Test method. European Committee for Standardization, 10 p.

Koo TK, Li MY (2016) A guideline of selecting and reporting intraclass correlation coefficients for reliability research. Journal of Chiropractic Medicine 15:155–163. https://doi.org/10.1016/j.jcm.2016.02.012

Bland MJ, Altman DG (1986) Statistical methods for assessing agreement between two methods of clinical measurement. The Lancet 327:307–310. https://doi.org/10.1016/S0140-6736(86)90837-8

Molnár S (2004) Knowledge of wood (Faanyagismeret). Mezőgazdasági Szaktudás Kiadó, Budapest

Mörath E (1932) Studien über die hygroskopischen Eigenschaften und die Härte der Hölzer. Verlag M. & H. Schaper, Hannover

MSZ 6786-11 (1982) Test methods for wood materials. Determination of hardness. Hungarian Standards Institute, 7 p.

Oliver WC, Pharr GM (1992) An improved technique for determining hardness and elastic modulus using load and displacement sensing indentation experiments. J Mater Res 7:1564–1583. https://doi.org/10.1557/JMR.1992.1564

Sitkei Gy (1994) Theory of woodworking operations (A faipari műveletek elmélete). Mezőgazdasági Szaktudás Kiadó, Budapest, Hungary

The Use of Adhesives Designed for Conifers on Oak

Dénes Horváth[1*], Sándor Fehér[1]

[1] University of Sopron, Faculty of Wood Engineering and Creative Industries. Bajcsy-Zs. Str. 4, Sopron, Hungary, 9400.

E-mail: hdenes68@gmail.com; feher.sandor@uni-sopron.hu

Keywords: delamination; polyurethane; poly-vinyl acetate; PUR; PVAc; *Quercus*.

ABSTRACT

This study investigated the applicability of adhesive systems developed for coniferous species in the manufacture of oak (*Quercus* spp.) glued-laminated timber (GLT). Laboratory-scale GLT beams were produced from low-grade oak lamellae containing natural wood defects and bonded using either one-component polyurethane (PUR) or polyvinyl acetate (PVAc) adhesives. Delamination resistance was evaluated according to EN 14080 using vacuum-pressure treatment and drying cycles. For PUR-bonded beams, total delamination reached 49.6%, while maximum delamination values of individual bond lines ranged from 44.1% to 53.8%, greatly exceeding the EN 14080 limit values of 4% total and 30% maximum delamination. PVAc-bonded specimens performed even more poorly, with severe bond-line separation and complete failure of several specimens during testing. Mechanical bending tests further demonstrated that insufficient bonding quality caused premature opening of finger joints and separation of lamellae under load. The results confirm that adhesive systems optimized for softwoods are unsuitable for oak under the applied manufacturing conditions. The findings emphasize the need for specialized adhesive formulations and bonding technologies specifically adapted to high-density hardwood species for reliable structural GLT production.

INTRODUCTION

The growing interest in environmentally sustainable construction materials has intensified research efforts directed toward engineered wood-based products, including glued-laminated timber (GLT, commonly referred to as glulam). Owing to its layered structure composed of adhesively bonded wooden lamellae, GLT enables more efficient utilization of timber resources while simultaneously improving structural reliability and mechanical performance. The present study focuses on the adhesive performance of GLT beams manufactured from lower quality oak lamellae, namely the delamination. The integration of finger-jointed connections parallel to the grain direction provides an effective means of reducing both the influence of natural wood defects and the high variability characteristic of hardwood timber, thereby improving mechanical behaviour under bending and other loading conditions. In the current investigation, wood was processed together with its naturally occurring imperfections. Consequently, during the preparation of lamellae suitable for GLT production, defects present in the lower-grade oak were intentionally retained. It should also be emphasized that GLT represents only one category within the broad range of sustainable engineered wood products currently available or under development. Other widely used examples include laminated veneer lumber (LVL), laminated strand lumber (LSL), oriented strand lumber (OSL), solid structural timber (SST), and cross-laminated timber (CLT) (Gong 2019; Van Acker 2021). The structural performance of GLT is primarily characterized by bending strength (*MoR*) and modulus of elasticity (*MoE*). These properties are affected by numerous parameters, including wood species, lamella quality, adhesive system, and the occurrence of finger joints. Several earlier studies have examined the mechanical behaviour of glued-laminated timber products (Fink et al. 2015; Kytka et al. 2022; Morin-Bernard et al. 2020). According to Gaff et al. (2017), modifications in lamella arrangement can significantly improve stiffness and bending resistance, particularly in engineered timber manufactured from lower-grade feedstock. The inclusion of finger joints introduces local discontinuities within the structure that may act as stress concentration zones, potentially decreasing both stiffness and strength (Morin-Bernard et al. 2021). Nevertheless, appropriately designed and accurately manufactured finger joints are capable of preserving a considerable proportion of the intrinsic bending capacity of solid wood.

Bonding and the Properties GLT

The adhesive system represents a critical factor influencing the performance of GLT, especially in the case of high-density hardwood species such as oak. Adhesive bonding of hardwoods presents specific challenges arising from high density, extractive content, and dimensional behaviour (Gáborík et al. 2016; Gržan et al. 2025). Consequently, proper adhesive selection and adequate surface preparation are essential for obtaining durable and mechanically reliable bonds. Adhesive formulation and bonding quality substantially influence the mechanical behaviour and long-term durability of glued-laminated products (Gáborík et al. 2016). Adhesives with improved penetration and curing characteristics may partially compensate for the inherent variability of wood, thereby improving resistance under cyclic loading conditions. Additional studies investigating adhesive-related parameters in laminated wood products further confirmed that optimization of the adhesive system is fundamental for maximizing GLT performance (Gáborík et al. 2016; Gaff et al. 2017). These results support the combined use of advanced adhesives and modern jointing technologies for the manufacture of high-performance engineered timber products. The specimens investigated in the present study were produced using industrial technologies currently available in commercial practice.

MATERIALS AND METHODS

Raw materials

One of the raw materials used in the study consisted of planed oak (*Quercus* spp.; mixed sortiment of pedunculate and sessile oak) lamellae with nominal dimensions of 20 × 50 × 500 mm (cross-section × length in grain direction), supplied by Zala-Fűrész Fafeldolgozó és Kereskedelmi Ltd. (Lenti, Hungary). The second material was planed thin oak timber measuring 4 or 5 × 100 × 1000 mm, hereinafter referred to as veneer. The total batch planed lamellae prepared for bonding contained several naturally occurring wood defects, including sapwood, slope of grain, occasional sawn surfaces resulting from reduced thickness, as well as both sound and decayed knots of varying size and distribution. According to the visual grading criteria specified in EN 975-1 (2009), the majority of the lamellae corresponded to the QF3 and QF4 appearance classes, indicating relatively low quality for the production of glued-laminated structural timber. In contrast, the veneer layers were free from visible defects.

2-5 layers laboratory-sized GLTs bonded with PVAc adhesive

After kiln drying, the timber was stored under workshop conditions until an average equilibrium moisture content of 10.95% was reached. Uniform climatic conditions were maintained during the entire manufacturing process. After planing, the lamellae were connected longitudinally by finger jointing and edge-glued in width, resulting in elements measuring 20 × 90 × 1000 mm. Bonding was performed using the one-component polyvinyl acetate adhesive Szolvegy Technobond D3 (Szolvegy Ltd., Szolnok, Hungary). The adhesive exhibited the following properties: density 1.08 g/cm^3; Brookfield viscosity 10.0 ± 2.0 Pa·s; pH 3.0 ± 0.4; gel time at 20 °C of 10 min; adhesive spread amount 120–180 g/m^2; pressing time 2 h; and bond strength 10.0 MPa (Szolvegy 2025). Subsequently, the elements were assembled into GLT beams by face gluing using the same adhesive system and pressing parameters.

5-9 layers laboratory-sized GLTs bonded with PUR adhesive

Following the same preparation and bonding procedures, additional elements with dimensions of either 15 × 100 × 2100 mm or 20 × 100 × 2100 mm were produced depending on the original lamella thickness. In this case, however, a one-component polyurethane adhesive (Henkel LOCTITE HB S209 PURBOND) was applied. The selected adhesive properties were as follows: kinematic viscosity at 20 °C of 17,241–27,586 mm^2/s; dynamic viscosity at 20 °C of 20,000–32,000 mPa·s; density at 20 °C of 1.15–1.17 g/cm^3; maximum allowable wood moisture content 8%; applicable wood temperature range 18–35 °C; maximum adhesive layer thickness 0.1 mm; spread rate 120–160 g/m^2; and open assembly time at 20 °C and 65% relative humidity of 10 min (DIBt 2025; Henkel 2025). All manufacturing operations were carried out at the production facility of Sokon Ltd. (Agárd, Hungary), a producer of structural softwood GLT beams employing industrially certified manufacturing technology. The same production methods used for certified load-bearing timber elements were applied in this study. Consequently, additional technological parameters, including exact adhesive quantities and pressing conditions, cannot be disclosed. The bonding procedures used for oak were consistent with those employed for coniferous species and complied with the adhesive manufacturers' recommendations.

Specimen preparation and measurement method

From the central region of the finished beams, specimens with a dimension along the grain of 75 mm were cut in accordance with EN 14080 (2013) for delamination testing. The procedure began with conditioning at 20 °C and 65% relative humidity, followed by individual weighing and visual inspection. All specimens were inspected prior to conducting the delamination test, and any existing delaminations were marked on the end-grains. These marked glue lines were not taken into account in the evaluation and were excluded from the results measured after the test. The specimens were subsequently placed into a large container separated by plastic spacers and mechanically restrained to prevent floating after water immersion. The prepared container was then transferred into a vacuum-pressure vessel, where Method B described in Annex C of the standard EN 14080 (2013) was applied. Specimens were subjected to vacuum treatment at 0.2 bar for 30 min, followed by a pressurization phase at 6 bars for 2 hours.

After the vacuum-pressure treatment, the specimens were dried at 70 °C for 15 h. During drying, mass was periodically monitored until the original mass was reached within the tolerance limits prescribed by the standard. Delamination was substantial in all specimen groups; therefore, additional testing cycles were not required. Total delamination ($Delam_{tot}$) and maximum delamination ($Delam_{max}$) were calculated in accordance with clauses C.5.2 and C.5.3 of the standard, respectively based on the total delamination length ($l_{tot,delam}$; mm), the entire length of all glue lines on the two end-grain surfaces of each test piece ($l_{tot,glue\ line}$; mm), the maximum delamination length ($l_{max,\ delam}$; mm), and the length of one glue line ($l_{glue\ \text{line}}$; mm).

$$Delam_{tot} = 100 \cdot \frac{l_{tot,delam}}{l_{tot,glue\ line}}\ [\%] \quad (1)$$

$$Delam_{max} = 100 \cdot \frac{l_{max,delam}}{2 \cdot l_{glue\ line}}\ [\%] \quad (2)$$

The results were evaluated based on the sub-section 5.5.5.2.2 of the EN 14080 (2013) standard. The total delamination of the GLT has to be less than or equal 4% if the test version ‘B’ has been used and one cycle has been performed. For the maximum delamination, the delamination percentage of a single glue line shall be less than or equal to 30%.

RESULTS, DISCUSSION AND CONCLUSIONS

The delamination behaviour of the GLT systems manufactured with the two different adhesive types is discussed separately due to the fundamentally different chemical and mechanical characteristics of the adhesives involved (Figure 1).

Figure 1: Images of some of the specimens made with PUR (a) and PVAc (b) adhesives

Sample bonded with PUR adhesive

One beam configuration, 65 specimens were tested assembled using polyurethan adhesive, each 99 mm wide and 41 mm thick (layer composition: 20 + 20 mm). For beams bonded with Henkel LOCTITE HB S209 PURBOND, the total delamination was 49.6%, while the maximum delamination was 53.8%; 45.6%; 49.2% and 44.1% in the four bond lines (Figure 2). Overall, the bonding performance achieved with the structural PUR adhesive and oak timber proved insufficient. The adhesive datasheet specifies suitability primarily for softwood species, including *Picea abies*, *Abies alba*, *Pinus sylvestris*, *Larix decidua*, and *Pseudotsuga menziesii*, which explains the limited effectiveness observed with oak (Henkel 2025). This suggests that adhesive performance depends on the specific adhesive formulation, the hardwood species involved, or the interaction of both factors. It is also recognized that adhesives developed for softwoods may exhibit inadequate performance even for certain coniferous species, such as larch in the case of the Henkel LOCTITE HB S209 PURBOND one-component polyurethane adhesive used here. The range of suitable adhesive systems is even more restricted for hardwood species, which are employed less frequently in structural timber production. Only recently have adhesive systems become available that are specifically optimized for broader species compatibility, whereas most commercially available products remain designed primarily for conventional softwoods (Kolbe et al. 2026; Konnerth et al. 2016). This explains why the present study employed a high-performance adhesive originally developed for softwood applications and why was its performance low. Of course, numerous additional factors influence bonding quality, including the moisture content of wood, adhesive anchorage within the wood structure, wood permeability, porosity, surface preparation, pressing pressure during curing. Many of these parameters are specified in the adhesive datasheets and were strictly followed during manufacturing, as the same procedures successfully used for coniferous structural products were applied. Since the manufacturing company routinely produces certified, high-quality structural timber from softwoods, extensive experience with this adhesive system was available.

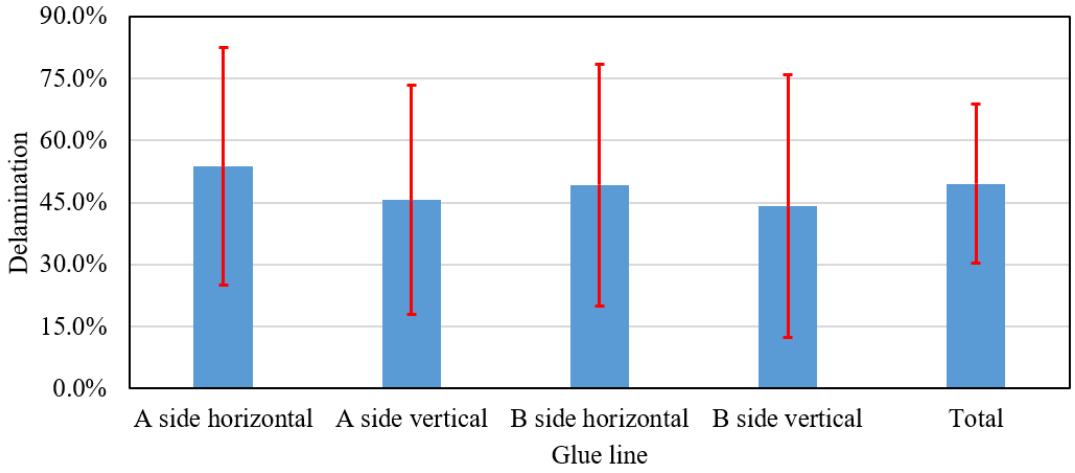

Figure 2: Maximum and total delamination of the beams bonded with PUR adhesive

Sample bonded with PVAc adhesive

Four types of beams with different configurations were tested assembled using polyvinyl acetate (PVAc) adhesive, each 90 mm wide:

- 40 mm thick (layer composition: 20 + 20 mm);
- 45 mm thick (layer composition: 20 + 5 + 20 mm);
- 40 mm thick (layer composition: 16 + 4 + 16 + 4 mm);
- 47 mm thick (layer composition: 5 + 16 + 5 + 16 + 5 mm).

For beams bonded with Szolvegy Technobond D3 PVAc, the delamination was noticeably more severe compared to the specimens made with PUR adhesive (Figure 1b), despite they were made with a D3 water-resistant adhesive. Given that the results of the PUR specimens fell far below the requirements, no delamination measurements were performed on the specimens bonded with PVAc adhesive after the delamination test. It is clear that the specimens bonded with PVAc adhesive did not meet the requirements; many specimens fell apart along the bond line. This clearly demonstrated that the adhesive is not compatible with oak, or that entirely different application and processing conditions should have been ensured. This could involve the surface quality of the oak as well as the viscosity of the adhesive, the amount of adhesive applied, the pressing pressure, and many other parameters. It should be noted that PVAc adhesives are not applied in structural applications because of their pronounced creep susceptibility. In the present investigation, however, the use of PVAc adhesive was considered worthwhile owing to the unexpectedly weak performance of the PUR adhesive system. This made it possible to evaluate, through bending tests, the structural applicability of low-grade raw materials in accordance with the original objectives of the study.

Other remarks

The bending experiments revealed that deficiencies in bonding quality considerably reduced the mechanical performance of the tested beams, regardless of the adhesive type applied. It was found that the bending tests performed after conditioning at 20 °C temperature and 65% relative humidity caused the opening of the finger joints that caused such a pronounced weakening that the entire structure failed suddenly. First, the finger joints shifted in the tension side of the beam, and then the lamellae separated from one another. Analysing the failures, it is typical that mostly the bond line between the flat surfaces split along the length of the beam, eliminating the tensile support of lamella layer on the tension side, consequently causing a fracture. The adhesive layers had separated from the wood, which clearly indicates a bonding problem. Consequently, it was also justified to perform delamination testing on the specimens bonded with PVAc adhesive. Delamination tests have also confirmed that, in general, adhesives developed for coniferous wood — as well as the application and pressing methods, or even the wood preparation processes — are not suitable for bonding oak timber.

At the finger joints, the strengths of adhesives applied in the presented tests cannot fully replace the natural tensile strength and shear strength of solid wood in the grain direction. Developing a specialized adhesive and its application for this purpose would be worthwhile, as it could significantly increase the strength values of oak beams. Although the bending test results showed appropriate values compared to conifers, significantly higher results are expected in bending tests due to the superior bond strength. This would suggest that much slimmer beams could be used as an oak product offering an excellent price-performance ratio.

REFERENCES

Deutschen Instituts für Bautechnik (DIBt) (2025) Allgemeine bauaufsichtliche Zulassung/ Allgemeine Bauartgenehmigung Nr. Z-9.1-802: Herstellung von Keilzinkenverbindungen mit berührungslosen Klebstoffauftragssystemen unter Verwendung von 1K-PUR-Klebstoffe LOCTITE HB S049 bis HB S209 PURBOND bzw. LOCTITE HB S049 bis HB S209 ECO PURBOND

EN 975-1:2009 Sawn timber. Appearance grading of hardwoods. Part 1: Oak and beech. European Committee for Standardization, 35 p.

EN 14080:2013 Timber structures - Glued laminated timber and glued solid timber - Requirements. European Committee for Standardization, 103 p.

Fink G, Frangi A, Kohler J (2015) Bending tests on GLT beams having well-known local material properties. Mater Struct 48:3571–3584. https://doi.org/10.1617/s11527-014-0424-2

Gáborík J, Gaff M, Ruman D, et al (2016) Adhesive as a Factor Affecting the Properties of Laminated Wood. BioResources 11:10565–10574. https://doi.org/10.15376/biores.11.4.10565-10574

Gaff M, Ruman D, Svoboda T, et al (2017) Impact bending strength as a function of selected factors: 2 – Layered materials from densified lamellas. BioRes 12:7311–7324. https://doi.org/10.15376/biores.12.4.7311-7324

Gong M (2019) Lumber-Based Mass Timber Products in Construction. In: Concu G (ed) Timber Buildings and Sustainability. IntechOpen

Gržan T, Novosel A, Špada V, et al (2025) Achieving maximum strength in oak wood (*Quercus robur*, L.) bonding: techniques for surface preparation and adhesive application. Eur J Wood Prod 83:44. https://doi.org/10.1007/s00107-024-02179-8

Henkel Magyarország Kft. (2025) Biztonsági adatlap az 1907/2006 / EK módosított rendelet szerint. LOCTITE HB S209 PURBOND 1100KG

Kolbe J, Koesling S, Steinberg T, et al (2026) Modified glutine adhesives for structural bonding of glued-in rods in timber engineering. International Journal of Adhesion and Adhesives 144:104164. https://doi.org/10.1016/j.ijadhadh.2025.104164

Konnerth J, Kluge M, Schweizer G, et al (2016) Survey of selected adhesive bonding properties of nine European softwood and hardwood species. Eur J Wood Prod 74:809–819. https://doi.org/10.1007/s00107-016-1087-1

Kytka T, Gašparík M, Sahula L, et al (2022) Bending characteristics of glued laminated timber depending on the alternating effects of freezing and heating. Construction and Building Materials 350:128916. https://doi.org/10.1016/j.conbuildmat.2022.128916

Morin-Bernard A, Blanchet P, Dagenais C, Achim A (2020) Use of northern hardwoods in glued-laminated timber: a study of bondline shear strength and resistance to moisture. Eur J Wood Prod 78:891–903. https://doi.org/10.1007/s00107-020-01572-3

Morin-Bernard A, Blanchet P, Dagenais C, Achim A (2021) Glued-laminated timber from northern hardwoods: Effect of finger-joint profile on lamellae tensile strength. Construction and Building Materials 271:121591. https://doi.org/10.1016/j.conbuildmat.2020.121591

Szolvegy Kft (2025) Technobond 3000 (D3) vízálló faipari ragasztó. Műszaki Leírás

Van Acker J (2021) Opportunities and challenges for hardwood based engineered wood products. In: Németh R, Rademacher P, Hansmann C, et al. (eds) 9th Hardwood Conference Proceedings. University of Sopron Press, Sopron, Hungary, pp 5–14

Method of Juvenile and Mature Wood Demarcation with Annual Growth Analysis

Péter Farkas[1*], Szabolcs Komán[1]

[1] University of Sopron, Faculty of Wood Engineering and Creative Industries, Bajcsy-Zs. Str. 4, Sopron, Hungary, 9400.

E-mail: farkaspeter@phd.uni-sopron.hu; koman.szabolcs@uni-sopron.hu

Keywords: juvenile wood demarcation, mature wood, *Celtis occidentalis*, annual growth dynamics, Basal Area Increment (BAI), dendrochronology, Cumulative Basal Area (CBA), non-linear growth modeling, Monte Carlo simulation.

ABSTRACT

The objective demarcation of the physiological boundaries of juvenile, mature, and senescent wood is crucial for dendroecology and the timber industry. This study presents a novel methodology based on cumulative growth analysis and biostatistical modeling. The procedure is demonstrated through a case study using samples from seven common hackberry *(Celtis occidentalis)* individuals. Tree-ring measurements were performed using CooRecorder 9.8.4, and the datasets were generated in standard **.rwl* (Tucson) format with the help of CDendro 9.8.4 software.

Within the presented method, we developed a complex approach in the R statistical environment using the dplR (Dendrochronology Program Library in R) package. Instead of the classical radial ring width, we examine the development of the Cumulative Basal Area, thereby eliminating age-related geometric distortions. An automated algorithm fits three non-linear growth models (Logistic, Gompertz, Richards) to the individual and stand (Regional Curve, RC) datasets, selecting the optimal one based on the Akaike Information Criterion (AIC). Due to the specific characteristics of the Gompertz and Richards models, biological stage boundaries are determined at the 15% and 85% values of the asymptote, while for the logistic model, they are defined at specific distances from the inflection point.

The uniqueness of the method lies in its in-depth analysis of tree growth dynamics by calculating the first three derivatives of the curves (growth velocity, acceleration, and jerk). Furthermore, to validate the empirical thresholds, the algorithm applies a Monte Carlo parameter simulation. This statistical procedure iteratively determines the 95% confidence intervals of the stage boundaries, exactly quantifying the uncertainty window of these limits in the form of density functions. The complex procedure, which can be executed by both biological age and calendar year and features edge-effect filtering, provides an objective and reproducible framework for the demarcation of tree-ring-based growth stage boundaries.

INTRODUCTION

During secondary thickening, the central wood layer around the pith is called juvenile or core wood, spanning 5–20 growth rings depending on species and stand. This layer differs from mature wood in its anatomical, chemical, physical, and mechanical properties. Juvenile wood formation is closely linked to crown development; in closed forest stands, the crown rises faster, causing the lower trunk to produce mature wood earlier (Larson 1969; Zobel and Buijtenen 1989). Juvenile wood is typically characterized by shorter fibers and tracheids, thinner cell walls, wider lumens, lower density, and a significantly larger microfibril angle (MFA) (Darmawan et al. 2013; Boruszewski et al. 2017). Because these properties impair wood strength and industrial processability, accurately determining the transition boundary to mature wood is crucial for both silviculture and the timber industry (Rahayu et al. 2021). However, this transition is a gradual, multi-year process rather than a sharp line, necessitating statistical and mathematical models for objective demarcation (Alteyrac et al. 2006; Delucis et al. 2014).

Indicators used for demarcation

Demarcating the juvenile-mature wood boundary relies on analyzing the radial variation (from pith to bark) of measurable wood properties, and considering the distance from the crown is also recommended. *Anatomical characteristics:* The literature uniformly considers anatomical features, particularly fiber length (or tracheid length) and microfibril angle, to be the most reliable parameters (Bhat et al. 2001; Darmawan et al. 2013; Kartikawati et al. 2024). As cambial age advances, fiber length increases steeply during the juvenile phase, while MFA decreases sharply, after which both stabilize at an approximately constant level upon reaching the mature zone. Several studies also utilize the radial progression of cell wall thickness and vessel diameter as reliable indicators (Rahayu et al. 2021; Lee et al. 2025).
Physical and mechanical characteristics: The physical density, modulus of elasticity (MOE), and modulus of rupture (MOR) also shows increasing trend from the direction of pith to bark (especially in fast-growing trees), but the fluctuation of that parameters are too high, and not sufficiently reliable to delimit the juvenile and mature wood, than microscopic anatomical features (Darmawan et al. 2013; Vega et al. 2020; Purba et al. 2021).

Mathematical and statistical methods for determining the transition

Because wood maturation is gradual, statistical models could define the exact juvenile-mature threshold:

1. *Segmented (piecewise) regression:* An objective, widely used method that models radial development using two functions: a steep curve (often a quadratic equation) describing the juvenile phase, and a fixed, flat plateau marking the mature phase. By iteratively minimizing the residual sum of squares, the method calculates the intersection point (join point) of the two segments, which yields the cambial age at the onset of mature wood (Bhat et al. 2001; Alteyrac et al. 2006; Gapare et al. 2006; Darmawan et al. 2013; Rahayu et al. 2021).
2. *Asymptotic growth models (Logistic, Gompertz, Richards):* Biological maturation can be effectively modeled using classical sigmoid growth curves, which are frequently applied to describe the attainment of wood stability through the curve's asymptote (Pödör 2014; Ukalska and Jastrzębowski 2019). In some methods, the boundary of juvenile wood is established where the predicted annual percentage change of the examined anatomical parameter falls below a predetermined, extremely low threshold, such as 1% (Vega et al. 2020; Zanuncio et al. 2022; Lee et al. 2025), or, in the case of mature wood, when the parameter reaches 95% of the theoretical mature asymptote (Purba et al. 2021).
3. *Increment thresholds and visual interpretation:* Some studies examine the annual increment of parameters (e.g., fiber length) by calculating the first derivative of polynomial or logarithmic functions. The boundary can be drawn where the first derivative falls below a critical level (Delucis et al. 2014; Kartikawati et al. 2024). Manual visual assessment of graphs is illustrative but highly subjective and prone to error (Bhat et al. 2001; Delucis et al. 2014; Boruszewski et al. 2017). Similarly, deterministic industry "rules of thumb" (e.g., a fixed threshold of 10 growth rings) severely lack accuracy (Zobel and Buijtenen 1989).

Factors influencing demarcation and difficulties

Calculating the transition age is statistically challenging because results vary depending on the measured parameter (Alteyrac et al. 2006; Darmawan et al. 2013). For example, fiber length often yields a shorter juvenile period than the microfibril angle (Gapare et al. 2006). Spatial distribution also matters: the transition occurs sooner higher up the stem (Burdon et al. 2004). Furthermore, the juvenile period is not solely dictated by age; mechanical, spacing, and environmental factors cause significant plasticity and adaptive responses (Alteyrac et al. 2006; Alméras et al. 2025). Consequently, modern wood science relies on the simultaneous mathematical modeling of multiple parameters for accurate spatial demarcation.

MATERIALS AND METHODS

In April 2024, seven common hackberry *(Celtis occidentalis)* trunks were collected by the University of Sopron from the south of Hungary, in the forestry district of Kelebia (location: Tompa 43/A). The site characteristics are as follows: forest-steppe climate, skeletal soil, and free-draining hydrology (NÉBIH 2026). The common hackberry is native to North America and it was introduced to Hungary as an ornamental tree. While past research has shown that it propagates easily in sandy lowland areas, it is now considered an invasive species (Bartha and Csiszár 2008). In the sampling area, the species forms nearly pure forest stands. A cross-sectional disk was cut from each log, but the sampling height is unknown. Photographs of the seven disks were taken alongside a measurement ruler for the preparation of annual ring analyses. Each sample was identified with a sequential number and a picture ID.

Measurement and data analyses

The aim of the data analysis was to develop a method relying exclusively on tree-ring data to demarcate the juvenile and senescence phases within individual trees, and to extend this assessment to the entire forest stand. Given that crown development is closely related to the developmental phases of wood (Larson 1969; Zobel and Buijtenen 1989), we are searching for the signal on the wood development curve that can indicate these stages. A sigmoid curve fitted to the CBA data can reveal this dynamic of growth, because we are not merely examining the basal area increment (BAI) data of individual tree rings or single years in isolation, but rather the cumulative growth resulting from accumulated biological and environmental effects since the onset of growth. Two input data files were required for the analysis:

1. Tree-ring measurements were performed using CooRecorder 9.8.4, and the datasets were generated in standard **.rwl* (Tucson) format with the help of CDendro 9.8.4 software (Maxwell and Larsson 2021). The last complete annual ring dated to the end of 2023.
2. Additionally, based on the raw measurement data, an additional **.csv* file was created. This file contained two columns: the sample ID and the estimated distance from the pith to the first identified annual ring (expressed in years).

For the analyses, a custom algorithm was developed in the R statistical computing environment (RStudio version 2024.09.0+375). The script utilizes the **dplR** (Dendrochronology Program Library in R) package (Bunn 2023) for processing **.rwl* file formats and the **MASS** package for Monte Carlo simulations, with development assisted by the Gemini 3.1 Pro model (Google 2026).

Using raw annual ring-width data, we calculated the Basal Area Increment (BAI) and Cumulative Basal Area (CBA), as well as their corresponding Regional Curves (RC), aligned by calendar age *(Figure 1)*. Depending on the research objective, these metrics can also be aligned by biological age. Drawing on established literature, the algorithm evaluates the fit of three asymptotic growth models (Logistic, Gompertz, and Richards) to the CBA data at both the individual sample and the RC levels. By applying the Akaike Information Criterion (AIC), the method objectively selects the best-fitting model among the three (Pödör 2014; Ukalska and Jastrzębowski 2019). In addition to the AIC, goodness-of-fit is assessed using the Residual Standard Error (RSE), relative error (RSE expressed as a percentage of the maximum CBA), and an indicative pseudo-R^2 value (due to the non-linear nature of the regression).

A primary objective of this method is to demarcate the ontogenetic stages of the trees: the juvenile, mature, and senescent phases. Depending on the mathematical characteristics of the winning model, these boundaries are estimated using distinct mathematical approaches. For the Logistic model, as the curve is symmetrical, the scale parameter (*scal*) is used to designate the boundaries around the inflection point (*xmid*): $\pm 1.5 \cdot scal$. The most intensive biomass production occurs within this range, representing the mature phase. For the Gompertz and Richards models, due to their inherent asymmetry, percentage thresholds of the maximum theoretical level (the Asymptote) are applied. The 15% threshold marks the end of the juvenile, exponential phase. Upon reaching the 85% threshold, the tree approaches its biological limits, growth decelerates significantly, and decline (senescence) begins.

To robustly quantify the uncertainty of these initial boundary estimations, the developed method incorporates a Monte Carlo (MC) simulation (Bonate 2001). When the earlier algorithm fits a sigmoid (non-linear) model to the CBA data points, it does more than just find the optimal parameters; it also measures the uncertainty of the model. This is stored in the variance-covariance matrix, which captures:

- The statistical variance of each fitted parameter.
- How the parameters correlate with one another (for example, if the S-curve is forced to be steeper, how much the inflection point must be shifted to maintain a good fit to the data).

Based on this matrix, the MC algorithm draws random parameter samples over 1000 iterations. The method applies the inverse functions of the sigmoidal models to these simulated parameters. Ultimately, it calculates the median and standard deviation (SD) of the resulting ages, and extracts the lower 2.5% and upper 97.5% percentiles to define the 95% confidence intervals. When the R script generates the comprehensive 5-panel diagnostic plot *(Figure 2)*, the thousands of simulated boundary values are visualized on the cumulative curve as filled green and red probability density curves (provided the senescence age is within a valid range). These visual objects are statistically valid density functions that illustrate a critical concept: given the inherent variance of the biological dataset, they show the precise probability of the actual transition wood zone falling on any specific year. To better understand the growth dynamics of individual trees and the forest stand, *Figure 2* presents the first, second, and third derivatives (growth velocity, acceleration, and jerk) of the fitted sigmoid curves as well. During the procedure, the user can review the results in a summary table and has the opportunity to run the script using manually chosen sigmoid models for specific samples in cases of high uncertainty.

RESULTS AND DISCUSSION

Given the extremely low sample size, these results primarily serve as an exploratory case study.
All seven common hackberry samples were collected simultaneously (last complete ring: 2023). Chronological alignment of the measurement data revealed that two samples originated from older, presumably lower stem sections, while five samples were 10 years younger, likely from higher stem positions. *Figure 1* supports this: the synchronized basal area increment (BAI) dynamics and individual juvenile boundaries overlaid on the cumulative basal area (CBA) curves vary slightly, falling between 2004 and 2008 (mean: 2006). Furthermore, the five younger samples influenced the initial rise of the average stand-level radial increment (RC) curve between 1998 and 2002. Consequently, the calculated stand-level juvenile boundary is 2003 (age 18). The upward trajectories of the curves indicate active growth at sample collection; thus, senescence cannot be accurately estimated. Therefore, the senescence phase is only flagged if its calculated onset falls within five years of the final measured year.

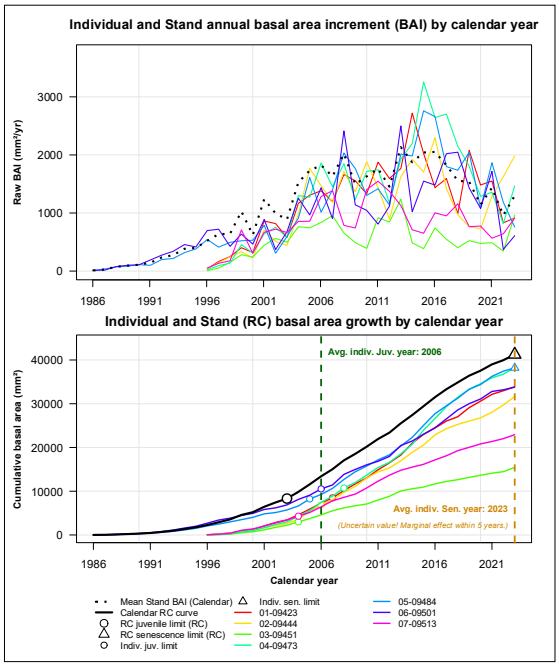

Figure 1: Two-panel comparative analysis of individual common hackberry (Celtis occidentalis) samples and computed Regional Curve (RC)-based forest stand data by calendar year

The R script generates a five-panel plot for each sample and the stand average. *Figure 2* exemplifies this using stand-level RC data. All panels share an x-axis displaying both biological age and calendar year.
Panel 1: Combines aggregated tree-ring data and BAI, displaying the basal area development dynamics based on raw data.

Panel 2: Displays CBA data, the fitted sigmoid model, fit quality metrics, and life-stage demarcations. MC simulations illustrate boundary uncertainties via green (juvenile) and red (senescence) bell curves. In this case, the juvenile phase metrics are: median 17.6 years, SD 0.98, range 14.4–17.9, what is means 3.5-year uncertainty span. The MC simulation estimates senescence between 40.2 and 45.8 years, falling beyond the plotted timeframe (values retrieved from the calculated summary table).
Panel 3: First derivative (y'), representing growth velocity. It is mathematically equivalent to a smoothed BAI curve. The y' maximum marks the growth velocity inflection point, indicating the year of peak of biomass production.
Panel 4: Second derivative (y''), representing acceleration/deceleration. It indicates shifts in growth vitality. Maximum acceleration (y'' max) highlights the juvenile phase's most intense surge, where the tree invests peak energy into increasing its growth rate. Maximum deceleration (y'' min) marks the late mature phase, where growth velocity drops most drastically (accelerating senescence).
Panel 5: Third derivative (y'''), representing "jerk" (the rate of change in acceleration). This precisely locates qualitative shifts in growth strategy. The downward zero-crossing identifies the exact year of maximum acceleration. The y''' minimum marks the sharpest transition from growth to deceleration (the jerk), often indicating canopy closure or root competition. The upward zero-crossing signifies peak deceleration, after which growth stabilizes at a slow, steady rate.

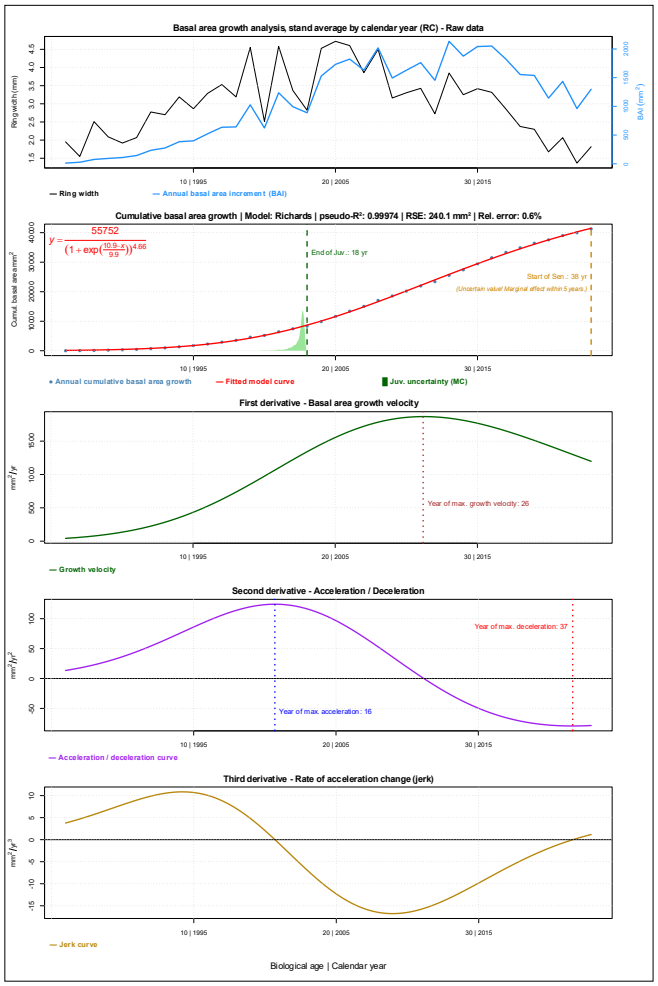

Figure 2: Five-panel analysis of Regional Curve (RC)-based forest stand data by calendar year for common hackberry (Celtis occidentalis)

CONCLUSIONS

The developed method for identifying juvenile, mature, and senescence phases using BAI and CBA data is currently in its initial stage. Monte Carlo simulations effectively demonstrate the uncertainty of these demarcation boundaries. Future comparative research using established anatomical methods (e.g., fiber length measurements) is required to validate these results.

ACKNOWLEGDEMENTS

The publication was supported by the project no. TKP2021-NKTA-43, which has been implemented with the support provided by the Ministry of Innovation and Technology of Hungary (successor: Ministry of Culture and Innovation of Hungary) from the National Research, Development and Innovation Fund, financed under the TKP2021-NKTA funding scheme. The research was supported by Foundation for University Research in Wood Industry (FAEKA).

REFERENCES

Alméras T, Jullien D, Liu S, et al (2025) The diversity of radial variations of wood properties in European beech (Fagus sylvatica L.) reveals the plastic nature of juvenile wood. Annals of Forest Science 82:15. https://doi.org/10.1186/s13595-025-01284-9

Alteyrac J, Cloutier A, Zhang SY (2006) Characterization of juvenile wood to mature wood transition age in black spruce (Picea mariana (Mill.) B.S.P.) at different stand densities and sampling heights. Wood Sci Technol 40:124–138. https://doi.org/10.1007/s00226-005-0047-4

Bartha D, Csiszár Á (2008) Common hackberry (Celtis occidentalis L.). In: The most important invasive plants in Hungary. Hungarian Academy of Sciences, Vácrátót, pp 95–102

Bhat KM, Priya PB, Rugmini P (2001) Characterisation of juvenile wood in teak. Wood Science and Technology 34:517–532. https://doi.org/10.1007/s002260000067

Bonate P (2001) A Brief Introduction to Monte Carlo Simulation. Clinical pharmacokinetics 40:15–22. https://doi.org/10.2165/00003088-200140010-00002

Boruszewski P, Jankowska A, Kurowska A (2017) Comparison of the Structure of Juvenile and Mature Wood of Larix decidua Mill. from Fast-Growing Plantations in Poland. BioResources 12:1813–1825. https://doi.org/10.15376/biores.12.1.1813-1825

Bunn A (2023) dplR - Dendrochronology Program Library in R, Version 1.7.6

Burdon RD, Kibblewhite RP, Walker JCF, et al (2004) Juvenile Versus Mature Wood: A New Concept, Orthogonal to Corewood Versus Outerwood, with Special Reference to Pinus radiata and P. taeda. For Sci 50:399–415. https://doi.org/10.1093/forestscience/50.4.399

Darmawan W, Nandika D, Rahayu I, et al (2013) Determination of juvenile and mature transition ring for fast growing sengon and jabon wood. J Indian Acad Wood Sci 10:39–47. https://doi.org/10.1007/s13196-013-0091-x

Delucis RDA, Gatto DA, Stangerlin DM, Beltrame R (2014) Métodos de delimitação dos lenhos juvenil e adulto de três folhosas e propriedades biométricas de suas fibras. Rev Árvore 38:943–950. https://doi.org/10.1590/S0100-67622014000500019

Gapare WJ, Wu HX, Abarquez A (2006) Genetic control of the time of transition from juvenile to mature wood in *Pinus radiata* D. Don. Ann For Sci 63:871–878. https://doi.org/10.1051/forest:2006070

Google (2026) Gemini (Gemini 3.1 Pro model) [Large language model].

Kartikawati E, Bienitta, Prastiwi FW, Nugroho WD (2024) Determination of the Boundary between Juvenile–Mature Wood of Diospyros kaki and Their Wood Anatomical Variations. J Korean Wood Sci Technol 52:191–203. https://doi.org/10.5658/WOOD.2024.52.2.191

Larson P (1969) Wood Formation and the Concept of Wood Quality. Yale School of the Environment Bulletin Series 69:

Lee Y-S, Kim JS, Seo J-W (2025) Determining the transition from juvenile to mature wood based on fibre characteristics in Fraxinus mandshurica Rupr. and Quercus mongolica Fisch. ex Ledeb. IAWA J 1–10. https://doi.org/10.1163/22941932-bja10208

Maxwell RS, Larsson L-A (2021) Measuring tree-ring widths using the CooRecorder software application. Dendrochronologia 67:125841. https://doi.org/10.1016/j.dendro.2021.125841

NÉBIH (2026) Erdőtérkép (Hungarian Foresty WebMap). In: https://erdoterkep.nebih.gov.hu/ Accessed 14 May 2026

Pödör Z (2014) Idősorok elemzési lehetőségeinek kiterjesztése és alkalmazhatósága erdészeti, faipari döntéstámogatásban. PhD Study, NymE

Purba CYC, Dlouha J, Ruelle J, Fournier M (2021) Mechanical properties of secondary quality beech (Fagus sylvatica L.) and oak (Quercus petraea (Matt.) Liebl.) obtained from thinning, and their relationship to structural parameters. Annals of Forest Science 78:81. https://doi.org/10.1007/s13595-021-01103-x

Rahayu I, Laksono G, Darmawan W, et al (2021) Demarcation area between juvenile and mature wood in Elaeocarpus angustifolius. Biodiversitas 22. https://doi.org/10.13057/biodiv/d220517

Ukalska J, Jastrzębowski S (2019) Sigmoid growth curves, a new approach to study the dynamics of the epicotyl emergence of oak. Folia Forestalia Polonica 61:30–41. https://doi.org/10.2478/ffp-2019-0003

Vega M, Hamilton M, Downes G, et al (2020) Radial variation in modulus of elasticity, microfibril angle and wood density of veneer logs from plantation-grown Eucalyptus nitens. Annals of Forest Science 77:65. https://doi.org/10.1007/s13595-020-00961-1

Zanuncio AJV, Possato EL, Carvalho AG, et al (2022) Basic density and scaling of juvenile and mature wood in Pinus caribaea trees. Cellulose Chem Technol 56:473–479. https://doi.org/10.35812/CelluloseChemTechnol.2022.56.40

Zobel BJ, Buijtenen JP (1989) Wood Variation (Its Causes and Control), 1st edn. Springer Berlin, Heidelberg

Exploring the Acoustic Properties of Different Hardwood Species

Antonius Androne[1*], Maria Violeta Guiman[2], Mariana Domnica Stanciu[2*], Camelia Coșereanu[1]

[1] Faculty of Furniture Design and Wood Engineering, Transilvania University of Brasov, B-dul Eroilor 29, 500036, Brasov, Romania
[2] Faculty of Mechanical Engineering, Transilvania University of Brașov, B-dul Eroilor 29, 500036 Romania.

E-mail:

antonius.androne@unitbv.ro; violeta.guiman@unitbv.ro; mariana.stanciu@unitbv.ro; cboieriu@unitbv.ro

Keywords: acoustic properties; hardwood; sound absorption coefficient; sound velocity.

ABSTRACT
Due to its biological nature, wood is characterized by a porous structure, with irregular pore shapes, different in the three main directions, which recommends it as a material with acoustic properties used either for sound amplification, as in the case of musical instruments, or in sound-absorbing applications, as in the case of cladding acoustic spaces. The mechanism of sound absorption in porous materials relies on three key phenomena: first, the interaction between vibrating air molecules and pore walls converts sound energy into dissipated heat; second, as longitudinal waves penetrate the material, the compression and decompression of air within the pores consumes energy; and third, the vibration of the pore walls themselves transforms sound into mechanical and thermal energy. The study explores the acoustic properties of four deciduous species: cherry (*Prunus avium*), beech (*Fagus Sylvatica L.),* oak (*Quercus robur*), and linden (*Tillia cordata*), with different anatomical characteristics. In the first stage, the sound propagation velocities in the main directions of the wood (longitudinal, radial, tangential) were determined by the time of flight (TOF) method with ultrasound, and in the next stage, samples were prepared for the determination of the acoustic absorption coefficient in the three directions by the impedance tube method (MTB). The results showed that the cross-section absorbs sound best, with acoustic absorption coefficients ranging from 0.3 to 0.7. The radial and tangential sections show close values for the acoustic absorption coefficient, regardless of the species, namely around 0.2.

INTRODUCTION

Wood is biologically defined by its porous structure, acting as a semi-phenomenological model with a rigid skeleton and arbitrary pore shapes (Bucur 2006, Watanabe *et al.* 1967). Its structure varies across three primary axes: longitudinal (L), radial (R), and tangential (T), forming three planes of elastic anisotropy: LR, RT, and TR (Guiman *et al.* 2023, Smardzewski *et al.* 2014). According to Cao *et al.* (2018), sound absorption in porous materials occurs through three stages: (a) energy conversion into heat via friction between vibrating air molecules and pore walls; (b) energy consumption as longitudinal waves compress and decompress air within the pores; and (c) the transformation of sound into mechanical and thermal energy through wall vibration. Analytical models developed by Yang *et al.* (2015), Delany *et al.* (1970), and Lee *et al.* (2021) predict wood's acoustic absorption based on morphology, ranging from simple cylindrical pores to non-uniform cross-sections with partial constrictions. Wood species are often categorized by their acoustic utility: some for resonance in instruments, others for sound insulation (Oliva & Hongisto 2013, Jiang *et al.* 2004, Isaac *et al.* 2020, and Stanciu *et al.* 2024). Research indicates that hardwood absorption coefficients vary significantly based on crystallinity, gas permeability, and pore structure (Plötze & Niemz 2011, Pentoś *et al.* 2016, Kolya 2020, Jang & Kang 2021a,b). For instance, high permeability correlates with better attenuation due to increased air flow. Studies by Smardzewski *et al.* (2014) and Guiman *et al.* (2023) revealed that density, porosity, and tortuosity significantly boost absorption at 2 and 4 kHz. While most research focuses on high frequencies (2–6 kHz) and longitudinal damping (Pentoś *et al.* (2016), Cao *et al.* (2018), the impact of radial and tangential directions remains a subject of debate. Research on the acoustic properties of some deciduous species in the temperate zone, such as cherry, linden, oak, and beech, remains limited. This study analyses the relationship between wood orthotropy and sound absorption coefficient of four hardwood species: cherry (*Prunus avium*), beech (*Fagus Sylvatica L.*), oak (*Quercus robur*), and linden (*Tillia cordata*).

MATERIALS AND METHODS

Sample preparation

In this study, 15 samples of each analyzed deciduous species were prepared, six samples cut in each main direction, according to the preparation methodology in previous studies (Guiman *et al.* 2023, Stanciu *et al.* 2024). Figure 1 shows the sample geometry. The main physical features of the samples are presented in Table 1.

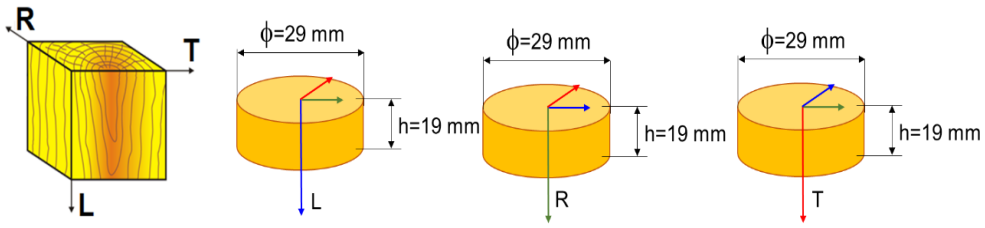

Figure 1: Geometry and cut direction of wood samples

Table 1: Physical features of wood samples

Wood species	Direction of sound	Code	No. of samples	MC (%) (Mean/ &STDV)	Density (kg/m^3) (Mean/ &STDV)
Beech	longitudinal	Beech L	5	10 (0.2)	0.684 (0.031)
	radial	Beech R	5	8 (0.5)	
	tangential	Beech T	5	9 (0.3)	
Cherry	longitudinal	Cherry L	5	8 (0.4)	0.531 (0.053)
	radial	Cherry R	5	9 (0.5)	
	tangential	Cherry T	5	8 (0.3)	
Linden	longitudinal	Linden L	5	7 (0.6)	0.525 (0.056)
	radial	Linden R	5	8 (0.4)	
	tangential	Linden T	5	8 (0.2)	
Oak	longitudinal	Oak L	5	10 (0.4)	0.705 (0.057)
	radial	Oak R	5	9 (0.8)	
	tangential	Oak T	5	9 (0.5)	

Experimental set-up

To evaluate the acoustic performance of the samples, the impedance tube method was employed to measure sound absorption, reflection, and transmission loss, according to ISO 11654 :1997 and ISO 10534:1998. Based on the decomposition of plane waves into incident and reflected components, this method measures acoustic pressure extrema to calculate the material's properties. Using the two-microphone transfer function (TFM) according to, both the resistance and reactance of the wood surface were identified (Nechita & Nastac 2018, Cherradi *et al.* 2021). All experimental tests were conducted using a small-scale Brüel & Kjær impedance system (Type 4206) with a 29 mm sample diameter, covering a broad frequency spectrum from 50 Hz up to 6.4 kHz. The experimental setup is presented in Figure 2.

Figure 2: Experimental set-up

RESULTS AND DISCUSSION

In Figure 3, the variation in the sound absorption coefficient (SAC) for each analyzed species is shown, grouped by the direction of sound propagation in wood. The highest SAC values were obtained for linden wood in the longitudinal directions. In radial direction, the highest values are obtained in the case of cherry wood samples, and in tangential direction, in the case of beech and linden. The anatomical structure of the wood is most evident in the longitudinal direction, specifically in the SAC variation in the cross-section in front of the wave. In this case, the highest acoustic absorption is recorded for all species (Figure 3a), compared to the other sections (Figure 3b,c). Table 2 summarizes the maximum SAC values and the frequency corresponding to these values.

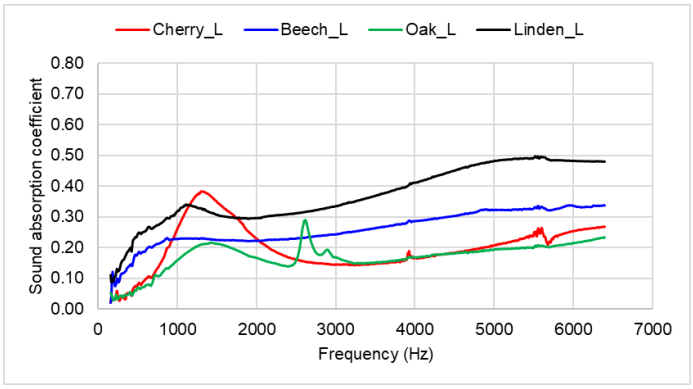

a)

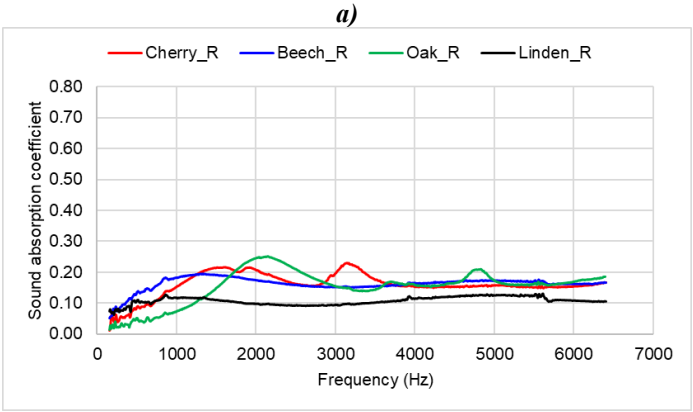

b)

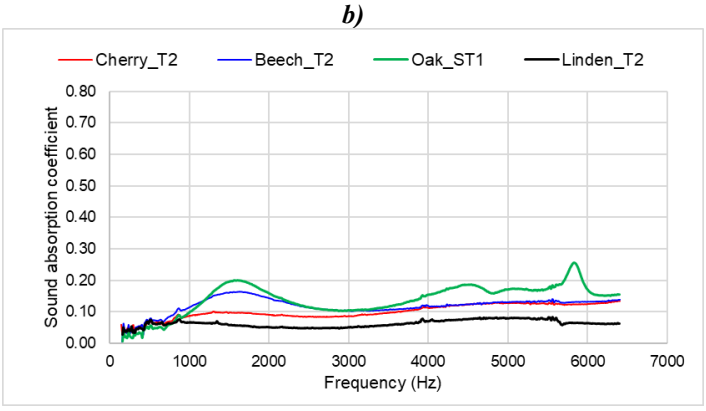

c)

Figure 3: Comparison of sound absorption coefficient for all studied wood species: a) sound transmission in longitudinal direction; b) sound transmission in radial direction; c) sound transmission in tangential direction

Analyzing the results, it is observed that there is a direct proportional relationship between the SAC values and the wood density. Thus, in the transverse plane (the longitudinal direction of sound propagation in the acoustic tube), SAC values are higher for linden. In the tangential plane (radial direction), cherry wood recorded the highest values, and in the radial plane (tangential sound direction), beech and linden wood are more sensitive to sound absorption.

Table 2: The average values of the sound absorption coefficient and the frequencies corresponding to the maximum absorption peak

Samples	SAC	Frequency (Hz)
Beech_L	0.29 – 0.41	1432
Beech_R	0.20 – 0.28	1576
Beech_T	0.24 – 0.43	1672
Cherry_L	0.22 – 0.41	1784
Cherry_R	0.22 – 0.47	1592
Cherry_T	0.15 – 0.32	1088
Linden_L	0.40 – 0.50	1216
Linden_R	0.10 – 0.17	968
Linden_T	0.20 – 0.38	944
Oak_L	0.23 – 0.31	1320
Oak_R	0.15 – 0.35	2000
Oak_T	0.13 – 0.31	1600

CONCLUSION

The paper analyzed the acoustic absorption capacity of four deciduous species from the temperate zone. The variation of the sound absorption coefficient was analyzed for each wood species depending on the main sections of the wood positioned in front of the wave front in the acoustic impedance tube. The most important results highlight the close relationship between the porosity of the sample surface, determined by the arrangement of the macroscopic anatomical elements, and the acoustic absorption coefficient. The applications of this research aim to select the optimal species for various fields, such as the architecture of concert halls and studios, building insulation, and the acoustics of musical instruments.

REFERENCES

Cao L, F. Q. (2018). Porous materials for sound absorption. Comp. Communications, 10:25–35.

Çavuş V, K. M. (2020). Experimental Determination of Sound Transmission Loss of Some Wood Species. Kastamonu Uni., Orman Fakültesi Dergisi, 20(2): 190-199.

Cherradi Y, R. I. (2021). Benyoucef, M. Acoustic properties for composite materials based on alfa and wood fibers. Appl. Acoust, 174:107759.

Delany ME, B. E. (1970). Acoustical Properties of fibrous absorbent materials. Appl. Acoust, 3:105-106.

Guiman M. V, S. M. (2023). Influence of the Grain Orientation of Wood upon Its Sound Absorption Proprerties. Materials.

Isaac CW, P. M. (2020). Comparative Study of Sound Transmission Losses of Sandwich Composite Double Panel Walls. Appl. Sci. 10:1543.

ISO. (1997). ISO 11654 :1997. Acoustics: sound absorbers for use in buildings. In: Rating of sound absorption. Geneva, Switzerland: International Organization for Standardization ISO.

ISO. (1998). Acoustics - determination of sound absorption coefficient and impedance in impedance tubes: Part 1: Method using standing wave ratio, Part 2: Transfer-function method. International Standard Organization ISO.

Jang ES, K. C. (2021a). Sound absorption characteristics of three species (binuang, balsa and paulownia) of low density hardwood. Holzforschung, 75(12):1115-1124.

Jang ES, K. C.-T. (2021b). Investigation of Sound Absorption Properties of Heat-Treated Indonesian Momala (Homalium foetidum (Roxb.) Benth.) and Korean Red Toon (Toona sinensis (A. Juss.) M. Roem.) Cross Sections. Forests, 12:1447.

Jiang ZH, Z. R. (2004). Sound absorption property of wood for five eucalypt species. Journal of Forestry Research, 15(3):207-210.

Kolya H, K. C. (2020). High acoustic absorption properties of hackberry compared to nine different hardwood species: A novel finding for acoustical engineers. Appl Acoust, 169:107475.

Lee HM, L. W. (2021). Studies on the sound absorption and transmission loss performances of wood-based, natural and waste materials. Acta Mech. Sin, 37:861-873.

Nechita P, N. S. (2018). Foam-formed cellulose composite materials with potential applications in sound insulation. J. Compos. Mater., 52:(6):747-754.

Oliva D, H. V. (2013). Sound absorption of porous materials – Accuracy of prediction method. Appl. Sci, 73:1473-1479.

Pentoś K, Ł. D.–2. (2016). The Use of Complex Impedance as a Parameter for Wood Differentiation. Wood Research, 61(1):13-24.

Plötze M, N. P. (2011). Porosity and pore size distribution of different wood types as determined by mercury intrusion porosimetry. Eur J Wood Wood Prod, 69:649-65.

Smardzewski J, B. W. (2014). Experimental study of wood acoustic absorption characteristics. Holzforschung, 467-476.

Stanciu MD, C. M. (2024). Tunable Acoustic Properties Using Different Coating Systems on Resonance Spruce Wood. Adv. Mat. Interfaces. 1:2300781.

V, B. (2006). Acoustics of Wood 2nd ed. In B. V, Acoustics of Wood 2nd ed (pp. 173-196). Berlin, Germany: Springer.

Watanabe T, M. T. (1967). Acoustical study of woods and wood products. In M. T. Watanabe T, Acoustical study of woods and wood products (pp. 177-1782). Japan: Japan wood Res.

Yang XH, R. S. (2015). A simplistic unit cell model for sound absorption of cellular foams with fully/semi-open cells. Composites Science and Technology, 118:276-283.

Chemical and Macromolecular Changes in Poplar Wood (*Populus tremula* L.)

Viera Kučerová[1*]

[1*] Technical University in Zvolen, Faculty of Wood Sciences and Technology, T. G. Masaryka 24, Zvolen, Slovakia, 960 01.

E-mail: kucerovav@tuzvo.sk

Keywords: Poplar wood (*Populus tremula* L.); hydrothermal pretreatment; chemical composition; cellulose; degree of polymerisation; polydispersity.

ABSTRACT

Poplar wood (*Populus tremula* L.) was hydrothermally pretreated in a Parr reactor at 200 °C for 30, 60, 120, and 240 minutes. The effects of hydrothermal pretreatment on the chemical composition of poplar wood were evaluated. In both untreated and pretreated wood, extractives were determined according to ASTM D1107-96, lignin content according to ASTM D1106-96, and cellulose content according to Seifert (1956). The extractive content increased up to 30 min, then decreased at longer pretreatment times. Lignin content decreased up to 60 min and subsequently increased with pretreatment time up to 240 min. A relative increase in cellulose content was also observed. Changes in the macromolecular traits of cellulose were investigated by gel permeation chromatography. The degree of polymerisation and polydispersity were decreased with time pretreatment.

INTRODUCTION

Lignocellulosic biomass is currently considered one of the most important renewable resources for the production of biofuels, chemicals, biomaterials, and other value-added products. Wood biomass is mainly composed of cellulose, hemicelluloses, and lignin, which form a complex and highly organized macromolecular structure resistant to chemical and biological degradation (Sjöström 1993). The structural arrangement and interactions among these components significantly influence the physical, chemical, and mechanical properties of wood, as well as its reactivity during industrial processing and biomass conversion technologies (Fengel, Wegener 1989). Among hardwood species, poplar wood represents a promising raw material because of its rapid growth, relatively low density, favourable fibre morphology, and lower lignin content compared to many other woody plants. Due to these characteristics, poplar wood is widely studied for applications in pulp and paper production, engineered wood products, and biorefinery technologies (Foston et al. 2011). In recent years, increasing attention has been focused on environmentally friendly pretreatment technologies capable of modifying lignocellulosic biomass while minimizing the use of harmful chemicals and energy consumption.

Hydrothermal pretreatment is one of the most effective and sustainable methods for biomass modification. During this process, wood is treated with hot compressed water at elevated temperatures, resulting in autohydrolysis reactions that primarily affect hemicelluloses and partially alter lignin and cellulose structures (Garrote et al. 1999). Water under hydrothermal conditions acts both as a reaction medium and catalyst, promoting cleavage of acetyl groups and glycosidic bonds in hemicelluloses, which subsequently leads to solubilization and degradation of polysaccharides (Mosier et al. 2005). Simultaneously, partial depolymerisation, condensation, and redistribution reactions occur within the lignin (Tjeerdsma, Militz 2005).

Hydrothermal treatment also influences the supramolecular and macromolecular characteristics of cellulose. Amorphous regions of cellulose are more susceptible to hydrolytic degradation, whereas crystalline domains are relatively resistant to thermal and hydrolytic attack. Consequently, pretreatment often leads to an increase in relative cellulose crystallinity accompanied by a decrease in degree of polymerisation and molecular weight distribution (Esteghlalian et al. 1997). These structural changes significantly affect enzymatic digestibility, chemical accessibility, thermal stability, and mechanical performance of lignocellulosic materials (Borrega, Kärenlampi 2011). Several studies have demonstrated that the severity of hydrothermal pretreatment, especially the combination of temperature

and exposure time, strongly determines the extent of chemical degradation and structural transformation in woody biomass (Garrote et al. 1999, Mosier et al. 2005). Prolonged exposure to elevated temperatures may result in increased degradation of hemicelluloses, formation of extractable degradation products, lignin condensation reactions, and progressive depolymerisation of cellulose chains. Monitoring these changes is essential for optimising pretreatment conditions in biorefinery applications and cellulose-based material production. The characterisation of chemical composition and cellulose macromolecular properties after hydrothermal pretreatment, therefore, represents an important aspect of biomass research. Analytical methods such as determination of extractives, lignin and cellulose contents, together with gel permeation chromatography for molecular weight distribution analysis, provide valuable information about degradation mechanisms occurring during thermal treatment processes.
Therefore, the purpose of this study was to investigate the influence of hydrothermal pretreatment at 200 °C with different reaction times on the chemical composition and macromolecular characteristics of cellulose in poplar wood (*Populus tremula* L.).

MATERIALS AND METHODS

Hot water pretreatment

From a 20-year-old poplar trunk (*Populus tremula* L.), we prepared samples measuring 2x2x10 mm, which we hydrolysed in a PARR 4561 reactor. We weighed 20 g of sample into the reaction vessel and added 80 ml of distilled water (hydromodulus 1:4). The reaction vessel was closed and heated to a temperature of 200 °C. The achieved temperature was maintained for 30, 60, 120 and 240 minutes. Then the reaction vessel was cooled in a vessel with cold water and ice. After drying, the samples were mechanically ground into sawdust and a fraction with a size of 0.5–1.0 mm was used for analysis. Each pretreatment was performed twice, and the solid residues were analysed in parallel, so that at each treatment level we obtained four results.

Determination of extractives, cellulose and lignin

Poplar wood samples before and after hot water pretreatment were extracted in the Soxhlet apparatus with a mixture of ethanol and toluene according to ASTM D 1107–96 (2013). Cellulose was isolated from samples using the Seifert method (Seifert 1956), and lignin content according to ASTM D1106-96 (2013).

Determination of macromolecular traits of cellulose

The molecular weight characteristics of the cellulose were determined after its conversion into cellulose tricarbanilates. Cellulose tricarbanilates were dissolved in tetrahydrofuran and filtered through a Puradisc 25 NYL filter (Whatman International) with a pore size of 0.45 μm and analysed by size-exclusion chromatography (Kučerová, Halajová 2009). Calculations of molecular weights were performed with the Clarity GPC module (DataApex). Degree of polymerisation (DP_w) values were calculated by dividing the molecular weight by the monomer equivalent weight of anhydroglucose ($DP_w = M_w/162$). Polydispersity index (PDI) of cellulose was calculated as the ratio M_w/M_n.

RESULTS AND DISCUSSION

Hydrothermal pretreatment significantly affected the chemical composition of poplar wood (*Populus tremula* L.), while the extent of the changes strongly depended on the treatment duration. The contents of extractives, cellulose, and lignin (Table 1) exhibited distinct trends during hydrothermal processing, indicating progressive dissolution, degradation, and redistribution of wood components.
The extractives content increased markedly during the initial stage of prehydrolysis. Untreated poplar wood contained only 4.32 % extractives; however, after 30 min of treatment, the value increased sharply to 33.07 %, representing the maximum recorded during the experiment. The increase can be attributed to the release of low-molecular degradation products, water-soluble compounds, and hydrolysis products of hemicelluloses generated during hydrothermal treatment (Scapini et al. 2021, Martín et al. 2022). With prolonged treatment, the extractives content gradually decreased to 19.94 %.
This decline may be associated with further decomposition of dissolved compounds into volatile substances or with secondary condensation reactions leading to the formation of less extractable structures **(**Demirbas 2008**)**.

The cellulose content continuously increased with increasing treatment time. The untreated sample contained 36.51 % cellulose, whereas after 240 min of prehydrolysis, the cellulose proportion reached 68.58 %. This behaviour is characteristic of hydrothermal pretreatment processes, during which hemicelluloses and extractives are preferentially removed, resulting in a relative enrichment of cellulose in the solid residue (Martín et al. 2022). The results further indicate that cellulose was considerably more resistant to hydrothermal degradation than the amorphous hemicellulosic fraction.

The lignin content showed a different trend compared to cellulose and extractives. Initially, lignin content decreased substantially from 21.94 % in untreated wood to 9.33 % after 60 min of treatment. This reduction may be explained by partial solubilization and redistribution of lignin fragments under hydrothermal conditions (Lu et al. 2009).

However, prolonged treatment resulted in an increase in lignin content to 22.66 % after 240 min. This phenomenon is likely associated with condensation reactions of lignin fragments and the formation of pseudo-lignin from carbohydrate degradation products, which are subsequently quantified as lignin during chemical analysis (Shinde et al. 2018). Similar lignin redeposition and pseudo-lignin formation during hydrothermal pretreatment were also described by Sarker et al. (2021).

Table 1: Content of extractives, cellulose and lignin

Time [min]	Extractives [%]	SE [%]	Cellulose [%]	SE [%]	Lignin [%]	SE [%]
untreated	4.32	0.02	36.51	0.01	21.94	0.13
30	33.07	0.47	42.16	0.43	9.56	0.63
60	30.75	0.36	48.48	0.68	9.33	0.61
120	24.91	0.00	60.64	0.48	12.12	0.30
240	19.94	0.37	68.58	0.12	22.66	0.32

Note: SE is standard error.

The results on the macromolecular traits of cellulose are presented in Table 2.

Table 2: Results of M_w and M_n of cellulose

Time [min]	M_w [g.mol^{-1}]	SE	M_n [g.mol^{-1}]	SE
untreated	218,954	374	27,470	371
30	52,225	840	21,531	36
60	55,790	1,711	22,903	14
120	54,376	2,961	21,239	122
240	38,299	4	19,320	146

Note: M_w is weight average molecular weight; M_n is number average molecular weight; SE is standard error.

The greatest degradation of cellulose occurred within 30 minutes after pretreatment. The cellulose fractions with high molecular weight cleave, and the proportion of low molecular weight fractions increases. The lower Mw value of 52,225 g.mol^{-1} of the pretreated sample at 30 minutes compared to the untreated sample suggested significant degradation of cellulose during pretreatment, which decreased by 76.15%. Further significant degradation of cellulose occurred above 120 minutes mark. M_w value decreased from 120 to 240 minutes by 29.57%. At higher temperatures, an important amount of acetic acid is released via deacetylation of hemicelluloses, which catalyses depolymerisation of the less ordered carbohydrates, such as hemicelluloses and amorphous cellulose (Candelier et al. 2016). This causes a decrease of DP_w.

The relationship between the degree of polymerisation and polydispersity of cellulose and time is shown in Table 3.

Table 3: Results of DP_w and PDI of cellulose

Time [min]	DP_w	SE	PDI	SE
untreated	1,352	1.33	7.97	0.05
30	322	6.25	2.43	0.06
60	344	15.91	2.44	0.11
120	336	23.14	2.57	0.20
240	236	1.48	1.98	0.01

Note: DP_w is a degree of polymerisation; PDI is polydispersity index; SE is standard error.

Polydispersity refers to the fact that, in most cases, there is a mixture of different-length cellulose chains in the system. The ratio of the weight average molecular weight to the number average molecular weight describes the polydispersity index (PDI). The PDI can change differently during degradation processes according to the types of degradation mechanisms occurring (random or systematic). In the case of a random degradation, the ratio does not change, and the molar mass distribution keeps the same profile. The ratio decreases if scissions near the centre are favoured and increases if scission is formed near the ends (Heywood, Emsley 1995). Our experimental results indicate that the greatest change of degree of polymerisation and polydispersity was observed within 30 minutes. The degree of polymerisation and polydispersity decreased within 240 minutes by 82.54% and 75.16%, respectively.

CONCLUSIONS

The results of the pretreatment at 200 °C for 30, 60, 120, and 240 minutes demonstrate that prehydrolysis markedly modified the chemical composition and molecular characteristics of poplar wood (*Populus tremula* L.). Short treatment times lead to a pronounced increase in extractive content, primarily due to the formation and accumulation of low-molecular-weight degradation products derived from hemicelluloses and related compounds. With increasing treatment duration, extractive content decreases, indicating further decomposition and possible involvement of secondary condensation reactions. Prolonged hydrothermal treatment results in substantial cellulose enrichment in the solid residue, accompanied by partial lignin removal at shorter times and subsequent lignin condensation and pseudo-lignin formation under more severe conditions. These findings confirm that hydrothermal prehydrolysis is an effective pretreatment method for poplar biomass intended for pulping and biorefinery applications.

ACKNOWLEDGEMENTS

This study was supported by the Grant Agency, Project No. VEGA 1/0599/25, Project No. KEGA 042SPU-4/2024.

REFERENCES

ASTM International. ASTM D1106-96(2013): Standard Test Method for Acid-Insoluble Lignin in Wood. West Conshohocken, PA: ASTM International, 2013.

ASTM International. ASTM D1107-96(2013): Standard Test Method for Ethanol-Toluene Solubility of Wood. West Conshohocken, PA: ASTM International, 2013.

Borrega M, Kärenlampi PP (2011) Cell wall properties of Norway spruce as affected by high-temperature drying. Wood Fiber Sci 43(2):206–214

Candelier K, Thevenon MF, Petrissans A, Dumarcay S, Gerardin P, Petrissans M (2016) Control of wood thermal treatment and its effects on decay resistance: A review. Ann For Sci 73:571–583. https://doi.org/10.1007/s13595-016-0541-x

Demirbas A (2008) Products from lignocellulosic materials via degradation processes. Energy Sources Part A 30:27–37. https://doi.org/10.1080/00908310600626705

Esteghlalian A, Hashimoto AG, Fenske JJ, Penner MH (1997) Modeling and optimization of the dilute-sulfuric-acid pretreatment of corn stover, poplar and switchgrass. Bioresour Technol 59(2–3):129–136. https://doi.org/10.1016/S0960-8524(97)81606-9

Fengel D, Wegener G (1989) Wood: Chemistry, Ultrastructure, Reactions. Walter de Gruyter, Berlin, Germany

Foston M, Hubbell CA, Samuel R, Jung S, Fan H, Ding SY, Zeng Y, Jawdy S, Davis M, Sykes R, Gjersing E, Tuskan GA, Kalluri U, Ragauskas AJ (2011) Chemical, ultrastructural and supramolecular analysis of tension wood in Populus tremula × alba as a model substrate for reduced recalcitrance. Energy Environ Sci 4:4962–4971. https://doi.org/10.1039/C1EE02073K

Garrote G, Domínguez H, Parajó JC (1999) Hydrothermal processing of lignocellulosic materials. Holz Roh Werkst 57:191–202. https://doi.org/10.1007/s001070050039

Heywood AM, Emsley RJ (1995) Computer modelling of the degradation of linear polymers. Polym Degrad Stab 48:145–149. https://doi.org/10.1016/0141-3910(95)00014-0

Kučerová V, Halajová L (2009) Evaluation of changes of the recycled pulps by method the gel permeation chromatography. Acta Facultatis Xylologiae 51(2):87–92.

Lu X, Yamauchi K, Phaiboonsilpa N, Saka S (2009) Two-step hydrolysis of Japanese beech as treated by semi-flow hot-compressed water. J Wood Sci 55:367–375. https://doi.org/10.1007/s10086-009-1040-6

Martín C, Dixit P, Momayez FM, Jönsson LJ (2022) Hydrothermal pretreatment of lignocellulosic feedstocks to facilitate biochemical conversion. Front Bioeng Biotechnol 10:846592. https://doi.org/10.3389/fbioe.2022.846592

Mosier N, Wyman C, Dale B, Elander R, Lee YY, Holtzapple M, Ladisch M (2005) Features of promising technologies for pretreatment of lignocellulosic biomass. Bioresour Technol 96(6):673–686. https://doi.org/10.1016/j.biortech.2004.06.025

Sarker TR, Pattnaik F, Nanda S, Dalai AK, Meda V, Naik S (2021) Hydrothermal pretreatment technologies for lignocellulosic biomass: A review of steam explosion and subcritical water hydrolysis. Chemosphere 284:131372. https://doi.org/10.1016/j.chemosphere.2021.131372

Scapini T, dos Santos MSN, Bonatto C, Wancura JHC, Mulinari J, Camargo AF, Klanovicz N, Zabot GL, Tres MV, Fongaro G, Treichel H (2021) Hydrothermal pretreatment of lignocellulosic biomass for hemicellulose recovery. Bioresource Technology 342:126033. https://doi.org/10.1016/j.biortech.2021.126033

Seifert K (1956) A procedure for the determination of cellulose in wood and pulp. Das Papier 10(23/24):301–306

Shinde SD, Meng X, Kumar R, Ragauskas AJ (2018) Recent advances in understanding the pseudo-lignin formation in a lignocellulosic biorefinery. Green Chem 20:2192–2205. https://doi.org/10.1039/C8GC00353J

Sjöström E (1993) Wood Chemistry: Fundamentals and Applications, 2nd ed. Academic Press, San Diego, CA, USA

Tjeerdsma BF, Militz H (2005) Chemical changes in hydrothermal treated wood: FTIR analysis of combined hydrothermal and dry heat-treated wood. Holz Roh Werkst 63:102–111. https://doi.org/10.1007/s00107-004-0532-8

Differences in the Resistance of Two Longitudinal Beech Wood Joints Under Bending Loads

Tomislav Gržan[1], Goran Mihulja[1*], Josip Miklečić[1], Tara Crnković[1], Martin Kašnar[1], Tomislav Sedlar[1]

[1] University of Zagreb, Faculty of Forestry and Wood Technology. Svetošimunska cesta 23, Zagreb, Croatia, HR-10000.

E-mail: gmihulja@sumfak.unizg.hr; tgrzan@sumfak.unizg.hr; jmiklecic@sumfak.unizg.hr; tcrnkovic@sumfak.unizg.hr; mkasnar@sumfak.unizg.hr; tsedlar@sumfak.unizg.hr

Keywords: wood joints; finger joint; conical tenon; bending strength.

ABSTRACT

Joints are one of the most important components in the production of furniture and other wood-based products. They significantly influence the overall behaviour of the structure of connected components. One of the key aspects in the consideration and design of wooden structures and furniture is the selection of a joint type that will ensure the required structural properties. Although longitudinal joints have found application in various structures and products, such as solid panels in furniture, laminated beams, and building joinery, their effects are the most difficult to achieve. Therefore, their application remains limited, as they are still significantly weaker than solid wood. In wood industry practice, the most reliable longitudinal joint is the finger joint, and this widely known and recognised technology for longitudinal wood joining has reached its peak in addressing the major issues in the use of wood as a raw material and its dimensional limitations. Consequently, it is necessary to investigate whether there are new possibilities for longitudinal wood joining that could bring the strength of a jointed element closer to that of solid wood or improve other functional properties. In addition to the quality of the finger joint, the most significant qualitative improvement lies in the application of bonding pressure at the interface of two adjacent elements during glueing. The main reason for the significantly weaker performance of longitudinal joints made with straight and rounded dowels, splits, and inserts is the bonding pressure, which reduces the adhesive layer thickness and improves bonding quality. Therefore, it can be assumed that a new qualitative advancement in longitudinal bonding systems may be achieved using conical dowels, which enable the development of bonding pressure by inserting the dowel into a conical hole. An additional major production advantage of such a joint is that only short-term pressure is required because self-locking develops at the contact surfaces, similar to that in finger joints.

The aim of this research was to analyse specific deformations resulting from bending loads on longitudinal joints of beech wood using glued conical mortise-and-tenon joints in two configurations: a longer and a shorter conical tenon, and to compare them with finger joints. Since the strength of the glued mortise-and-tenon joint was compared with the finger joint, it was necessary to precisely determine the bonding surface area through which stresses are transferred. Both joints were designed with truncated conical tenons of different lengths. Two variants of the mortise-and-tenon joint were tested: one with 75% of the contact surface area of the finger joint and another with 50%.

PVAC adhesive was used for bonding the samples, with a pressing pressure of at least 0.5 N/mm² applied for 80 seconds. Mechanical testing of the bonded samples was conducted on a Shimadzu universal testing machine in accordance with HRN EN 408, and the modulus of elasticity (MOE) and modulus of rupture (MOR) were determined. Alongside mechanical testing, the ARAMIS system was used to measure optical deformation using the digital image correlation (DIC) method.

The results of the study showed that both variants of the mortise-and-tenon joints, despite the reduced contact area, performed better than the finger joint in terms of load-bearing capacity and resistance to deformation. The good performance of the mortise-and-tenon joints can be attributed to their truncated-conical geometry, which promotes a more uniform stress distribution across the joint, even with reduced contact area. The larger bonding surface in the version with the longer conical tenon allowed greater force absorption and higher structural integrity (i.e., increased stiffness), while the version with the shorter tenon, despite the reduced contact area, still showed better performance than the finger joint. The finger joint, although easier to manufacture and assemble, suffered from localised stress concentrations, which led to earlier deformation and failure under load.

The final version of this abstract and the full scientific article are scheduled to be published in the Special Issue "12th Hardwood Conference—Sopron" of the journal MDPI Forests, available at the following link:

MDPI Forests Special Issue: 12th Hardwood Conference—Sopron

Concept for Utilisation of Beech False Heartwood Based on the Correlation Between Colour and Hardness

Miroslava Mamoňová[1*], Peter Truban[2], Tatiana Hýrošová[3]

[1*, 2] Technical University in Zvolen, Faculty of Wood Sciences and Technology, Department of Wood Science, T. G. Masaryka 24, Zvolen, Slovakia, 960 01
[3] Technical University in Zvolen, Faculty of Wood Sciences and Technology, Department of Mathematics and Descriptive Geometry, T. G. Masaryka 24, Zvolen, Slovakia, 960 01.

E-mail: mamonova@tuzvo.sk; petertruban@tuzvo.sk; tatiana.hyrosovatuzvo.sk

Keywords: beech; false heartwood; hardness; colour; CIEL*a*b*; spectral analysis; scanning electron microscopy.

ABSTRACT
This paper focuses on the study of false heartwood in European beech (*Fagus sylvatica* L.), analyzing its colour and mechanical properties with the goal of proposing a concept for its more effective use in interior furniture components. The primary objective was to examine the correlation between hardness and CIEL*a*b* color coordinates across different zones of false heartwood. Regression analysis revealed a strong correlation between the b* coordinate and wood hardness. Additional spectral charakteristics analyses and SEM microscopy (via Tescan Vega and UHR-SEM Tescan Amber) allowed the distinction between degraded and non-degraded zones based on their structural condition. The findings suggest that optical parameters can serve as reliable indicators for automated and objective grading of beech wood containing false heartwood, thereby improving its utilization in the wood processing industry.

As demonstrated in Figure 1, a clear correlation exists between the dependent hardness values and the independent b* colour coordinate values. The graph reveals a strong linear relationship between them. The coefficient of determination, $r^2 = 0.7162$, indicates that 71.62% of the variation in hardness is attributable to changes in the b* colour coordinate, with the remaining 28.38% being attributable to other factors. The correlation coefficient, r, is measured at 0.8463, indicating a very strong correlation between hardness and the colour coordinate b*.

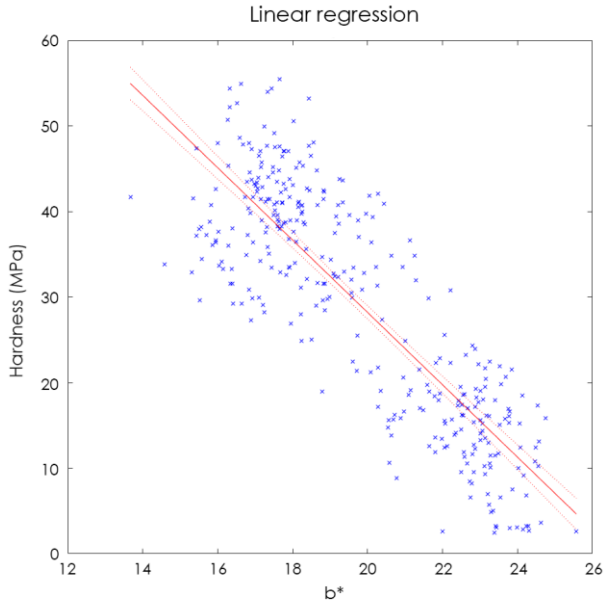

Linear regression model
$Y = b_0 + b_1x$
$Y = 112,7 + (-4,228x)$
Parameters
$b_0 = <107;118,4>$
$b_1 = <-4,513;-3,942>$

Figure 1: Linear regression of hardness and b*

The histogram (Figure 2) illustrates the categorisation of hardness values into intervals based on a statistical set of values from the zones of the false heartwood, excluding values from the sapwood (n = 338). Spectral lines representing individual intervals are generated from the mean reflectance values of the wavelengths (Figure 3). Along the spectral curves of intervals 6–12, characteristic undulations (wavelength 360–460 nm) are observed for undegraded and slightly degraded false heartwood zones (hardness 25–60 MPa). In contrast, the spectral curves for intervals 1–5 exhibit a substantially more linear course. The hardness values of these samples, ranging from 0 to 25 MPa, are indicative of degraded zones within the false heartwood. The spectral lines of the undegraded false heartwood (intervals 6–12) delineate the upper limit. It is possible to reliably distinguish degraded zones from undegraded zones of the false heartwood based on the described specific profiles and characteristic undulations.

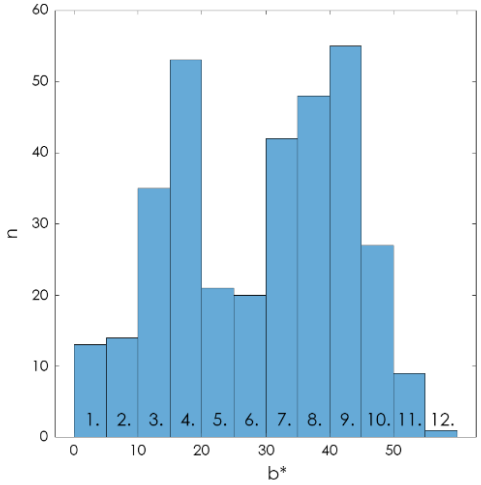

Figure 2: Hardness histogram

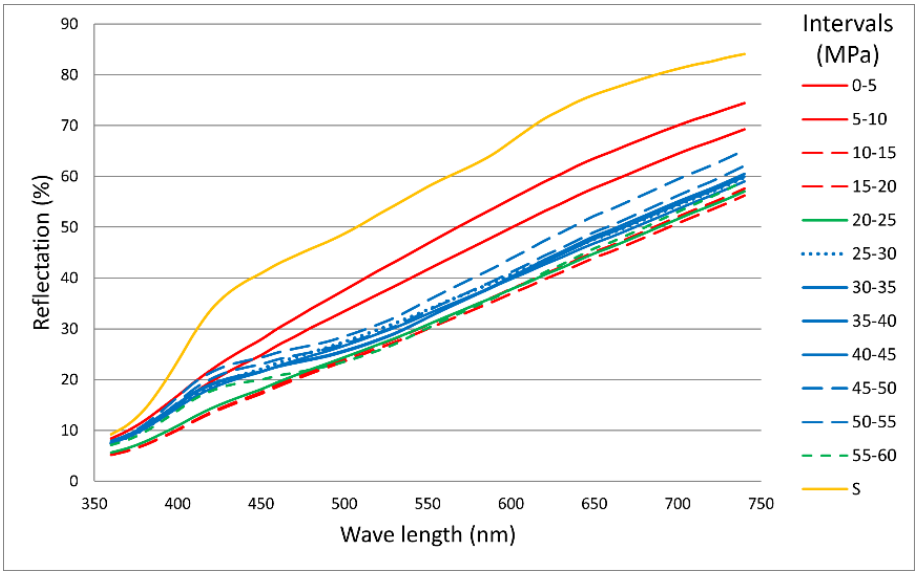

Figure 3: Spectral lines of hardness intervals

SEM analysis - Boundary black line (BL)

The preparation was made from the black borderline (Figure 4a) separating the degraded false heartwood (located on the left) and the sapwood (located on the right). As illustrated in the available images, this boundary zone, characterised by completely encrusted lumen vessels (Figure 5a), effectively delineates the degraded portion of the false heartwood with hyphae from the sapwood, which has undergone a gradual transformation into false heartwood.

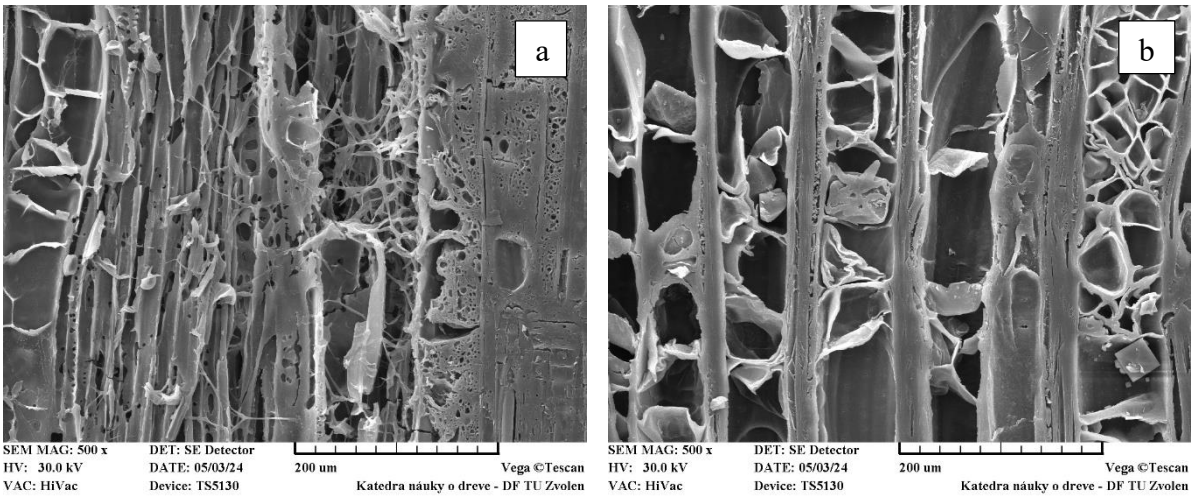

Figure 4: Scanning electron microscopy (SEM) images from borderline zone

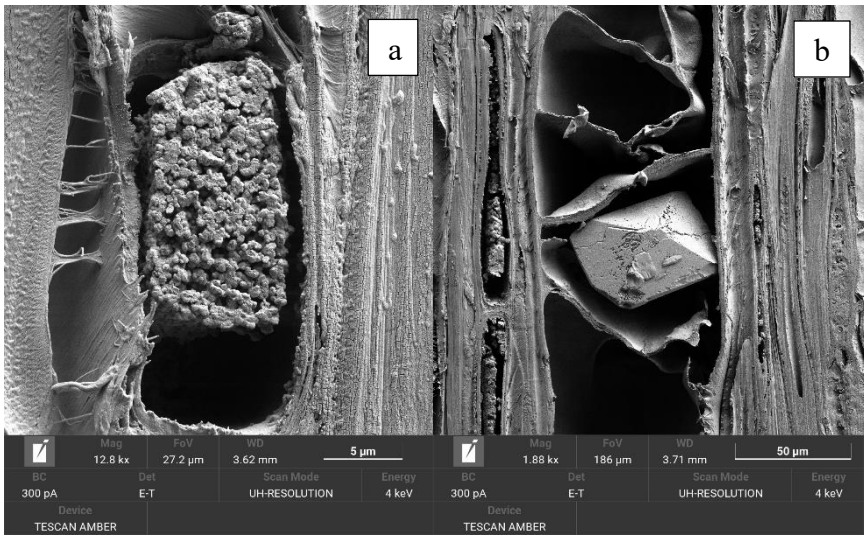

Figure 5: Scanning electron microscopy (SEM Tescan Amber) images from borderline zone. Details of the encrustations (a) and crystalline structures (b) in the vessels, which were analyzed by EDS

The final version of this abstract and the full scientific article are scheduled to be published in the Special Issue "12th Hardwood Conference—Sopron" of the journal MDPI Forests, available at the following link:
MDPI Forests Special Issue: 12th Hardwood Conference—Sopron

Evaluating the Impact of Adhesive Selection on Bonding Strength in Multi-Layered Floor Elements (GRIpod)

Tomislav Sedlar[1], Vjekoslav Živković[1*], Goran Mihulja[1], Mihael Gazilj[1], Andrija Novosel[1]

[1] University of Zagreb, Faculty of Forestry and Wood Technology. Svetošimunska cesta 23, Zagreb, Croatia, HR-10000.

E-mail: tsedlar@sumfak.unizg.hr; vzivkovic@sumfak.unizg.hr; gmihulja@sumfak.unizg.hr; mgazilj@sumfak.unizg.hr; anovosel@sumfak.unizg.hr

Keywords: adhesives; bonding strength; delamination; composite materials.

ABSTRACT

This article presents a comprehensive investigation into the influence of various adhesives on the bonding strength between different materials within multi-layered floor elements (GRIpod), which are composed of both wood and non-wood components. The study is motivated by the need to enhance the structural integrity and reliability of composite materials, particularly in applications where diverse components must be joined effectively. The research focuses on adhesives commonly used in woodworking, including polyurethane, polyvinyl acetate, epoxy, and silane glue, examining their performance in connecting wood to non-wood elements under standard room conditions.

A series of mechanical tests was conducted to evaluate the bond strength between adjacent layers formed with these adhesives. In addition to quantitative strength measurements, the study also involved the observation and analysis of delamination events, utilising both macroscopic inspection and microscopic examination of fractured surfaces. This multifaceted approach enabled a thorough understanding of the adhesive interactions at both the macro and micro levels, shedding light on the mechanisms that contribute to or hinder effective bonding.

The findings provide valuable insights into the selection of adhesives for composite manufacturing, identifying key factors that influence the durability and stability of the bonded interfaces. These results are expected to inform future developments in composite technology, especially flooring, supporting the creation of new high-quality materials. The outcomes of this research will contribute to the broader knowledge base in the field of advanced materials engineering.

ACKNOWLEDGEMENT

This work was supported by the Croatian Science Foundation under the project number HRZZ IP-2024-05-9506

A Collaborative Robotic System for Automated Measurement of Wood Sorption Isotherms and Associated Shrinkage and Swelling

Edit Földvári-Nagy[1*], Jakub Sandak[1]

[1]InnoRenew CoE, IAM, University of Primorska, Slovenia, 6310 Izola, Livade 6a.

E-mail: edit.foldvari-nagy@innorenew.eu, jakub.sandak@innorenew.eu

Keywords: automatization, collaborative robots, wood, moisture content, sorption isotherms, near infrared spectroscopy, shrinkage and swelling.

ABSRACT

Moisture-induced dimensional changes strongly affect the performance and durability of wood-based materials, making the accurate determination of moisture content and associated shrinkage and swelling essential for sorption studies. It is especially relevant for hardwood species, which usually present higher shrinkage coefficients than softwoods (Schroeder, 1972). Conventional experimental approaches rely on manual handling, sequential gravimetric and optical measurements, and are therefore time-consuming, error-prone, and susceptible to moisture drift between measurement steps (Sandak et al., 2016).

This study presents a fully automated measurement system based on a collaborative dual-arm robot for the integrated assessment of wood moisture content and moisture-induced dimensional changes. Moisture content is determined using high-precision gravimetric measurements combined with near-infrared (NIR) spectroscopy in the 1750–2150 nm range. Automated white and black reference measurements accompany each sample to minimise calibration drift and improve reproducibility, while the robotic workflow reduces the time delay between weighing and spectral acquisition to a few seconds. In parallel, shrinkage and swelling are quantified using a vision-based system with a CCD camera and telecentric optics, enabling distortion-free, non-contact dimensional analysis under successive climate conditions. By synchronising gravimetric, spectroscopic, and imaging measurements within a single robotic cycle, the system improves throughput, repeatability, and data integrity, providing a robust platform for high-resolution analysis of wood hygroscopic behaviour and dimensional stability. The robotised measurement station presented in the **Hiba! A hivatkozási forrás nem található.**.

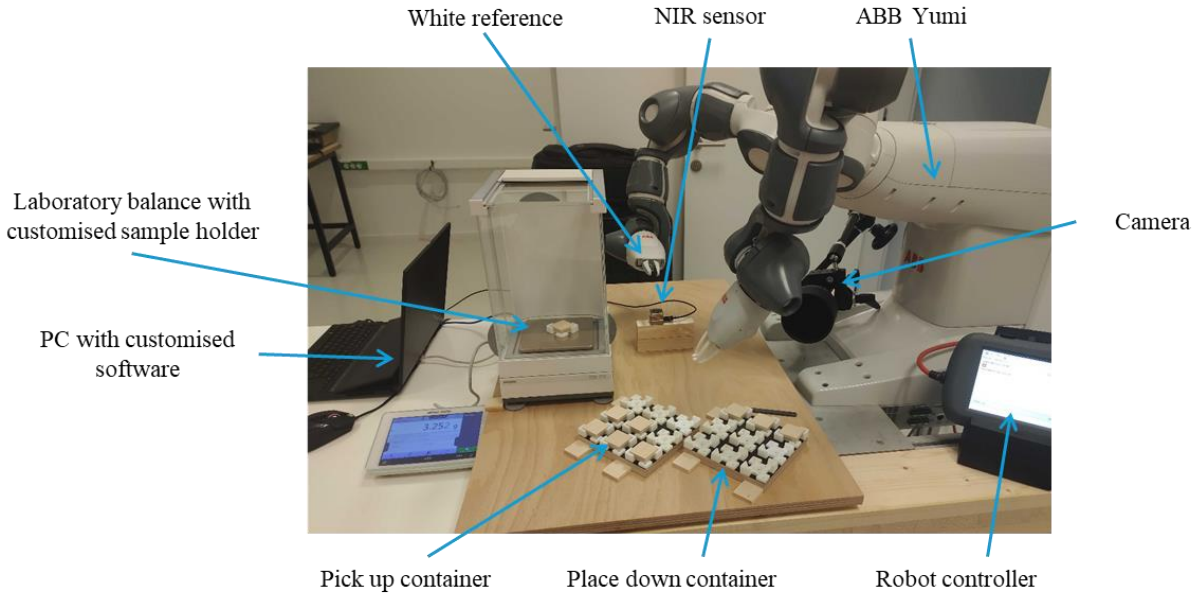

Figure 9: Outline of the robotised measurement station

INTRODUCTION

The interaction between wood and ambient humidity strongly influences its physical, mechanical, and dimensional behaviour. Sorption isotherms describe the equilibrium relationship between relative humidity (RH) and moisture content (MC) (Yang et al., 2013) are fundamental for understanding dimensional stability, shrinkage and swelling behaviour, and long-term performance of wood in service. Accurate characterisation of these relationships requires repeated measurements of mass, moisture-sensitive material properties, and dimensional changes under controlled environmental conditions (USDA Forest Service, 2021).

Near-infrared (NIR) spectroscopy has become a widely applied, non-destructive tool for estimating wood moisture content due to its sensitivity to O–H vibrations associated with water and wood polymers (Thapa et al., 2024). Combined with chemometric techniques such as partial least squares (PLS) regression (Wold et al., 2001), NIR spectroscopy allows rapid MC prediction once suitable calibration models are established. In parallel, image-based methods for dimensional analysis offer a contactless way to quantify shrinkage and swelling, particularly when distortion-free imaging systems such as telecentric lenses are used.

Despite these advances, conventional laboratory workflows for sorption studies remain largely manual. Samples are repeatedly transferred between balances, spectrometers, and imaging systems, resulting in long time delays between individual measurements (directly altering the moisture of characterised samples), increased risk of handling errors, and limited throughput. These drawbacks reduce data consistency, particularly when mass and spectral measurements are not sufficiently synchronised, allowing moisture redistribution to occur between steps.

The aim of this study is to present and evaluate a fully automated robotic measurement workflow that integrates sample handling, mass measurement, NIR spectroscopy, and machine-vision-based imaging into a single, synchronised process. The study focuses on two key outcomes: the performance of PLS regression models for moisture content estimation derived from robotically acquired NIR spectra, and the applicability of image-based dimensional analysis for quantifying shrinkage and swelling within the same automated framework. The novelty of the approach lies in the tight temporal coupling of all measurements and the generation of consistent, high-quality datasets suitable for combined chemometric and dimensional analyses.

MATERIALS AND METHODS

Materials

The objective of this study was to develop a custom measurement system rather than to analyse the specific characteristics of the investigated samples. For this reason, the wood species and sample dimensions were chosen to support the system-development focus. To represent a broad range of wood variability, samples of beech, larch, pine, and spruce were included in the experiments. Each sample measured 30 mm × 30 mm × 5 mm in the longitudinal, tangential, and radial directions, respectively. Only limited information was available regarding the geographical origin of these samples.

Automated Measurement Workflow

All measurements were carried out in a robotic work-cell built around a dual-arm collaborative robot. The system was designed to automatically execute the complete measurement cycle without human intervention. Each cycle consisted of sample pickup, optical image acquisition, mass measurement, NIR spectral acquisition, and deposition of the sample into a post-measurement container.

Automation ensured that each sample followed an identical measurement path, with the sequence and timing of individual steps controlled by a supervisory state machine. The time interval between mass measurement and NIR acquisition was reduced to a few seconds, thereby minimising moisture content changes between measurements. The workflow also enabled systematic data logging, ensuring traceability between image, spectral, and gravimetric data for each sample.

NIR Spectroscopic Measurements

NIR spectra were acquired using a compact NIRONE S2.2 sensor produced by Spectral Engines (Steinbach (Taunus), Germany) operating in the wavelength range of 1750–2150 nm, which includes absorption bands associated with water and hydroxyl groups in wood. Attention was given to the spectral

region around 1950 nm, which is known to exhibit strong sensitivity to moisture content (Hein et al., 2017; Leblon et al., 2013; Schwanninger et al., 2011).
To compensate for sensor drift and temperature sensitivity, white and black reference spectra were recorded before and after each sample measurement. For every measurement point, multiple spectra were collected and averaged to improve the signal-to-noise ratio. All raw and reference spectra were stored together with metadata, including timestamp and sample identification code, allowing transparent post-processing and quality control.
Reference moisture content values were obtained gravimetrically using a precision balance with milligram resolution. During weighing, the balance enclosure was closed to minimise the influence of air currents. A measurement was accepted once the mass reading stabilised, defined as a sequence of identical values over multiple consecutive readings.
Moisture content was calculated based on changes in mass relative to the sample's dry reference mass.

Chemometric Modelling Using PLS Regression

PLS regression was employed to establish quantitative relationships between NIR spectra and reference moisture content values. Prior to modelling, spectral data were pre-processed to reduce the influence of scattering effects and baseline variations. Common pre-processing approaches, such as 2nd derivative correction and mean centring, were applied.
Calibration models were developed using a subset of the measured samples, while model performance was evaluated using cross-validation. The number of latent variables was selected based on minimisation of prediction error and avoidance of overfitting. Model quality was assessed using the coefficient of determination (R^2) and root mean square error of prediction (*RMSEP*) (Westad & Marini, 2015).

Image Acquisition and Dimensional Analysis

Images were captured using a camera equipped with a telecentric lens, providing distortion-free imaging independent of small variations in sample position along the optical axis. Each sample was imaged at a fixed orientation and distance, ensuring consistent scale across measurement cycles.
Image processing involved feature detection and image correlation-based measurement of sample dimensions along orthogonal axes. Dimensional changes were evaluated by comparing measured dimensions at different moisture contents. Shrinkage and swelling were expressed as relative changes (%) with respect to reference dimensions at the dry state, allowing direct comparison between samples and measurement conditions. The concept of the image analysis approach used for the shrinkage/swelling coefficient determination is shown in **Hiba! A hivatkozási forrás nem található.**. T he mathematical formula for converting image-derived coordinates into the shrinkage coefficient is presented in Equation 1.

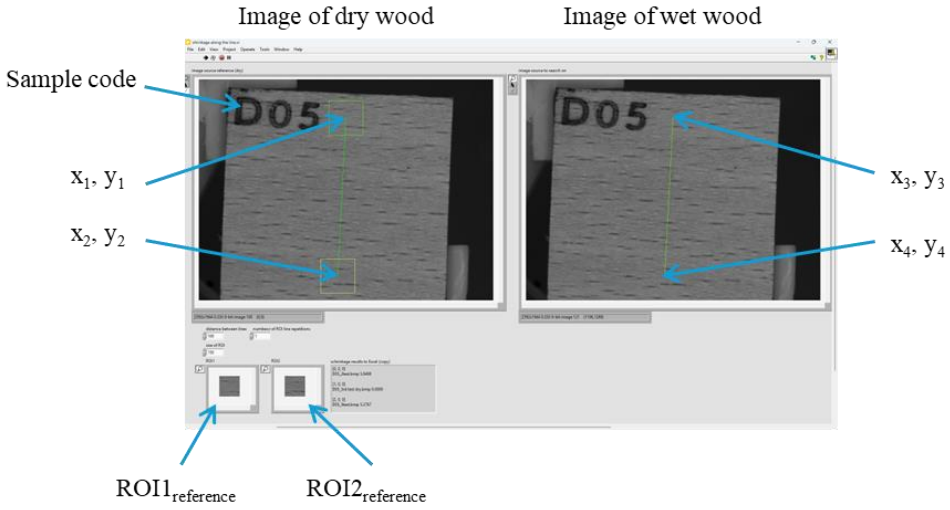

Figure 10: PLS model linking NIR spectra and moisture content measured on different species of wood

$$Shrinkage = \frac{\sqrt{(x_4-x_3)^2+(y_4-y_3)^2}-\sqrt{(x_2-x_1)^2+(y_2-y_1)^2}}{\sqrt{(x_2-x_1)^2+(y_2-y_1)^2}} \times 100\ \% \quad (1)$$

RESULTS AND DISCUSSION

Performance of the PLS Moisture Content Model

PLS regression models derived from the robotically acquired NIR spectra showed strong predictive performance for moisture content estimation. The relationship between predicted and reference MC values exhibited high linearity, with coefficients of determination indicating that a substantial proportion of variance in moisture content could be explained by the spectral data. R^2 of the prediction is 0.93; RMSEP is 1,10% using the 2nd derivative and mean centre as the pre-processing. The reference to predicted values of MC for beech and three alternative softwood species is shown in **Hiba! A h ivatkozási forrás nem található.**.

Prediction errors remained low across the investigated moisture range, and no systematic bias was observed. The reduced time delay between mass and NIR measurements contributed to improved model consistency, as moisture redistribution effects were minimised. Compared to typical manually collected datasets, the automated workflow resulted in fewer outliers and more uniform residual distributions.

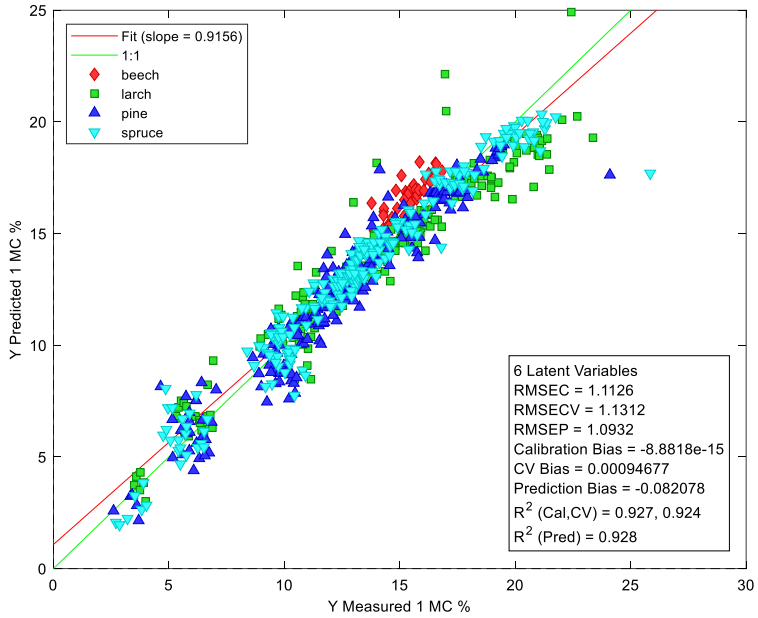

Figure 11: PLS model linking NIR spectra and moisture content measured on different species of wood

Relationship Between Moisture Content and Dimensional Change

A clear qualitative relationship was observed between gravimetrically determined moisture content and image-derived dimensional changes. Dimensional variation followed expected trends with increasing or decreasing MC, supporting the physical relevance of the image-based measurements.

These results suggest that combined datasets linking NIR-predicted MC and dimensional changes could serve as a foundation for future multivariate models that simultaneously describe moisture content and dimensional response.

CONCLUSION

This study demonstrates that a fully automated robotic workflow can successfully integrate mass measurement, NIR spectroscopy, and machine-vision-based dimensional analysis for wood sorption studies. The resulting datasets enable reliable PLS regression models for moisture content estimation and simultaneous quantification of shrinkage and swelling behaviour.

The approach offers clear advantages in terms of throughput, repeatability, and data coherence, providing a scalable platform for advanced wood-water interaction studies. Beyond sorption research, the presented methodology applies to a wide range of laboratory automation tasks requiring synchronised, multi-modal measurements.

ACKNOWLEDGEMENTS

This research was conducted as a part of the research project DendroSpec: "Spectroscopic Methods for Rapid Phenotyping of Trees Reflecting their Ecological Resilience", co-financed by Polish National Science Centre (NCN) No UMO-2021/43/I/NZ9/02809 and Slovenian Research Agency (ARRS) No N4-0274.

REFERENCES

Hein, P. R. G., Pakkanen, H. K., & Dos Santos, A. A. (2017). Challenges in the use of Near Infrared Spectroscopy for improving wood quality: A review. Forest Systems, 26(3), eR03–eR03. https://doi.org/10.5424/FS/2017263-11892

Leblon, B., Adedipe, O., Hans, G., Haddadi, A., Tsuchikawa, S., Burger, J., Stirling, R., Pirouz, Z., Groves, K., Nader, J., & Larocque, A. (2013). A review of near-infrared spectroscopy for monitoring moisture content and density of solid wood (Vol. 89). https://doi.org/https://doi.org/10.5558/tfc2013-111

Sandak, J., Sandak, A., & Meder, R. (2016). Assessing Trees, Wood and Derived Products with Near Infrared Spectroscopy: Hints and Tips, 24(6), 485–505. https://doi.org/10.1255/JNIRS.1255

Schroeder, H. A. (1972). Shrinking and Swelling Differences Between Hardwoods and Softwoods. Wood and Fiber Science, 20–25. https://wfs.swst.org/index.php/wfs/article/view/2030

Schwanninger, M., Rodrigues, J. C., & Fackler, K. (2011). A Review of Band Assignments in Near-Infrared Spectra of Wood and Wood Components. Journal of Near Infrared Spectroscopy, Vol. 19, Issue 5, Pp. 287-308, 19(5), 287–308. https://doi.org/10.1255/jnirs.955

Thapa, S., Li, L., Rubert-Nason, K., Wang, J., Mirtes, C., Brown, T., Pelletier, E., & Zhang, Y.-J. (2024). Wood Moisture Content Determination By Handheld Near-Infrared Reflectance Spectrometer. Wood and Fiber Science, 56(4), 197–206. https://doi.org/10.22382/wfs-2024-18

Westad, F., & Marini, F. (2015). Validation of chemometric models – A tutorial. Analytica Chimica Acta, 893, 14–24. https://doi.org/10.1016/J.ACA.2015.06.056

Wold, S., Sjöström, M., & Eriksson, L. (2001). PLS-regression: a basic tool of chemometrics. Chemometrics and Intelligent Laboratory Systems, 58(2), 109–130. https://doi.org/10.1016/S0169-7439(01)00155-1

USDA Forest Service, F. P. L. (2021). Wood Handbook, Wood as an Engineering Material. (General Technical Report FPL-GTR-282). Moisture Relations and Physical Properties of Wood, Chapter 4

Yang, S.-Y., Han, Y., Chang, Y.-S., Kim, K.-M., & Yeo, H. (2013). Moisture Content Prediction Below And Above Fiber Saturation Point By Partial Least Squares Regression Analysis On Near Infrared Absorption Spectra Of Korean Pine. In Wood and Fiber Science (Vol. 45, Number 4).

Prediction of Durability Based on Wood Color

Szabolcs Komán[1*], Zalán Mátyás Balogh[1], Tamás Hofmann[2]

[1] University of Sopron, Faculty of Wood Engineering and Creative Industries, Institute of Basic Sciences. Bajcsy-Zs. Str. 4, Sopron, Hungary, 9400
[2] University of Sopron, Faculty of Forestry, Institute of Environmental Protection and Natural Conservation, Bajcsy-Zs. Str. 4, Sopron, Hungary, 9400.

E-mail: koman.szabolcs@uni-sopron.hu; balmaza23@student.uni-sopron.hu;; hofmann.tamas@uni-sopron.hu

Keywords: iron(III) chloride, iron(III) sulfate, antioxidant, total phenol, color, durability.

ABSTRACT

Wood, as a fundamentally important natural and renewable building material, is inherently susceptible to various environmental and biological deteriorating agents due to its organic origin. The service life and applicability of wood products are largely determined by their natural durability, defined as the inherent resistance against wood-decaying fungi and insects. The investigation of the relationship between wood color and this durability is of great significance, as color is an easily and non-destructively measurable physical attribute that can provide insight into the internal chemical properties and defense mechanisms of the wood.

The connection between color and biological resistance is primarily attributed to the presence of secondary metabolites, known as extractives, within the wood. During the biochemical process of heartwood formation, various compounds, including polyphenols (tannins, flavonoids, etc.) accumulate in the wood cells. These substances serve a dual function within the wood structure. On the one hand, they are responsible for creating the unique color hues—such as reddish, yellowish, or dark brown tones—characteristic of different species, as well as the visual contrast between heartwood and sapwood. On the other hand, these compounds are often toxic to degrading organisms; thus, through their fungicidal and biocidal properties, they provide natural protection. As a result, darker and more intensely colored wood typically indicates a higher extractive content and, consequently, an enhanced resistance to decay.

However, the development of wood color and durability is influenced by numerous factors, leading to significant variability not only among different species but also between individuals of the same species, and even within different parts of a single tree trunk. Physiological characteristics, genetic background, tree age, and site conditions (such as climate and soil properties) all affect the synthesis and accumulation of extractives.

The aim of the present study was to investigate the polyphenolic content of the sapwood and heartwood tissues of various industrially important wood species originating from various growing sites in Hungary and find relationships with with color and durability parameters to predict possible connections for future assessment of wood quality.

Grey Poplar (*Populus* × *canescens*) in Hungary: Introductory Remarks on Its Underutilization

Hasan Celik[1*], Csilla Csiha[1], Endre Magoss[1]

[1] University of Sopron, Faculty of Wood Engineering and Creative Industries, Sopron, 9400, Hungary.

E-mail: CelHasaHuseyin25@student.uni-sopron.hu; csiha.csilla@uni-sopron.hu; magoss.endre@uni-sopron.hu

Keywords: grey poplar; *Populus* × *canescens*; CLT; hybrid engineered wood products; structural timber; Hungary; scoping review; LCA; sustainable construction.

ABSTRACT

The transition to low carbon construction has renewed interest in engineered wood products, but the European mass timber sector remains strongly dependent on a narrow softwood feedstock, particularly spruce and pine. This creates both a supply chain vulnerability and a missed opportunity for regions with underused domestic hardwood resources. This scoping review provides a brief introductory overview of the existing knowledge on grey poplar (*Populus* × *canescens*) as a potential structural timber resource in Hungary, particularly for cross-laminated timber (CLT) and hybrid engineered wood products. The review synthesizes evidence both from forestry and wood science, with focus on grey poplar resource base.

Current evidence suggests that grey poplar is a credible candidate but not yet a validated direct substitute for conventional softwoods in CLT and hybrid engineered wood products. The main barriers are insufficient data on drying procedure, processing parameter optimization, convenient adhesive types and bonding process, standardized bending at panel scale, variability linked to provenance, durability constraints etc. The review positions grey poplar as a promising but still understudied material and proposes a standards aware research agenda for its responsible integration into European mass timber construction.

INTRODUCTION

The global construction industry is actively seeking viable bio-based structural materials to lower the carbon footprint associated with classical concrete and steel-dominated building systems. This shift has driven a rapid growth in the European engineered wood market, particularly in the production of cross-laminated timber (CLT) and glue-laminated timber (glulam). However, the resource foundation of this industry remains highly narrow, with softwoods, mainly Norway spruce (*Picea abies*) and Scots pine (Pinus sylvestris), constituting over 90% of the feedstock. This intense reliance on coniferous monocultures presents severe supply chain risks due to escalating climate stressors, such as droughts, windthrows, and beetle infestations, which continue to degrade spruce plantations across Central Europe.

Diversifying the structural timber basket by integrating underutilized hardwood species is key to securing resilient, regional forest-product chains. Fast-growing soft-hardwoods represent a valuable but under-commercialized biomass resource in Central and Eastern Europe. In Hungary, poplars (genus *Populus*) represent a highly significant part of regional forestry, covering sandy soils and alluvial floodplains.

While hybrid euramerican clones (such as I-214) are cultivated under intensive short-rotation forestry for pulpwood, native poplar species remain underutilized. Grey poplar (*Populus* × *canescens* Sm.), a natural, fertile hybrid of European aspen (*Populus tremula* L.) and white poplar (*Populus alba* L.), occupies an important ecological and silvicultural niche in Hungary, particularly on the sandy lowlands of the Danube-Tisza interfluve.

Due to historical paradigms, grey poplar wood is currently restricted to low-grade industrial uses, such as shipping pallets, light packaging, wood-based particleboard, and bioenergy. Its application in load-bearing mass timber products has been hindered by a lack of species-specific structural grading rules, processing guidelines, and mechanical characterization. This scoping review addresses these knowledge gaps by synthesizing forestry inventory records, wood anatomy assessments, and engineering compliance guidelines to evaluate the structural viability of Hungarian grey poplar.

MATERIALS AND METHODS

To compile an objective baseline of grey poplar's structural suitability, a scoping review methodology was adopted. The review integrates data from national forest inventories, wood anatomy archives, physical-mechanical test records, and European design standards. Literature searches targeted peer-reviewed wood science databases and academic archives at the University of Sopron, focusing on the mechanical properties, visual and machine grading, and adhesive bonding characteristics of Populus × canescens.

The extracted technical data were cross-examined with the current European regulatory frameworks governing mass timber structures:

- **Mechanical classification:** EN 338 (Strength classes for structural timber) and EN 408 (Structural sizes determination of physical and mechanical properties).
- **Adhesive compliance:** EN 301 and EN 302 series (Adhesives for load-bearing timber structures; testing methods for shear strength and delamination resistance).
- **Composite timber manufacturing:** EN 16351 (Cross-laminated timber product requirements) and EN 14080 (Glued laminated timber and glued solid timber).
- **Physical baseline testing:** ISO 13061-1 (Determination of moisture content for physical and mechanical tests on small clear specimens).

Data obtained from small clear wood specimens were contrasted with structural-sized boards to assess the typical downscaling effect associated with growth defects like knots and reaction wood.

RESULTS AND DISCUSSION

Resource base and regional distribution in Hungary

Poplar stands account for approximately 10% of Hungary's total forest area. Unlike intensive hybrid euramerican plantations, grey poplar is well-suited to marginal lands. It exhibits high drought tolerance and grows effectively on the low-nutrient sandy soils of the Great Plain (Alföld).

Hungary's national growing stock of grey poplar consists of several million cubic meters, with a stable annual increment. Historically, however, silvicultural treatments have treated grey poplar as an accessory resource, resulting in highly variable log assortments. Standardizing structural applications for this hardwood would provide regional forest owners with higher economic incentives, promoting sustainable silvicultural management of native broadleaved stands.

Anatomical challenges: tension wood

The wood anatomy of grey poplar (*Populus* × *canescens*) is diffuse-porous, with vessels distributed relatively evenly throughout the growth ring. Similar to other poplar species, grey poplar may develop tension wood in response to mechanical stresses such as wind loading, stem inclination, or asymmetric crown development. Tension wood in poplar is characterized by the presence of gelatinous fibres containing a cellulose-rich gelatinous layer (G-layer), in which the cellulose microfibrils are oriented nearly parallel to the fibre axis. This specialized tissue contributes to stem reorientation but may also influence the technological properties of the wood. (Goswami et al. 2008; Lautner et al. 2012).

The occurrence of tension wood is of particular importance for the utilization of grey poplar in engineered wood products. Studies on poplar species have shown that the presence of G-fibres can increase longitudinal shrinkage and contribute to dimensional instability during drying, resulting in warp, crook, and twist of sawn timber. In addition, the gelatinous layer may detach or fibrillate during machining, producing fuzzy surfaces that can adversely affect surface quality and potentially reduce bonding efficiency if not adequately removed during planing operations. Consequently, careful material selection, drying control, and surface preparation are essential when processing grey poplar for structural applications such as glulam and CLT. (Jourez et al. 2001; Clair et al. 2005).

Physical and mechanical property profiles

The mechanical performance of grey poplar indicates a competitive profile compared to conventional softwoods. At 12% moisture content, its mean density ranges from 450 to 520 kg/m³, which is higher than that of Norway spruce (~440 kg/m³) and conventional plantation poplar clones (~380 kg/m³). Bending strength (MOR) and compression strength parallel to grain are highly favorable, meeting or exceeding standard spruce properties when tested on small, clear specimens.

Table 1: Physical and mechanical properties comparison of grey poplar with reference species

Property [Unit]	Grey Poplar (*P.* × *canescens*)	Norway Spruce (*P. abies*)	Plantation Poplar Clones[b]
Density at 12% MC [kg/m³]	450 – 520	430 – 470	350 – 410
Bending Strength (MOR) [MPa]	75 – 90	70 – 85	55 – 70
Modulus of Elasticity (MOE) [GPa]	9.2 – 11.5	10.0 – 12.0	7.2 – 8.8
Compression parallel to grain [MPa]	35 – 45	38 – 48	28 – 35
Radial Shrinkage [%][a]	4.2	3.6	3.8

[a] Determined according to ISO 13061-1; [b] Data adapted from plantation poplar clones (Báder et al. 2022).

However, the Modulus of Elasticity (MOE) displays significant variation. When scaling up to full-size structural boards, defects like knots and grain deviation lead to localized stress concentrations, reducing strength. Because hardwoods are subject to a steep strength reduction with scale, visual or machine-assisted grading rules must be established to classify grey poplar under EN 338.

Characteristics of adhesive bonding of grey poplar

The performance of cross-laminated timber manufactured from grey poplar (Populus canescens) is highly dependent on bond-line quality and the interaction between the adhesive system and the wood substrate. Due to its relatively low density (approximately 575 kg m^{-3}) and diffuse-porous anatomical structure, grey poplar exhibits high permeability and pronounced adhesive penetration behaviour compared with denser hardwood species. While this characteristic can enhance mechanical interlocking between adhesive and wood, excessive penetration may reduce effective bond-line thickness and result in locally starved bond lines if adhesive spread rates and processing parameters are not carefully controlled.

A detailed evaluation of the bonding characteristics of grey poplar conducted by Csiha (2026) demonstrated that the species possesses adhesive properties comparable to those of Scots pine when bonded with commonly used PUR and PVAc adhesive systems. Although the tensile shear strength values remained lower than those obtained for beech, the results confirmed the suitability of grey poplar for both structural and non-structural bonded wood products. The study highlighted that the relatively low density and porous anatomical structure of grey poplar significantly influence adhesive penetration and bond formation, emphasizing the need for optimized bonding parameters in engineered wood applications. These findings suggest that grey poplar can provide satisfactory bond performance and should be considered a promising raw material for value-added wood products, including glulam and CLT.

Adhesion performance and adhesive selection

Experimental investigations by Csiha et al. (2025) further demonstrated that grey poplar can be successfully bonded using both polyurethane (PUR) and polyvinyl acetate (PVAc) adhesive systems. Satisfactory bond performance was achieved using adhesive application rates of approximately 85 g m^{-2} for PUR and 155 g m^{-2} for PVAc under a pressing pressure of 0.8 MPa. Although tensile shear strength values were lower than those obtained for red eucalyptus (Eucalyptus camaldulensis), the results confirmed the suitability of grey poplar for bonded wood products and building applications. The observed differences were attributed primarily to the substantially lower density and different anatomical structure of grey poplar compared with eucalyptus.

The chemical composition of grey poplar may further contribute to its favourable bonding behaviour. Csiha et al. (2025) reported a cellulose content of 48.21%, exceeding that measured for eucalyptus (45.18%). Together with its porous microstructure, this composition supports efficient adhesive penetration and bond formation. Nevertheless, optimization of adhesive viscosity, spread rate, assembly

time, and pressing pressure remains necessary to prevent excessive adhesive absorption and ensure a continuous bond line throughout the panel thickness. For structural applications, bond quality should be verified through shear strength and delamination testing according to EN 302 and relevant CLT product standards. Moisture-curing PUR adhesives have shown particularly good compatibility with grey poplar; however, maintaining wood moisture content within the recommended range of approximately 10–12% remains essential for complete curing and consistent bond performance.

Surface roughness and wettability

Recent research on the surface characteristics and wettability of grey poplar has provided additional evidence of its suitability for engineered wood products. Surface roughness measurements on planed grey poplar sapwood showed values comparable to those of spruce (Ra ≈ 6–7 μm; Rz ≈ 35–40 μm), while dynamic contact-angle measurements revealed rapid liquid spreading after initial wetting. Although the initial contact angles of grey poplar were slightly higher than those measured for spruce, the subsequent spreading behaviour indicated favourable conditions for adhesive interaction and bond development.

These findings suggest that grey poplar possesses surface characteristics compatible with structural bonding applications, including glulam and CLT manufacture. The observed wettability behaviour indicates that, despite minor differences in initial surface energy compared with traditional softwood species, grey poplar provides favourable conditions for adhesive spreading, penetration, and mechanical interlocking. Consequently, its surface properties support the development of durable adhesive bonds required for engineered wood products.

Synthesis of recent research findings on bondability of grey poplar

Recent studies have provided a comprehensive assessment of the suitability of grey poplar (*Populus canescens*) for bonded wood products through the investigation of its bonding performance, adhesive behaviour, and surface characteristics. Bonding tests demonstrated that grey poplar exhibits adhesive properties comparable to those of Scots pine and can achieve satisfactory performance with both PUR and PVAc adhesive systems. Complementary adhesion studies confirmed the compatibility of grey poplar with structural bonding technologies, while highlighting the need to optimize adhesive spread rates and processing parameters due to the species' relatively low density and high permeability. Furthermore, investigations of surface roughness and wettability revealed favourable surface characteristics that support adhesive spreading and bond formation. Taken together, these findings indicate that grey poplar possesses the physical, chemical, and technological properties required for application in engineered wood products and mass timber systems, supporting its consideration as an alternative raw material for glulam, CLT, and other value-added structural products.

Mechanical validation formulations

Structural design requires predicting the nominal bending capacity (M_R) of rectangular cross-sections, calculated via the Navier-Bernoulli equation (Equation 1):

$$M_R = f_m \cdot (b \cdot h^2) / 6 \quad (1)$$

where f_m is the characteristic bending strength [MPa], b is the section width [mm], and h is the section height [mm]. For composite panels, these calculations must incorporate rolling shear resistance ($f_{v,R}$).

CONCLUSIONS

Grey poplar (Populus × canescens) represents a promising, fast-growing domestic hardwood resource in Hungary that remains critically underutilized. Its physical and mechanical profile suggests that it has the raw mechanical capacity to serve as a structural feedstock. However, its industrial application in mass timber products (such as CLT) is currently barred by several key technical limitations:

- The lack of systematic, standardized grading rules for structural-sized grey poplar boards in EN 1912.
- Anatomical instability resulting from high concentrations of tension wood, leading to processing and drying failures.
- The need for optimized bonding parameters to handle its porosity and surface characteristics.

To address these gaps, we propose a research roadmap focused on destructive testing of full-scale grey poplar lamellas to establish characteristic values, developing hybrid CLT layouts (e.g., combining spruce core layers with grey poplar face layers), and executing Life Cycle Assessments (LCA) to fully quantify the ecological advantages of grey poplar in low-carbon regional supply chains.

ACKNOWLEDGEMENTS

The authors express their gratitude to the Faculty of Wood Engineering and Creative Industries, University of Sopron, for providing the experimental infrastructure and regional research databases that made this scoping review possible.

REFERENCES

Báder M, Németh R, Benke A, Köbölkuti ZA, Borovics A, Takács D (2022) Bending test results of plantation poplar clones. In: Németh R, Hansmann C, Rademacher P, Bak M, Báder M (eds) 10th Hardwood Conference Proceedings. University of Sopron Press, Sopron, Hungary, pp 75–82. https://doi.org/10.35511/978-963-334-446-0

Clair B, Thibaut B, Sugiyama J (2005) On the detachment of the gelatinous layer in tension wood fiber. Journal of Wood Science 51(3):218–221. https://doi.org/10.1007/s10086-004-0648-9

Csiha CsM (2026) Evaluation of bonding characteristics of grey poplar (Populus × canescens). Acta Facultatis Xylologiae Zvolen 68(1):5–16. https://doi.org/10.17423/afx.2026.68.1.01

Csiha CsM, Alpár TL, Németh L, Magoss E (2026) Comparative analysis of surface roughness and wettability of grey poplar (Populus × canescens) and spruce (Picea abies). Forests 17(4):400. https://doi.org/10.3390/f17040400

Csiha CsM, Hofmann T, Zinad OS (2025) Investigation into adhesion of coatings and adhesives of eucalyptus and grey poplar for building applications. Forests 16(2):287. https://doi.org/10.3390/f16020287

EN 338 (2016) Structural timber - Strength classes. European Committee for Standardization, Brussels, Belgium.

EN 408 (2010+A1:2012) Timber structures - Structural timber and glued laminated timber - Determination of some physical and mechanical properties. European Committee for Standardization, Brussels, Belgium.

EN 16351 (2021) Timber structures - Cross laminated timber - Requirements. European Committee for Standardization, Brussels, Belgium.

Goswami L, Dunlop JWC, Jungnikl K, Eder M, Gierlinger N, Coutand C, Jeronimidis G, Fratzl P, Burgert I (2008) Stress generation in the tension wood of poplar is based on the lateral swelling power of the G-layer. The Plant Journal 56(4):531–538. https://doi.org/10.1111/j.1365-313X.2008.03617.x

ISO 13061-1 (2014) Physical and mechanical properties of wood - Test methods for small clear wood specimens - Part 1: Determination of moisture content for physical and mechanical tests. International Organization for Standardization, Geneva, Switzerland.

Jourez B, Riboux A, Leclercq A (2001) Comparison of basic density and longitudinal shrinkage in tension wood and opposite wood in young stems of Populus euramericana cv. Ghoy when subjected to a gravitational stimulus. Canadian Journal of Forest Research 31(10):1676–1683. https://doi.org/10.1139/x01-096

Komán Sz (2012) Nemesnyár-fajták korszerű ipari vegyészeti és energetikai hasznosítását befolyásoló faanatómiai és fizikai jellemzők. PhD dissertation, Nyugat-Magyarországi Egyetem, Sopron, Hungary (in Hungarian).

Lautner S, Zollfrank C, Fromm J (2012) Microfibril angle distribution of poplar tension wood. IAWA Journal 33(4):431–439. https://doi.org/10.1163/22941932-90000105

The Effect of Ageing and Finishing Type on the Service Properties of Lacquer Coatings on Oak Wood (*Quercus robur*)

Tomasz Krystofiak[1*], Ahmet Can[2], Dimitar Angelski[3], Barbara Lis[1]

[1] Poznan University of Life Sciences, Poznan, Poland
[2] University in Bartin, Türkiye
[3] University of Forestry, Sofia, Bulgaria.

E-mail: tomasz.krystofiak@up.poznan.pl; acan@bartin.edu.tr; d.angelski@ltu.bg; barbara.lis@up.poznan.pl

Keywords:

ABSTRACT

The aim of the study was to evaluate the utility properties of lacquer products used for finishing flooring elements. Four variants of oxidative varnishes were analysed: standard, white, matte, and additionally brushed, applied to a two-layer parquet made of pedunculate oak wood (*Quercus robur*), obtained under industrial conditions. The aesthetic characteristics, adhesion properties, and mechanical resistance of the coating systems were evaluated in the context of their durability and functional performance. As part of the accelerated ageing tests, after exposure to IR radiation, gloss stability was determined using a Pico Gloss glossmeter, while colour changes were evaluated by visual assessment.

The conducted experiments showed that the analysed coating systems were characterised by high visual qualities, particularly in terms of colour and gloss. It was found that the accelerated ageing process affected the optical properties of the coatings, resulting in a reduction in gloss values and visually perceptible colour changes. All tested variants exhibited very good adhesion to the substrate, with the highest values obtained for the brushed lacquers. The matte coatings showed the greatest resistance to scratching, whereas, in visual assessment, the brushed varnish exhibited the lowest visibility of surface damage. The best results in terms of abrasion resistance were obtained for the white-coated systems, which showed the lowest mass loss. In the impact resistance test, the best properties were demonstrated by the matte-finished elements.

The results indicate that the appropriate selection of a coating system influences the functional and aesthetic properties of flooring elements, including the reduction of visible surface scratches.

The final version of this abstract and the full scientific article are scheduled to be published in the Special Issue "12th Hardwood Conference—Sopron" of the journal MDPI Forests, available at the following link:

MDPI Forests Special Issue: 12th Hardwood Conference—Sopron

Natural Regeneration of European Ash Under Severe Ash Dieback Pressure in Fjugstad Nature Reserve, Norway

Nina Elisabeth Nagy[1*], Mari Mette Tollefsrud[2*], Ane Vollsnes[2], Volkmar Timmermann[1], Isabella Børja[1], Ari Hietala[1]

[1] Norwegian Institute of Bioeconomy Research (NIBIO), Dept. Fungal Plant Pathology in Forestry, Agriculture and Horticulture, Høgskoleveien 8, 1433 Ås, Norway
[2] Norwegian Institute of Bioeconomy Research (NIBIO), Dept. Forest genetics and Regeneration, Høgskoleveien 8, 1433 Ås, Norway.

E-mail: nina.elisabeth.nagy@nibio.no; mari.mette.tollefsrud@nibio.no

Keywords: *Fraxinus excelsior*; *Hymenoscyphus fraxineus*; ash dieback; natural regeneration; seedling survival; environmental gradients; forest health.

ABSTRACT
European ash (*Fraxinus excelsior*) is a key broadleaved tree species in Norwegian temperate deciduous forests, but it is severely threatened by ash dieback caused by the pathogenic fungus *Hymenoscyphus fraxineus*. In Fjugstad Nature Reserve in south-eastern Norway, mature ash trees are heavily affected, while natural regeneration is still abundant. This study examines whether natural regeneration may contribute to maintaining ash in forests under severe disease pressure, and which local environmental factors influence establishment, growth and survival.

In 2025, we established a standardized monitoring system with three main transects covering variation in topography, vegetation and soil moisture. Within 2 m × 20 m plots, adult trees, shrub layer composition, crown damage, decay symptoms and deadwood were recorded. Associated 2 m × 2 m subplots were used to quantify ash regeneration, disease symptoms and mean seedling height. Selected seedlings were harvested for age determination by annual-ring counts and measurements of height and root collar diameter. These data were combined with long-term monitoring data from approximately 240 marked ash seedlings followed from 2019 to 2025 in two permanent plots.

The adult ash population was in poor condition. Among 75 large ash trees recorded in the plots, only two had no crown damage, 70% were dead and 80% showed extensive decay, mainly associated with secondary rot fungi. No healthy seed trees were found within the main plots. In the shrub layer, 80% of 68 ash individuals showed symptoms of ash dieback. Nevertheless, regeneration was abundant: more than 3,015 ash seedlings were recorded in 50 subplots, and 33% showed disease symptoms (Figure 1A). At subplot level, the proportion of symptomatic seedlings increased significantly with mean regeneration height (Figure 1B; Pearson $r = 0.66$, $p < 0.001$), whereas no clear relationship was found with mean seedling age and density. Individual seedling height was strongly related to root collar diameter ($R^2 = 0.86$), but more weakly related to age ($R^2 = 0.39$), indicating large variation in growth rate among seedlings of similar age.

Long-term data showed declining survival from 2019 to 2025, with faster and higher mortality in one of the two permanent plots. Cumulative mortality ranged from 20.5% to 35.7% among age classes in the drier plot, compared with 50.0% to 63.1% in the plot with generally higher soil moisture. Preliminary mixed-model analyses suggested that slightly drier microsites supported higher densities of regeneration and more healthy seedlings. Higher light exposure was associated with a lower proportion of healthy regeneration, but this relationship should be interpreted cautiously, as light may also influence growth rate and seedling height, which in turn were related to disease incidence. Further analyses are needed to separate direct effects of light from indirect effects mediated through growth and local infection pressure.

Our results show that natural regeneration of ash is still extensive in Fjugstad, but that transition from seedling and shrub layers into the tree layer represents a critical bottleneck. Local moisture conditions, light environment, growth rate and infection pressure appear to influence seedling performance. Continued spatial monitoring may help identify microsites and individual trees with potential for future ash persistence and inform targeted conservation and management of ash-dominated hardwood forests affected by ash dieback.

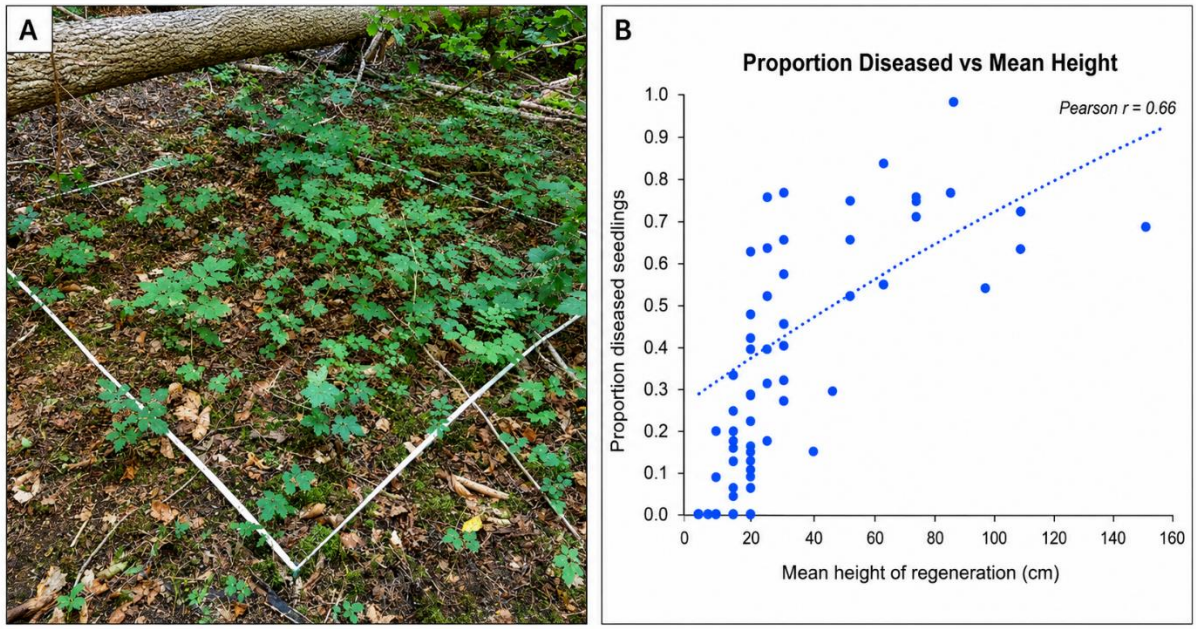

Figure 1: (A) Example of a 2 m × 2 m subplot used to assess natural regeneration of European ash (Fraxinus excelsior). (B) Relationship between mean regeneration height and the proportion of symptomatic ash seedlings in subplots. Disease incidence increased with mean regeneration height (Pearson r = 0.66, p < 0.001)

Hardwood's Role in Sustainable Construction: A Multidimensional Analysis

Konstantin Schneider[1], Sascha Bicke[1*]

[1] University of Applied Sciences Erfurt, Faculty of Landscape Architecture, Horticulture and Forestry. Leipziger Str. 77, Erfurt, Germany, 99085.

E-mail: konstantin.schneider@fh-erfurt.de; sascha.bicke@fh-erfurt.de

Keywords: hardwood utilization, sustainable construction, climate-effective building solutions.

ABSTRACT

The climate change-induced restructuring of forests in Central Europe leads to a long-term shift in the composition of tree species, increasing the proportion of hardwood-rich stands.

However, established scenario models, such as the forest development and timber resource model (WEHAM), show that the absolute proportion of hardwood will stagnate in the medium term under current conditions, while forest policy objectives, particularly biodiversity and carbon sink targets, limit the utilization potentials. According to the WEHAM baseline scenario, a general decrease in the raw timber potential of all hardwood species of almost 5.5 % is expected between the projection periods 2023-2027 and 2058-2062. The proportion of the main hardwood species, beech (Fagus sylvatica), is expected to decline by approximately 10 %, while the proportion of oak (Quercus spp.) is expected to increase by almost 14 %. At the same time, the high-quality material use of hardwood in timber construction remains marginal. A significant portion of harvested hardwood is used for energy, leaving potentials for long-term carbon storage in building products and for substituting emission-intensive materials untapped.

Against this background, the project investigates the strategic potentials of hardwood for multi-story construction and modernization. The core question is under which technical, market-related, and regulatory conditions hardwood can contribute to the development of climate-effective construction methods. A systematic literature review shows that hardwoods exhibit their strengths notably in high-stress, material-efficient constructions. Due to their high strength and stiffness values, species like beech, oak, ash, or birch are particularly suitable for wide-span beams, slender columns, load-bearing nodes, and hybrid constructions (Table 1).

Table 3: Comparison of existing hardwood and softwood products' raw-density and flexural modulus (mean values)

Designation	Wood type	Raw-Density [kg/m^3]	Flexural modulus [GPa]
1 *BauBuche* GL70	**1** *Fagus sylvatica*	**1** 800	**1** 16.80
2 *Hasslacher GLT Birch*	**2** *Betula spp.*	**2** 620	**2** 15.00
3 Moulded beech (SSH 48)	**3** *Fagus sylvatica*	**3** 690	**3** 16.00
4 Moulded Ash (SSH 48)	**4** *Fraxinus excelsior*	**4** 680	**4** 15.00
5 Standardized beech beam	**5** *Fagus sylvatica*	**5** 732	**5** 14.15
6 Cross-laminated timber (CLT)	**6** Softwood	**6** 500	**6** 8.00
7 Structural timber (KVH)	**7** Softwood	**7** 500	**7** 11.60

Laminated or veneer-based materials, molded profiles, or hybrid systems are examples of how constructive principles from steel construction can be transferred to hardwood. This enables material-efficient cross-sections and reduced component dimensions. Simultaneously, combining with softwoods or mineral materials opens new optimization approaches. Even perceived disadvantages, such as stronger swelling and shrinkage, can be constructively harnessed, for example, to create pre-stressing in floor beams using moisture from cast-in-place concrete, potentially saving traditional support systems.

The central potential thus does not lie in the volumetric substitution of softwood in the mass market, but in targeted high-performance applications with substantial value creation.

To evaluate innovative product developments in the hardwood segment, a scoring model was developed, that summarizes technical, sustainability-oriented, and economic product properties into a defined score. It confirmed that hardwood materials display high to very high mechanical properties, although dimensional stability remains a persistent issue. Given the low global warming potential of hardwood materials during production phases A1-A3, according to DIN EN ISO 14040, they are considered sustainable despite increased energy requirements for processing and bonding. The technical and sustainable potentials face structural obstacles. The absence of standardizations, as known in the softwood industry, and the lack of systems tailored to the advantages of hardwood constructions (e.g., standard dimensions for panel materials), lead to difficulties in building code integration and market unawareness. Conducted market analyses indicate low demand, weak capacity utilization of hardwood processing enterprises, and a lack of investment incentives.

The results illustrate that future hardwood utilization is determined less by raw material supply than by demand stimuli and policy frameworks. Sustainability regulations, such as CO_2 limits in construction, Environmental, Social, and Governance criteria (ESG), the EU taxonomy, and CO_2-oriented financing instruments can create options that represent a significant economic factor for the use of hardwood in construction. When emissions and material efficiency become financially relevant, high-performance hardwood products gain strategic importance. Thus, hardwood can act as a "nature-based solution" bridging forest development, construction transition, and financial transition.

Birch Plywood in Connections of Timber Structures

Roberto Crocetti[1,2], Tianxiang Wang[1], Lars Blomqvist[3], Dániel Honfi[4,2*]

[1] KTH Royal Institute of Technology, Department of Civil and Architectural Engineering, Brinellvägen 23, 114 28 Stockholm, Sweden
[2] TBS Timber Bridge Specialists, Kvarnbergsgatan 2, 411 05 Göteborg, Sweden
[3] SCI TECH WOOD, Tomtebyholm 670, 395 91 Kalmar, Sweden
[4] Uppsala University, Department of Civil and Industrial Engineering, Regementsvägen 10, 751 04 Uppsala, Sweden.

E-mail: crocetti@kth.se; tiawan@kth.se; lars@lbwoodtech.se; daniel.honfi@angstrom.uu.se

Keywords: birch plywood, wooden connections, timber construction.

ABSTRACT
Load-bearing timber structures often rely on steel components in their connections, which makes them relatively costly, carbon-intensive, and prone to long lead times. Timber-based alternatives offer several advantages, including lower cost, easier storage and transport, easier assembly, and reduced environmental impact.
In Sweden, with 68& of its area covered by forests, softwood species such as spruce and pine dominate. Thus, these species are the primary raw materials used in construction. At the same time, sustainable forest management is shifting from uniform conifer stands towards more mixed and structurally diverse forests. In the Nordic region, birch is increasingly introduced into forest mixtures to reduce climate-related risks and enhance biodiversity. This also increases the potential to convert forest carbon into long-lived wood products. As a result, the supply of hardwood is expected to grow.
In this context, local hardwoods such as birch offer a promising alternative to steel components in timber connections. Birch is relatively fast-growing, readily available domestically, and easier to process than steel, while providing suitable strength and stiffness for structural applications. In addition, its visual appearance makes it attractive for use in exposed surfaces.
This contribution presents recent research investigations and pilot projects arising from collaborations between academia and industry, with a focus on the use of birch plywood in connections for timber structures, such as shown in Figure 1.

Figure 1: Truss connection prototype made with sheets of birch plywood inserted into glulam members (a) and application of the concept in a real structure (b)

Integrating Genomics and Transcriptomics to Explore Wood Properties and Stress Responses in Poplar Species

Zoltán Attila Köbölkuti[1*], Klára Cseke[1], Botond Boldizsár Lados[1], Katalin Bereczki[1], Roland Takács[1], Valter Toldi[1], Attila Benke[1]

[1] Department of Forest Tree Breeding, Forest Research Institute, University of Sopron, Sárvár, Hungary.

E-mail: kobolkuti.zoltan@uni-sopron.hu; cseke.klara@uni-sopron.hu; lados.botond@uni-sopron.hu; bereczki.katalin@uni-sopron.hu; takacs.roland@uni-sopron.hu; toldi.valter@uni-sopron.hu; benke.attila@uni-sopron.hu

Keywords: *Populus*; ddRAD-seq; SNP markers; heartwood formation; comparative genomics; RNA-seq; drought stress; stress adaptation.

ABSTRACT

Poplars (*Populus* spp.) are economically and ecologically important tree species whose key traits are still only partially understood at the genetic level. The aim of our research is to establish an integrated framework for investigating the genetic basis of wood properties and responses to environmental stress. The work is organized into three parallel research directions. The first component focuses on the development of a ddRAD-seq-based genomic resource using natural populations of three poplar taxa: European aspen (*Populus tremula*), white poplar (*Populus alba*), and their natural hybrid, grey poplar (*Populus* × *canescens*). Bioinformatic processing resulted in the identification of nearly 80,000 high-confidence SNP markers, providing a foundation for subsequent population genetic analyses and for exploring genetic variation associated with heartwood colour. The second research direction aims to identify candidate genes involved in heartwood formation through comparative genomics and to develop molecular markers based on these genes. Primer pairs have been designed and are being tested for genes associated with several biochemical pathways involved in colour formation, including flavonoid and phenylpropanoid metabolism. The third component involves the establishment of an RNA-seq-based experimental system to investigate gene expression responses of poplar species to drought stress. This work will enable the identification of genes and regulatory pathways associated with stress adaptation. Together, these three complementary research directions may provide new tools and genetic resources for studying economically important wood properties and adaptive traits in poplar species, while also supporting future breeding and conservation efforts.

Characterization of UV-Assisted Lignin-Modified Beech Veneer as an Initial Step Towards Transparent Wood Preparation

Dávid Takács[1*], Miklós Bak[1]

[1] University of Sopron, Faculty of Wood Engineering and Creative Industries. Bajcsy-Zs. Str. 4, Sopron, Hungary, 9400.

E-mail: takacs.david@uni-sopron.hu, bak.miklos@uni-sopron.hu

Keywords: transparent wood; beech veneer; lignin modification; UV-A irradiation; colour change; FTIR spectroscopy.

ABSTRACT

Transparent wood preparation commonly requires the reduction of light absorption associated with lignin and lignin-derived chromophores. This study investigated two UV-A-assisted lignin-modification treatment variants applied to European beech (*Fagus sylvatica*) veneer as an initial step towards transparent wood preparation. Sodium hydroxide and hydrogen peroxide solutions were applied to both surfaces of the specimens by brushing, followed by UV-A irradiation in six consecutive 30-min treatment blocks. In the Delig 3.1 variant, the same veneer surface was exposed to the UV-A source throughout the treatment, whereas the Delig 3.2 specimens were turned after the second and fourth treatment blocks. Treatment-induced changes were evaluated by mass, thickness, CIELab colour measurements, and FTIR difference spectroscopy.

Both treatment variants caused considerable mass loss, reaching 20.456 ± 2.413% for Delig 3.1 and 21.807 ± 2.174% for Delig 3.2. At the same time, veneer thickness increased by 25.177 ± 4.913% and 22.707 ± 4.148%, respectively. Colour measurements indicated pronounced lightening, with ΔL* values of 30.91 and 28.95 and total colour differences of 35.71 and 34.34 for Delig 3.1 and Delig 3.2, respectively. FTIR difference spectra showed treatment-induced changes in the 1900–900 cm^{-1} region, indicating chemical modification of the veneer.

The two treatment variants produced broadly similar physical, optical, and chemical responses. Under the applied conditions, turning the specimens during UV-A exposure did not result in a clearly distinguishable overall improvement. The results provide a basis for further optimization and subsequent transparent wood preparation.

INTRODUCTION

Wood is a renewable hierarchical material with favourable mechanical properties and considerable potential for functional modification. In recent years, transparent wood has received increasing attention as a wood-based optical material combining the structural framework of natural wood with light-transmitting and light-scattering properties. Potential applications include energy-efficient building elements, light-management systems, photonic devices, and multifunctional wood composites (Li T et al. 2016; Li Y et al. 2018).

The optical opacity of natural wood is caused by both light absorption and light scattering. Lignin and lignin-derived chromophoric structures contribute substantially to the absorption of visible light, while differences in refractive index between the wood cell-wall components and the air-filled cellular structure cause strong light scattering. Conventional transparent wood preparation therefore generally consists of two main steps: partial or extensive lignin removal followed by infiltration of the porous wood structure with a transparent polymer having a refractive index close to that of the cell wall. Although effective, extensive delignification may require long processing times and substantial chemical consumption and may affect the structural integrity of the wood template.

As an alternative to complete lignin removal, recent approaches have focused on the chemical modification of lignin chromophores while retaining a larger proportion of the lignin within the cell wall. Oxidative treatments based on hydrogen peroxide, combined with light-assisted activation, can reduce wood colour and visible-light absorption through modification of lignin-associated chromophoric groups. Chemical brushing and irradiation-based approaches may also enable more localised and potentially scalable processing compared with conventional immersion-based

delignification methods (Xia et al. 2021a, b). However, treatment efficiency may depend on chemical concentration, irradiation conditions, treatment duration, specimen dimensions, and the orientation of the wood surface relative to the radiation source.
In the present study, a modified UV-A-assisted lignin treatment was applied to beech veneer using sodium hydroxide and hydrogen peroxide. Two treatment variants were compared: in Delig 3.1, the same veneer surface was oriented towards the UV-A source throughout the repeated treatment blocks, whereas in Delig 3.2, the specimens were turned between treatment blocks. Treatment-induced changes were evaluated by mass, thickness, CIELab colour measurements, and FTIR difference spectroscopy. The aim was to characterise the physical, optical, and chemical effects of the two treatment variants and to provide a basis for the future optimisation of beech-based transparent wood preparation.

MATERIALS AND METHODS

European beech (*Fagus sylvatica*) veneer was used in this study. The specimen dimensions were 40 × 40 mm and 40 × 10 mm, with a thickness of 0.5 mm. Hydrogen peroxide (30% H_2O_2 solution) and sodium hydroxide (10% NaOH solution) were used for lignin modification. The UV-A light source consisted of three light tubes, each with a rated power of 30 W. The specimens were oven-dried at 103 ± 2 °C before the measurements performed both before and after treatment.
The lignin-modification procedure was based on the method reported by Xia et al. (2021 a) and on our previous work (Takács et al. 2024). The H_2O_2 and NaOH solutions were applied to both surfaces of the specimens using a brush. The specimens were then placed under UV-A light. The specimen holder was positioned 3 cm below the light tubes. At this distance, the measured UV-A irradiance was 0.579 ± 0.087 mW cm^{-2}.
The treatment was carried out in six consecutive blocks of 30 min each. During the first, third, and fifth blocks, both NaOH and H_2O_2 were applied to the specimen surfaces. During the second, fourth, and sixth blocks, only H_2O_2 was applied. Two treatment variants, designated Delig 3.1 and Delig 3.2, were investigated. For Delig 3.1, the same side of each specimen was exposed to the UV-A source throughout the entire treatment. For Delig 3.2, the specimens were turned over after the second and fourth treatment blocks.
Following treatment, the specimens were successively immersed in distilled water, ethanol, and acetone. Each immersion step lasted 24 h.
Mass measurements were performed both before and after treatment. Mass loss (ML) was calculated from the oven-dry mass before treatment (m_{b0}) and the oven-dry mass after treatment (m_{a0}), according to Equation 1:

$$ML = \frac{m_{b0} - m_{a0}}{m_{b0}} \cdot 100 \quad (1)$$

Thickness was measured before and after treatment at three points on each specimen. The relative thickness change (ΔT) was calculated from the dry thickness before treatment (t_{b0}) and the dry thickness after treatment (t_{a0}) according to Equation 2:

$$\Delta T = \frac{t_{a0} - t_{b0}}{t_{a0}} \cdot 100 \quad (2)$$

Colour was measured before and after treatment using a Konica Minolta CM2600d spectrophotometer under D65 illumination and a d/8 standard observer. Measurements were performed at same positions on each specimen. The changes in the colour coordinates (ΔL*, Δa* and Δb*) were determined as the differences between the values measured after treatment and the initial values. The total colour difference (ΔE*) was calculated using the following equation (Eq. 3):

$$\Delta E^* = \sqrt{(\Delta L^*)^2 + (\Delta a^*)^2 + (\Delta b^*)^2} \quad (3)$$

FTIR spectra were recorded before and after treatment using a JASCO, FT/IR-6300 spectrometer equipped with a DRITS accessory. Spectra were collected over the range of 4000–400 cm^{-1} at a spectral resolution of 4 cm^{-1} using 50 scans per measurement. Measurements were performed at same positions on each specimen. The resulting Kubelka–Munk spectra were vector-normalized over the 1900–900 cm^{-1} spectral range. The difference spectra were calculated by subtracting the initial spectrum from the corresponding treated spectrum.

RESULTS AND DISCUSSION

Physical changes

Both UV-A-assisted treatment variants resulted in a substantial decrease in the mass of the beech veneer specimens. The mean mass loss was 20.456 ± 2.413% for Delig 3.1 and 21.807 ± 2.174% for Delig 3.2. This mass loss suggests that some wood components were degraded and subsequently leached out during treatment and washing. Further analyses would be required to determine which wood constituents contributed most to the observed mass loss.

In contrast to the mass loss, the thickness of the veneers increased after treatment. The mean thickness increase was 25.177 ± 4.913% for Delig 3.1 and 22.707 ± 4.148% for Delig 3.2. This increase may be associated with swelling and structural loosening of the veneer caused by the alkaline and oxidative treatment (Chen et al. 2025). The relatively large increase in thickness indicates that the treatment affected not only the surface colour but also the dimensional state of the thin veneer specimens. Although the mean thickness increase was slightly greater for Delig 3.1 than for Delig 3.2, the values were within a similar range.

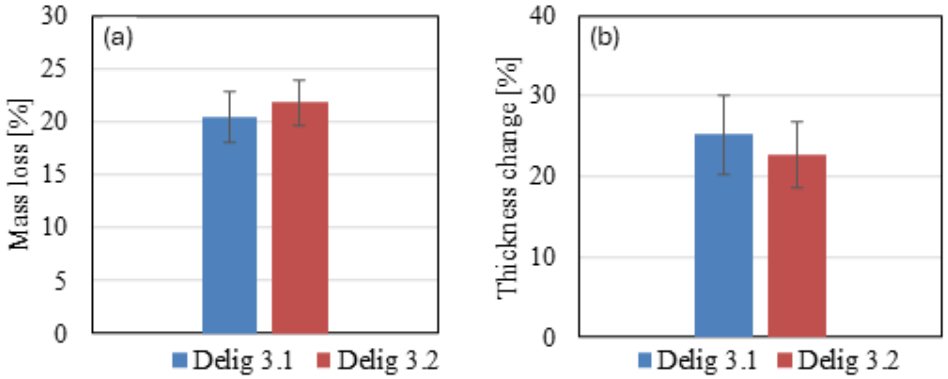

Figure 1: Physical changes of beech veneer after UV-A-assisted lignin modification: mass loss (a) and thickness change (b). Bars represent mean values with error bars showing standard deviation

Colour changes

The colour measurements revealed pronounced treatment-induced optical changes for both treatment variants. The positive ΔL* values indicated a substantial increase in lightness, reaching 30.91 for Delig 3.1 and 28.95 for Delig 3.2. These results indicate that the UV-A-assisted $NaOH/H_2O_2$ treatment effectively lightened the surface of the beech veneers. At the same time, both Δa* and Δb* were negative. The decrease in a* indicates a shift away from the red colour component, whereas the decrease in b* reflects a reduction in yellowness. These changes are consistent with the expected effects of lignin modification, since lignin and lignin-derived chromophores contribute substantially to the natural colour of wood.

The total colour difference was high for both treatment variants, with ΔE* values of 35.71 for Delig 3.1 and 34.34 for Delig 3.2. These values correspond to clearly visible colour changes after treatment. The slightly higher ΔE* and ΔL* values observed for Delig 3.1 suggest somewhat more pronounced lightening, whereas Delig 3.2 showed a slightly greater decrease in b*. Overall, the two treatment variants produced similar optical changes, and the effect of specimen orientation during UV-A exposure could not be clearly distinguished based on the colour measurements alone. Nevertheless, it should be noted that, although the specimens reached a sufficiently lightened appearance by the end of the treatment, the bleaching process was not uniform during the intermediate treatment stages.

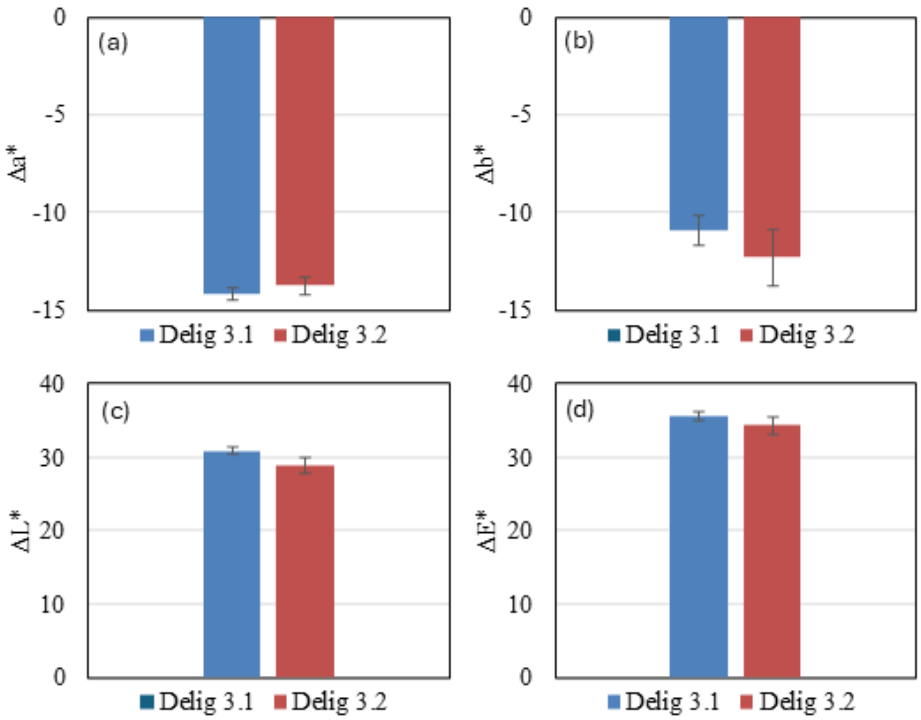

Figure 2: CIELab colour changes of beech veneer after UV-A-assisted lignin modification: Δa* (a), Δb* (b), ΔL* (c), and ΔE* (d). Bars represent mean values, and error bars indicate standard deviations

FTIR difference spectra

FTIR spectra were baseline corrected and vector normalized in the 1900–900 cm^{-1} region. Difference spectra were calculated for each specimen by subtracting the pre-treatment spectrum from the post-treatment spectrum measured at the same location. The resulting difference spectra were averaged for each treatment variant. This paired approach reduces the influence of natural variability within the veneer specimens and allows treatment-induced spectral changes to be evaluated more directly.

The FTIR difference spectra showed clear changes in the 1900–900 cm^{-1} region for both treatment variants. The observed positive and negative bands indicate chemical changes in lignin- and carbohydrate-related spectral regions. These changes are consistent with the expected effect of alkaline peroxide treatment combined with UV-A exposure, which can modify chromophoric structures and functional groups associated with lignin. The two treatment variants showed broadly similar spectral patterns, although Delig 3.2 appeared to exhibit somewhat stronger changes in selected regions. Without statistical analysis or detailed band assignment, these differences should be interpreted cautiously.

Comparison of treatment variants

The two treatment variants produced broadly similar physical, optical, and chemical responses. Delig 3.2 showed a slightly greater mean mass loss and somewhat larger FTIR difference intensities in selected spectral regions. In contrast, Delig 3.1 showed a slightly greater thickness increase and slightly higher ΔL* and ΔE* values.

The observed differences did not indicate a consistent advantage for either treatment variant. In particular, turning the specimens between treatment blocks did not result in a clearly distinguishable improvement in the measured physical or optical properties. Since no statistical analysis was performed, the differences between Delig 3.1 and Delig 3.2 should be interpreted as tendencies rather than confirmed treatment effects.

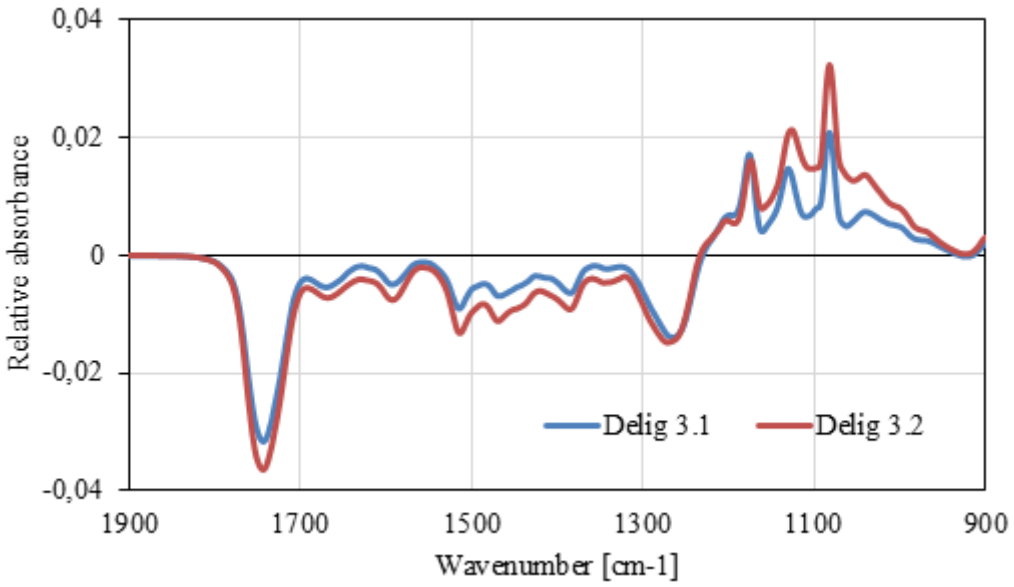

Figure 3: Average FTIR difference spectra of UV-A-assisted lignin-modified beech veneer

CONCLUSIONS

The UV-A-assisted NaOH/H_2O_2 treatment caused substantial physical, optical, and chemical changes in beech veneer. Both treatment variants resulted in considerable mass loss, increased veneer thickness, pronounced lightening, and detectable changes in the FTIR difference spectra.

Delig 3.1 and Delig 3.2 produced broadly similar results. Although small differences were observed in mass loss, thickness increase, colour parameters, and FTIR difference intensities, neither treatment variant showed a consistent overall advantage. Based on the present measurements, the effect of turning the specimens during UV-A exposure could not be clearly distinguished.

The results demonstrate that the applied treatments are promising approaches for the preliminary modification of beech veneer. However, their suitability for transparent wood preparation can only be confirmed after polymer impregnation and subsequent optical characterization. Further work should therefore include statistical evaluation, optimization of the chemical and irradiation parameters, and the preparation and testing of transparent wood samples.

<u>Ongoing work</u>

Preliminary transparent wood specimens have already been prepared from the lignin-modified beech veneers. However, further optimization and quantitative optical and physical characterization are required before the suitability of the treatment variants can be evaluated.

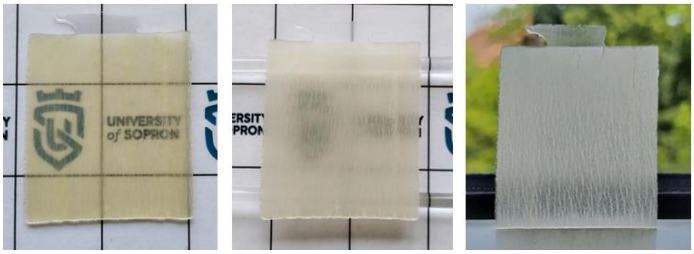

Figure 4: Preliminary transparent wood specimens prepared from lignin-modified beech veneer. Optical characterization has not yet been performed

ACKNOWLEDGEMENTS

This article was made in the framework of the project TKP2021-NKTA-43, which has been implemented with the support provided by the Ministry of Culture and Innovation of Hungary from the National Research, Development and Innovation Fund, financed under the TKP2021-NKTA funding scheme.

REFERENCES

Chen H, Garemark J, Li L, et al (2025) Green Nanotechnology of Cell Wall Swelling for Nanostructured Transparent Wood of High Optical Performance. Small 21:2406749. https://doi.org/10.1002/smll.202406749

Li T, Zhu M, Yang Z, et al (2016) Wood Composite as an Energy Efficient Building Material: Guided Sunlight Transmittance and Effective Thermal Insulation. Advanced Energy Materials 6:1601122. https://doi.org/10.1002/aenm.201601122

Li Y, Vasileva E, Sychugov I, et al (2018) Optically Transparent Wood: Recent Progress, Opportunities, and Challenges. Advanced Optical Materials 6:null. https://doi.org/10.1002/adom.201800059

Takács D, Hanzséros O, Bak M (2024) Production of transparent wood with UV assisted lignin modification using beech and oak wood,. In: Proceedings of the 2020 Society of Wood Science and Technology International Convention 63-67 p.

Xia Q, Chen C, Li T, et al (2021a) Solar-assisted fabrication of large-scale, patternable transparent wood. Sci Adv 7:eabd7342. https://doi.org/10.1126/sciadv.abd7342

Xia Q, Chen C, Yao Y, et al (2021b) In Situ Lignin Modification toward Photonic Wood. Adv Mater 33:2001588. https://doi.org/10.1002/adma.202001588

Session II
-
Hardwood Structure and Properties

Correlations Among Select Properties and Anatomical Parameters of *Simarouba Amara* Wood

Clara Gaspar Fossi de Souza[1*], André Luis Christoforo[2], Francisco Antonio Rocco Lahr[1]

[1] University of São Paulo / Department of Materials Science and Engineering – 13566-590 – São Carlos – SP, Brazil
[2] Federal University of São Carlos / Department of Civil Engineering - 13565-905 - São Carlos, SP – Brazil.

E-mail: clara.gaspar@hotmail.com; christoforoal@yahoo.com.br; frocco@sc.usp.br

Keywords: wood anatomy; mechanical properties; apparent density, tropical hardwood.

ABSTRACT

Wood anatomy plays a fundamental role in determining physical and mechanical behaviour; however, structure–property relationships are still insufficiently understood for most lightweight tropical species. In this study, correlations between anatomical features and physical–mechanical properties were evaluated for *Simarouba amara* (Caixeta), a fast-growing Amazonian hardwood with potential for engineered applications. Twelve clear specimens were extracted from structural beams, and mechanical properties were determined following ABNT NBR 7190-3:2022, resulting in characteristic values of compressive strength ($f_{c0,k}$ = 38.43 MPa), tensile strength parallel to the grain ($f_{t0,k}$ = 47.84 MPa), shear strength ($f_{v0,k}$ = 7.29 MPa), and modulus of elasticity in compression (E_{c0} = 7,939 MPa), classifying the species as D30. Apparent density averaged 0.33 g/cm³ (CV = 2.75%). Anatomical characterization, performed by optical microscopy, included fiber dimensions (length, diameter, lumen diameter, and wall thickness), as well as vessel diameter and frequency, and ray dimensions. Correlations were quantified using Pearson's coefficient and tested by ANOVA at a 5% significance level. Fiber wall thickness (Twf) and lumen diameter (Dl) showed the strongest relationships with density (r = 0.356 and −0.404), while vessel frequency (Frv) and vessel diameter (Dv) were significantly associated with shear strength (r = 0.701 and 0.863, respectively). Ray width (Wr) correlated with compressive strength (r = 0.753), and lumen diameter showed a negative relationship with stiffness (E_{c0}; r = −0.727). A strong inverse correlation between lumen diameter and fiber wall thickness (r = −0.809) highlights the importance of cell wall fraction in controlling mechanical behaviour. Overall, the findings demonstrate that anatomical parameters can serve as reliable predictors of structural performance in *S. amara*, supporting the development of more efficient characterization approaches for lesser-known tropical woods.

INTRODUCTION

Wood has been a fundamental structural material in human civilization for millennia, and its relevance in contemporary construction has been significantly renewed in the face of growing environmental and sustainability demands (Ramage et al. 2017; Joung et al. 2024). As a renewable, carbon-sequestering resource with a favorable strength-to-weight ratio, timber has attracted increasing scientific and engineering interest as a substitute for energy-intensive materials such as concrete and steel (Lestari and Ikaputra 2024).

Physical and mechanical characterization of wood is essential for its safe use in structural applications. In Brazil, this process is regulated by the ABNT NBR 7190 codes, recently updated by NBR 7190-3:2022, which refines experimental procedures and emphasizes key properties such as the modulus of elasticity and modulus of rupture. In this context, the inclusion of lesser-known species represents both a scientific challenge and a strategic opportunity to expand the sustainable use of wood in civil engineering (Aguiar et al. 2025).

Wood anatomy occupies a central position in the understanding of timber performance. The cellular architecture of wood encompassing the dimensions and proportions of fibers, vessels, rays, and parenchyma directly conditions the physical and mechanical responses of the material (Hugo I. Martínez-Cabrera et al. 2011). Species with high wood density typically exhibit thick-walled fibers,

while low-density species tend to present fibers with proportionally thinner walls and larger lumen diameters (Chave et al. 2009). However, recent investigations have demonstrated that physical properties such as density and dimensional stability are not solely determined by fiber dimensions, but emerge from the combined effects of all wood cell types including vessel area and density, ray width and height, and the proportion of axial parenchyma (Monteiro et al. 2026).
The use of anatomical parameters as predictors of mechanical performance is a research frontier of considerable practical relevance. Establishing statistically significant correlations between anatomical traits and properties such as compression strength parallel to the grain (f_{c0}), tensile strength (f_{t0}), shear strength (f_{v0}), and elastic moduli would enable more efficient characterization protocols, potentially reducing the reliance on large sample sets and costly destructive testing (Lukovic et al. 2024).
Caixeta (*Simarouba amara*) is a tropical native species widely distributed in the Amazon, characterized by rapid growth and a pioneer role in secondary forests. Its wood is lightweight, with low density (< 0.40 g/cm³), featuring a diffuse-porous structure and large vessel diameters (ITTO 2024). Despite its use in light applications, comprehensive studies on its physical and mechanical properties according to ABNT NBR 7190-3:2022, as well as their relationship with anatomical characteristics, are still lacking.
In this framework, the present study investigates the correlations among selected anatomical parameters and physical-mechanical properties of Caixeta wood, with the objective of determining whether anatomical features specifically fiber length, fiber and lumen diameter, fiber wall thickness, vessel diameter, vessel frequency, and ray dimensions can serve as statistically reliable predictors of mechanical performance.

MATERIALS

This study focused on Caixeta wood (*Simarouba amara*), a native species sourced from the southern region of Brasnorte, Mato Grosso State, Brazil. Structural timber pieces twelve beams ranging from 4.0 to 4.5 m in length were collected from mature trees with estimated ages exceeding 50 years.
A total of twelve specimens were extracted from the Caixeta beams and prepared for mechanical and physical testing in accordance with the procedures set forth in ABNT NBR 7190-3:2022 (ABNT 2022a). For microscopic characterization, wood blocks were cut to expose the three principal anatomical planes: longitudinal, radial, and tangential.
Histological preparation comprised twelve permanent slides four sections per anatomical orientation (radial, longitudinal, and tangential). An additional set of eight slides was produced from macerated wood material for the quantitative assessment of individual anatomical parameters.

METHODS

Determination of apparent density and dimensional stability

Apparent density (ρap) was calculated as the ratio between the mass and volume of the specimens conditioned to a moisture content of 12%, as shown in Equation (1):

$$\rho_{ap} = m_{12} / V_{12} \quad (1)$$

where m_{12} corresponds to the specimen mass at 12% moisture content (kg), and $\mathbf{V_{12}}$ is the respective volume at the same moisture condition (m³).
The cross-sectional dimensions were measured using a digital caliper with 0.1 mm precision, while mass was determined with an analytical balance with 0.01 g resolution.
Dimensional stability was assessed through the linear shrinkage coefficient (εr), calculated separately for the radial (R) and tangential (T) directions, in accordance with ABNT NBR 7190-3:2022 (ABNT 2022a), as presented in Equation (2):

$$\varepsilon r = (L_{i,sat} - L_{i,dry}) / L_{i,sat} \quad (2)$$

where $L_{i,sat}$ represents the dimension at moisture content equal to or above the fiber saturation point, and $L_{i,dry}$ corresponds to the dimension at 0% moisture content.

Mechanical testing

All mechanical tests were performed in compliance with ABNT NBR 7190-3:2022 (ABNT 2022a), using a servo-controlled universal testing machine (AMSLER, 250 kN capacity). The evaluated properties for Caixeta wood included compressive strength and modulus of elasticity parallel to the grain (f_{c0} and E_{c0}), shear strength parallel to the grain (f_{v0}), radial and tangential shrinkage (RS and TS), tensile strength and modulus of elasticity parallel to the grain (f_{t0} and E_{t0}), as well as tensile strength perpendicular to the grain (f_{t90}). The obtained results were corrected to a standard moisture content of 12% using the procedures specified in Section 5.6.1 of ABNT NBR 7190-1:2022 (ABNT 2022b).

Microscopic analysis

Quantitative wood anatomy focused on three categories of cellular elements: fibres (length, wall thickness, and total diameter), vessel elements (frequency per mm² and mean diameter), and rays (height and width). All measurements followed the guidelines established by ABNT NBR 15066 (ABNT 2004) and the International Association of Wood Anatomists (IAWA) (IAWA 1989).

Individual fibre characteristics were obtained from macerated material. Small wood chips (30–40 fragments per sample) were isolated from each Caixeta specimen and subjected to the Franklin maceration protocol (Johansen 1940; Sass 1951). Briefly, chips were transferred to Erlenmeyer flasks, submerged in a 1:1 (v/v) mixture of glacial acetic acid and 30% hydrogen peroxide, sealed, and held at 50 °C in a forced-air oven for 24 hours, following the procedures described by Marini *et al*. (Marini et al. 2022b, a) and Souza *et al.* (Souza et al. 2025). After the thermal treatment, macerated fibres were rinsed three times with distilled water to remove residual reagents and subsequently stained with a 1% aqueous safranin solution.

A small volume of stained suspension was deposited onto a glass slide, covered with a coverslip care being taken to exclude air bubbles and examined under an optical microscope (Olympus EX51). All fibre measurements were performed on this material. Wall thickness (T_{wf}) was derived from fibre diameter and lumen diameter data using Equation (3) (ABNT 2004):

$$Twf = (Wf - Dl) / 2 \quad (3)$$

where Twf represents the fiber wall thickness (mm), Wf corresponds to the total fiber diameter (mm), and Dl denotes the lumen diameter (mm).

For vessel and ray measurements, cubic wood blocks (10 mm × 10 mm × 10 mm) were softened by immersion in boiling water and then sectioned in the three anatomical planes using a rotary sliding microtome, producing histological sections 18–20 µm thick. Sections were mounted on permanent slides, labelled by orientation, and stored for microscopic examination. Digital images captured from each slide served as the basis for quantifying vessel frequency and diameter, as well as ray height and width (Souza et al. 2025).

Statistical analysis

For each anatomical variable, as well as for all physical and mechanical properties including apparent density, radial and tangential shrinkage, and strength and stiffness parameters twelve measurements were obtained. Since the number of observations differed among variables, the statistical treatment was based on average values.

The relationships between variables were assessed using the Pearson correlation coefficient (r, ranging from −1 to 1), with statistical significance verified through one-way analysis of variance (ANOVA) at a 5% significance level ($\alpha = 0.05$). This procedure was applied both to correlations among anatomical features and to their relationships with the physical and mechanical properties of Caixeta.

RESULTS AND DISCUSSION

Table 1 shows a synthesis of the mean results for the physical and mechanical properties of the Caixeta species. These values are in accordance with the prescriptions of ABNT NBR 7190-3:2022 (ABNT 2022a).

Table 1: Mean physical and mechanical properties of Caixeta

SPECIES		$\rho_{ap,12}$ g/cm	RS %	TS %	f_{c0} MPa	f_{t0} MPa	f_{t90} MPa	f_{v0} MPa	E_{c0} MPa	E_{t0} MPa
Caixeta	Mean	0.33	4.33	7.74	37.10	49.26	2.48	8.14	7939.23	9.689
	CV%	2.75	11.50	11.76	5.19	7.38	30.91	14.92	20.76	5.97

Table 1 indicates that Caixeta is a low-density wood ($\rho \approx 0.33$ g/cm³), with mechanical properties consistent with strength class D30, including moderate strength and stiffness. The elastic moduli confirm its limited rigidity, while shrinkage values suggest moderate dimensional stability. Overall, the results reinforce that its mechanical performance is primarily governed by apparent density, consistent with typical behaviour of lightweight tropical woods (Arriaga et al. 2023).

Table 2 presents the characteristic strength values ($f_{w,k}$) for Caixeta, which were used to determine its inclusion in the tropical wood strength classes (CR) according to the criteria established by ABNT NBR 7190-3:2022 (ABNT 2022a). These categories include:

Table 2: Characteristic mechanical strength values (fw,k) of Caixeta

SPECIES	$f_{c0,k}$ MPa	$f_{t0,k}$ MPa	$f_{t90,k}$ MPa	$f_{v0,k}$ MPa	CR
Caixeta	38.43	47.84	1.64	7.29	D30

$f_{c0,k}$: Characteristic value of compression parallel to the grain; $f_{t0,k}$: Characteristic value of tension parallel to the grain; $f_{t90,k}$: Characteristic value of tension parallel to the grain; $f_{v0,k}$: Characteristic value of shear stress perpendicular to the grain; CR: Strength class.

Caixeta wood exhibited relatively low strength values (Table 2), consistent with its classification as a lightweight tropical species. The characteristic values obtained in this study place it in a lower strength class according to the standard [20], indicating its suitability primarily for light structural applications.

A synthesis of the anatomical characteristics for the Caixeta species is provided in Table 3, where the dispersion of the data is quantified by the coefficient of variation (CV).

Table 3: Mean anatomical properties of Caixeta

SPECIES		Dv mm	Frv Vessel/mm²	Hr mm	Wr mm	Lf mm	Df mm	Dl mm	Twf mm
Caixeta	Mean	0.17377	3.19952	0.53213	0.02871	1.14326	0.00748	0.00472	0.00137
	CV%	16.44	9.72	16.33	19.87	20.97	6.56	17.36	27.47

Vessel elements are illustrated in Figures 1(a) and 1(b), supporting the anatomical characterization proposed in this study. The mean vessel diameter was 0.17 mm, indicating relatively large conduits typical of low-density woods. Ray elements are shown in Figures 1(c) and 1(d), with a mean height of 0.53 mm and a mean width of 0.03 mm, reflecting the presence of narrow rays. Fiber dimensions showed mean values of 1.14 mm for length and 0.0075 mm for diameter, while the lumen diameter averaged 0.0047 mm and the fiber wall thickness 0.00137 mm, consistent with the lightweight anatomical structure of Caixeta.

Regarding the fibers, their diameters can be classified as narrow, with a mean value of 0.0075 mm (Figure 2a). In terms of length, short fibers predominated, with an average of 1.14 mm (Figure 2b). The lumen diameter was also narrow, with a mean value of 0.0047 mm (Figure 2c). Fiber wall thickness was relatively thin, averaging 0.00137 mm (Figure 2d), consistent with the low-density structure of Caixeta.

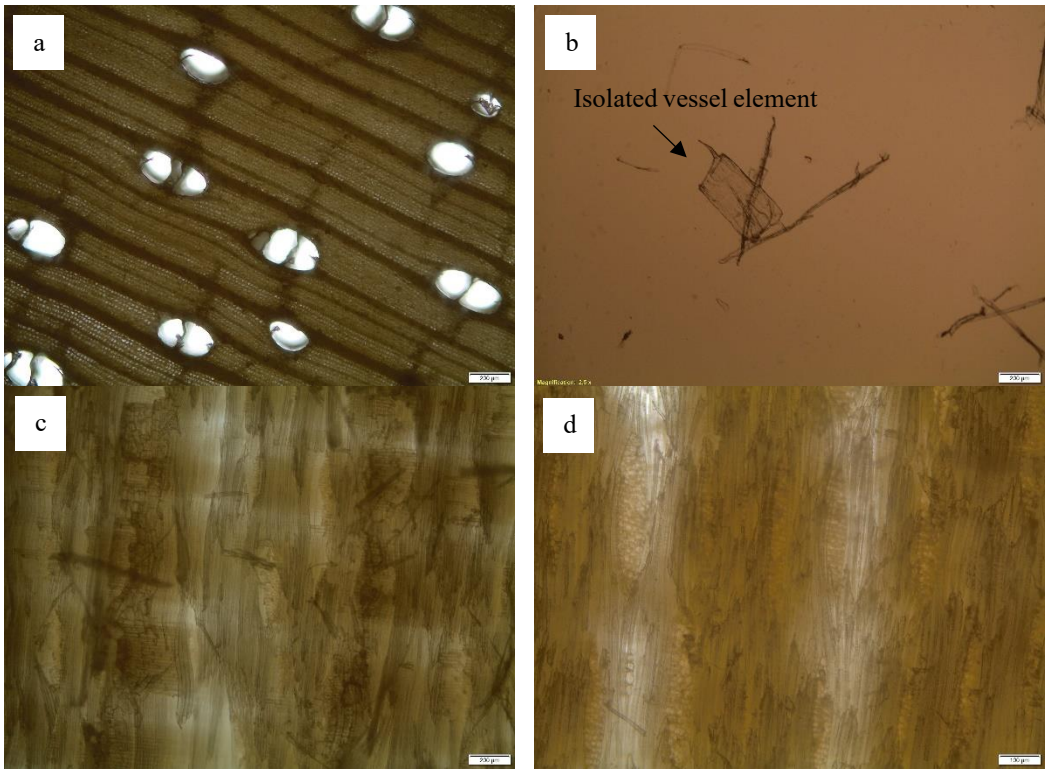

Figure 1: Transverse section showing (a) vessel elements of Caixeta, (b) an isolated vessel element, (c) tangential section, and (d) radial section

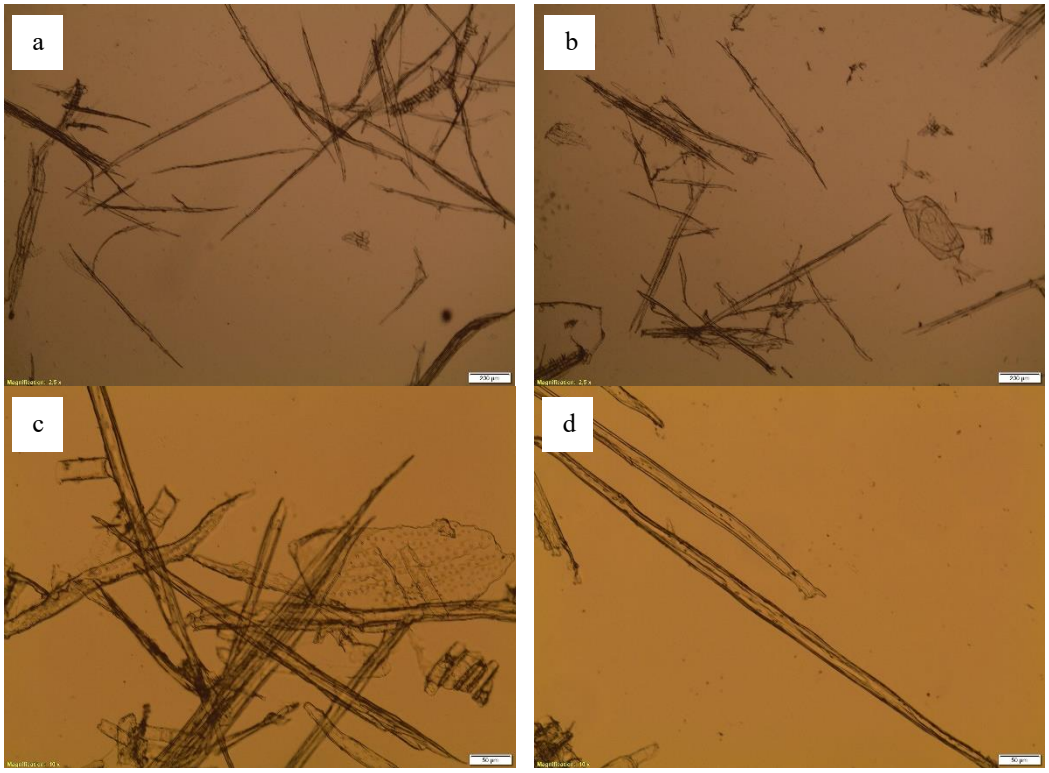

Figure 2: Fiber characteristics of Caixeta wood, including (a) fiber diameter (Df), (b) fiber length (Lf), (c) lumen diameter (Dl), and (d) fiber wall thickness (Twf)

Table 4 presents the Pearson correlation coefficients (Pearson's r) describing the relationships among the seven anatomical parameters evaluated for Caixeta, in which statistically significant correlations are underlined.

Table 4: Pearson correlation coefficients (−1 ≤ r ≤ 1) between the evaluated anatomical properties

Stat.	Dv	Frv	Hr	Wr	Lf	Df	Dl
Frv	0.541						
Hr	0.679	0.258					
Wr	-0.188	-0.433	-0.533				
Lf	0.234	-0.472	0.061	0.035			
Df	-0.042	-0.497	-0.270	0.507	0.474		
Dl	-0.577	-0.326	-0.432	-0.245	0.235	0.425	
Twf	0.599	0.031	0.294	0.595	0.052	0.187	-0.809

**At the 5% significance level, correlations identified as significant based on analysis of variance (ANOVA) are highlighted with underlining.*

Pearson's correlation coefficients show that the anatomical structure of Caixeta is strongly influenced by the inverse relationship between lumen diameter and cell wall thickness ($r = –0.809$; $p < 0.05$). This pattern is particularly significant for modeling mechanical performance, since cell wall thickness is a determining factor in compressive strength and stiffness in many tropical woods. Conversely, the weak association between fiber length and other anatomical characteristics suggests that longitudinal variation plays a small role in determining cell wall density in this species.

Table 5 presents a comprehensive overview of the relationships between anatomical parameters and the physical and mechanical properties of Caixeta with statistically significant correlations underlined.

Table 5: Pearson correlation coefficients (−1 ≤ r ≤ 1) between anatomical, physical, and mechanical properties

Stat.	$\rho_{ap,12}$	RS	TS	f_{c0}	f_{t0}	f_{t90}	f_{v0}	E_{c0}	E_{t0}
Dv	-0.176	0.165	0.162	0.013	-0.056	-0.008	0.863	0.179	0.203
Frv	-0.543	0.559	0.076	-0.282	-0.072	-0.155	0.701	0.146	0.048
Hr	0.022	-0.348	-0.153	-0.265	0.306	-0.407	0.781	-0.137	0.440
Wr	0.421	0.247	0.028	0.753	-0.487	0.266	-0.380	0.406	-0.418
Lf	0.175	-0.272	0.132	-0.014	0.075	0.411	-0.145	-0.174	0.049
Df	-0.127	-0.033	0.176	0.227	-0.124	-0.062	-0.296	-0.403	0.115
Dl	-0.404	-0.158	0.069	-0.453	0.264	-0.119	-0.577	-0.727	0.195
Twf	0.356	0.150	0.039	0.639	-0.367	0.089	0.434	0.528	-0.137

**At the 5% significance level, correlations identified as significant based on analysis of variance (ANOVA) are highlighted with underlining*

The negative correlation between vessel diameter (Dv) and apparent density ($\rho_{ap,12}$) reflects the increase in void volume caused by larger vessels, which reduces wood density. This inverse relationship is well established in the literature, indicating that species with larger vessels tend to have lower density. In *S. amara*, the presence of large vessels is consistent with its low apparent density (≈ 0.33 g/cm³), typical of lightweight diffuse-porous woods (Rungwattana and Hietz 2018).

Vessel frequency (Frv) showed positive correlations with compressive strength (f_{c0}) and modulus of elasticity (E_{c0}). This can be explained by the inverse relationship between vessel size and frequency: a higher number of smaller vessels results in a more compact and mechanically efficient structure. Studies such as Monteiro *et al.* (Monteiro et al. 2026) confirm that vessel-related parameters significantly contribute to wood physical and mechanical behavior.

Fiber diameter (Df) and lumen diameter (Dl) showed significant negative correlations with apparent density ($\rho_{ap,12}$), indicating that larger lumens reduce the proportion of cell wall material and, consequently, wood density. This pattern is well established in the literature and aligns with findings by Marini *et al.* (Marini et al. 2022b), who demonstrated that fiber-related anatomical parameters are strong predictors of mechanical properties when combined with density. The results for Caixeta are also

consistent with Monteiro *et al.* (Monteiro et al. 2026), confirming that lower-density woods are associated with larger lumen fractions and thinner fiber walls.
Fiber wall thickness (Twf) showed a significant positive correlation with stiffness (E_{c0}) and tensile strength (f_{t0}), highlighting its key role as a load-bearing structural element in wood. Thicker fiber walls increase structural rigidity and strength, a relationship well supported by cellular solid mechanics and previous studies (Ajuziogu, G.C., Nwosu, M.O., Nzekwe, U., Onyeke, C.C., Odo, G.E,.Ejikeme, P.M . And Onyeonagu 2014). In Caixeta, the relatively thin fiber walls explain its moderate mechanical properties, while the observed correlations suggest that Twf can serve as a useful predictor of mechanical performance, reducing reliance on extensive destructive testing.
Apparent density ($\rho_{ap,12}$) showed significant correlations with compressive strength (f_{c0}) and stiffness (E_{c0}), acting as an integrative parameter of anatomical features such as vessel size, lumen proportion, and fiber wall fraction. This dual role both influenced by anatomy and predictive of mechanical performance is well established in the literature (Marini et al. 2022b). The results for Caixeta confirm that anatomical parameters affect density, which in turn governs strength and stiffness properties.
The lack of significant correlations for ray width (Wr) and fiber length (Lf) in Caixeta is attributed to its high anatomical homogeneity. The limited variance of these parameters reduces their statistical power to explain mechanical fluctuations. Furthermore, fiber length, often influenced by ontogenetic factors, does not necessarily reflect cell wall stiffness or load transfer capacity in clear wood. This pattern of selective correlations supports the literature, indicating that the structural uniformity of diffuse-porous, low-density species results in a correlation structure distinct from more heterogeneous timbers (Menezes IS, Ferreira TR, Souza CGF, Prataviera R, Lahr FAR, Freitas L, Santos HF, Christoforo 2024).

Table 6 provides a detailed overview of the relationships between the physical and mechanical properties of Caixeta, with statistically significant correlations underlined.

Table 6: Pearson correlation coefficients (−1 ≤ r ≤ 1) between physical and mechanical properties

Stat.	f_{c0}	f_{t0}	f_{t90}	f_{v0}	E_{c0}	E_{t0}
$\rho_{ap,12}$	0.189	0.177	0.064	-0.137	0.315	-0.094
RS	-0.155	-0.187	-0.128	0.276	0.078	-0.212
TS	0.360	0.037	0.508	-0.115	0.372	0.275

**At the 5% significance level, correlations identified as significant based on analysis of variance (ANOVA) are highlighted with underlining.*

The Pearson correlation analysis for Caixeta shows a pattern of generally weak linear relationships among its physical and mechanical properties. Unlike higher-density woods where specific gravity typically governs mechanical behaviour Caixeta exhibits a more complex and less density-driven response.
The correlation between apparent density and compressive strength (f_{c0}) is only 0.189, while for the modulus of elasticity (E_{c0}), it is 0.315. In wood science literature, density is generally regarded as the primary predictor of strength. However, for low-density species such as Caixeta (≈0.33 g/cm³), the mass variation is so subtle that it ceases to be the determining factor. This reinforces the thesis of this study: for these species, anatomical traits (such as fiber wall thickness and lumen diameter) may serve as far more reliable predictors than density alone.
The strongest correlation in the dataset appears between Tangential Shrinkage (TS) and tensile strength perpendicular to the grain (f_{t90}), with r = 0.508. Although this value does not meet the strict threshold for statistical significance, the moderate association suggests that tangential dimensional stability is linked to the internal cohesion of the fibers. Woods that shrink more tangentially tend to show higher tensile strength in the same direction, likely reflecting a more compact or tightly bonded cellular structure.
The correlations with ft0 (tension parallel to the grain) and f_{v0} (shear strength) are extremely low or even negative (e.g., –0.137 for shear). This indicates that failure mechanisms involving fiber tension or fiber-sliding in Caixeta do not follow a linear pattern with density or shrinkage. Instead, they are likely

governed by microscopic defects or by the spatial organization of vessels, rather than by the overall mass of the material.

At present, the literature offers limited data for direct comparison with the results obtained for Caixeta in this study. Although some research has addressed the relationship between anatomical features and mechanical properties in tropical woods, studies specifically focused on low-density species remain scarce. This gap emphasizes both the novelty of the present work and the need for further investigations aimed at better understanding how anatomical characteristics influence the structural performance of lightweight woods.

CONCLUSIONS

Simarouba amara (Caixeta) was characterized according to ABNT NBR 7190-3:2022, showing low apparent density (0.33 g/cm³) and mechanical properties consistent with strength class D30, confirming its suitability for light structural applications with moderate dimensional stability. Anatomically, the species exhibits a diffuse-porous structure with large vessels and thin fiber walls, typical of lightweight woods.

Correlation analyses revealed that anatomical parameters, especially vessel diameter and frequency, ray dimensions, lumen diameter, and fiber wall thickness, are significant predictors of mechanical behavior, particularly shear and compressive properties. In contrast, apparent density showed no significant correlations with mechanical properties, likely due to its low variability in this species.

Overall, the results highlight that anatomical features provide more sensitive and mechanistically meaningful predictors of mechanical performance than density alone, supporting their use as efficient, low-cost tools for the characterization of lesser-known tropical woods.

Expanding this approach to a broader range of tropical species with different anatomical characteristics, densities, and porosity patterns is an important next step to verify how widely these structure–property relationships apply and to build more robust, anatomy-based prediction models for practical and normative use.

ACKNOWLEDGEMENTS

Authors thank Dept of Science and Materials Engineering; Dept of Structural Engineering, University of São Paulo, for supplying materials used in experiments; National Council for Scientific and Technological Development (CNPq), process 313198 2023 3; Foundation for Coordination of Improvement of Higher Education Personnel (CAPES); and São Paulo Research Foundation (FAPESP) for their financial support, processer 2024/01589-2.

REFERENCES

ABNT (2022a) Associação Brasileira de Normas Técnicas NBR:7190-PARTE3. Métodos de ensaio para corpos de prova isentos de defeitos para madeiras de florestas nativas. Rio de Janeiro

ABNT (2022b) Associação Brasileira de Normas Técnicas NBR:7190-PARTE1. Critérios de dimensionamento. Rio de Janeiro

ABNT (2004) Associação Brasileira de Normas Técnicas NBR 15066. Madeira e pasta celulósica – Determinação das dimensões de fibras – Método de microscopia óptica. Rio de Janeiro

Aguiar F da S, Silva G dos S, Santos HF dos, et al (2025) Estimation of longitudinal and transverse elastic moduli of wood in bending: comparison of test configurations and standards. BioResources 20:6680–6691

Ajuziogu, G.C., Nwosu, M.O., Nzekwe, U., Onyeke, C.C., Odo, G.E,.Ejikeme, P.M . And Onyeonagu CC (2014) Biomechanics, an aspect of the relationships between Wood Anatomical Parameters and Mechanical Strength in Ten Nigerian Timber species. International Journal of Scientific and Engineering Research 5:628–645

Arriaga F, Wang X, Íñiguez-González G, et al (2023) Mechanical Properties of Wood: A Review. Forests 14:1202. https://doi.org/https://doi.org/10.3390/f14061202

Chave J, Coomes D, Jansen S, et al (2009) REVIEW AND Towards a worldwide wood economics spectrum. Ecology Letters 12:351–366. https://doi.org/10.1111/j.1461-0248.2009.01285.x

HUGO I. MARTÍNEZ-CABRERA, SCHENK HJ, CEVALLOS-FERRIZ SRS, JONES CS (2011) Integration of vessel traits, wood density, and height in angiosperm shrubs and trees. American Journal of Botany 98:915–922

IAWA (1989) International Association of Wood Anatomists. List of microscopic features for hardwood identification. IAWA Bulletin 3 219–332

ITTO (2024) Marupa (Simarouba amara). Tropical Timber Species Database. Yokohama: ITTO, 2024. In: INTERNATIONAL TROPICAL TIMBER ORGANIZATION – ITTO

Johansen DA (1940) Plant microtechnique. New York: McGraw-Hill. 523

Joung J, Kwon D, Im H, et al (2024) Timber Construction Materials in Modern Timber Buildings : Domestic and Global Market Trends. Trends Agric Life Sci 62:13–32

Lestari L, Ikaputra I (2024) Toward Sustainable Construction Using Wood Material. International Journal of Environment, Architecture, and Societies 04:77–90. https://doi.org/10.26418/ijeas.2024.4.02.77-90

Lukovic M, Ciernik L, Müller G, et al (2024) Probing the complexity of wood with computer vision : from pixels to properties. J R Soc Interface 21:. https://doi.org/https://doi.org/10.1098/rsif.2023.0492

Marini LJ, Cavalheiro RS, Araujo VA de, et al (2022a) Estimativa da resistência à tração nas madeiras de dez espécies de eucalipto em função de parâmetros anatômicos e da densidade aparente. Matéria (Rio de Janeiro) 27:. https://doi.org/10.1590/1517-7076-rmat-2022-0196

Marini LJ, Cavalheiro RS, De Araujo VA, et al (2022b) Estimation of mechanical properties in Eucalyptus woods towards physical and anatomical parameters. Construction and Building Materials 352:. https://doi.org/10.1016/j.conbuildmat.2022.128824

Menezes IS, Ferreira TR, Souza CGF, Prataviera R, Lahr FAR, Freitas L, Santos HF, Christoforo AL (2024) Relationship between characteristic values of shear strength parallel to grain and tensile strength perpendicular to grain for tropical woods. BioResources 19:7408–7417

Monteiro RDO, Dória LC, Ribeiro ES, Gonçalez JC (2026) Wood anatomy and its effects on physical properties in nineteen commercial species. Brazilian Journal of Botany 49:

Ramage MH, Burridge H, Busse-wicher M, et al (2017) The wood from the trees : The use of timber in construction. Renewable and Sustainable Energy Reviews 68:333–359. https://doi.org/10.1016/j.rser.2016.09.107

Rungwattana K, Hietz P (2018) Radial variation of wood functional traits reflect size- - related adaptations of tree mechanics and hydraulics. 260–272. https://doi.org/10.1111/1365-2435.12970

Sass JE (1951) Botanical microtechnique. 2nd ed. Ames: Iowa State College Press. 228

Souza CGF De, Christoforo AL, Lahr FAR (2025) Correlations among select properties and anatomical parameters of Dipteryx odorata wood

Comparative Analysis of Chemical Composition, Anatomical Features and FTIR Spectra in Maple Wood: Implications for Musical Instrument Quality

Mariana Domnica Stanciu[1*], Olga A. Shapchenkova[2], Maria A. Plyashechnik[2], Marina A. Sheller[3], Antonina A. Aniskina[2], Florin Dinulică[4]

[1] Faculty of Mechanical Engineering, Transilvania University of Brașov, B-dul Eroilor 29, 500036 Romania
[2] V.N. Sukachev Institute of Forest SB RAS – separate subdivision of the Federal Research Center "Krasnoyarsk Science Center SB RAS", Akademgorodok 50/28, 660036 Krasnoyarsk, Russia
[3] Siberian Federal University, Svobodny pr. 79, 660041 Krasnoyarsk, Russia
[4] Faculty of Silviculture and Forest Engineering, Transilvania University of Brașov, B-dul Eroilor 29, 500360 Brașov, Romania.

E-mail: mariana.stanciu@unitbv.ro; shapchenkova@mail.ru; lilwood@ksc.krasn.ru; maralexsheller@mail.ru; aniskina_a@ksc.krasn.ru; dinulică@unitbv.ro

Keywords: maple wood; thermal degradation; anatomic pattern; musical instruments.

ABSTRACT

The paper presents the comparative analysis of four categories of anatomical models of *Acer Pseudoplatanus* used for the construction of stringed musical instruments. The maple wood samples were grouped according to the degree of grain waviness, being measured in the first stage, different anatomical parameters such as the width of the annual rings and the degree of grain waviness. Based on FTIR analysis, ratios of absorbance intensities were calculated using the characteristic wavenumbers of the main chemical components, thus identifying the differences between the categories of maple wood analysed. Using thermogravimetric analysis with a heating rate of 10 °C/min from 25 °C to 600 °C under an air atmosphere, the mass loss associated with the thermal degradation of hemicelluloses, cellulose, and lignin was determined. The PCA thus provides a more integrated view of the differences among the series, capturing synergistic patterns that univariate tests cannot detect. The PCA demonstrates that the wavy (PA) and slightly wavy (PC) groups are separated by a coordinated suite of traits. Straight grain (PD) and rare wavy (PB) are less distinct and more variable. Strong contributions of cellulose, lignin, hemicellulose, and specific FTIR ratios confirm that these variables are the significant discriminators among the aesthetic quality classes of sycamore maple.

INTRODUCTION

Acer pseudoplatanus L. (maple) is utilized for musical instrument back plates, with species displaying aesthetic fiber patterns categorized as curly, fiddleback, flame, or bird's-eye (Beldeanu 2001, Bucur 1992, Dinulica et al 2023). In Romania, this wavy-grained wood is prevalent in the Carpathian mountainous and premontane regions (Dinca et al 1996, 1998). From anatomically point of view, maple features complex, distinct annual rings, diffuse-porous microstructure with helical thickenings, and distinct waviness metrics—wavelength, amplitude, and grain angle—used to analyze fiber patterns (Bucur 2006, Alkadri et al 2018). Luthiers classify this wood into four quality grades based on wave intensity, with studies indicating that wavy-grained, high-grade wood possesses higher ring regularity (RRI) compared to straight-grained samples (Spycher et al 2008, Stanciu et al 2020). Wavy-fiber maple wood is a structural anomaly consisting in the arrangement of fibers and other anatomical elements along slightly sinuous lines, mainly in the radial and tangential planes, giving the appearance of a three-dimensional drawing. There are hypotheses regarding the formation of wavy fibers: one hypothesis supports the hereditary character of this type of maple; another hypothesis is based on the mechanical aspect during the life of the tree, when under the weight of the crown, the fibers in the tree stem suffer a phenomenon of mechanical instability (buckling) thus giving rise to the wavy-fiber structure or stationary causes; another hypothesis is related to the natural reaction of the maple tree to the attack of fungi at the root level, the waviness of the fiber leading to the obstruction of the penetration of hyphae

into the wood. The modification of the anatomical architecture of maple wood implies the modification of the proportions of the main chemical components of the wood, as shown by previous studies (Stanciu et al 2024). There are few studies that analyse the chemical differences between straight-grained and wavy-grained maple wood, which is why these paper focuses on the analysis of the chemical composition in relation to anatomical features of maple wood used for stringed musical instruments.

MATERIALS AND METHODS

Sample preparation

The wood samples of sycamore maple (Acer pseudoplatanus L.) were classified into four groups: PA (wavy grain), PB (rare wavy grain), PC (slightly wavy grain), and PD (straight grain). Wavy wood (PA) is potentially favourable for resonance (Dinulica et al., 2023). Each group consisted of five replicates, giving a total of 20 samples, as can be seen in Figure 1a. In Figure 1b can be seen how was measured the fiber curl pitch. The evaluation of the anatomical characteristics of the sycamore maple wood and their division into the four groups was carried out in previous studies by visual methods and measurements with the WinDENDRO Density image analysis system (Régent Instruments Inc., Québec City, QC, Canada, 2007). Each sample was scanned in transverse and radial sections to measure the width of the annual rings, denoted RW, and the pitch of the sycamore maple wood fibers (denoted CWL) (Dinulica et al., 2023, Stanciu et al 2025). From the initial cube samples, the wood specimens for each type of test were carefully sawed manually using a fine-tooth metal saw. The resulting fine sawdust was used for thermal analysis and FTIR spectroscopy.

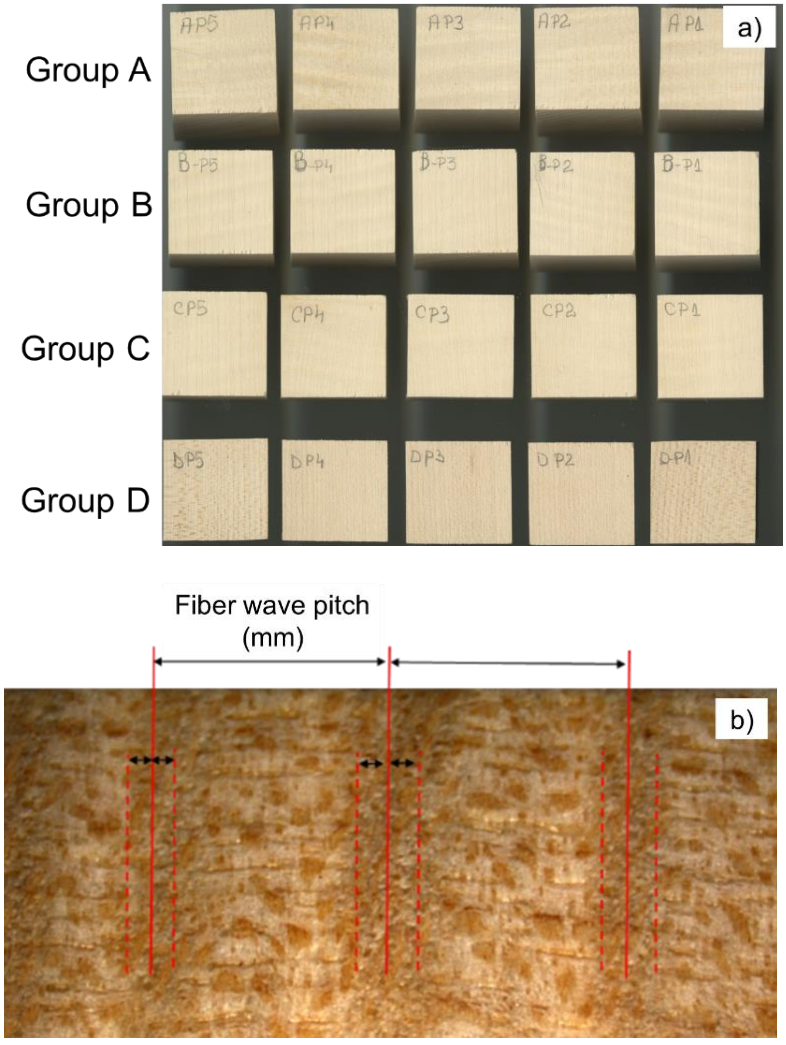

Figure 1: The four maple groups (a) and method to measure the fibre wave pitch (b)

Methods

Thermogravimetry

Thermogravimetry (TG) was carried out under an air atmosphere with a gas flow of 20 mL/min and a heating rate of 10 °C/min from 25 to 600 °C. Mass loss in the temperature ranges of 200–295°C (I), 295–380°C (II), and 380–480°C (III) was determined from TG and DTG (differential thermogravimetric) curves (Figure 2) and was attributed to thermal degradation of mainly hemicellulose, cellulose, and lignin, respectively (Gao et al., 2004; Shen et al., 2009; Brebu & Vasile 2010, Shapchenkova et al 2022). The TG curve indicates the mass loss of the sample, whereas the DTG curve shows the rate of mass loss as can be seen in Figure 2. The inorganic residue measured at the end of the TG analysis indicates the sample's ash content.

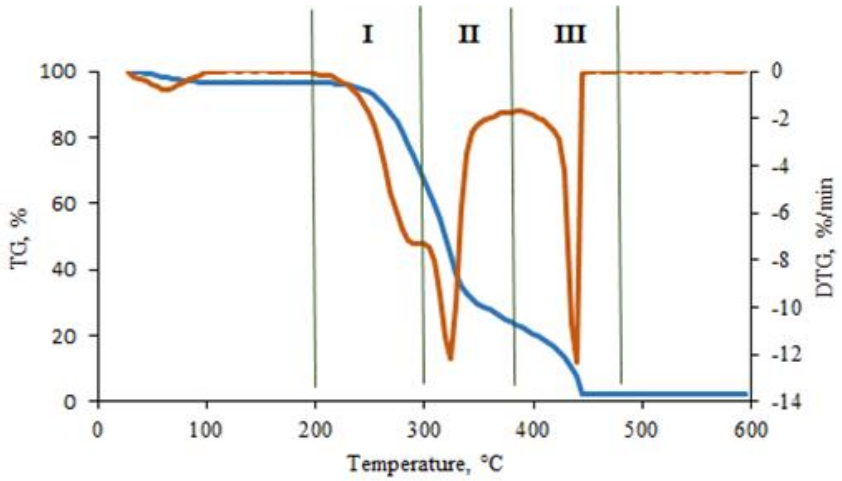

Figure 2: TG and DTG curves of maple wood (PC samples as an example) in an air atmosphere at heating rate 10 °C min^{-1}

Fourier Transform Infrared Spectroscopy

Fourier transform infrared (FTIR) spectra were recorded using a Vertex 80 spectrometer (Bruker Optics, Germany). The samples were ground with KBr and pressed into tablets. Measurements were performed over the range 4000–400 cm^{-1} with a resolution of 4 cm^{-1}. For each sample, the following FTIR absorbance ratios were calculated: 1373/2902 (carbohydrate C–H deformation / total C–H stretching), 1424/897 (cellulose crystallinity index, the band at 1424 cm^{-1} is characteristic of the crystalline domains of cellulose, whereas the band at 897 cm^{-1} corresponds to its amorphous regions), 1507/1740 (lignin / carbonyl, mainly hemicellulose), 1507/1373 (lignin / carbohydrate, C–H deformation), 1507/1160 (lignin / carbohydrate, C–O–C stretching), and 1507/1050 (lignin / carbohydrate, C–O stretching) (Poletto et al., 2012; Li et al., 2024). In Figure 3 are presented the FTIR spectra of maple wood – group C.

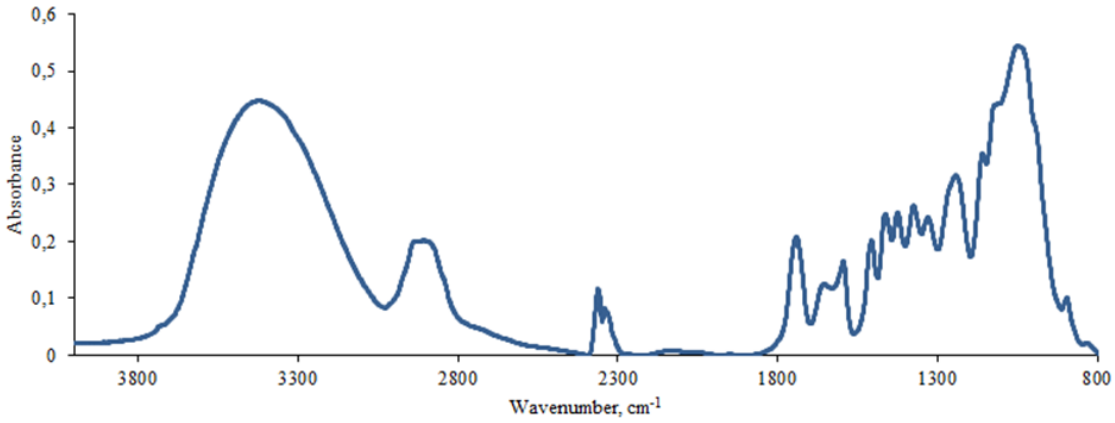

Figure 3: FTIR spectra of maple wood (PC as an example)

Scanning electron microscopy (SEM)

The intraspecies peculiarities because of the organization and growth of the anatomical cells of the wood are reflected in the surface morphology. The surface morphology of the samples was examined using a TM-1000 microscope (Hitachi, Japan), as can be seen in Figure 4.

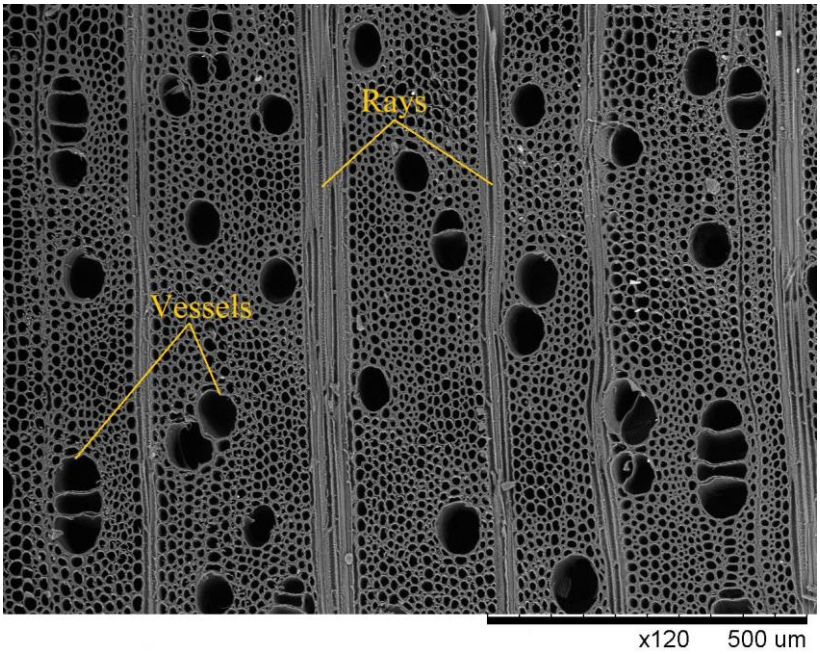

Figure 4: SEM image of maple wood (PC) cross section as an example. SEM image at 120x magnification. Scale bar = 500 µm

Statistical analysis of data

Statistical analyses were performed using Statistica 10. Homogeneity of variances among the four groups was examined using Levene's test. To determine whether significant differences existed among the groups for each parameter, a one-way analysis of variance (ANOVA) was performed. Tukey's honestly significant difference (HSD) post hoc test was used to identify which specific pairs of groups differed. When the assumption of homogeneity of variances was not met, the non-parametric Kruskal–Wallis's test was employed, followed by Dunn's post hoc test with Bonferroni correction. Principal component analysis (PCA) was performed using R to explore multivariate patterns among the variables.

RESULTS AND DISCUSSION

Univariate analysis

Having carried out numerous experimental investigations, the data obtained were statistically processed, this analysis highlights the links between the various the physical, chemical and anatomical properties. For variables meeting the assumption of equal variances (Levene's test $p > 0.05$), one way ANOVA followed by Tukey's HSD post hoc test was applied (Table 1). For annual ring width, where variances were heterogeneous (Levene's test $p < 0.05$), the non-parametric Kruskal Wallis test was used, followed by Dunn's post hoc test with Bonferroni correction ($\alpha = 0.05/6 = 0.0083$). For number of vessels per mm², the Kruskal Wallis test was not significant; therefore, no post hoc comparisons were performed. Univariate ANOVA with Tukey HSD revealed significant differences among the four groups for hemicellulose (PA–PC, PB–PC, PC–PD), cellulose (PA–PC), and FTIR ratio I_{1373}/I_{2902} (PC–PD). All other pairwise comparisons were non-significant. The Kruskal Wallis test revealed a significant difference in annual ring width among the four series. Post hoc pairwise comparisons using Dunn's test indicated a potential difference between PA and PC (raw $p = 0.0277$). However, after applying a Bonferroni correction for six comparisons (adjusted $\alpha = 0.0083$), none of the pairwise differences remained statistically significant. Thus, the overall significant effect reflects a general trend rather than a specific contrast between any two series.

Table 1: Results of the test

Variable	Test used	Global test statistic	df	p value	Significant pairwise comparisons (direction, p < 0.05)
Hemicellulose, %	One-way ANOVA + Tukey HSD	F(3.16) = 11.032	3.16	0.000358	PC > PA. PC > PB. PC > PD
Cellulose, %	One-way ANOVA + Tukey HSD	F(3.16) = 6.33	3.16	0.004913	PC < PA
I_{1373}/I_{2902}	One-way ANOVA + Tukey HSD	F(3.16) = 3.40	3.16	0.043468	PC > PD

Note: No other variables showed significant differences.

Principal component analysis

Principal component analysis was performed on all variables to explore the multivariate relationships among the four sycamore maple groups (PA, PB, PC, PD). The first two principal components explained 34.5% and 26.7% of the total variance, respectively (cumulative 61.2%).

Score plot (individual samples)

The score plot (Figure 5) revealed a clear separation between the pronounced wavy series (PA) and the slightly wavy series (PC) along PC1. All PA samples were in the left-upper quadrant, whereas all PC samples occupied the right-lower quadrant (with one PC sample on the right border). In contrast, the straight grain series (PD) was split: two samples (PD1, PD5) were found in the right-upper quadrant, two samples (PD2, PD4) in the left-lower quadrant, and one sample (PD3) on the right border. The rare wavy series (PB) was scattered across the top half of the plot, with samples appearing in both left-upper (PB2, PB3) and right-upper (PB1, PB4) quadrants, and one sample (PB5) on the left border. Thus, while PA and PC form two distinct and coherent clusters, PD and PB exhibit greater within-group heterogeneity and overlap with both PA and PC.

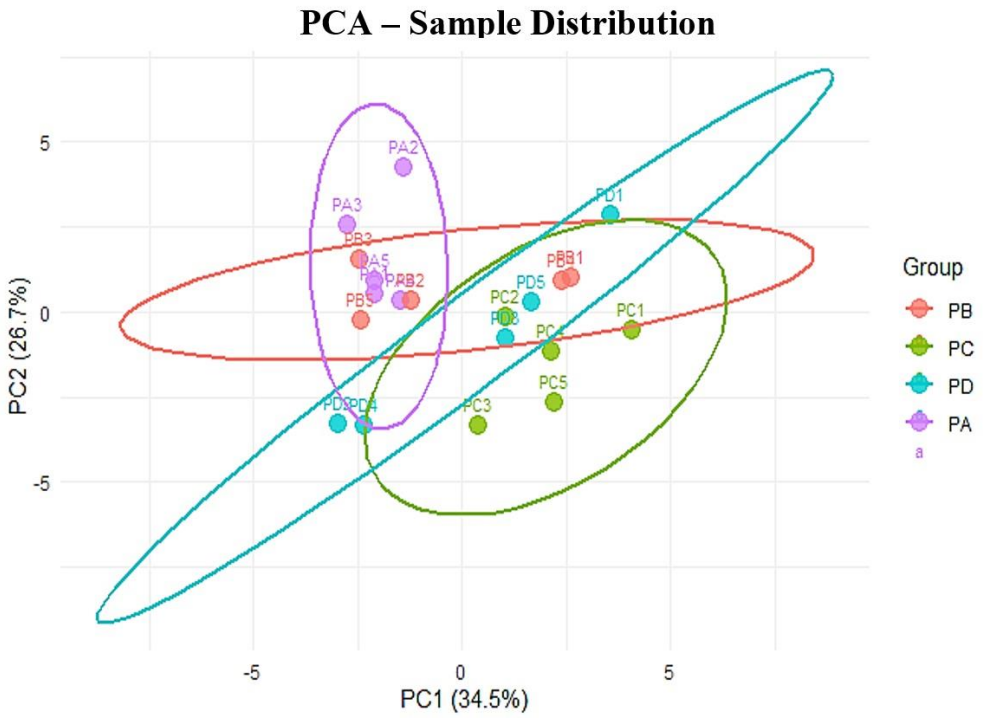

Figure 5: Score plot of individual samples coloured by groups obtained by PCA of anatomical, physical and chemical variables for sycamore maple groups PA (wavy), PB (rare wavy), PC (slightly wavy), and PD (straight grain), n = 5 per group

Loading plot (variables)

The loading plot (Figure 6) and the contribution analysis (Table 2) revealed the variables driving the separation. PC1 separates PA (negative side) from PC (positive side). PC1 (34.5%) was primarily driven by negative loadings from carbohydrate/lignin ratio (−0.397, 15.8% contribution), cellulose (−0.388, 15.1%), vessel area (−0.331, 11.0%), carbohydrate (−0.279, 7.8%), and annual ring width (−0.238, 5.7%), and positive loadings from lignin (0.369, 13.6%), hemicellulose (0.346, 12.0%), and number of vessels (0.313, 9.8%).

Thus, PA (negative PC1) is characterized by higher cellulose, wider annual rings, larger vessel area, and higher carbohydrate/lignin ratio, whereas PC (positive PC1) is characterized by higher lignin, higher hemicellulose, and higher vessel density. PC2 (26.7%) was dominated by positive loadings from FTIR ratio I_{1507}/I_{1050} (0.455, 20.7% contribution), I_{1507}/I_{1160} (0.434, 18.9%), and I_{1507}/I_{1375} (0.383, 14.6%), as well as ash content (0.307, 9.4%). Conversely, PC2 received a strong negative loading from FTIR ratio I_{1424}/I_{897} (−0.366, 13.4%), which is associated with cellulose crystallinity. Examination of the raw FTIR I_{1424}/I_{897} values showed that PC (mean 2.63) and PD (mean 2.61) had higher values than PA (mean 2.51), placing them on the negative side of PC2, while PA (on positive PC2) exhibited lower crystallinity. This indicates that, despite the lack of statistical significance in univariate tests, PCA reveals a trend toward higher cellulose crystallinity in slightly wavy and straight grain wood compared to pronounced wavy wood. PC2 thus captures subtle spectral variations that differentiate the waviness classes beyond the primary chemical gradient described by PC1. The PCA demonstrates that the wavy (PA) and slightly wavy (PC) groups are separated by a coordinated suite of traits. Straight grain (PD) and rare wavy (PB) are less distinct and more variable. The strong contributions of cellulose, lignin, hemicellulose, and specific FTIR ratios confirm that these variables are the significant discriminators among the aesthetic quality classes of sycamore maple.

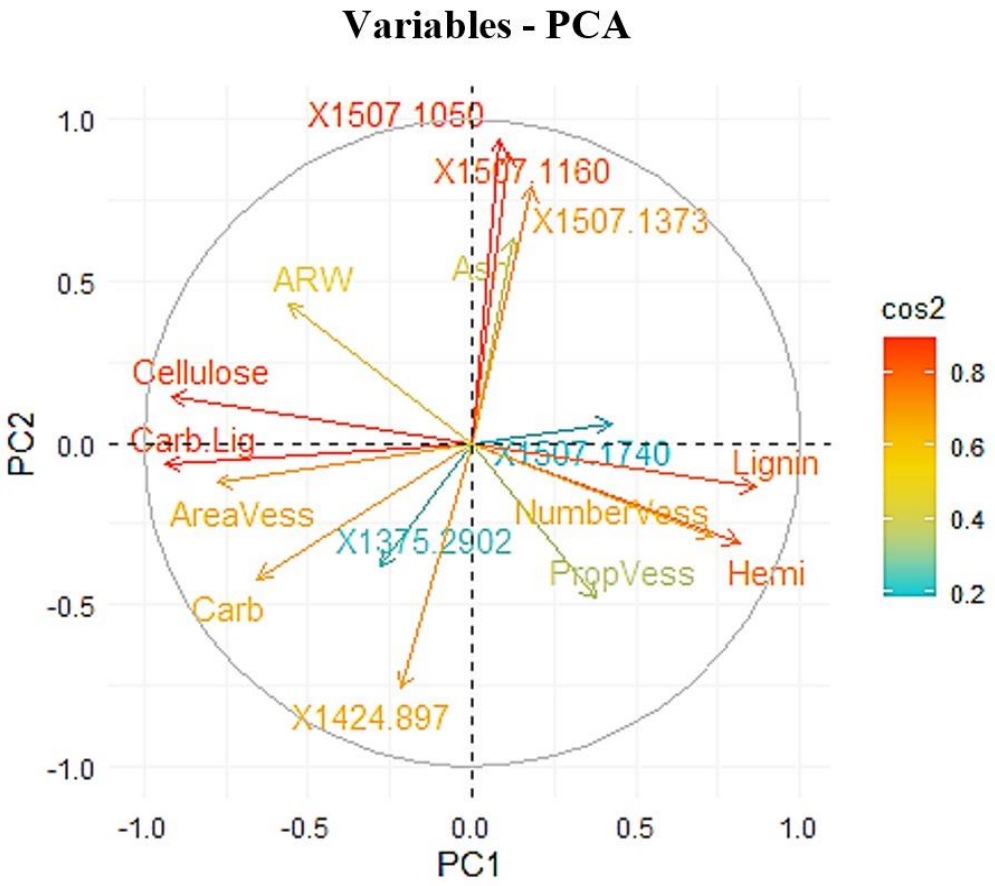

Figure 6: Loading plot shows variable contributions (right side). Arrows represent the original variables from principal component analysis of anatomical, physical and chemical variables for sycamore maple groups PA (wavy), PB (rare wavy), PC (slightly wavy), and PD (straight grain), n = 5 per group

Table 2: PCA loadings and contributions (%) of variables to PC1 and PC2

Variable	PC1 Loading	PC1 Contrib (%)	PC2 Loading	PC2 Contrib (%)
Carbohydrate/Lignin	-0.397	15.8	-0.032	0.1
Cellulose, %	-0.388	15.1	0.069	0.5
Lignin, %	0.369	13.6	-0.067	0.5
Hemicellulose, %	0.346	12.0	-0.149	2.2
Vessel area, mm^2	-0.331	11.0	-0.06	0.4
Number of vessels per 1 mm^2	0.313	9.8	-0.139	1.9
Carbohydrate	-0.279	7.8	-0.203	4.1
Annual ring width, mm	-0.238	5.7	0.207	4.3
I_{1507}/I_{1740}	0.181	3.3	0.03	0.1
Proportion of vessels per 1 mm^2	0.161	2.6	-0.233	5.4
I_{1373}/I_{2902}	-0.119	1.4	-0.186	3.4
I_{1424}/I_{897}	-0.091	0.8	-0.366	13.4
I_{1507}/I_{1373}	0.079	0.6	0.383	14.6
Ash, %	0.053	0.3	0.307	9.4
I_{1507}/I_{1160}	0.049	0.2	0.434	18.9
I_{1507}/I_{1050}	0.036	0.1	0.455	20.7

According to the results obtained, the most important properties influencing the difference between the groups of maple samples analyzed are presented in Figure 7.

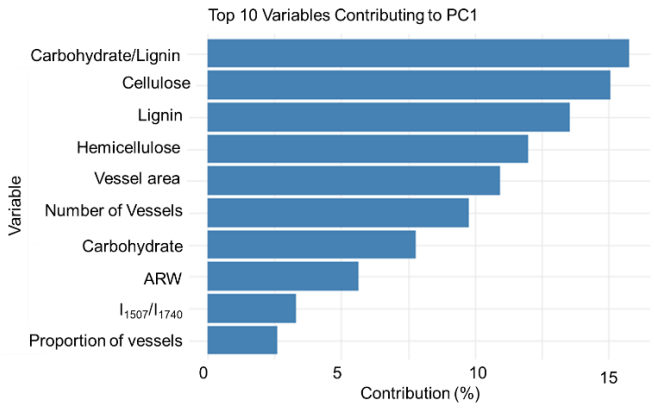

a)

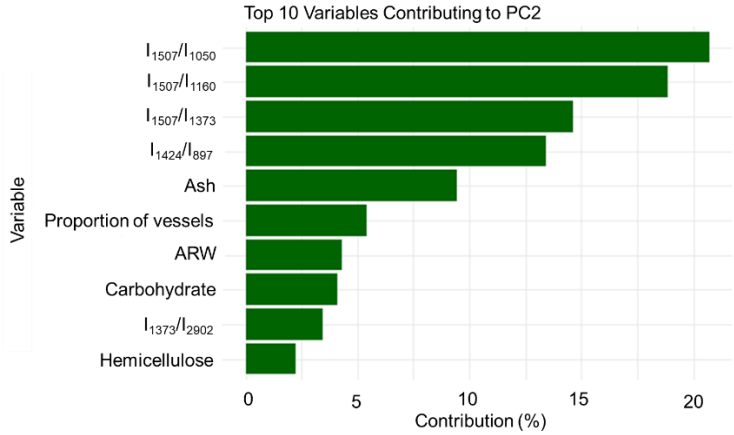

b)

Figure 7: Ranking of variables by their contribution to PC1(a) and PC2 (b)

CONCLUSION

The study presented a comparative analysis of the physical, chemical and anatomical properties of four categories of maple wood used for musical instruments. Principal component analysis (PCA) highlights a clear separation between the wavy (PA) and slightly wavy (PC) texture groups, based on a correlated set of features. In contrast, the straight-fiber (PD) and sparsely wavy (PB) groups present a greater variability and a weaker delimitation. The determining factors in differentiating the aesthetic quality classes are the concentrations of cellulose, lignin and hemicellulose, along with the specific FTIR ratio.

ACKNOWLEDGMENTS

This research was supported by a grant of the Ministry of Research, Innovation and Digitization, CNCS/CCCDI – UEFISCDI, project number 61PCE/2022, PN-III-P4-PCE2021-0885, ACADIA – Qualitative, dynamic and acoustic analysis of anisotropic systems with modified interfaces.

REFERENCES

Alkadri A, Carlier C, Wahyundi I, Grill J, Langbour P, Bremaud I (2018) Relationships between anatomical and vibrational properties of wavy sycamore maples. IAWA - Intern. Assoc. Wood Anatomists J. 39, 1: 63-86

Beldeanu EC (2001) Produse forestiere şi studiul lemnului (in Romanian Laguage). Editura Universităţii Transilvania, Braşov, Brasov, Romania

Brebu M, Vasile C (2010) Thermal degradation of lignin – a review. Cellulose Chem Technol. 44(9): 353−363.

Bucur V (2016) Handbook of Materials for String Musical Instruments, Springer International Publishing Switzerland

Dincă L, Dincă M (1996) Paltinul creţ: caracteristici, răspândire, recunoaştere. Revista de Silvicultura

Dincă L, Dincă M (1998) Gestionarea durabilă a unor resurse de foioase preţioase (sorb de câmpie şi paltin creţ) existente în fondul forestier autohton. Sesiunea de comunicări ştiinţifice "Cercetarea ştiinţifică pentru gestionarea durabilă a pădurilor", I.C.A.S. Bucureşti, 05.03.1998

Dinulica F, Savin A, Stanciu MD (2023) Physical and Acoustical Properties of Wavy Grain Sycamore Maple (Acer pseudoplatanus L.) Used for Musical Instruments. Forests, 14:197

Gao M, Li S, Sun C (2004) Thermal degradation of wood in air and nitrogen treated with basic nitrogen compounds and phosphoric acid. Combust Sci Technol 176: 2057-2070.

Li R, Zhang Z, Jiao L. et al. (2024) Combining microscale ATR-FTIR and chemometrics to interpret degradation characteristics of earlywood, latewood, and compression wood in waterlogged archaeological pine wood. Herit Sci 12:387

Poletto M, Zattera AJ, Santana RMC (2012) Structural differences between wood species: Evidence from chemical composition, FTIR spectroscopy, and thermogravimetric analysis. J. Appl. Polym. Sci., 126: E337-E344

Shen DK, Gua S, Luo KH, Bridgwater AV, Fang MX (2009). Kinetic study on thermal decomposition of woods in oxidative environment. Fuel 88(6):1024

Shapchenkova O, Loskutov S, Aniskina A et al. (2022) Thermal characterization of wood of nine European tree species: thermogravimetry and differential scanning calorimetry in an air atmosphere. Eur. J. Wood Prod. 80:409–417

Spycher M, Schwarze FWMR, Steiger R (2008) Assessment of resonance wood quality by comparing its physical and histological properties. Wood Sci. Technol. 42:325–342

Stanciu MD, Cosereanu C, Dinulică F, Bucur V (2020) Effect of wood species on vibration modes of violins plates. Eur. J. Wood Prod., 78, 785–799

Stanciu MD, Gurau L, Dinulica F, Roibu CC, Hiciu C, Mursa A, Stirbu M (2024) The surface morphology of sanded curly maple in comparison with straight grain maple selected for musical instruments. 11th Hardwood Conference Proceedings, Sopron, Hungary, 30-31 May 2024, 178 – 182.

Stanciu MD, Teodorescu HD, Vlase S, Mihalcica M, Cosnită M, Savin A (2024) Multiscale assessment of artificial aging treatment of polysaccharides from tonewood species, Int. J. Biol. 274(1):133310

Stanciu MD, Dinulică F, Roibu CC, Guiman MV, Cerbu C, Savin A (2025). Quality Classes of Blanks for Violins and Some Relevant Physical Parameters of Wood. In: Stanciu, M.D., Bucur, V. (eds) Interdisciplinary Approach to the Violin. Springer, Cham

Strength Grading of Lesser Used Hardwood Assortments – Examples for Birch and Beech

Philipp Schlotzhauer[1*], Tom Jansen[2], Florian Gonzalo Fleer, Hieronymus Bischoff, Susanne Bollmus[1], Thomas Uibel[2], Holger Militz[1]

[1] Wood Biology and Wood Products, Burckhardt Institute, Georg-August University of Göttingen, Büsgenweg 4, 37077 Göttingen, Germany
[2] Department 2 – Civil Engineering, FH Aachen University of Applied Sciences, Bayernallee 9, 52066 Aachen, Germany.

E-mail: philipp.schlotzhauer@uni-goettingen.de; tom.jansen@fh-aachen.de; susanne.bollmus@uni-goettingen.de; uibel@fh-aachen.de; holger.militz@uni-goettingen.de

Keywords: strength grading; birch; beech; bending; tension.

ABSTRACT

Medium-dense European hardwoods have been investigated for structural applications for over two decades, primarily highlighting their superior mechanical properties compared to softwoods. However, decreasing softwood availability in Central Europe increases the need for efficient utilization of all timber resources, including hardwoods. This study presents three experimental approaches to enhance hardwood utilization through alternative applications of underused materials such as low-value beech and Central European birch.

In the first experimental series, beech side-products from furniture production were analysed. Boards close to pith were processed and divided into two groups: BC (higher quality) and BH (lower quality, typically used as firewood). The boards were intended for a use as structural timber. Therefore, 4-point-bending tests (upright) were performed. The mechanical testing revealed characteristic strengths of 14.7 N/mm² for BH and 18.95 N/mm² for BC.

The second series focused on strength grading of Central European birch for structural timber. After processing and 4-point-bending testing (upright), visual and machine grading was developed. A machine grading approach based on dynamic modulus of elasticity divided the material into strength classes, enabling the production of high-strength beams ($F_{m,0.05}$ = 45.7 N/mm²) alongside standard-grade beams ($F_{m,0.05}$ = 30.7 N/mm²), albeit with reduced yield.

The third series investigated tensile strength properties of birch lamellas for glulam production from four growth regions in Germany to derive suitable grading approaches. It shows that tensile strength exhibits high variability, while density and dynamic modulus of elasticity are more consistent. A hybrid grading system combining knot characteristics and dynamic MOE enables reliable strength classification. Even visually lower-quality lamellas with pith or heartwood can achieve sufficient strength, highlighting the strong potential of birch wood for load bearing applications – e.g. as glulam or CLT.

INTRODUCTION

The increasing use of hardwoods in structural timber engineering is closely related to their high mechanical properties. Compared with softwoods, many hardwood species have higher densities, higher moduli of elasticity, and especially high tensile and bending strengths. These properties make hardwoods attractive for high-performance glued laminated timber, cross-laminated timber, and other timber products. At the same time, their practical use in structural applications is challenging. The mechanical properties of natural wood lamellas show large scatter and are influenced by growth characteristics such as grain deviation and knots, or wood moisture content. They are also influenced by density. Reliable strength grading is therefore required for load-bearing applications. It must represent characteristic values safely and allow assignments to suitable strength classes (cf. Glos and Lederer 2000).

4-poing-bending strength (beams tested upright) is the most important characteristic for structural timber and finger-jointed structural timber, since in rafters and floor or ceiling joists the structural timber is stressed in this manner. Also, the vibration and the deformation behaviour expressed by MOE_{dyn} and MOE_{stat} is important. For German hardwoods (maple, ash, poplar, beech, oak) in the years between 2000 and 2010 visual grading systems for the allocation into EN 1912 were developed in Munich, Germany (Glos and Näher 2005, Glos and Torno 2008). Machine grading systems may be commercially available, but to the knowledge of the authors are not used at the moment.

Tensile strength parallel to the grain is particularly important for glulam lamellas. The characteristic tensile strength of individual lamellas therefore determines the bending capacity of glued laminated timber. Studies on beech glued laminated timber show that machine grading and the characteristic tensile strength of the lamellas are key factors for the strength classes that can be achieved (cf. Blaß et al. 2005). For hardwoods, further research is still needed on suitable tensile strength classes. Kovryga et al. (2019) therefore proposed a separate system of tensile strength classes for European hardwoods with medium density. This was necessary, because the property profiles of hardwoods such as beech, ash, maple and birch do not fully match the classification systems derived from softwoods. The authors analysed tensile strength (f_t), tensile modulus of elasticity (MOE_{stat}), lamella properties and their inter-relationships. They showed that specific hardwood tensile strength classes (DT classes) can enable a more efficient use of the available strength potential.

More recent studies also confirm the relevance of this issue. Based on more than 900 beech boards, Rais et al. (2022) derived grading models and machine settings for beech tensile strength classes. They studied lamellas from different origins, as well as different cross-sections and quality groups. Their results showed that grading based on the dynamic modulus of elasticity can enable a reliable prediction of tensile strength.

The most comprehensive study to date on tensile loading of silver birch in the context of strength grading was published by Collins and Fink (2022). In that study, the variability of tensile strength and tensile stiffness of Finish silver birch boards was analysed. Prediction models were developed at the global board level and at the local defect level. In addition to destructive tensile tests, visual and non-destructive indicators were considered. The results show that tensile strength can be predicted reliably, especially by combining dynamic modulus of elasticity, grain angle, and knot parameters. The study therefore supports the assumption that separate or adapted grading models are required for birch lamellas. It also shows that hybrid grading approaches can offer advantages over pure visual grading. The study is therefore an important reference for deriving tensile strength classes, even though a direct normative classification of birch lamellas was not derived from it.

Jansen et al. (2025) examined German birch lamellas from several growth regions with regard to density, dynamic modulus of elasticity, visual grading characteristics, and tensile strength. The study showed that pure visual grading already allows high characteristic tensile strengths. The additional consideration of the dynamic modulus of elasticity allows classification up to DT30. The work therefore demonstrates both the potential of birch for structural timber engineering and the need for adapted grading procedures and further studies. These studies are needed to verify strength classes, finger-joint connections, and glued laminated timber members.

Medium-dense European hardwoods for structural applications have been the subject of research for two decades. Most studies have focused on products with superior mechanical properties compared to softwoods, aiming to demonstrate the high potential of hardwoods that could justify their higher prices. With decreasing availability of softwood in Central Europe for structural purposes, the efficient use of all timber resources - including hardwood - is becoming increasingly important. This manuscript aims to present three examples of a more efficient hardwood utilization by introducing alternative applications that have not been widely explored. These include:

- **Experimental Series 1** – low quality beech structural timber,
- **Experimental Series 2** – birch structural timber, and
- **Experimental Series 3** – birch lamellas for glulam.

For these three series strength, density and stiffness data is listed and different example strength grading approaches are presented.

EXPERIMENTAL SERIES 1 – LOW QUALITY BEECH STRUCTURAL TIMBER

Material and Methods (Experimental Series 1)

The following mechanical test was carried out:

- 4-point-bending (upright) testing (see Figure 1) of 302 beech boards (*Fagus sylvatica*) according to EN 408:2012 (conditioned at 20 °C and 65% relative humidity)
- The global MOE_{stat} was determined according to EN 408:2012 (see Figure 1)
- Two sub-samples BH & BC (lowest quality assortments) from a local beech sawmill
  - from furniture production using a "cutting all around" sawing pattern (see Figure 1 in Kovryga et al. 2019)
  - sawmill wants to find uses for these assortments other than firewood
  - beech wood from one growth region: Lower Saxony and Hesse, Germany
- two lamella cross-sections tested: 38 × 80 mm and 38 × 120 mm
  - 38 mm boards of different width (130 - 400 mm) were cut to the two test widths of 80 mm and 120 mm
  - Quality was optimized by cutting out cracks and minimizing big knots, cupping and warping
- The characteristic values ($Q_{0.05}$) were calculated in accordance with EN 14358:2016 as 5th percentile values, assuming a normal distribution and considering a confidence level of 75 %.

Before mechanical testing, the following visual grading parameters were recorded:

- knot characteristics single-knot parameter (SK) and knot-cluster parameter (KC) according to DIN 4074-5:2008,
- bark inclusions,
- pith,
- heartwood,
- grain deviation, and
- annual ring structure.

Additionally, the non-destructive machine grading parameters density and dynamic modulus of elasticity using longitudinal frequency measurements (Timbergrader MTG or Grindosonic MK7) were determined.

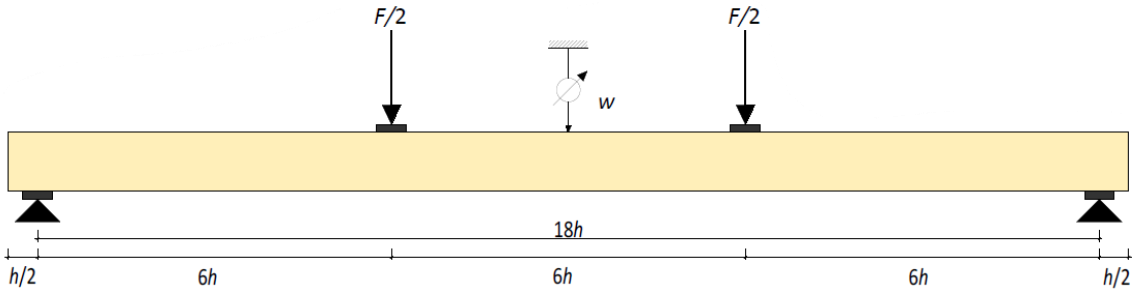

Figure 1: Test setup for 4-point-bending testing according to EN 408:2012

Results and Discussion (Experimental Series 1)

The mechanical properties of the investigated beech boards were evaluated separately for the two assortments BH and BC. The BH group, representing lower-quality material, is usually sold as firewood due to pith presence and pronounced bowing, while the BC group shows less bowing and no pith content and is sold as low-grade sawn timber.

Table 1 shows different densities for the two different assortments. Differences in strength and stiffness values cannot be explained by density differences, though. Bending strength showed much larger scatter than density and dynamic modulus of elasticity. For the total sample (BH & BC), the mean value was 59.00 N/mm², with a coefficient of variation of 42.65 %. The static modulus of elasticity was evaluated for 286 boards instead of 308 due to measurement errors in some boards. The strength values are not

affected by this. For the total sample, the mean value for $MOE_{stat,mean}$ was 13,409 N/mm², with a coefficient of variation of 19.46 %. It is notable that the coefficients of variation of the static modulus of elasticity are generally higher than those of the dynamic modulus of elasticity. Overall, the assortment-related evaluation shows that the investigated beech boards show higher densities, but lower MOE (dynamic and static) for the lower quality BH assortment. The boards of this assortment originate from regions in the trunk close to the pith. 23 % of the BH boards contained pith. The BC assortment boards originate from regions in the trunk further away from the pith. Here 0 % of the BC boards contained pith. Thus, the lower mean bending strengths of 53.31 N/mm² of the BH assortment compared to 67.05 N/mm² for the BC assortment can also be explained. Due to a few very low strength values in each assortment (in BH lowest F_m = 1.94 N/mm²; in BC lowest F_m = 7.39 N/mm²), the characteristic strength values (5 % quantiles calculated according to EN 14358:2016) are with 14.70 (BH) and 18.95 (BC) very low. By excluding boards with large cracks, rot and big size knots and knot clusters, these values can be substantially raised. For each sawmill (sawing pattern) and assortment available, these threshold values need to be determined separately by empiric testing. In order to use these assortments as load bearing products, in Germany a national technical approval (abZ) or a European Technical Assesment (ETA) can be developed, which is then issued by the German Institute for Building Technology (DIBt). Info on data and documents necessary for an abZ is given by the DIBt, for an ETA this info can also be given by the DIBt or another European Technical Assessment Body (TAB).

Table 1: Mechanical properties of beech 4-point-bending-tested (upright) boards from the two lowest quality assortments from furniture producing hardwood sawmill

Parameter	Statistics	Assortment BH	Assortment BC	Total
MOE_{dyn} [N/mm²]	*n*	179	123	302
	μ	12.554	14.224	13.234
	CV	0.1515	0.1164	0.1499
	$Q_{0.05}$	9.198	11.298	9.738
ρ_{12} [g/cm³]	*n*	181	127	308
	μ	0.73	0.68	0.71
	CV	0.047	0.0588	0.065
	$Q_{0.05}$	0.672	0.609	0.63
F_m [N/mm²]	*n*	181	127	308
	μ	53.31	67.05	59.00
	CV	0.4104	0.4060	0.4265
	$Q_{0.05}$	14.70	18.95	14.64
MOE_{stat} [N/mm²]	*n*	173	113	286
	μ	12.632	14.599	13.409
	CV	0.1988	0.1567	0.1946
	$Q_{0.05}$	8.199	10.554	8.809

EXPERIMENTAL SERIES 2 – BIRCH STRUCTURAL TIMBER

Material and Methods (Experimental Series 2)

The following mechanical test was carried out:

- 4-point-bending (upright) testing (see Figure 1) of 210 birch boards (*Betula pendula*) according to EN 408:2012 (conditioned at 20 °C and 65% relative humidity)
- The global MOE_{stat} was determined according to EN 408:2012 (see Figure 1)
- sub-samples originated from two growth regions - 1 in Brandenburg and 1 in Lower Saxony, Germany
- sawing pattern “cant sawing” (see Figure 1 in Schlotzhauer et al. 2019, patterns A-C)
    - no further optimization
    - only technical drying, planing to lamella cross sections and cutting to test lengths
- two lamella cross-sections tested: 40 × 80 mm and 40 × 120 mm
- The characteristic values ($Q_{0.05}$) were calculated in accordance with EN 14358:2016 as 5th percentile values, assuming a normal distribution and considering a confidence level of 75 %.

Before mechanical testing, visual grading parameters were recorded and the non-destructive machine grading parameters density and dynamic modulus of elasticity were determined like specified for EXPERIMENTAL SERIES 1.

Results and Discussion (Experimental Series 2)

Characteristics after growth regions

The mechanical properties of the investigated birch boards (tested upright) were evaluated separately for the two growth regions respectively origins. This was done to identify possible origin-related differences within the sample population.

Table 2 shows that the investigated origins are relatively homogeneous with regard to density. The differences in strength and stiffness values therefore cannot be explained by density differences alone. As expected, 4-point-bending strength showed much larger scatter than density and dynamic modulus of elasticity. For the total sample, the mean value was $F_{m,mean}$ = 61.61 N/mm², with a coefficient of variation of 29.93 %. The mean bending strengths of the individual origins ranged from 60.61 N/mm² to 63.57 N/mm². For the total sample, the mean value for $MOE_{stat,mean}$ was 12,910 N/mm², with a coefficient of variation of 15.32 %. It is notable that the coefficients of variation of the static modulus of elasticity are generally higher than those of the dynamic modulus of elasticity. Overall, the origin-related evaluation shows that the investigated birch boards have comparable dynamic moduli of elasticity across the two origins.

Table 2: Mechanical properties of birch 4-point-bending-tested (upright) boards from two different German growth regions (origin 1-2)

Parameter	Statistics	Origin 1	Origin 2	Total
MOE_{dyn} [N/mm²]	*n*	137	73	210
	μ	13.957	13.791	13.899
	CV	0.1269	0.1064	0.1204
	$Q_{0.05}$	10.828	11.117	10.946
ρ_{12} [g/cm³]	*n*	144	73	217
	μ	0.643	0.652	0.646
	CV	0.0448	0.0513	0.0475
	$Q_{0.05}$	0.592	0.591	0.592
F_m [N/mm²]	*n*	144	73	217
	μ	60.61	63.57	61.61
	CV	0.3085	0.2792	0.2993
	$Q_{0.05}$	27.59	31.23	29.08
MOE_{stat} [N/mm²]	*n*	144	73	217
	μ	12.794	13.137	12.910
	CV	0.1641	0.1285	0.1532
	$Q_{0.05}$	9.086	10.062	9.421

Grading approach using MOE_{dyn}

The MOE_{dyn} presents a non-destructive machine grading parameter that can be attained easily with a hand-held device (Görlacher 1984). The device measures the longitudinal frequency, from which – together with the board's dimensions and mass – the dynamic modulus of elasticity is calculated. Costs for such a system are rather low and the measured values are highly repeatable. Therefore, grading approaches using only the MOE_{dyn} are especially suited for small sawmills that want to provide structural timber. Figure 2 presents a simple division of the original sample (all, i.e. all origins and cross-sections) into three grades.

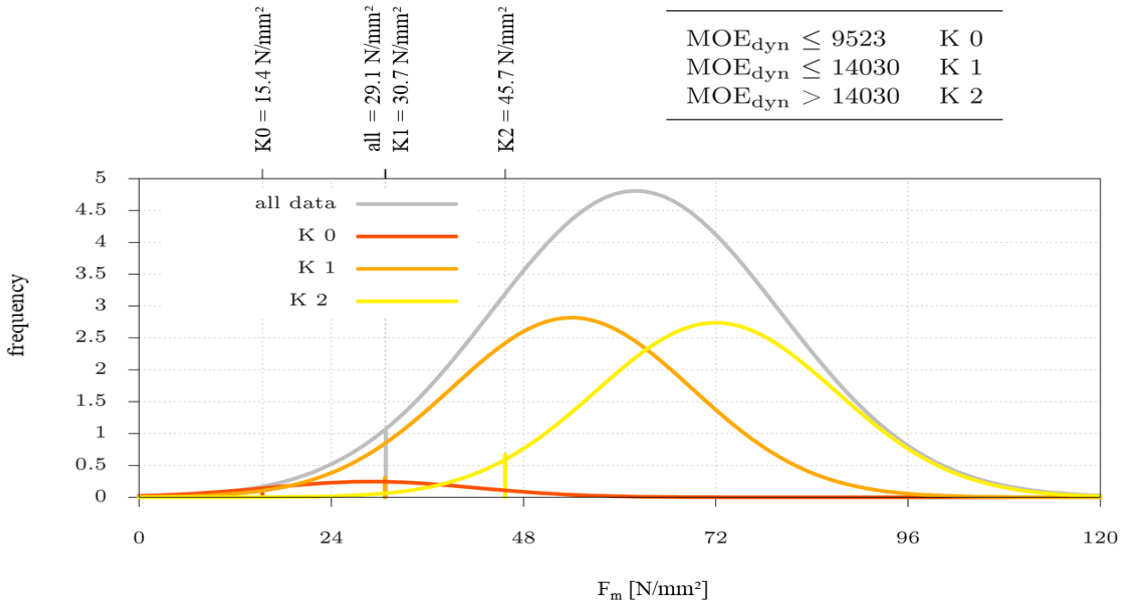

Figure 2: Frequency distribution curves of the 4-point-bending strength (F_m) for three different strength grading proposals (K0, K1, K2) and the entire tested population (all) plus characteristic values ($Q_{0.05}$) for each grade and all

The lowest grade (K0) includes all boards with MOE_{dyn} lower than 9,523 N/mm². This threshold value produces a grade with a very low characteristic strength of 15.4 N/mm². Mainly this threshold value excludes boards with very big knots, which were very rare in the original sample (population). The grades K1 and K2 are separated by the MOE_{dyn} value 14,030 N/mm². This threshold value separates the original sample into two grades of nearly the same size (n). It produces the K1 grade with a characteristic strength of 30.7 N/mm², which is almost the same value the entire original sample produces without grading (29.1 N/mm²). It also produces the higher quality grade K2 with a characteristic strength of 45.7 N/mm². Thus, the effort of measuring the MOE_{dyn} and using it for simple machine grading results in an overall higher quality yield.

EXPERIMENTAL SERIES 3 – BIRCH LAMELLAS FOR GLULAM

Material and Methods (Experimental Series 3)

The following mechanical test was carried out:

- tension testing (see Figure 3) of 474 birch lamellas (*Betula pendula* and *Betula pubescens*) according to EN 408:2012 (conditioned at 20 °C and 65% relative humidity)
- sub-samples originated from four growth regions - 2 in North Rhine-Westphalia and 2 in Lower Saxony, Germany
- sawing pattern "through and through"
    - afterwards optimization by sawing boards to lamellas with less characteristics and cracks
    - afterwards technical drying, planing to lamella cross sections and cutting to test lengths
- four lamella cross-sections tested: 20 × 80 mm, 30 × 100 mm, 30 × 150 mm, and 40 × 150 mm
- The characteristic values ($Q_{0.05}$) were calculated in accordance with EN 14358:2016 as 5th percentile values, assuming a normal distribution and considering a confidence level of 75%.

Before mechanical testing, visual grading parameters were recorded and the non-destructive machine grading parameters density and dynamic modulus of elasticity were determined like specified for EXPERIMENTAL SERIES 1.

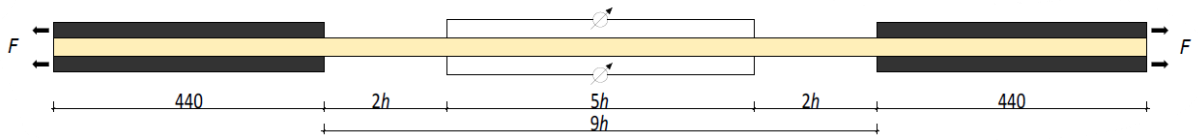

Figure 3: Test setup for tension testing according to EN 408:2012

Results and Discussion (Experimental Series 3)

Characteristics after growth regions

The mechanical properties of the investigated birch lamellas were evaluated separately for the four growth regions respectively origins. This was done to identify possible origin-related differences within the sample population.

Table 3 shows that the investigated origins are relatively homogeneous with regard to density. The differences in strength and stiffness values therefore cannot be explained by density differences alone. As expected, tensile strength showed much larger scatter than density and dynamic modulus of elasticity. For the total sample, the mean value was $F_{t,mean}$ = 46.82 N/mm², with a coefficient of variation of 36.49 %. The mean tensile strengths of the individual origins ranged from 43.34 N/mm² to 50.89 N/mm². The static modulus of elasticity was evaluated for 436 lamellas instead of 473 due to measurement errors in some lamellas. The strength values are not affected by this. For the total sample, the mean value for $MOE_{stat,mean}$ was 13,156 N/mm², with a coefficient of variation of 18.39 %. It is notable that the coefficients of variation of the static modulus of elasticity are generally higher than those of the dynamic modulus of elasticity. Overall, the origin-related evaluation shows that the investigated birch lamellas have comparable densities and dynamic moduli of elasticity (MOE_{dyn}) across all four origins, while strength and MOE_{stat} values differ to a greater extent. Origin 4 shows the most favourable tensile strengths, while Origin 2 tends to show lower stiffness and strength values.

Table 3: Mechanical properties of birch tension-tested lamellas from four different German growth regions (origin 1-4)

Parameter	Statistics	Origin 1	Origin 2	Origin 3	Origin 4	Total
MOE_{dyn} [N/mm²]	*n*	129	111	117	116	473
	μ	15.436	13.712	14.751	14.634	14.665
	CV	0.1292	0.1528	0.1429	0.1039	0.1387
	$Q_{0.05}$	11.927	10.024	11.042	11.957	11.087
ρ_{12} [g/cm³]	*n*	129	111	117	116	473
	μ	0.672	0.654	0.643	0.646	0.654
	CV	0.0634	0.0654	0.0703	0.0637	0.0678
	$Q_{0.05}$	0.597	0.579	0.564	0.573	0.576
F_t [N/mm²]	*n*	129	111	117	116	473
	μ	47.23	43.34	45.63	50.89	46.82
	CV	0.3679	0.3676	0.3673	0.3437	0.3649
	$Q_{0.05}$	16.65	15.30	16.14	20.11	16.75
MOE_{stat} [N/mm²]	*n*	108	95	117	116	436
	μ	14.135	12.123	13.188	13.060	13.156
	CV	0.1617	0.1972	0.2067	0.1397	0.1839
	$Q_{0.05}$	10.113	7.795	8.391	9.850	8.898

Grading approach for visual grading (plus MOE_{dyn})

To derive tensile strength classes for birch lamellas, Jansen et al. (2025) used a hybrid grading approach. In this approach, visually detectable grading characteristics were combined with the non-destructively determined longitudinal dynamic modulus of elasticity. Knot clusters were used as the governing visual criterion. The grading limits were defined so that the classes LS 7m, LS 10m, and LS 13m each had grading requirements for knot clusters and for the MOE_{dyn} (see Table 4). They were used, because they showed the strongest individual relationship with tensile strength in the investigations. For the classes LS 7m, LS 10m, and LS 13m, minimum values of the dynamic modulus of elasticity of 10,000 N/mm², 12,500 N/mm², and 15,000 N/mm² were applied. Pith and brown heartwood were permitted in the classes LS 7m and LS 10m, but excluded in the highest class LS 13m. Grain deviation and annual ring width were not used as limiting grading criteria.

Table 4: Grading parameters with limits and corresponding tensile strength based on Jansen et al. (2025)

Parameter	Unit	LS 7m	LS 10m	LS 13m
Grading parameters				
Knot cluster	-	<1/2	<1/3	<1/5
Brown heartwood	-	Yes	Yes	No
Pith	-	Yes	Yes	No
MOE_{dyn}	[N/mm²]	>10.000	>12.500	>15.000
Tensile Strength				
Number	[pcs]	81	267	105
Yield	[%]	17.9	58.9	23.2
$f_{t,mean}$	[N/mm²]	33.97	44.79	62.41
$f_{t,0.05}$	[N/mm²]	16.39	22.17	31.63
CV	-	0.2859	0.2870	0.2802
MOE_{stat}				
Number	[pcs]	77	241	104
MOE_{mean}	[N/mm²]	10.817	13.211	15.271
$MOE_{0.05}$	[N/mm²]	8.199	10.435	12.229
CV	-	0.1338	0.1478	0.1132

Regression model for machine grading

Grading machines use regression models. Various regression approaches can be found in the literature for estimating the mechanical properties of solid wood lamellas, particularly tensile strength, on the basis of non-destructively or easily determined input parameters. An early approach is the Karlsruhe calculation model according to Ehlbeck and Colling (1987), which was developed for spruce lamellas. In this model, the MOE_{stat} is first described as a function of knot area ratio (KAR) and density. Subsequently, the tensile strength is modelled by MOE_{stat} and an interaction term between KAR and the MOE_{stat}. Building on this, the Karlsruhe calculation model was transferred and adapted to beech wood by Blaß et al. (2005). In this model, the MOE_{stat} is additionally described by linear and quadratic terms of density, while the tensile strength is formulated as a function of MOE_{stat} and KAR. Fink (2014) used a further regression approach for spruce lamellas, in which both the MOE_{stat} and the tensile strength are described directly as functions of MOE_{dyn} and KAR. As a more recent development, the study by Collins and Fink (2022) on silver birch should be mentioned. In this work, models were developed for predicting the tensile strength and stiffness of birch boards. For the strength models, the MOE_{dyn}, the mean grain angle determined by laser light scattering, and KAR were considered in particular.

Building on the regression approaches described in the literature, a model structure based on Fink (2014) was applied to the present birch dataset, and the regression parameters were re-estimated using the least squares method. After removing outliers with standardized residuals greater than |3|, 466 datasets remained for the regression analysis. The model based on MOE_{dyn} (E_{dyn}) and KC (knot cluster parameter) achieved a coefficient of determination of $R^2 = 0.486$ and an adjusted coefficient of determination of $R_{adj}^2 = 0.484$ for the logarithmic tensile strength. The correlation coefficient between measured and predicted values was $r = 0.697$ on the logarithmic scale and $r = 0.713$ on the strength scale. Both the individual parameters and the overall model were statistically highly significant. The residual scatter on the logarithmic strength scale was $RMSE_{ln(ft)} = 0.251$. On the strength scale, an RMSE of 11.83 N/mm² and an MAE of 9.16 N/mm² were obtained. The regression equation is then as follows:

$$\ln(f_t) = 2{,}70 + 8.5 \cdot 10^{-5} \cdot E_{dyn} - 0.86 \cdot KC + \varepsilon \quad (1)$$

Compared with the correlation coefficient of about $r \approx 0.74$ reported by Collins and Fink (2022), the model developed in this study shows a similar level of predictive performance. This is notable, since the present model does not include grain deviation or the tracheid effect as an input parameter. The remaining scatter in the predictions may therefore be explained by structural features that were not recorded in this study, such as grain deviations, local wood defects, or other material-related influences.

CONCLUSIONS

This manuscript showed the strength determination and different strength grading approaches for three lesser used hardwood assortments. The goal of this elaboration was to show that for any given resource respectively assortment (or sample) a strength grading system can be developed. The economic use of the resource depends on a series of other factors, though, mainly the product yield, which directly affects the prize.

For each product a strength grading system optimized for its main use/stress needs to be developed. If a board or beam is to be used mainly as rafter or floor and ceiling joist, its 4-point-bending strength is most relevant. And therefore, a strength grading system optimized for 4-point-bending strength needs to be established. For glulam lamellas a tension strength grading system is most suitable. For boards used as bottom or top plates in wall framing a strength grading system predicting the compression strength perpendicular to grain or the nail holding strength (nail withdrawal resistance) might be a viable alternative. These strength grading systems need to be developed and afterwards proposed to the DIBt or another European Technical Assessment Body (TAB). Other characteristic and mean values also need to be provided - like Table 1 of EN 338:2016 does for structural timber. Here either more date determination is necessary or the use of available date or other EADs can be discussed with the DIBt or another European Technical Assessment Body (TAB).

REFERENCES

Blaß HJ, Denzler J, Frese M, et al (2005) Biegefestigkeit von Brettschichtholz aus Buche. Band 1 Karlsruher Berichte zum Ingenieurholzbau, Universitätsverlag Karlsruhe, Karlsruhe

Collins S, Fink G (2022) Modeling the tensile mechanical properties of silver birch timber boards. Construction and Building Materials 344:121-128. https://doi.org/10.1080/17480272.2020.1801836

DIN 4074-5 (2008) Strength grading of wood - Part 5: Sawn hardwood. German Institute for Standardization (DIN), Berlin

Ehlbeck J, Colling F (1987) Biegefestigkeit von Brettschichtholz in Abhängigkeit von Rohdichte, Elastizitätsmodul, Ästigkeit und Keilzinkung der Lamellen, der Lage der Keilzinkung sowie von der Trägerhöhe. Versuchsanstalt für Stahl, Holz und Steine, Universität Fridericiana Karlsruhe, Karlsruhe, Germany

EN 338 (2016) Structural timber - Strength classes. European Committee for Standardization, Brussels

EN 408 (2012) Timber structures - Structural timber and glued laminated timber - Determination of some physical and mechanical properties. European Committee of Standartization, Brussels

EN 1912 (2013) Structural timber - Strength classes - Assignment of visual grades and species. European Committee for Standardization, Brussels

EN 14358 (2016) Timber structures - Calculation and verification of characteristic values. European Committee of Standartization, Brussels

Fink G (2014) Influence of varying material properties on the load-bearing capacity of glued laminated timber. ETH Zurich

Glos P, Lederer B (2000) Sortierung von Buchen-und Eichenschnittholz nach der Tragfähigkeit und Bestimmung der zugehörigen Festigkeits-und Steifigkeitskennwerte. Final report. Institut für Holzforschung, Technische Universität München, Munich

Glos P, Näher T (2005) Aufnahme der einheimischen Holzarten Buche (Fagus sylvatica), Eiche (Quercus petraea, Quercus robur) und Douglasie (Pseudotsuga menziesii) in die europäische Norm EN 1912. Holzforschung München, Technische Universität München, Munich

Glos P, Torno S (2008) Aufnahme der einheimischen Holzarten Ahorn, Esche und Pappel in die europäische Norm EN 1912: „Bauholz – Festigkeitsklassen – Zuordnung von visuellen Sortierklassen und Holzarten“. Holzforschung München, Technische Universität München, Munich

Görlacher R (1984) Ein neues Meßverfahren zur Bestimmung des Elastizitätsmoduls von Holz. Holz als Roh-und Werkstoff 42:219–222. https://doi.org/10.1007/BF02607231

Jansen T, Wieland S, Emmerich L, Uibel T (2025) Synchronisation der Wertschöpfungskette Forst-Holz – Etablierung der Verwendung von Birkenholz im Ingenieurholzbau. In: Tagungsband Aachener Holzbautagung 2025. Aachen

Kovryga A, Schlotzhauer P, Stapel P, et al (2019) Visual and machine strength grading of European ash and maple for glulam application. Wood Material Science & Engineering. https://doi.org/10.1515/hf-2018-0142

Rais A, Kovryga A, Pretzsch H, Van De Kuilen J-WG (2022) Timber tensile strength in mixed stands of European beech (Fagus sylvatica L.). Wood Sci Technol 56:1239–1259. https://doi.org/10.1007/s00226-022-01398-7

Schlotzhauer P, Kovryga A, Emmerich L, et al (2019) Analysis of Economic Feasibility of Ash and Maple Lamella Production for Glued Laminated Timber. Forests 10:529. https://doi.org/10.3390/f10070529

Circular Economy in Structural Timber

Daniel F. Llana[1,2*], Guillermo Íñiguez-González[2,3], Mônica Ruy[4], Katarzyna Ostapska[5]

[1] Timber Products Laboratory, ICIFOR-INIA, CSIC, Ctra. La Coruña 7,5, 28040, Madrid, Spain
[2] Timber Construction Research Group (GICM - UPM), Madrid, Spain
[3] School of Forestry Engineering and Natural Resources. Universidad Politécnica de Madrid, Spain
[4] Structural Timber Engineering Platform, PEMADE, USC, Lugo, Spain
[5] SINTEF Community, Trondheim, Norway.

E-mail: daniel.llana@inia.csic.es; guillermo.iniguez@upm.es; m.ruy@usc.es; Katarzyna.Ostapska@sintef.no

Keywords: Cascading; non-destructive testing; reclaimed timber; recovered timber; salvaged timber; secondary timber; TiReX project.

ABSTRACT

The growing demand for timber in structural applications, together with the transition toward sustainable construction and the policies promoted by the European Union and other international organizations, has highlighted the need to implement circular economy principles within the timber construction sector. In recent years, concepts such as design for disassembly, material recovery, reusability, and recycling have received increasing research attention. However, a critical challenge remains: how should recovered timber be graded for structural applications?

Current visual strength grading standards tend to downgrade most recovered timber elements, thereby underestimating their actual mechanical properties. In contrast, non-destructive testing methods, which are widely applied to new timber grading, appear to provide more reliable estimations of structural performance.

Within the framework of the ongoing European TiReX project, four batches of recovered timber were evaluated using several non-destructive testing techniques. The material included two batches of European oak from Spain, one batch of Norway spruce from Norway, and one batch of Scots pine from Norway. The results showed that longitudinal vibration techniques provided more accurate estimations of modulus of elasticity and bending strength (R^2 values up to 70%) than time-of-flight devices (R^2 values up to 60%).

Furthermore, the reuse of recovered timber depends not only on its mechanical properties but also on additional factors such as specimen's length, wanes, warp, the presence of metallic inclusions, and hazardous substances, among others, all of which must be considered when assessing its potential for reuse.

INTRODUCTION

The use of timber and timber products as structural materials increases every year in the construction sector due to their favorable strength-to-weight ratio, advantages in industrialized construction, sustainability, decarbonization potential, and recyclability. Consequently, the growing demand for wood for these purposes is raising concerns about the limits of sustainable use and the availability of raw materials. There is also increasing interest in implementing circular economy principles in the timber construction sector, supported by European Union and international policies that promote extended building service life and the reuse and recycling of materials (European Commission COM/2020/98 2020, Commission delegated regulation (EU) 2023/2486 2023).

Several research studies have addressed the circular economy in the timber construction sector in different aspects like Design for Disassembly, how to build today in order to recover as much timber in the future and in the best conditions (Ottenhaus et al. 2023, Torres et al. 2025). Recycling timber into high-value products, mainly Engineering Recovered Wood Products (ERWPs). In most cases, these

studies have produced construction-suitable products, although with very low timber yields during the manufacturing process (Rose et al. 2018, Irle et al. 2019, Uí Chúláin et al. 2023). Due this low yield during manufacturing process, directly reuse of recovered timber in its original shape or with minimal would be a better option to explore (Llana et al. 2023).

Most or the research studies have identified a key issue: the determination of mechanical properties. How recovered timber should be graded? Current visual strength grading standards were developed for new timber and tend to underestimate the properties of recovered timber, resulting in excessively high rejection rates, Llana et al. (2022) reported 77% rejection in recovered European oak and Llana et al. (2023) reported 95% rejection in recovered Norway spruce. Non-destructive testing (NDT) techniques are the most common method used nowadays for new timber grading and have shown reliable results in the assessment of existing timber structures when combined with visual inspection (Llana et al. 2023; Dietsch et al. 2025).

The present research study is part of the TiReX project (https://www.tirex.info/), a three-year European research project involving partners from six European countries (Norway, Finland, Latvia, Poland, Slovenia and Spain). The project aims to create a comprehensive database of recovered timber to support the development of a European grading standard combining both non-destructive tests and visual assessment techniques, based on an extensive testing campaign. This large campaign of structural size specimens, includes timber from various European regions (Northern, Eastern, and Southern Europe), covering both softwoods and hardwoods.

MATERIALS AND METHODS

Geometry

Two batches with a total number of 156 recovered specimens of European oak (*Quercus robur* L.) were used. These specimens were mainly floor beams recovered from the demolition of several structures of more than 100 years old in the Basque Country (Spain). Furthermore, 26 specimens of Norway spruce (*Picea abies* (L.) Karst) and 4 of Scots pine (*Pinus sylvestris* L.) recovered from a riverside wharf building in Trondheim, Norway were studied (Fig. 1).

Regarding dimensions, while in new timber cross-section is regular with CoV lower than 1.5 % (Íñiguez-González et al. 2019), in recovered timber usually present an irregular cross-section due to ancient sawn methods, wanes and round wood inclusion. There are differences between specimens and also differences within each specimen. Therefore, it is not easy to define a homogenous cross-section, the method to determine the average cross-section was described by Osuna-Sequera et al. (2020) measuring in 3 cross-sections with a forest calliper. Table 1 shows dimensions and coefficients of variation (CoV) of cross-section measurements.

Table 1: Timber specimens geometry

Species	Batch	N	MC [%]	Thickness		Width		Length [mm]
				b [mm]	CoV (%)	h [mm]	CoV (%)	
QCXE[a]	Q1	30	20.4	136	8.4	151	7.9	3,010
	Q2	126	23.4	136	9.3	148	9.2	3,258
PCAB[b]	P1	26	14.1	174	19.4	190	16.1	2,543
PNSY[c]	P2	4	9.2	168	6.3	208	28.0	3,912

[a]QCXE: European oak (Quercus robur L.); [b]PCAB: Norway spruce (Picea abies (L.) Karst.); [c]PNSY: Scots pine (Pinus sylvestris L.) Species codes according to the European standard EN 13556 2003

Figure 1: European oak specimens from Spanish's provenance at the laboratory (left). Norway spruce specimens salvaged from one riverside wharf building in Trondheim (right)

Non destructive testing experiments

Portable Lumber Grader PLG (Fakopp Enterprise Bt., Sopron, Hungary) device was used for longitudinal vibration in batches Q1 and Q2. Specimens were simply supported at the ends, and one end was struck by a hammer (Fig. 2). A microphone recorded the signal and the first mode natural frequency was obtained from the signal recorded through Fast Fourier Transform (FFT) software. Velocity (V) was calculated as two times length by frequency. Furthermore, MicroSecond Timer (Fakopp Enterprise Bt., Sopron, Hungary) device was used to record Time-of-Flight (ToF) end-to-end in all batches (Fig. 2) and velocity calculated as length divided by ToF.

The dimensions and mass of boards were recorded to determine their density. Edyn was calculated according to Eq. 1.

$$E_{dyn} = \rho \ V^2 \tag{1}$$

In the case of batches P1 and P2, MicroSecond Timer MST (Fakopp Enterprise Bt., Sopron, Hungary) device was used to record Time-of-Flight (ToF).

Mechanical testing experiments

Mechanical properties of specimens were determined according to EN 408 (2012) standard. Four-point bending test was conducted to obtained global modulus of elasticity (MOE) and bending strength (MOR).

All measurements were adjusted to a reference moisture content (MC) of 12%.

Figure 2: Portable Lumber Grader PLG (left) and MicroSecond Timer MST (right) measurements on European oak specimens

RESULTS AND DISCUSSION

Mechanical properties estimation

As significant differences in MOE and MOR were found between batches Q1 and Q2, separate estimation models were developed. Estimation of mechanical properties of recovered specimens were done through linear regressions from NDT measurements. Figure 3 shows linear regression for batches Q1 and Q2 estimating MOE from Edyn calculated from PLG results. Table 2 presents determination coefficients and standard errors for all batches.

Table 2: Determination coefficients (R2) and Standard Errors (StE) for mechanical properties estimation from Edyn

Species	Batch	MOE				MOR			
		Edyn PLG		Edyn MST		Edyn PLG		Edyn MST	
		R^2 [%]	StE [N/mm^2]	R^2 [%]	StE [N/mm^2]	R^2 [%]	StE [N/mm^2]	R^2 [%]	StE [N/mm^2]
QCXE	Q1	70	793	60	920	50	5.89	30	6.96
	Q2	45	1307	33	1442	36	7.31	25	7.91
PCAB	P1	-	-	20	2144	-	-	3	11.1
PNSY	P2	-	-	79	450	-	-	88	2.8

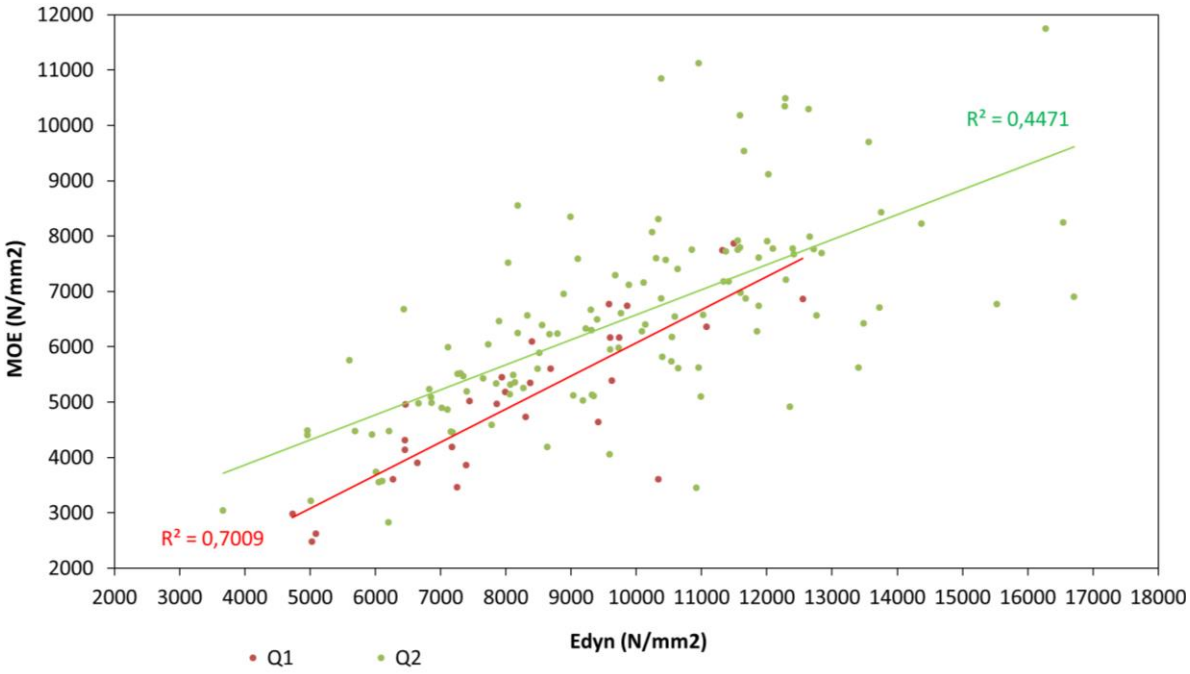

Figure 3: Linear regression of batches Q1 and Q2 between MOE and Edyn calculated from Portable Lumber Grader PLG

From results of recovered oak (Q1 and Q2) in Table 2, the most accurate mechanical properties estimations were obtained based on longitudinal vibration measurements as was also reported in previous research works (Llana et al. 2022 and 2023). However, results varied a lot between the two batches due to the high variability of the recovered timber. Osuna-Sequera et al. (2024), using longitudinal vibration on recovered Salzmann pine to estimate MOE and MOR, obtained an R^2 of 61% and StE of 1046 N/mm^2 for MOE and R^2 of 55% and StE of 6.17 N/mm^2 for MOR. Regarding Norway spruce, the coefficients of determination were low and the standard errors were high. This may be related to the round shape of the timber, the limited number of specimens, and the short specimen length used for mechanical testing. These models will be further improved in future work by incorporating visual parameters. In the case of Scots pine, values similar to those reported for new timber were obtained. These are preliminary results from the TiReX project in Spain and Norway and should be interpreted with caution, as they were developed from a limited number of specimens. The testing campaign of the TiReX project is ongoing, and by the end of the project in April 2027, models based on a substantially larger number of specimens are expected to be developed.

Reusability aspects

The estimation of mechanical properties alone is insufficient for grading recovered timber for structural reuse. Additional factors affecting reusability, beyond physical and mechanical performance, must also be considered.

Dimensional limitations are common in recovered timber. Reduced lengths frequently result from historical construction practices and the removal of decayed beam ends previously embedded in masonry walls. Irregular cross-sections, caused by traditional sawing techniques and the presence of wanes, are particularly common in older timber and may also affect the accuracy of non-destructive testing methods. In addition, significant warp is often observed in large cross-section elements, complicating handling and installation during construction (Fig. 4).

Figure 4: Twist in a 11-m length recovered Salzmann pine specimen (left), wane and mortises in recovered European oak (right)

Recovered timber also commonly contains embedded metallic elements such as nails, screws, and connector plates. While some can be removed, corroded nails in older timber are often difficult to extract and may remain inside if further machining work is unnecessary. Another relevant issue is the potential presence of hazardous chemical treatments applied in the past, which are difficult to identify and remove, especially in relatively recent recovered timber.

CONCLUSIONS

The circularity of timber should be fully implemented within the timber construction sector through strategies such as design for disassembly, material recovery, reuse, and recycling. Recovered timber can subsequently be reused or recycled into new engineered timber products for structural applications. However, one of the main barriers to this transition is the reliable assessment of the mechanical properties of recovered timber, particularly for strength grading purposes. In this context, non-destructive testing methods, especially resonance-based techniques, appear to be more promising than conventional visual strength grading methods.

Nevertheless, grading cannot rely exclusively on mechanical properties, as several additional factors influencing reusability must also be considered. These include geometric characteristics (e.g., length, warp, and wane), the presence of metallic inclusions, and potentially hazardous chemical treatments.

The European project TiReX is currently conducting an extensive testing campaign on recovered structural timber sourced from several European countries. The main objective of the project is to develop a comprehensive database that will support the establishment of a grading standard based on both non-destructive testing results and visual assessment parameters.

ACKNOWLEDGEMENTS

The TiReX project has received funding in Spain from Ministerio de Ciencia, Innovación y Universidades (MICIU) Spain [PCI2024-153432], and in Norway from grant No. 351968 from The Research Council of Norway. Both under the ForestValue2 Joint Call program 2023 from European Union's Horizon Europe under grant agreement No. 101094340.

REFERENCES

Commission delegated regulation (EU) 2023/2486 (2023). Official Journal of the European Union. Document 32023R2486. http://data.europa.eu/eli/reg_del/2023/2486/oj

Dietsch P, Ehrenlechner C, Frese M, Winter S (2025) Reuse: Guideline on the assessment of technical integrity of disassembled timber members. World Conference on Timber Engineering (WCTE 2025) 1786-1795. https://doi.org/10.52202/080513-0218

European Commission COM/2020/98 (2020) A new Circular Economy Action Plan for a cleaner and more competitive Europe. https://eur-lex.europa.eu/resource.html?uri=cellar:9903b325-6388-11ea-b735-01aa75ed71a1.0017.02/DOC_1&format=PDF

European standard EN 408:2010+A1 (2012) Timber structures - Structural timber and glued laminated timber - Determination of some physical and mechanical properties. European Committee of Standardization (CEN) Brussels Belgium.

European standard EN 13556 (2003) Round and sawn timber - Nomenclature of timbers used in Europe. European Committee of Standardization (CEN) Brussels Belgium.

Íñiguez-González G, Arriaga F, Osuna-Sequera C, Esteban M, Ridley-Ellis D (2019) Nondestructive measurements in reclaimed timber from existing structures. 21st International Nondestructive Testing and Evaluation of Wood Symposium. September 24-27 2019. Freiburg im Breisgau, BW, Germany. Pp. 462-472.

Irle M, Privat F, Couret L, Belloncle C, Déroubaix G, Bonnin E, Cathala B (2019) Advanced recycling of post-consumer solid wood and MDF. Wood Mater Sci Eng 14(1):19-23. https://doi.org/10.1080/17480272.2018.1427144

Llana DF, González-Alegre V, Portela M, Íñiguez-González G (2022) Cross Laminated Timber (CLT) manufactured with European oak recovered from demolition: structural properties and non-destructive evaluation. Constr Build Mater 339:127635. https://doi.org/10.1016/j.conbuildmat.2022.127635

Llana DF, Íñiguez-González G, Plos M, Turk G (2023) Grading of recovered Norway spruce (*Picea abies*) timber for structural purposes. Constr Build Mater 398:132440. https://doi.org/10.1016/j.conbuildmat.2023.132440

Osuna-Sequera C, Llana DF, Íñiguez-González G, Arriaga F (2020) The influence of cross-section variation on bending stiffness assessment in existing timber structures. Eng. Struct. 204:110082. https://doi.org/10.1016/j.engstruct.2019.110082

Osuna-Sequera C, Arriaga F, Llana DF, Íñiguez-González G (2024) Predicting the mechanical properties of timber from existing structures by the longitudinal vibration method, visual grading and definition of the nominal cross-section. Wood Mater. Sci. Eng. 19(2):366-374 https://doi.org/10.1080/17480272.2023.2243673

Ottenhaus LM, Yan Z, Brandner R, Leardini P, Fink G, Jockwer R (2023) Design for adaptability disassembly and reuse - A review of reversible timber connection systems. Constr Build Mater 400:132823. https://doi.org/10.1016/j.conbuildmat.2023.132823

Rose CM, Bergsagel D, Dufresne T, Unubreme E, Lyu T, Duffour P, Stegemann JA (2018) Cross-Laminated Secondary Timber: Experimental testing and modelling the effect of defects and reduced feedstock properties. Sustainability 10(11):4118. https://doi.org/10.3390/su10114118

TiReX project (European ForestValue2 Joint call program) website. https://www.tirex.info/ Accessed 14 April 2026

Torres V, Íñiguez-González G, Blanchet P, Giorgio B (2025) Challenges in the design for disassembly of light timber framing panelized components. Buildings 15(3):321. https://doi.org/10.3390/buildings15030321

Uí Chúláin C, Llana DF, Hogan P, McGetrick P, Harte AM (2023) Bending characteristics of CLT from recovered spruce. World Conference on Timber Engineering (WCTE 2023) 888-894. https://doi.org/10.52202/069179-0121

Static and Dynamic Investigation of the Bending Strength and Modulus of Elasticity of Oak Timber

Mikael Perstorper[1], Joan W. Gikonyo[2]

[1] Karlstad University, Universitetsgatan 2, 651 88 Karlstad and Limab AB, Sweden, Almedalsvägen 15, 412 63 Göteborg
[2] Karlstad University, Universitetsgatan 2, 651 88 Karlstad.

E-mail: mikael.perstorper@kau.se; joan.wangui.gikonyo@kau.se

Keywords: dynamic modal testing; modulus of elasticity; bending strength; bending tests; non-destructive techniques; strength grading, oak

ABSTRACT
Norway spruce is the dominating species for structural purposes in northern Europe. However, other species have come into focus as alternatives. Hardwoods such as beech, birch and oak etc. are of interest as alternatives due to their superior strength properties. For integration of these hardwood species in structural engineered wood products, knowledge of the strength and stiffness properties as well as methods for strength grading is essential. The dynamic modal testing method is an efficient tool to determine the elastic properties of wood and has become the most common technique for strength grading of softwood timber in Europe. However, more studies are needed to investigate how well this and other non-destructive techniques (NDT) methods work for hardwoods.

The aim of this study was to investigate the modulus of elasticity and bending strength of oak timber including defects and to study methods for strength grading including dynamic modal tests, stress wave techniques and knot inspection. A semi-destructive method based on cut-out miniature specimens was also evaluated, in view of in-situ quality assessment of old oak structures. The material for this study was chosen carefully to cover the complete variation in raw material quality and included 101 oak boards from Sweden with the average cross section 29x78 mm.

The global and local modulus of elasticity ($E_{m,l}$ $E_{m,g}$) and bending strength of oak beams were determined using both static and dynamic methods. For the static tests, the four-point static bending test method according to the European standard EN 408 was used for the experiments. Additionally, the knot area ratio (KAR) was determined for the worst defect zone in the centre of the specimen. Dynamic moduli of elasticity were determined based on resonance frequencies from the following vibration modes: axial/longitudinal (E_{AX}), flatwise bending (E_{BF}) and edgewise bending (E_{BE}), refer to

Figure 12. The dynamic shear modulus was determined based on torsional vibration (G_T) and from analysis of edgewise bending modes using Timoshenko beam theory (G_{BE}). The dynamic modulus of elasticity from the speed of a stress wave was determined from measurements along all four sides of the boards, (E_{SW}).

Figure 12: Test set-up for stress-wave measurement (left) and dynamic modal test (right)

On average, the density recorded was 710 kg/m^3, which is in the range for typical values for European oak. The average local modulus of elasticity $E_{m,l}$ was 9.97 GPa, which is slightly lower compared to other studies and 10% higher than the global stiffness, $E_{m,g}$. This is expected due to the influence of shear deformations for the global stiffness. The average bending strength recorded was 53 MPa and is in line with previous research. The average shear modulus was 706 GPa. Compared to typical softwood in Sweden, the results indicate that oak has considerably higher bending strength (+20%) but slightly lower modulus of elasticity (-10%) and similar shear modulus (+-0%). Variation in bending strength (CoV=37%) and stiffness (CoV=22%) was high.

Stronger than expected correlations were found between the modulus of elasticity from dynamic modal tests and the bending test results (stiffness: R^2=0.98, strength: R^2=0.62), see Figure 13. Noteworthy is that an indicating property based only on axial resonance frequency and board length shows an unusually strong correlation to bending stiffness (R^2=0.82) and strength (R^2=0.56). It seems that the density information is of lesser importance compared to softwood. Less strong correlations were found for the modulus of elasticity from stress waves and knot data (*KAR*).

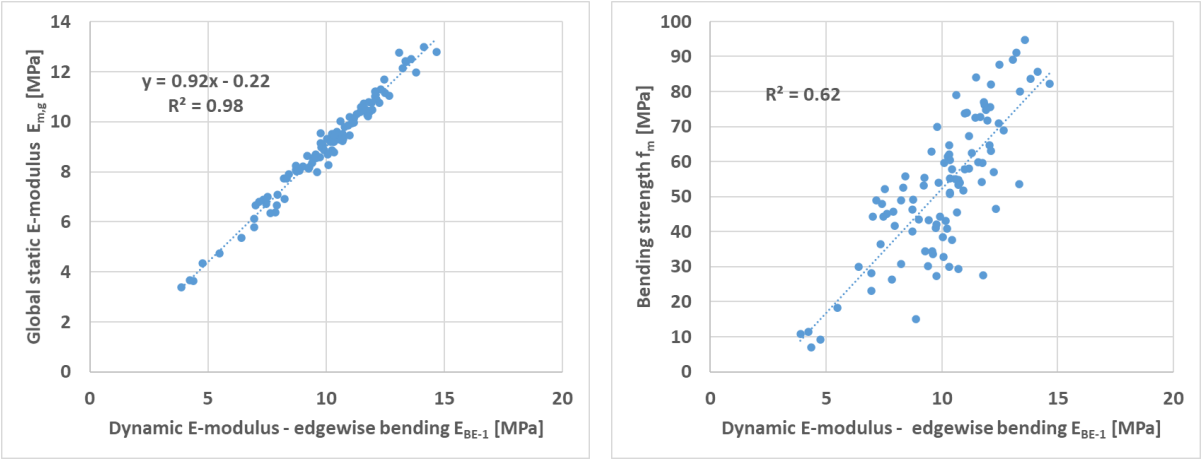

Figure 13: Relationship between dynamic modulus of elasticity and bending test results

The final version of this abstract and the full scientific article are scheduled to be published in the Special Issue "12th Hardwood Conference—Sopron" of the journal MDPI Forests, available at the following link:
MDPI Forests Special Issue: 12th Hardwood Conference—Sopron

State-of-Art NIRS Technology for Wood Products

Satoru Tsuchikawa[1*]

[1] Graduate School of Bioagricultural Sciences, Nagoya University, Nagoya, Japan, 464-8601

E-mail: st3842@agr.nagoya-u.ac.jp

Keywords: Near Infrared Spectroscopy (NIRS); Non-destructive measurement; Hyperspectral imaging (HSI); Artificial intelligence (AI); Convolutional neural networks (CNNs).

ABSTRACT

Near-infrared spectroscopy (NIRS) has been widely studied for the non-destructive quality evaluation of organic materials, including agricultural and forest products. This technique analyzes reflected and transmitted light in the wavelength range of approximately 800 to 2500 nm. Compared with mid-infrared spectroscopy, NIRS has lower absorption energy, allowing non-destructive measurements of dense organic materials. In addition, because of its lower molar absorptivity, NIRS is particularly suitable for analyzing samples with high moisture content, such as standing trees and green wood.

INTRODUCTION

Several state-of-the-art technologies have further expanded the applicability of NIRS in wood science. In particular, spectroscopic and imaging methods, combined with advanced data analysis, provide powerful tools for investigating the properties and structure of wood and other organic materials. This presentation highlights how spectroscopic and imaging approaches can contribute to a sustainable wood supply. Owing to recent advances in hyperspectral imaging and data analysis, these techniques now offer greater analytical capability than ever before.

Prediction and mapping of wood properties using NIRS and hyperspectral imaging

NIRS and hyperspectral imaging (HSI) have become powerful tools for the rapid and non-destructive evaluation of wood properties. In wood science, these techniques have been applied to the prediction of moisture content, density, stiffness, fiber orientation, and chemical composition, as well as to the visualization of their spatial distributions. Early studies demonstrated the applicability of NIRS to non-destructive measurements of wood moisture content and subsurface structural characteristics. Subsequent investigations clarified the optical behavior of NIR light in anisotropic cellular materials such as wood, providing the theoretical basis for advanced spectroscopic analyses.

Recent advances in HSI have further expanded these applications by enabling simultaneous acquisition of spectral and spatial information. This has allowed researchers not only to predict wood properties but also to visualize their two-dimensional and three-dimensional distributions. For example, NIRS-HSI has been successfully used for mapping moisture content and density in Japanese Cedar, as well as for evaluating stiffness and microfibril angle with high spatial resolution. Furthermore, recent studies have demonstrated the feasibility of monitoring moisture transport dynamics during wood drying processes using NIR-HSI combined with computational modeling approaches.

Cognitive spectroscopy for wood species identification using NIR hyperspectral imaging combined with a convolutional neural network

Recent advances in NIR-HSI and artificial intelligence (AI) have significantly expanded the capability of non-destructive wood identification. Conventional NIRS has long been used for wood discrimination based on spectral differences associated with chemical composition and anatomical structure. However, the combination of HSI and deep learning techniques has enabled more sophisticated analyses that simultaneously utilize spectral and spatial information.

Cognitive spectroscopy, which integrates spectroscopic sensing with AI, has recently emerged as a promising approach for wood science applications. In particular, convolutional neural networks (CNNs) combined with NIR-HSI allow automatic extraction of complex spectral–spatial features that are difficult to interpret using conventional chemometric methods. This approach improves the robustness

and accuracy of wood species identification while reducing the need for extensive manual feature engineering.
Recent studies demonstrated that NIR-HSI can effectively capture subtle differences in wood structure, density, grain orientation, and chemical characteristics. These properties contribute to species-dependent optical responses, which can be learned efficiently by deep learning models. Furthermore, hyperspectral imaging enables visualization of spatial variations within wood samples, providing additional information beyond point-based spectroscopic measurements.
The integration of cognitive spectroscopy with hyperspectral imaging is expected to contribute to rapid and reliable wood identification systems for sustainable forest management, timber grading, traceability, and automated industrial applications.

COCLUSION

Near-infrared spectroscopy and hyperspectral imaging have evolved into powerful non-destructive techniques for evaluating wood properties and structure. Recent advances in imaging technology, chemometrics, and artificial intelligence have significantly improved the capability of these methods for predicting and visualizing moisture content, density, stiffness, grain orientation, and other wood characteristics. In particular, the integration of hyperspectral imaging with deep learning approaches, such as convolutional neural networks, has enabled rapid and accurate wood species identification through cognitive spectroscopy.
These technologies provide not only high analytical performance but also the possibility of real-time and on-site applications for timber grading, traceability, quality control, and sustainable forest resource management. Furthermore, the combination of spectroscopy, imaging, and data science is expected to play an increasingly important role in future wood science and forest products engineering. Continued development of advanced sensing systems and computational approaches will further expand the applicability of NIRS and hyperspectral imaging toward sustainable utilization of wood resources.

ACKNOWLEDGEMENTS

This work was financially supported by JSPS (KAKENHI： 25H00941).

REFERENCES

Kanayama, H, Ma T, Tsuchikawa, S, Inagaki T (2019) Cognitive spectroscopy for wood species identification: Near infrared hyperspectral imaging combined with convolutional neural network. Analyst, 144, 6438-6446

Schimleck, L, Ma T, Inagaki, T, Tsuchikawa, S (2023) Review of near infrared hyperspectral imaging applications related to wood and wood products. Applied Spectroscopy Reviews, 58, 585-609, https://doi.org/10.1080/05704928.2022.2098759

Tsuchikawa S, Inagaki, T, Ma, T (2023) Application of near-infrared spectroscopy to forest and wood products. Current Forestry Reports, 9, 401-412

Mechanical Characterisation of *Milicia excelsa* (Iroko) from Angola: Experimental Basis for the Structural Valorisation of a Tropical Hardwood

Jorge M. Branco[1*], Wander B. João[1,2]

[1] TiMLAB, ISISE, University of Minho, 4800-058 Guimarães, Portugal
[2] Military Technical Higher Institute, Luanda, Angola.

E-mail: jbranco@civil.uminho.pt; pg28671@alunos.uminho.pt

Keywords: *Milicia excelsa*; Iroko; tropical hardwood; mechanical characterization; Angolan timber.

ABSTRACT

Milicia excelsa (Iroko/Câmbala/Moreira) is a tropical hardwood species widely distributed across sub-Saharan Africa, including Angola. Despite its recognised traditional use and natural durability, the absence of standardised physical and mechanical data has limited its integration into modern structural engineering applications. This study presents an experimental characterisation of *Milicia excelsa* of Angolan origin, including the determination of moisture content, density, static bending strength, compression strength parallel and perpendicular to the grain, shear strength, and tensile strength parallel to the grain. The results indicated moisture content values ranging from 12.7% to 22.7%, densities between 503 and 673 kg/m³, and mean mechanical strengths of approximately 154 MPa in bending, 48 MPa in compression parallel to the grain, 7 MPa in shear, and 53 MPa in tension parallel to the grain. The findings confirm the significant structural potential of *Milicia excelsa* and provide experimental reference data to support future strength grading, standardisation procedures, and the sustainable structural utilisation of tropical hardwoods in Angola.

INTRODUCTION

Timber has long been recognised as one of the most efficient structural materials due to its favourable strength-to-weight ratio, renewability, low embodied energy, and compatibility with sustainable construction principles (Bodig & Jayne, 1982). In recent decades, the growing demand for low-carbon construction solutions has intensified international interest in timber engineering, particularly through advances in engineered timber systems capable of competing with conventional structural materials such as reinforced concrete and steel (Glass & Zelinka, 2010; Ramage et al., 2017).

Despite the extensive forest resources available across tropical Africa, the structural utilisation of indigenous hardwood species remains comparatively limited. One of the principal constraints affecting their integration into structural design is the lack of standardised experimental data compatible with internationally recognised testing and grading procedures. In many African countries, timber species traditionally employed in vernacular construction continue to be used empirically, without sufficient mechanical characterisation to support modern engineering applications (PROTA, 2022). This limitation is particularly relevant in Angola, where the technical valorisation of native timber species remains underdeveloped despite the considerable availability of tropical hardwoods.

Among the tropical hardwoods available in Angola, *Milicia excelsa* (Welw.) C.C. Berg- commercially known as Iroko and locally designated as Moreira or Câmbala - exhibits significant technological and structural potential. The species is naturally distributed across West, Central, and East Africa, including Angola (Berg, 1982; Orwa et al., 2009). Due to its natural durability, dimensional stability, biological resistance, and favourable mechanical performance, *Milicia excelsa* has traditionally been used in carpentry, flooring systems, bridge components, exterior applications, and heavy timber construction (LNEC, 2010). However, the currently available information remains fragmented and insufficiently aligned with modern structural frameworks such as Eurocode 5, EN 338, and EN 408. Moreover, the species is not currently included in the EN 338 strength classification system, limiting its direct implementation in structural design.

In timber engineering, the determination of intrinsic material properties through small clear specimens remains fundamental for evaluating wood behaviour independently of natural defects and geometric discontinuities. International standards such as ASTM D143, EN 408, and EN 384 provide recognised

methodologies for the physical and mechanical characterisation of timber and strength grading procedures applicable to structural materials.
The present study aims to contribute to the technical valorisation of Angolan timber resources through the physical and mechanical characterisation of *Milicia excelsa* using small clear specimens prepared according to standardised procedures. The experimental programme included the determination of moisture content, density, bending strength, compression strength parallel and perpendicular to the grain, shear strength, and tensile strength parallel to the grain, following internationally recognised ASTM, ISO 13061, and EN procedures, including ISO 13061-1 for moisture content determination, ISO 13061-2 for density, ISO 13061-3 for static bending, and ISO 13061-5 for compression-related testing. The study further evaluates the structural potential of the species through comparison with reference tropical hardwoods and an approximate strength class assessment according to EN 338, contributing to future timber grading and structural implementation initiatives in Angola.

MATERIALS AND METHODS

Material Description

Timber of *Milicia excelsa* (Welw.) C.C. Berg, commercially known as Iroko and locally designated as Moreira or Câmbala in Angola, was obtained from commercially processed boards supplied by a Portuguese importer specialising in tropical hardwoods. The material originates from Angola, although the precise harvesting region could not be identified due to commercial supply chain constraints. Prior to specimen preparation, all boards were visually inspected to minimise the influence of natural defects. Specimens containing knots with diameter exceeding 5 mm, checks, biological degradation, grain deviation greater than 10°, resin pockets, or visible discontinuities were excluded from the experimental programme. This selection procedure ensured compatibility with the requirements for small clear specimens according to ASTM D143 (2022), allowing the intrinsic physical and mechanical properties of the species to be assessed independently of structural-scale irregularities.

Physical Characterisation

Moisture content and apparent density were determined according to ASTM D4442 (2021), ASTM D2395 (2021), ISO 13061-1 (2014), and ISO 13061-2 (2014), respectively. All specimens were conditioned in a controlled environment at 20 ± 2°C and 65 ± 5% relative humidity until constant mass was achieved (mass variation < 0.1% over 24 hours).

Mechanical Testing

All mechanical tests were performed using a universal testing machine (MTS) under displacement-controlled loading. Table 1 summarises the specimen dimensions and number of specimens (N) adopted for each test, following ASTM D143 (2022) unless otherwise specified.

Table 1: Summary of mechanical test configurations

Test	Specimen dimensions [mm]	N	Standard
Static bending	20 x 20 x 340	35	ASTM D143
Compression //	20 x 20 x 60	55	ASTM D143
Compression ⊥	45 x 90 x 70	41	ASTM D143
Shear //	Standard shear block	50	ASTM D143
Tension //	Prismatic with reduced section	43	ASTM D143 (adapted)

Static bending tests were conducted using a three-point bending configuration with a span of 280 mm, resulting in a span-to-depth ratio of 14:1. Bending strength (f_m) was calculated from the maximum load recorded during the test. Compression parallel to the grain tests ($f_{c,0}$) were performed by loading specimens longitudinally along the fibre direction. Compression perpendicular to the grain tests ($f_{c,90}$) used specimens loaded transversely across the full width of the cross-section. Shear tests followed ASTM D143 procedures using standard shear block specimens designed to promote longitudinal shear failure parallel to the grain (f_v). Tension parallel to the grain tests ($f_{t,0}$) were conducted on prismatic specimens with a reduced central section (dog-bone shape) to ensure failure within the effective gauge length, following an adaptation of ASTM D143.

Data Analysis

For each property, the mean value and coefficient of variation (CV%) were calculated according to standard statistical procedures. Outliers were identified using the Chauvenet criterion and excluded from the analysis when justified. Specimens exhibiting premature failure due to visible defects (e.g., knots, grain deviation) were excluded from the calculation of intrinsic mechanical properties but were documented separately for completeness.

RESULTS

Physical Properties

Moisture Content

The moisture content of the specimens at the time of testing varied between 12.7% and 22.7% (Table 2), reflecting the hygroscopic nature of *Milicia excelsa* and the difficulty of achieving complete equilibrium in tropical hardwoods under standard laboratory conditioning (20 ± 2°C, 65 ± 5% RH). The mean moisture content values for each test group ranged from 12.7% (shear) to 22.7% (compression parallel to grain), as summarised in Table 2. The observed variability, while relatively high, falls within ranges commonly reported for conditioned tropical hardwoods and remains compatible with the procedures described in ASTM D143 (2022) and ISO 13061-1 (2014) and ISO 13061-2 (2014). Nevertheless, the influence of moisture content on mechanical properties (particularly mechanical strength) was considered when interpreting the results.

Density

The apparent density values obtained ranged from 503 kg/m³ to 673 kg/m³ (Table 2), classifying *Milicia excelsa* as a medium- to high-density tropical hardwood. The mean density varied between 476 kg/m³ (compression perpendicular group) and 658 kg/m³ (tension group), with coefficients of variation (CV%) between 3.0% and 11.6%, indicating satisfactory material consistency. These values are consistent with density ranges reported in Angolan forestry classification systems and international technical references, where the species is generally described within the range of 550–750 kg/m³ (LNEC, 2010; PROTA, 2022). The density levels observed are compatible with the elevated mechanical performance subsequently obtained in bending and compression tests.

Table 2: Moisture content and density of Milicia excelsa specimens per test group

Test group	N	Moisture content [%]	Density [kg/m³]
Static bending	35	16.8 (8.8)	647.7 (3.0)
Compression //	55	17.4 (10.1)	654.4 (4.3)
Compression ⊥	41	22.7 (13.8)	476.1 (6.9)
Shear //	50	19.8 (13.5)	629.6 (11.6)
Tension //	43	12.7 (11.0)	658.8 (4.0)

Values in parentheses are coefficients of variation (CV%).

Mechanical Properties

Bending

The static bending tests yielded an average bending strength (f_m) of approximately 154 MPa (Table 3), demonstrating the high flexural resistance of *Milicia excelsa*. The failure modes were predominantly governed by tension parallel to the grain in the tensile zone of the specimens, including classical tensile rupture, fibrous tension failure, and longitudinal splintering (Figure 1). Premature failures associated with local discontinuities or accidental defects were excluded from the analysis. The bending strength values place *Milicia excelsa* among the most mechanically competitive tropical hardwoods, comparable to Sapelli (130–160 MPa) and exceeding Khaya (110–140 MPa) and Ayous (70–100 MPa) (LNEC, 2010; PROTA, 2022).

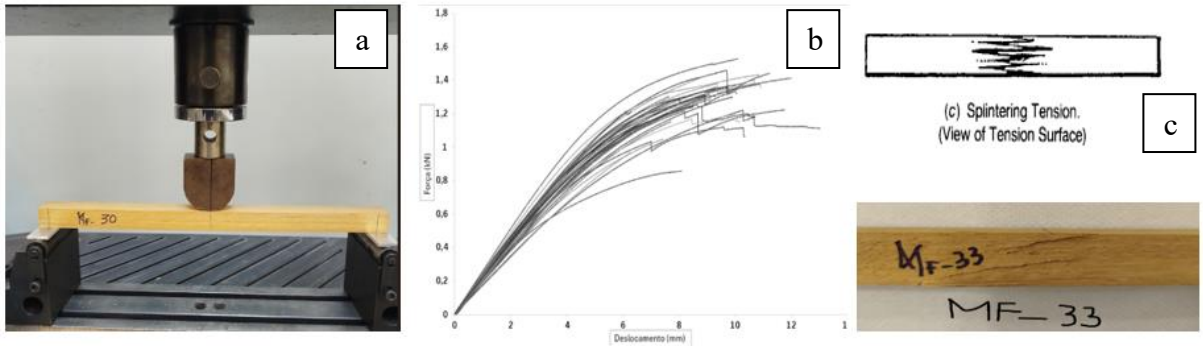

Figure 1: Static bending test of Milicia excelsa: (a) test setup using MTS universal testing machine with three-point bending configuration; (b) representative force-displacement curves; (c) typical failure mode showing tensile rupture along the grain

Compression Parallel to Grain

The compression parallel to grain tests yielded an average compressive strength ($f_{c,0}$) of approximately 48 MPa (Table 3), indicating significant resistance capacity under axial compressive loading. This property is particularly relevant for columns, compressed members, and timber framing systems where compressive stresses govern structural performance. The observed behaviour during testing was characterised predominantly by progressive fibre crushing and local instability mechanisms typical of hardwoods subjected to compression parallel to the grain (see Figure 2). The force-displacement curves exhibited an initial linear-elastic region, followed by a non-linear plateau corresponding to progressive crushing of the cellular structure, and finally a post-peak softening branch associated with local buckling and collapse.

Compared with softwood structural species commonly used in Europe (e.g., C24: $f_{c,0}$ =21 MPa), the obtained values demonstrate considerably higher compressive resistance, reflecting the dense fibre arrangement and favourable anatomical structure of *Milicia excelsa*. The coefficient of variation (CV%) observed in the compression tests was approximately 4.3% (Table 2), indicating satisfactory mechanical consistency for engineering applications. The relatively moderate variability suggests that the species responds predictably under axial compression when defects are minimised.

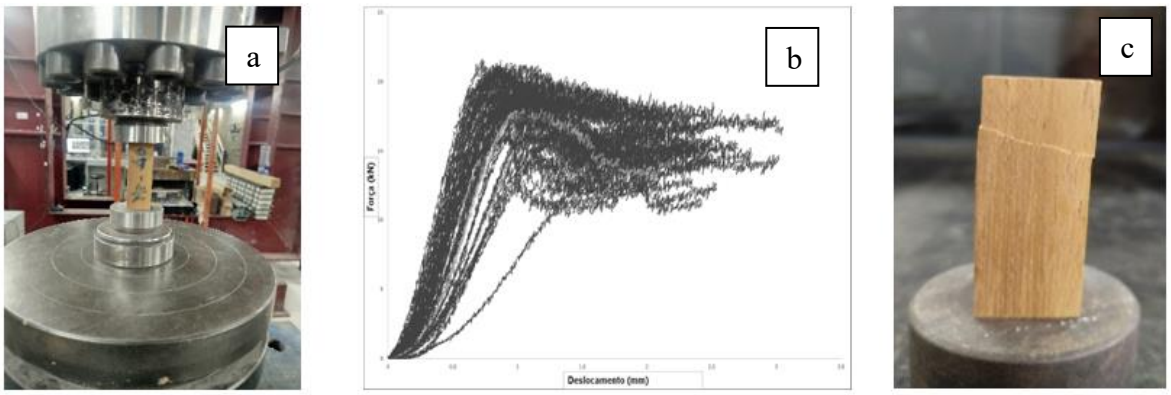

Figure 2: Compression parallel to grain test of Milicia excelsa: (a) test setup using MTS universal testing machine; (b) representative force-displacement curves; (c) typical failure mode showing progressive fibre crushing and local buckling

Compression Perpendicular to Grain

The compression perpendicular to grain tests revealed behaviour dominated by progressive local crushing and plastic deformation of the cellular structure (Figure 3). Unlike compression parallel to the grain, the perpendicular loading configuration produced significantly lower resistance values, reflecting the anisotropic nature of wood and the reduced load-transfer efficiency across the fibre direction.

The force-displacement curves exhibited an initial non-linear response from the onset of loading, corresponding to the gradual densification of the cellular structure, followed by a sustained plateau without a clear peak load.

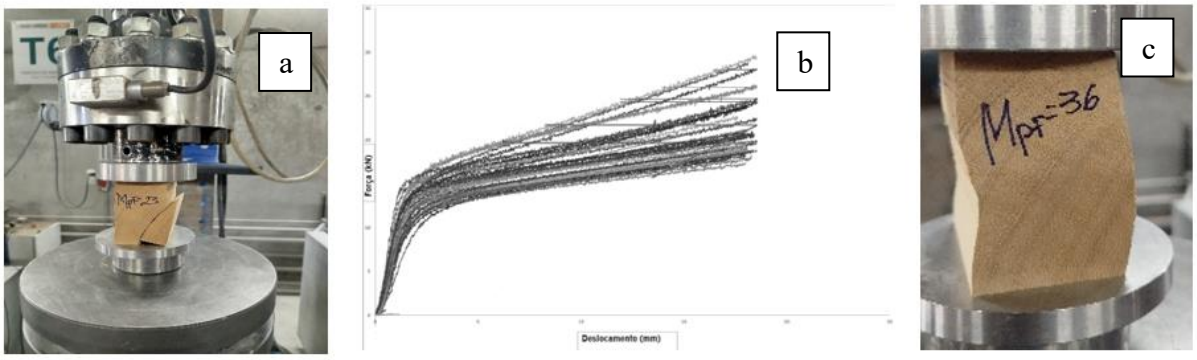

Figure 3: Compression perpendicular to grain test of Milicia excelsa: (a) test setup with specimen positioned transversely; (b) representative force-displacement curves showing progressive crushing without clear peak load; (c) typical failure mode with local fibre crushing

This behaviour is characteristic of hardwoods subjected to perpendicular compression, where failure is defined not by brittle collapse but by a predefined deformation limit (typically 2.5 mm or 5% of the specimen height), as prescribed by ASTM D143 (2022). Despite the lower strength levels inherent to perpendicular loading, the obtained behaviour remained stable and predictable throughout testing. The proportional limit stress (stress at the onset of non-linear behaviour) and the stress at the reference deformation limit were recorded to characterise the material's performance under localised bearing stresses. The mean values obtained for *Milicia excelsa* ($f_{c,90} \approx 6.7$ MPa) are slightly below but generally consistent with those reported for tropical hardwoods of similar density, such as Sapelli and Khaya, where perpendicular compression strength typically ranges between 8 and 15 MPa at fibre saturation (LNEC, 2010). The coefficient of variation (CV%) observed was approximately 6.0% (Table 2), indicating satisfactory consistency for this property. From a structural engineering perspective, compression perpendicular to grain governs the behaviour of bearing regions, supports, contact surfaces, and connection zones where localised stresses develop (e.g., beam seats, column bases, and bolted connections). The results indicate adequate performance of *Milicia excelsa* in such applications, provided that appropriate bearing areas and stress limits are adopted in design.

Shear Parallel to Grain

The shear parallel to grain tests yielded an average shear strength (f_v) of approximately 7 MPa (Table 3). The failures observed during testing were predominantly characterised by longitudinal fibre separation and shear cracking along the grain direction (Figure 4), which is the typical failure mode for wood subjected to shear stresses parallel to the fibres.

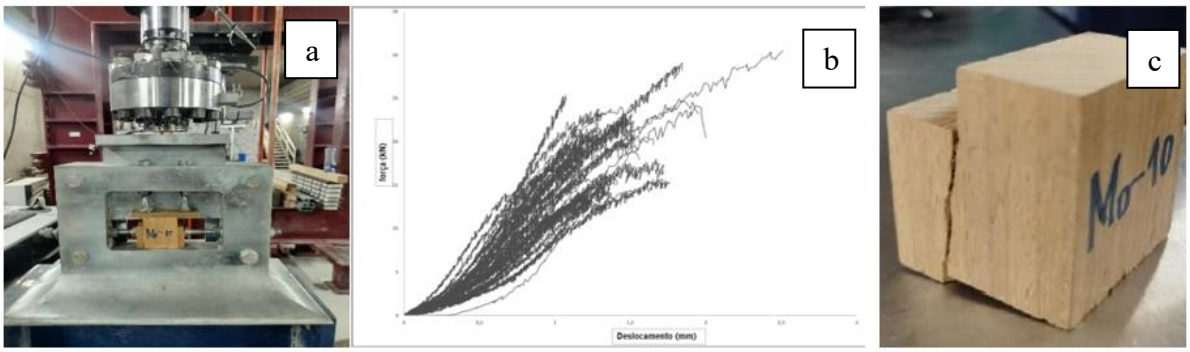

Figure 4: Shear parallel to grain test of Milicia excelsa: (a) test setup with standard shear block specimen; (b) representative force-displacement curves; (c) typical failure mode showing longitudinal shear cracking along the grain

The force-displacement curves exhibited an initial linear-elastic response, followed by a sudden drop after peak load, reflecting the brittle nature of shear failure in hardwoods. Unlike bending or compression, shear failures occurred with limited plastic deformation, confirming the low ductility of the material under this loading configuration. Shear resistance in timber is strongly influenced by fibre orientation, local anatomical discontinuities, and density distribution. The values obtained for *Milicia excelsa* ($f_v \approx 7$ MPa) are consistent with those reported for structural tropical hardwoods traditionally employed in engineering applications, particularly Sapelli (6–10 MPa) and Khaya (6–9 MPa) (LNEC, 2010). The coefficient of variation (CV%) observed in the shear tests was approximately 11.0% (Table 2), which is within the typical range for this property in hardwoods. The moderate variability reflects the sensitivity of shear strength to local anatomical features, such as growth ring orientation and the presence of rays, even in clear specimens. From a structural engineering perspective, the results indicate satisfactory shear performance for applications involving connections, notched beams, support regions, and combined stress states where longitudinal shear stresses become significant. However, as shear strength is derived from small clear specimens, the characteristic values for structural design should be adjusted with appropriate factors (k_{mod}, γ_M) and, ideally, verified through structural-scale testing.

Tension Parallel to Grain

The tension parallel to grain tests yielded an average tensile strength ($f_{t,0}$) of approximately 53 MPa (Table 3). Failures occurred predominantly in a brittle manner, with crack propagation rapidly developing along the fibre direction after the attainment of peak load (see Figure 5).

Characteristic failure modes included straight grain tension rupture, fibrous separation, and localised splitting originating from minor surface irregularities or anatomical features. The force-displacement curves exhibited a nearly linear-elastic response up to failure, with negligible plastic deformation. This behaviour reflects the low ductility of wood under tension parallel to the grain, where failure is governed by fibre rupture rather than by yielding or crushing. The sudden load drop after peak load is characteristic of brittle tensile failure and emphasises the importance of using appropriate safety factors in structural design applications.

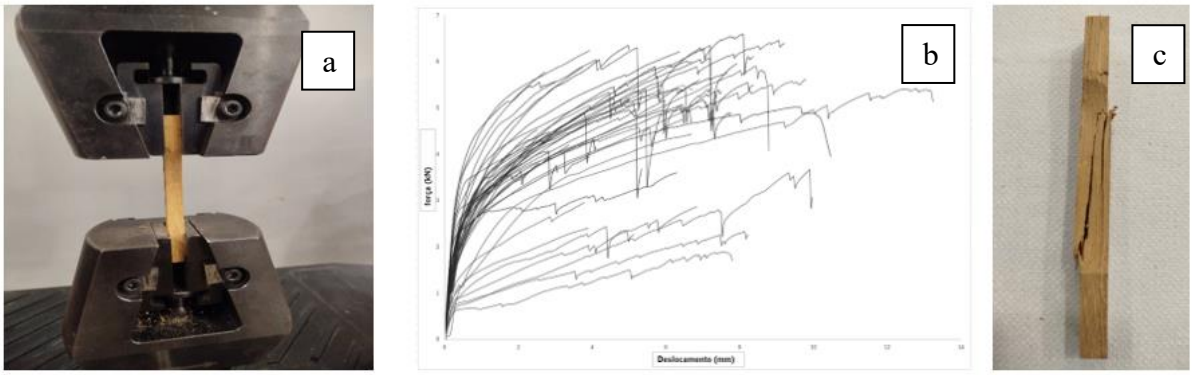

Figure 5: Tension parallel to grain test of Milicia excelsa: (a) test setup with dog-bone specimen configuration; (b) representative force-displacement curves showing linear-elastic response and brittle failure; (c) typical failure mode with straight grain tension rupture

The obtained tensile resistance (53 MPa) is approximately 35% lower than the bending strength (154 MPa) and about 10% higher than the compression strength parallel to the grain (48 MPa) of the same species. This relationship ($f_{t,0} < f_m > f_{c,0}$) is characteristic of hardwoods, where bending strength is generally enhanced by the combined action of tensile and compressive stresses within the cross-section. Compared with reference tropical hardwoods (Table 4), the tensile strength of *Milicia excelsa* (53 MPa) falls within the lower range reported for Sapelli (50–80 MPa) and is comparable to Khaya (45–70 MPa), while significantly exceeding Ayous (30–50 MPa) (LNEC, 2010; PROTA, 2022). The coefficient of variation observed in the tension tests (CV = 14.9%; Table 3) indicates moderate variability and reflects satisfactory experimental consistency for a mechanical property known to be sensitive to fibre orientation and local anatomical irregularities. Such variability is commonly reported for tropical hardwoods and may be attributed to minor fibre deviations, surface imperfections, and local stress

concentrations, even in carefully selected clear specimens. Premature failures associated with visible surface defects or irregular grain orientation were excluded from the analysis to ensure representative mechanical behaviour. From a structural engineering perspective, the tensile strength of *Milicia excelsa* appears adequate for applications governed by tension parallel to the grain, including the tensile zone of bending members, truss bottom chords, and timber connections subjected to tensile stresses. Nevertheless, due to the inherently brittle nature of tensile failure in wood, characteristic values for structural design should be established using appropriate statistical procedures (e.g., 5th percentile) and applied together with the partial safety factors prescribed by Eurocode 5 (EN 1995-1-1, 2004).

Summary of Mechanical Properties

Table 3 summarises the mechanical properties obtained for *Milicia excelsa* from the small clear specimen tests. For each property, the number of valid specimens (N), mean value and coefficient of variation (CV%) are presented.

Table 3: Summary of mechanical properties of Milicia excelsa (small clear specimens)

Property	N	Mean [MPa]	CV [%]
Bending Strength (f_m)	35	154.2	11.4
Compression // to grain ($f_{c,0}$)	55	48.2	7.4
Compression ⊥ to grain ($f_{c,90}$)	41	6.7	16.7
Shear // to grain (f_v)	50	7.3	25.7
Tension // to grain ($f_{t,0}$)	43	52.9	14.9

The bending strength (fm) of approximately 154 MPa confirms the high flexural performance of *Milicia excelsa*, positioning the species among the strongest tropical hardwoods currently used in structural applications. Compression strength parallel to the grain (fc,0), averaging approximately 48 MPa, demonstrated satisfactory performance under axial loading conditions, while shear strength (fv), averaging approximately 7 MPa, remained within the expected range for hardwood species of comparable density. Tensile strength parallel to the grain (ft,0), with a mean value of approximately 53 MPa, although lower than bending strength, is consistent with the mechanical behaviour typically observed in hardwoods, where tensile resistance is strongly influenced by local stress concentrations and minor fibre deviations. The coefficient of variation observed for tensile strength (CV = 14.9%) reflects the intrinsic sensitivity of this property to small anatomical irregularities, even in carefully selected clear specimens. Compression perpendicular to the grain (fc,90) values were determined at the proportional limit in accordance with ASTM D143 procedures. Additional details regarding the stress–deformation behaviour are presented in Section 3.2.3 and Figure 3.

Comparison with Literature and Tropical Hardwoods

The mechanical properties obtained for *Milicia excelsa* in this study are generally consistent with values reported in international literature and technical reference documents, including the Portuguese LNEC M3 sheet for Iroko LNEC (2010) and the database PROTA (2022). Small discrepancies may be attributed to differences in geographic origin, growth conditions, moisture content at testing, and specimen preparation procedures. Table 4 compares the mechanical properties of *Milicia excelsa* with selected tropical hardwood species commonly employed in structural applications. The reference species were chosen based on their commercial availability, established use in timber engineering, and comparable density ranges.

Table 4: Comparative mechanical properties of Milicia excelsa and selected tropical hardwoods (mean values, MPa)

Species	f_m	$f_{c,0}$	f_v	$f_{t,0}$	Source
Milicia excelsa (Câmbala)	~154	~48	~7	~53	Present
Entandrophragma cylindricum (Sapelli)	130-160	45-60	6-10	50-80	CIRAD (2020); Wagenführ (2007)
Khaya ivorensis (Khaya)	110-140	40-55	6-9	45-70	CIRAD (2020); Meier (2023)
Triplochiton scleroxylon (Ayous)	70-100	25-35	4-6	30-50	CIRAD (2020); Wagenführ (2007)

The bending strength of *Milicia excelsa* (~154 MPa) is at the upper range of Sapelli (130–160 MPa) and significantly higher than Khaya (110–140 MPa) and Ayous (70–100 MPa). Among commonly traded African hardwoods, only Azobé exhibits systematically higher bending strength (150–200 MPa), although Azobé is considerably denser (800–1100 kg/m³) and more challenging to machine. Compression parallel to grain (~48 MPa) is comparable to Sapelli (45–60 MPa) and Khaya (40–55 MPa), confirming the suitability of *Milicia excelsa* for axially loaded members such as columns, truss elements, and piled foundations. Shear strength (~7 MPa) falls within the typical range for these species (6–10 MPa), indicating adequate performance for connections, notched beams, and support regions where longitudinal shear stresses develop. Tension parallel to grain (~53 MPa) is within the lower range of Sapelli (50–80 MPa) and comparable to Khaya (45–70 MPa), while significantly exceeding Ayous (30–50 MPa). The coefficient of variation observed for tension parallel to grain (CV = 14.9%) indicates moderate variability, which is consistent with values commonly reported for tropical hardwoods. Tensile strength parallel to the grain remains sensitive to local fibre deviations, anatomical discontinuities, and minor surface irregularities, even in carefully selected clear specimens (Dinwoodie, 2000). From a structural engineering perspective, the results confirm that *Milicia excelsa* is mechanically competitive with established African hardwoods and suitable for structural applications requiring high strength, natural durability, and dimensional stability. The species exhibits significant potential for application in bridge structures, heavy timber construction, flooring systems, and exterior structural applications where resistance to biological degradation is required.

DISCUSSION

Influence of moisture content on mechanical properties

The moisture content at testing varied between 12.7% and 22.7% (Table 2), representing a relatively wide range for a laboratory characterisation study. This variability is attributed to the relatively high density and low permeability of *Milicia excelsa*, which may prolong the time required to achieve complete hygroscopic equilibrium. Since a 1% variation in moisture content below fibre saturation typically results in an approximate 3–5% variation in mechanical strength (Dinwoodie, 2000), the observed moisture range may have contributed, to some extent, to the variability of the mechanical results. Nevertheless, the moderate variability observed for tension parallel to the grain (CV = 14.9%) indicates satisfactory experimental consistency and remains within acceptable limits commonly reported for tropical hardwood characterisation. Despite this limitation, the mean moisture content values remained within acceptable ranges for comparative studies involving tropical hardwood species (LNEC, 2010; PROTA, 2022).

Density as a predictor of mechanical performance

The density values (503–673 kg/m³) classify *Milicia excelsa* as a medium- to high-density tropical hardwood, consistent with literature references (550–750 kg/m³) [LNEC, 2010]. A positive correlation between density and mechanical strength was observed, with higher-density specimens exhibiting higher bending and compression strength, which is expected for hardwoods [Bodig and Jayne, 1982]. The mean density (~640 kg/m³) is comparable to Sapelli and slightly higher than Khaya, explaining the high strength values obtained.

Comparison with EN 338 strength classes

Although *Milicia excelsa* is not currently covered by EN 338, an approximate classification can be proposed. Based on the characteristic bending strength (estimated 5th percentile ~120–130 MPa), the species would likely fall within strength classes D40 to D50 (EN 338, 2016). However, the mean density (~640 kg/m³) is slightly below the D40 threshold (720 kg/m³), suggesting a cautious classification between D35 and D40. It should be emphasised that EN 338 classification requires structural-size testing according to EN 384 (2016); the present results from small clear specimens provide an upper-bound estimate.

Failure mechanisms and anisotropic behaviour

The observed failure modes were consistent with typical hardwood behaviour. Bending failures were governed by tension parallel to grain, compression parallel to grain exhibited progressive fibre crushing, and compression perpendicular to grain showed local crushing without a clear peak load. Shear and tension failures were brittle, with rapid crack propagation along the grain. This consistency supports the applicability of established design rules (Eurocode 5) for the species, provided appropriate characteristic values are adopted.

Limitations and future research

This study has several limitations: (i) tests were performed on small clear specimens, excluding natural defects; (ii) moisture content varied over a relatively wide range; (iii) material originated from a single commercial supply chain; (iv) long-term properties were not investigated. Future research should include structural-size testing according to EN 408, strength grading trials, evaluation of creep behaviour, and connection testing.

Implications for Angolan timber construction

The results provide a scientific basis for the structural use of *Milicia excelsa* in Angola, potentially reducing import dependency and promoting sustainable local value chains. The species is suitable for bridges, heavy timber framing, industrial flooring, and exterior applications. However, adoption will require complementary efforts in sustainable forest management and the development of national timber grading standards aligned with Eurocode 5.

CONCLUSIONS

This study presented the physical and mechanical characterisation of *Milicia excelsa* from Angola. The following conclusions are drawn:

1. Physical properties: Moisture content ranged from 12.7% to 22.7%, and density from 503 to 673 kg/m³, classifying the species as a medium- to high-density tropical hardwood.
2. Mechanical strength: the species exhibited high bending strength (~154 MPa), adequate compression parallel to grain (~48 MPa), shear strength (~7 MPa), and tension parallel to grain (~53 MPa).
3. Comparative performance: *Milicia excelsa* is mechanically competitive with established African hardwoods such as Sapelli and Khaya, and suitable for structural applications requiring high strength and natural durability.
4. Strength class estimate: Based on characteristic values, the species would likely fall within EN 338 classes D35–D40, pending confirmation from structural-size testing.
5. Limitations: The study is based on small clear specimens; structural-size testing is required for design values.
6. Future research: Priorities include structural-size testing, strength grading, creep behaviour, and connection performance.
7. Valorisation: This study provides experimental reference data supporting the technical valorisation of Angolan timber resources and future standardisation initiatives.

ACKNOWLEDGEMENTS

This research was supported by the R&D Project ‘R2U Technologies | Modular Systems’, reference C644876810-00000019, funded by the Recovery and Resilience Plan (RRP) and by the European Union’s Next Generation EU Funds, under the incentive programme ‘Agendas for Business Innovation’. This work was also supported by the Foundation for Science and Technology (FCT/MCTES) through the R&D Unit Institute for Sustainability and Innovation in Structural Engineering (ISISE), under references UID/4029/2025, UID/PRR/04029/2025, and UID/PRR2/04029/2025.

REFERENCES

ASTM D143-22 (2022). Standard test methods for small clear specimens of timber. ASTM International.

ASTM D2395-17 (2021). Standard test methods for density and specific gravity of wood and wood-based materials. ASTM International.

ASTM D4442-20 (2021). Standard test methods for direct moisture content measurement of wood and wood-based materials. ASTM International.

Berg, C. C. (1982). The identity of *Milicia excelsa*. Bulletin du Jardin Botanique National de Belgique, 52(3–4), 225–229.

Bodig, J., & Jayne, B. A. (1982). *Mechanics of wood and wood composites*. Van Nostrand Reinhold.

CIRAD (2020). Tropix 7: Tropical timber database. https://tropix.cirad.fr

Dinwoodie, J. M. (2000). *Timber: Its nature and behaviour* (2nd ed.). E & FN Spon.

EN 1995-1-1 (2004). Eurocode 5—Design of timber structures—Part 1-1: General—Common rules and rules for buildings.

EN 408 (2012). Timber structures—Structural timber and glued laminated timber—Determination of some physical and mechanical properties.

EN 338 (2016). Structural timber—Strength classes. European Committee for Standardization.

EN 384 (2016). Structural timber—Determination of characteristic values of mechanical properties and density. European Committee for Standardization.

Glass, S. V., & Zelinka, S. L. (2010). Moisture relations and physical properties of wood. In R. J. Ross (Ed.), *Wood handbook: Wood as an engineering material* (General Technical Report FPL-GTR-190). U.S. Department of Agriculture, Forest Service, Forest Products Laboratory.

ISO 13061-1 (2014). Physical and mechanical properties of wood—Test methods for small clear wood specimens—Part 1: Determination of moisture content for physical and mechanical tests. International Organization for Standardization.

ISO 13061-2 (2014). Physical and mechanical properties of wood—Test methods for small clear wood specimens—Part 2: Determination of density for physical and mechanical tests. International Organization for Standardization.

ISO 13061-3 (2014). Physical and mechanical properties of wood—Test methods for small clear wood specimens—Part 3: Determination of ultimate strength in static bending. International Organization for Standardization.

ISO 13061-5 (2014). Physical and mechanical properties of wood—Test methods for small clear wood specimens—Part 5: Determination of strength in compression perpendicular to grain. International Organization for Standardization.

LNEC (2010). Ficha M3—Madeiras tropicais: Iroko (*Milicia excelsa*). Laboratório Nacional de Engenharia Civil.

Louppe, D., Oteng-Amoako, A. A., & Brink, M. (Eds.). (2008). *Plant resources of tropical Africa* 7(1): Timbers 1. PROTA Foundation.

Meier, E. (2023). The wood database. https://www.wood-database.com

Orwa, C., Mutua, A., Kindt, R., Jamnadass, R., & Simons, A. (2009). Agroforestree database: A tree reference and selection guide. World Agroforestry Centre (ICRAF).

Ramage, M. H., Burridge, H., Busse-Wicher, M., Fereday, G., Reynolds, T., Shah, D. U., Wu, G., Yu, L., Fleming, P., Densley-Tingley, D., Allwood, J., Dupree, P., Linden, P. F., & Scherman, O. (2017). The wood from the trees: The use of timber in construction. Renewable and Sustainable Energy Reviews, 68, 333–359.

Wagenführ, R. (2007). *Wood atlas* (6th ed.). Hanser Publishers.

The Potential of Grey Poplar as Load-Bearing Material

Laszlo Bejo[1*], Ruben Acs[1], Zoltan Hantos[2]

[1]University of Sopron, Faculty of Wood Engineering and Creative Industries.
Bajcsy-Zs. Str. 4, Sopron, Hungary, 9400.
[2] Wood Structural Engineer, self-employed.

E-mail: bejo.laszlo@uni-sopron.hu; rbnacs@gmail.com; faiparimernok@gmail.com

Keywords: grey poplar; hybrid poplar; MOE; MOR; vibration characteristics.

ABSTRACT
Grey Poplar (*Populus* × *Canescens*) is an underutilised indigenous wood species that grows abundantly in Hungary. *Populus* × *Euramericana* hybrids, bred selectively for their superior growth, appearance and technical characteristics, are much more popular for various applications, including plywood production, packaging and wood-based materials, as well as certain structural applications. Unfortunately, these hybrids require large amounts of water to grow, and recent aridification trends are unfavourable for their cultivation. In addition, environmental regulations also favour indigenous species like grey poplar. This means that, in the future, indigenous species, which are better adapted to dry climates, will increasingly dominate the raw material base.
Unfortunately, the Hungarian wood industries are not prepared for this shift in the raw material mix. Construction products, in particular, are in increasingly high demand, and it is important to assess the future raw material base to establish their potential as structural material. This paper reports on the results of an extensive comparative investigation of the physical and mechanical characteristics of *Populus* × *Canescens* and *Populus* × *Euramericana*, using small specimens for testing. Parameters measured included density, MOE and MOR. MOE was measured using vibration techniques (dynamic MOE), as well as bending MOE determination during destructive testing. The results showed no significant difference in the density of the two species. Grey poplar proved to be superior to the I-214 hybrid in terms of MOE and MOR. As expected, MOE was found to be a good predictor of MOR in case of both varieties. Based on the results, indigenous grey poplar may be a viable substitute for hybrid poplar in structural applications.

INTRODUCTION

Wood is a well-established material in the construction of traditional family houses, but based on the European Commission's sustainable built environment policy (European Parliament and Council 2024) it is also a potential candidate as a major construction material of the future. It can be used as simple construction lumber, glued construction elements or wood based composites. Softwoods are especially well suited for these purposes, but, due to climate change and intensive use, their availability is increasingly limited, and alternatives are needed for the traditional coniferous wood species in the construction sector.
Poplars represent a significant component of European forest resources. In Hungary alone, the standing volume reaches approximately 37.9 million m³, amounting to around 9.4% of the total forest stock (NFK 2024, Komán et al. 2023). This considerable biomass is largely associated with short rotation cycles, typically 10–30 years, which enhance productivity and make poplars suitable for both industrial raw material supply and bioenergy production (Lindegaard et al. 2016). A limited number of taxa often dominates species composition. For example, grey poplar (*Populus* × *canescens*) and the 'Pannonia' hybrid (*Populus* × *euramericana* cv. Pannonia) together constitute roughly two-thirds of the poplar area of Hungary. Such dominance reflects both natural adaptability and the outcomes of long-term breeding programs aimed at optimizing yield and wood quality (Santon et al. 2010).
Hybrid poplars have been created by artificial hybridization of various species. The most prominent group of poplar hybrids in Hungary have been created by crossing Populus nigra and Populus deltoides, to create the so-called Euramerican poplars (*Populus* × *euramericana*, a.k.a. *Populus* × *canadensis*), which have many varieties, each with their particular characteristics. Most of these varieties typically have light color, homogeneous structure and excellent growth characteristics, not unlike those of soft-

woods (Bondor 2011). Their extensive use to create fast-growing plantations in Hungary in the second half of the 20th century means that currently there are high quantities of hybrid poplar harvested and available as industrial raw material. However, hybrid poplar cultivation requires high quantities of water. Due to climate change trends and increasingly stringent environmental regulations, their availability in Hungary is expected to slowly decline in the coming decades, and the industry will have to contend with lower quality indigenous poplar (Borovics et al. 2024). In addition, indigenous poplars are available in large quantities, while their amount used in industry is quite low.
Due to their current ubiquity and superior growth characteristics, much attention has been paid to the physical and mechanical properties of hybrid poplars (e.g. Báder et al. 2022). Indigenous poplar species received less attention, although some measurement results from the previous century are available in the literature (Molnár and Bariska 2002.) The purpose of the research presented in this paper was to revisit and reassess some of the most important mechanical and physical characteristics of grey poplar, one of the most ubiquitous indigenous poplar species, and compare it to that of hybrid poplar. Furthermore, the suitability of non-destructive predictors was also examined for estimating the mechanical characteristics of grey poplar.

MATERIALS AND METHODS

Investigations involved two poplar raw materials: grey poplar (*Populus* × *canescens*), and Euramerican poplar (*Populus* × *euramericana* – the exact variety is unknown.) Grey poplar was sourced from the KEFAG LC (Kecskemét, Hungary), while hybrid poplar was supplied by JAF Holz Ungarn Ltd. (Dunaharaszti, Hungary). Investigations included measuring the density, dynamic modulus of elasticity (MOE), bending strength and MOE of both materials.

Specimen preparation and physical characteristics

Investigations in this study were limited to small clear bending specimens. The dimensions of the specimens were 450 × 50 × 20 mm. The relatively small size of bending specimens was due to the growth characteristics of grey poplar that limited the length of clear specimens. 50 bending specimens of both species were manufactured. Specimens were randomly selected from a limited number of poplar boards, and the sample was treated as random.
A capacitive moisture meter was used to measure and record the moisture content of each specimen. The density of the bending specimens was determined by measuring the average dimensions and mass of each specimen using digital calipers and a laboratory scale. Density values were converted to normal conditions (12% MC).

Dynamic modulus of elasticity determination

The dynamic MOE of each bending specimen was measured based on longitudinal and bending vibrations as well.
Longitudinal vibration measurement involved hitting the end of each bending specimen (Figure 1a). A sensitive microphone picked up the vibrations and forwarded it to a computer, where the vibration frequency was determined using an FFT analyser. Sound velocity was determined based on the vibration frequency, and MOE was calculated using the following equation, derived from Hooke's law:

$$MOE_{long} = \rho v^2, \quad (1)$$

where ρ is the calculated density (before conversion to normal conditions) and v is the sound velocity. Note that 10 of the 50 measurement on hybrid poplar specimens were unsuccessful. The exact reason is unknown, but the probable cause was the disturbed grain structure of some specimens, which distorted the acoustic signal.
Bending vibration frequency was measured in the first bending mode, simply supported, by placing the specimen on elastic supports at the two nodes, and hitting the middle of the specimen with a hammer (Figure 1b). Frequency determination occurred the same way as in the case of longitudinal vibration. Transverse dynamic modulus of elasticity was calculated using the Euler equation (Weaver et al. 1991):

$$MOE_{trans} = \left(\frac{2f_n}{\gamma_n \pi}\right)^2 \frac{mL^3}{I}, \quad (2)$$

where f_n is the vibration frequency, m, L and I are the mass, length and 2nd order moment of inertia of the specimen, respectively, and the value of γ_n is 2.267 in case of first modus vibrations.

a *b*

Figure 1: Dynamic MOE determination based on longitudinal (a) and bending vibrations (b)

Bending tests

4-point bending tests were performed based on global bending EN 408:2010+A1, using an INSTRON 4208 (Illinois Tool Works Inc., IL, USA) universal testing machine equipped with 30 mm dia. supports and a self-aligning loading attachment. The measurement was controlled with the Bluehill analytical software version 4.44 (Illinois Tool Works Inc.) Bending tests were performed using a span of 360 mm, and crosshead movement of 2.4 mm/min. Deformation was measured using a strain gage, which was removed once bending load reached 3000 N. Bending strength (MOR) and MOE were determined using the following equations (based on EN 408:2010+A1):

$$MOR = \frac{M_{max}}{I}\frac{h}{2}, \quad (3)$$

$$MOE_b = \frac{3aL^2 - 4a^3}{2bh^2\left(2\frac{w_2 - w_1}{F_2 - F_1} - \frac{6a}{5Gbh}\right)}, \quad (4)$$

where: M_{max} - the max. bending moment ($M_{max} = F_{max}\, a$, where Fmax is the maximum load
b, h - specimen width and height, respectively
a - the distance between the support and the closest loading point
F_1, F_2 - load values measured at 20% and 30% of the maximum load, respectively
w_1, w_2 - deflection values measured at 20% and 30% of the maximum load, respectively
G - shear modulus (literature values taken from Molnár and Bariska 2002)

Bending strength and all MOE values were adjusted to normal conditions according to ISO 13061-3:2014 and ISO 13061-4:2014, respectively:

$$MOR' = MOR[1 + \alpha_1(mc - 12)], \quad (5)$$

$$MOE' = {MOE}/{[1 - \alpha_2(mc - 12)]}, \quad (6)$$

where *mc* is the moisture content (inserted as percentage value), and correction factors $\alpha_1 = 0.04$ and $\alpha_2 = 0.02$, as specified in the respective standards. (Note: these standards refer to 3-point bending, but it was assumed that they hold true for MOR and MOE determined in 4-point bending, as well as vibration-based MOE values.)

RESULTS AND DISCUSSION

Table 1 summarizes the basic descriptive statistics of all measured values, as well as the results of the unpaired t-tests performed on each parameter to compare the results of indigenous and hybrid poplar. The average density of the two species were very close, grey poplar's being slightly higher, but statistical significance was not found. The mechanical performance of indigenous and hybrid poplar, on the other hand, was highly significantly different.

Table 1: Comparing the various parameters of indigenous and hybrid poplar

Parameter[a]	Material	Mean	Std.	Min.	Max.	Statistics[b]
Density (kg/m^3)	Indigenous	493	23.3	441	541	t = 0.556
	Hybrid	490	36.4	429	590	p = 0.580
MOR' (MPa)	Indigenous	102.6	11.9	70.6	128.5	t = 9.570
	Hybrid	75.6	16.0	31.4	120.6	p < 0.001
MOE'$_{long}$ (GPa)	Indigenous	17.7	1.85	12.9	22.8	t = 10.776
	Hybrid [c]	13.2	2.11	8.4	16.9	p < 0.001
MOE'$_{trans}$ (GPa)	Indigenous	16.4	1.57	12.2	20.2	t = 10.931
	Hybrid	12.2	2.18	6.2	18.1	p < 0.001
MOE'$_b$ (GPa)	Indigenous	17.2	1.64	13.4	21.1	t = 12.093
	Hybrid	12.2	2.46	5.1	17.9	p < 0.001

[a]All values adjusted to 12% moisture content; [b]two-tailed unpaired t-test, df=98 (except for MOE'$_{long}$)
[c]A total of 10 measurements were unsuccessful and were excluded from the evaluation.

The similar densities of the two species is also evident in Figure 2a. Figure 2b shows that, even though the two materials did not differ significantly in terms of density, grey poplar's bending strength was approx. 35% higher.

Figure 3 compares the Moduli of Elasticity, measured using the three different methods. Again, grey poplar performed much better, surpassing the MOE of Euramerican poplar by about 35 % again. The difference in the results between MOE measured by bending vibrations and static bending was not significantly different (t = 0.902; p = 0.368). MOE measured by longitudinal vibrations was, on the other hand, significantly lower than the static MOE values (t = 2.216; p = 0.028).

Figure 4 shows the relationship between density and bending strength for both materials. This diagram further demonstrates the fact that grey poplar had much better load bearing capacity, while its density is similar. There is a moderately close relationship between the density and MOR of Euramerican poplar, but no relationship was found for grey poplar.

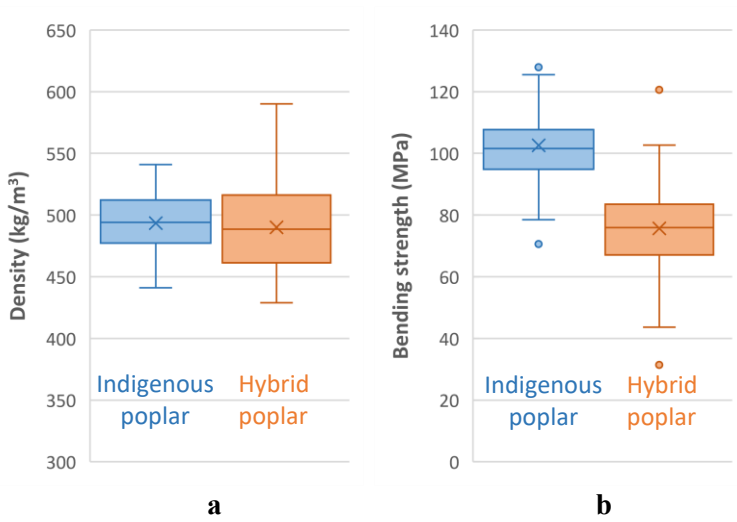

Figure 2: Measured density (a) and Bending strength (b) values of indigenous grey poplar and Euramerican hybrid poplar. All values adjusted to 12% MC

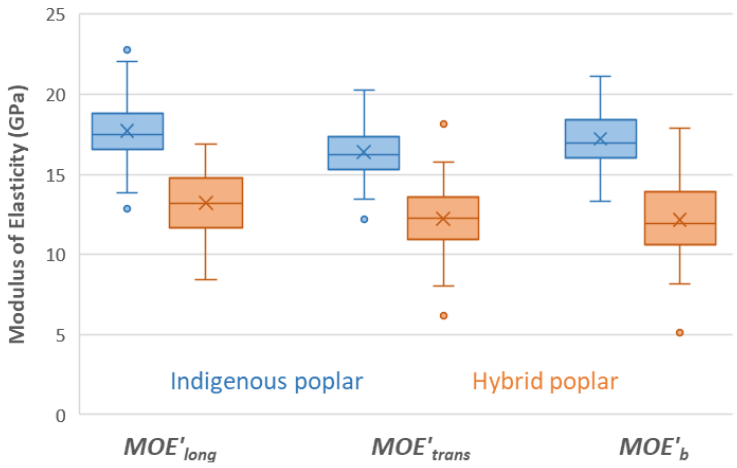

Figure 3: Modulus of Elasticity of indigenous grey poplar and Euramerican hybrid poplar measured by three different methods. All values adjusted to 12% MC

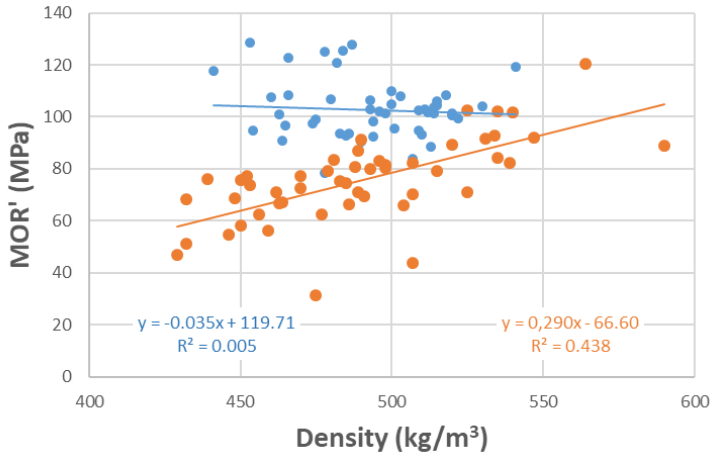

Figure 4: The relationship between the measured density and bending strength values. All values adjusted to 12% MC

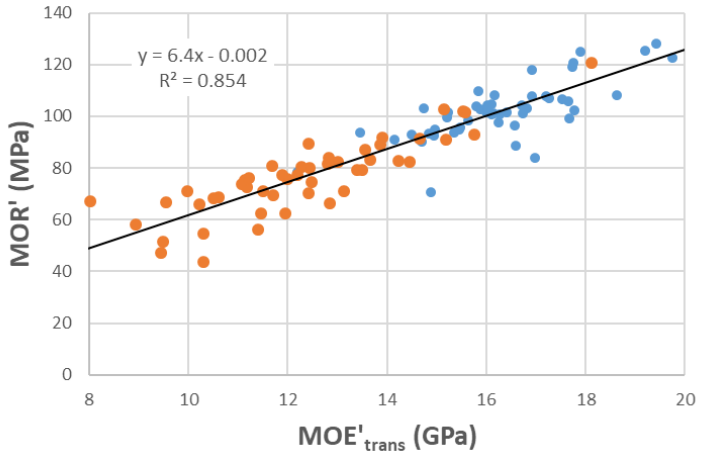

Figure 5: The relationship between MOE measured by bending vibrations and bending strength values. All values adjusted to 12% MC

Figure 5 depicts the relationship between the MOE and the bending strength of poplar. There is a very close relationship between MOE measured by bending vibrations and MOR, and this relationship is species-independent; all data points clearly fit a single linear model. The linear fit is somewhat worse for static bending MOE and that measured by longitudinal vibrations (r^2 = 0.813 and 0.785, respectively), but the relationship is still fairly tight.

Literature data on the technical properties of grey poplar is scarce to non-existent. In various sources (Molnár and Bariska 2002, Kozakiewicz et al. 2020, Noskowiak et al 2014, Chen et al. 2022, Bier 1985) the characteristics of *P. nigra* and *P. deltoides* (the two species that combined to form the *P.* × *canescens* hybrid) range from 372 to 470 kg/m^3 (density), 35 to 65 MPa (MOR), 6.0 to 9.8 GPa (MOE). The material investigated in this study had slightly higher density than the values found in the literature. The MOR and MOE, on the other hand, was much higher, about twice as high as the values found in the literature.

In the literature, the density and mechanical properties of hybrid Euramerican poplar ranges from 320 to 420 kg/m^3 (density), 58 to 82 MPa (MOR), 5.2 to 9.8 GPa (MOE) (Molnár and Bariska 2002, Báder et al. 2022). The experimental results in this study are, again, somewhat higher than the literature values, but the difference is not as striking as in the case of grey poplar.

The results of the present study show the excellent potential of grey poplar, but the large discrepancy compared to the literature calls for caution. The material examined in this study is may have been an outlier with excellent mechanical properties, and may not represent Hungarian grey poplar in general. This was confirmed in a recent study aimed at creating grey poplar CLT, where the lamellas were graded as C14 to C22, except for one outlier with a C45 grade (Fabrice 2026). Another concern is the growth characteristics of grey poplar, which prevents the production of structural lumber with appropriate dimensions, although grey poplar may be a good raw material for glued construction lumber and structural wood based composites.

Non-destructively measured MOE values are expected to be higher than the static bending MOE, due to the viscoelastic nature of wood, which doesn't allow viscous deformation to develop at fast deformation rates during vibration testing (Divos and Tanaka 2000). In this study, there was no marked difference between the MOE values determined with static and dynamic methods, and MOE_{long} values were even lower than those measured using static bending. The exact cause of this is unknown.

Bulk density was found an unreliable predictor of bending strength in this study. Density predicted the *MOR* of Euramerican poplar relatively well, but there was no correlation between the MOR and density of indigenous grey poplar. MOE measured with vibration techniques, as well as static bending MOE, on the other hand, proved to be a very reliable strength predictor. The relationship between MOE and MOR is also independent of species; data points for both materials fit the same linear model well (with r^2 values ranging from 0.785 to 0.854.) Bending vibrations are especially well suited to predict the MOR of small clear specimens.

CONCLUSIONS

A comparative investigation of small clear specimens made of indigenous grey poplar () and Euramerican hybrid poplar *Populus* × *canescens*), and Euramerican poplar (*Populus* × *euramericana*) revealed the following conclusions:

- At similar densities, grey poplar had significantly higher bending strength and MOE values, which shows the excellent potential of grey poplar as a structural raw material.
- While grey poplar specimens investigated in this study had excellent mechanical properties, this may not be representative of Hungarian grey poplar in general. Another issue is the unfavourable growth characteristics of this species. Nevertheless, grey poplar may be used as raw material for glued structural products and structural wood based composites.
- Density is a reliable strength predictor, but MOE values in general, and MOE measured by bending vibrations in particular, are excellent strength predictors for small clear specimens of indigenous and hybrid poplar. The same linear model can be used to predict the MOR of both species.

While the results are encouraging, further studies are needed to get a more representative picture of the physical and mechanical properties of grey poplar, and to verify the results on structural-size lumber that contains defects.

ACKNWOLEDGEMENTS
This article was made in the frame of the project TKP2021-NKTA-43, which has been implemented with support provided by the Ministry of Culture and Innovation of Hungary from the National Research, Development and Innovation Fund, financed under the TKP2021-NKTA funding scheme. The authors are grateful for the help of research associate Mátyás Báder and research engineer Olivér Hanzséros.

REFERENCES

Báder M, Németh R, Benke A, Köbölkuti ZA, Borovics A, Takács D (2022) Bending test results of plantation poplar clones. In: Németh R, Hansmann C, Rademacher P, Bak M, Báder M (eds) 10th Hardwood Conference Proceedings. University of Sopron Press, Sopron, Hungary, pp 75–82. https://doi.org/10.35511/978-963-334-446-0

Bier H (1985) Structural Properties Of Timber From Two Poplar Varieties. New Zealand Journal of Forestry Science 15(2): 223-32.

Bondor A (2011) A nemesnyár-termesztés fejlesztésének újabb eredményei [Latest results in the development of hybrid poplar cultivation]. Doctoral Dissertation, University of West-Hungaty, Faculty of Forestry, Hungary (in Hungarian)

Borovics A, Király É, Kottek P (2024) Projection of the Carbon Balance of the Hungarian Forestry and Wood Industry Sector Us-ing the Forest Industry Carbon Model. Forests, vol. 15, no. 4, p. 600 https://doi.org/10.3390/f15040600

Chen Y, Wu, H, Dai, X, Li W, Qiu Y, Yang Y, Yin T (2022). Sex effect on growth performance and marker-aided sex discrimination of seedlings of *Populus deltoides*. Journal of Forestry Research. 34. 1-7. https://doi.org/10.1007/s11676-022-01567-1

Divos F, Tanaka T (2000). Effects of creep on modulus of elasticity determination of wood. Journal of Vibration and Acoustics-Transactions of the ASME 122(1):89-92.

EN 408:2010+A1:2012; Timber Structures. Structural Timber and Glued Laminated Timber. Determination of Some Physical and Mechanical Properties. European Committee for Standardization: Brussels, Belgium, 2012; 39p.

European Parliament and Council of the European Union. Regulation (EU) 2024/3110 of 27 November 2024 laying down harmonised rules for the marketing of construction products and repealing Regulation (EU) No 305/2011. Off. J. Eur. Union 2024, L 123. pp. 1-106.

Fabrice S (2026) CLT made of Hungarian indigenous poplar material. MSc. Thesis, University of Sopron, Faculty of Wood Sciences and Creative Industries. 49 pp.

ISO 13061-3:2014. Physical and mechanical properties of wood — Test methods for small clear wood specimens. Part 3: Determination of ultimate strength in static bending. International Organization for Standardization, 5 pp.

ISO 13061-4:2014. Physical and mechanical properties of wood — Test methods for small clear wood specimens Part 4: Determination of modulus of elasticity in static bending. International Organization for Standardization, 6 pp.

Kozakiewicz P, Drożdżek M, Laskowska A, Grzeskiewicz M, Bytner O, Radomski A, Mróz A, Betlej I, Zawadzki J. (2020). Chemical composition as factor affecting the mechanical properties of thermally modified black poplar (*Populus nigra* L.). BioResources. 15. 3915-3929. https://doi.org/10.15376/biores.15.2.3915-3929

Komán S, Németh R, Báder M (2023) An Overview of the Current Situation of European Poplar Cultures with a Main Focus on Hungary Applied Sciences-Basel 2023 13 : 23 Paper: 12922 https://doi.org/10.3390/app132312922

Lindegaard KN, Adams PWR, Holley M, Lamley A, Henriksson A, Larsson S, von Engelbrechten H-G, Esteban Lopez G, Pisarek M (2016) Short Rotati on Plantations Policy History in Europe: Lessons from the Past and Recommendations for the Future. Food Energy Secur. 2016 vol. 5, pp. 125–152. https://doi.org/10.1002/fes3.86

Molnár S, Bariska M (2002) Wood Species of Hungary. Szaktudás Publishing House, Budapest, Hungary, 210 pp.

NFK (National Land Centre) (2024). Hungarian Forest Related Data (Magyarország Erdeivel Kapcsolatos Adatok); National Land Centre of the Ministry of Agriculture; Budapest, Hungary, 2022. https://foldalap.am.gov.hu/Magyarorszag_erdeivel_kapcsolatos_adatok_news_513

Noskowiak A, Pajchrowski G, Szumiński G, Jabłoński L. (2014) Properties of black poplar wood (Populus nigra L.) in terms of structural applications. Annals of WULS - SGGW. Forestry and Wood Technology. 86:189-192.

Stanton BJ, Neale DB, Li S. (2010) Populus Breeding: From the Classical to the Genomic Approach. In: Jansson S, Bhalerao R, Groover A (eds) Genetics and Genomics of *Populus*; Springer: New York, NY, USA, pp. 309–348, ISBN 978-1-4419-1540-5.

Weaver W, Timishenko SP, Young DH (1991). Vibration Problems in Engineering. 5th edition. John Wiley and Sons, 624 pp.

The Impact of *Hymenoscyphus fraxineus* and Associated Fungal Pathogens on the Material Structure and Chemical Composition of Common Ash (*Fraxinus excelsior*)

Anett Sütő[1*], Róbert Németh[1]

[1] University of Sopron, Faculty of Wood Engineering and Creative Industries. Bajcsy-Zs. Str. 4, Sopron, Hungary, 9400.

E-mail: suto.anett@phd.uni-sopron.hu; nemeth.robert@uni-sopron.hu

Keywords: ash dieback, associated fungal infections, FT-IR spectroscopy, tree-ring analysis, material structure.

ABSTRACT

The decline of European ash populations is driven by *Hymenoscyphus fraxineus* infections, often compounded by other fungal pathogens. In Hungary, as a result of this complex pathological process, a significant portion of the stands is suffering from decline, leading to changes in the structural and chemical properties of the standing timber. The aim of our research was to explore these alterations, with a particular focus on wood anatomical distortions and molecular-level modifications.

Tree-ring analysis of the collected samples revealed that individuals suffering from long-term decline underwent a drastic reduction in growth, with the most recent tree rings becoming extremely narrow. This physical change is a direct indicator of disturbances in the tree's vital physiological processes. During the research, infrared spectroscopy was employed to examine the chemical footprint of the altered wood structure, seeking changes in the main wood components (cellulose, hemicelluloses, lignin, and extractives).

Although spectroscopic analyses show certain deviations in the fingerprint regions of healthy and infected samples, the interpretation of these results is subject to significant uncertainty. The multi-factorial infection process, the presence of secondary pathogens, and the varying defense mechanisms of individual trees result in a heterogeneous pattern that prevents the establishment of clear regularities at this stage. The presentation demonstrates these measurement anomalies, the challenges in finding correlations between the observed spectra and anatomical characteristics, and outlines the further research directions necessary to resolve these uncertainties.

INTRODUCTION

European ash (Fraxinus excelsior L.) is an ecologically and economically important native hardwood species in Europe and Hungary, playing a significant role in forest ecosystems (Bartha et al., 2015). During recent decades, European ash populations have been severely affected by ash dieback, a disease primarily caused by *Hymenoscyphus fraxineus*. The disease has spread rapidly throughout Europe and has become one of the most serious health problems affecting European ash (Gross et al., 2014; Pautasso et al., 2013).

The infection results in crown thinning, shoot dieback, and a gradual decline in tree vitality. The decline process is often accompanied by secondary pathogens; therefore, the observed damage cannot always be attributed exclusively to the presence of *H. fraxineus*. Several studies have demonstrated that infected stands may also host other fungal species, including *Armillaria* spp., *Diplodia fraxini*, *Diaporthe eres*, and various members of the *Botryosphaeriaceae* (Kowalski et al., 2017; Langer, 2017; Linaldeddu et al., 2020, 2022).

Prolonged decline may also be reflected in tree growth. Reduced cambial activity can lead to the formation of narrower annual rings, indicating a deterioration in tree vitality. However, only limited information is available regarding the extent to which these anatomical changes are accompanied by modifications in the chemical composition of the wood.

Fourier-transform infrared spectroscopy (FTIR) is a widely used method for the chemical characterization of wood and is suitable for investigating the structural characteristics of cellulose, hemicelluloses, lignin, and extractives (Tolvaj, 2024; Faix, 1991; Pandey & Pitman, 2003). The

technique is particularly useful in exploratory studies aimed at identifying chemical patterns and relative differences.
The aim of the present study was to determine whether European ash samples affected by ash dieback and exhibiting different growth histories show detectable differences in annual ring structure and FTIR spectra that may be associated with prolonged decline. The study was exploratory in nature and focused on investigating relationships between anatomical changes and infrared absorption bands associated with the major wood constituents.

MATERIALS AND METHODS

Wood Material and Sampling Background

The study was conducted on disc samples and increment cores. As the investigation was exploratory in nature, the objective of sample selection was to compare ash samples with different growth histories. The material included samples with relatively uniform annual ring structures, which could be interpreted as control-like samples, as well as samples originating from trees in which the annual rings formed during the last years showed pronounced narrowing (Figure 1).

Figure 1: Samples with narrowing rings

Particular emphasis was placed on differences in growth history during sample evaluation. In samples with a uniform annual ring structure, no marked reduction in radial growth was observed. In contrast, samples interpreted as declining exhibited considerably narrower outer annual rings formed during the most recent years, suggesting a prolonged reduction in tree vitality.

FTIR Spectroscopic Analysis

Fourier-transform infrared spectroscopy (FTIR) was used to investigate the chemical characteristics of the wood. Several deliberately selected measurement points were examined within each sample. The locations of the measurement points were not determined according to an evenly spaced geometric profile but were selected on the basis of anatomical features and growth history.
For each sample, measurements were taken from the outermost annual rings formed during the most recent years, from the inner part of the sapwood, from the sapwood–heartwood transition zone, and from the heartwood. Additional measurement points were selected whenever justified by the macroscopic annual ring pattern or by structural differences in the wood.

Selected Absorption Bands

The evaluation of FTIR results focused on five selected wavenumbers:
1170 cm^{-1}: band associated with hemicelluloses;
1270 cm^{-1}: band associated with guaiacyl lignin;
1510 cm^{-1}: band associated with the aromatic lignin skeleton;
1657 cm^{-1}: band reflecting carbonyl groups and certain extractive-related compounds;
1740 cm^{-1}: band associated with acetyl and carbonyl groups of hemicelluloses as well as certain ester bonds.
The interpretation of the selected bands was based on assignments commonly used in FTIR studies of wood (Tolvaj, 2024; Faix, 1991; Pandey & Pitman, 2003).
The objective was to determine whether consistent or partially consistent FTIR spectral differences could be observed among samples with different growth histories.

RESULTS

Annual Ring Observations

Considerable differences were observed in the annual ring structure of the investigated ash samples. Some samples exhibited a relatively uniform annual ring pattern, whereas others showed pronounced narrowing of the outer annual rings formed during the most recent years.

General Characteristics of the FTIR Spectra

The investigated FTIR bands were associated with hemicelluloses, lignin, and certain carbonyl-containing and extractive-related compounds (Tolvaj, 2024; Faix, 1991; Pandey & Pitman, 2003). Considerable differences were observed among the samples in terms of radial variability. The sample with a uniform annual ring structure generally exhibited smaller fluctuations, whereas samples interpreted as declining showed larger-amplitude variations in several absorption bands (Figures 2-7).

Figure 2: Increment core sample from a declining tree

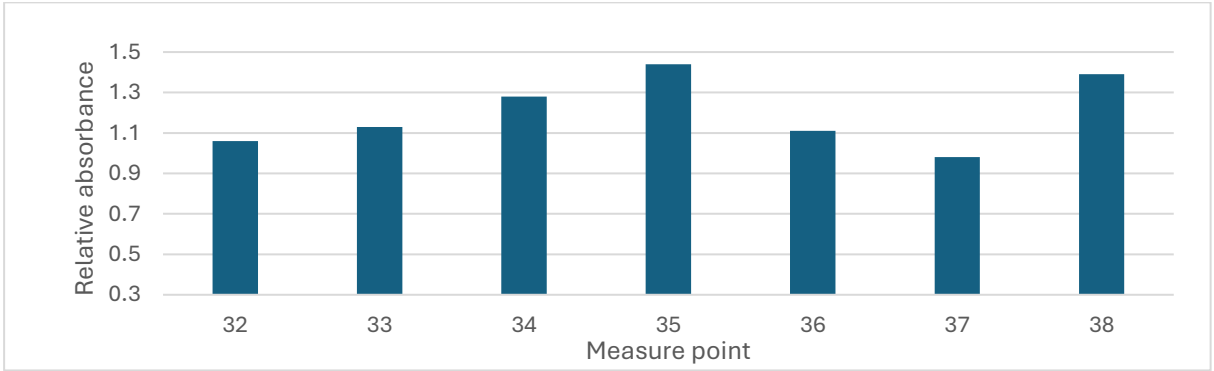

Figure 3: 6 12 Sample, 1170 Wavenumber (cm^{-1})

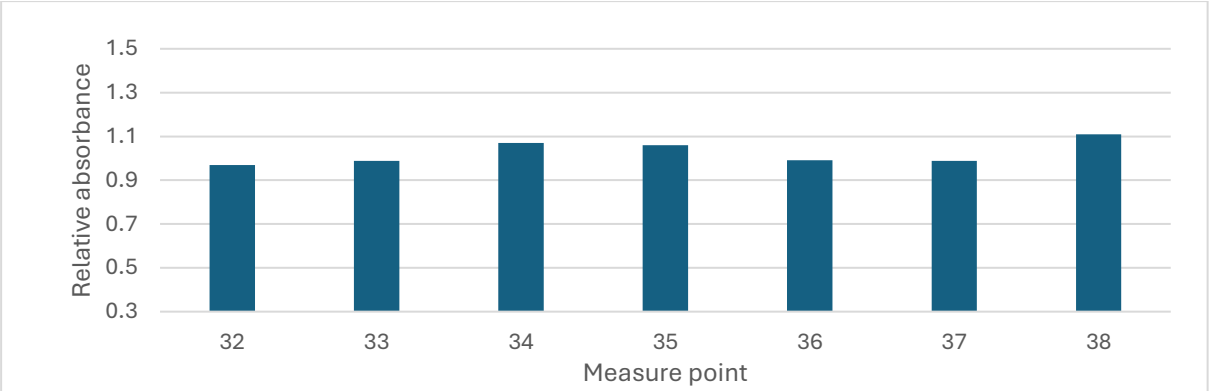

Figure 4: 6 12 Sample, 1270 Wavenumber (cm^{-1})

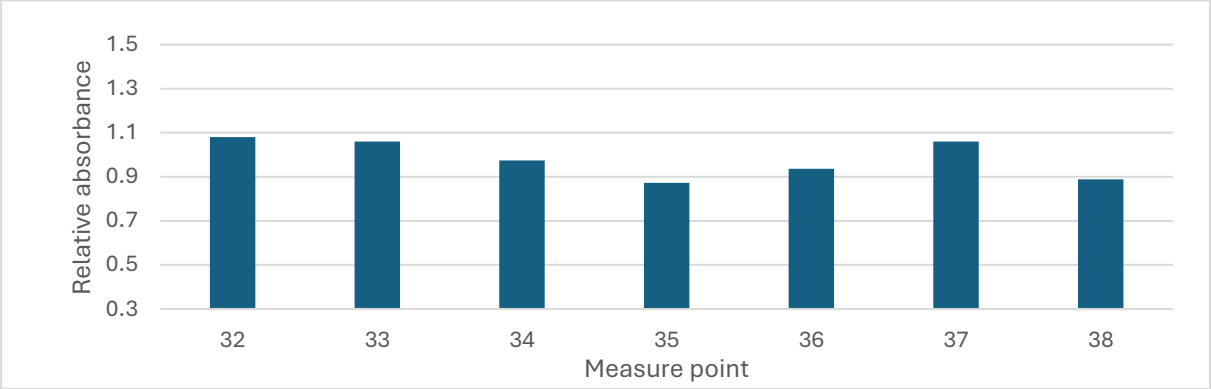

Figure 5: 6 12 Sample, 1510 Wavenumber (cm^{-1})

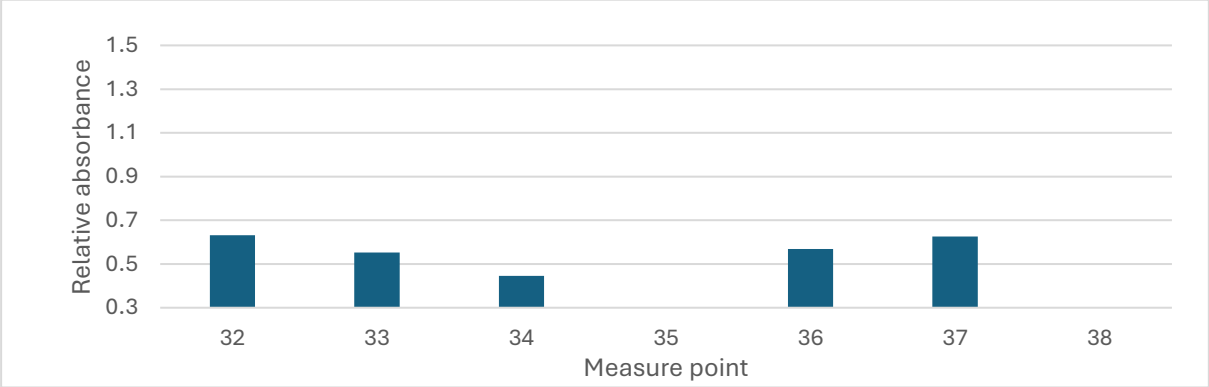

Figure 6: 6 12 Sample, 1657 Wavenumber (cm^{-1})

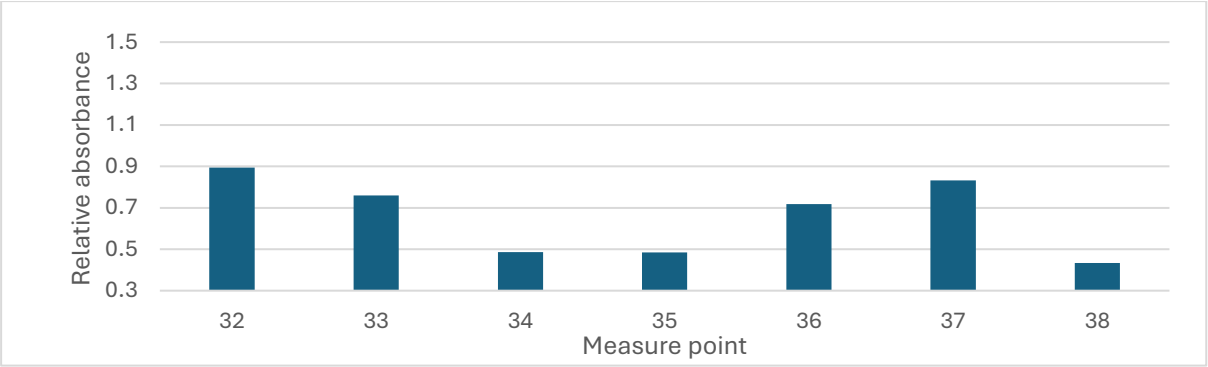

Figure 7: 6 12 Sample, 1740 Wavenumber (cm^{-1})

Comparison of the Investigated Absorption Bands

The band around 1170 cm^{-1} exhibited the greatest within-sample variability. In several samples, an inverse relationship was observed between the 1170 cm^{-1} and 1740 cm^{-1} absorption bands.

The lignin-related bands around 1270 cm^{-1} and 1510 cm^{-1} proved to be relatively stable in the investigated samples and showed no clear relationship with the degree of decline.

The band around 1657 cm^{-1} displayed considerable variability both among and within samples. Overall, the highest variability was observed for the 1170 cm^{-1} and 1657 cm^{-1} bands, whereas the 1270 cm^{-1} band remained comparatively stable.

DISCUSSION

Relationship Between Growth Reduction and Changes in Wood Chemistry

Annual ring analysis revealed a marked reduction in radial growth in several samples, manifested by the narrowing of the outer annual rings. This observation is consistent with the progressive loss of vitality commonly associated with ash dieback (Gross et al., 2014; Pautasso et al., 2013).

The FTIR analyses indicated that this reduction in growth may be accompanied by changes in wood chemistry. The greatest variability was observed in bands associated with hemicelluloses and certain extractive-related compounds. However, the observed differences did not follow a uniform pattern among the investigated samples.

These findings suggest that the relationship between decline and chemical changes cannot be described by a simple cause-and-effect mechanism. Individual trees may respond differently to the same pathological process.

Challenges in the Interpretation of FTIR Results

One of the most important findings of the study was the absence of a consistent FTIR spectral response among samples interpreted as declining. Although increased radial heterogeneity was frequently observed, no absorption band exhibited the same pattern of change in all declining samples.

This may be explained by the fact that FTIR spectra represent the combined signal of a complex chemical system. Individual absorption bands often reflect the contribution of several chemical components; therefore, their interpretation is not always straightforward (Pandey & Pitman, 2003; Tolvaj, 2024).

Particular attention should be paid to the band around 1657 cm^{-1}, which may be influenced by various carbonyl-containing compounds and extractive-related components. Consequently, the observed differences cannot be attributed to a single biological process.

Complexity of the Disease Process and the Role of Associated Pathogens

Ash dieback can no longer be regarded as a disease caused exclusively by Hymenoscyphus fraxineus. Several studies have demonstrated that additional fungal species may contribute to the deterioration of affected trees (Kowalski et al., 2017; Langer, 2017; Linaldeddu et al., 2020).

This aspect is particularly important when interpreting the present results. No detailed microbiological investigation was carried out on the analysed samples; therefore, it is not possible to determine the extent

to which the observed chemical differences can be attributed directly to H. fraxineus or to associated fungal species.
The duration and stage of the decline process may also represent important sources of variability. It is likely that the investigated trees were affected to different degrees and at different stages of decline, which may have contributed to the heterogeneous spectral patterns observed.

Relationship Between the 1170 cm^{-1} and 1740 cm^{-1} Bands

An interesting observation was the apparent inverse relationship between the 1170 cm^{-1} and 1740 cm^{-1} absorption bands in several samples. In measurement points where the intensity of the 1170 cm^{-1} band was higher, the 1740 cm^{-1} band generally exhibited lower values, whereas decreases in the 1170 cm^{-1} band were often accompanied by increases in the 1740 cm^{-1} band.
Because the 1170 cm^{-1} band is mainly associated with hemicelluloses, while the 1740 cm^{-1} band is related to carbonyl and acetyl groups as well as certain ester bonds, this observation may indicate structural modifications rather than simple quantitative changes in wood constituents. However, the present dataset does not allow a definitive interpretation of this relationship.

Limitations of the Study and Future Research Directions

The exploratory nature of the study imposes several limitations. The number of samples was limited, the infection history of the investigated trees was not known in detail, and no parallel microbiological or molecular analyses were performed to identify the fungal species present.
Future studies should include larger sample sets, well-documented stages of decline, combined FTIR and microscopic investigations, and molecular identification of associated pathogens. In addition, the relationship between chemical changes and the mechanical properties of the wood deserves further investigation.
The combined evaluation of annual ring characteristics and radial FTIR profiles appears to be a promising approach for improving our understanding of the effects of ash decline on wood structure and chemistry.

CONCLUSIONS

The investigated ash samples exhibited considerable differences in annual ring structure. Several samples showed progressive narrowing of the outer annual rings, indicating a prolonged decline in tree vitality.
FTIR analyses revealed differences in absorption bands associated with hemicelluloses, lignin, and certain extractive-related compounds; however, these differences did not follow a consistent pattern. The greatest variability was observed in the 1170 cm^{-1} and 1657 cm^{-1} bands, whereas lignin-related bands remained comparatively stable.
In several samples, an inverse relationship was observed between the 1170 cm^{-1} and 1740 cm^{-1} absorption bands, suggesting the possibility of structural modifications associated with hemicellulose-related components.
Samples interpreted as declining generally exhibited greater radial chemical heterogeneity than the sample with a uniform annual ring structure. Nevertheless, the present study did not identify an FTIR marker that could serve as a reliable diagnostic indicator of ash dieback on its own.
The results demonstrate that the combined application of annual ring analysis and FTIR spectroscopy can provide valuable information on wood alterations associated with ash decline. However, a more detailed understanding of these relationships will require larger sample sets and complementary investigations involving pathogen identification and additional wood property analyses.

AKNOWLEDGEMENTS

I would like to express my deepest gratitude to Dr. László Tolvaj for their invaluable assistance and guidance throughout this research. Their immense help with the infrared spectroscopy measurements and data analysis was essential to the completion of this work, and I am truly grateful for their time and support.

Project no. 2025-2.1.1-EKÖP-2025-00002 has been implemented with the support provided by the Ministry of Culture and Innovation of Hungary from the National Research, Development and Innovation Fund, financed under the EKÖP-25-3-I funding scheme.

REFERENCES

Bartha, D., Király, G., Schmidt, D., Tiborcz, V., Barina, Z., Csiky, J., Jakab, G., Lesku, B., Schmotzer, A., Vidéki, R., Vojtkó, A., & Zólyomi, Sz. (Eds.). (2015). Magyarország edényes növényfajainak elterjedési atlasza / Distribution atlas of vascular plants of Hungary. Nyugat-magyarországi Egyetem Kiadó

Carroll, D., Boa, E., Cleary, M., Ghelardini, L., Gonthier, P., Martín-García, J., O'Hanlon, R., Prospero, S., & Scanu, B. (2024). Ash dieback: From Asia to Europe. Plant Pathology, 73(5), 1127–1145. https://doi.org/10.1111/ppa.13859

Faix, O. (1991). Classification of lignins from different botanical origins by FT-IR spectroscopy. Holzforschung, 45(Suppl.), 21–27. https://doi.org/10.1515/hfsg.1991.45.s1.21

Gross, A., Holdenrieder, O., Pautasso, M., Queloz, V., & Sieber, T. N. (2014). Hymenoscyphus pseudoalbidus, the causal agent of European ash dieback. Molecular Plant Pathology, 15(1), 5–21. https://doi.org/10.1111/mpp.12073

Kowalski, T., Bilański, P., & Kraj, W. (2017). Pathogenicity of fungi associated with ash dieback towards Fraxinus excelsior. Plant Pathology, 66(8), 1228–1238. https://doi.org/10.1111/ppa.12667

Langer, G. (2017). Collar rots in forests of northwest Germany affected by ash dieback. Baltic Forestry, 23(1), 4–19. https://www.nw-fva.de/fileadmin/nwfva/publikationen/pdf/langer_collar_rots_in_forests.pdf

Linaldeddu, B. T., Bregant, C., Montecchio, L., Brglez, A., Piškur, B., & Ogris, N. (2022). First report of Diplodia fraxini and Diplodia subglobosa causing canker and dieback of Fraxinus excelsior in Slovenia. Plant Disease, 106(1), 26–29. https://doi.org/10.1094/PDIS-06-21-1204-SC

Pandey, K. K., & Pitman, A. J. (2003). FTIR studies of the changes in wood chemistry following decay by brown-rot and white-rot fungi. International Biodeterioration & Biodegradation, 52(3), 151–160. https://doi.org/10.1016/S0964-8305(03)00052-0

Pautasso, M., Aas, G., Queloz, V., & Holdenrieder, O. (2013). European ash (Fraxinus excelsior) dieback—A conservation biology challenge. Biological Conservation, 158, 37–49. https://doi.org/10.1016/j.biocon.2012.08.026

Tolvaj, L. (2024). Optical properties of wood: Measurement methods and result evaluations. Springer Cham. https://doi.org/10.1007/978-3-031-46906-0

Acoustic Emission Monitoring of Moisture Uptake in Beech

Alexander Schneider[1,2], Mehieddine Derbas[1], Martin Riegler[1,2*]

[1] Wood K plus - Competence Center for Wood Composites & Wood Chemistry, Kompetenzzentrum Holz GmbH, Linz, Austria
[2] BOKU University, Institute of Wood Technology and Renewable Materials, Department of Natural Sciences and Sustainable Resources, Vienna, Austria.

E-mail: a.schneider@wood-kplus.at; m.derbas@wood-kplus.at; m.riegler@wood-kplus.at

Keywords: European beech; acoustic emission; moisture uptake; swelling; structural health monitoring; hardwood construction.

ABSTRACT
Fagus Sylvatica (European beech) plays an increasingly important role as hardwood species in modern timber construction, as it is an environmentally friendly alternative to concrete. But, as with most wood species and wood products, moisture-induced degradation remains a major concern. This study investigates whether acoustic emission (AE) monitoring can be used to detect moisture uptake in beech under controlled climatic conditions (20°C, 65% RH). A fully dried beech specimen was exposed to a humid environment while its mass, cross-sectional dimensions and AE were recorded over time. The results showed a pronounced increase in moisture content (MC) accompanied by dimensional swelling, with a strong correlation between mass increase and cross section change. Despite substantial noise in the AE signals, the AE median followed a similar trend and showed a reasonably strong correlation with moisture uptake. The findings indicate that AE monitoring has potential as a technique for detecting MC changes in wood. At the same time, further studies are required to improve signal stability and reduce the sensitivity to external disturbances.

INTRODUCTION
The use of wood is a great alternative to concrete, as it has a lower CO_2 emission prior, during and after construction, with concrete showing more than 200% higher global warming potential than wooden buildings (Adekunle Mofolasayo 2022; Gustavsson et al. 2006). However, rising temperatures pose a major challenge for the wood industry, particularly due to the widespread decline of spruce forests caused by bark beetle infestations (Lisztes-Szabó et al. 2026; Sommerfeld et al. 2021). In this context, European beech, the most abundant broadleaved tree species, is gaining importance because it thrives across a wide range of soil conditions and utilizes light very efficiently (Brunet et al. 2010). However, since wood is a hygroscopic material, it constantly interacts with the surrounding climate, leading to a change in its physical, chemical, mechanical and biological properties (Niemz et al. 2023). As the moisture content (MC) reaches approximately 20%, fungi start to degenerate wood (Arango et al. 2021). Therefore, monitoring the MC of wood is of great importance. Acoustic emission (AE) monitoring has increasingly gained attention in the wood industry. It can be applied not only to monitor wood drying processes (Kowalski et al. 2004) and wood machining or processing operations (Nasir et al. 2019) but also for structural health monitoring (SHM), although the latter has so far mainly been investigated at laboratory scale (Palma and Steiger 2020).
In this work, the measurement of AE during moisture absorption is investigated. Building upon the results of a previous master's thesis (Schneider 2026), the experimental methodology was further optimized in which the challenges identified in the original work were specifically addressed and reduced.

MATERIALS AND METHODS
For this study, *Fagus sylvatica* (beech) with dimensions of 90 * 90 * 45 mm was used. Prior to the experiment, the sample was stored in an oven (103°C) until it reached mass stability (±0.01 g over 24 h). To monitor the change in MC during the experiment, a precision scale of the company Sartorius (Model: Entris II BCE3202-ix) was used to measure the mass of the sample. To determine the dimensional change of the cross section of the sample, a Sony α 6100 digital camera was used.

Additionally, to measure the AE signals, Q-WT MCX structure-borne piezoelectric sensors (QASS GmbH, Wetter, Germany) were used. The sensor was mounted on the radial side of the sample using a threaded socket and a M5 screw. The sampling time for all measurements was set to 60 s and the data was then evaluated using MATLAB (Version R2023b) and Python (Version 3.12.3) (Figure 1). The MC of the sample was calculated according to equation 1.

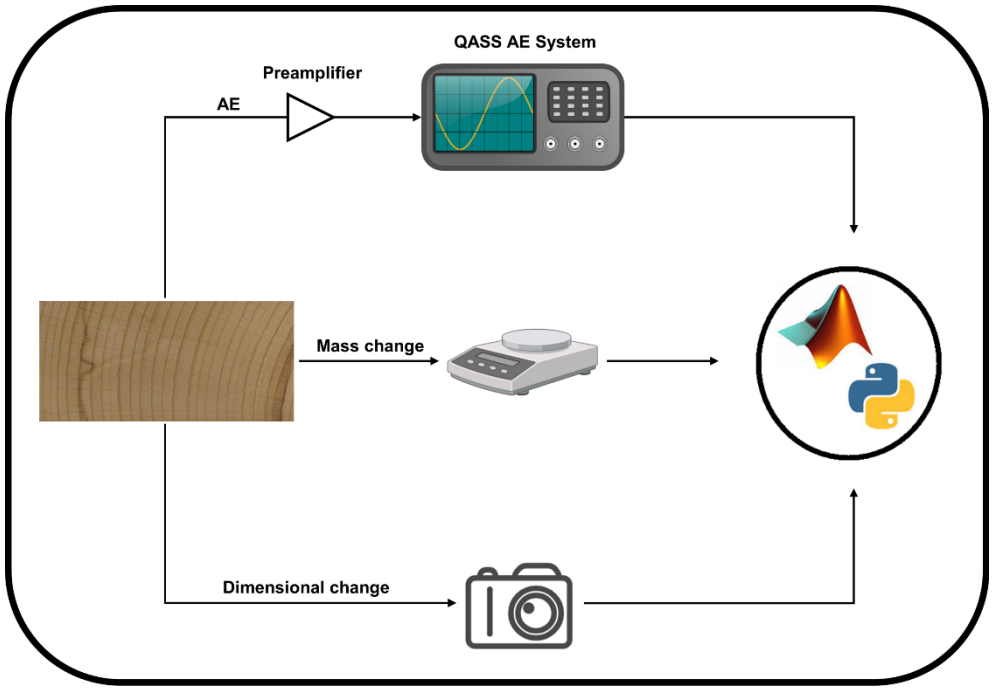

Figure 1: Experimental setup

$$w = \frac{(m_{w-}\, m_0)}{m_0} * 100\ (\%) \quad (1)$$

With:
w… Moisture content (%)
mw… Mass of wood in moist condition (g)
m0… Mass of wood in oven-dry condition (g).

Data acquisition

To separate the sample from the background, a mask was created by modifying the colour values of the images. After distinguishing the edges of the sample from the background, the border coordinates were applied to the original image, making it possible to determine properties such as the sample area, width and thickness (Figure 2).

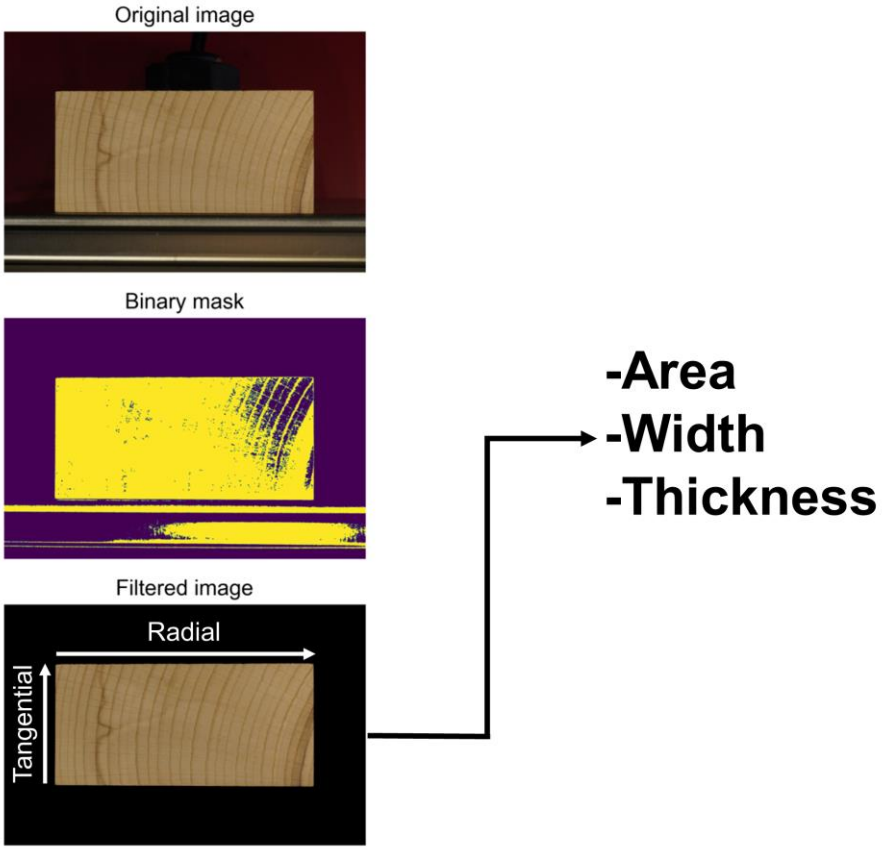

Figure 2: Image processing. Top: original image; middle: modified image for edge detection; bottom: filtered image without background for further analysis

As the generated raw data from the AE measurements exceeded 4 TB, the energy calculations were performed directly by the measurement system (QASS GmbH), which reduces the file size to 2-3 GB. The signal output is calculated as the sum of the amplitudes across all frequencies. According to the manufacturer, the resulting output is dimensionless.

RESULTS AND DISCUSSION

Figure illustrates the change in MC and the samples dimensions. During the experiment, the sample experienced an increase in MC of 3.45%. As expected, the moisture uptake had a rapid increase in the initial phase and gradually transformed into an approximate linear progression after around 20 h into the experiment (Niemz et al. 2023). Regarding the dimensional changes, the radial direction exhibited an increase of 1.15%, while the tangential direction increased by 2.19%. Further, the overall cross section of the sample increased by 3.23%. Similar to MC, the dimensional change had the same trend with a rapid increase at the start of the experiment and a linear progression after around 20 h. A sudden change after approximately 45 h can be observed for all properties. Since this behaviour occurred simultaneously across all measured properties, it is assumed that the change was caused by an external disturbance, such as electrical fluctuations. It is also evident that the data in the tangential direction are highly noisy and remain relatively constant after the occurrence of the fluctuations, despite the continued increase in MC. Therefore, MC and the cross section were selected for further comparisons.

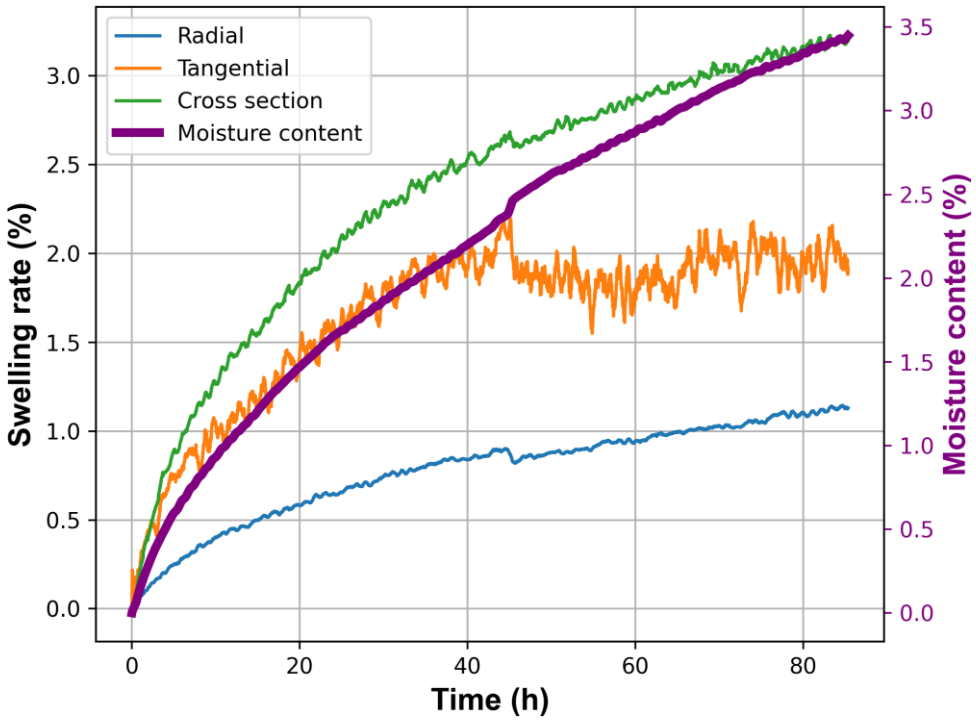

Figure 3: MC and dimensional change of beech

When plotting the mass increase against the increase in cross-sectional area (Figure 4), a very strong correlation can be observed ($r^2 = 0.99$). It is assumed that the previously described disturbance reduced the overall correlation. Due to the occurrence of a disturbance, a correlation approach was selected that accounts for its influence. The breaking point represents the transition point at which the relationship between mass- and cross section increase changes its behaviour.

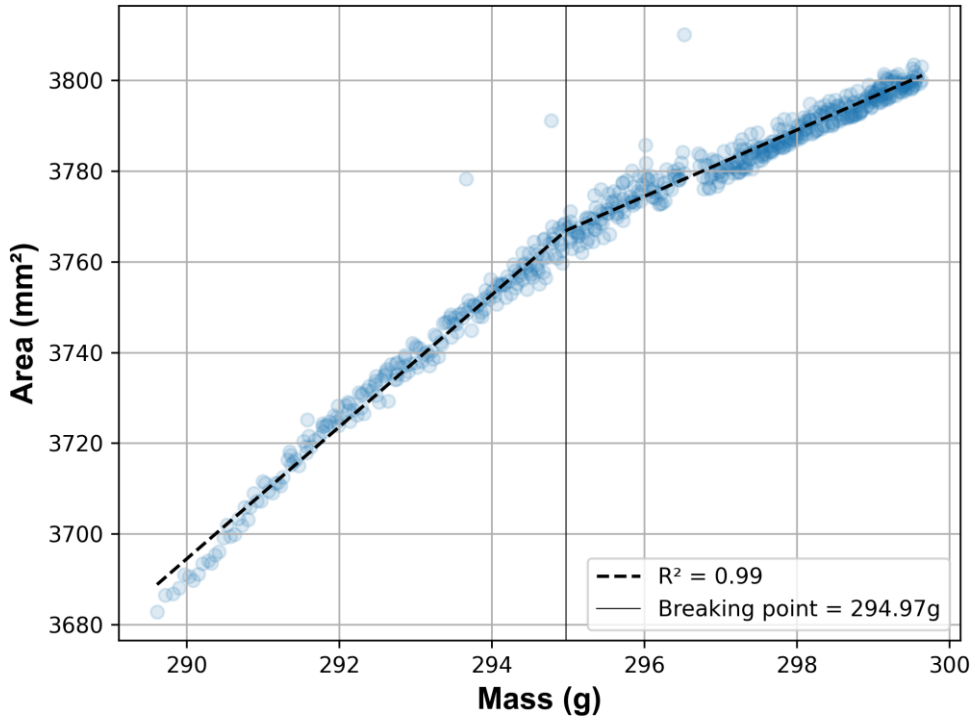

Figure 4: Correlation between change in mass and cross section

For AE Median, a very similar trend can be observed as for the MC and the cross section. Similar to Derbas et al. (2026), these results suggest that increasing MC either leads to crack formation or increases the pre-tension between the sensor and the specimen, both of which are detectable by the sensor. Since piezoelectric sensors and acoustic emission measurements are highly sensitive, the AE Median data are rather noisy.

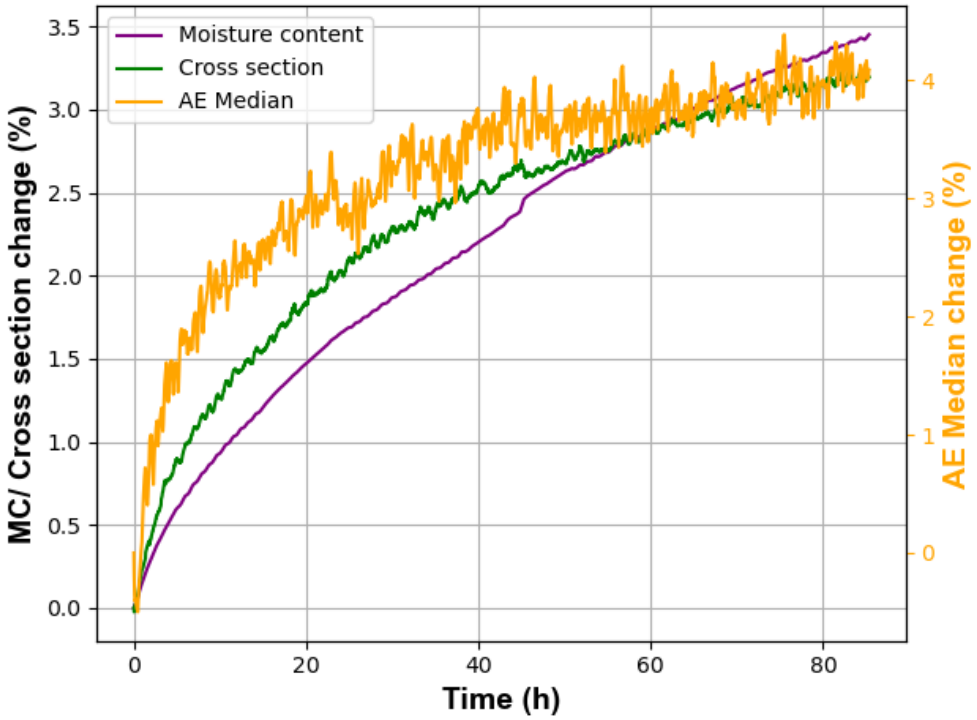

Figure 5: Increase of MC, cross section and AE median over time

Figure 14 illustrates the correlation between MC and AE median. Similar to the correlation between mass and cross section, the correlation was divided into two segments because a distinct breaking point was observed. Although the AE measurement data were relatively noisy, AE median and mass still exhibited a reasonably strong correlation ($r^2 = 0.82$). It is also noticeable that the breaking point between AE median and mass occurs at a different position compared to the correlation between cross section and mass. This difference may be related to the use of separate measurement systems, as the camera and scale were connected to the same computer, whereas the piezoelectric sensor was connected to a different system.

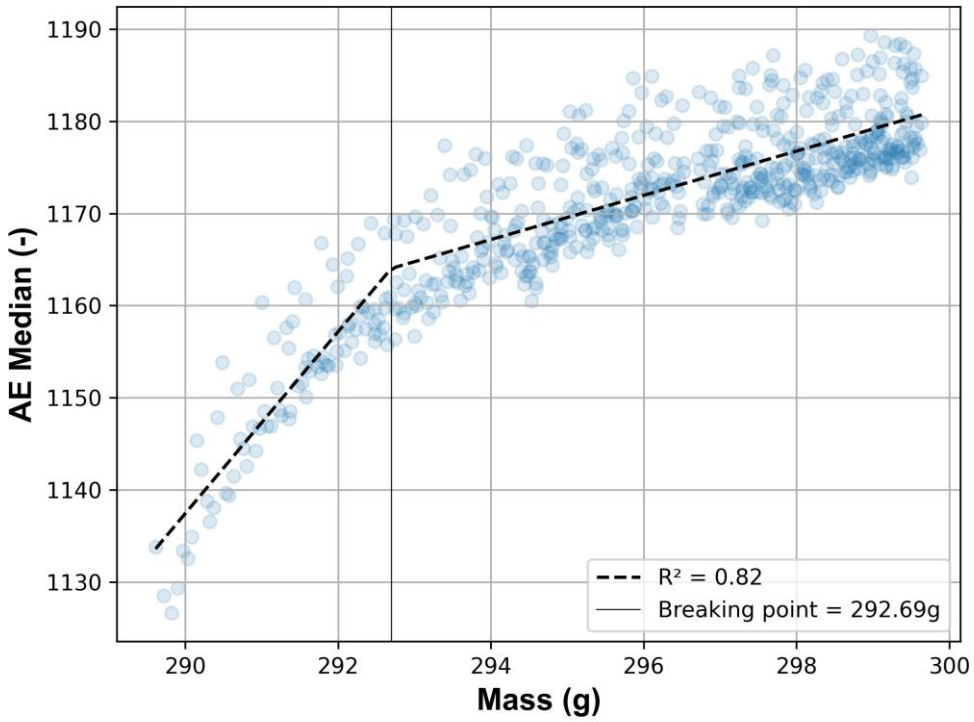

Figure 14: Correlation between change in mass and AE median

To verify fluctuations in RH, it was continuously measured during the experiment (Figure 7). It is noticeable that periodically recurring fluctuations in RH occurred throughout the experiment, which also affected the cross section and mass measurements. This suggests that the observed noise was not solely caused by signal noise, but was also influenced by continuous slight changes in mass and cross section, which may ultimately have affected the AE measurements as well.

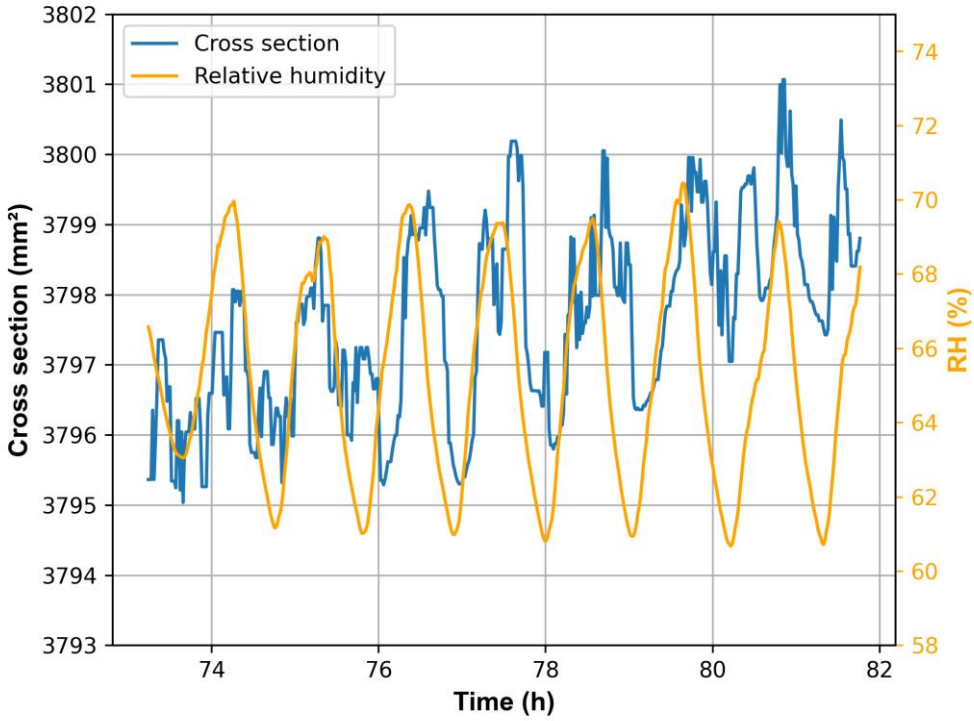

Figure 7: Simultaneously occurring fluctuations of RH measurements and cross section during the experiment

CONCLUSIONS

This study demonstrates the feasibility of AE monitoring for capturing moisture uptake in European beech. A beech sample was dried until mass stability was achieved, indicating a completely dry condition. During the experiment, mass, cross section and AE were continuously measured. Over the course of the experiment, the sample exhibited a total mass increase of 3.45%, a cross section increase of 3.23% and an AE median increase of more than 4%. The results show a clear relationship between increasing MC, dimensional swelling and the AE measurements. Although the AE signals were affected by considerable noise, a meaningful correlation with moisture uptake could still be established. The observed behaviour indicates that AE monitoring could serve as a promising method for monitoring MC changes in wood. However, the results also underline the sensitivity of the measurement setup to external disturbances, such as fluctuations in relative humidity and possible electrical interference. Further research should therefore focus on improving measurement stability, enhancing signal processing and extending the method to different materials, such engineered wood products.

REFERENCES

Adekunle Mofolasayo (2022): A Comparison of Life Cycle Impact of Mass Timber and Concrete in Building Construction. In World Journal of Civil Engineering and Architecture 1 (1), p. 47. DOI: http://doi.org/10.31586/wjcea.2022.449

Arango, Rachel; Lebow, Stan; Glaeser, Jessie A. (2021): Chapter 14: Biodeterioration of wood. Available online at https://research.fs.usda.gov/treesearch/62262

Brunet, Jörg; Fritz, Örjan; Richnau, Gustav (2010): Biodiversity in European beech forests - a review with recommendations for sustainable forest management. In Ecological Bulletins (53), pp. 77–94. Available online at http://www.jstor.org/stable/41442021

Derbas, Mehieddine; Schneider, Alexander; Riegler, Martin (2026): Detecting real-time moisture uptake in spruce samples by acoustic emissions. In Wood Material Science & Engineering, pp. 1–11. DOI: http://doi.org/10.1080/17480272.2026.2637793

Gustavsson, Leif; Pingoud, Kim; Sathre, Roger (2006): Carbon Dioxide Balance of Wood Substitution: Comparing Concrete- and Wood-Framed Buildings. In Mitigation and Adaptation Strategies for Global Change 11 (3), pp. 667–691. DOI: http://doi.org/10.1007/s11027-006-7207-1

Kowalski, Stefan Jan; Moliński, Waldemar; Musielak, Grzegorz (2004): The identification of fracture in dried wood based on theoretical modelling and acoustic emission. In Wood Science and Technology 38 (1), pp. 35–52. DOI: http://doi.org/10.1007/s00226-003-0211-7

Lisztes-Szabó, Zsuzsa; Tóth, Albert; Filep, Anna F.; Szentes, Olivér; László, Elemér; Braun, Mihály (2026): Climate-driven decline of Norway spruce in Central Europe: a threshold crossing in the warming Carpathian Basin. In International Journal of Biometeorology 70 (4), p. 121. DOI: http://doi.org/10.1007/s00484-026-03174-9

Nasir, Vahid; Cool, Julie; Sassani, Farrokh (2019): Acoustic emission monitoring of sawing process: artificial intelligence approach for optimal sensory feature selection. In The International Journal of Advanced Manufacturing Technology 102 (9), pp. 4179–4197. DOI: http://doi.org/10.1007/s00170-019-03526-3

Niemz, Peter; Teischinger, Alfred; Sandberg, Dick (2023): Springer Handbook of Wood Science and Technology. With assistance of Alfred Teischinger, Peter Niemz, Dick Sandberg. 1st ed. Cham (Springer Handbooks).

Palma, Pedro; Steiger, René (2020): Structural health monitoring of timber structures – Review of available methods and case studies. In Construction and Building Materials 248, p. 118528. DOI: http://doi.org/10.1016/j.conbuildmat.2020.118528

Schneider, Alexander (2026): Acoustic emission monitoring of moisture uptake in solid wood. Vienna. Available online at https://permalink.obvsg.at/bok/AC17789575

Sommerfeld, Andreas; Rammer, Werner; Heurich, Marco; Hilmers, Torben; Müller, Jörg; Seidl, Rupert (2021): Do bark beetle outbreaks amplify or dampen future bark beetle disturbances in Central Europe? In J. Ecol. 109 (2), pp. 737–749. DOI: http://doi.org/10.1111/1365-2745.13502

Physical and Mechanical Properties of Hardwood from Invasive Species in an Urban Forest in the City of Rio de Janeiro, Brazil

Alexandre Monteiro de Carvalho[1*], Carolina Nogueira Xavier[1], Andrea Vanini[2]

[1] Department of Forest Products, Forest Institute, Federal Rural University of Rio de Janeiro (UFRRJ), Rodovia BR 465, km 07, Seropédica/RJ, Brazil, 23890-000.
[2] Oswaldo Cruz Foundation (FIOCRUZ) – Fiocruz Atlantic Forest, Avenida Sampaio Correia, s/n, Jacarepaguá, Rio de Janeiro/RJ, Brazil, 22713-560.

E-mail: amcarvalho.ufrrj@gmail.com; ncarolx@gmail.com; vanini.andrea@gmail.com

Keywords: invasive species wood; wood artifacts; small wooden objects; wood waste utilization.

ABSTRACT

Trees of invasive exotic species cause several problems to the global biota. The removal of these trees is important for restoring ecosystem balance. However, after their removal, an impasse arises regarding the destination of the generated material. The lack of knowledge about the characteristics of these woods makes it difficult to indicate the most suitable uses, resulting in low added value for the material. The objective of this study was to evaluate the physical and mechanical properties and indicate possible uses for wood derived from invasive exotic species from the Fiocruz Atlantic Forest Biological Station, Rio de Janeiro, RJ, Brazil. Three species were studied: *Artocarpus heterophyllus* Lamarck (jackfruit tree), *Syzygium cumini* (L.) Skeels (jambolan), and *Clitoria fairchildiana* R.A. Howard (sombreiro). The physical properties were determined according to NBR 7190 (ABNT 1997), and the mechanical properties according to ASTM D143 (ASTM 2014). The basic density of jackfruit wood was classified as low, while jambolan and sombreiro woods were classified as medium density. The anisotropy coefficient of the three analyzed wood species was considered normal. jambolan wood showed the highest mechanical strength among the species studied. All three species exhibited physical properties suitable for use in the furniture industry, while jambolan wood showed adequate mechanical strength for use in civil construction.

INTRODUCTION

According to the definition adopted by the Convention on Biological Diversity (CBD) at the Sixth Conference of the Parties (COP-6 2002), an invasive exotic species is one that, once established in a new habitat, expands its distribution and threatens native biological diversity. Invasive exotic species contribute to landscape homogenization, reduce biodiversity, and undesirably alter ecosystem functioning (Cardinale et al. 2012, Gaertner et al. 2011). They are among the main causes of native species extinction and therefore should be excluded from areas established for ecosystem conservation (Dechoum et al. 2018). Actions aimed at removing invasive exotic species are necessary to restore biodiversity balance. However, the removal of these trees generates another challenge: the destination of the woody material.

According to the guidance manual for the management of invasive exotic species in federal protected areas published by ICMBio (2019), the most common destination for woody material from removed trees is to leave it in the field for decomposition. Alternatives for transforming this material into higher value-added products are therefore necessary. Its use as an alternative raw material for timber purposes is a viable option. However, studies enabling the use of wood from invasive exotic species are still nonexistent, since basic research on biological invasions predominates over management and control studies (Zenni et al. 2016).

Thus, the objective of the present study was to evaluate the physical and mechanical properties of wood from invasive exotic species found at the Fiocruz Atlantic Forest Biological Station and to indicate possible alternatives for their utilization.

MATERIALS AND METHODS

Study Area and Tree Sampling

The trees were located at the Fiocruz Atlantic Forest Campus, belonging to the Oswaldo Cruz Foundation (CFMA/FIOCRUZ), situated within the buffer zone of the Pedra Branca State Park, in the municipality of Rio de Janeiro.

A study conducted on the control of invasive exotic tree species at the Fiocruz Atlantic Forest Biological Station (EFMA) analyzed ecological characteristics of the species, such as dispersal, phenology, regeneration capacity, biotic and abiotic interactions, and population structure. The study also evaluated tree size, spatial distribution, and stem diameter distribution. Based on these analyses, it was possible to observe the greater invasive potential of jackfruit and jambolan, both presenting zoochoric dispersal, followed by sombreiro with autochoric dispersal (FIOTEC - BNDES Mata Atlântica 2016).

Thus, three invasive exotic species were studied in the aforementioned conservation unit: *Syzygium cumini* (L.) Skeels (jambolan), *Artocarpus heterophyllus* Lamarck (jackfruit tree), and *Clitoria fairchildiana* R.A. Howard (sombreiro). For each species, nine trees were selected and georeferenced. Tree removal was carried out in accordance with cutting permit No. 002920, granted by the Municipal Secretariat for Environment and Culture of Rio de Janeiro (SMAC). The distances between trees ranged from 20 to 400 m, 30 to 250 m, and 20 to 500 m for jackfruit, jambolan, and sombreiro, respectively. The selection of trees farther apart from one another aimed to reduce the possibility that the sampled trees originated from the same mother plant.

Studied species

The species *Artocarpus heterophyllus* (Lamk.), popularly known as jackfruit tree, belongs to the family Moraceae and is an exotic fruit species native to India. The jackfruit tree is considered a large-sized tree, reaching more than 10 m in height. It is monoecious and exhibits cauliflory (Figure 1A) (Crane et al. 2002). It is an evergreen species, flowering from October to January (Barbosa 2016). Individuals of this species bear fruit throughout the year, with most fruiting occurring preferentially during the summer months (December–February) (Cunha et al. 2006).

In Indonesia, jackfruit wood is used in shipbuilding and is classified as a strong and durable timber according to the requirements established for vessel construction (Thaib et al. 2019). In India, jackfruit wood is also used in textile dyeing processes (Samanta, Agarwal and Datta, 2009).

The species *Syzygium cumini* (L.) Skeels, whose scientific synonyms include *Eugenia jambolana* Lam. and *Syzygium jambolanum* DC., is popularly known as jambolão, olive tree, purple olive, jambolan, sweet olive, or jambul. It is an exotic fruit species of Indian origin, belonging to the family Myrtaceae, characterized by simple leaves and dark purple fruits (Figure 1B). It has a dense and broad crown and is therefore widely cultivated as an ornamental and shade tree (Lorenzi et al. 2006). The species can reach heights of up to 20 m, flowers between September and November (Lorenzi et al. 2003), and bears fruit from January to May (Vizzotto and Fetter, 2009).

Ramananantoandro et al. (2016) reported that *Syzygium cumini* may serve as an alternative timber species to replace high-value woods in Madagascar; however, further studies on aesthetics and mechanical properties are still required. In India, wood from the genus *Syzygium* is used for construction, furniture, flooring, and poles, with *Syzygium cumini* being the most important species (Wangkhem, Sharma and Sharma, 2020).

The species *Clitoria fairchildiana* R.A. Howard, native to the Amazon region and popularly known as faveira, sombreiro, or palheteira, is a medium- to large-sized tree species belonging to the family Fabaceae and subfamily Papilionoideae. It has a leafy crown and reaches heights between 6 and 12 m (Figure 1C), flowering during the summer and fruiting from May to July, when leaf fall begins. The species produces a large quantity of viable seeds annually, with approximately 1,800 seeds per kilogram (Lorenzi 1992). Studies regarding the wood properties of sombreiro were not found in the literature.

Sombreiro presents invasive potential due to its high seed production, elevated germination capacity, and rapid growth (Santana 2020). Another characteristic that may facilitate the establishment of this species outside its native range is its potential allelopathic effect, as observed in the study conducted by Soares et al. (2002). The same author emphasizes that this species is recommended as a pioneer species in restoration models for degraded areas. However, caution is required because if the phytotoxic effects observed also occur under field conditions, sombreiro may compromise the normal development of the

successional process by inhibiting root development of seeds present in the natural seed bank of the environment.
Figure 1 presents images of the studied tree species, while Tables 1 and 2 show the results of the physical and mechanical properties analyses.

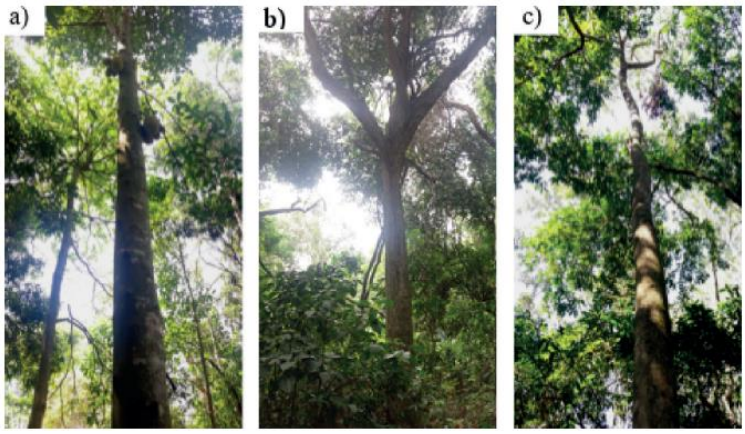

Figure 1: Specimens of jackfruit (A), jambolan (B), and sombreiro (C) from the Fiocruz Atlantic Forest Biological Station used in the study

Jackfruit tree, jambolan, and sombreiro are listed among the invasive species found in federal Conservation Units in Brazil (Sampaio and Schmidt 2014). They are also included in the list of invasive exotic plant species in the Municipality of Rio de Janeiro, according to SMAC Resolution No. 544 of March 28, 2014, issued by the Municipal Secretariat for the Environment.
The jackfruit tree and jambolan are also included in the official list of exotic species in the state of Santa Catarina, established by CONSEMA Resolution No. 8 of September 14, 2012.
In the state of Rio Grande do Sul, jambolan is recognized as an invasive exotic species according to Ordinance No. 79/2013 issued by SEMA.

Primary processing of logs

After tree removal, logs measuring two meters in length were collected from the basal region of the trees (Figure 2A).
The logs were transported to the Federal Rural University of Rio de Janeiro (UFRRJ) for primary processing at the sawmill of the Forestry Institute. The sawing operation was carried out using a vertical band saw (Figure 2B) to obtain boards with a thickness of 3 cm and a central cant with a thickness of 8 cm for the manufacture of test specimens used in the determination of physical and mechanical properties.

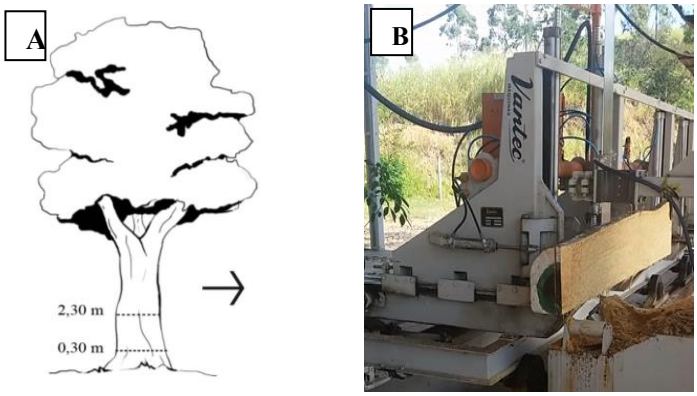

Figure 2: Illustration of log removal from the basal region of the tree (A) and primary processing (B)

Physical properties

Physical properties are directly related to wood quality. Among the main physical properties, density and dimensional stability stand out.

There is a strong relationship between density and several wood characteristics. In general, as density increases, the mechanical strength and natural durability of wood also increase. Conversely, higher density reduces permeability to preservative and finishing solutions (Cardin 2011).

The dimensional stability of wood can be characterized by its shrinkage or swelling when in contact with water and is related to the wood's capacity to absorb hygroscopic moisture (Delucis et al. 2013).

The ratio between tangential and radial shrinkage is called the anisotropy coefficient. This value indicates the dimensional stability of wood; the closer the value is to one, the more dimensionally stable the material will be (Durlo and Marchiori 1992). Greater dimensional stability results in reduced warping and cracking during the drying process. The classification according to the anisotropy coefficient proposed by Durlo and Marchiori (1992) is presented in Table 1.

Table 1: Classification according to the anisotropy coefficient

Anisotropy coefficient	Classification
1.2 to 1.5	Excellent dimensional stability
1.5 to 2.0	Normal dimensional stability
>2.0	Poor dimensional stability

Source: Durlo and Marchiori (1992)

High anisotropy coefficients are characteristics that limit wood applications (Trianoski 2012). Dimensional instability is one of the main causes of resource waste in wood processing, especially in fast-growing species (Manhiça et al. 2013).

To determine the physical properties, nine trees of each species were used. From each log, three boards were removed from different regions in the pith-to-bark direction: near the pith, near the bark, and between these two regions. Three repetitions were performed for each board, totaling 81 test specimens per species. The specimens were prepared based on ASTM D143 (ASTM 2014), with dimensions of 100 × 25 × 25 mm, ensuring that the radial, tangential, and longitudinal directions were properly oriented (Figure 3A).

The test specimens were submerged in water and saturated using a vacuum pump. After saturation, the specimens were weighed on a digital scale with an accuracy of 0.01 g, and their dimensions in the radial, tangential, and axial directions were measured using a digital caliper with an accuracy of 0.01 mm (Figure 3B). For the drying process, the specimens were placed in an oven at a temperature of 103°C ± 2°C, and their dimensions were measured periodically until constant weight was achieved.

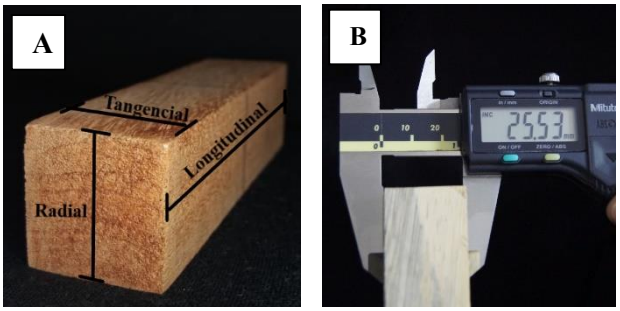

Figure 3: Test specimens with oriented radial, tangential, and longitudinal directions (A), and measurement of the test specimen using a digital caliper (B)

The determination of the physical properties was carried out at the Wood Physical and Mechanical Properties Laboratory, Department of Forest Sciences, Federal University of Lavras (UFLA).

Based on the collected data, calculations were performed to determine radial and tangential shrinkage (Equation 1), volumetric shrinkage (Equation 2), anisotropy coefficient (Equation 3), basic density (Equation 4), and wood moisture content (Equation 5).

$$\varepsilon_i = \frac{(L_{sat} - L_{u(\%)})}{L_{sat}} \text{x}100 \quad (1)$$

Where: ε_i = shrinkage, in which "i" may refer to the radial or tangential direction; Lsat = dimension of the saturated test specimen in the radial or tangential direction; Lu(%) = dimension of the test specimen at the considered moisture content in the radial or tangential direction.

$$\text{C } volumetric = \frac{(Vsat - Vu_{(\%)})}{V_{sat}} \text{x}100 \quad (2)$$

Where: $C_{volumetric}$ = volumetric shrinkage; Vsat = volume of the saturated test specimen; Vu(%) = volume of the test specimen at the considered moisture content.

$$CA = \frac{\varepsilon_T}{\varepsilon_R} \quad (3)$$

Where: CA = anisotropy coefficient; ε_T = tangential shrinkage; ε_R = radial shrinkage.

$$\rho_{basic} = \frac{m_s}{V_{sat}} \quad (4)$$

Where: ρ_{basic} = Specific gravity - density (g/cm³); ms = oven-dry mass (g); V_{sat} = saturated volume (cm³).

$$U_{(\%)} = \frac{(m_i - m_s)}{m_s} \text{x}100 \quad (5)$$

Where: $U_{(\%)}$ = moisture content of the sample (%); mi = initial mass of the wood (g); ms = oven-dry mass (g).

Mechanical properties

Mechanical properties of wood are associated with its elasticity and strength characteristics. Wood strength refers to the material's ability to resist external forces or loads that tend to alter its shape (Rocha et al.1988). Mechanical strength is one of the most important properties of wood as a construction material and is a fundamental factor in the construction of houses, bridges, and other wooden structures (Oliveira 1997).

The determination of mechanical properties is necessary for the proper structural design of wooden constructions such as bridges, sheds, and residential buildings (Dadzie and Amoah 2015).

The determination of mechanical properties was carried out using seven trees of each species. After primary processing, the material was air-dried for six months. Subsequently, test specimens were prepared according to the dimensions specified in Table 2 for each test, following ASTM D143 (ASTM 2014). A total of 84 test specimens were produced for each species and each test. The specimens were obtained from three distinct regions along the pith-to-bark direction: near the pith, near the bark, and between these two regions.

The test specimens were stored under controlled conditions at a temperature of 22°C ± 2°C and relative humidity of 60% ± 5% until they reached an approximate moisture content of 12%.

Four mechanical tests were performed: compression parallel to the grain, shear strength, hardness parallel and perpendicular to the grain, and static bending, with four repetitions for each sampled region.

Table 2: Dimensions of the test specimens for each mechanical test

Test	Dimensions of the test specimen (mm)		
	Length	Width	Thickness
Compression	100	25	25
Shear	63	50	50
Hardness	150	50	50
Static bending	410	25	25

For the tests used to determine the mechanical properties, a universal testing machine equipped with a load cell and different loading rates for each test was used (Table 4). Connected to the universal testing machine was a computer running Tesc software (version 1.13), in which the parameters for each mechanical test were configured according to ASTM D143 (ASTM 2014). The software was also used for data acquisition and for generating reports containing the mechanical property data described in Table 3. The mechanical property tests were carried out at the Wood Physical and Mechanical Properties Laboratory, Department of Forest Sciences, Federal University of Lavras (UFLA).

Table 4: Load cell used and mechanical properties obtained in each test

Test	Load cell (ton)	Speed (mm/min)	Mechanical property
Compression Shear	30	0.076	Compression strength parallel to the grain (f_{c0}) Modulus of elasticity in compression (E_{c0})
Hardness	30	0.60	Shear strength (f_v)
Compression	10	0.60	Hardness strength parallel to the grain (f_{H0}) Hardness strength perpendicular to the grain (f_{H90})
Static bending	10	1.30	Modulus of elasticity (E_M) Modulus of rupture (MOR)

In the Janka hardness test, the steel ball with a diametral area of 1 cm² was embedded six times in each test specimen: twice parallel to the grain (transverse faces) (Figure 4C) and four times perpendicular to the grain (radial and tangential faces) (Figure 4D), at the center of the analyzed surface. For the static bending test, the test specimens were positioned so that the growth rings were parallel to the applied load, using a span length of 36 cm (Figure 4E).

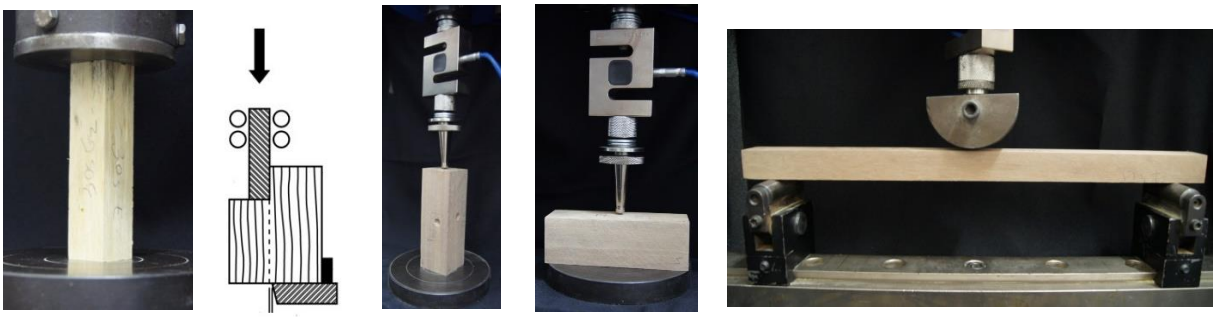

Figure 4: Compression test parallel to the grain performed on sombreiro wood (A), assembly method for the shear test (B), Janka hardness test parallel (C) and perpendicular (D) to the grain on jambolan wood, and static bending test on jambolan wood (E). Source: B - ASTM D143 (2014)

RESULTS AND DISCUSSION

Physical properties

Table 4 presents the physical properties of jackfruit, jambolan, and sombreiro wood.

Table 4: Physical properties of jackfruit, jambolan, and sombreiro wood. Values in parentheses represent coefficients of variation

Physical properties	Jackfruit	Jambolan	Sombreiro
Radial shrinkage (%)	3.33 (32.53)	5.38 (18.67)	4.79 (27.46)
Tangential shrinkage (%)	5.81 (17.43)	8.81 (13.34)	7.18 (17.06)
Volumetric shrinkage (%)	10.24 (15.43)	14.22 (8.93)	14.09 (16.06)
Anisotropy coefficient (%)	1.95 (38.31)	1.74 (29.29)	1.59 (25.54)
Specific gravity-density ($g \cdot cm^{-3}$)	0.466 (8.78)	0.623 (4.23)	0.523 (11.28)

Values in parentheses represent the coefficients of variation.

The radial (3.33%) and tangential (5.81%) shrinkage of jackfruit wood may be compared to that of purpleheart wood (*Peltogyne* spp.), which presents 3.5% radial and 6.5% tangential shrinkage (IPT, 1989). In jambolan wood, radial shrinkage was 5.38% and tangential shrinkage was 8.81%, values close to those reported for cumaru wood (*Dipteryx odorata*), with radial and tangential shrinkage values of 5.94% and 8.4%, respectively (ANPM 2015). The radial (4.79%) and tangential (7.18%) shrinkage of sombreiro wood showed values similar to those of muiracatiara wood (*Astronium lecointei*), whose radial and tangential shrinkage values are 4.6% and 7.6%, respectively (ANPM 2015). Therefore, jackfruit, jambolan, and sombreiro woods showed good performance regarding shrinkage parameters and have potential for furniture manufacturing, since they exhibit shrinkage values compatible with woods recommended for the furniture industry.

Wood shrinkage is an important characteristic for the furniture industry because it indicates the orientation of cracks and gaps that may occur between wooden components, compromising fittings and joints (Lopes et al. 2011).

Regarding the anisotropy coefficient, the three analyzed wood species were classified as presenting normal dimensional stability (1.5–2.0), indicating their suitability for products such as tables, shelves, and cabinets.

The basic density of jackfruit wood was classified as low (≤ 0.50 g/cm³), whereas jambolan and sombreiro woods were classified as medium density (0.50–0.72 g/cm³) according to Coradin (1991).

Mechanical Properties

Table 5 presents the mechanical properties of jackfruit, jambolan, and sombreiro wood.

Table 5: Mechanical properties of jackfruit, jambolan, and sombreiro wood. Values in parentheses represent coefficients of variation

Mechanical properties (MPa)	Jackfruit	Jambolan	Sombreiro
Compressive strength parallel to the grain (fc0) - MPa	44 (13.74)	52 (10.49)	34 (24.26)
Modulus of elasticity in compression (Ec0) - MPa	6015 (14.17)	7035 (12.90)	4966 (29.83)
Shear strength (fv) - MPa	13 (19.44)	14 (12.70)	11 (23.23)
Janka hardness parallel to the grain (fH0) - MPa	58 (15.71)	88 (11.72)	57 (23.35)
Janka hardness perpendicular to the grain (fH90) - MPa	47 (21.56)	76 (14.13)	54 (29.35)
Modulus of elasticity in bending (MOE) - MPa	10685 (12.87)	12698 (17.63)	8297 (27.77)
Modulus of rupture (MOR) - MPa	84 (17.17)	103 (17.36)	77 (32.49)

Values in parentheses represent the coefficients of variation.

According to the strength classes of NBR 7190 (ABNT 1997), jackfruit and sombreiro are classified as C20, while jambolan is classified as C30. Among the three studied species, sombreiro wood showed the lowest mechanical strength values.

The transverse faces of jackfruit and jambolan wood exhibited higher hardness resistance, a behavior similar to that observed in *Eucalyptus benthamii*. This is associated with the arrangement of fibers in the axial direction, since fibers are the main anatomical element responsible for wood support and mechanical resistance (Benin et al. 2017).

Jackfruit wood is mechanically similar to cedrinho (*Erisma uncinatum*), which is recommended for light external and internal structural construction (IPT 2009). The mechanical properties of jambolan wood are suitable for heavy construction as well as light external, internal, and structural uses. Sombreiro wood showed the lowest mechanical resistance among the studied species and is therefore recommended for temporary applications, such as concrete formwork.

Jackfruit, jambolan, and sombreiro woods were classified as medium hardness according to the classification of hardness perpendicular to the grain proposed by the National Association of Hardwood Flooring (ANPM 2015) and show similarity to cedrinho wood (*Erisma uncinatum*).

jambolan wood presents mechanical resistance and density suitable for use as fence posts, since it meets the minimum requirements of NBR 9480 (ABNT 2009), which establishes a minimum static bending strength of 52 MPa and a specific gravity (density) greater than or equal to 0.540 g/cm³ for this application. However, it is important to emphasize the need for studies on natural durability in order to define appropriate preservative treatment for this use.

Potential Uses

The appropriate timber use for each species depends on the properties observed. Thus, after analyzing the physical and mechanical properties of jackfruit, jambolan, and sombreiro wood, it is possible to indicate the most suitable applications according to the studied characteristics. Table 6 presents the potential uses for each species.

Table 6: Potential uses of jackfruit, jambolan, and sombreiro wood

Jackfruit	Jambolan	Sombreiro
Furniture; flooring; window and door frames (joinery).	Furniture; flooring; structural use; fence posts.	Low value-added, temporary use applications, such as concrete formwork.

Based on the physical properties presented by the wood of the three studied species, all of them show potential for use in the furniture industry.

Regarding mechanical properties, the three species exhibit satisfactory hardness for flooring applications; however, specific tests for flooring use are still required.

jambolan wood presents adequate mechanical strength for structural applications and for use as fence posts, although studies on natural durability are necessary to define appropriate preservative treatments.

CONCLUSIONS

It is possible to use the wood from the invasive exotic species found at the Fiocruz Atlantic Forest Biological Station—jackfruit, jambolan, and sombreiro—as raw material for timber purposes. This provides a new alternative use and destination for these species, which must be removed due to the various negative impacts they cause on biodiversity.

The wood of the studied species can be utilized within the mentioned Conservation Unit as fence posts (jambolan), in civil construction (jambolan), in furniture and flooring production (jambolan and jackfruit), and in low-value, temporary applications such as concrete formwork (sombreiro).

ACKNOWLEDGEMENTS

The authors thank the Fiocruz Atlantic Forest team for their support and donation of the material. They also acknowledge the Federal University of Lavras and the Federal Rural University of Rio de Janeiro for the laboratory infrastructure where the experimental tests were carried out. This study was financed in part by the Coordination for the Improvement of Higher Education Personnel – Brazil (CAPES) – Finance Code 001.

REFERENCES

American Society for Testing and Materials. ASTM D-143 (2014) Standard methods of testing small clear specimens of timber, Philadelphia, USA, 32 p.

Barbosa UM (2016). Aspectos ecológicos e influência de *Artocarpus heterophyllus* Lam na estrutura do componente arbóreo de fragmento florestal urbano, Recife, PE. Dissertation (Master's degree in Forest Sciences). Recife, Brazil. 79 f.

Benin CC, Watzlawick LF, Hillig E (2017) Propriedades físicas e mecânicas da madeira de E*ucalyptus benthamii* sob efeito do espaçamento de plantio. Ciência Florestal, Santa Maria, Brazil, 27 (4): 1375-1384.

Brazilian Association of Technical Standards – ABNT-NBR 7190 (1997) – Projeto de Estruturas de Madeira – São Paulo, Brazil. 107p.

Brazilian Association of Technical Standards – ABNT-NBR 9480 (2009) Peças roliças preservadas de eucalipto para construções rurais - Requirement. Rio de Janeiro, Brazil: ABNT; 12 p.

Cardin VS (2011) Ensaios não destrutivos aplicados à madeira serrada e estruturas: técnicas potenciais para uso no Brasil. Dissertation de Master's degree, São Carlos-SP: Federal University of São Carlos.

Cardinale BJ, Duffy JE, Gonzalez A, Hooper DU, Perrings C, Venail P, Narwani A, Mace GM, Tilman D, Wardle DA, Kinzig AP, Daily GC, Loreau M, Grace JB, Larigauderie A, Srivastava DS, Naeem S (2012) Biodiversity loss and its impact on humanity. Nature, 486 (7401): 59-67, 2012.

Conference of the Parties to the Convention on Biological Diversity – COP-6 da CDB. 2002. Report of the Sixth Meeting of the Conference of the Parties of the Convention on Biological Diversity. 341p. Available at: <https://www.cbd.int/doc/meetings/cop/cop-06/official/cop-06-20-en.pdf>.

Coradin VTR (1991) Normas de procedimentos em estudos de anatomia de madeira: I. Angiospermae. II. Gimnospermae. IBAMA, Forest Products Laboratory, Brasília, Brazil.

Crane JH, Balerdi CF, Campbell RJ (2002) The Jackfruit (*Artocarpus heterophyllus* Lam.) in Florida. University of Florida IFAS Extension. Fact Sheet HS-882.

Cunha AA, Vieira MV, Grelle CE (2006) Preliminary observations on habitat, support use and diet in two non-native primates in an urban Atlantic forest fragment: The capuchin monkey (*Cebus* sp.) and the commom marmoset (*Callithrix jacchus*) in the Tijuca forest, Rio de Janeiro. Urban Ecosystems 9: 351-359.

Dadzie PK, Amoah M (2015) Density, some anatomical properties and natural durability of stem and branch wood of two tropical hardwood species for ground applications. European Journal of Wood and Wood Products, 73 (6): 759-773.

Dechoum MDS, Sampaio AB, Ziller SR, Zenni RD (2018) Invasive species and the Global Strategy for Plant Conservation: how close has Brazil come to achieving Target 10? Rodriguésia, 69 (4): 1567-1576.

Delucis RA, Gatto DA, Stangerlin DM, Cademartori PHG, Weinert LC, De Avila Vega R (2013) Segregação e variação radial das propriedades físicas da madeira juvenil e adulta de cedro (*Cedrela fissilis* Vellozo), Scientia Florestalis, 41 (100): 549-556, Piracicaba, Brazil.

Durlo MA, Marchiori JNC (1992) Tecnologia da madeira: retratibilidade. Santa Maria, Brazil: CEPEF/FATEC, 33p. (Série Técnica, 10).

FIOTEC - Foundation for Scientific and Technological Development in Health – BNDES Mata Atlântica (2016) Final Report: Ecological restoration of 344 hectares of the Atlantic Forest using native species; Reactivation of the Campus Fiocruz Atlantic Forest School Nursery (Horto-Escola).

Gaertner M, Richardson DM, Privett SDJ (2011) Effects of alien plants on ecosystem structure and functioning and implications for restoration: insights from three degraded sites in South African fynbos. Environmental management, 48 (1): 57-69.

ICMBio - Chico Mendes Institute for Biodiversity Conservation (2019). Guia de orientação para o manejo de espécies exóticas invasoras em unidades de conservação federais. ICMBio, Brazil.135p.

IPT - Instituto de Pesquisas Tecnológicas do Estado de São Paulo (1989). Fichas de Características das Madeiras Brasileiras. 2a ed, nº 1791. São Paulo, Brazil: IPT, 418p.

IPT - Instituto de Pesquisas Tecnológicas do Estado de São Paulo (2009). Madeira: uso sustentável na construção civil. São Paulo, Brazil: IPT, no 3010, 103p.

Lopes CSD, Nolasco AM, Tomazello Filho M, Dias CTDS, Pansini A (2011) Estudo da massa específica básica e da variação dimensional da madeira de três espécies de eucalipto para a indústria moveleira. Ciência Florestal, Santa Maria, 21 (2): 315-322.

Lorenzi H (1992). Árvores brasileiras: manual de identificação e cultivo de plantas arbóreas nativas do Brasil. Nova Odessa, SP, Brazil: Plantarum.

Lorenzi H et al (2003). Árvores exóticas no Brasil: madeireiras, ornamentais e aromáticas. Nova Odessa, SP, Brazil: Instituto Plantarum.

Lorenzi H, Bacher L, Lacerda M, Sartori S (2006) Frutas brasileiras e exóticas cultivadas. Nova Odessa, SP, Brazil: Instituto Plantarum.

Manhiça AA, Rocha MP, Junior RT (2013). Eficiência operacional no desdobro de Pinus utilizando modelos de corte numa serraria de pequeno porte. Cerne, 19 (2): 339-346.

National Association of Hardwood Flooring Producers – ANPM (2015) Pisos de madeira: características de espécies brasileiras. Piracicaba, Brazil. 184p.

Oliveira JTS (1997) Caracterização da madeira de eucalipto para a construção civil. Doctoral thesis, São Paulo, Brazil: Polytechnic School, University of São Paulo.

Ramananantoandro T, Ramanakoto MF, Rajoelison GL, Randriamboavonjy JC, Rafidimanantsoa HP (2016) Influence of tree species, tree diameter and soil types on wood density and its radial variation in a mid-altitude rainforest in Madagascar. Annals of forest science, 73 (4): 1113-1124.

Rio de Janeiro (2014) Resolução SMAC nº 544 de 28 de março de 2014. Atualiza a lista de Espécies Vegetais Exóticas Invasoras. Rio de Janeiro Municipal Secretariat for the Environment, Rio de Janeiro, Brazil.

Rio Grande do Sul (2013). Portaria no 79/2013. Reconhece a Lista Oficial de Espécies Exóticas Invasoras do Estado do Rio Grande do Sul. State Secretariat for the Environment (Brazil).

Rocha JS, Paula EVCM, Siqueira, ML (1988) Flexão estática em amostras pequenas livres de defeitos. Acta Amazonia, 18 (½): 147- 162.

Samanta, AK, Agarwal P, Datta S (2009) Studies on color interaction parameters and color fastness properties for dyeing of cotton fabrics with binary mixtures of jackfruit wood and other natural dyes. Journal of Natural Fibers, 6 (2): 171-190.

Sampaio AB, Schmidt IB (2014) Espécies exóticas invasoras em Unidades de Conservação federais do Brasil. Biodiversidade Brasileira, 2: 32-49.

Santa Catarina (2012) Resolução nº 8 de 14 de setembro de 2012. Reconhece a Lista Oficial de Espécies Exóticas Invasoras no Estado de Santa Catarina e dá outras providências. State Council for the Environment of Santa Catarina, CONSEMA-SC, Brazil.

Santana CAA (2020) Estrangeiros na cidade do Rio de Janeiro: características e histórias de algumas espécies exóticas presentes no cotidiano carioca (recurso eletrônico). Rio de Janeiro, Brazil, 2020.

Soares GLG, Scalon VR, Pereira TODO, Vieira DDA (2002) Potencial alelopático do extrato aquoso de folhas de algumas leguminosas arbóreas brasileiras. Floresta e Ambiente, Seropédica/RJ, Brazil, 9 (1): 119-126.

Thaib R, Lubis RZ, Rusydi I, Chaliluddin C, Affan JM, Putra DF, Yusrizal Y (2019) The assessment of wood utilization rate at UD. Karya Lomba Shipyard, Aceh Besar, Indonesia. IOP Conference Series: Earth and Environmental Science. 348 (1).

Trianoski R (2012). Avaliação da qualidade da madeira de espécies de Pinus tropicais por meio de métodos convencionais e não destrutivos. Doctoral Thesis, Curitiba: Federal University of Paraná -UFPR, Brazil.

Vizzotto M, Fetter Mr (2009). Jambolão: o poderoso antioxidante. Embrapa, Brasilia, Brazil.

Wangkhem M, Sharma M, Sharma CL (2020) Comparative wood anatomical properties of genus Syzygium (family Myrtaceae) from manipur, India. Indonesian Journal of Forestry Research, 7 (1): 27-42.

Xavier CN, Granato-Souza D, Barbosa ACM, Da Silva JRM (2019) Tropical dendrochronology applied to invasive tree species in the Brazilian Atlantic Forest. Journal of Forestry Research, p. 1-11.

Zenni RD, De Sá Dechoum M, Ziller SR (2016) Dez anos do informe brasileiro sobre espécies exóticas invasoras: avanços, lacunas e direções futuras. Biotemas, Santa Catarina, Brazil, 29, (1): 133-153, 2016.

Comparison of Radial Growth and Mechanical Properties of Sessile and Downy Oaks Grown in a Mixed Forest Stand

Dimitrios Tsalagkas[1*], Sergei Mikhailov[1,2], Marko Stojanović[2], Lenka Foltýnová[2], Petr Horáček[1,2], Kyriaki Giagli[1], Vladimír Gryc[1], Hanuš Vavrčík[1], Luka Krajnc[3]

[1] Mendel University in Brno, Faculty of Forestry and Wood Technology, Department of Wood Science, Zemědělská 3, 61300, Brno, Czech Republic
[2] Global Change Research Institute of the Czech Academy of Sciences, Bělidla 986/4a, 60300, Brno, Czech Republic
[3] Slovenian Forestry Institute, Department of Forest Yield and Silviculture, Večna pot 2, 1000, Ljubljana, Slovenia.

E-mail: dimitrios.tsalagkas@mendelu.cz; mikhailov.s@czechglobe.cz; stojanovic.m@czechglobe.cz; foltynova.l@czechglobe.cz; horacek.p@czechglobe.cz; kyriaki.giagli@mendelu.cz; gryc@mendelu.cz; vavrcik@mendelu.cz; luka.krajnc@gozdis.si

Keywords: tree-ring width; bending strength; *Quercus petraea*; *Quercus pubescens.*

ABSTRACT

Global wood harvest and demand are projected to continue growing to meet the needs of a sustainable forest products market, with a focus on efforts to promote a circular bioeconomy and contribute to climate mitigation. As global demand for wood material is expected to grow, likewise, the research on the contribution of underutilised (lesser-used timber species) oak species as feedstock is widening. Sessile oak (*Quercus petraea* (Matt.) Liebl.) and downy oak (*Quercus pubescens* Willd.) are two native, dominant oak species in a wide variety of biomes and habitats in Central and sub-Mediterranean Europe.

The projected rise in timber supply and wood-based products is responsive not only to changes in production costs and economic growth, but also to factors such as climate change impact and water availability, which have crucial implications on trees' growth and forest productivity and as a consequence, wood quality and properties. The response of temperate forests to climate change is uncertain. Several studies have reported or projected, from forest declines to increased growth and vegetation shifts triggered by drought in tree species across Europe. The more drought-tolerant oak species, such as the mesophilous sessile and heliophilous and thermophilous downy oaks, will likely cope better in the forthcoming years and become competitive in Central Europe compared to other tree species than they do today.

Physical and mechanical properties of wood are crucial indicators for wood quality prediction. The objective of this study was to compare wood density and bending strength values and to assess how oak (sessile and downy) species grown under identical meteorological conditions might differ. The wood samples were taken from a mixed forest in the northwestern part of the Czech Republic, in Karlštejn National Nature Reserve, located in Central Bohemia. The mean age of sessile oak trees was 129.0 (diameter 26.9 ± 0.3 cm; tree height 18.4 ± 1.2 m), and 120.5 (24.1 ± 2.0 cm; tree height 16.6 ± 0.7 m) for downy oak trees. A 40 cm log was cut at breast height level (1.3 m above ground level) along with a 10 cm thick cross-sectional disc for mechanical tests and dendrochronological examination, respectively. From strength and stiffness characteristics, the bending strength (MOR) and modulus of elasticity (MOE) were measured in accordance with the following standards ČSN 490115 and ČSN 490116. The logs were segmented using a circular saw into specialised orthotropic blocks (20 mm × 20 mm × 300 mm) for three-point bending tests and labelled according to the stem radius with a direction from bark to pith. Data for radial growth and dendrochronology analysis were performed using WinDendro 2009 Regular software (Regent Instruments Inc., Canada). Tree-ring increment series were individually cross-dated using PAST4 software. The testing samples were conditioned at 20 ºC and 65% relative humidity to achieve a 12% moisture content in the wood. Statistical analyses and significant differences were conducted in Statistica v.13 (TIBCO Software Inc., USA).

In terms of species differences, similar diameter increment variability was observed between sessile oak (tree-ring width 0.98 ± 0.5 mm) and downy oak (tree-ring width 0.91 ± 0.6 mm). Likewise, latewood percentage (approximately 50%) and mean wood density (~ 770 kg/m³) – with an increasing trend from bark to pith – were not found statistically significant. In contrast, the differences in mean values of bending strength properties (MOR and MOE) were statistically significant. Sessile oak presented higher MOR (79.29 ± 5.94 MPa) and MOE (6.94 ± 0.9 GPa), relevant to downy oak (68.99 ± 2.39 MPa; 5.39 ± 0.5 GPa).

FUNDING
This research was conducted with funding from the Czech Science Foundation (GAČR), Grant No. 24-14324L and the support of the Slovenian Research and Innovation Agency (ARIS), Program and Research Core Funding No. P4-0430 and J4-50130. The European Union additionally supported the work of Lukas Krajnc, contract no. 0005-404, Recovery and Resilience Facility (NOO) and 'NextGenerationEU'.

The final version of this abstract and the full scientific article are scheduled to be published in the Special Issue "12th Hardwood Conference—Sopron" of the journal MDPI Forests, available at the following link:
MDPI Forests Special Issue: 12th Hardwood Conference—Sopron

Session III
-
Surface Coating and Bonding Characteristics of Hardwoods

Surface Bonding Performance of Birch and Birch-Based Hybrid Combinations for Structural Applications: A Preliminary Study

Maik Slabohm[1], Philipp Schlotzhauer[1], Holger Militz[1*]

[1] Wood Biology and Wood Products, Burckhardt Institute, Georg-August University of Göttingen, Büsgenweg 4, 37077 Göttingen, Germany.

E-mail: E-mail: maik.slabohm@uni-goettingen.de; philipp.schlotzhauer@uni-goettingen.de; hmilitz@gwdg.de

Keywords: bonding; birch; load-bearing construction.

ABSTRACT
This study presents preliminary results on the surface bonding performance of birch and birch-based hybrid bonding based on EN 302-1 (2023). For the birch hybrid bonding, spruce, pine, and maple were selected. In addition, each species was bonded to itself to serve as a reference. One melamine-urea-formaldehyde (MUF) and one polyurethane (PUR) adhesive system were applied, based on the supplier's recommendation. Bonding performance was evaluated by determining tensile shear strength (TSS) and wood failure percentage (WF) in dry and wet conditions. Depending on the adhesive system, test condition, and wood species combination, high bonding performance was achieved.

INTRODUCTION
Cross-laminated timber (CLT) and glue-laminated timber (GLT) are well-established engineered wood products widely used in load-bearing applications. Currently, spruce represents the predominant wood species used in such products. However, the use of wood species with superior mechanical properties in the outer layers may provide structural advantages and enable new design approaches in timber construction. In this context, hardwood species such as birch, which are often used in plywood but rarely used in load-bearing structures, show high potential.

Extensive research has been conducted on the bonding performance of European hardwood species, particularly beech. However, due to the specific chemical and anatomical characteristics of the wood species, the results for one species cannot be directly transferred to other species, including birch (Konnerth et al., 2016). The fundamental research conducted by Engelhardt et al. (2023, 2024) and Böger et al. (2024) provides further insights and valuable guidance for the adhesive bonding of birch wood in structural applications.

However, application-oriented research on surface bonding of birch wood and hybrid bonding of birch has not been investigated to date. Therefore, the present study provides initial insights into the bonding behaviour of birch-based hybrid structures.

MATERIALS AND METHODS
Solid wood from birch (*Betula pendula*), maple (*Acer spp.*), Scots pine (*Pinus sylvestris*), and spruce (*Picea abies*) was selected for the bonding. The wood was assembled in both homogeneous configurations (Birch–Birch, Maple–Maple, Pine–Pine, Spruce–Spruce) and hybrid combinations (Birch–Maple, Birch–Pine, Birch–Spruce).

Two adhesives were employed: one polyurethane (PUR) system and one melamine-urea-formaldehyde (MUF) adhesive, both suitable for load-bearing applications. Detailed bonding parameters, including application rate, open assembly time, closed assembly time, pressing time, and pressure, are summarized in Table 1 and were defined according to manufacturer recommendations.

The experimental procedure followed EN 302-1 (2023). For each adhesive–wood combination, two boards with a total bonded area of 400 × 150 × 5 mm were prepared and bonded face-to-face using a

hydraulic press (LAP-40, Gottfried Joos Maschinenfabrik GmbH & Co. KG, Germany). Bond performance was assessed via longitudinal tensile shear strength (TSS) and wood failure percentage (WF). Specimens were tested under two conditioning regimes: (A1) dry condition at 20 °C and 65% RH, and (A2) wet conditions after 96 h water immersion at 20 °C. Tests were conducted on a 10kN Zwick/Roell universal testing machine with the software textXpert® II V3.5 (Zwick/Roell, Ulm, Germany).

Table 1: Bonding parameters

Adhesive	**MUF**	**PUR**
Application rate [g/m²]	260	170
Open assembly time [min]	<5	<5
Closed assembly time [min]	10	1
Pressing time [min]	360	90
Pressure [N/mm²]	0.8	1

RESULTS AND DISCUSSION

The experimental data presented in Figure 1 and Figure 2 demonstrate a consistent reduction in bonding performance under wet conditions compared to dry states, especially for specimens bonded with PUR. A reduction in TSS of wood in wet state compared to dry state is often found in other studies (Konnerth et al., 2016; Ammann et al., 2015). This degradation is driven by two distinct but interrelated mechanisms: the hygroscopic nature of the wood substrate and the moisture sensitivity of the adhesive interface.

On the one hand, it is well-known that the mechanical properties of wood decrease with increasing moisture in the cell wall, and therefore also the shear strength. For example, in the birch–birch configurations bonded with the MUF, the WF remains high even in wet states. In these cases, the reduced TSS is primarily attributed to the mechanical weakening of the wood substrate itself, rather than a failure of the adhesive bond.

On the other hand, moisture can penetrate the bond line, compromising both the cohesive strength of the polymer and the adhesive bond at the interface. For example, in birch–birch assemblies bonded with PUR, wet conditions lead to a significant decrease in WF. This shift indicates a transition toward adhesive-dominated failure, where the water molecules weaken the bonding.

For the homogeneous hardwood bonding (birch-birch, maple-maple), the highest TSS was found, especially in the dry state. The reason for this can be explained by the superior mechanical properties of the used hardwoods compared to the used softwoods. In general, the TSS of a wood bonding increases with increasing density (Konnerth et al., 2016). The hybrid combination (birch-maple) showed comparable performance to the homogeneous hardwoods, which could be due to the comparable mechanical properties of both wood species and their comparable bonding characteristics.

The TSS of the birch-softwood combinations with pine and spruce was lower compared to the TSS of the hardwoods. This could be due to the limited shear strength of the softwoods, which depends on the wood density as stated above. This is further evidenced by the fact that spruce and pine homogeneous configurations have a low TSS, despite maintaining high WF. At the same time, the lowered shear strength of the softwoods resulted in higher WF of the hybrids (birch-spruce, birch-pine), especially for the PUR.

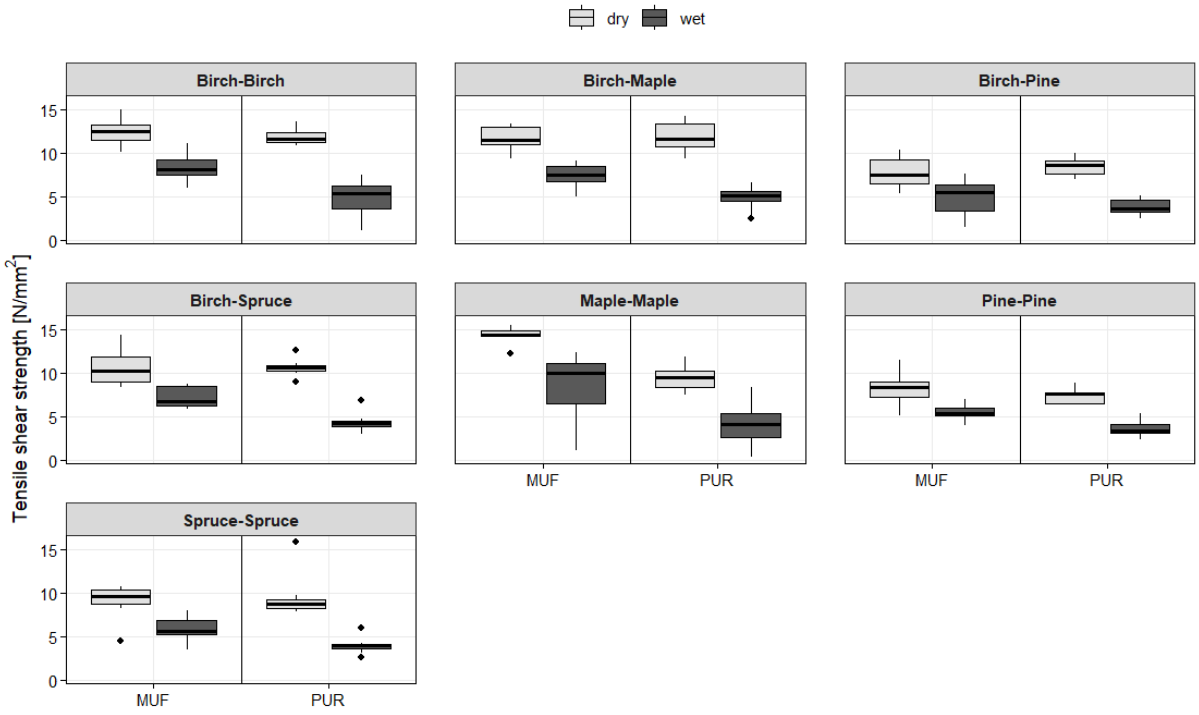

Figure 1: Tensile shear strength (TSS) in dry and wet state of birch wood and birch wood hybrids bonded with MUF and PUR

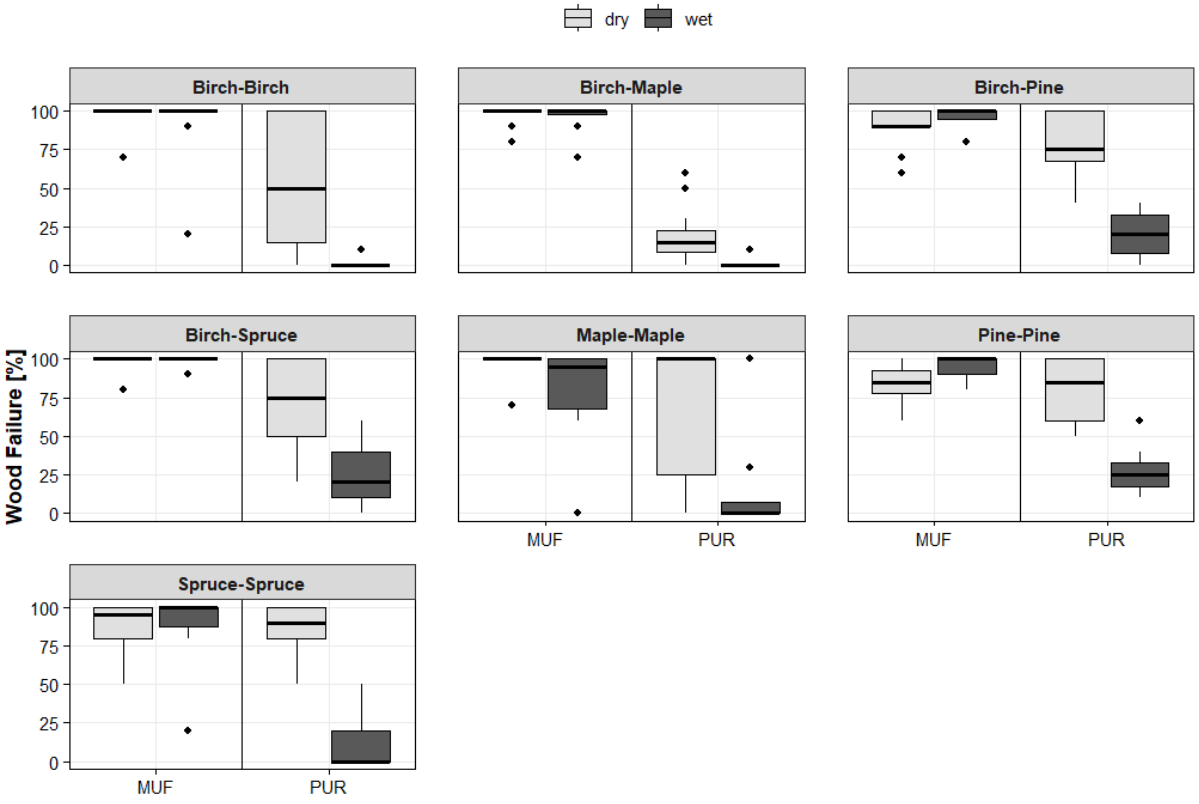

Figure 1: Wood failure percentage (WF) in dry and wet state of birch wood and birch wood hybrids bonded with MUF and PUR

CONCLUSIONS AND OUTLOOK

Based on the preliminary results the following conclusion can be drawn:

- Water treatment led to a decrease in bond strength for all tested combinations, indicating a moisture-induced effect on the wood, the adhesive, and their interaction.
- The tested MUF system exhibited higher moisture resistance compared to the PUR system, shown by higher shear strengths after water treatment and higher wood failure percentages. The simultaneous reduction in TSS and WF signals a failure of the bonding, especially for the PUR-bonded systems.
- The ultimate bonding performance is capped by the mechanical properties of the wood species; dense hardwoods like birch and maple provide higher strength, while softwoods fail at lower thresholds regardless of adhesive quality.

This study is limited to two adhesive systems. Changing process parameters (open assembly time, primer, pressing time, etc.) may improve the bonding, especially for the PUR system. Further investigation on the adhesive penetration and the bonding performance using various adhesive systems is ongoing.

ACKNOWLEDGEMENTS

This study was conducted as part of the *BirkeKleb*t research project (Project No. 10.08.18.7-25.04), funded by the German *ZukunftBau* research initiative.

REFERENCES

Ammann, S., Schlegel, S., Beyer, M., Aehlig, K., Lehmann, M., Jung, H., & Niemz, P. (2016). Quality assessment of glued ash wood for construction engineering. European Journal of Wood and Wood Products, 74(1), 67–74. https://doi.org/10.1007/s00107-015-0981-2

Böger, T., Engelhardt, M., Suh, F. T., Richter, K., & Sánchez-Ferrer, A. (2024). Wood–water interactions of primers to enhance wood–polyurethane bonding performance. Wood Science and Technology, 58, 135–160. https://doi.org/10.1007/s00226-023-01508-z

EN 302-1:2023. Adhesives for load-bearing timber structures—Test methods—Part 1: Determination of longitudinal tensile shear strength. European Committee for Standardization (CEN), Brussels, Belgium.

Engelhardt, M., Böger, T., Gigl, M., Meng, C., Soprunyuk, V., Schranz, W., Richter, K., & Sánchez-Ferrer, A. (2023). Interactions of hydrophilic birch wood (Betula pendula Roth) extractives with adhesives for load-bearing timber structures. International Journal of Adhesion and Adhesives, 125, 103447. https://doi.org/10.1016/j.ijadhadh.2023.103447

Engelhardt, M., Gilg, H. A., Richter, K., & Sánchez-Ferrer, A. (2024). Adhesion-related properties of silver birch (Betula pendula Roth) wood as affected by hydrophilic extraction. Wood Science and Technology, 58(2), 379–402. https://doi.org/10.1007/s00226-023-01526-x

Konnerth, J., Kluge, M., Schweizer, G., Miljković, M., Gindl-Altmutter, W. (2016). Survey of selected adhesive bonding properties of nine European softwood and hardwood species. European Journal of Wood and Wood Products, 74, 809–819. https://doi.org/10.1007/s00107-016-1087-1

Comparative Analysis of Accelerated Weathering and Protective Coating Efficacy on Six Wood Species

M. Pilar Giraldo[1*], Alina Avellaneda[2], Laia Haurie[2], Ana M. Lacasta[2], Vicente Guallart[3], Marcel Vilches-Casals[1]

[1] Centre de Ciència i Tecnologia Forestal de Catalunya (CTFC), Crta. Sant Llorenç de Morunys, km 2, 25280 Solsona, Lleida, Spain
[2] Universitat Politècnica de Catalunya (UPC), Av. Dr. Marañón 44-50, 08028, Barcelona, Spain
[3] Institute for Advanced Architecture of Catalonia (IaaC), C/ Pujades 102, 08005, Barcelona, Spain.

E-mail: pilar.giraldo@ctfc.cat; alina.avellaneda@upc.edu; laia.haurie@upc.edu; ana.lacasta@upc.edu; vicente.guallart@gmail.com; marcel.vilches@ctfc.cat

Keywords: Accelerated weathering; wood degradation; waterborne coating; colorimetry; service durability of wood.

ABSTRACT

This study, conducted within the framework of the ForestED project, evaluates the degradation behaviour of six wood species (Birch, Catalan Chestnut, Galician Chestnut, Beech, Aleppo Pine, and Oak) under accelerated weathering conditions. The investigation aims to assess the influence of external abiotic agents on the degradation mechanisms of wood and to determine the protective efficacy of a commercial surface coating, specifically a waterborne semi-transparent coating, on physical integrity and colour stability. Particular attention is given to the concept of service durability, understood as the capacity of wood products and protection systems to maintain their functional and aesthetic performance under environmental exposure conditions over time. Samples were subjected to four weekly exposure cycles in a QUV/spray tester, simulating solar radiation, condensation, and rain according to the UNE-EN 927-6:2019 standard.

Colorimetric analysis was performed using the CIE Lab* system to quantify variations in luminosity (L*) and global colour difference (ΔE*). Results indicate that the protective finish treatment significantly enhances physical stability, preventing cracking and dimensional deformations across all species, whereas uncoated Aleppo Pine, Beech, Oak, and Galician Chestnut exhibited severe physical degradation. Regarding aesthetic performance, uncoated Birch and Oak showed a tendency toward increased brightness, while the remaining species progressively darkened. The effectiveness of the treatment in mitigating colour change was species-dependent: although it significantly reduced chromatic variation in Birch and Oak, it proved counterproductive for Aleppo Pine and Beech, where coated samples exhibited higher colour variability than uncoated specimens. Furthermore, coating durability also varied according to species, with visible surface degradation appearing in Beech, Oak, and Galician Chestnut after three to four weeks of exposure. These findings highlight the species-dependent behaviour of wood protection systems and the critical role of surface treatments in preserving the dimensional stability and service durability of wood intended for exterior applications.

INTRODUCTION

Spain possesses one of the largest and most diverse forest resources in Europe. Nevertheless, a considerable proportion of these forests has progressively lost economic and productive value due to forest abandonment, landscape homogenization, and the replacement of native species by fast-growing monocultures with higher short-term commercial demand. This process has important implications for biodiversity, forest resilience, and wildfire risk. In this context, the ForestED project was conceived as an applied research initiative focused on evaluating the industrial and constructive potential of several native and underutilized wood species from Galicia and Catalonia, with special emphasis on hardwood broadleaf species capable of diversifying the current timber industry.

The project investigates the potential use of birch (Betula pubescens), Catalan chestnut (Castanea sativa), Galician chestnut (Castanea hybrida), beech (Fagus sylvatica), Aleppo pine and oak (Quercus robur) for industrialized construction systems such as cross-laminated timber (CLT), glued laminated timber (GLT), laminated veneer lumber (LVL), and finger-jointed products. Figure 1 shows the selected harvesting areas for the studied timber species in Galicia and Catalonia. Within this broader framework, understanding the durability-in-service behaviour of these species under exterior exposure conditions becomes essential for their implementation in building envelopes and outdoor applications.

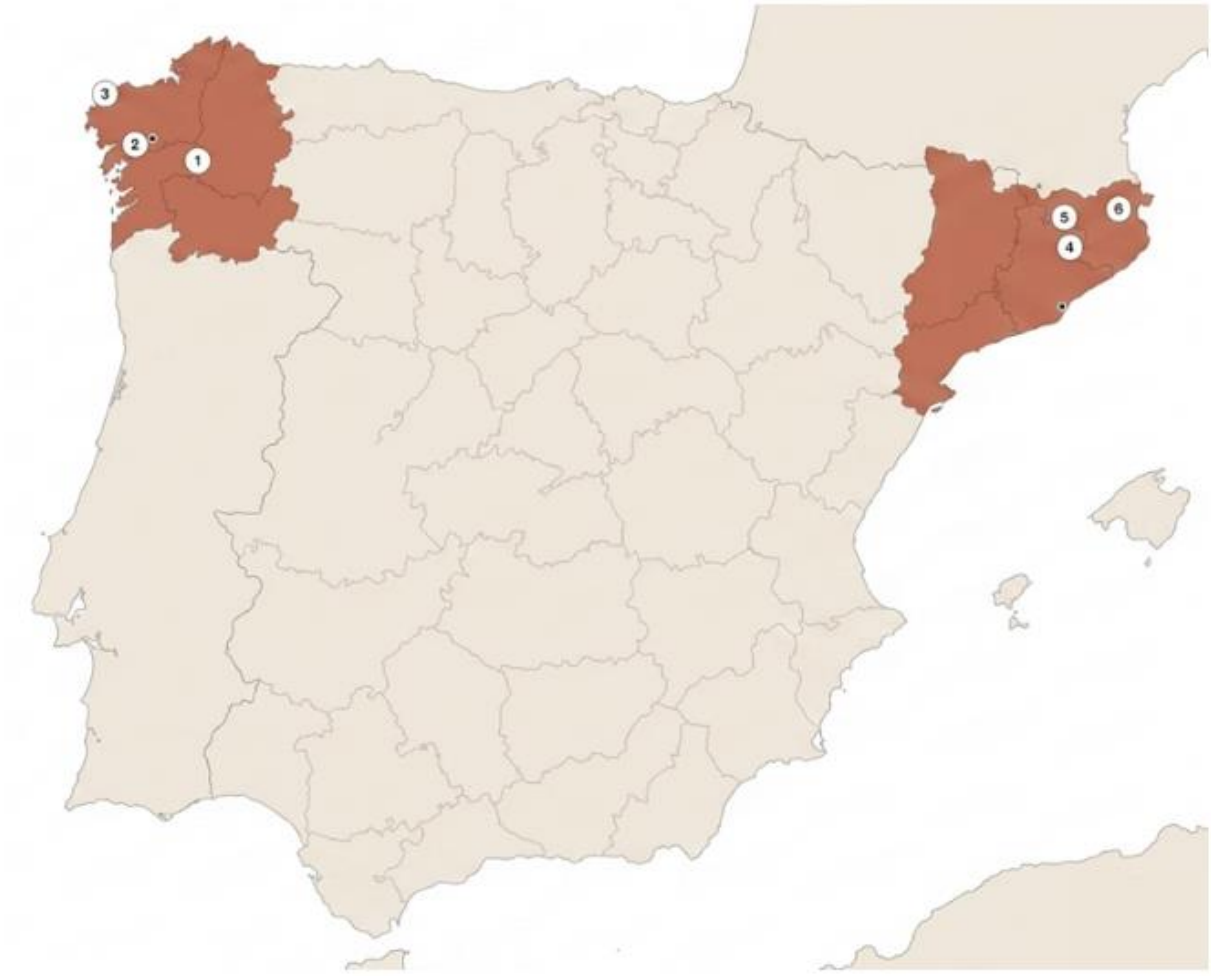

Figure 1: Selected harvesting areas in Galicia and Catalonia for the timber species included in the study: (1) oak, (2) birch, (3) Galician chestnut in Galicia, and (4) Catalan chestnut, (5) beech and (6) Aleppo pine in Catalonia

Wood exposed outdoors undergoes progressive degradation caused by ultraviolet radiation, moisture fluctuations, oxygen, temperature changes, and biological colonization. Photodegradation of lignin, dimensional instability associated with cyclic moisture variations, and surface checking are among the principal deterioration mechanisms affecting service life and aesthetic performance (Özgenç et al., 2022). Surface coatings are commonly used to mitigate these effects by reducing moisture penetration and limiting ultraviolet exposure. However, their effectiveness strongly depends on wood anatomy, density, extractive content, porosity, and dimensional stability.

The present study evaluates the degradation behaviour of six wood species selected within the ForestED project under accelerated weathering conditions, with particular attention to the influence of a commercial waterborne wood coating on physical integrity and colour stability. The study aims to provide comparative information regarding the service durability potential of these species for exterior construction applications.

MATERIALS

The experimental campaign included six wood species in two conditions: uncoated and coated with a commercial waterborne semi-transparent coating for exterior applications. The studied materials comprised five hardwood species and one softwood species, namely oak, birch, beech, European chestnut from Galician and Catalan provenances, and Aleppo pine.

For each species, five uncoated and five coated specimens were prepared. During the four-week accelerated weathering campaign, one specimen from each condition was removed after each weekly cycle for evaluation, while one additional specimen was kept as an unexposed reference sample. All specimens had approximate dimensions of 320 × 80 × 18 mm.

The coding system distinguished uncoated and coated specimens, with the prefix "T" indicating samples treated with the coating finish. The nomenclature employed throughout the study was as follows: B/TB for birch, CC/TCC for Catalan chestnut, CG/TCG for Galician chestnut, F/TF for beech, P/TP for Aleppo pine, and R/TR for oak. Table 1 summarizes the tested wood species, specimen coding, and mean density values.

Table 1: Tested specimens characteristics

Uncoated specimens	Coated specimens	Wood species	Wood type	Mean density (kg/m^3)
B	**TB**	Birch	Hardwood	647.7
CC	**TCC**	Catalan chestnut	Hardwood	599.5
CG	**TCG**	Galician chestnut	Hardwood	659.8
F	**TF**	Beech	Hardwood	729.2
P	**TP**	Aleppo pine	Softwood	629.2
R	**TR**	Oak	Hardwood	826.0

Mean density values were obtained from representative specimens belonging to the same timber batches used for the mechanical tests.

METHODS

Accelerated weathering procedure

The accelerated weathering tests were performed using a QUV/spray accelerated weathering chamber equipped with UVA-340 fluorescent lamps and a water spray system. The experimental procedure followed the UNE-EN 927-6:2019 protocol. Each weekly exposure cycle consisted of an initial 24 h condensation stage, followed by 48 sub cycles of 3 h combining 2.5 h of UV-A 340 radiation and 0.5 h of water spray. Table 2 shows the total exposure time corresponding to each stage of the artificial weathering procedure.

Table 2: Accelerate weathering exposure periods according to UNE-EN 927-6:2019

Standard	Exposure periods throughout the trial [h]			
	Condensation	UV-A	Water spray	Total test time
UNE-EN 927-6:2019	96	480	96	672

Before exposure, all specimens were conditioned for one week in a climatic chamber at 20 ± 2 °C and 65 ± 5% relative humidity. Initial photographs and colour measurements were then recorded. A total of four weekly cycles were completed. According to previous literature, four weeks of artificial weathering under similar conditions may correspond approximately to two years of natural outdoor exposure, depending on climatic conditions and orientation (Aydin et al., 2025; Liu et al., 2019).

After each weekly cycle, the specimens were reconditioned for at least 24 h under climatic chamber conditions prior to visual inspection and colorimetric analysis.

Colorimetric analysis

Colour measurements were performed using a PCE-TCR 200 colorimeter operating in the CIE Lab* colour space. The analysed parameters included: L^*, a^* and b^*. L^* is the lightness, going from 0 (black) to 100 (white), whereas a^* and b^* are the colour coordinates, from green (negative) to red (positive) and from blue (negative) to yellow (positive), respectively. These parameters were used to evaluate changes in surface lightness and chromatic variation associated with the weathering process. The overall colour difference (ΔE_{ab}^*) was calculated according to:

$$\Delta E_{ab}^* = \sqrt{(L^* - L_0^*)^2 + (a^* - a_0^*)^2 + (b^* - b_0^*)^2} \quad (1)$$

where L^*, a^* and b^* are the measured values after aging and L_0^*, a_0^* and b_0^* are the corresponding reference values from non-weathered specimens.

RESULTS AND DISCUSSION

Visual and physical degradation

Visual evaluation revealed clear differences in weathering behaviour depending on wood species and surface condition (coated or uncoated). Progressive changes in colour, surface texture, deformation and cracking became evident throughout the exposure period, with uncoated specimens generally exhibiting more pronounced degradation patterns (Fig. 2).

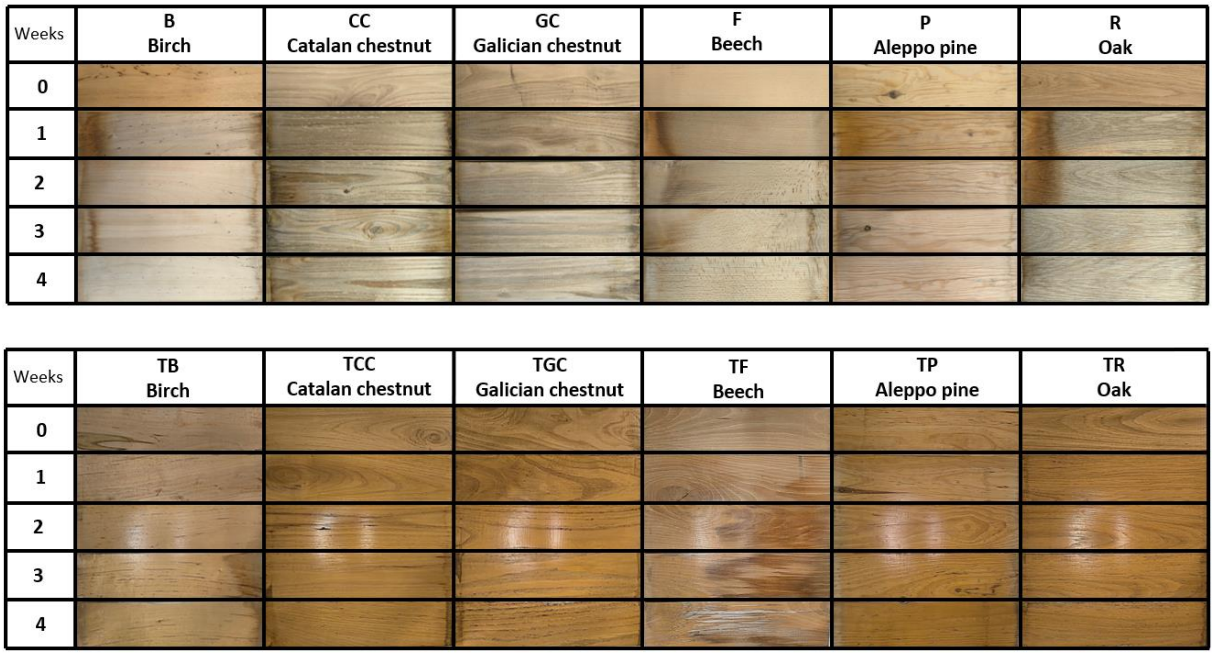

Figure 2: Samples before and after each week of the four-week accelerated weathering test. Top uncoated specimens; bottom coated specimens

Birch and Catalan chestnut showed the highest dimensional stability, with no significant fissures or deformations throughout the test duration. In contrast, Aleppo pine developed surface cracking from the early stages of exposure, while beech, oak, and Galician chestnut presented progressive fissuring and warping that intensified during the later stages of the experiment (Fig. 3).

Figure 3: Surface degradation associated with warping and cracking in uncoated specimens after accelerated weathering exposure. (a) Galician chestnut, week 2. (b) beech, week 3. (c) Aleppo pine, week 3

The comparison between Catalan chestnut (Castanea sativa) and Galician chestnut (Castanea hybrida) revealed noticeable differences in weathering behaviour despite their close taxonomic relationship. Under the accelerated weathering conditions, Galician chestnut showed more pronounced deformation and surface cracking than Catalan chestnut (Fig. 4). Although the specific causes were not analysed in detail in the present study, previous research has shown that factors such as density, anatomical characteristics and moisture-related dimensional movement can significantly influence the weathering and checking behaviour of wood exposed outdoors (Kropat et al., 2020).

Coated specimens generally acquired a more orange-toned appearance with satin gloss characteristics. More importantly, all coated specimens maintained satisfactory dimensional stability and remained free of visible fissures after four weeks of exposure. These results confirm the effectiveness of the waterborne wood coating in limiting moisture-induced stresses and reducing surface degradation mechanisms.

Figure 4: Comparison of the degradation observed between Galician chestnut (Castanea hybrida) specimens (front) and Catalan chestnut (Castanea sativa) specimens (back) after accelerated weathering exposure

Nevertheless, coating durability varied among species throughout the exposure period. While the coating remained comparatively stable on birch, Catalan chestnut, and Aleppo pine, visible surface degradation appeared after three weeks in beech and oak, and after four weeks in Galician chestnut. These differences may be associated with substrate-dependent factors such as adhesion performance, extractive migration, moisture-induced dimensional movements, or other species-specific interactions occurring during repeated wetting and drying cycles. Similar tendencies have been reported in previous studies, which indicate that coating performance is strongly influenced by wood anatomy and moisture-related behaviour (Petrillo et al., 2019).

Colourimetry results

Luminosity evolution (L*)

Colorimetric analysis confirmed the visual changes observed during the accelerated weathering exposure. As shown in Figure 5, uncoated birch and oak exhibited an increase in luminosity (L*),

indicating progressive surface whitening. In contrast, Catalan chestnut, Galician chestnut, beech, and Aleppo pine showed decreasing L* values, corresponding to progressive darkening during exposure.

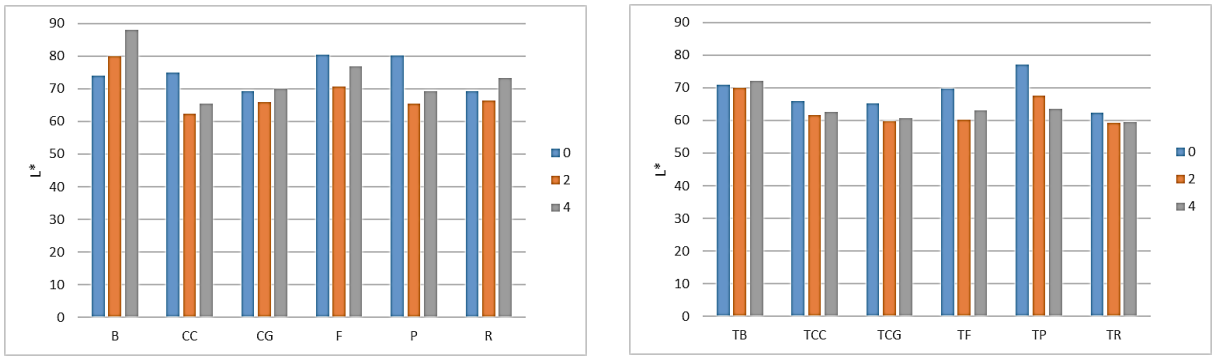

Figure 5: Evolution of luminosity (L*) before and after 2 and 4 weeks of accelerated weathering exposure. Left: uncoated specimens; right: surface-coated specimens treated with the waterborne wood finish. Higher L* values indicate surface lightening, while decreasing values correspond to progressive darkening

For coated specimens, the general tendency was also toward reduced luminosity, although the magnitude of the variation differed among species. This behaviour may be associated with coating ageing, oxidation phenomena, and surface modifications induced by weathering exposure.

The increase in luminosity observed in uncoated birch and oak is consistent with lignin photodegradation mechanisms commonly reported for weathered wood surfaces. Ultraviolet radiation promotes the degradation of lignin-rich surface layers, generating lighter cellulose-rich surfaces after leaching of degradation products (Kropat et al., 2020).

Global Colour Difference (ΔE*)

The evolution of ΔE* revealed that the coating did not provide uniform chromatic stabilization across all studied species (Fig. 6). Significant differences were observed depending on the wood substrate and exposure time.

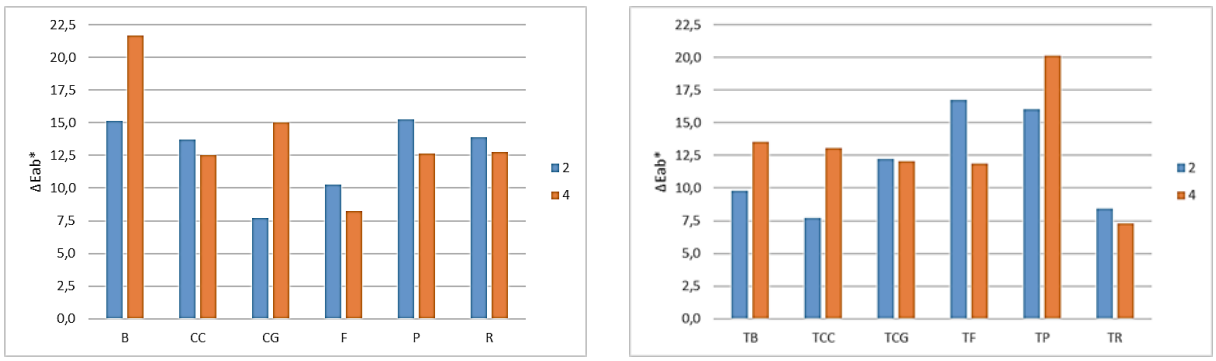

Figure 6: Evolution of the global colour difference (ΔE*) after 2 and 4 weeks of accelerated weathering exposure. Left: uncoated specimens; right: surface-coated specimens treated with the waterborne wood finish. Higher ΔE* values indicate greater chromatic variation with respect to the initial unweathered condition

Birch and oak showed the most favourable response to the coating treatment. Uncoated birch reached ΔE* values above 20 after four weeks of exposure, whereas coated specimens remained close to 13. Similarly, coated oak exhibited lower colour variation than uncoated samples throughout the exposure period.

In contrast, coated Aleppo pine and beech exhibited greater chromatic variation than their uncoated counterparts. However, despite the high ΔE* values observed for coated Aleppo pine, the visual appearance of the specimens suggested relatively homogeneous colour changes rather than severe surface degradation. A similar tendency was observed for beech, where the coating appeared to undergo ageing-related optical modifications during exposure. These observations indicate that high ΔE* values do not necessarily correspond to pronounced physical deterioration but may also reflect uniform chromatic changes associated with coating ageing and surface oxidation phenomena.

Galician chestnut exhibited a marked increase in ΔE* between the second and fourth weeks under uncoated conditions, whereas the coated specimens showed lower colour variation, indicating a partial stabilizing effect of the protective treatment.

Overall, the results indicate that chromatic stability depends not only on the protective coating itself, but also on substrate–coating interactions. Factors such as wood anatomy, extractive content, porosity, permeability, and dimensional stability may significantly influence coating performance and weathering behaviour. Previous studies have also highlighted the important influence of wood extractives on the photo discoloration processes of weathered wood surfaces (Arpaci et al., 2021). However, further research would be necessary to better understand the specific mechanisms governing the different chromatic responses observed among the studied species.

CONCLUSIONS

This study evaluated the durability-in-service behaviour of six native wood species under accelerated weathering conditions following UNE-EN 927-6:2019, comparing uncoated and waterborne wood coating specimens.

The main conclusions are as follows:

The waterborne surface coating improved the physical and dimensional stability of all evaluated species, reducing the occurrence of fissures and deformation during the exposure period.
Uncoated Aleppo pine, beech and Galician chestnut exhibited the most pronounced physical degradation, particularly in terms of warping and surface cracking. In contrast, birch and Catalan chestnut showed comparatively better dimensional stability under the applied weathering conditions.
Significant differences were observed between Catalan chestnut (Castanea sativa) and Galician chestnut (Castanea hybrida), despite their close taxonomic relationship. Galician chestnut exhibited greater deformation and cracking during exposure, suggesting differences in weathering behaviour associated with material characteristics and botanical origin.
Chromatic evolution was strongly species-dependent. Uncoated birch and oak exhibited increased luminosity associated with surface whitening, whereas the remaining species generally showed progressive darkening during exposure.
The coating did not provide uniform chromatic stabilization across all species. It effectively reduced colour variation in birch and oak, while higher ΔE* values were observed in coated Aleppo pine and beech. However, these changes appeared to be associated mainly with homogeneous optical modifications and coating ageing rather than severe visual surface degradation.
The results demonstrate the importance of considering species-specific behaviour when selecting protective systems for exterior wood applications. The study also highlights the usefulness of accelerated weathering methodologies for assessing service durability within the context of developing diversified forest-based value chains and promoting the use of underutilized hardwood species in construction.

ACKNOWLEDGMENTS

The authors acknowledge the support of the ForestED project, led by the Institute for Advanced Architecture of Catalonia in partnership with the Forest Science and Technology Centre of Catalonia, the Forestry Consortium of Catalonia, and the Galician Forestry Association. The authors also gratefully acknowledge the financial support provided by the Fundación Biodiversidad for the development of the ForestED project within the framework of the ecological transition actions of the Recovery, Transformation and Resilience Plan, funded by the European Union – NextGenerationEU.

REFERENCES

Aydın, M. A., Can, A., Tomak, E. D., & Ermeydan, M. A. (2025). Weathering of wood under indoor and outdoor environmental conditions. Coloration Technology, 142, 456–473. https://doi.org/10.1111/cote.12833

Arpaci, S. S., Tomak, E. D., Ermeydan, M. A., & Yildirim, I. (2021). Natural weathering of sixteen wood species: Changes on surface properties. Polymer Degradation and Stability, 183, 109415. https://doi.org/10.1016/j.polymdegradstab.2020.109415

Kropat, M., Hubbe, M. A., & Laleicke, F. (2020). Natural, accelerated, and simulated weathering of wood: A review. BioResources, 15(4), 9998–10082. https://doi.org/10.15376/biores.15.4.Kropat

Liu, R., Zhu, J., Lu, Y., Gong, M., & Zhou, J. (2019). Comparison on the aging of woods exposed to natural sunlight and artificial xenon light. Polymers, 11(4), 709. https://doi.org/10.3390/polym11040709

Özgenç, Ö., Bilici, E., Durmaz, S., Söğütlü, C., & Emik, S. (2022). Enhancing weathering durability of pre-protected and unprotected wood by using bark extracts as natural UV absorbers in waterborne acrylic coating. Journal of Coatings Technology and Research, 19(1), 303–321. https://doi.org/10.1007/s11998-021-00528-3

Petrillo, M., Sandak, J., Grossi, P., & Sandak, A. (2019). Chemical and appearance changes of wood due to artificial weathering–dose–response model. Journal of Near Infrared Spectroscopy, 27(1), 26–37. https://doi.org/10.1177/0967033518825364

UNE-EN 927-6:2019. Paints and varnishes. Coating materials and coating systems for exterior wood. Part 6: Exposure of wood coatings to artificial weathering using fluorescent UV lamps and water. Asociación Española de Normalización (UNE), Madrid, Spain.

Hardwood Lignin for Phenolic Resins: More Reactive Than its Reputation

Peter Bliem[1,2], Hendrikus W. G. van Herwijnen[1,2*]

[1] Wood K plus – Competence Center of Wood Composites and Wood Chemistry, Kompetenzzentrum Holz GmbH, Linz, Austria
[2] BOKU University, Institute of Wood Technology and Renewable Materials, Department of Natural Sciences and Sustainable Resources, Tulln an der Donau, Austria.

E-mail: p.bliem@wood-kplus.at; e.herwijnen@wood-kplus.at

Keywords: hardwood lignin, lignophenolic resins, plywood, CBC pulping.

ABSTRACT

Lignin is the most abundant renewable aromatic polymer in lignocellulosic biomass and represents a promising bio-based substitute for fossil-based phenol in phenol-formaldehyde (PF) adhesives. While most research has focused on softwood lignin due to its higher theoretical reactivity, hardwood lignin remains an abundant but underutilized resource. Recent advances in lignin isolation technologies, such as Continuous Batch Cooking (CBC), enable the recovery of lignin with improved structural integrity and reactivity. In this study, hardwood lignin obtained from an industrial CBC pulping process was investigated as a renewable raw material for lignin-phenol-formaldehyde (LPF) resins for plywood applications. The CBC-derived hardwood lignin exhibited lower molecular weight, narrower molecular weight distribution, and improved accessibility of reactive hydroxyl groups compared to conventional softwood Kraft lignin. LPF resins were synthesised with phenol substitution levels of 30 wt.% and 50 wt.% and characterised regarding viscosity, solids content, pH, free formaldehyde content, curing behaviour (B-time), and bonding strength development (ABES).

The results showed that hardwood lignin-based LPF resins had suitable processing properties and significantly shorter B-times than softwood lignin-based formulations, indicating faster curing behaviour. In birch plywood bonding tests according to the plywood standard EN 314, all formulations with 30 wt.% phenol substitution fulfilled the requirements for bonding classes 1 and 2 and showed promising performance for bonding class 3. At 50 wt.% substitution, the bonding performance decreased but still met the requirements for bonding classes 1 and 2. Overall, the findings demonstrate that CBC-derived hardwood lignin can be directly utilised in high-performance wood adhesives and represents a promising sustainable alternative for reducing fossil-based phenol in plywood adhesive systems.

INTRODUCTION

Lignin is a renewable, wood-derived biopolymer with a phenolic structure and therefore represents a promising sustainable alternative to fossil-based phenol in phenol-formaldehyde (PF) adhesives used in wood-based panels and engineered wood products (Sarika et al., 2020). Partial substitution of phenol by lignin in lignin-phenol-formaldehyde (LPF) resins has been extensively investigated, with several studies demonstrating the technical feasibility of such systems in plywood and other structural wood applications (Ghorbani et al., 2018; Mansouri et al., 2007; Solt et al., 2019). However, the industrial use of lignin in adhesive formulations remains limited due to its structural heterogeneity, variable reactivity, and the often insufficient curing performance of lignin-based resins (Jääskeläinen et al., 2017; Karthäuser et al., 2021; Lourençon et al., 2020).

Among the different lignin sources, softwood Kraft lignins have been more widely studied because of their higher proportion of guaiacyl (G) and p-hydroxyphenyl (H) units, which provide more reactive ortho positions for formaldehyde condensation reactions (Kalami et al., 2018). In contrast, hardwood lignins contain a higher proportion of syringyl (S) units (indicative values in Figure 1), whose additional methoxyl groups reduce the number of reactive sites on the phenolic rings and may limit their direct use in PF resin synthesis (Kalami et al., 2018).

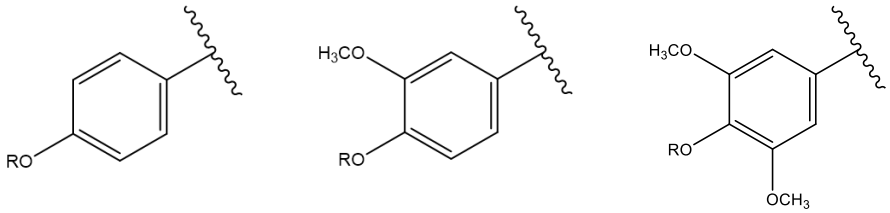

	p-hydroxyphenyl (H)	Guaiacyl (G)	Syringyl (S)
Softwood:	~0-10%	~90-100%	trace
Hardwood:	~0-5%	~25-50%	~40-65%

Figure 1: Composition of lignin, values shown are indicative estimated averages based on experience and internal discussions

The pulping process strongly influences lignin structure and therefore its suitability for adhesive applications. Conventional Kraft lignins are typically produced in continuous Kamyr digesters under harsh conditions, promoting depolymerisation and condensation reactions that reduce lignin reactivity (Jardim et al., 2020; Karthäuser et al., 2021). In contrast, the Continuous Batch Cooking (CBC) process applies more controlled delignification conditions, including optimized alkali concentration, high initial hydrosulfide concentration, reduced dissolved lignin concentration in later stages, and lower temperature profiles (Nadányi et al., 2024; Sixta et al., 2006b; Wizani et al., 2000). These process conditions minimize lignin degradation and condensation, resulting in more homogeneous lignin fractions with improved accessibility of reactive functional groups (Sixta et al., 2006a). Especially for hardwood feedstocks, CBC-derived lignin may offer significant advantages for adhesive synthesis.
This study investigates hardwood lignin from an industrial CBC process as a partial phenol substitute in LPF resins for plywood applications. Its performance was compared with conventional softwood Kraft lignin-based LPF resins at phenol substitution levels of 30 wt.% and 50 wt.%. The resins were characterised for viscosity, free formaldehyde content, and curing behaviour, while bonding performance was evaluated in plywood according to EN 314. The results highlight the potential of CBC-derived hardwood lignin as a sustainable raw material for high-performance wood adhesives.

MATERIALS AND METHODS

Lignin raw materials

Hardwood (HW) lignin was supplied by a central European pulp mill and recovered from black liquor generated in an industrial Continuous Batch Cooking (CBC) process. The feedstock comprised over ten hardwood species in varying proportions. Owing to the CBC conditions, the lignin showed relatively low molecular weight, narrow molecular weight distribution, and low condensation. Softwood (SW) lignin was precipitated from black liquor at laboratory scale using the LignoBoost® process. The black liquor originated from a northern European pulp mill using softwood feedstock and conventional Kraft pulping in a Kamyr digester. Both lignins were air-dried and oven-dried at 60°C for 96 h before resin synthesis. The molecular weight distribution of the lignins was analysed by gel permeation chromatography (GPC), while hydroxyl group contents were determined by ^{31}P NMR spectroscopy followed the methodology described in the literature (Korntner et al., 2015). Methoxyl group contents were measured by GC-MS according to established methods (Sumerskii et al., 2017).

LPF resin synthesis and characterisation

Lignin-phenol-formaldehyde (LPF) resins were synthesised using hardwood (HW) and softwood (SW) lignins at phenol substitution levels of 30 wt.% and 50 wt.% based on the total phenolic component (L/(L+P)). Formulations were slightly adjusted according to lignin content, while the formaldehyde-to-phenol molar ratio (F/P) was kept constant at 2.4. Sodium hydroxide was added in two stages to control condensation. Synthesis consisted of two condensation stages. In the first stage, phenol was heated and mixed with the initial sodium hydroxide portion, followed by lignin powder and formaldehyde addition. Condensation continued until an intermediate viscosity of ~400 mPa·s (25°C, 100 s^{-1}) was reached. In the second stage, deionised water and the remaining sodium hydroxide were added, and condensation

proceeded to a final viscosity of ~500 mPa·s (25°C, 100 s^{-1}). The resins were then cooled to room temperature and stored at +7°C for further analysis.
The synthesised LPF resins were characterised with respect to their suitability for wood bonding applications. Solid content was determined according to ÖNORM EN ISO 3251 (2019)by drying the resin at 135°C to constant mass. Viscosity was measured immediately after synthesis and after storage at +7°C using a rheometer at 25°C and a shear rate of 100 s^{-1} to assess storage stability and further condensation. The pH value was measured on diluted resin samples (50:50 with deionised water) according to ÖNORM EN ISO 8975 (1995). The free formaldehyde content of the resins was determined using the hydroxylamine hydrochloride method according to ÖNORM EN ISO 11402 (2004). B-time, representing the time required to reach the B-stage during curing, was measured at 130°C according to ÖNORM EN ISO 8987 (2005) to assess curing speed and lignin reactivity. Bonding strength development during hot pressing was evaluated using an Automated Bonding Evaluation System (ABES) following the ASTM D7998-15 (2015) standard. Beech veneers were bonded at a pressing temperature of 120°C under a pressure of 1.6 MPa with varying pressing times between 0.5 and 20 min. The tensile shear strength of the bonded overlap area was measured immediately after pressing.

Plywood production and testing

To improve processability for plywood production, LPF resins were modified with wheat flour and deionised water in a 100:10:10 ratio (wet resin:wheat flour:water). Such additives improve viscosity, flow behaviour, and cost efficiency (Aydin et al., 2017; Dunky & Niemz, 2002).
Nine-layer plywood panels were manufactured using 1.5 mm rotary-cut birch (*Betula*) veneers (500 × 500 mm^2). Prior to bonding, the veneers were conditioned at approximately 23°C and 40% relative humidity to an equilibrium moisture content of 7–8%. Modified LPF resins were applied to one veneer side at 155 g/m^2. Panels were hot pressed at 135°C and 1.6 MPa for 22 min, then conditioned at 20°C and 65% relative humidity before testing.
Lap-joint specimens were prepared according to ÖNORM EN 314-1 (2005). The bonding performance was evaluated separately for the core and face layers of the plywood. Prior to tensile shear testing, specimens were subjected to different pre-treatments according to ÖNORM EN 314-1 (2005) and ÖNORM EN 314-2 (1997) to simulate different service conditions:

- Bonding class 1: 24 h water storage at 20°C (interior use)
- Bonding class 2: 6 h boiling water followed by 1 h cooling in water at 20°C (covered exterior use)
- Bonding class 3: 4 h boiling water, drying in a ventilated oven at 60 ± 3°C for 16 to 20 hours, 4 h boiling water followed by 1 h cooling in water at 20°C (exterior use)

Tensile shear strength was measured using a universal testing machine at a constant crosshead speed of 1 mm/min. In addition to tensile shear strength, wood failure content was visually assessed according to the plywood standard.

RESULTS AND DISCUSSION

Lignin characterisation

The molecular weight distribution analysis revealed clear structural differences between hardwood (HW) and softwood (SW) lignins. The HW lignin obtained from the Continuous Batch Cooking (CBC) process exhibited a lower number-average molecular weight (Mn = 400 Da) and weight-average molecular weight (Mw = 1375 Da) compared to the SW lignin (Mn = 685 Da; Mw = 3736 Da), as well as a lower dispersity (Đ = 3.4 vs. 5.5). These results indicate a more homogeneous and less condensed lignin structure for the CBC-derived HW lignin.
The ^{31}P NMR analysis showed similar total hydroxyl group contents for both lignins, with 5.69 mmol/g for HW and 5.82 mmol/g for SW lignin. However, structural differences in aromatic unit composition were observed. HW lignin contained a higher proportion of syringyl and condensed units, whereas SW lignin contained more guaiacyl and catechol units. In addition, the methoxyl group content was higher in HW lignin (5.98 mmol/g) than in SW lignin (4.17 mmol/g), confirming the typical syringyl-rich structure of hardwood lignin.
Based on these structural features, SW lignin would be expected to show higher reactivity toward formaldehyde due to the greater availability of reactive ortho positions. However, the practical results

of this study indicate that the CBC-derived HW lignin performed similarly or even better under the investigated conditions. This may be attributed to its lower molecular weight, narrower molecular weight distribution, and improved accessibility of reactive hydroxyl groups.

LPF resin properties and curing behaviour

An overview of the key properties of the synthesised hardwood- and softwood-based LPF resins at 30 and 50 wt.% phenol substitution is provided in Table 1. The synthesised LPF resins showed solid contents between 50.0% and 51.4%, with only minor differences between lignin types and substitution levels. Prior to resin synthesis, the technically dried lignins still exhibited different residual moisture contents, with an average of 14.2% for HW lignin and 25.6% for SW lignin before oven drying. After oven drying at 60°C for 96 h, the moisture content was substantially reduced. However, residual moisture and slight differences in drying efficiency may still have influenced the final solid content of the resins. In addition, the measured values were lower than the theoretical value due to the formation of condensation water during resin synthesis.

The target viscosity after synthesis was approximately 500 mPa·s and was achieved for most formulations. At 30 wt.% phenol replacement, both HW and SW lignin-based LPF resins exhibited an initial viscosity after resin synthesis of 510 mPa·s. At 50 wt.% replacement, the HW-based resin showed a viscosity of 486 mPa·s, whereas the SW-based resin reached 582 mPa·s. After 7 days of storage at +7°C, viscosity increased in all formulations, indicating ongoing condensation reactions during storage. The viscosity of the HW lignin-based resins increased to 734 mPa·s (30 wt.%) and 667 mPa·s (50 wt.%), while the SW lignin-based resins increased to 720 mPa·s (30 wt.%) and 799 mPa·s (50 wt.%). Particularly at 50 wt.% substitution, HW lignin-based resins showed better viscosity stability during storage compared to SW lignin-based resins.

The pH values ranged from 10.4 to 11.1 and were similar for both lignin types comparable to literature (Ruohola, 2019). Free formaldehyde contents remained low, ranging between 0.2% and 0.4%, indicating acceptable environmental and processing properties. HW lignin-based LPF resins maintained relatively stable formaldehyde contents over storage, whereas SW lignin-based resins showed slight variations depending on substitution level and storage time. A further reduction of free formaldehyde content could potentially be achieved by post-addition of formaldehyde scavengers such as urea, as reported by Pizzi and Ibeh (2014).

A major difference between lignin types was observed in B-time. HW lignin-based LPF resins showed significantly shorter B-times (2:16–2:50 min) than SW lignin-based resins (6:30–6:46 min), indicating faster curing and higher practical reactivity. This result is particularly notable because hardwood lignin is often assumed to be less reactive due to its syringyl-rich structure. The improved curing behaviour may be explained by the lower molecular weight and reduced condensation of the CBC-derived HW lignin, resulting in improved accessibility of functional groups.

ABES measurements (Figure 2) showed that all LPF resins exhibited relatively slow bonding strength development compared to conventional PF resins, which is consistent with previous findings (Bliem et al., 2025a; Sailer-Kronlachner et al., 2024; Solt, et al., 2018a; Solt et al., 2018b; Solt et al., 2019). During the first minutes of pressing, no major differences between lignin types were observed. After longer pressing times, the LPF resins with 30 wt.% substitution achieved higher bond strengths than those with 50 wt.% substitution. At 50 wt.% substitution, SW lignin-based resins showed slightly higher bond strength development than HW lignin-based resins.

Table 1: Key properties of hardwood- and softwood-based LPF resins at 30 and 50 wt.% phenol substitution by lignin

Parameter	Unit	HW30	SW30	HW50	SW50
Solid content of the LPF resin	%	50.2 ± 0.1	50.0 ± 0.1	50.3 ± 0.1	51.4 ± 0.1
Viscosity after resin synthesis	mPa·s	510	510	486	582
Viscosity after 7 days of storage	mPa·s	734	720	667	799
pH of the LPF resin	-	11.0	11.1	10.4	10.4
Free formaldehyde content 1 day after resin synthesis	%	0.3	0.2	0.3	0.4
Free formaldehyde content 7 days after resin synthesis	%	0.4	0.2	0.3	0.2
B-time at 130°C	min:s	02:50 ± 00:08	06:30 ± 00:08	02:16 ± 00:04	06:46 ± 00:12

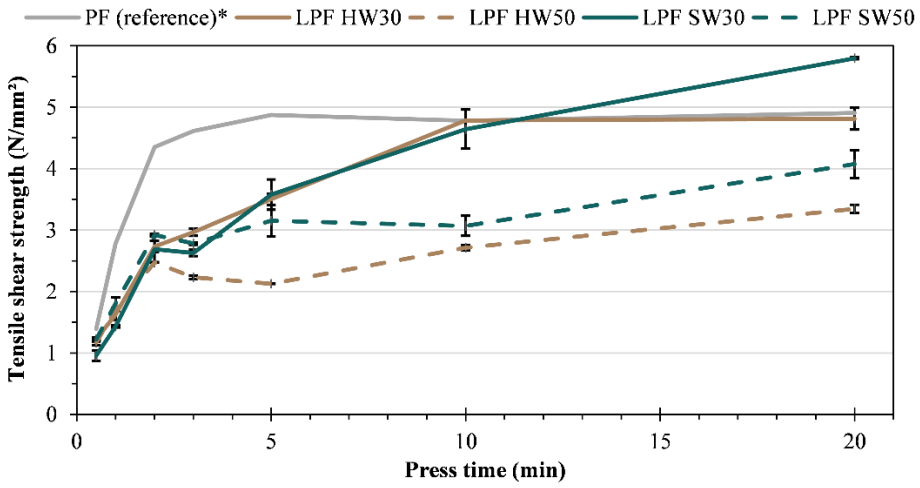

Figure 2: Bonding strength development curves of LPF resins based on hardwood (HW) and softwood (SW) lignin at 30 wt.% and 50 wt.% phenol substitution by lignin, measured at a pressing temperature of 120°C and different pressing times. *) reference values based on Bliem et al. (2025a); Sailer-Kronlachner et al. (2024)

Plywood bonding performance

Before plywood production, the viscosity of the LPF resins increased significantly after the addition of wheat flour and deionised water (100:10:10 wt.%). For the 30 wt.% phenol replacement formulations, viscosity increased from 483 to 600 mPa·s for HW lignin-based resins and from 514 to 613 mPa·s for SW lignin-based resins. At 50 wt.% phenol replacement, viscosity increased more strongly, from 498 to 800 mPa·s for HW lignin-based resins and from 590 to 740 mPa·s for SW lignin-based resins. This increase improved the applicability of the adhesive on the veneer surfaces and reduced excessive penetration into the wood structure.

The tensile shear strength results of the plywood panels are shown in Figure 3 and demonstrated that both hardwood (HW) and softwood (SW) lignin-based LPF resins are suitable for structural wood bonding applications. The bonding performance was evaluated separately for the core and face layers and under different pre-treatment conditions according to the plywood standard, representing bonding classes 1, 2, and 3.

At 30 wt.% phenol replacement by lignin, all tested variants clearly exceeded the minimum tensile shear strength requirement of 1 N/mm² for bonding classes 1 and 2. For bonding class 1, representing dry interior applications, mean tensile shear strength values ranged from 2.7 to 3.0 N/mm² for the core layers and from 2.5 to 2.6 N/mm² for the face layers. After the more severe pre-treatment for bonding class 2, representing covered exterior applications, the strength values decreased but still remained well above the standard requirement, ranging from 2.1 to 2.3 N/mm² for the core layers and approximately 1.9 to 2.0 N/mm² for the face layers. For bonding class 3, representing non-covered exterior applications, only two specimens per variant were tested as an indication. The measured values ranged from 1.9 to 2.1 N/mm² for the core layers and from 1.5 to 2.3 N/mm² for the face layers, indicating promising performance even under severe pre-treatment.

At 50 wt.% phenol replacement, tensile shear strength values were generally lower than those obtained at 30 wt.% replacement, confirming the negative effect of higher lignin substitution on bonding performance. Nevertheless, all variants still fulfilled the minimum requirement of 1 N/mm² for bonding classes 1 and 2. For bonding class 1, mean tensile shear strength values ranged from 1.9 to 2.3 N/mm² for the core layers and from 2.1 to 2.3 N/mm² for the face layers. For bonding class 2, values ranged from 1.5 to 1.8 N/mm² for the core layers and from 1.4 to 1.7 N/mm² for the face layers. For bonding class 3 at 50 wt.% phenol replacement, only the face layers exceeded the minimum requirement of 1 N/mm², with mean values between 1.1 and 1.2 N/mm². The core layers showed lower values between 0.3 and 0.7 N/mm² and therefore did not meet the requirement. However, since only two specimens per variant were tested, these results should be interpreted cautiously and considered as indicative.

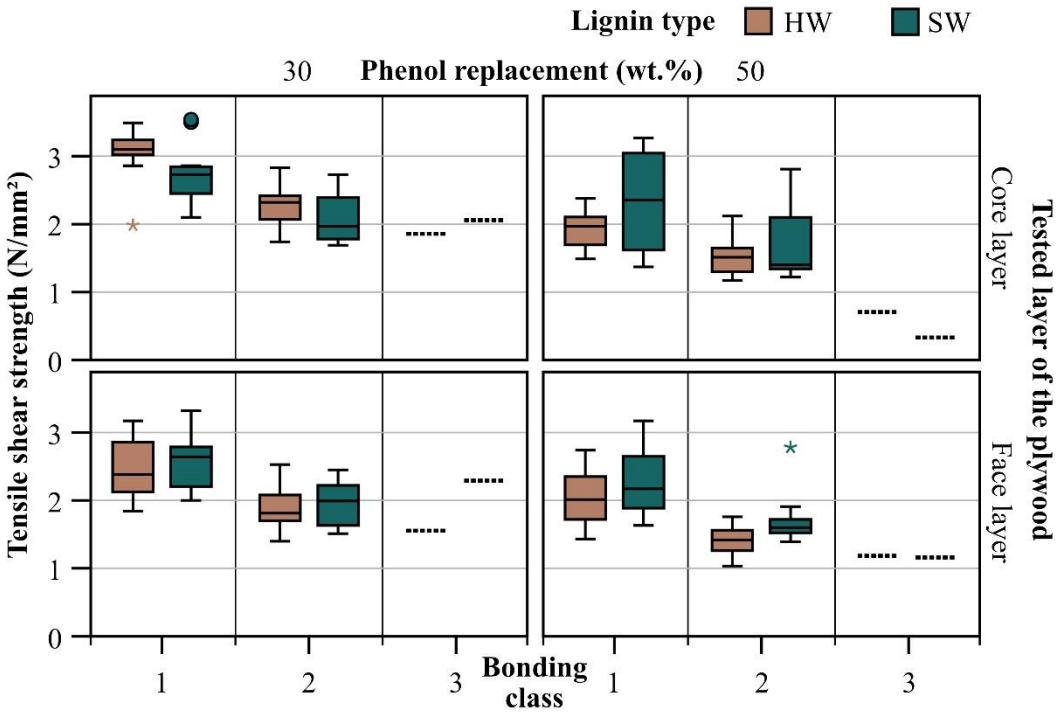

Figure 3: Tensile shear strength of plywood bonded with LPF resins based on different lignin types (HW = hardwood, SW = softwood) and phenol substitution levels (30 wt.% and 50 wt.%) for the core and face layers of lap-joint specimens.
Note: For bonding classes 1 and 2, boxplots represent 12 specimens each; for bonding class 3, the dashed line indicates the mean value of two specimens as an orientation. The minimum strength requirement according to EN 314-2 is 1 N/mm² at 0% wood failure

The visually assessed wood failure content generally decreased with increasing bonding class and more severe pre-treatment conditions, indicating a shift toward more adhesive-related failure under harsher moisture and thermal stresses (Table 2 and Table 3). Nevertheless, no delamination of the plywood panels was observed during the cyclic water soaking and drying procedures.

Table 2: Mean wood failure content of plywood bonded with LPF resins based on different lignin types (HW = hardwood, SW = softwood) and bonding classes at a phenol substitution level of 30 wt.% for the core and face layers of lap-joint specimens

Phenol replacement (wt.%)	**30**					
Bonding class	**1**		**2**		**3**	
Lignin type	**HW**	**SW**	**HW**	**SW**	**HW**	**SW**
Core layer	49	19	27	19	25	0
Face layer	19	22	6	15	0	25

Table 3: Mean wood failure content of plywood bonded with LPF resins based on different lignin types (HW = hardwood, SW = softwood) and bonding classes at a phenol substitution level of 50 wt.% for the core and face layers of lap-joint specimens

Phenol replacement (wt.%)	**30**					
Bonding class	**1**		**2**		**3**	
Lignin type	**HW**	**SW**	**HW**	**SW**	**HW**	**SW**
Core layer	8	28	3	15	0	0
Face layer	10	4	0	1	0	0

In general, both HW and SW lignin-based LPF resins showed similar bonding performance at the same substitution level, with only minor differences between lignin types. This demonstrates that hardwood lignin obtained from the CBC process can be directly utilised for adhesive synthesis without further

modification (as reported in literature by Hu et al. (2011); Jardim et al. (2020); Liu et al. (2024)) and can achieve bonding performance comparable to conventional softwood Kraft lignin.
The reduced bonding performance observed at 50 wt.% phenol replacement and under severe pre-treatment conditions may be improved by post-curing or stack maturation processes, which allow further curing of the resin after hot pressing (Carvalho et al., 2010; Dunky & Niemz, 2002). Previous studies demonstrated that such post-curing strategies can improve bonding performance sufficiently to meet bonding class 3 requirements (Bliem et al., 2025a; Sailer-Kronlachner et al., 2024).

CONCLUSION

This study demonstrated that hardwood (HW) lignin obtained from an industrial Continuous Batch Cooking (CBC) process can be used as a partial substitute for fossil-based phenol in lignin-phenol-formaldehyde (LPF) adhesives for plywood applications. Compared to conventional softwood (SW) Kraft lignin, the CBC-derived HW lignin showed a lower molecular weight, narrower molecular weight distribution and a less condensed structure. Despite its syringyl-rich composition, HW lignin exhibited comparable or even superior curing behaviour, reflected by significantly shorter B-times. The synthesised LPF resins showed suitable properties for industrial application, including appropriate viscosity, solid content, pH and low free formaldehyde content. In plywood testing according to EN 314, all formulations with 30 wt.% phenol replacement fulfilled the requirements for bonding classes 1 and 2 and showed promising results for bonding class 3. At 50 wt.% substitution, bonding performance decreased, but the requirements for bonding classes 1 and 2 were still met.
Overall, the results indicate that CBC-derived hardwood lignin can be directly utilised in adhesive synthesis and achieve bonding performance comparable to softwood Kraft lignin (Bliem et al. 2025b). Further optimisation of resin formulation and post-curing conditions may enable higher substitution rates and improved performance under severe conditions.

ACKNOWLEDGMENTS

The authors gratefully acknowledge the financial support provided by the Austrian Research Promotion Agency FFG within the COMET program (grant number 892416). The authors acknowledge the support of the Institute of Chemistry of Renewable Resources at BOKU University.

REFERENCES

ASTM D7998-15. (2015) Standard Test Method for Measuring the Effect of Temperature on the Cohesive Strength Development of Adhesives using Lap Shear Bonds under Tensile Loading.

Aydin I, Demirkir C, Colak S, Colakoglu G (2017) Utilization of bark flours as additive in plywood manufacturing. Eur J Wood Wood Prod 75(1):63-69. https://doi.org/10.1007/s00107-016-1096-0

Bliem P, Sailer-Kronlachner W. van Herwijnen HWG (2025a) Blend Technology to Enable Lignophenolic Resins on Industrial Scale. In: da Silva LFM, Adams RD, Sato C, Dilger K (eds.) 3rd International Conference on Industrial Applications of Adhesives 2024, Springer Nature Switzerland pp. 3-13. https://doi.org/10.1007/978-3-031-69503-2_1

Bliem P, Zinovyev G, van Herwijnen HWG (2025b) High-performance lignin-phenol-formaldehyde resins synthesed with hardwood lignin from continuous batch cooking-CBC process. J Adh 101(16):1842-1868. https://doi.org/10.1080/00218464.2025.2502093

Carvalho L, Martins J, Costa C (2010) Transport Phenomena. In: Thoemen H, Irle M, Sernek M (eds.) Wood-based Panels: An Introduction to Specialists (pp. 123-176). Brunel University Press.

Dunky M. Niemz P (2002). Holzwerkstoffe und Leime: Technologie und Einflussfaktoren. Springer Berlin Heidelberg.

Ghorbani M, Liebner F, van Herwijnen, HWG, Solt P, Konnerth J (2018) Ligneous resole adhesives for exterior-grade plywood. Eur J Wood Wood Prod 76(1):251-258. https://doi.org/10.1007/s00107-017-1249-9

Hu L, Pan H, Zhou Y, Zhang M (2011). Methods to improve lignin's reactivity as a phenol substitute and as replacement for other phenolic compounds: A brief review. BioRes 6(3):3515-3525.

Jääskeläinen AS, Liitiä T, Mikkelson A, Tamminen T (2017) Aqueous organic solvent fractionation as means to improve lignin homogeneity and purity. Ind Crops Prod 103:51-58. https://doi.org/10.1016/j.indcrop.2017.03.039

Jardim JM, Hart PW, Lucia L, Jameel H (2020) Insights into the Potential of Hardwood Kraft Lignin to Be a Green Platform Material for Emergence of the Biorefinery. Poylmers 12(8):1795. https://doi.org/10.3390/polym12081795

Kalami S, Chen N, Borazjani H, Nejad M (2018) Comparative analysis of different lignins as phenol replacement in phenolic adhesive formulations. Ind Crops Prod 125:520-528. https://doi.org/10.1016/j.indcrop.2018.09.037

Karthäuser J, Biziks V, Mai C, Militz H (2021) Lignin and Lignin-Derived Compounds for Wood Applications—A Review. Molecules 26(9):2533. https://doi.org/10.3390/molecules26092533

Korntner P, Sumerskii I, Bacher M, Rosenau T, Potthast A (2015) Characterization of technical lignins by NMR spectroscopy: optimization of functional group analysis by 31P NMR spectroscopy. Holzforschung 69(6):807-814. https://doi.org/doi:10.1515/hf-2014-0281

Liu LY, Chiang WS, Chang HM, Yeh TF (2024) Phenolation to Improve Hardwood Kraft Lignin for Wood Adhesive Application. Polymers 16(13):1923. https://doi.org/10.3390/polym16131923

Lourençon TV, Alakurtti S, Virtanen T, Jääskeläinen AS, Liitiä T, Hughes M, Magalhães WLE, Muniz, GIB, Tamminen T (2020) Phenol-formaldehyde resins with suitable bonding strength synthesized from "less-reactive" hardwood lignin fractions. Holzforschung 74(2):175-183. https://doi.org/doi:10.1515/hf-2018-0203

Mansouri NEE, Pizzi A, Salvado J (2007) Lignin-based polycondensation resins for wood adhesives. J Appl Pol Sci 103(3):1690-1699. https://doi.org/10.1002/app.25098

Nadányi R, Zinovyev G, Majerčiak M, Štosel M, Jablonský M, Ház A (2024) Optimizing Hardwood Lignin Precipitation from Kraft Black Liquor: A Study of Temperature and pH Effects. Forests 15(6):1028. https://doi.org/10.3390/f15061028

ÖNORM EN 314-1. (2005) Plywood - Bonding quality - Part 1: Test methods.

ÖNORM EN 314-2. (1997) Plywood - Bonding quality - Part 2: Requirements.

ÖNORM EN ISO 3251. (2019) Paints, varnishes and plastics - Determination of non-volatile-matter content.

ÖNORM EN ISO 8975. (1995) Plastics - Phenolic resins - Determination of pH.

ÖNORM EN ISO 8987. (2005) Plastics - Phenolic resins - Determination of reactivity on a B-transformation test plate.

ÖNORM EN ISO 11402. (2004) Phenolic, amino and condensation resins - Determination of free-formaldehyde content.

Pizzi A, Ibeh CC (2014) Phenol–Formaldehydes. In: Dodiuk H, Goodman SH (eds.) Handbook of Thermoset Plastics (Third Edition). William Andrew Publishing, pp13-44. https://doi.org/10.1016/B978-1-4557-3107-7.00002-6

Ruohola PAI (2019) Curing characteristics of lignin-phenol-formaldehyde resins for OSB panel [Master thesis, Lappeenranta University of Technology].

Sailer-Kronlachner W, Bliem P, van Herwijnen HWG. (2024) From Phenol-Lignin Blends towards birch plywood board production. In: Németh R, Hansmann C, Miliz H, Bak M, Báder M (eds) 11th Hardwood Conference Proceedings University of Sopron Press, Sopron, Hungary, pp 386–394. https://doi.org/10.35511/978-963-334-518-4

Sarika PR, Nancarrow P, Khansaheb A, Ibrahim T (2020) Bio-Based Alternatives to Phenol and Formaldehyde for the Production of Resins. Polymers 12(10):2237. https://doi.org/10.3390/polym12102237

Sixta H, Potthast A, Krotschek AW (2006a) Chemical Pulping Processes: Sections 4.1–4.2.5. In Sixta H (ed.) Handbook of Pulp, pp 109-229. https://doi.org/10.1002/9783527619887.ch4a

Sixta H, Potthast A, Krotschek AW (2006b) Chemical Pulping Processes: Sections 4.2.6–4.2.7. In Sixta H (ed.), Handbook of Pulp, pp 229-365. https://doi.org/10.1002/9783527619887.ch4b

Solt P, Jääskeläinen AS, Lingenfelter P, Konnerth J, van Herwijnen HWG (2018a) Impact of Molecular Weight of Kraft Lignin on Adhesive Performance of Lignin-Based Phenol-Formaldehyde Resins. For Prod J 68(4):365-371. https://doi.org/10.13073/fpj-d-17-00079

Solt P, Rößiger B, Konnerth J, van Herwijnen HWG (2018b) Lignin Phenol Formaldehyde Resoles Using Base-Catalysed Depolymerized Kraft Lignin. Polymers 10(10):1162. https://doi.org/10.3390/polym10101162

Solt P, van Herwijnen HWG, Konnerth J (2019) Thermoplastic and moisture-dependent behavior of lignin phenol formaldehyde resins. J Appl Pol Sci 136(40):48011. https://doi.org/10.1002/app.48011

Sumerskii I, Zweckmair T, Hettegger H, Zinovyev G, Bacher M, Rosenau T, Potthast A (2017) A fast track for the accurate determination of methoxyl and ethoxyl groups in lignin. RSC Adv 7(37):22974-22982. https://doi.org/10.1039/C7RA00690J

Wizani W, Juljanski W, Krotscheck A, Bito R (2000) CBC - Continuous batch cooking the revolution in kraft cooking. Kraft Pulp Yield Symposium.

The Feasibility of Black Locust Wood (*Robinia Pseudoacacia* L.) for Use in Load-Bearing Construction

Dominique Streib[1*], Gerhard Dill-Langer[1], Max Lutz[1], Rupert Nieberle[2], Philippe Grönquist[1,3]

[1] University of Stuttgart, Materials Testing Institute, Pfaffenwaldring 4b, Stuttgart 70569, Germany
[2] Duale Hochschule Sachen (Cooperative State University of Saxony), Campus Dresden, Hans-Grundig-Str. 25, Dresden 01307, Germany.
[3] University of Stuttgart, Institute of Construction Materials, Pfaffenwaldring 4, Stuttgart 70569, Germany.

E-mail: Dominique.Streib@mpa.uni-stuttgart.de; Gerhard.Dill-Langer@mpa.uni-stuttgart.de; Max.Lutz88@yahoo.com; Rupert.Nieberle@dhsn.de; Philippe.Groenquist@iwb.uni-stuttgart.de

Keywords: bonding, Black locust (*Robinia pseudoacacia* L.), adhesive systems, structural timber products, delamination, grading.

ABSTRACT

Black locust (*Robinia pseudoacacia* L.) exhibits significant potential for application as a primary structural element in timber engineering. Characteried by exceptional natural durability and robustness, this hardwood species is particularly well-suited for outdoor applications. Its potential for superior mechanical properties facilitates the optimisation of structural cross-sections, enabling the design of slender, material-efficient components. However, the transition of black locust into standardised engineered wood products (EWP) is contingent upon both accurate strength grading of lamellas and reliable bonding performance. This paper provides a comprehensive overview of several research projects dedicated to the structural utilisation of this species. A primary objective involves the development of a specialised strength grading model tailored to the unique characteristics of black locust. Subsequently, roundwood grading will be conducted and directly contrasted with the strength classes of the resulting lamellas. This comparative analysis aims to identify synergies between both methods to optimise overall material yield. Parallel to grading, adhesive performance constitutes a fundamental component of this research. Bond line integrity will be evaluated through rigorous delamination and block shear testing. Furthermore, the study aims to define an optimised geometry for longitudinal joints (finger jointing) specifically adapted to the properties of the species. Collectively, this research can provide a decisive foundation for establishing black locust as a viable material for high-performance structural timber applications.

INTRODUCTION

The utilisation of hardwood species in structural timber engineering is anticipated to gain significant importance. Climate change is fundamentally altering growth conditions for traditional softwoods, such as Norway spruce (*Picea abies*), leading to a decline in both availability and timber quality. Furthermore, common deciduous species like oak (*Quercus* spp.) and beech (*Fagus sylvatica*) are increasingly compromised by biotic and abiotic disturbances, including prolonged drought periods and xylophagous insect infestations (BMEL 2024). Consequently, there is an urgent need to investigate climate-resilient alternatives, among which black locust (*Robinia pseudoacacia* L.) emerges as a highly promising candidate.

Despite its principally superior mechanical properties and natural durability, the industrial integration of black locust into mass timber products—such as glued laminated timber (GLT) or cross-laminated timber (CLT)—is i.a. currently constrained by its challenging bonding characteristics. Previous investigations have highlighted a high degree of variability in bond quality, often attributed to the species' high density and its distinct chemical extractive composition. (Kamperidou und Barboutis 2017) demonstrated that while satisfactory shear strength can be achieved under specific laboratory conditions, the choice of adhesive system and the calibration of processing parameters, such as clamping pressure, are critical and often produce inconsistent results compared to other hardwoods like beech. This suggests that the complex interfacial interaction between conventional adhesives and the extractive-rich heartwood of black locust necessitates a more fundamental understanding of the bonding process.

To date, comprehensive data regarding the bonding integrity of *R. pseudoacacia* remains sparse. (Konnerth et al. 2016) evaluated the performance of various hardwoods using standard structural adhesives, including polyurethane (PUR), melamine-urea-formaldehyde (MUF), and phenol-resorcinol-formaldehyde (PRF). In their study, delamination tests yielded substandard results for black locust, highlighting a critical requirement for further investigation. This necessitates the exploration of alternative adhesive formulations or the implementation of chemical surface pre-treatments to enhance long-term bond durability. Mechanical assessments of finger-jointed members have been documented in select studies, most notably by Müller (2006), whose extensive work contrasts different adhesive types and joint configurations. Further investigations into PUR-bonded finger joints identified these connections as a primary structural weakness in laminated black locust elements (Frühwald et al. 2003). The longitudinal jointing of black locust (*Robinia pseudoacacia* L.) lamellas is essential for the production of continuous layers required in the manufacture of engineered wood products, such as GLT and CLT. To establish a technical foundation for this process, this research objective is to optimize conventional finger-jointing techniques while simultaneously developing innovative joining methodologies. To contextualise these technological challenges, a comprehensive understanding of the species' ecological background, availability, and inherent material characteristics is required.

CHARACTERISTICS AND DISTRIBUTION OF BLACK LOCUST

Robinia pseudoacacia L., a pioneer deciduous species within the *Fabaceae* family, is indigenous to the temperate regions of eastern North America, with its primary evolutionary centre located in the Appalachian Mountains (Vítková et al. 2017). In the contemporary global landscape, it represents one of the most widely propagated non-native deciduous hardwoods, having naturalised extensively across the European continent, predominantly concentrating in the thermophilic, continental regions of Central and Southeastern Europe.

The European centre of distribution is located in Hungary, where it accounts for roughly 20% of the total forested area, covering an estimated 460,000 hectares (Rédei et al. 2014). In contrast, according to the most recent National Forest Inventory, the area occupied by this species in Germany amounts to approximately 47,000 hectares, representing only 0.4% of the total forest cover (BMEL 2024). As a typical pioneer species, the black locust is characterised by rapid early growth and high resilience to prolonged drought and nutrient-poor soils, making it a preferred choice for initial afforestation and reclamation sites (Cierjacks et al. 2013). Concurrently, its vigorous capacity for vegetative reproduction via root suckers contributes to a high expansion potential, often leading to its classification as an invasive or invasive-hazardous species in certain European ecosystems.

Mature black locust trees can reach terminal heights of 20 to 25 meters, with a diameter at breast height (DBH) of up to 80 cm (Wagenführ 2021). However, silvicultural management often contends with a frequently irregular, asymmetrical stem development, characterised by a brownish-grey, deeply furrowed, reticulate bark. Due to this inherently poor stem form, the merchantable log length is typically limited to approximately 10 meters, frequently exhibiting sweep and taper. This morphological limitation directly underscores the necessity for efficient roundwood grading and subsequent conversion into smaller, standardied lamellas for engineered applications.

Despite these growth-related challenges, the clear wood of *R. pseudoacacia* exhibits exceptional mechanical-technological properties driven by its high average raw density. A defining attribute of the species is its superior natural resistance to biotic degradation, specifically against wood-destroying fungi and insects. According to EN 350, the heartwood is categorised into durability classes 1 to 2 ('very durable' to 'durable'). This inherent bio-resistance renders the untreated heartwood fully suitable for structural applications under direct weathering conditions (Use Service Class 3 and 4) as well as for permanent soil or aquatic contact, rendering anthropogenic chemical preservation redundant.

In this regard, black locust surpasses all other indigenous commercial timber species in Europe, representing a high-performance regional alternative to imported tropical hardwoods. Historically, *R. pseudoacacia* has been restricted to specialised niche applications; in exterior construction, it is predominantly used for landscaping elements, palisades, playground equipment, and viticulture stakes. However, the synergy of superior natural durability and exceptional mechanical strength positions black locust as a prime candidate for high-performance structural timber engineering, provided the technical challenges of grading and bonding can be structurally resolved.

STRENGTH GRADING OF BLACK LOCUST LAMELLAS

To safely utilise *Robinia pseudoacacia* L. in structural engineered wood products (EWP) such as glued laminated timber (GLT), precise and reliable non-destructive strength grading methodologies are mandatory. Due to the high variability in material properties and the frequently irregular growth characteristics of black locust, conventional visual grading rules often fail to accurately predict actual mechanical performance.

To address this challenge, the first phase of the research project focused on establishing optimised grading models specifically for black locust lamellas, the comprehensive results of which have been previously published by the authors (Dill-Langer et al. 2025). Within this completed stage, the evaluation was based on adapted visual grading rules. The visual sorting criteria were adopted in accordance with DIN 4074-5. Additionally, the density (ρ) and dynamic modulus of elasticity ($E_{dyn,l}$) were determined for each lamination. A statistical analysis of the criteria recorded is provided in Table 1.

Table 1: Statistical analysis of the properties of the lamellas

Parameter	Knot area ratio [-]	Global slope of grain [°]	Raw density ρ [kg/m³]	Dynamic MOE $E_{dyn,l}$ [N/mm²]
Mean value	0.08	9	775	16800
Max. value	0.47	25	977	24700
Min value	0.00	1	677	12000
Stand. Dev.	0.08	5	47	2200
COV	1.02	0.50	0.06	0.13

Tensile strength was evaluated through the execution of tensile tests in accordance with EN 408. The development of these visual grading models was driven by the objective of enhancing yield while ensuring the attainment of optimal characteristic tensile strengths. Figure 1 illustrates the effect of visual grading on the cumulative frequency of tensile strength for model 1, 2 and 3.

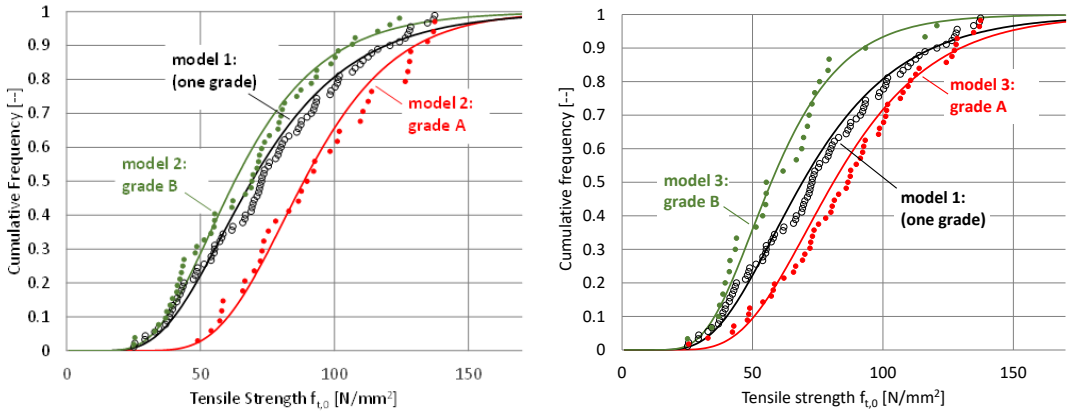

Figure 1: Comparison of model 1 (only one grade, no rejects) and model 2 (left) and model 3 (right) with two grades each. The individual strength values and the respective lognormal distributions are given (Dill-Langer et al. 2025)

ROUNDWOOD GRADING (LOG GRADING)

In addition to the strength grading of individual lamellas, a primary objective of the research involves the qualitative grading of black locust roundwood. In German forestry, roundwood grading is traditionally executed in accordance with the Framework Agreement for Roundwood Trade (RVR). Although the RVR encompasses hardwoods, its sorting criteria are primarily calibrated for more prevalent species, such as oak (*Quercus* spp.) and beech (*Fagus sylvatica*). Furthermore, the European standards EN 1316-1 to 3, which provide criteria for the quality sorting of various hardwoods, do not explicitly include black locust within their specific frameworks.

To address this technical gap, approximately 20 solid cubic metres (m³) of roundwood will be graded within the scope of this study. The batch consists of lower-quality black locust timber harvested from the Lusatia region in northeastern Germany. Evaluating this specific material pool aims to determine the structural potential and viable material yield of lower-grade assortments, which have historically been excluded from high-performance timber applications.

BONDABILITY OF BLACK LOCUST

Surface Bonding

A critical requirement for the structural implementation of laminated timber components is the long-term integrity and durability of the adhesive bond line. Due to its high density, distinct anatomical structure, and extractive-rich chemical composition, black locust is traditionally categorised as a wood species that is highly challenging to bond.

Building upon a completed research project that initiated the testing of various adhesive systems to optimie the surface bonding (Dill-Langer et al. 2025), the current study continues these investigations and implements prior findings. Two distinct structural adhesive systems - a one-component polyurethane (1K PUR) and a melamine-urea-formaldehyde (MUF) resin - are under investigation. For the 1K PUR system, the application of a specific primer is implemented as a surface pre-treatment. To determine the optimal bonding conditions for black locust, a comprehensive parameter study is being conducted, systematically adjusting variables such as adhesive spread rate, open and closed assembly times, and clamping pressure.

A further objective of the current research involves assessing the feasibility of hybrid configurations, combining black locust in the high-stress outer zones with birch (*Betula* spp.) in the core of the cross-section. In this context, the optimal bonding conditions for this specific hardwood-hardwood combination will be evaluated.

The resulting bonding performance will be evaluated through delamination tests in accordance with EN 302-2, with classification to be performed according to the requirements specified in EN 301. Furthermore, block shear tests will be conducted on both the bond lines and the solid wood, following the methodology of EAD 130320-00-0304. These shear strength assessments will be performed on dry (unconditioned) as well as pre-treated (moisture-exposed) specimens to verify long-term durability.

Glued Finger Joints and Alternative Joining Methods for Longitudinal Bonding

Previous studies have investigated the performance of conventional finger-jointed connections in black locust lamellas, utilising specimens manufactured under both laboratory and industrial conditions (Dill-Langer et al. 2025). In both instances, milling was performed using industrial-scale equipment, while the adhesive was applied manually to the finger joints. In the laboratory setting, the performance of three distinct adhesive systems—polyurethane (PUR), melamine-urea-formaldehyde (MUF), and phenol-resorcinol-formaldehyde (PRF)—was compared, whereas the industrial production phase focused exclusively on the application of the PRF adhesive. Bending and tensile strengths were determined in accordance with EN 14080, while the long-term bonding durability was evaluated through delamination tests following the protocols of EN 301 Annex A.

The results of this experimental series demonstrated that the PRF system achieved the highest bonding performance. However, as the industrial use of PRF adhesives is steadily declining in favour of more modern alternatives, the further research efforts within this project will concentrate on MUF and PUR systems to ensure industrial relevance. Further findings from these investigations indicated that the clamping pressure during the assembly of finger joints must be optimised to prevent the splitting of the fingers while simultaneously ensuring the tight fit of small finger dimensions. In addition, the wear of the milling cutters must be strictly monitored, as a reduction in milling quality significantly impairs the interfacial bonding strength and the overall structural integrity of the finger-jointed connections.

Future investigations will incorporate all aforementioned optimisations for the production of finger-jointed connections, while introducing several novel approaches. A new MUF adhesive system will be implemented. Regarding PUR bonding, the efficacy of a chemical surface pretreatment via primer application will be examined, despite the inherent technical challenges associated with applying primers to complex finger-joint geometries.

In addition to conventional finger joints, alternative joining methods will be developed to enhance bond performance:

- Scarf joints: This method involves joining beveled board ends, which likewise simplifies access for primer application. While scarf joints are well-established in non-structural applications, comprehensive and generalised knowledge regarding their mechanical properties in structural hardwood components remains insufficient. Historically, scarf joints have been associated with low material yield; however, this project aims to reduce such losses by optimising grading specifications. Key parameters for refining scarf joints into a high-quality, material-efficient joining method will include evaluation of various adhesive systems and surface treatments, the impact of the flank-to-fibre angle, and the required timber sorting quality within the immediate area of the joint. Figure 2 depicts a schematic representation of the scarf joint configuration.

Figure 2: Potential scarf joint configuration

- "Mega-finger-joints": By significantly increasing the dimensions of the finger-joint geometry, accessibility to the joint flanks will be improved, thereby facilitating a controlled primer application. Research in this area will prioritise the quality of surface treatments, the resulting tensile strength, the overall manufacturability of these larger geometries, and the influence of the flank-to-fibre angle. Figure 3 illustrates a potential configuration for the mega finger joint geometry.

Figure 3: Potential mega finger joint configuration

In addition to the determination of tensile and bending strengths in accordance with EN 14080, a comprehensive durability assessment of the bonded joints will be established. In order to quantify bonding durability, the delamination tests prescribed in EN 301 Annex A will be systematically modified and implemented as a benchmark for the durability of the various joining methods.

ACKNOWLEDGEMENTS

The underlying research projects were conducted in collaboration with STRAB Ingenieurholzbau Hermsdorf GmbH, Gebrüder Noack Holzfachmarkt GmbH & Sägewerk GbR, Holzbau Plan+Werk GmbH, WMS Werkzeugmaschinen-Service GmbH, Häberlein GmbH, the Duale Hochschule Sachsen (Saxony State Cooperative University), the Materials Testing Institute (MPA) of the University of Stuttgart, the Fraunhofer Institute for Material and Beam Technology (IWS), EBF Innovation GmbH, and Eurobinia.

The authors wish to express their gratitude to all participating partners and funding organisations for their support. This project was supported by the Federal Ministry for Economic Affairs and Climate Action (BMWK) on the basis of a decision by the German Bundestag.

REFERENCES

BMEL (2024): Der Wald in Deutschland - Ausgewählte Ergebnisse der vierten Bundeswaldinventur. Online verfügbar unter https://www.bundeswaldinventur.de

Cierjacks, Arne; Kowarik, Ingo; Joshi, Jasmin; Hempel, Stefan; Ristow, Michael; Lippe, Moritz von der; Weber, Ewald (2013): Biological Flora of the British Isles: Robinia pseudoacacia. In: Journal of Ecology 101 (6), S. 1623–1640. https://doi.org/10.1111/1365-2745.12162

Dill-Langer, Gerhard; Nieberle, Rupert; Hänsel, Andreas (2025): Glued laminated Robinia hardwood timber for structural use. In: BioRes 20 (2), S. 3848–3865. https://doi.org/10.15376/biores.20.2.3848-3865

DIN 4074-5:2008: Sortierung von Holz nach der Tragfähigkeit - Teil 5: Laubschnittholz

DIN EN 301:2023: Klebstoffe, Phenoplaste und Aminoplaste, für tragende Holzbauteile – Klassifizierung und Leistungsanforderungen (German version EN 301:2023)

DIN EN 302-2:2023: Klebstoffe für tragende Holzbauteile – Prüfverfahren – Teil 2: Bestimmung der Delaminierungsbeständigkeit (German version EN 302-2:2023)

DIN EN 408:2012: Holzbauwerke – Bauholz für tragende Zwecke und Brettschichtholz – Bestimmung einiger physikalischer und mechanischer Eigenschaften (German version EN 408:2010+A1:2012)

DIN EN 1316-1:2013: Laub-Rundholz – Qualitäts-Sortierung – Teil 1: Eiche und Buche (German version EN 1316-1:2012)

DIN EN 1316-2:2013: Laub-Rundholz – Qualitäts-Sortierung – Teil 2: Pappel (German version EN 1316-2:2012)

DIN EN 1316-3:2013, Laub-Rundholz – Qualitäts-Sortierung – Teil 3: Esche, Ahorn, Kirsche und Linde (German version EN 1316-3:2012)

EN 350:2016: Durability of wood and wood-based products - Testing and classification of the durability to biological agents of wood and wood-based materials.

EN 14080:2013: Timber structures - Glued laminated timber and glued solid timber - Requirements.

EOTA (2021). EAD 130320-00-0304: Glued laminated products made of specific hardwood species. European Organisation for Technical Assessment.

Frühwald, A., Ressel, J. B., Becker, P., Pohlmann C. M., and Wonnemann, R. (2003). Verwendung von Laubhölzern zur Herstellung von Leimholzelementen – Abschlussbericht, Hamburg: Universität Hamburg - Zentrum Holzwirtschaft.

Kamperidou, Vasiliki; Barboutis, Ioannis (2017): Bondability of Black locust (Robinia pseudoacacia) and Beech wood (Fagus sylvatica) with polyvinyl acetate and polyurethane adhesives. In: Maderas, Cienc. tecnol. (ahead), S. 0. https://doi.org/10.4067/S0718-221X2017005000008

Konnerth, Johannes; Kluge, Marcel; Schweizer, Georg; Miljković, Milica; Gindl-Altmutter, Wolfgang (2016): Survey of selected adhesive bonding properties of nine European softwood and hardwood species. In: Eur. J. Wood Prod. 74 (6), S. 809–819. https://doi.org/10.1007/s00107-016-1087-1

Rédei, Károly; Csiha, Imre; Keseru, Zsolt; Rásó, János; Kamandiné Végh, Ágnes; Antal, Borbála (2014): Growth and Yield of Black Locust (Robinia pseudoacacia L.) Stands in Nyírség Growing Region (North-East Hungary). In: SEEFOR 5 (1). https://doi.org/10.15177/seefor.14-04

Vítková, Michaela; Müllerová, Jana; Sádlo, Jiří; Pergl, Jan; Pyšek, Petr (2017): Black locust (Robinia pseudoacacia) beloved and despised: a story of an invasive tree in Central Europe. In: Forest ecology and management 384, S. 287–302. https://doi.org/10.1016/j.foreco.2016.10.057

Wagenführ, André Aubin (2021): Holzatlas. 7th, newly revised and expanded edition. Munich: Carl Hanser Verlag

Water Vapor Transport Through Adhesive Layers on Eucalyptus (Eucalyptus Camaldulensis) Wood: Pre-Steady and Steady-State Behavior

Omar Saber Zinad[1*], Csilla Csiha[1]

[2] University of Sopron, Faculty of Wood Engineering and Creative Industries. Bajcsy-Zs. Str. 4, Sopron, Hungary, 9400.

e-mail: omar.saber.khalaf.zinad@phd.uni-sopron.hu; csiha.csilla@uni-sopron.hu

Keywords:

ABSTRACT

Eucalyptus (*Eucalyptus camaldulensis*), as a high-density hardwood species ($\rho = 952.18$ kg/m³), exhibits distinct water-vapor diffusion behavior when combined with different adhesive layers. This study evaluates the diffusion characteristics of eucalyptus under different surface conditions, including uncoated (EUW), lasure-coated (EUWL), commercial adhesive-coated (EUWAJ) and (EUWAX), and coated with custom-made synthesized polymer systems with varying molecular weights (EUWS1–EUWS5). Lasure coated samples served as reference for controlled diffusion properties. The experiments were conducted using the cup method according to ISO 12572 and ASTM E96 standards under accelerated conditions, with analysis performed in both pre-steady and steady-state zones. In the steady-state zone, EUW exhibited a permeability coefficient of $\delta = 2.62 \times 10^{-14}$ kg/(m·s·Pa), while EUWAJS showed a reduced value of $\delta = 0.326 \times 10^{-14}$ kg/(m·s·Pa) and G = 0.000258 g/h, confirming strong vapor-blocking behavior. Similar results were observed for EUWAXS ($\delta = 0.212 \times 10^{-14}$, G = 0.000168 g/h) and EUWS1S ($\delta = 0.213 \times 10^{-14}$, G = 0.000169 g/h). EUWLS exhibited semi-permeable behavior with $\delta = 1.345 \times 10^{-14}$ kg/(m·s·Pa) and G = 0.001068 g/h, reaching the transition point at 262.8 h. Intermediate systems EUWS2S ($\delta = 0.350 \times 10^{-14}$, G = 0.000278 g/h) and EUWS3S ($\delta = 0.520 \times 10^{-14}$, G = 0.000413 g/h) showed controlled diffusion, while higher MW systems EUWS4S ($\delta = 0.736 \times 10^{-14}$) and EUWS5S ($\delta = 1.077 \times 10^{-14}$, G = 0.000855 g/h) approached lasure behavior. In the pre-steady zone, EUW exhibited $\delta = 46.40 \times 10^{-12}$ kg/(m²·s·Pa) with a mass change of 7.77 g, confirming the strong influence of density on early-stage diffusion. The results show that vapor diffusion in eucalyptus is governed by wood density and adhesive molecular weight, while the pre-steady zone provides a more sensitive evaluation than steady-state parameters.

The final version of this abstract and the full scientific article are scheduled to be published in the Special Issue "12th Hardwood Conference—Sopron" of the journal MDPI Forests, available at the following link:

MDPI Forests Special Issue: 12th Hardwood Conference—Sopron

Interactions on Steamed Beech Wood-Epoxy Resin Phase Boundary During Wood Moisture Content Changes

Barbora Slováčková[1*]

[1] Technical University of Zvolen, Faculty of Wood Sciences and Technology, Department of Wood Science, T. G. Masaryka 24, Zvolen, Slovakia, 96001.

E-mail: xslovackova@tuzvo.sk

Keywords: beech wood, epoxy resin, adhesion, phase boundary, stresses.

ABSTRACT

Combining casting epoxy resin and wood as materials to produce various types of furniture and decorative items has been very popular in recent years. Epoxy resin is a material with very small dimensional changes and water uptake due to changes in moisture, whereas wood is a hydrophilic material with significant dimensional changes due to moisture content changes. Therefore, the behavior of the phase boundary between wood and casting epoxy resin during changes in wood moisture content needs to be studied. The focus of this article was deformation of the wood – resin phase boundary during exposure of the beech wood-epoxy resin samples to a high relative air humidity environment. Dimensional and equilibrium moisture content changes of the untreated and steamed beech wood samples were monitored to support the findings. To evaluate the stability of the wood-epoxy resin phase boundary, pictures of the samples were taken after each stage of the experiment and a ratio of intact area of adhesion was calculated with the help of a graphic software. Samples treated with Mode II steaming regime showed the best adhesion of epoxy resin to the substrate, even though the dimensional changes of these samples were about the same as in the other sample sets. A noticeable color change of the epoxy resin was noticed after the experiment was concluded, the epoxy resin was therefore gently removed from the wood samples and the color was measured. Lightness of the epoxy resin decreased in all sample sets and the epoxy resin color shifted towards a greener and noticeable yellow color.

INTRODUCTION

Wood as a natural, organic, composite material has specific properties in comparison to other materials. There are many positive properties, like mechanical properties and workability, but on the other hand, there are also many negative properties. Among the negative properties, heterogeneity, hydrophilicity, dimensional instability to name a few, pose a significant obstacle in various technological processes, especially surface finishing. These properties can be enhanced by modification of wood. Wood modification has been a focus of research for a long time and there is currently a wide variety of physicochemical wood modification methods available (Hill 2006, Reinprecht 2016, Sandberg et al. 2021, Spear et al. 2021).

One of the first chemical modification methods is the modification of wood with resins (Stamm and Seborg 1943, 1944). Pores in wood, especially lumens of cell elements, were filled out with these modifying substances. The goal of this modification was to enhance the mechanical properties of the modified wood, as well as its dimensional stability during changes in moisture content (Kurjatko et al. 1987, Liptáková et al. 1991, Deka and Saikia 2000, Homan and Jorissen 2004, Dieste et al. 2008). In comparison to wood, epoxy resin has a negligible water uptake (Vanlandingham et al. 1999). Moreover, epoxy resins exhibit a greater dimensional stability under varying moisture conditions than wood (Kovařík and Tesařová 2022). According to the last cited authors and Guo et al. (2022) Wondmagegnehu and Legesse (2023), Zhou et al. (2025) and Slováčková and Kovařík (2025), the main problems of the wood-epoxy resin phase boundary stability are stresses from moisture, mechanical load and heat. When wood samples with epoxy resin were exposed to a high relative humidity environment, the wood swelled and the epoxy resin detached from the wood in a cohesive failure within the epoxy resin (Slováčková and Kovařík 2025). The loss of adhesion and a deformation of the phase boundary between the solid epoxy resin layer and wood due to the dimensional instability of wood is a serious issue for finished products, and it needs to be studied further.

Epoxy resins are synthetic materials; they consist of mono- or oligomers in the raw state. During polymerization of the resin, mono- and oligomers chemically crosslink to form a three-dimensional polymer structure. Epoxy resins are widely used in adhesives, paints, coatings, medical implants, and electrical devices, and also in furniture production as table tops or even jewellery (Bilyeu et al. 1999, Frihart 2005, Kumosa 2006, Kovařík and Tesařová 2022). Epoxy adhesives and coatings have excellent environmental resistance and the ability to bond to a variety of surfaces, including wood (Bilyeu et al. 1999, Kovařík 2025), they are easy to work with and lack volatile byproducts (Kovařík and Tesařová 2022). Tabletops made with epoxy resin and wood can be made from wood of varying quality – wood with defects, burnt wood, rotten wood, recycled wood. The transparency and glass like look of the resin emphasize the beauty of the wood and together they create a one-of-a-kind product with added value.
The research on interactions in the wood-epoxy resin system is scarce and needs to be enhanced. The main goal of this article was observing interactions on the wood-epoxy resin phase boundary during wood moisture content changes. Untreated and steamed beech wood was selected as the substrate for the epoxy resin. The samples were exposed to high relative air humidity; the dimensional changes of the wood and the deformations of the phase boundary between the solid epoxy resin layer and the beech wood were observed. A colour change of the epoxy resin was noticed after the experiment was concluded, the colour of the epoxy resin after the exposure to high relative air humidity without the exposure to light was measured.

MATERIALS AND METHODS

A preliminary experiment and a main experiment were performed. Beech wood (*Fagus sylvatica*, L.) lumber was used in both experiments, due to its extensive dimensional changes (Kúdela and Čunderlík 2012). Beech wood steamed with saturated steam was selected because steaming changes its properties in a complex way (Slováčková et al. 2026).
For the preliminary experiment, only untreated beech sapwood samples were used; 24 samples were prepared. The samples were cut to dimensions of 120x50x20 mm (LxRxT) and the surfaces of the samples were milled. The average oven dried density of the samples was 692 kg·m^{-3}. Prior to casting the epoxy resin layers, these samples were placed into a climatic chamber at a relative air humidity (RH) of 50±5% and an air temperature of 20±2°C until they reached equilibrium moisture content (EMC). The EMC of these samples was 9.87%.
For the main experiment, untreated and saturated steam treated samples by two modes (Mode I and Mode II) from both false heartwood (FHW) and sapwood (SW) were used. The detailed description of the saturated steam treatment, moisture content, temperatures, pressures and treatment durations are described in Slováčková et al. (2026). Sixteen samples per treatment were used – 48 samples in total. These samples were cut to 100x50x10 mm (LxRxT) and the surfaces of the samples were milled. After the samples were oven dried at 103±2°C, weighed and their dimensions were measured, they were placed into a climatic chamber at a RH of 50±5% and an air temperature of 20±2°C until they reached EMC. The EMCs of the samples from the main experiment are listed in Tab. 1 along with their oven-dried densities.

Table 1: Oven dried densities and EMCs of untreated and steam treated beech FHW and SW samples

	Basic statistical characteristics	Untreated		Steamed with Mode I		Steamed with Mode II	
		Density [kg·m^{-3}]	EMC [%]	Density [kg·m^{-3}]	EMC [%]	Density [kg·m^{-3}]	EMC [%]
FHW	x̄	683	9.40	594	9.44	725	7.60
	s	30.0	0.22	10.9	0.07	24.7	0.14
SW	x̄	675	9.70	592	9.41	695	7.84
	s	8.26	0.36	12.6	0.09	15.5	0.03

Note: Eight samples per both FHW and SW were used in the experiment.

Two types of epoxy resin were used to cast a layer on all samples. For the preliminary experiment, a bisphenol A type with UV stabilizer (Epoxy 2020, Epoxy s. r. o. Vysoká pri Morave, Slovakia) epoxy resin was used. For the main experiment, a bisphenol F type epoxy resin (Stachema, Stachema CZ, Brno, Czech Republic) was used. The epoxy resin was casted on radial or mid-radial faces of the samples in

both experiments. Edges on all samples were sanded, to ensure leak-proof adhesion of the forms. White sanitary silicone was applied to the edges of the samples and a 4cm wide tape was used to wrap around the silicone covered edges of the samples to create a casting form for the resin. The silicone was left to solidify for 24 hours. The epoxy resins were mixed according to the manufacturer 's instructions. An approximately 1 cm thick layer was casted in the preliminary experiment, and a 0.5 cm thick layer was casted in the main experiment. The resin was left to cure at an RH of 50±5% and an air temperature of 20±2°C for two days. The tape forms and the silicone were removed after the initial curing and then the samples were left to fully cure for 5 additional days.

When the samples were fully cured, they were subjected to cycles of changing relative air humidities. One cycle consisted of an exposure to a high RH and then to a low RH at an air temperature of 20±2°C. The samples were left in these environments until they reached EMCs. The samples for the preliminary experiment were placed into desiccators with deionised water at the bottoms of the desiccators (RH=99.9%) and then back to a climatic room at an RH of 50±5%. Three cycles were repeated for the preliminary experiment to establish a time frame for the main experiment. The samples in the main experiment were subjected to one cycle, and they were placed into desiccators with a saturated solution of potassium chloride (RH=85%) at the bottom and then back to the climatic chamber at an RH of 50±5%.

Dimensions of the samples were measured in three places in each anatomical direction with a slide calliper twice during a cycle – after the wood swelled in the high RH environment and after the wood shrunk in the low RH environment. The samples were also weighed on laboratory scales and images of the samples were taken to evaluate the area of resin adhesion to wood. Radial and tangential swelling $\beta_{R,T}$ were calculated as:

$$\beta_{R,T} = \frac{r,t_w - r,t_0}{r,t_0} \cdot 100 \quad (1)$$

Where r,t_w are average radial and tangential dimensions at a certain EMC and r,t_0 are the average radial and tangential dimensions of oven-dried samples. Radial and tangential shrinking $\alpha_{R,T}$ was calculated as:

$$\alpha_{R,T} = \frac{r,t_w - r,t_0}{r,t_w} \cdot 100 \quad (2)$$

The area of resin adhesion to wood was calculated as a ratio of the area with intact adhesion to the area of the sample surface. The areas were measured in a graphic software (GIMP 2.10.28).

For the colour measurement, epoxy resin samples with dimensions 100x50x5 mm (length x width x height) were casted as reference samples. The cured epoxy resin layers were carefully removed from the wood samples, and the transmittance and colour coordinates of the resin layers were measured. The equipment used was a CM-5 (Konica Minolta, Tokyo, Japan) spectrophotometer, with the Colour Data Software CM-S100W Spectra MagicTNNX 2.81 (Konica Minolta, Tokyo, Japan). The measurement was performed with the specular component excluded, at 2° standard observer and a D65 illumination. The colour coordinates were expressed in the CIEL*a*b* colour space system. The total colour difference ΔE of the epoxy resin was evaluated as:

$$\Delta E = \sqrt{\Delta L^{*2} + \Delta a^{*2} + \Delta b^{*2}} \quad (3)$$

Where ΔL* is the change in lightness, Δa* is the change in parameter a* which is the green-red chromatic coordinate, and Δb* is the change in parameter b* which is the blue-yellow chromatic coordinate of the epoxy resin samples.

RESULTS AND DISCUSSION

Changes in equilibrium moisture contents (EMC) and dimensional changes of untreated and steamed beech samples are presented in Tab. 2. Since the table presents results from both preliminary and main experiments and these experiments were conducted at different relative air humidities, the corresponding EMC change is listed above each dimensional change value. The average values for the main experiment were calculated by combining FHW and SW data, since there was very little difference between the dimensional changes of FHW and SW.

Table 2: EMC changes, swelling and shrinking of the beech wood samples

		Statistical characteristics	Swelling		Shrinking	
			Radial	Tangential	Radial	Tangential
Untreated beech wood	EMC change		11.1→25.6%[a]		25.6→13.1%[a]	
		$\bar{x}$ [%]	3.07[a]	6.96[a]	2.94[a]	6.29[a]
		s [%]	0.98[a]	1.22[a]	0.81[a]	0.88[a]
	EMC change		5.55→14.2%		14.2→10.8%	
		$\bar{x}$ [%]	1.59	3.23	0.66	1.42
		s [%]	0.27	0.57	0.12	0.24
Steamed beech wood	EMC change		5.42→13.8%		13.8→10.4%	
	1st regime	$\bar{x}$ [%]	1.31	2.48	0.69	1.15
		s [%]	0.22	0.24	0.14	0.19
	EMC change		3.72→10.2%		10.2→7.53%	
	2nd regime	$\bar{x}$ [%]	1.46	2.51	0.67	1.11
		s [%]	0.28	0.33	0.11	0.13

Note: Average and standard deviations of values with uppercase "a" are from the preliminary experiment and were calculated from 72 measurements. Values without uppercase "a" are from the main experiment, and they were calculated from 48 measurements.

Samples treated by Mode II steaming regime reached a lower EMC than untreated samples and samples treated by Mode I steaming regime. However, the increases and decreases in the EMCs are similar for both untreated and steam treated samples: an increase around 6.5 – 8.6% during the exposure to a high RH and a decrease 2.7 - 3.4% during the exposure to a lower RH. Average values of the dimensional changes of untreated and steamed beech wood samples in the main experiment are therefore similar too. When coatings dry or harden on the wood surface, they create a system with the wood through adhesion between the solid coating film and wood. When stresses form in either wood or the solid coating film, these stresses are propagated into the other part of the system, if the adhesion between the solid coating film and wood in the system is adequate (Totemeier 2004). It is a well-known fact that wood is a hydrophilic material, while the amount of water epoxy resin can absorb is negligible in comparison to wood (Vanlandingham et al., 1999, Kovařík and Tesařová 2022). The solid layer of epoxy resin on the radial or mid-radial faces of the samples in this experiment can therefore be considered a constraint to dimensional changes of the wood. The tangential direction swelled and shrunk without constraints. Such constraint created stresses in wood during the dimensional changes, and these stresses were presented as cracks in the wood (Figure 1) and deformation of the wood-epoxy resin phase boundary (Figure 3). Figure 1 presents the end grain face of a sample from the preliminary experiment right after epoxy resin layer curing and after the first swelling.

In Figure 1, the distortion of the right-angled rectangular end grain face of the sample after the first swelling is clearly visible. The moisture stress and the one-sided swelling constraint are presented as numerous cracks in the wood running along the rays (Figure 1).

As it was already established, the moisture stress and dimensional changes in wood cause stresses to the wood-epoxy resin system especially on the phase boundary (Kovařík and Tesařová 2022, Kovařík et al. 2023, Wondmagegnehu and Legesse 2023, Zhou et al. 2025, Slováčková and Kovařík 2025). Stresses caused by various factors can affect coating adhesion and/or cohesion and provoke delamination and/or cracking. Stresses originate in coatings as a result of their adhesion to the substrate. Good adhesion is, on the one hand, indispensable for adequate substrate protection, but on the other hand it prevents the normal movement of a coating (Perera 1995).

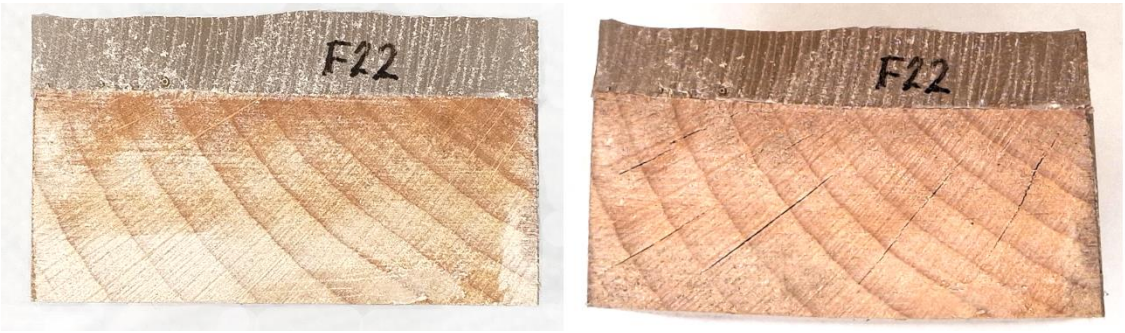

Figure 1: End grain face of a preliminary experiment sample right after epoxy resin curing (reference, on the left) and after first swelling (on the right)

Another form in which the moisture stress presented in the wood-epoxy resin samples was deformation in the phase boundary between the epoxy resin layer and wood. Because of the dimensional changes of the wood samples, the epoxy resin layer partially detached from the wood. A complete detachment of the epoxy resin layer from the wood did not happen in any sample set. The loss of the adhesion area in both experiments is presented in Figure 2.

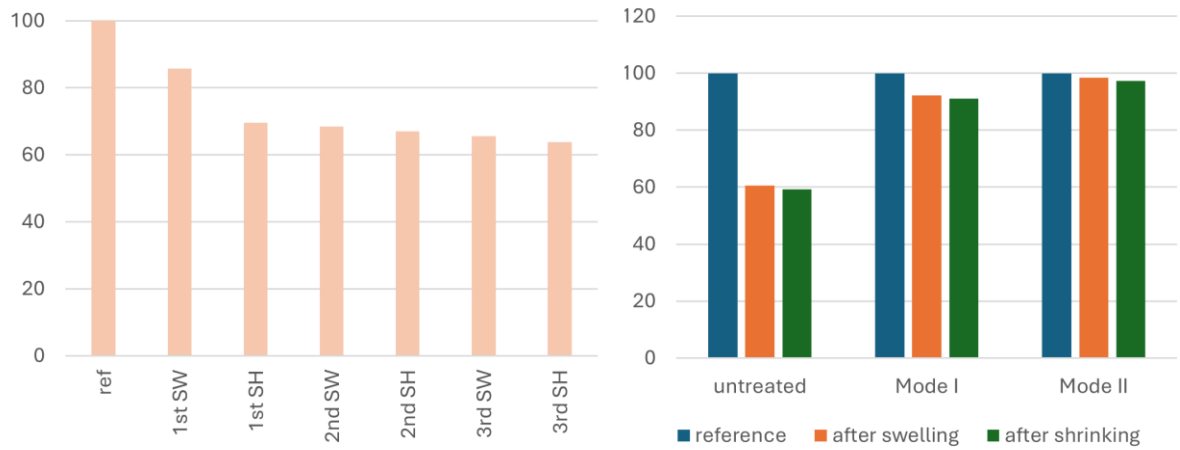

Figure 2: Loss of adhesion area in the preliminary experiment (on the left) and in the main experiment (on the right). The bars represent the intact adhesion area, SW – swelling, SH - shrinking

The largest adhesion area losses happened within the first high RH cycle; 30.35% of adhesion area was lost by the end of the first cycle in the preliminary experiment. The adhesion area losses by the end of the second cycle were 33.0% and by the end of the third cycle 36.2%. That is an increase of only 2.61 and 3.20% respectively (from the previous average value). It was therefore concluded that the main experiment will consist of only one humidity exposure cycle.

In the main experiment, the biggest adhesion area losses happened also after swelling (Fig. 2). The loss of adhesion after the shrinking was lower by only around 1%. Despite the similar average dimensional changes of these sample sets (Tab. 2), the adhesion of the epoxy resin to the samples was different for each sample treatment in the main experiment. In the main experiment, the loss of adhesion was observed in 50% of untreated samples, in 11.1% of the samples steamed by Mode I regime and in 12.5% of the samples steamed by Mode II regime. In the preliminary experiment, 79.2% of the samples recorded a loss of adhesion area. The samples in the preliminary experiment were exposed to a higher relative humidity and therefore presented higher dimensional changes, so a higher ratio of samples with detached epoxy resin layer was expected. The Mode II steamed samples retained over 95% area with intact adhesion of the epoxy resin to the substrate, which was the highest among the sample sets. The area with intact adhesion was the lowest in untreated beech samples, the area dropped to around 60% after the exposure to a high relative humidity. Progress of the adhesion area loss or delamination of the epoxy resin from the wood is presented in Figure 3.

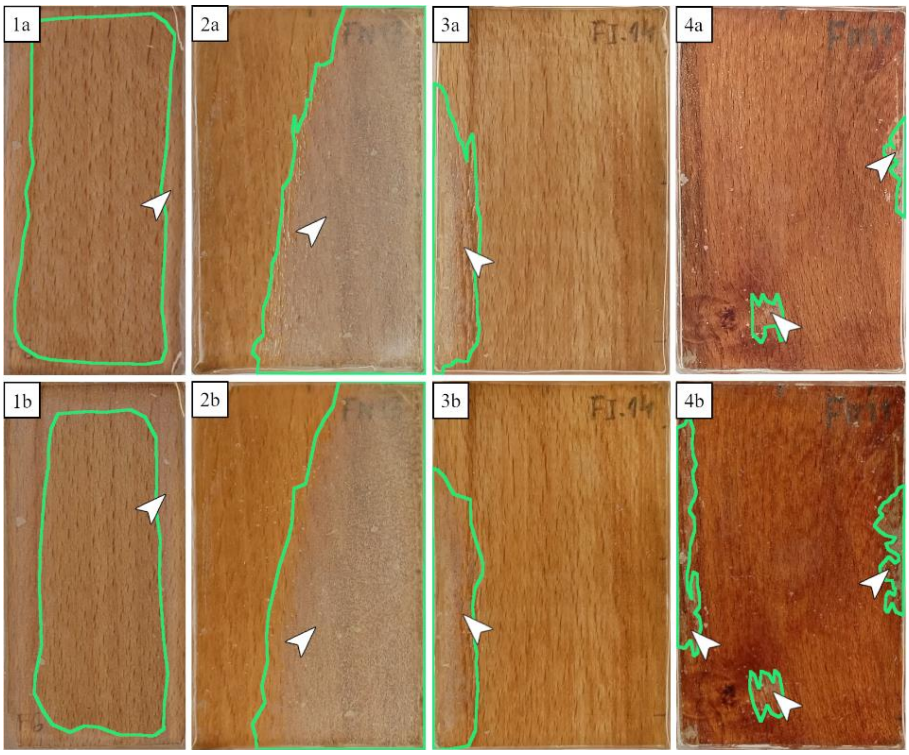

Figure 3: Detachment of the epoxy resin layer from the wood. 1a and 1b are untreated samples in the preliminary experiment, 2a and 2b are untreated samples in the main experiment, 3a and 3b are samples treated with Mode I regime and 4a and 4b are samples treated with Mode II regime. "a" are images after swelling, "b" after shrinking

The white arrowheads with black outline point to the detached area, the area is outlined with the green line. Different patterns of detachment can be seen in Figure 3. The preliminary experiment samples showed delamination starting along both longer sides of the samples. The delamination usually spread along the entire circumference of the sample, starting multiple sites of detachment, as can be seen in Figure 3, 1a and 1b. A different epoxy resin was used for the main experiment, and it is assumed that this is the reason for the different delamination pattern. The detachment started usually on only one longer side of the samples and spread along the radial direction of the wood (Figure 3, 2a and b, and 3a and b). In Figure 3, 4a and b, there is a delamination site further from the edge of the sample. A knot is present near this site, the wood grain has therefore a different direction, which is the cause for this type of delamination.

Steaming of wood changes many of its properties in a complex way (Fengel and Wegener 1989, Sundqvist et al. 2006, Varga and van der Zee 2008, Yin et al. 2011, Kaygin et al. 2014, Rautkari et al. 2014, Dzurenda 2014, Geffert et al. 2017, Novák et al. 2020, Klement et al. 2025). The change in properties of steamed wood can affect the adhesion of coatings to steamed wood in comparison to untreated wood (Slováčková et al. 2026). According to the last cited authors, beech wood steamed with Mode II regime had a lower average surface free energy in comparison to untreated beech wood and beech wood steamed by Mode I. Despite that, the disperse component of the surface free energy of the beech wood steamed by Mode II was notably higher than its polar component, and the average value of the disperse surface free energy component was higher than in Mode I steamed beech wood. According to Kovařík (2025) the adhesion of epoxy resin to wood is high, owing especially to the high disperse surface free energy component. When the same surface free energy components of the substrate and of the coating are of similar values, an excellent adhesion between the substrate and the coating film is expected (van Acker et al. 2023). This is presented in Figures 2 and 3, 4a and b for the Mode II steamed beech wood. Despite similar dimensional and moisture content changes of these samples, the adhesion of epoxy resin was the highest among the sample sets, because of the high disperse surface free energy components of the wood and the epoxy resin.

Yellowing of the resin was noticed after both experiments were concluded. The epoxy resin layers were carefully removed from the wood, and the colour of the epoxy resin was measured and the total colour difference ΔE was calculated. As reference samples, epoxy resin samples were casted. The colour of the reference epoxy resin samples was measured right after the samples cured completely. The results are presented in Table 3.

Table 3: Colour coordinates and total colour differences of the epoxy resin

Epoxy resin type	Substrate and treatment	Colour coordinate	Colour coordinate values		Total colour difference
			Reference	After humidity cycles exposure	
Bisphenol A type epoxy resin	Untreated beech wood	L*	96.4 (1.50)	89.0 (1.28)	14.8
		a*	0.39 (0.14)	-2.45 (0.23)	
		b*	0.47 (0.15)	13.0 (0.66)	
Bisphenol F type epoxy resin	Untreated beech wood	L*		89.2 (2.48)	8.28
		a*		-0.35 (0.22)	
		b*		5.93 (1.06)	
	Beech wood steamed with Mode I	L*	95.9 (0.30)	89.6 (2.36)	7.85
		a*	-0.21 (0.03)	-0.35 (0.24)	
		b*	1.08 (0.14)	5.79 (1.21)	
	Beech wood steamed with Mode II	L*		88.5 (2.24)	9.36
		a*		-0.43 (0.17)	
		b*		6.87 (0.65)	

Note: 24 measurements per sample set were performed, 4 samples per set were used. Average values are presented; standard deviations are listed in the round brackets.

The colour of bisphenol A type resin was measured after the beech wood-epoxy resin samples were stored for 15 months in darkness, exposed to 3 humidity cycles. Lightness of these samples decreased substantially, as well as colour coordinate a* value. The colour coordinate b* value increased noticeably; overall the colour of bisphenol A type resin shifted from achromatic towards greener and more noticeable yellow colour. The total colour difference value in this resin was the highest among the sample sets.

The colour of the bisphenol F type resin samples was measured after the samples were stored for 9 months in darkness, and they were exposed to one humidity cycle. The lightness of the bisphenol F type epoxy resin samples decreased, the average values are about the same as L* values of the bisphenol A type epoxy resin. The colour coordinate a* values decreased only faintly in the bisphenol F type resin, while the b* values increased noticeably. The average a* values are about the same for the three sample sets. The average b* values are about the same for epoxy resin samples which were casted on untreated and Mode I steam treated beech samples. For the epoxy resin casted on the Mode II steam treated beech samples, the average b* value was higher than in the other sample sets. The total colour difference in the epoxy resin samples casted on the Mode II samples is therefore also the highest among the bisphenol F type sample sets. To confirm whether this difference is significant, a one-way ANOVA analysis was performed on the b* data. The p-value was 0.00052, which showed that the average b* values of the epoxy resin samples casted on Mode II steamed beech wood are significantly different from the other two sample sets.

Various types of resins are known to yellow due to a variety of factors – UV radiation (Tennent 1979, Cabral-Fonseca et al. 2012, Wang et al. 2017, Wu et al. 2022), oxygen (Buch and Shanahan 2000), moisture and temperature (Ksouri and Haddar 2018, Wu et al. 2022), resin type (Fiorentino and Borelli 1975), curing agents (Down 1984, 1986) or even additives (Tennent 1979). The question, whether the difference of the particular epoxy resins used in this experiment was caused by a chemical reaction between the epoxy resin and the beech wood and/or in combination with other factors, arises.

CONCLUSIONS

The main goal of this article were interactions on the wood-epoxy resin phase boundary during moisture content and dimensional changes of the wood. Untreated and steamed beech wood were selected for the experiment.

Beech wood samples steamed with Mode II regime reached lower average equilibrium moisture contents than the other samples, however the dimensional changes were about the same as in other sample sets. Despite similar dimensional changes, the Mode II steam treated samples showed the best phase boundary stability. The ratio of samples with epoxy resin delamination from the substrate was very low in this sample set and the area with intact adhesion remained the highest. The worst wood-epoxy resin phase boundary stability was in untreated beech wood samples. These samples also had the highest ratio of samples with partially detached epoxy resin layer and the area with loss of adhesion was also the highest among the sample sets. The exceptional phase boundary stability was the result of similar surface free energies components.

The colour of the epoxy resin changes during the storage in a dark room and exposure to high relative air humidity. In both epoxy resin types, the lightness decreased and the colour shifted towards a greener and noticeably yellower colour.

ACKNOWLEDGEMENTS

This work was supported by the Slovak Research and Development Agency under the contract No. APVV-21-0051 “Research of False Heartwood and Sapwood of Fagus sylvatica L Wood in Order to Eliminate Color Differences by the Process of Thermal Treatment with Saturated Water Steam” and by the Scientific Grant Agency of the Ministry of Education, Science, Research and Sport of the Slovak Republic, VEGA contract number 1/0599/25 “Účelová zmena vlastností dreva pôsobením rôznych foriem energie pre efektívne spracovanie dreva a dlhodobú trvanlivosť drevených výrobkov” (The intentional change of wood properties by the action of energy various forms for efficient wood processing and long-term durability of wooden products).

REFERENCES

Bilyeu B, Brostow W, Menard K P (1999) Epoxy Thermosets and Their Applications I: Chemical Structures and Applications. J. Mater. Educ. 21(5&6):281-286.

Buch X, Shanahan M E R (2000) Thermal and thermo-oxidative ageing of an epoxy adhesive. Polym. Degrad. Stabil. 68(3):403–411. https://doi.org/10.1016/S0141-3910(00)00028-8

Cabral-Fonseca S, Correia J, Rodrigues M, Branco F (2012) Artificial accelerated ageing of GFRP pultruded profiles made of polyester and vinylester resins: characterisation of physical-chemical and mechanical damage. Strain 48:162–173. https://doi.org/10.1111/j.1475-1305.2011.00810.x

Deka M, Saikia C N (2000) Chemical modification of wood with thermosetting resin: effect on dimensional stability and strength property. Bioresource Technology 73:179–181. https://doi.org/10.1016/s0960-8524(99)00167-4

Dieste A, Krause A, Bollmus S, Militz H (2008) Physical and mechanical properties of plywood produced with 1.3-dimethylol-4.5-dihydroxyethyleneurea (DMDHEU)-modified veneers of Betula sp. and Fagus sylvatica. Holz Als Roh- Werkstoff 66:281. https://doi.org/10.1007/s00107-008-0247-3

Down J L (1984) The yellowing of epoxy resin adhesives: report on natural dark aging. Stud. Conserv. 29(2):63–76. https://doi.org/10.1179/sic.1984.29.2.63

Down J L (1986) The yellowing of epoxy resin adhesives: report on high-intensity light aging. Stud. Conserv. 31(4):159–170. https://doi.org/10.2307/1506247

Dzurenda L (2014) Colouring of Beech Wood during Thermal Treatment using Saturated Water Steams. Acta Fac Xylologiae Zvolen 56(1):13–22. https://df.tuzvo.sk/sites/default/files/02-1-14-dzurenda_1.pdf

Fengel D, Wegener G (1989) Wood: Chemistry, Ultrastructure, Reactions. Walter de Gruyter: Berlin, Germany, 1989; p. 613; ISBN 978-3-11-008481-8.

Fiorentino P, Borrelli L V (1975) A preliminary note on the use of adhesives and fillers in the restoration of ancient materials with special reference to glass. Stud. Conserv. 20(4):201–205. https://doi.org/10.1179/sic.1975.20.4.020

Frihart C R (2005) Wood adhesion and adhesives. Handbook of wood chemistry and wood composites. Boca Raton, Florida: CRC Press, 2005, pp. 215-278.

Geffert A, Výbohová E, Geffertova, J (2017) Characterization of the changes of colour and some wood components on the surface of steamed beech wood. Acta Fac. Xylologiae Zvolen 59(1):49–57. https://df.tuzvo.sk/sites/default/files/05-01-17_3_0_0_1_1_0_0_0_0_0_0_0_0.pdf

Guo D, Guo N, Fu F, Yang S, Li G, Chu F (2022) Preparation and mechanical failure analysis of wood–epoxy polymer composites with excellent mechanical performances. Composites Part B: Engineering, 235, 109748. https://doi.org/10.1016/j.compositesb.2022.109748

Hill C (2006) Wood Modification: Chemical, Thermal and Other Processes. John Wiley & Sons 2006. https://doi.org/10.1002/0470021748

Homan W J, Jorissen A J M (2004) Wood modification developments. Heron 49(4): 361 – 385.

Kaygin B, Koc K H, Hiziroglu S (2014) Surface quality and hardness of eastern redcedar as function of steaming. J. Wood Sci. 60:243–248. https://doi.org/10.1007/s10086-014-1399-x

Klement I, Vilkovská T, Vilkovský P, Uhrín M (2025) Comparison of Pressure and Atmospheric Steaming Processes and Their Effects on Selected Properties of Beech Wood (Fagus sylvatica L.). Appl. Sci. 15(24):13066. https://doi.org/10.3390/app152413066

Kovařík R (2025) Vybrané vlastnosti materiálov na báze dreva a epoxidových živíc a ich povrchová úprava. PhD. dissertation. Zvolen: Technical University at Zvolen. Faculty of Wood Sciences and Technology. (in Czech)

Kovařík R, Tesařová D (2022) Surface treatment of composite materials based on epoxy casting resins and solid wood. In: XV. Konference pigmenty a pojiva: sborník/Conference Proceedings. Pardubice: Chemagazín, 2022, pp.71-79.

Kovařík R, Tesařová D, Kúdela J (2023) Analysis of durability characteristics of composite material based on epoxy casting resins and solid wood with focus on surface finish. In: XVI. Konference pigmenty a pojiva: sborník/conference proceedings. Pardubice: Chemagazín, 2023, pp. 66-74.

Ksouri I, Haddar N (2018) Long term ageing of polyamide 6 and polyamide 6 reinforced with 30% of glass fibers: temperature effect. J. Polym. Res. 25(7):12. https://10.1007/s10965-018-1551-1

Kumosa M S (2006) Damage Mechanisms in Polymer Matrix Composites in Extreme Environments. Key Engineering Materials. Vol. 324–325, pp. 663–666. Trans Tech Publications, Ltd. https://doi.org/10.4028/0-87849-413-8.663

Kurjatko S, Kúdela J, Lawniczak M, Lübke H (1987) Modifikácia imisného smrekového dreva metylmetakrylátom a styrénom. Modyfikacja drewna '87. Rydzyna, AR Poznań, pp. 156–166. (in Slovak)

Kúdela J, Čunderlík I (2012) Bukové drevo – štruktúra, vlastnosti, použitie. Technical University at Zvolen, Zvolen. ISBN 987-80-228-2318-0 (in Slovak)

Liptáková E, Kúdela J, Paprzycki O (1991) The adhesion of polystyrene to wood. Holz als Roh-Werkstoff 49(1):31–37. https://doi.org/10.1007/bf02627548

Novák I, Kleinová A, Janigová I, Mičušík M, Sedliačik J, Šlouf M, Bekhta P, Matyšovský J, Jurkovič P (2020) Properties of Water Steam-Treated Maple Wood (Acer pseudoplatanus L.). Wood Res. 65(6):865–876. https://doi.org/10.37763/wr.1336-4561/65.6.865876

Perera D Y (1995) Stress Phenomena in Organic Coatings. In: Paint and Coating Testing manual, 1995, 513 – 524, 14th edition of the Gardner – Sward Handbook, ed. Joseph V. Koleske.

Rautkari L, Honkanen J, Hill C A S, Ridley-Ellis D, Hughes M (2014) Mechanical and physical properties of thermally modified Scots pine wood in high pressure reactor under saturated steam at 120, 150 and 180 ◦C. Eur. J. Wood Wood Prod. 72:33–41. https://doi.org/10.1007/s00107-013-0749-5

Reinprecht L (2016) Wood Deterioration, Protection and Maintenance. John Wiley & Sons, p. 357.

Sandberg D, Kutnar A, Karlsson O, Jones D (2021) Wood Modification Technologies: Principles, Sustainability, and the Need for Innovation, 1st ed.; CRC Press: Boca Raton, FL, USA. https://doi.org/10.1201/9781351028226-1

Slováčková B, Kovařík R (2025) Deformation of wood-resin phase boundary by moisture content changes in wood. Acta Fac Xylologiae Zvolen 67(1):89 – 100. https://doi.org/10.17423/afx.2025.67.1.08

Slováčková B, Dudiak M, Schmidtová J (2026) Evaluation of Wettability, Surface Free Energy, and Janka Hardness of Steamed Beech Wood. Appl Sci 16:4346. https://doi.org/10.3390/app16094346
Spear M J, Curling S F, Dimitriou A, Ormondroyd G A (2021) Review of Functional Treatments for Modified Wood. Coatings 11:327. https://doi.org/10.3390/coatings11030327
Stamm A J, Seborg R M (1943) Resin treated wood (Impreg). USDA Forest Service Forest Products Laboratory Report No. 1380. Madison, WI.
Stamm A J, Seborg R M (1944) Resin treated laminated compressed wood (Compreg). USDA Forest Serv. Forest Prod. Lab. Rep. No. 1381, Madison, WI.
Sundqvist B, Karlsson O, Westermark U (2006) Determination of formic-acid and acetic acid concentrations formed during hydrothermal treatment of birch wood and its relation to color, strength and hardness. Wood Sci. Technol. 40:549–561. https://doi.org/10.1007/s00226-006-0071-z
Tennent N H (1979) Clear and pigmented epoxy resins for stained glass conservation: light ageing studies. Stud. Conserv. 24(4):153–164. https://doi.org/10.2307/1505777
Totemeier T C, Wright R N, Swank, W D (2004) Residual Stresses in high-velocity oxy-fuel metallic coatings. Metall Mater Trans A 35:1807–1814. https://doi.org/10.1007/s11661-004-0089-5
van Acker J, van der Bulcke J, Forsthuber B, Grüll G (2023) Wood Preservation and Wood Finishing. In: Springer Handbook of Wood Science and Technology, (eds) Niemz P, Teischinger A, Sandberg D, Springer Cham, Cham, Switzerland, pp 793-872. https://doi.org/10.1007/978-3-030-81315-4
Vanlandingham M R, Eduljee R F, Gillespie J R (1999) Moisture diffusion in Epoxy Systems. J. Appl. Polym. Sci., 71(5): 787-798. https://doi.org/10.1002/(SICI)1097-4628(19990131)71:5<787::AID-APP12>3.0.CO;2-A
Varga D, van der Zee M E (2008) Influence of steaming on selected wood properties of four hardwood species. Holz Roh-Werkst. 66:11–18. https://doi.org/10.1007/s00107-007-0205-5
Wang G, Sun Y, Wang X, Jiang W (2017) Effect of UV irradiation on glass fiber reinforced unsaturated polyester resin composite under warm-wet environment. Mater. Mech. Eng. 41(7):34–38, 42. https://10.11973/jxgccl201707007
Wondmagegnehu B T, Legesse A A (2023) Experimental Investigation of Mechanical and Physical Properties on Epoxy Resin with Wood Timber for Furniture Application. J. Nat. Fibers 20(2): 2286327. https://doi.org/10.1080/15440478.2023.2286327
Wu C, Meng B C, Tam L, He L (2022) Yellowing mechanisms of epoxy and vinyl ester resins under thermal, UV and natural aging conditions and protection methods. Polym. Test. 114:107708. https://doi.org/10.1016/j.polymertesting.2022.107708
Zhou A, Li K, Yang G, Liu T, Qin R, Zou D (2025) Effect of temperature and humidity on the mechanical behavior of basalt FRP bonded wood under sustained load: An experimental and atomistic study. J. Build. Eng. 104:112325. https://doi.org/10.1016/j.jobe.2025.112325
Yin Y, Berglund L, Salmén L (2011) Effect of Steam Treatment on the Properties of Wood Cell Walls. Biomacromolecules 12(1):194–202. https://doi.org/10.1021/bm101144m

Session IV
-
Hardwood Processing and Modification Technologies

Effect of Anhydrides Modification on the Properties of Plantation Rubber (*Hevea brasiliensis*), Acacia (*Acacia* spp.), and Oil Palm (*Tinnera* spp.) Trees Grown in Peninsular Malaysia

Norul Hisham Hamid[1,2*], Mohd. Afiq Mokhtar[1], Ummi Hani Bin Abdullah[1,2], Paiman Bawon[1*]

[1] Department of Wood and Fibre, Faculty of Forestry and Environment, Universiti Putra Malaysia, 43400, UPM, Serdang, Selangor Darul Ehsan
[2] Institute of Tropical Forestry and Forest Product, Universiti Putra Malaysia, 43400, UPM, Serdang, Selangor Darul Ehsan.

E-mail: h_noroul@upm.edu.my; ummi@upm.edu.my; paiman@upm.edu.my

Keywords: plantation; rubber wood; acacia wood; modification; anhydrides; properties.

ABSTRACT

The microstructure, physical and mechanical properties of Rubber, Acacia, and Oil palm woods reacted with acetic, propionic, and butyric anhydrides were studied. Samples dimension of 300mm×100mm×25mm (*L*×*W*×*T*) were impregnated with the anhydrides followed by microwave heated for 4 minutes. This study found that no damage occurred to the cell wall structures during the modification procedure as observed by the scanning electron microscope (SEM). The basic properties such as density increment and void volume changes were not significantly different with the anhydrides. The compression strength was improved in modified rubberwood and acacia, but not in modified oil palm wood. The hardness was not improved with either treatment with anhydride and this trend was consistent with all wood species. Generally, the highest improvement in mechanical properties was obtained by modification of Rubber and Acacia woods with butyric anhydride.

INTRODUCTION

Rubberwood, acacia and oil-palm wood are three wood species that has abundant resources in Malaysia. The resource is ready able and sustainable. However, these three wood species need to undergo pre-treatment processes to make it possible to be used especially outdoor applications. For example, rubberwood need to be treated with wood preservatives such as Copper Chrome Arsenic (CCA) and creosote to improve its decay resistance, dimensional stability, strength and durability. As well as acacia and oil-palm wood, which need to be coated, apply wax during forming process for reconstituted woods or impregnation with phenolic resin to enhance the performance of wood. However, such treatments are not permanent, which the coating may be failed by cracking, the chemical leach out and erode during the lifetime of the product. The loss of performance occurs because the treating agent is not chemically bonded to or otherwise immobilized within the wood structure (Rowell et al. 1994). During the lifetime of the treated product may be a very low hazard associated with in service use, this may well change at the end of life of the product. Therefore, potential loss of the preservative into the environment may become a problem in disposal or recycling situations. When this occurs, the biocidal action of the preservatives remains and this can cause a negative impact to the environment.

Chemical modification of wood can be defined as any chemical reaction between some reactive part of a wood cell wall component and a simple single chemical reagent, with or without catalyst that forms a covalent bond between the two components (Rowell 1991). The chemicals are including acetic, butyric and propionic anhydrides. Chemical modification of wood by using acetic anhydride is called acetylation and has been extensively studied all over the world. It has been reported that acetylation is a very effective way for enhancing wood properties. Wood properties can be improved considerably by converting hydrophilic hydroxyl (OH) groups into larger more hydrophobic groups. Dimensionally stable of material is created because the cell wall itself will be permanently in swollen state that will attract no or very little water (Homan and Jorissen 2004).

Chemical modification of wood with anhydride provides a process that alters the properties of the material such that during the lifetime of a product no loss of the enhanced performance of the wood should occur. These modification processes with anhydride requires a lot of time using conventional heating to acquire the optimum properties wood and obtain maximum performance possible. However, using microwave, the reaction temperature of 120-130°C can be reached in a comparatively short time and provide a uniform heating.

Acetic anhydride has been widely used in chemical modification experiments and the results compared to other chemical were also better while wood treated with anhydride leave no harm to the environment (Rowell 2006). Wood treated with anhydride provides consistent and optimum result for Anti-Swelling Efficiency (ASE) and biological resistance. However, the effect of modification on strength properties such as static bending, compression, hardness and impact strength were dependent on the degree of modification as well as species.

Recent studies by Larsson and Simonson (1999) reported that, microwave heating can be used for the acetylation of wood in lumber thickness which aimed to reduce reaction time and to provide a uniform heating pattern in wood. However, chemical modification using a microwave heating has not been studied on rubberwood, acacia and oil palm wood. The reaction of these woods with anhydrides and its effect on anatomy, chemical structure, dimensional stability, physical and mechanical properties are still not completely known. A specific research on this subject is crucially needed so that these woods can be used beyond its natural limits.

The aim of this study is to modify rubberwood (*Hevea brasiliensis*), acacia (*Acacia mangium*) and oil-palm wood (*Elaeis guineensis*) with carboxylic acid anhydrides (acetic anhydride, butyric anhydride and propionic anhydride). The target output from this research is not only to help releasing the great demands of timber from natural forest but also to promote the use of low quality wood as a main material for high end furniture and building materials.

METHODOLOGY

Preparation and selection of samples

Rubberwood (*Hevea brasiliensis*), aged 25 to 30 years, acacia (*Acacia mangium*), aged 5 to 7 years old and oil palm (*Elaeis guineensis*), aged more than 25 years old was studied. The rubberwood were obtained from a local rubberwood furniture factory at Semenyih, Selangor, acacia from pallet factory at Jalan Reko, Kajang, Selangor, and oil-palm wood from Felda Jengka 25, Pahang. A total of 60 samples consist of 45 modified and 15 unmodified samples was used.

Rubberwood and acacia samples were received in the form of sawn timber while the oil palm samples were in log form. Rubberwood and acacia samples were cut into desired dimension of 300 × 100 × 25 mm (length (L) x width
(W) x thickness (T)) for modification process. After trimmed, the samples were oven dried until it reaches 8 to 10% MC. The method of drying samples before reaction process was adapted from Militz (1994) and Rowell et al. (1990).

Selection of chemicals

Acetic anhydride, propionic anhydride and butyric anhydride were used in this study for the reaction procedure. The chemicals were bought from a Europe company called Sigma-Aldrich Co. LLC. All of the chemical were used as supplied without further purification (neat) and the chemicals were analytical reagent grade.

Impregnation procedure

The impregnation process was conducted using a vacuum-pressure impregnation process. The samples were arranged separately by species and anhydride. They were submerged in anhydrides, ballasted with brick wrapped with aluminium-foil in a steel container. The container contained submerged sample was inserted in the vacuum vessel. The vacuum was applied for 20 minutes using a vacuum machine and slowly released to allow the atmospheric pressure occurred. After vacuum process, additional pressure was applied using air-compressor at 0.8 MPa for 30 minutes. To make sure that the samples were fully impregnated with the anhydride, the samples were re-pressured again for another 15 minutes.

Reaction procedure

The Panasonic Microwave NN-CD997S with 2450MHz frequency and 50W output was used in this study. The impregnated wood was transferred into microwave and the reaction was conducted for 2 and 4 minutes. After 2 minutes, the reacted wood was taken out from microwave to measure its weight and volume and then it was reacted again for another 2 minutes. This procedure was to minimize the damage/crack to the samples. It was previously observed that the crack occurred when the wood reacted for more than 4 minutes (Figure 3.9). The method of reaction procedure using microwave was adapted from Chang and Chang (2003).

Post treatment

After the reaction procedure, the modified wood were submerged in a steel container contained a cold acetone for 24 hours to stop the reaction. The acetone was removed and the container with reacted wood was vacuumed again to remove any unreacted anhydride and other residues using the impregnation chamber. Finally, the modified woods were oven-dried at 70°C for 24 hours to determine its WPG. This method was adapted from Obataya (2005).

Confirmation of bonding

SEM observation

Scanning electron microscopy (SEM) was used to observe the structure of modified and unmodified woods. The SEM analysis was performed at the Institute of Bio-science, UPM, Serdang. The specimens 10mm x 10mm x 10mm (L x T x W) were prepared from all modified and unmodified wood. The specimen surface was then cut with a sharp razor- blade to get a smooth surface. The specimen was oven dried at 70°c overnight to ensure a clear image was obtained during the SEM observation. Scanning electron microscope was performed using PHILIPS XL30 ESEM. A total of 12 clear images were selected for a comparison purpose.

Determination of basic properties of modified wood

Solution uptake (SU)

The amount of anhydrides uptake was calculated by comparing the weight of sample before and after impregnation process. The amount of anhydrides uptake was expressed as solution uptake (SU) (%) and was calculated as the following formula (3.1) (Rowell 1991).

$$Solution\ uptake\ (SU)\ (\%) = [(W_1 - W_0)/W_0] \times 100$$

Where, W_1= weight of sample after impregnation.
W_0= weight of sample before impregnation.

Weight percent gain (WPG)

In order to determine the WPG, the initial weight of oven dried sample before modification was recorded. The oven dried weight of the same sample after modification was also noted. Then, the WPG can be calculated using the following formula (3.2) (Hill 2006).

$$Weight\ percent\ gain\ (WPG)\ (\%) = [(M_m - M_u)/M_u] \times 10$$

Where, M_m= oven-dry weight of sample after modification.
M_u= oven-dry weight of sample before modification.

Determination of physical properties of modified wood

Density increment

The density of the sample before and after modification was determine to calculate the density increment for each modified wood samples. The density and density increment was calculated using the following formula.

$$Density\ (kg/m^3) = W/V$$

Where, W= weight of sample before or after modification
V= volume of sample before or after modification.

$$Density\ increment\ (\%) = [(D1 - D0)/D0] \times 100$$

Where, D_1= density of wood after modification
D_0= density of wood before modification.

Void volume changes

The void volume was calculated to measure the void volume of the wood before and after modification take place. The void volume of wood before and after modification; and percent void volume changes were calculated as the formula adapted from Bowyer et al. (2003).

$$Void\ volume\ (\%) = [\ (1- (SG_{od}/1.5)\ ]\ x\ 100$$

Where, SG_{od}= specific gravity of wood before or after modification.

Then,

$$void\ vol.\ changes(\%) = [(VM_m - VM_{um})/\ VM_{um}]\ x\ 100$$

Where, VM_m= void volume of wood after modification
VM_{um}= void volume of wood before modification.

Determination of mechanical properties of unmodified and modified wood

Compression

The compression strength parallel to the grain of unmodified and modified specimens was tested according to the BS 373:1957 standard. The specimen dimension of 60mm x 20mm x 20mm (L x W x T) was prepared and the test was conducted at crosshead speed of 0.06350cm/min. The test piece was placed vertically parallel to the grain along the load direction. The load moved downward and pressed the specimen until it was cracked. The data was automatically calculated by the control panel of the testing machine. The compression strength can also be calculated using following formula:

$$Compression\ strength\ (CS)\ (MPa) = Pm/A$$

Where, Pm= load at maximum limit proportionally (N)
A= area of cross-sectional to the direction of load (mm^2).

Hardness

The hardness strength was tested using the Janka indentation test according to the BS 373:1957 standard for the unmodified and modified specimens. The test required the determination of the load necessary to force into the test piece to a depth of 0.564cm by a hemispherical end of a steel ball with diameter of 0.005cm. The specimen dimension of 60 mm x 20 mm x 20 mm (L x W x T) was placed at the center of a solid wood plank designed for this test. The rate of penetration of the hardness tool was 0.635cm/min. Once the test was started, the pin was pull and push constantly towards and backwards horizontally until the test cycle was completed. The data of hardness strength was automatically calculated by a computer. The data collected from all the experiments were analysed with analysis of variance (ANOVA) and the Duncan (post hoc test) at 95% confident level. All the analysis was done by using SPSS (version 22).

RESULT AND DISCUSSION

Confirmation of bonding

Scanning Electron Microscopy (SEM) Observation

The SEM observation focused on the cross sectional area of the unmodified and modified specimens. The SEM observation images were shown in Figure 1 (unmodified and modified rubberwood).

The SEM observation indicates that the cell walls were slightly thickened in modified rubberwood with acetic, propionic and butyric anhydrides compared to the unmodified (Figure 1). Similar behaviour can be seen for the acacia and oil palm. The cell wall swelling due to acetylation was also reported by Sander et al. (2003). The images shows that the chemical modification of wood using microwave did damage the cell walls of any wood species**.** Sander et al. (2003) also reported that acetylation procedure did not damage the wood cell wall.

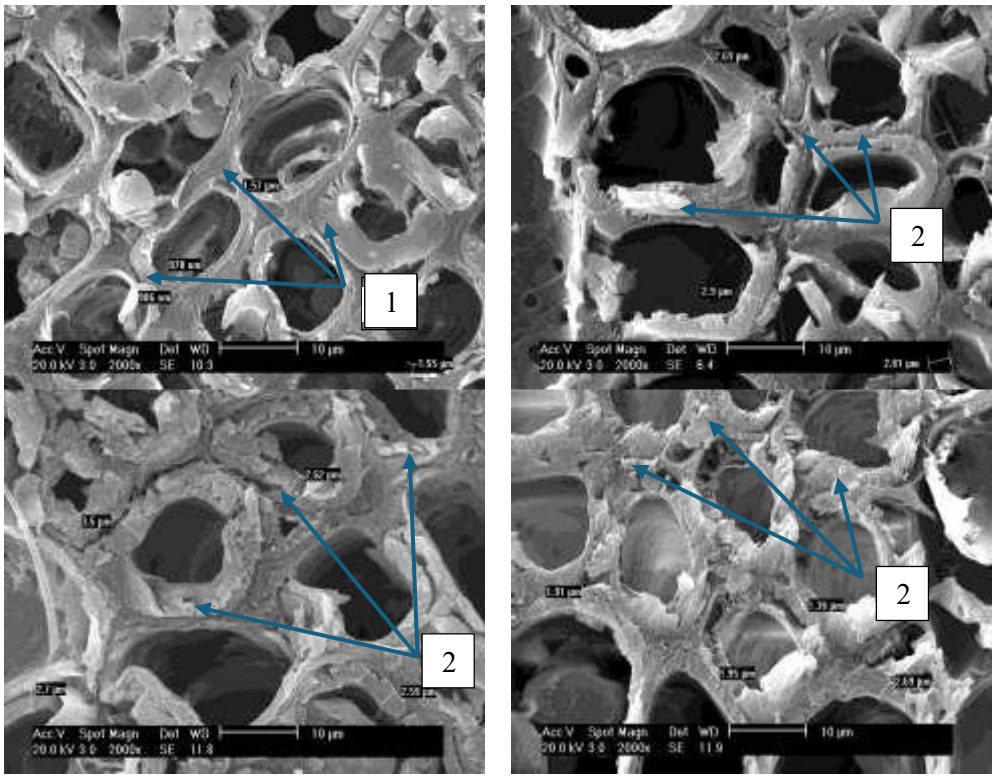

Figure 1: The SEM images of cross-sectional view of rubberwood. (a)=unmodified rubberwood, (b)=acetylated rubberwood, (c)=propionylated rubberwood and (d)=butyrylated rubberwood. Arrows indicate the smooth (1) and rough (2) surfaces

Basic properties of modified woods

Summary of analysis of variance (ANOVA) results show that the basic properties of modified wood were varied with species (Table 1). Regardless of anhydride, the solution uptake and WPG were not significantly different for rubberwood, but not for the BC. However, all the basic properties were not significantly different for acacia. In contrast, only WPG was significantly different for oil palm wood but not for the SU and BC.

Table 1: Summary of ANOVA of basic properties of modified wood

Basic properties	df	F	p-value
Rubberwood			
Solution uptake	2	0.231	0.799Ns
Weight percent gain	2	0.578	0.581Ns
Acacia			
Solution uptake	2	0.393	0.686Ns
Weight percent gain	2	2.791	0.114Ns
Oil palm wood			
Solution uptake	2	2.906	0.145Ns
Weight percent gain	2	10.373	0.011*

*Ns: not significant; *: significant at p<0.05; **: significant at p<0.01*

Solution uptake (SU)

Regardless of anhydrides (Figure 2, left), the oil palm wood wood took up the highest anhydride solutions followed by rubberwood and acacia, which indicates its highest permeability. In oil palm wood, the solution uptake were not significantly different where butyric anhydride took up 127.8% of solution uptake followed by propionic anhydride 123.6% and 114.5% for acetic anhydride. The percent void volume in oil palm wood was highest among the three species which leads to its higher solution uptake. In rubberwood, the solution uptake was not significantly different with the anhydrides. The averages were 75.8% for acetic anhydride, 72.8% for propionic anhydride and 74.2% for butyric anhydride. In acacia, the solution uptake was also not significantly different with anhydrides ranging from 23.3% for acetic anhydride, and 24.5% for propionic anhydride and 24.2% for butyric anhydride. This indicates that the molecular weight of anhydrides did not influenced the uptake all species.

Weight percent gain (WPG)

In contrast to uptake, the WPG (Figure 2, right) was highest in rubberwood followed by oil palm wood and acacia with regardless of anhydride. This generally means that the reactivity of rubberwood with anhydrides were greater than acacia and oil palm wood. Chemical modification of wood can be defined as any chemical reaction between some reactive part of a wood cell wall component and a simple single chemical reagent, with or without catalyst that forms a covalent bond between the two components. Therefore, the amount of chemical constituents for each wood species influenced the WPG. Among the structural chemical component, cellulose was the fastest react with acetic anhydride followed by hemicelluloses and lastly lignin (Rowell 1980, 1982 and 1984). However, Stamm (1964) estimated that, only 35% of OH groups in amorphous cellulose are accessible for reaction and the remaining 65% is inaccessible crystalline cellulose.

The highest WPG obtained in rubberwood was probably be caused by its higher hemicelluloses and lignin contents as compared to Acacia and oil palm wood. Regardless of anhydrides, the averages WPG was ranging from 39 to 42.2% for rubberwood, from 9.7 to 14.7% for acacia and from 19.6 to 26.3% for oil palm wood. This indicates that the anhydrides molecular weight did not significantly influence the weight gain for each wood species.

For comparison, acetylation of Pine wood sized 4.5 × 12 × 14 cm (tangential × radial × longitunal) using a microwave (460 W) had a maximum 20 WPG after 200 minutes reaction (Larsson et al. 1999). Modification of hinoki wood with acetic, propionic, butyric, isobutyric, and hexanoic anhydrides using a conventional heating method gave a maximum WPG ranging from 20 to 40 after reacted at temperature of 140 °C for 24 hours (Li et al. 2000).The averages WPG of modified oil palm wood either anhydride was higher than acetylated rattan (14-15 WPG) reacted for 24 hours using conventional heating method as reported by Hamid and Hale (2012). This was probably due to lower hemicellulose (13-14.5 %) and lignin (17.3-19.4%) contents in rattan compared to oil palm wood. The lower WPG obtain by conventional heating method might be due to the uneven distribution of the heat throughout the sample.

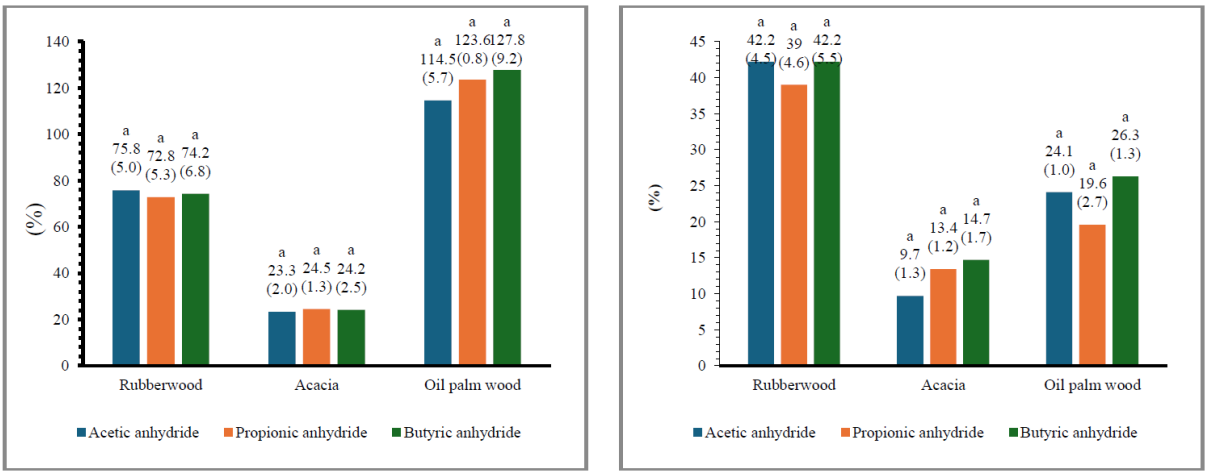

Figure 2: The solution uptake (left) and weight percent gain (right) of wood modified with different anhydride. Figures in the parentheses are standard deviations. Means followed by the same letter(s) in the same bar are not significantly different at the 0.05 probability level according to the Duncan test

Physical properties of modified woods

The summary of ANOVA results show that the physical properties of modified wood were almost identical for all wood species (Table 2). Regardless of anhydride, all of the physical properties of modified woods were not significantly different for all wood species and between the anhydride.

Table 2: Summary of ANOVA of physical properties of modified wood

Physical properties	Df	F	p-value
Rubberwood			
Density increment	2	0.431	0.659^{Ns}
Void volume changes	2	0.185	0.833^{Ns}
Acacia			
Density increment	2	0.160	0.854^{Ns}
Void volume changes	2	0.438	0.655^{Ns}
Oil palm wood			
Density increment	2	0.912	0.428^{Ns}
Void volume changes	2	0.744	0.496^{Ns}

^{Ns}: not significant; *: significant at $p<0.05$; **: significant at $p<0.01$

Density increment

The densities for all wood species were generally higher after modified with any anhydrides. The density increments were found to be not significantly different with the anhydrides for all wood species, despite a slightly higher increment in butrylated wood in Figure 3 (left). The increments were largest in rubberwood followed by oil palm wood and acacia, with regardless of anhydrides. They ranged from 25.6% to 37.5% for modified rubberwood, from 22.2% to 25.3% for modified oil palm wood and from 3.2% to 8.2% for modified acacia. This indicates that the anhydrides molecular weight did not influence the density increment of modified woods. The density increment of rubberwood were highest among the three species may probably cause by its highest WPG. The higher density increment in modified oil palm wood compared to modified acacia was probably due to the high solution uptake which leads to weight increment and result in high density. Even though oil palm wood had the highest solution uptake, however its reaction with the anhydrides was low. This was probably due to that the oil palm wood was not solvent extracted before reaction. The excess oil in the fiber and parenchyma cells may probably obstructed the reaction between structural organic chemicals and anhydrides which result in low bulking coefficient. A similar low density increment also occurred for modified acacia.

Void volume changes due to modification

The untreated oil palm wood had a higher percent void volume than those of rubberwood and acacia (Figure 3, right). The averages percent void volume was ranged from 41.57 to 45.90% for oil palm wood, from 22.80 to 26.40% for acacia and from 23.18 to 24.82% for rubberwood. This was probably due to the low density of oil palm wood as compared to rubberwood and acacia, which have more void volume theoretically. The averages percent void volume of modified wood was not significantly different with anhydrides for all species, ranging from 36.04 to 41.43% for oil palm wood, 22.53 to 27.52% for acacia and 12.03 to 13.87% for rubberwood. This indicates that the percent void volume of modified wood was not influenced by the anhydride molecular weights. The rubberwood modified with any anhydrides had the highest percent void volume changes, followed by oil palm wood and acacia. The highest BC obtained by the modified rubberwood may probably be caused by its lowest percent void volume changes. In contrast, acacia and oil palm wood obtained a lower BC probably be caused by its higher percent void volume changes. The averages percent void volume changes for modified woods were ranged from -49.64 to -42.84% for rubberwood, from -13.47 to -9.03% for oil palm wood and from -7.95 to 22.51% for acacia. The percent void volume changes for rubberwood and Oil palm wood modified with anhydrides were higher than those of acetylated rattan (ranged from -10.1 to 8.8) as reported by Hamid and Hale (2012).

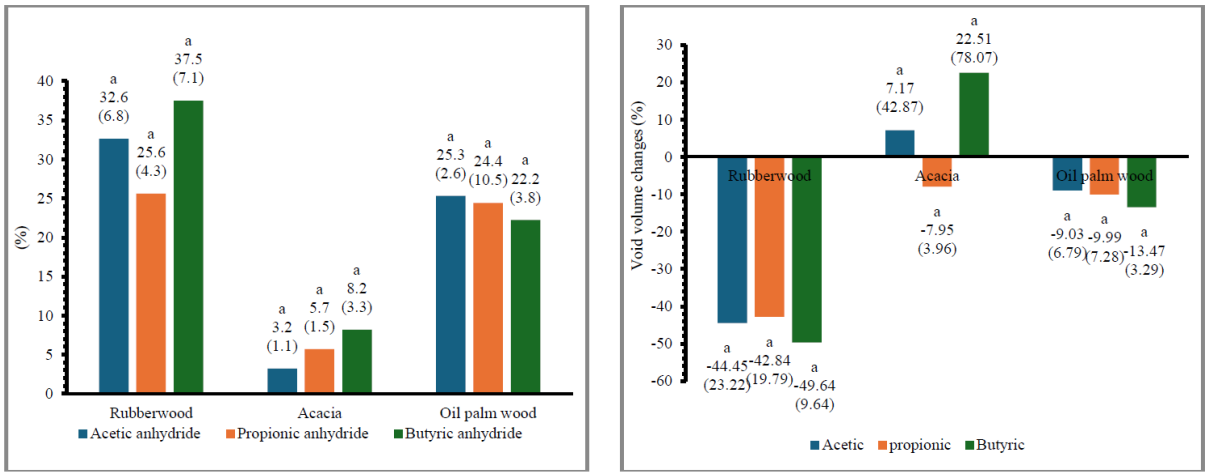

Figure 3: The averages density increment and void volume changes of modified wood with different anhydride. Figures in the parentheses are standard deviations. Means followed by the same letter(s) in the same bar are not significantly different at the 0.05 probability level according to the Duncan test

Compression

The compression strength parallel to the grain is important to determine the load a short post or column will carry (Haygreen and Bowyer 1982). The averages compression strength was significantly different with the anhydrides for rubberwood and oil palm wood, but not in the case of acacia (Table 3). In rubberwood (Figure 4, left), the averages compression strength was significantly increased with increasing molecular weight. The highest compression strength was obtained by modifying with butyric anhydride (29.5 MPa) followed by acetic anhydride (29.3 MPa) and propionic anhydride (28.2 MPa). The unmodified rubberwood obtained lower compression strength as compared to those modified rubberwood. In contrast, the averages compression strength was not significantly different with the anhydrides in acacia, ranging from 42.9 to 52 MPa. However, the averages compression strength for all the modified acacia was double than the untreated wood (22. 6 MPa). The oil palm wood modified with acetic anhydride (4.5 MPa) had significantly higher compression strength than the untreated (3.4 MPa). However, the compression strengths of oil palm wood modified with propionic (2.3 MPa) and butyric (2.8 MPa) anhydrides were significantly lower than the unmodified wood.

According to Dinwoodie et al. (2000); Panshin and Dezeeuw (1980), hexanyolated wood recorded an increase in compression strength compared to acetylated wood due to un-substitute hydroxyl groups which imparts a high tension and compression strengths. A same finding was reported by Papadopoulos

and Pougioula, (2010) for modified Corsican pine (Pinus Nigra S.) with acetic, propionic, butyric, valeric and hexanoic anhydrides. The compression strength was increased with increasing molecular weight of anhydride due to lower hydroxyl group's substitution for a higher molecular weight of anhydrides. Brelid et al, (2000) states that compression strength of wood was mainly contributed by the hemicelluloses and lignin contents, followed by cellulose content. Therefore, a higher un- substituted hydroxyl groups in hemi-cellulose, lignin and cellulose will leads to increase the compression strength.

Hardness

The trend of hardness was same for all wood species (Figure 4, right). The averages hardness of rubberwood modified with anhydrides were not significantly different with unmodified wood, ranging from 6.35 to 8.47 MPa (Figure 4, right). The hardness was ranged from 6.57 to 7.74 MPa in modified acacia and 0.58 to 0.77 MPa for modified oil palm wood. The hardness was also highest in untreated rubberwood (8.47 MPa) followed by acacia (6.58 MPa) and oil palm wood (0.73 MPa). This indicates that the anhydride molecule weight did not influence the hardness of modified wood. For comparison, Larsson and Simonson (1994) found the increased of Brinell hardness strength in acetylated pine compared to unmodified wood for both tangential and radial surface from 1.82 to 2.28 and from 2.47 to 2.96 respectively. Lower moisture content in modified wood was probably the main factor for the hardness increment.

Table 3: Summary of ANOVA of mechanical properties of modified wood

Mechanical Properties	df	F	p-value
Rubber wood			
Compression	3	20.979	0.000**
Hardness	3	1.650	0.218Ns
Acacia spp.			
Compression	3	13.512	0.000**
Hardness	3	1.056	0.395Ns
Oil palm			
Compression	3	3.373	0.045Ns
Hardness	3	1.399	0.280Ns

*MOR: modulus of rupture; MOE: modulus of elasticity; Ns: not significant, *: significant at p<0.05, **: significant at p<0.01*

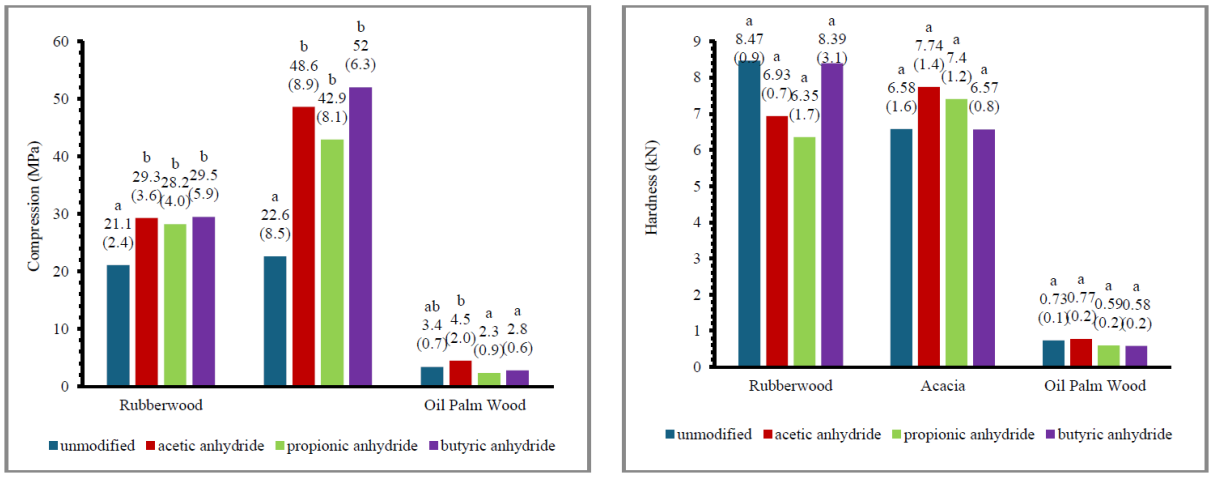

Figure 4: The Compression (Left) and Hardness (right) of woods modified with different anhydrides. Figures in the parentheses are standard deviations. Means followed by the same letter(s) in the same bar are not significantly different at the 0.05 probability level according to the Duncan test

CONCLUSION

From these studies, it can be concluded that regardless of species, no damage occur to the cell wall structure due to the modification process using microwave heating at temperature of more than 100°C. This was observed using the SEM. The result of basic properties shows that, even oil palm wood had the highest solution uptake, it will not result in a higher WPG and BC. The basic properties were dependent to the species properties and characteristics. Overall, the density of wood were increased due to the modification where density increment of rubberwood recorded the highest density increment as well as void volume changes. the modified wood with anhydride shows a higher compression strength value compared to the unmodified wood. The hardness value of modified wood with anhydride did not indicate for any significant improvement

ACKNLOWLEDGEMENT

The authors would like to thank to the Universiti Putra Malaysia for the Putra Research Grant Scheme

REFERENCES

Brelid P, Simonson R and Risman PO (1999) Acetylation of wood using microwave heating.Part 1. Studies of ielectric properties. HolzalsRoh- und Werkstoff: 57(4): 259-263.

BS 373(1957) Methods of Testing Small Clear Specimens of Timber.

Chang, HT and Chang ST (2003) Improvements in dimensional stability and lightfastness of wood by butyrylation using microwave heating. Journal of Wood Science. 49(5): 455-460.

Dinwoodie JM (2000). Timber: its Nature and Behaviour, 2nd edn. E. and F.N. Spon, London, UK.

Hamid NH and Hale M (2012) Decay threshold of acetylated rattan against white and brown rot fungi. International Wood Products Journal. 3(2): 96-106.

Haygreen JG and Bowyer JL (1982) Forest Products and Wood Science: an Introduction,4thedn. Iowa State University Press, USA.

Hill CAS (2006) Wood Modification: Chemical, Thermal and Other Processes, John Wiley & Sons, England, UK. Homan WJ and Jorissen AJM (2004) Wood modification development. Netherlands.

Larsson P and Simonson R (1994) A study of the strength, hardness and deformation of acetylated Scandinavian softwoods. Holz als Roh- und Werkstoff. 52(2): 83-86.

Larsson P and Simonson R (1999) Acetylation of solid wood using microwave heating.Part 2. Experiment in laboratory scale. Holz als Roh- und Werkstoff 57(5): 383-389.

Li JZ, Furuno T, Katoh S and Uehara, T (2000) Chemical modification of wood without solvents or catalysts. Journal of Wood Science 46(3): 215-221.

Panshin A J and DeZeeuw C (1980) Textbook of Wood Technology, fourth ed. McGrawhill Inc

Papadopoulos AN and Pougioula G (2010). Mechanical behavior of pine wood chemically modified with a homologous series of linear chain carboxylic acid anhydrides. Bioresource Technology 101(3): 6147-6150.

Rowell RM (1980) Distribution of reacted chemicals in southern pine treated with methyl isocyanate. Wood Science 13(2): 102-110.

Rowell RM (1982) Distribution of acetyl groups in southern pine reacted with acetic anhydride. Wood Science 15(2): 172-182.

Rowell RM (1991). Chemical modification of wood. Wood and Cellulosic Chemistry. New York : Marcel Dekker, Inc, (15):703-756.

Rowell RM, Simonsen R, Hess S, Plackett DV, Cronshaw D and Dunningham E (1994). Acetyl distribution in acetylated whole wood and reactivity of isolated cell wall components to acetic anhydride. Wood and Fiber Science 26(1): 11-18.

Sander C, Beckers EPJ, Militz H and Van Veenendaal W (2003) Analysis of acetylated wood by electron microscopy. Wood Science and Technology 37(1): 39-46.

Simulating the Sawing of Beech and Birch Logs

Urs Buehlmann[1*], R. Edward Thomas[2]

[1] Virginia Tech, Department of Sustainable Biomaterials, Brooks Forest Products Center, 1650 Research Center Drive, Blacksburg, VA 24061-1072, United States
[2] USDA Forest Service, Forest Product Laboratory, Brooks Forest Products Center, 1650 Research Center Drive, Blacksburg, VA 24061-1072, United States.

E-mail: ubuehlm@vt.edu; ralph.thomas@usda.gov

Keywords: hardwood, sawmill, log yield, recovery, simulation.

ABSTRACT
One of the most important metrics for analyzing hardwood sawmill performance with respect to profitability is knowing the expected yield from any specific log. The Log Recovery Analysis Tool (LORCAT) is a spreadsheet-based sawmill simulation and analysis tool that was developed to provide this information. As such, LORCAT depends on recorded grade recovery data to determine the quality and volume using the NHLA grade of the sawn lumber. Recently, the grade recovery data of LORCAT was expanded to include beech (*Fagus grandifolia*) and paper birch (*Betula papyrifa*), allowing the software to simulate sawing and analysis of these species. While the data are based on North American species, grading systems, and economic assumptions, with differences in species, silvicultural, logging (bucking), and sawing practices acknowledged, LORCAT can be used to emulate the sawing of European logs. Overall, LORCAT can simulate and analyze the sawing of 13 common North American hardwood species (red oak, white oak, black oak, scarlet oak, chestnut oak, red maple, sugar maple, yellow poplar, American beech, paper birch, yellow birch, black cherry, and basswood) for small-end diameters ranging from 20 cm to 90 cm, and report the volume and the quality of lumber produced, as well as the volume and weight of residual products.

The final version of this abstract and the full scientific article are scheduled to be published in the Special Issue "12th Hardwood Conference—Sopron" of the journal MDPI Forests, available at the following link:
MDPI Forests Special Issue: 12th Hardwood Conference—Sopron

https://doi.org/10.3390/f17060665

Optimization of Beech Wood Cutting with Circular Saw Blades Using ANN and RSM

Mihai Ispas[1], Bogdan Bedelean[1*], Sergiu Răcășan[1], Ana - Maria Angelescu[1]

[1] Transilvania University of Brașov, Faculty of Furniture Design and Wood Engineering, B-dul Eroilor nr.29, Brașov, Romania.

E-mail: ispas.m@unitbv.ro; bedelean@unitbv.ro; sergiu.racasan@unitbv.ro; ana.angelescu@unitbv.ro

Keywords: wood sawing; optimization; ANN modelling; beech wood; wood machining.

ABSTRACT

Several parameters like blade design, rotational speed, feed rate, tooth geometry, wood moisture content, and wood species affect the efficiency of wood sawing processes. Identifying the optimal combination of these factors can reduce energy consumption during processing of wood. In this study, a novel approach was applied to optimize wood cutting using circular saw blades. The investigated variables included: wood density, blade rotational speed, feed rate, blade type (defined by the number of teeth and their geometry). The beech (*Fagus sylvatica*) samples were longitudinally cut using two different circular saw blades (one with 18 cutting teeth and the other with 54 cutting teeth). Cutting power consumption were experimentally measured using an active/reactive electrical power transducer connected to a DAQ system and computer. After collecting and processing the experimental data, artificial neural network (ANN) modelling was used to develop one predictive model that is able to predict the cutting power with high accuracy (R=0.99). Subsequently, response surface methodology (RSM) was employed to analyse the influence of each factor on cutting power and to determine optimal operating conditions. The results indicated that feed rate had the greatest influence on the cutting power followed by blade rotational speed, sample density and blade type. The optimal machining conditions recommended by the optimization algorithm in the case of a saw blade with 18 cutting teeth were a feed rate of 3.5 m/min., a rotational speed of 3000 rpm at sample density of 520 kg/m^3. One the other hand, in the case of a saw blade with 54 cutting teeth, a feed rate of 3.6 m/min, a rotational speed of 4036 rpm and at a sample density of 720 kg/m^3 was revealed by the optimization algorithm. Future research will focus on further investigating the behaviour of different wood species during circular sawing and clarifying the influence of blade design parameters, such as teeth number and geometry, on cutting performance.

The final version of this abstract and the full scientific article are scheduled to be published in the Special Issue "12th Hardwood Conference—Sopron" of the journal MDPI Forests, available at the following link:

MDPI Forests Special Issue: 12th Hardwood Conference—Sopron

Investigation of Surface Properties of Poplar Wood Impregnated with Lauryl Alcohol After Densification

Ahmet Can[1,2*], Tomasz Krystofiak[2], Barbara Lis[2]

[1] Bartin University, Department of Faculty of Forestry, 74100 Bartin, Türkiye
[2] Poznan University of Life Sciences, Department of Gluing and Finishing of Wood, 60 637, Poznan, Poland.

E-mail: acan@bartin.edu.tr; tomasz.krystofiak@up.poznan.pl; barbara.lis@up.poznan.pl

Keywords: poplar wood; impregnation; densification; surface properties.

ABSTRACT

Impregnation and densification processes, widely used to enhance wood performance, can substantially modify not only mechanical properties but also surface characteristics. In this study, poplar (*Populus* × *canadensis*) wood samples were impregnated with lauryl alcohol (LOH) and subsequently subjected to densification (Dw). The resulting changes in color, gloss, and surface roughness were systematically evaluated. Surface color was measured using the CIE Lab* system, and color differences (ΔL*, Δa*, Δb*, ΔE) were calculated for control, impregnated, and densified samples. A ΔE value of 2.303 for control samples indicated minimal color variation, whereas LOH-treated samples exhibited a notable color change (ΔE = 10.84), primarily due to surface darkening (ΔL = −6.36) and a marked increase in yellow tones (Δb = 7.49). Densified samples (LOH/Dw) showed trends like LOH-only treatment. Surface roughness parameters (Ra, Rq, Rz), measured according to ISO 1997, decreased significantly after both impregnation and densification, with the lowest values observed in Dw and LOH/Dw groups. Gloss measurements at 20°, 60°, and 85° angles revealed that densified samples exhibited the highest gloss values, particularly at 85°, indicating improved surface reflectivity. In contrast, LOH-treated samples showed lower gloss, while the combined LOH/Dw treatment resulted in moderate gloss enhancement compared to the control. Overall, densification played a dominant role in improving surface smoothness and gloss.

INTRODUCTION

The most effective way to improve the physical properties of wood materials is wood modification. Among these, impregnation modification is a highly efficient approach, particularly for fast-growing wood species, as it enhances material performance by filling cell lumens and altering the cell wall structure. In this method, one or more chemical agents are introduced into the wood using vacuum, atmospheric pressure, pressurization, or a combination of these techniques, taking advantage of the wood's multilayered structure. Impregnation modification not only improves key properties such as dimensional stability and mechanical strength but can also impart flame retardancy and resistance to biological degradation. Although conventional modifiers (e.g., thermosetting resins, organic monomers, and N-hydroxymethylamide compounds) provide effective improvements, their fossil-based origin presents environmental drawbacks. Therefore, recent studies have increasingly focused on more sustainable, biomass-based alternatives such as furfuryl alcohol, low-molecular-weight sugars, and polybasic acids. In addition, hybrid modifiers combining organic and inorganic components offer synergistic potential for enhancing wood performance (Guo et al. 2019; Yang et al. 2021; Yonggui et al. 2025). In literature research summarizes impregnation modification methods, mechanisms, and current approaches aimed at improving dimensional stability in fast-growing wood species, providing a comprehensive framework for future research (Guo et al. 2019; Yang et al. 2021; Yonggui et al. 2025).

Another effective method for improving the physical and mechanical properties of low-density, fast-growing wood is densification (Kutnar et al. 2008; Bekhta et al. 2014; Salca and Bekhta, 2021). In this process, wood is compressed in the transverse direction, leading to the collapse of cell lumens and an increase in density (Blomberg et al. 2005; Kutnar et al. 2009; Rautkari et al. 2010; Laskowska 2017; Pelit et al. 2018; Sandberg et al. 2013). Prior to densification, wood can be impregnated with chemicals

or resins to enhance treatment efficiency (Laine et al. 2016; Brischke et al. 2007; Lykidis et al. 2020). In a study by Song et al. (2018), wood samples were treated with aqueous solutions containing sodium hydroxide (NaOH) and sodium sulfite (Na_2SO_3), followed by densification resulting in an 80% reduction in volume. This process significantly increased density and markedly improved mechanical properties compared to untreated wood, with notable enhancements in bending strength, compression strength parallel to the grain, tensile strength, and hardness. In addition to solid wood, densification has also been investigated to improve veneer properties (Gaff and Gašparík 2015; Bekhta et al. 2017). The simple and effective strategy developed by Song et al. (2018) enables veneers to be directly transformed into high-performance materials, achieving more than a tenfold increase in strength, toughness, and ballistic resistance, along with improved dimensional stability. After densification, aesthetic quality assessment must consider wood color, its modification, and its stability over time (Ayadi et al. 2003; González-Peña and Hale 2009; Bekhta et al. 2014). Veneers are used not only in plywood and LVL production but also for coating particleboard and MDF in furniture manufacturing. In such applications, surface color is critically important both for aesthetic quality and as an economic parameter influencing the final product value. By adjusting densification parameters, less decorative wood species can be modified to exhibit color and texture characteristics like exotic woods.

Since the effectiveness of densification depends not only on process parameters but also on wood species and anatomical characteristics, poplar (*Populus × canadensis*) veneers, a hardwood species, were used in this study. The aim of this research is to quantitatively determine the changes in density, color, gloss, and surface roughness of veneers impregnated with lauryl alcohol (LOH) and subjected to densification.

MATERIALS AND METHODS

Materials

In In this research, veneers obtained from a single hardwood species were used for plywood production: poplar (*Populus × canadensis*). Poplar was chosen as a low-value and infrequently used wood species in Türkiye. Although this hardwood species has low density and strength, it has been used in plywood production before (Madhoushi et al. 2010). The veneers were purchased from the Çaycuma factory. The veneers were obtained according to the rotary-peeling method. After the peeling process, the veneer matt was cut into sheets with dimensions of 30 × 50 cm² using a guillotine. Then, the veneers were dried in an oven.

Lauryl alcohol (LOH) is a long-chain fatty alcohol, typically with a 12-carbon backbone ($C_{12}H_{26}O$). It was supplied from Sigma-Aldirch Company (m.p: 22–26 °C; purity ≥98 %; density 0.83 g/mL at 25 °C).

Methods

The impregnation process of the veneer samples was carried out within a controlled and repeatable procedure. Poplar veneers with dimensions of 30 × 50 cm² were used in the experiments. The veneers were impregnated by immersion in molten LOH for 1 hour under atmospheric pressure. The weight percent gain (WPG, %) ratio was calculated using Equation 1.

$$WPG\ (\%) = \frac{(W2-W1)}{W1} \times 100 \quad (1)$$

Where W2 and W1 are oven-dried weight after and before impregnation.

Following the impregnation process, the samples were densified by a mechanical process at Bartın University. Densified veneers samples with dimensions of 30 × 50 cm2 were produced. The samples were conditioned at 20 ± 2 °C and 65 ± 5% RH until they reached equilibrium moisture content before densification. Densification was performed at room temperature. The veneers were uniaxially compressed between plates. The targeted compression ratio was to compress approximately 40%, starting from initial thicknesses of 1.5 mm. The pressing cycle was initiated after the samples were placed on the plate. Densification took place for ten minutes at 24°C and 30 MPa. The compression ratio (CR,%) was calculated using Equation 2.

$$CR\ (\%) = \frac{(T2-T1)}{T1} \times 100 \quad (2)$$

Where T2 and T1 are oven-dried thicknesses before and after densification.

The color measurements of all specimens were recorded on the surface of veneer with a colorimeter Testan DT-145 (Anticorr, Gdansk, Poland). The sensor head was 6 mm in diameter. Measurements were made using a D65 illuminant and 10-degree standard observer. Color was determined in the CIE L*a*b* system, where L* represents lightness, while a* and b* define chromatic coordinates along the green–red and blue–yellow axes, respectively. Based on the obtained L*a*b* values, color uniformity was evaluated as differences in lightness (ΔL*) and chromatic parameters (Δa* and Δb*) between treated and untreated veneer samples, according to Equations 3–5. Color measurements were performed always on the same marked locations on the sample. In addition, total color difference (ΔE) was calculated as Equation 6.

$$\Delta \boldsymbol{L}^* = \Delta \boldsymbol{L}^*_{\boldsymbol{t}} - \Delta \boldsymbol{L}^*_{\boldsymbol{n}} \quad (3)$$
$$\Delta \boldsymbol{a}^* = \Delta \boldsymbol{a}^*_{\boldsymbol{t}} - \Delta \boldsymbol{a}^*_{\boldsymbol{n}} \quad (4)$$
$$\Delta \boldsymbol{b}^* = \Delta \boldsymbol{b}^*_{\boldsymbol{t}} - \Delta \boldsymbol{b}^*_{\boldsymbol{n}} \quad (5)$$

where "t" refers to treated and "n" to non-treated samples.

$$\Delta \boldsymbol{E} = \sqrt{\Delta \boldsymbol{L}^{*2} + \Delta \boldsymbol{a}^{*2} + \Delta \boldsymbol{b}^{*2}} \quad (6)$$

For each sample, ten random measurements of surface color were taken. Positive values of ΔL* show whitening, and negative indicate a shift toward gray. Positive values of Δa* indicate reddening, and negative values show a shift towards green. Positive values of Δb* represent yellowing, and negative values represent a shift towards blue.

Changes in the surface gloss units were evaluated according to ASTM D523, at least ten measurements on each sample in different locations (ASTM D523-14, 2014). Specular reflectance was assessed with incidence angles of 20°, 65° and 85°, assuring the incident ray direction being parallel and across to the fiber direction.

The surface roughness measurements of the veneer before and after processing were performed using a portable Mitutoyo Surftest SJ-210 series 178 profilometer, in accordance with ISO 4287 [45]. All measurement results were processed using a digital Gaussian filter. The measurement error of unevenness did not exceed ±10%. Six measurements were taken from the surface of each sample, six parallel and across to the fiber direction. The following parameters of wood surface roughness were evaluated: arithmetic average height (Ra), average peak-to-valley roughness (Rz), root mean square (Rq).

RESULT AND DISCISSION

The initial density of the control samples was 0.32 g/cm³, which increased to 0.84 g/cm³ after the densification process. For the LOH-impregnated samples, the value changed from 0.53 to 0.67 g/cm³.

The weight gain rate (WPG) of the samples after impregnation with LOH was calculated as 54.82%, indicating a high penetration of the impregnating agent into the wood structure.

When the compression ratios obtained after the densification process were examined, it was determined that the control samples were compressed by 16%, while the samples impregnated with LOH were compressed by 26.36%. These results show that LOH impregnation has a positive effect on the densification behavior. The higher compression ratio obtained in LOH-impregnated samples compared to control samples can be explained by the plasticizing and lubricating effect of lauryl alcohol on the wood structure. The WPG value of 54.82% obtained because of the impregnation process shows that

lauryl alcohol penetrates the cell lumens and partially the cell wall to a high degree, creating a significant increase in mass in the anatomical structure of the wood. This weakens the interactions between cell wall polymers, increasing the viscoelastic behavior of the material and allowing for easier deformation of the cell wall during compression. In addition, the hydrophobic and lubricating character of lauryl alcohol reduces interfiber friction, contributing to the formation of a higher permanent compression set during the deformation process (Shi et al. 2020; Yue et al. 2020; Cabral et al. 2022). Therefore, the compression ratio, which was determined as 16% in control samples, increased to 26.36% in LOH-impregnated samples, and the main reason for this difference is the decrease in the mechanical resistance of the wood and the increase in its deformation ability after impregnation.

Table 1 shows the surface color parameters of the control and test samples. Compared to the control sample, a slight increase in the L* value (from 95.38 to 98.45) was observed in the Dw sample. Similarly, the a* value increased from 2.26 to 3.19, while the b* value decreased from 13.92 to 13.28. The resulting ΔE value is 3.26, a difference that is visually barely discernible. In the samples impregnated with LOH, the L* value showed a significant decrease to 89.03. While the a* value remained close to the control at 2.65, the b* value increased to 21.42. Following this change in the LOH samples, the ΔE value was found to be 9.83, indicating a significantly different color from the control group. Similarly, in the LOH/Dw sample, the following values were obtained: L* = 89.47, a* = 2.87, b* = 20.08, and ΔE = 8.55. These findings reveal that both LOH and LOH/Dw treatments darken the color, significantly increasing the yellow tone (b*) and causing a large color deviation (ΔE > 8) from the control group. The Dw treatment, on the other hand, resulted in a more limited color change.

Table 1: Color parameters and total color change

	L*	**a***	**b***	**ΔE**
Control	95.38 (1.88)	2.26 (0.55)	13.92 (0.78)	
Dw	98.45 (1.54)	3.19 (0.75)	13.28 (0.84)	3.26
LOH	89.03 (3.69)	2.65 (0.91)	21.42 (2.14)	9.83
LOH/Dw	89.47 (2.59)	2.87 (0.79)	20.08 (2.32)	8.55

Figure 1 shows gloss values (GU) measured at three different angles. In control samples, the specular reflectance initially increases with increasing angle of incidence, but at angles over 60° it rapidly subsides. A similar situation is observed in Dw samples. However, the decrease at 60° is not as severe as in control samples. In fact, the results at 85°, measured parallel to the fibers, are like those at 60°. A similar situation is seen in LOH impregnation and LOH/Dw samples. The gloss values measured at 20° and 85° are practically the same. However, higher gloss values are obtained at 85° after the densification process. This is probably due to the very high surface roughness of the control samples. A typical finding for 60° and 85° gloss measurements for all variation is that gloss values when measured along the grain are higher than those measured across the grain. The anatomical structure and surface imperfections of wood veneers provide an explanation for this. When assessing gloss across the grain, surface roughness has a greater impact on light scattering. The diffuse component rises because of increased light scattering.

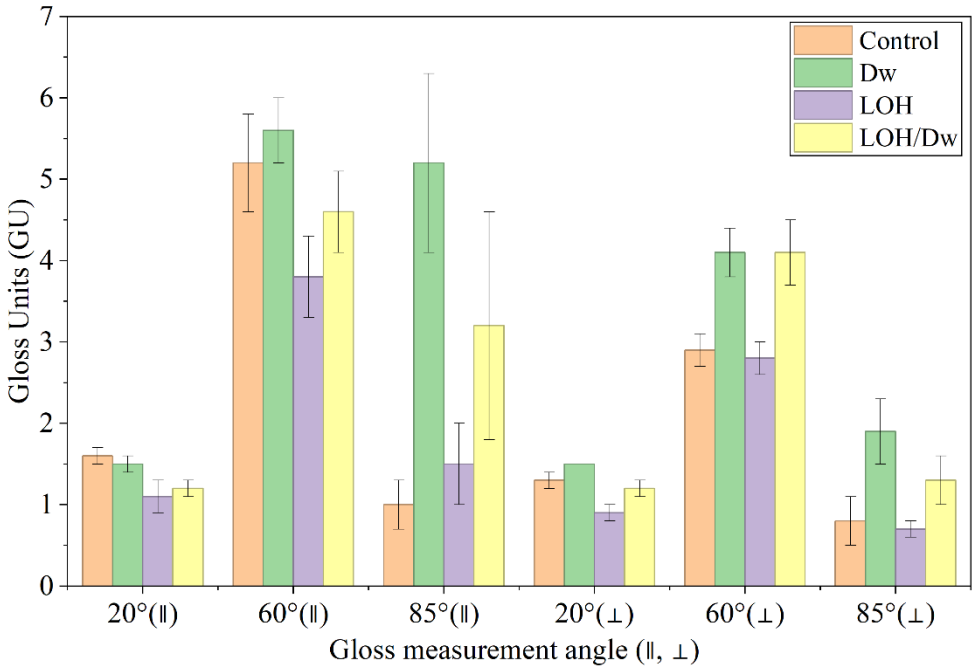

Figure 1: Gloss measured at three different angles: parallel to the fibers (∥) and perpendicular to the fibers (⊥)

Table 2 shows the surface roughness values of the control and test samples. According to Table 2, the roughest surfaces were obtained in the control samples (Ra: 12.10), while the least rough surface was obtained in the samples that underwent the densification process (Ra: 6.78).

Table 2: Test results of the surface roughness

Specimen	Ra	Rq	Rz
Control	12.10 (1.75)	15.48 (1.91)	73.61 (5.52)
Dw	6.78 (0.07)	8.62 (0.33)	42.00 (2.10)
LOH Imp.	9.64 (2.57)	13.83 (3.35)	63.62 (14.76)
LOH/Dw	7.33 (1.42)	9.17 (1.85)	42.12 (9.32)

It can be said that the densification process reduces the roughness of poplar veneers due to the decrease in void volume and the more regular arrangement of fibers. Furthermore, the fact that compressed veneers exhibit a more homogeneous structure compared to control samples may also affect the surface roughness results. A literature review indicates that the surface roughness of densified wood decreases with increasing compression ratio, and this may be due to the reduction in intercellular spaces and the increase in density, resulting in a tighter structure (Pelit et al. 2015). Similar studies show that the surface roughness of veneers decreases depending on the applied densification parameters (Diouf et al. 2011; Santos et al. 2012; Bekhta et al. 2014; Pelit and Arısüt 2023).

The roughness values of the samples showed a slight decrease after the LOH impregnation process. The Rz value, which was 73.61 in the control samples, decreased to 63.62 in the samples impregnated with LOH. However, it is understood from the standard deviation values that this decrease is not statistically significant. Literature studies have reported that the roughness values of samples decrease after impregnation because the cell voids of wood samples or veneers are filled with the impregnating agent (Pelit and Arısüt 2023). It has been reported that the surface roughness of samples impregnated with water-based agents increases (Ors et al. 2006; Dundar et al. 2008).

CONCLUSIONS

This study revealed that the surface properties of poplar (*Populus* × *canadensis*) wood can be significantly altered by both lauryl alcohol (LOH) impregnation and densification processes. LOH application caused noticeable changes in surface color, particularly darkening and an increase in yellow tones, but had a limited and negative effect on surface gloss. In contrast, densification reduced surface roughness, resulting in a smoother structure and increased surface gloss, leading to higher reflectivity. The combined LOH/Dw application preserved the LOH effect in terms of color change, while partially reflecting the positive contribution of densification in terms of surface smoothness and gloss. Overall, it appears that densification plays a dominant role in improving surface quality. Future studies could investigate the long-term performance and outdoor resistance of systems using densification in combination with different phase change materials or bio-based impregnation agents in detail.

ACKNOWLEDGEMENTS

Ahmet CAN gratefully acknowledges support from NAWA (The Director of The Polish National Agency for Academic Exchange) Program, under grant BPN/ULM/2025/1/00306.

REFERENCES

ASTM D523-14 (2014) Standard test method for specular gloss. ASTM International, West Conshohocken, PA, USA

Ayadi N, Lejeune F, Charrier F, Charrier B, Merlin A (2003) Color stability of heat-treated wood during artificial weathering. Holz Roh Werkst 61(3):221–226

Bekhta P, Proszyk S, Krystofiak T (2014) Color in short-term thermo-mechanically densified veneer of various wood species. Eur J Wood Wood Prod 72(6):785–797

Bekhta P, Proszyk S, Krystofiak T, Sedliačik J, Novák I, Mamoňová M (2017) Effects of short-term thermomechanical densification on the structure and properties of wood veneers. Wood Mater Sci Eng 12(1):40–54

Bekhta P, Proszyk S, Krystofiak T, Mamonova M, Pinkowski G, Lis B (2014) Effect of thermomechanical densification on surface roughness of wood veneers. Wood Mater Sci Eng 9(4):233–245

Blomberg J, Persson B, Blomberg A (2005) Effects of semi-isostatic densification of wood on the variation in strength properties with density. Wood Sci Technol 39(5):339–350

Brischke C, Welzbacher CR, Brandt K, Rapp AO (2007) Quality control of thermally modified timber: interrelationship between heat treatment intensities and CIE Lab* color data on homogenized wood samples. Holzforschung 61(1):19–22

Cabral JP, Kafle B, Subhani M, Reiner J, Ashraf M (2022) Densification of timber: a review on the process, material properties, and application. J Wood Sci 68(1):20

Diouf PN, Stevanovic T, Cloutier A, Fang CH, Blanchet P, Koubaa A, Mariotti N (2011) Effects of thermo-hygro-mechanical densification on the surface characteristics of trembling aspen and hybrid poplar wood veneers. Appl Surf Sci 257(8):3558–3564

Dundar T, Ayrilmis N, Candan Z (2008) Evaluation of surface roughness of laminated veneer lumber (LVL) made from beech veneers treated with various fire retardants and dried at different temperatures. For Prod J 58(1):71–76

Salca, E. A., & Bekhta, P. (2021). Effects of thermo-mechanical densification applied to veneers of fast-growing species to produce value-added plywood panels. Cut. Edge Res. Agric. Sci, 9, 161-177.

Gaff M, Gašparík M (2015) Influence of densification on bending strength of laminated beech wood. BioResources 10(1):1506–1518

González-Peña MM, Hale MDC (2009) Color in thermally modified wood of beech, Norway spruce and Scots pine. Part 1: color evolution and color changes. Holzforschung 63(4):385–393

Guo W, Xiao Z, Xie Y (2019) Modification of Scots pine with activated glucose and citric acid: physical and mechanical properties. BioResources 14(2):3445-3458

ISO 4287 (1997) Geometrical Product Specifications Surface Texture Profile Method Terms, Definitions and Surface Texture Parameters. International Organization for Standardization (ISO): Geneva, Switzerland.

Kutnar A, Kamke FA, Sernek M (2008) The mechanical properties of densified VTC wood relevant for structural composites. Holz Roh Werkst 66(6):439–446

Kutnar A, Kamke FA, Sernek M (2009) Density profile and morphology of viscoelastic thermal compressed wood. Wood Sci Technol 43(1–2):57–68

Laine K, Segerholm K, Wålinder M, Rautkari L, Hughes M (2016) Wood densification and thermal modification: hardness, set-recovery and micromorphology. Wood Sci Technol 50(5):883–894

Laskowska A (2017) The influence of process parameters on the density profile and hardness of surface-densified birch wood (Betula pendula Roth). BioResources 12(3):6011–6023

Lykidis C, Moya R, Tenorio C (2020) The effect of melamine formaldehyde impregnation and hot-pressing parameters on the density profile of densified poplar wood. Eur J Wood Wood Prod 78:433–440

Madhoushi M, Gray M, Tabarsa T (2010) Influence of wood densification on withdrawal strength of fasteners in eastern cottonwood (Populus deltoides). In: Proc 11th World Conf Timber Eng (WCTE 2010), Trentino, Italy, 20–24 June 2010, Vol 1

Ors Y, Atar M, Keskin H, Colakoglu MH (2006) Impacts of impregnation with boron compounds on surface roughness of woods and varnished surfaces. J Appl Polym Sci 102(5):4952–4957

Pelit H, Budakçı M, Sönmez A (2018) Density and some mechanical properties of densified and heat post-treated Uludağ fir, linden and black poplar woods. Eur J Wood Wood Prod 76(1):79–87

Pelit H, Budakçı M, Sönmez A, Burdurlu E (2015) Surface roughness and brightness of Scots pine (Pinus sylvestris) applied with water-based varnish after densification and heat treatment. J Wood Sci 61(6):586–594

Pelit H, Arısüt U (2023) Roughness, wettability, and morphological properties of impregnated and densified wood materials. BioResources 18(1):429–446

Rautkari L, Properzi M, Pichelin F, Hughes M (2010) Properties and set-recovery of surface densified Norway spruce and European beech. Wood Sci Technol 44(4):679–691

Sandberg D, Haller P, Navi P (2013) Thermo-hydro and thermo-hydro-mechanical wood processing: an opportunity for future environmentally friendly wood products. Wood Mater Sci Eng 8(1):64–88

Santos CMT, Del Menezzi CH, de Souza MR (2012) Properties of thermomechanically treated wood from Pinus caribaea var. hondurensis. BioResources 7(2):1850–1865

Shi J, Peng J, Huang Q, Cai L, Shi SQ (2020) Fabrication of densified wood via synergy of chemical pretreatment, hot-pressing and post mechanical fixation. J Wood Sci 66(1):5

Song J, Chen C, Zhu S, Zhu M, Dai J, Ray U, Li Y, Kuang Y, Li Y, Quispe N, Yao Y, Gong A, Leiste UH, Bruck HA, Zhu JY, Vellore A, Li H, Minus ML, Jia Z, Martini A, Li T, Hu L (2018) Processing bulk natural wood into a high-performance structural material. Nature 554(7691):224–228

Yang ML, Xiao ZF, Wang HG, Wang YG, Liang DX, Xie YJ, Zhang SQ (2021) Physical properties of Chinese fir wood modified with the mixing agent of citric acid and sucrose. 49(12):120-125

Yonggui W, Fanjun Y, Yijie Z, Zefang X, Yanjun X (2025) Research progress on impregnation to improve the dimensional stability of fast-growing wood. Chin J Wood Sci Technol 39(1):10–21

Yue K, Wu J, Xu L, Tang Z, Chen Z, Liu W, Wang L (2020) Use of impregnation and densification to improve mechanical properties and combustion performance of Chinese fir. Constr Build Mater 241:118101

Combined Wood Modification Using Bark Extractive Impregnation and Ammonia Fuming

Miklós Bak[1*], Fanni Fodor[1], Zsolt Kajli[1], Tamás Hofmann[2]

[1] Faculty of Wood Engineering and Creative Industries, University of Sopron, H-9400 Sopron, Bajcsy-Zsilinszky St. 4
[2] Institute of Environmental Protection and Natural Conservation, Faculty of Forestry, University of Sopron, H-9400 Sopron, Bajcsy-Zsilinszky St. 4.

E-mail: bak.miklos@uni-sopron.hu; fodor.fanni@uni-sopron.hu; KajliZs20@student.uni-sopron.hu; hofmann.tamas@uni-sopron.hu

Keywords: ammonia fuming; bark extractives; wood impregnation; wood modification; wood durability, physical properties, color change.

ABSTRACT
The present study investigated, for the first time, the synergistic effects of combining bark extractive impregnation with ammonia fuming, revealing promising enhancements in both aesthetic and functional attributes of wood. This combined approach not only leverages the bioactive and protective qualities of natural extractives but also extends ammonia fuming treatment to those wood species that are naturally low in extractive content. The novel approach offers a pathway toward more sustainable, high-performance wood products. Bark extracts of pedunculate oak and European beech were investigated on wood specimens of European beech (with and without red heartwood), hornbeam and gray poplar.

Figure 1: Arrangement of the wood specimens in the fuming chamber. On the left, the specimens are placed in before fuming (the photo was taken here without lid). On the right, the color darkening can be seen after fuming. There is a Petri dish at the bottom of the chamber holding the treatment medium (30% NH_4OH solution)

Oak bark extract contained substantially higher total extractives and polyphenols than beech bark extract. Treatments caused only minor changes in density and equilibrium moisture content (generally within ±8%), while some shrinkage parameters changed more noticeably. The largest improvement occurred in beech false heartwood, where volumetric shrinkage decreased by up to 16%. Both treatments darkened the wood surface, with oak bark extract producing significantly larger color changes; ammonia fuming further intensified these effects, especially in poplar.

Durability improved markedly: mass loss caused by *Coniophora puteana* and *Trametes versicolor* decreased from 27–38% in untreated samples to 0.58–7.73% after treatment, improving durability classification from Durability Class 4 to Classes 1–2. Bark extract treatments slightly reduced hardness but generally maintained or slightly increased compression strength.

Overall, the treatments produced significant color changes and enhanced their durability greatly, which may be beneficial where improved durability and aesthetic modification are the primary objectives, like indoor and outdoor decorations and furniture. However, since hardness decreased and compression strength did not improve substantially, the treated wood is not suitable for applications requiring higher mechanical performance. Future research should focus on bigger samples sizes and outdoor testing to evaluate the feasibility of these treatment methods.

This article was made in frame of the project TKP2021-NKTA-43 which has been implemented with the support provided by the Ministry of Innovation and Technology of Hungary (successor: Ministry of Culture and Innovation of Hungary) from the National Research, Development and Innovation Fund, financed under the TKP2021-NKTA funding scheme.

The final version of this abstract and the full scientific article are scheduled to be published in the Special Issue "12th Hardwood Conference—Sopron" of the journal MDPI Forests, available at the following link:
MDPI Forests Special Issue: 12th Hardwood Conference—Sopron

Session V
-
Hardwoods in Composites and Engineered Materials

LVL from Hungarian Under-Utilized Hardwood Species

Tibor L. Alpár[1*], Szili-Török György[1], György Péter Horváth[1], László Bejó[1], József Garab[1]

[1] University of Sopron, Faculty of Wood Engineering and Creative Industries. Bajcsy-Zs. Str. 4, Sopron, Hungary, 9400.

E-mail: tibor.alpar@uni-sopron.hu, torok.gyorgy@uni-sopron.hu; horvath.peter.gyorgy@uni-sopron.hu, bejo.laszlo@uni-sopron.hu, garab.jozsef@uni-sopron.hu

Keywords: LVL, Turkey oak, poplar, MUF, PF, MDI**,** bending strength, SEM, finite element analysis.

ABSTRACT

Laminated Veneer Lumber (LVL), defined by the MSZ EN 14279 standard, has become one of the most important engineered wood materials in modern construction due to its excellent mechanical properties, versatility, and compliance with sustainability requirements. The global LVL market, however, is shaped by numerous external factors, including the growing demand for sustainable building materials, fluctuations in supply chains, regional economic conditions, as well as the effects of pandemics and geopolitical conflicts on the construction sector. Demand is primarily driven by rapidly developing construction markets such as China, the United States, and Northern Europe, while supply is dominated by Europe and North America due to their significant wood resources and advanced manufacturing technologies.

In Hungary, the wood industry is currently dominated by furniture production, partly due to the greater availability of hardwood species. However, rising construction and timber prices have begun to shift attention toward lightweight timber structures and wood-based architectural solutions, where LVL can play a key role. A fundamental requirement for the domestic expansion of LVL use is the ability to produce high-quality LVL from local wood species—such as Turkey oak and grey poplar—thereby reducing import dependency and potentially enabling the development of new export markets.

This research explores the physical and mechanical properties of LVL produced from selected Hungarian hardwoods (Turkey oak, poplar) and examines the effects of different adhesives (PF – phenol-formaldehyde; MUF – melamine-urea-formaldehyde; MDI – methylene-diphenyl-diisocyanate). Building on previous findings, MUF adhesives exhibited stable performance, while MDI generally demonstrated superior mechanical behavior. The PF adhesive used in the present study also provided high strength; however, due to its stiffer and more brittle nature, it may be more suitable for static loading, whereas the more flexible MDI adhesive performs better under dynamic loads.

Mechanical testing – including three-point bending strength and perpendicular-to-grain tension tests – showed overall satisfactory results, although greater variability occurred in the control samples due to manual adhesive application. The experimental results were integrated into Finite Element Analysis (FEM) models, allowing the numerical reproduction of specimen behavior. While the models successfully represented stiffness characteristics, further development is recommended, particularly through the use of full 3D orthotropic modelling, examination of the adhesive–wood transition zone, and the experimental determination of the complete set of orthotropic elastic constants for the domestic species.

In summary, Turkey oak and various poplar species represent promising raw materials for domestic LVL production. Turkey oak veneers provided outstanding strength, while poplar species contribute favorable strength-to-weight ratios and good manufacturability, enabling efficient and sustainable LVL manufacturing. The examination of different adhesives and layups revealed that mechanical performance can be significantly optimised depending on the intended application.

This research contributes to the development of LVL technology and innovation in engineered timber structures, supporting a more sustainable and economically viable construction sector in which local resources can be used efficiently and with high added value.

ACKNOWLEDGEMENT
This article was made in frame of the project TKP2021-NKTA-43 which has been implemented with the support provided by the Ministry of Innovation and Technology of Hungary (successor: Ministry of Culture and Innovation of Hungary) from the National Research, Development and Innovation Fund, financed under the TKP2021-NKTA funding scheme.

The final version of this abstract and the full scientific article are scheduled to be published in the Special Issue "12th Hardwood Conference—Sopron" of the journal MDPI Forests, available at the following link:
MDPI Forests Special Issue: 12th Hardwood Conference—Sopron

From ABES to Panels: Wood-Species Effects on Adhesive Curing and Mechanical Performance in Strand-Based Composites

Andrej Fašalek[1], Lukas Malzl[1], Maximilian Pramreiter[1], Hendrikus van Herwijnen[2], Jan Stroobants[3], Johann Moser[4], Wolfgang Kantner[4], Johannes Konnerth[1*]

[1] BOKU University, Institute of Wood Technology and Renewable Materials, Department of Natural Sciences and Sustainable Resources, Tulln an der Donau, Austria
[2] Wood K plus - Competence Center of Wood Composites and Wood Chemistry, Kompetenzzentrum Holz GmbH, Linz, Austria
[3] Huntsman Corporation - Advanced Materials, Performance Products, Polyurethanes, Tienen, Belgium
[4] KremsChem Austria GmbH, Krems an der Donau, Austria.

E-mail: andrej.fasalek@boku.ac.at; lukas.malzl@boku.ac.at; maximilian.pramreiter@boku.ac.at; e.herwijnen@wood-kplus.at; jan_stroobants@huntsman.com; Johann.Moser@kremschem.com; wolfgang.kantner@kremschem.com; johannes.konnerth@boku.ac.at

Keywords: strand based panels, USB, hardwood, softwood.

ABSTRACT

This work addresses a practical question for the next generation of strand-based composites: how to efficiently integrate alternative wood species into panel production without sacrificing bond quality or increasing pressing times. Our overarching aim is to connect rapid laboratory screening of adhesive curing (ABES) with realistic panel-scale outcomes, so manufacturers can make faster, better-informed choices about wood–adhesive combinations and process settings.

We adapted ABES to reliably evaluate moisture-reactive isocyanate adhesives and compared three established systems—pMDI, modified MDI, and MUF—across pine (reference) and various soft- and hardwood species. Typically, modified MDI cures fastest and is least sensitive to species, MUF shows intermediate behaviour, and pMDI is most species-dependent. Within this, pine–pMDI cures notably fast, while beech and birch can achieve very high final strengths with pMDI but require longer pressing. These insights emphasize that species-specific factors matter and that quick screening can reveal promising and risky combinations early.

To translate screening into practice, we produced lab panels across the same species–adhesive matrix and determined the minimal sufficient press time under closer to practise conditions. The press-time trends mirrored ABES: fast-curing pairs in ABES also needed shorter press times in panels. While denser woods often required longer times, poplar surprisingly needed about 30% more pressing than pine with pMDI, underscoring that density alone does not govern curing; wood structure and extractives also play a role. Despite differences in panel density, internal bond was similar across all panel series. Depending on wood species and panel density a wide range of mechanical properties could be covered with average tensile strength ranging from 34 to 70 MPa and modulus from 9.5 to 17.5 GPa. When normalized by specimen density, Douglas fir and beech showed significantly superior performance while oak exhibited significantly lower specific properties.

Taken together, this ABES-to-panels strategy provides a pragmatic pathway: starting with ABES to rapidly rank wood–adhesive combinations and guide press-time targets, then validate with a limited set of panels to capture heat–moisture dynamics and confirm mechanical performance. Practically, pine with pMDI remains an efficient baseline; when introducing other species, modified MDI or MUF may offer more robust curing with less species sensitivity under variable press conditions.

INTRODUCTION

Climate change is altering the composition of Central European forests from predominantly coniferous to more mixed stands. These developments challenge wood supply chains that have been optimized for relatively uniform raw materials and increase the need to use a broader spectrum of wood species and assortments. Also, for strand-based panel materials like oriented strand board (OSB) raw-material

quality and quantity plays a critical role. Hereby, European production currently relies mainly on softwoods such as pine and spruce (Akrami, Barbu et al. 2014). Adapting the wood-based panel industry to future wood resources will therefore be essential.
As wood-based structural products for building applications are expected to increase in demand, improved resource efficiency is becoming a key objective for producing engineered wood products (Pramreiter, Nenning et al. 2023). Panel producers are well positioned to contribute, since disintegration processes such as stranding can offer high material yields, con potentially be combined with other disintegration strategies and enable the use of wood assortments that are unsuitable for sawn timber. Uniaxially oriented strand products like laminated strand lumber, oriented strand lumber and oriented strand boards have high potential in this regard, as they may be suitable for Cross Laminated Timber analogue products (Malzl, Fašalek et al. 2025), although they are currently not produced in Europe in meaningful quantity.
Several studies have evaluated the suitability of alternative wood species for strand-based products (Akrami, Barbu et al. 2014, Pipíška, Nociar et al. 2024), typically focusing on the mechanical and physical properties of boards produced under defined manufacturing parameters. A range of hardwood and softwood species were shown to be processable, even fulfilling standard requirements of OSB.
To achieve target properties, typically varying compaction ratios (CR) have been used which superimpose species intrinsic effects and reduce comparability between species.
Specifically relevant for industrial production is the hot pressing behaviour, which is the costliest production step and often determines production-line capacity (Thoemen and Humphrey 2006).
In our previous study we investigated the strength development of veneer lap joints of eight wood species using the Automated Bonding Evaluation System (ABES) (Fašalek, Malzl et al. 2026). The results showed that wood species can significantly influence bond formation. As the method deviates significantly from conditions occurring during hot pressing of panels, we now extended the study by evaluating the processing of lab-scale unidirectional strand boards (USB) produced with a selection of these wood species (Fašalek, Malzl et al. 2026).
In addition to production relevant parameters like achievable press factor we extended the evaluation to further mechanical properties relevant when panels are used within mass timber products, i.e. in plane tensile properties (Malzl, Fašalek et al. 2025) as an example. Focusing on density corrected specific mechanical properties a comparison of the potential of wood species without a density bias will be provided.

MATERIALS AND METHODS

2.1 Materials

For the evaluation of bond strength development (ABES measurements) (Fašalek, Malzl et al. 2026), commercially available sliced veneers from eight wood species, namely beech (*Fagus sylvatica* L.), birch (*Betula pendula* Roth), oak (*Quercus* spp.), and poplar (*Populus balsamifera* L.), Douglas fir (*Pseudotsuga menziesii* Franco), larch (*Larix decidua* Mill.), pine (*Pinus sylvestris* L.), and spruce (*Picea abies* Karst) were used. The average density ranged from 430 kg/m³ (spruce) to approx. 630 kg/m³ (beech, larch, Douglas fir). Samples were cut to a size of 20 × 117 mm with a thickness of 0.5to 0.7 mm for most wood species and 0.9 mm for oak.
Lab-scale OSL panels were produced using strands of the same wood species. These strands were produced using a laboratory ring strander (Kadant Carmanah, Surrey, Canada) with a nominal strand length of 150 mm, kiln-dried at 80 °C for several hours to a moisture content (MC) of 1–3%. Before panel production, the strands were sieved to remove fines, dust, and folded or curled strands. The strand production procedure is described in more detail here (Malzl, Fašalek et al. 2025).
As adhesives a modified MDI and a pMDI (Huntsman, Tienen, Belgium), and two melamine–urea–formaldehyde (MUF) adhesive with different formaldehyde emission level from KremsChem (Krems, Austria) were used. For the MUF adhesive, a hardener consisting of a 33% aqueous solution of ammonium nitrate (Sigma-Aldrich, St. Louis, Missouri, USA) was added at 3.6 wt% hardener solids, based on resin solids.

2.2. Methods

Bond strength development was assessed using an Automated bonding evaluation system (ABES) equipped with a miniature hot-press contacting the overlapping area of the joint. Immediately after hot pressing the shear strength of the lap-joint specimens are tested in tensile mode. The detailed experimental protocol is available here (Fašalek, Malzl et al. 2026). Tests were conducted at a pressing temperature of 110 °C. For isocyanate adhesives, 30 g/m² water was applied to the overlap area, followed by 30 g/m² adhesive; water and adhesive were applied to both veneers (two-sided application). For MUF, adhesive was applied one-sided at 200 g/m².

Lab scale unidirectional strand panels (USB) were produced from face layer strands of single species (Figure 1). To allow for a fair comparison of wood species, panels were manufactured at a compaction ratio of 1.2, defined as the ratio of oven-dry panel density to oven-dry wood density. To ensure comparable adhesive coverage despite differences in strand density and thickness, and thus specific surface (m²/kg), the surface-specific adhesive amount was calculated. Pine panels served as the reference, with adhesive contents of 5% (based on dry panel mass) for isocyanate adhesives and 15% for MUF resulting in 11 g/m² of adhesive coverage for isocyanate adhesives and 35 g/m² (solids) for MUF. This adhesive coverage was kept constant for all species, resulting in different adhesive contents based on the dry weight of the panel.

Figure 1: Stages of Unidirectional Strand board production, from left to right: strand production, mat forming, halved USB panels after pressing with different press factors

The total strand mat moisture content was set to 10%. Blending was performed in a Coil laboratory blender (Model 6 × 3) equipped with an EL-4 atomiser (Coil Manufacturing Ltd., B.C., Canada). Single-layer mats were oriented using a self-built vibrating orienting device and formed to dimensions of 36.5 cm × 57 cm. Pressing was carried out in a laboratory hot press (LZT-OK 175 L, Langzauner GmbH, Lambrechten, Austria) at 200 °C. Panel thickness was set to 25 mm using metallic spacers. The press factor was calculated as the total press time (press closing + curing) divided by the target thickness. For each series, four panels were produced. Within each series, curing times were varied in steps of approximately 20 s to obtain at least one under-cured panel (target thickness not reached due to excessive spring back) and two panels considered fully cured (target thickness reached). Panel thickness was measured immediately after pressing using a thickness gauge.

As exemplary mechanical properties internal bond strength (IB) and in plane tensile properties were tested. Specimen density was determined for all samples. For IB according to EN 319 only panels that reached the target thickness were used with a specimen size of 50 × 50 mm. Samples were sanded prior to bonding to the metallic sample holders.

Tension was tested with an adapted version of EN 408 on the full length of the panels (550 × 50 × 23.6 mm^3, L × W × T) using a universal testing machine (Z250, Zwick-Roell, Ulm, Germany), while clamping with the help of two custom-made hydraulic clamps. Due to the limitation of the specimen length, the free clamping length was set to 200 mm Deformation was measured by a 50 mm axial extensometer (3542-050M-010-ST, Epsilon Technology Corp., Jackson, USA) that was placed in the middle of the specimens. The tensile modulus was determined by linear regression within 10% to 40% of Fmax, tested with a testing speed of 0.6 mm/min to achieve failure within 320 ± 120 s and Fmax was used to calculate tensile strength.

All specimens were conditioned prior to testing at 20 °C and 65% relative humidity until constant mass was reached.

RESULT AND DISCUSSION

The evolution of bond strength using veneer lap joints of different wood adhesive combinations is displayed in Figure 2. Clear differences can be found for the slope of bond strength development in the first phase of the hot pressing, indicating a strong dependence of the curing on wood-adhesive combination. Furthermore, the maximum tensile shear strength shows again a strong dependence on the wood-adhesive combination, that cannot be attributed to the strength of the wood alone, even though wood failure was achieved for most cases after completing the steepest increase.

Among the adhesives, pMDI showed the highest sensitivity in strength development to species variation, while modified MDI was less species dependent. MUF1 showed the most consistent performance and outperformed MUF2, a low emitting adhesive, in bond strength development and final strength, likely due to its higher formaldehyde-to-amino group ratio. Larch exhibited the slowest strength development with all adhesives except MUF1. pMDI achieved the highest final strengths, especially with diffuse-porous species. Good compatibility was observed between pine and pMDI, while oak heartwood bonded nearly twice as fast as sapwood when using pMDI.

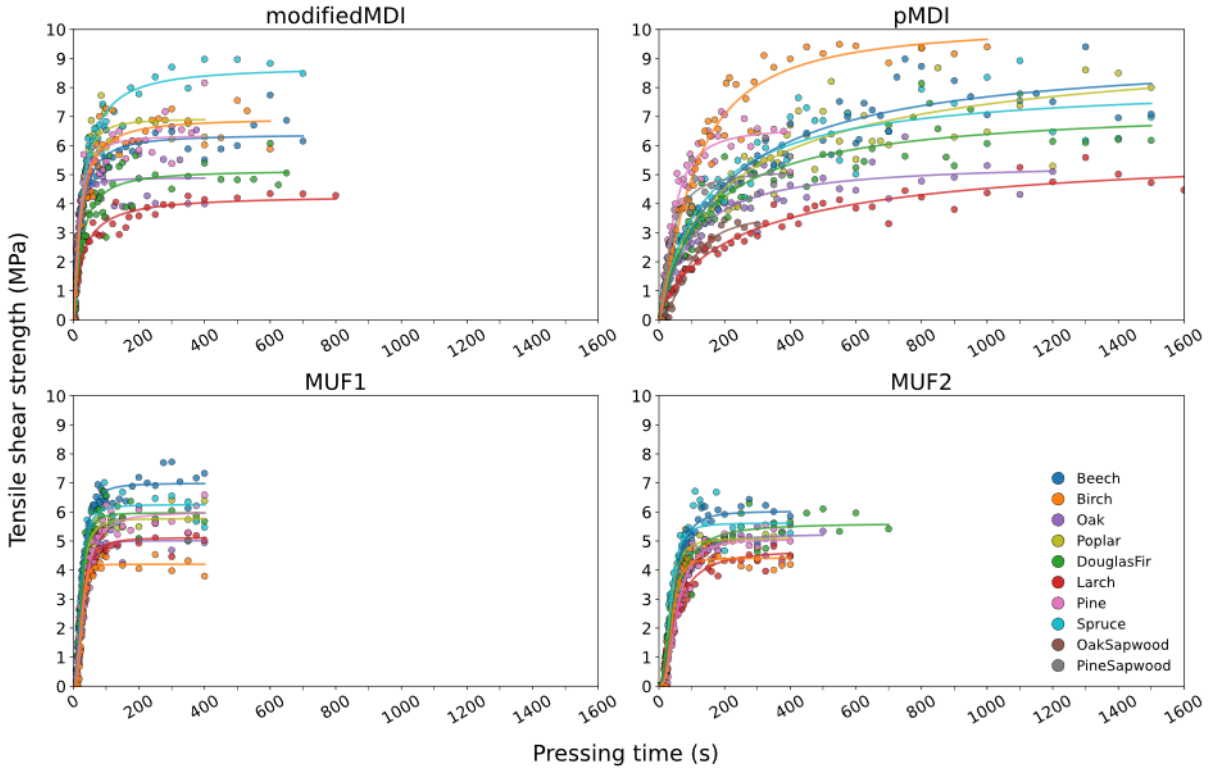

Figure 2: Tensile shear strength development of veneer lap joints using different adhesives and eight different wood species at a pressing temperature of 110 °C

Figure 3 (left) shows the maximum bond strength development rates, defined as the slope of the tangent at the inflection point of the fitted curve. For datasets with pronounced hyperbolic growth, instead the slope of the tangent at 20% of the asymptotic value was used to avoid overestimation. Among all adhesives tested, MUF1 exhibited the smallest variation in bond strength development rates across different wood species followed by modified MDI. MUF2 showed slightly more sensitivity to the wood species but generally performed in a similar way to MUF1, although with lower overall rates most likely due to its lower ratio of formaldehyde to amino groups. In most cases, pMDI cured more slowly than the other adhesives, except when applied to pine. Of all the wood species tested, bonding beech with pMDI proved to be the most difficult. It was the only combination that required an increased pressing pressure to achieve full curing. For pine, sapwood and heartwood performed similarly while oak sapwood showed only about half the bond strength development rate of heartwood, along with a delay in strength development that was more than five times longer.

The pronounced differences in bond strength development rates of pMDI across wood species, compared to other adhesives, is assumed to be associated with wood extractives (Solt-Rindler, van Herwijnen et al. 2026).

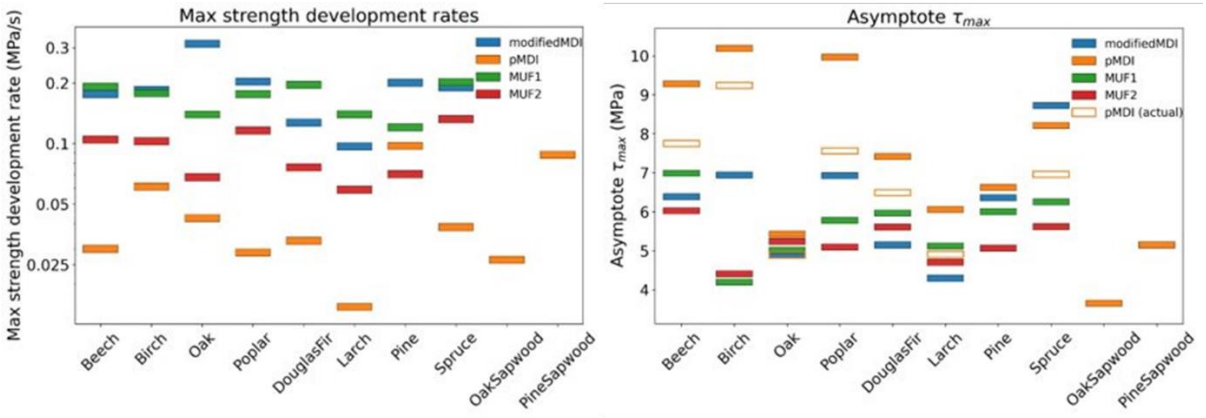

Figure 3: Maximal strength developing rate (left) and theoretical maximum shear strength ((right, asymptote) of veneer lap joints using different adhesives and wood species at a pressing temperature of 110 °C

In Figure 3 (right) the maximum achievable strength of wood-adhesive combinations is shown. The highest bond strengths in our study were achieved with pMDI using beech, birch and poplar, exceeding 9 MPa, while oak sapwood reached less than 4 MPa. Spruce despite its low density achieved tensile shear strengths of nearly 9 MPa with modified MDI, while larch, with over 630 kg/m³ density, averaged below 5 MPa despite reaching 100% wood failure.
According to Marra's (Marra 1992) chain-link model, the strength of the adhesive bond depends on its weakest link, suggesting that denser wood species should achieve higher strength due to higher mechanical properties of the adherend in case of wood failure. However, differences in final strength can be attributed to adhesive properties such as cross-linking degree and stiffness and other factors that are discussed in more detail (Fašalek, Malzl et al. 2026).
The results show that the bond strength development of adhesives varies depending on the wood species, with pMDI being the most sensitive. This is particularly relevant for European OSB producers, where pine and pMDI are commonly used. Introducing new wood species into production may result in longer pressing times. In such cases, less species-sensitive adhesives like modified MDI or MUF may be more suitable.

To validate whether the strength development rate observed in the model veneer-based lap joints is also transferable to the conditions occurring in panel production, selected wood species - adhesive combinations were manufactured in laboratory scale using different press factors. The press factor resulting in well performing panels is displayed in Figure 4 (left).
Overall, the minimum press factor depended again on both the adhesive system and the wood species. Across most wood species, modified MDI required the lowest press factors, pMDI the highest, and MUF was generally intermediate. Within the isocyanate systems, a largely consistent wood-species trend was observed: for both modified MDI and pMDI, pine reached full cure at the lowest press factors, while birch and poplar were typically similar and intermediate. Beech deviated slightly from this pattern, with Beech–pMDI requiring slightly higher and Beech–modified MDI slightly lower press factors than the birch and poplar combinations. The difference between modified MDI and pMDI was smallest for pine, but more pronounced for the hardwood species, suggesting that the faster curing of modified MDI is particularly advantageous for hardwood panels. For MUF, press factors differed across all species; pine reached full cure at the lowest values, whereas beech required the highest.
The lower press factors for modified MDI are consistent with its higher reactivity of the adhesive.
Comparing the observations with bond strength development from ABES (Figure 2 and 3) captured relative curing behaviour is best within a given wood species.

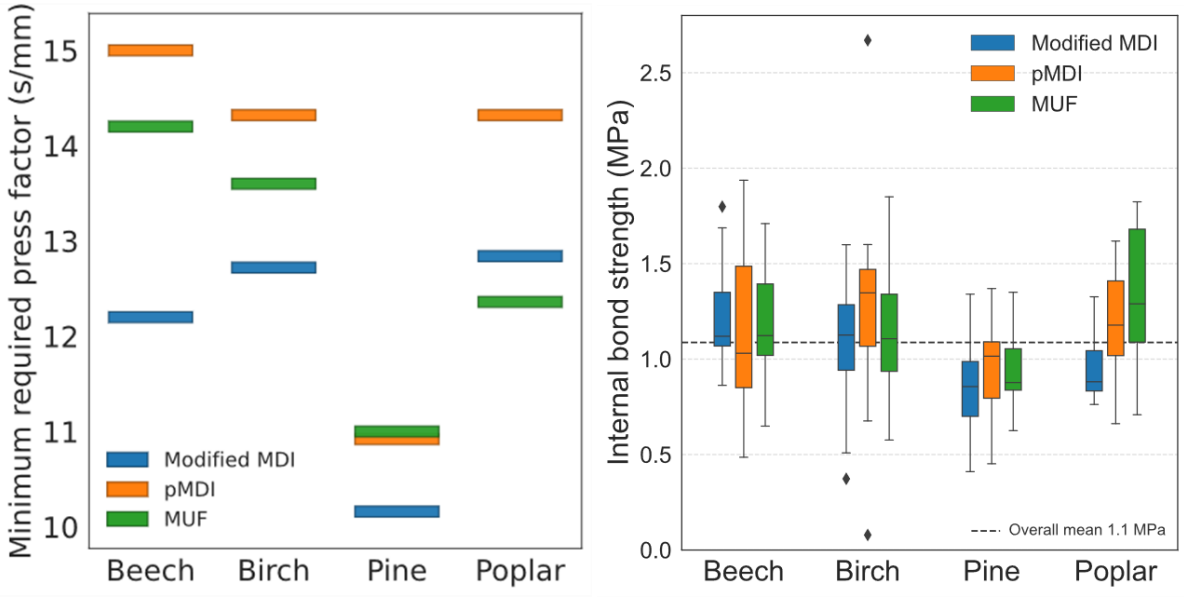

Figure 4: Minimum required press factor (left) and internal bond strength (right) of selected wood adhesive combinations of lab scale unidirectional strand boards

While minimum required press factor depended on both wood species and adhesive internal bond strength (Figure 4, right) varied only to a minor degree, despite large density differences. It is assumed, that incomplete adhesive coverage of the strands (compared to the conditions in ABES) and consequently bond failure might play a more dominant role in the case of panels.

As exemplary mechanical property relevant for USB application in plane tensile properties are shown in Figure 5, opposing various wood species – here all bonded with pMDI as adhesive. Based on the targeted compaction ratio of 1.2 based on raw material density, resulting panel densities for different wood species ranged from almost 550 kg/m³ for spruce to 950 kg/m³ for beech. As a reference, pine was produced in three different compactions ratios.

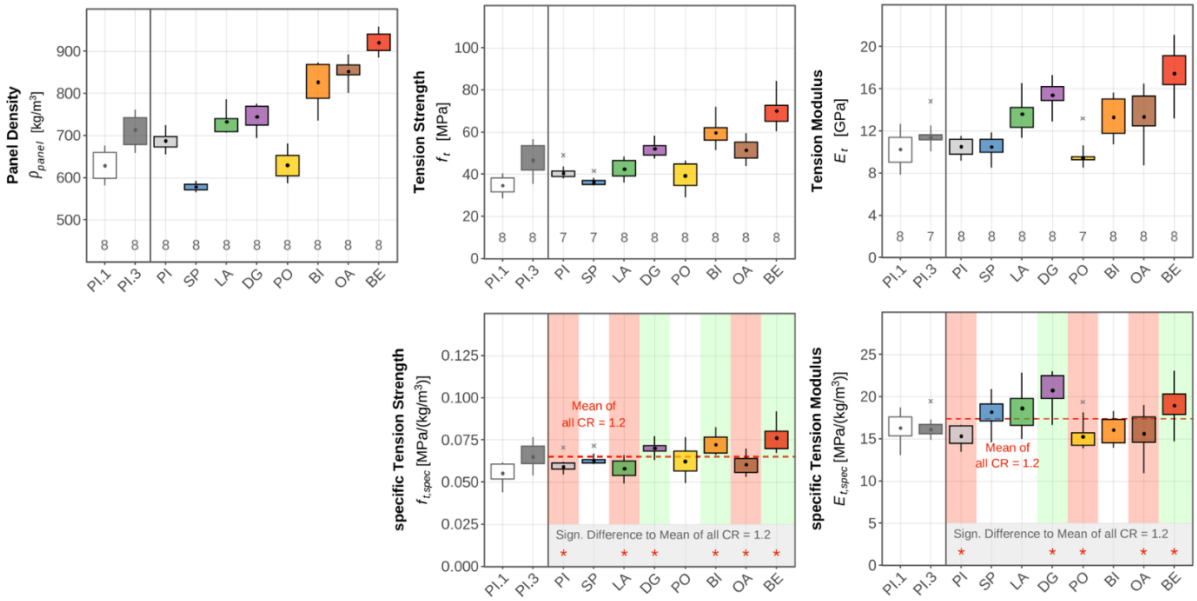

Figure 5: Properties of unidirectional strand boards produced from different wood species (SP spruce, LA larch, DG Douglas fir, PO poplar, BI birch, OA oak, BE beech), with pine (PI) at three different densities as a reference

The tension properties parallel to preferred strand-orientation covered a range from 34 to 70 MPa for tensile strength and the tensile modulus ranged from 9.5 to 17.5 GPa. Beech and birch delivered the highest overall performance with mean tension strength values of 70 MPa and 60 MPa and tensile moduli of 17.5 GPa and 13.3 GPa. Only Douglas fir showed a similar tension modulus of 15.4 GPa, but at lower strength of 52 MPa. Spruce performed lowest in tension with 36 MPa strength and 10.5 GPa modulus. In order to eliminate the sole effect of varying density, the comparison of specific tension strength rendered beech, birch and Douglas fir above the average of all species, respectively. Oak, pine, and larch, performed significantly below the average. In terms of the specific tension modulus only beech and Douglas fir showed significantly higher values above average. Again, oak and pine, but also poplar performed below the mean specific modulus.

CONCLUSIONS

With the data at hand, it can be concluded that the speed of bond formation is largely depending on wood – adhesive combination. This is a highly relevant factor for the productivity and consequently cost structure of large-scale panel production. On the positive side, for all wood species standard adhesives of different chemistry are available resulting in proper bond performance.

Using different wood species may result in mechanical properties currently not covered with strand-based materials using currently dominant species for strand products, namely pine and poplar. However, high density wood species may be difficult to process in today's hot presses, as they require high pressure for proper compaction of high-density species such as beech, oak or birch. Furthermore, these wood species typically show very different behaviour also in other processing steps like stranding, occurrence of fines, strand geometry and blending.

REFERENCES

Akrami A, Barbu MC, Fruehwald A (2014) Characterization of properties of oriented strand boards from beech and poplar. Europ J Wood Wood Products 72(3): 393-398. https://doi.org/10.1007/s00107-014-0793-9

Fašalek A, Malzl L, Konnerth J, van Herwijnen HWG, Stroobants J, Moser J, Kantner W, Gabler C, Pramreiter M (2026) Evaluation of bondability of different wood species using adhesives for wood-based panels. Int J Adhes Adhes. https://doi.org/146. 10.1016/j.ijadhadh.2025.104230

Fašalek A, Malzl L, Konnerth J, van Herwijnen HWG, Thoemen H, Stroobants J, Moser J, Kantner W, Gabler C, Solt-Rindler P, Czasch A, Pramreiter M (2026) Bond Performance Development of Lab-Scale Oriented Strand Lumber Panels with Pressing Time and Its Comparison with ABES Results. Accepted by Europ J Wood Wood Products.

Malzl L, Fašalek A, Konnerth J, Pramreiter M (2025) Unidirectional Strand Board (USB) from Underutilized European Wood Species: Mechanical Performance and Technical Suitability. submitted to Construction and Building Materials.

Marra AA (1992). Technology of Wood Bonding, Principles in practice. New York, Van Nostrand Reinhold.

Pipíška T, Nociar M, Král P, Ráheľ J, Bekhta P, Réh R, Krišťák L, Jopek M, Pijáková B, Wimmer R, Šernek M (2024) Characterization of randomly oriented strand boards manufactured from juvenile wood of underutilized wood species. Europ J Wood Wood Products 82(4): 927-941. https://doi.org/10.1007/s00107-024-02080-4

Pramreiter M, Nenning T, Huber C, Müller U, Kromoser B, Mayencourt P, Konnerth J (2023) A review of the resource efficiency and mechanical performance of commercial wood-based building materials. Sust Mat Tech 38. https://doi.org/10.1016/j.susmat.2023.e00728

Solt-Rindler P, van Herwijnen HWG, Mitter R, Konnerth J (2026) Influence of wood species and pine extractives on the curing behaviour of pMDI. Int Journal Adhes Adhes 146. https://doi.org/10.1016/j.ijadhadh.2025.104248

Thoemen H, Humphrey PE (2006) Modeling the physical processes relevant during hot pressing of wood-based composites. Part I. Heat and mass transfer. Holz Roh Werkst 64(1): 1-10. https://doi.org/ 10.1007/s00107-005-0027-2

Enhanced Thermal Mass of Mycelium-Based Biocomposites for Timber Constructions: A Comparative Study

Benjamín Petržela[1*], Tadeáš Zachara[1], Miroslav Jozífek[2], Miloš Pavelek[1], Štěpán Hýsek[1]

[1] Department of Wood Processing and Biomaterials, Faculty of Forestry and Wood Sciences, Czech University of Life Sciences Prague, Prague, Czech Republic
[2] Department of Horticulture, Faculty of Agrobiology, Food and Natural Resources, Czech University of LifeSciences Prague, Prague, Czech Republic.

E-mail: petrzela@fld.czu.cz; zachara@fld.czu.cz; jozifek@af.czu.cz; pavelek@fld.czu.cz; hyseks@fld.czu.cz

Keywords: mycelium-based biocomposite; thermal mass; thermal inertia; bio-based insulation; timber construction; hardwood; volumetric heat capacity; summer overheating; building physics; fungal biocomposite.

ABSTRACT

Summer overheating is an escalating challenge for lightweight timber constructions, which inherently lack the thermal mass of traditional masonry. This study investigates the thermo-physical properties of a mycelium-based biocomposite (MBB) insulation produced from industrial wood waste, with particular focus on volumetric heat capacity (C_v). The C_v and thermal conductivity (λ) of MBB were experimentally measured and benchmarked against seven reference insulation materials spanning bio-based, mineral, and petroleum-derived categories, with results visualized on an Ashby diagram. The areal heat capacity (κ) of nine representative wall assemblies was theoretically calculated per EN ISO 13786. Even though the MBB achieved the highest thermal conductivity (λ = 0.0641 ± 0.0024 $W \cdot m^{-1} \cdot K^{-1}$) among the tested insulation materials, it offers 4.7 times higher C_v than EPS. Analytical modeling indicates a thermal phase shift of 8.2 h for a 185 mm layer, compared to 4.6 h for EPS. The softwood timber + MBB wall assembly achieved an areal heat capacity approaching the lower boundary of traditional masonry performance. These findings demonstrate MBB's potential as a bio-based, waste-derived insulation for significantly enhancing the thermal inertia of lightweight timber buildings and mitigating summer overheating risk.

The final version of this abstract and the full scientific article are scheduled to be published in the Special Issue "12th Hardwood Conference—Sopron" of the journal MDPI Forests, available at the following link:

MDPI Forests Special Issue: 12th Hardwood Conference—Sopron

https://doi.org/10.3390/f17070763

Birch Becomes Structural: Valorizing Small-Diameter Silver Birch (*Betula pendula Roth.)* Into Innovative Glue Laminated Beams for Sustainable Construction

Tom Mortelmans[1*], Tom De Mil[1], Thierry Descamps[2]

[1] University of Liège, Faculty of Gembloux Agro Bio-Tech, 2 passage des déportés 5030 Gembloux
[2] Université of Mons, Faculty of Polytechnics.

E-mail: tmortelmans@uliege.be; tomdemil@uliege.be; thierrydescamps@umons.ac.be

Keywords: silver birch, glue laminated timber, small diameter, construction, engineered wood product.

ABSTRACT
Silver birch (Betula pendula sp.) has recently gained significant attention across Europe as a hardwood species with high potential for valorization in timber products. Owing to its favorable natural regeneration and rapid growth dynamics, birch has become the third most prevalent hardwood species in Belgium in terms of standing volume. However both forest management and the wood quality assessment has been understudied and birch is mostly used as fuelwood or pulpwood in Belgium.
Currently, softwood remains the predominant material for timber constructions, whilst hardwoods constitute approximately half of the forested area in Wallonia. A large portion of hardwoods are being valorized into shorter-lived Harvested Wood Products (HWP), fuelwood or exported outside Belgium for transformation. Here, we aim at valorizing birch-based HWP that are largely composed of small-diameter logs, in order to develop innovative valorization strategies to increase the carbon residence time of these products: glued laminated timber (glulam) for use in construction. The first steps toward that goal is to characterize mechanical properties of small diameter birches.
Further investigation into the material quality of birch, with a focus on its juvenile form (thinning products), is pursued. Due to its rapid growth rate, juvenile birch may achieve mechanical performance comparable to that of Norway spruce (Picea abies) in roughly half the rotation time(Gil-Moreno et al., 2025). Preliminary experimental data indicate a mean local modulus of elasticity of 14 529.15 MPa (CoV = 15.07%; n = 118) for birch specimens with a diameter at breast height (DBH) below 30 cm.
To explore its potential, beam prototypes will be tested mechanically. Hence, low-values wood can be used for high-value structural applications that can replace fossil-based construction materials.

Tables

Table 1: Characteristics of small diameter Walloon birches

Properties	Value	Units	n
Length	292.26 ± 55.23	cm	58
Diameter thin side	14.26 ± 2.48	cm	60
Diameter large side	17.17 ± 3.41	cm	60
Circumference scrolling	3.22 ± 1.99 (61.92 %)	cm/m	57

Results presented as Mean ± SD (CoV)

Figures

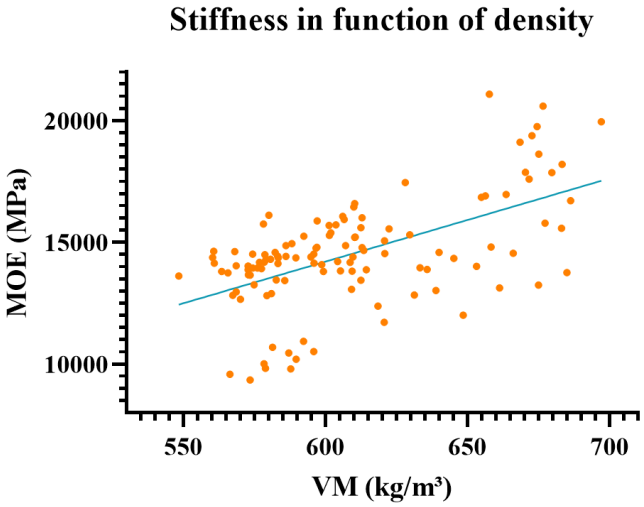

Figure 1: Relation between elasticity module (MOE) and volumetric mass (VM) for small specimens

The relationship between elasticity module (MOE) and volumetric mass (VM), as shown in Figure 1, has been established for 128 specimens with a coefficient of correlation (R^2) of 0.3291 and a formula as such: MOE = 34.199*VM-6310.4. The 128 specimens of 2x2x36cm, tested according to the EN 408 norm, have been made from 6 birches from the 60 birches that serves the whole study.
This result is part of the on going research on small diameter birches that grew up without sylvicultural practices and aims to reflect the current stage of Walloon birches and how this material can compare to conventional woods used in wood engineering.

The final version of this abstract and the full scientific article are scheduled to be published in the Special Issue "12th Hardwood Conference—Sopron" of the journal MDPI Forests, available at the following link:
MDPI Forests Special Issue: 12th Hardwood Conference—Sopron

Pretreatment of Beech Chips with Compression for Accelerated Maceration and Pulp Production

Richard Hrčka[1*], Viera Kučerová[2], Rastislav Lagaňa[1], Oľga Mišíková[1]

[1] Department of Wood Science, Faculty of Wood Sciences and Technology, Technical University in Zvolen, T.G. Masaryka, 96001 Zvolen, Slovak Republic
[2] Department of Chemistry and Chemical Technology, Faculty of Wood Sciences and Technology, Technical University in Zvolen, Slovak Republic.

E-mail: hrcka@tuzvo.sk; viera.kucerova@tuzvo.sk; lagana@is.tuzvo.sk; misikova@tuzvo.sk

Keywords: beech, sapwood, red heartwood; chip, pretreatment; compression; accelerated maceration.

ABSTRACT
Manufacturers of pulp are seeking strategies to reduce production costs while preserving product quality. Pretreatment of wood in the form of chips represents an important contribution of wood science to cost reduction. The accelerated maceration of wood is achieved by applying compression perpendicular to the grain orientation. Faster wood permeability and the exclusion of air or free water from the wood structure serve as the key mechanisms of pretreating nearly impermeable wood using perpendicular compression. The liquid maceration solution penetrates the chip structure in the longitudinal direction, reaching the target cell wall and moving deeper toward the chip centre. Evidence of this functional mechanism is provided by the maceration of impermeable red beech heartwood in a solution of peroxide and acetic acid. The chemical composition of pretreated and macerated red beech heartwood significantly differed from that of untreated and macerated red beech heartwood. Similar results were obtained for permeable sapwood. The ratio of cellulose to lignin shifted significantly toward a higher cellulose fraction of the pretreated samples. Direct measurement of the chemical composition of macerated wood was validated and subsequently replaced by a rapid inverse determination of chemical composition based on the colour of wood chemical compounds.

The final version of this abstract and the full scientific article are scheduled to be published in the Special Issue "12th Hardwood Conference—Sopron" of the journal MDPI Forests, available at the following link:
MDPI Forests Special Issue: 12th Hardwood Conference—Sopron

SMADBatt Sustainable Materials and Design for Electric Vehicle Batteries

Stefan Pinkl[1,2*], Peter Bliem[1,2], Kevin Vitzthum[3,4], Thomas Krenke[4]

[1] Wood K plus - Competence Center for Wood Composites & Wood Chemistry, Kompetenzzentrum Holz GmbH, Altenberger Straße 69, Linz, Austria, 4040
[2] BOKU University, Institute of Wood Technology and Renewable Materials, Department of Natural Sciences and Sustainable Resources, Gregor-Mendel-Straße 33, Vienna, Austria, 1180
[3] Innovationszentrum W.E.I.Z., Franz-Pichler-Straße 30, Weiz, Austria, 8160
[4] Wood Vision Lab, Franz-Pichler-Straße 30, Weiz, Austria, 8160.

E-mail: s.pinkl@wood-kplus.at; p.bliem@wood-kplus.at;
kevin.vitzthum@innovationszentrum-weiz.at; thomas.krenke@wood-vision-lab.com

Keywords: Poplar fibres, bio-based composites, recyclability, battery tray.

ABSTRACT

This study investigates the use of binder-free poplar fibre materials derived from low-diameter timber (<10 cm) for structural applications in steel–wood hybrid battery housings. Building on the Bio!Lib project, the aim is to replace solid wood cores with more resource-efficient fibre-based fillings while maintaining mechanical performance and enabling improved recyclability.

Three defibration approaches - strand production, crushing-roller-based macrofibres, and scrimber - were applied to juvenile poplar (*Populus x canadensis* MOENCH). The resulting fibre assortments were characterized using image-based analysis and integrated into steel profiles at densities between 250 and 550 kg/m³. Mechanical performance was evaluated using three-point bending tests and compared to glued laminated timber (GLT) references.

The results show a strong dependence of bending performance on both fibre morphology and densification. Macrofibres exhibited the highest apparent bending strength, reaching up to 162 MPa at 550 kg/m³, approaching the performance of GLT-based steel–wood hybrids (172 MPa). In contrast, strands showed lower performance and a high proportion of fines (79 wt.%), attributed to less controlled fibre orientation during processing.

The study demonstrates that crushing-roller-based defibration enables favourable fibre alignment and improved mechanical behaviour. Overall, binder-free poplar fibre fillings show significant potential for load-bearing hybrid structures while supporting circular design principles through material efficiency and full recyclability.

INTRODUCTION

At first glance, wood may appear unsuitable for applications in the automotive industry due to its susceptibility to biological degradation, combustibility, brittle failure behaviour, sensitivity to moisture, and inherent material heterogeneity. However, the combination of steel and wood has already been demonstrated in the previous Bio!LIB project, where structural components of a battery housing successfully met the requirements of the automotive sector.

Building on this work, the present project utilizes an existing demonstrator of a steel–wood hybrid battery housing and investigates the substitution of the solid wood core used therein. Compared to particle-based materials, solid wood exhibits lower material yield efficiency (Pramreiter, et al. 2023), highlighting the potential advantages of alternative wood-based material concepts.

At the outset of the project, it was defined that timber with a diameter of less than 10 cm would be used as the primary raw material. Such assortments are currently predominantly utilized in forestry as wood chips for energy production. Upgrading this material for structural applications with higher added value represents a promising development from both ecological and economic perspectives.

Poplar wood was selected as the raw material. This choice was motivated by its low density, which enables high densification ratios, as well as its comparatively high splitting resistance among native wood species. The high splitting resistance of poplar can be attributed to its homogeneous, diffuse-porous anatomical structure (Wagenführ and Wagenführ 2021), which lacks distinct planes of weakness. In addition, poplar fibres are described as elastic and tough (Wu et al. 2023). Notably, the fibres are

approximately twice as long as the vessels (Balatinecz and Kretschmann 2001), which plays a key role in the fracture behaviour. Under loading, the vessels tend to fail first, while the longer fibres bridge the crack (fibre bridging), undergo elongation across the vessels, and are gradually pulled out of the matrix (fibre pull-out). This mechanism is generally applicable to diffuse-porous hardwoods, whereas softwoods do not contain fibres in the same anatomical sense. Against this background, the following study investigates the use of juvenile poplar wood in combination with a steel casing as a structural component for automotive battery systems.

MATERIALS AND METHODS

The processing of this non-sawable timber into fibres involved the identification of three defibration approaches: (1) strand production, (2) a crushing-roller process for the generation of macrofibres, and (3) the production of continuous macrofibre mats (scrimber).

Eight trees of Canadian hybrid poplar (*Populus x canadensis* MOENCH) were harvested during a thinning operation (July 2nd 2025; GPS: 48.1524, 16.9766). The trees had an average diameter of 10 cm, an age of 11 years, a wood moisture of 51% and a density of 0.35 g/cm³. The harvested raw material was evenly divided into three batches (Figure 1) to evaluate the different defibration processes and debarked.

Figure 1 left: three assortments out of 8 poplar trees for the production of strands, macrofibres and scrimber. Right: debarked, cut to 30 cm and split for the production of strands

Strand production was carried out at the Department of Wood Science and Wood Technology at Mendel University in Brno with a MSF 1400 Strand flaker (Maier Dieffenbacher, Brno, Czech Republic). In parallel, macrofibres and macrofibre mats were produced at Wood K plus in Tulln using a crushing-roller process (Figure 2). The resulting fibres were subsequently dried and pre-sorted, using a vibrating screen with a built-in screen having a 5 cm mesh size over a screening length of 1 m. Afterwards characterized, packaged and delivered to the project partner W.E.I.Z. for bending tests on filled steel profiles.

Fibre geometry was characterized using an image-based analysis approach. Images were captured with a Nikon D3100 camera equipped with a remote shutter release, maintaining a fixed camera-to-sample distance to ensure consistent scaling. A black background was used to enhance contrast and a photo light box provided controlled lighting conditions, minimizing the influence of external light sources. To facilitate accurate evaluation, individual fibres were analysed separately. The acquired images were processed in Python, where fibre geometry was quantified using Principal Component Analysis.

Figure 2: crushing roller process to produce macrofibres and scrimber, strand flaker at Mendel University in Brno, band saw for solid wood production

As a reference material, sawn timber (34 mm thickness) was produced from the same poplar trees and subsequently dried. Afterwards glue laminated timber (GLT) was produced out of 4 lamellas. This reference material was also used for filling the steel profiles to ensure comparability with results from the preceding project.
The produced assortments were subsequently introduced into a steel frame. The optimal geometry of the steel profiles was defined as two overlapping C-shaped shells that fully enclose the particle filling. Filling and densification were carried out in a single combined process step. The aim was to investigate the mechanical stability as a function of the filling density, which was targeted in the range of 250–550 kg/m³. Following this, the two C-shaped shells were joined by laser welding to minimize heat input, as excessive heating can cause outgassing of the wood and result in poor weld quality.
Three-point bending tests were prepared to evaluate the mechanical performance. The 600 mm long test specimens consisted of steel profiles filled with different particle types (strands, macrofibres and scrimber) and three density levels (250, 400, and 550 kg/m³) are shown in Figure 3.

Figure 3: steel-wood hybrid (60x30 mm²) filled with strands, macrofibres and scrimber (left to right) at 550 kg/m³

RESULTS AND DISCUSSION

The crushing-roller process produces both macrofibres and scrimber. These two assortments are closely related, as scrimber represents an intermediate product in which the process is stopped at an earlier stage. In both cases, the process is iterative, with the fibre bundles progressively reduced in size. For the scrimber fraction, processing is terminated once the fibre bundle begins to lose its structural integrity. In contrast, macrofibres are produced until no further size reduction can be achieved by the crushing rollers.
The results of the measured assortments are presented in Figure 4. Pre-sorting resulted in a classification into large and small fractions; however, only macrofibres and strands were subjected to detailed measurement. The fine fraction of the strand assortment accounted for 79 wt.% of the total, indicating a need for adjustments in processing parameters such as knife configuration and cutting depth. Differences were also observed in the initial length of the split wood: strands were cut to 30 cm, whereas macrofibres

and scrimber were processed at 60 cm. Consequently, macrofibres were approximately twice as long as strands, regardless of whether coarse or fine fractions were considered.
In terms of width, the opposite trend was observed: macrofibres were narrower than strands. This is attributed to the crushing-roller process, which defines the fibre width, with a spacing of 8 mm between the roller profile peaks.
In general, the production of macrofibres and scrimber allows for a high degree of fibre alignment. During processing, the wood pieces are manually fed into the crushing-roller system, resulting in little to no compression or cutting perpendicular to the grain. In contrast, the strand flaker operates with a 65 cm knife processing wood pieces of 30 cm length, which can lead to cutting across the grain. This mechanism also explains the high proportion of fine particles observed in the strand fraction.
As an alternative, ring flakers are available for pilot- and laboratory-scale applications. Similar to their industrial counterparts, these systems fix the wood bundle in place while the knife ring rotates enabling more controlled processing and improved alignment.

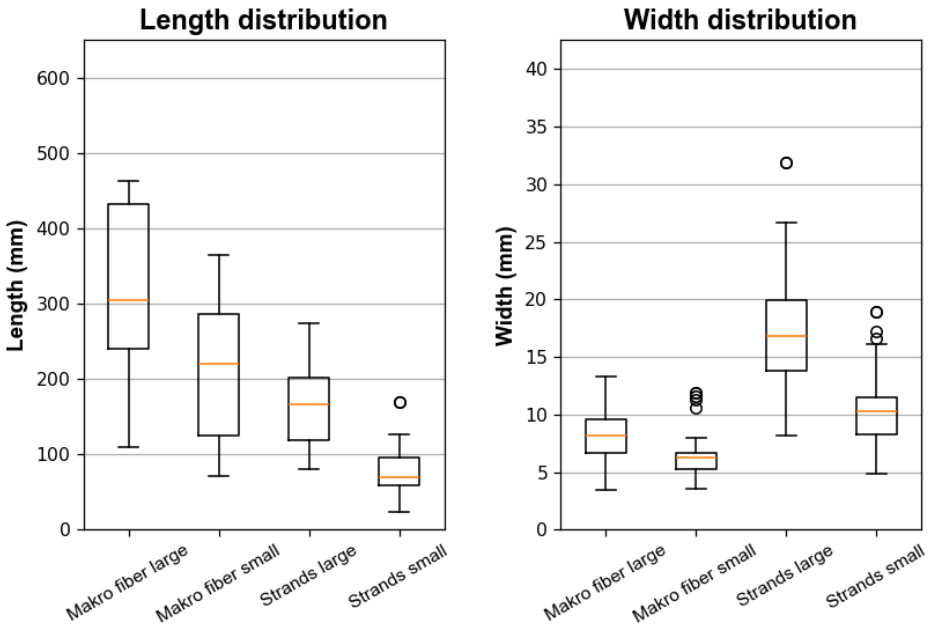

Figure 4: Length and width of poplar macrofibres and strands, grouped into coarse (large) and fine (small) fractions

The empty steel profile exhibited an apparent bending strength of 83 MPa. Figure 5 includes results for glued laminated timber (GLT) produced from both juvenile and mature wood. In this context, "juvenile" refers to poplar wood sourced from the same trees used for the production of macrofibers, strands, and scrimber. For comparison with the preceding Bio!Lib project, GLT from mature wood was also manufactured. This material showed approximately 20 MPa higher apparent bending strength, both as a standalone material and when integrated into the steel–wood hybrid.
In comparison, strand-based fillings exhibited a clear density-dependent behaviour. The apparent bending strength ranged from 94 to 140 MPa, depending on the density and remained below the 172 MPa achieved by the steel–wood hybrid incorporating GLT.
In Figure 6 macrofibres, at a filling density of 550 kg/m³, an apparent bending strength of 162 MPa was achieved, which is only 10 MPa lower than that of the steel–wood hybrid incorporating GLT. However, this density is significantly higher than that of the GLT produced from the same trees (319 kg/m³).
A clear relationship between density and apparent bending strength can be observed for strands, macrofibres, and scrimber. Among these, macrofibres exhibited the highest apparent bending strength, followed by scrimber, while strands showed the lowest values.

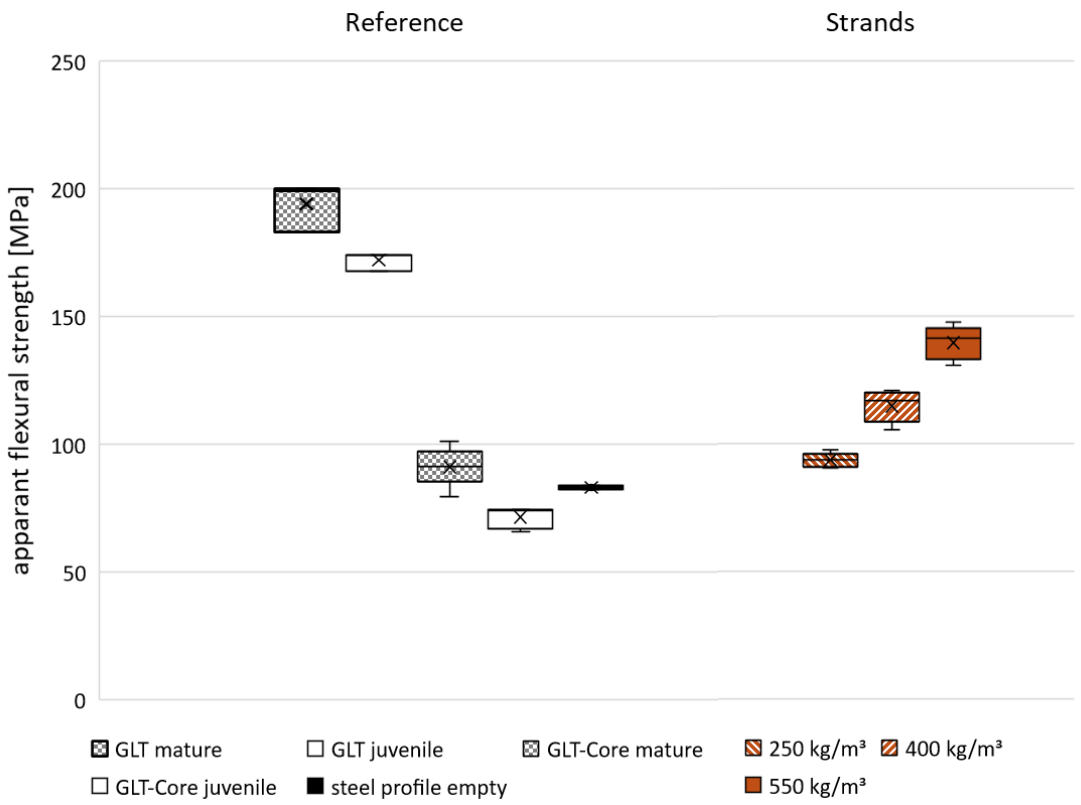

Figure 5: Flexural strength of empty steel profile, solid poplar wood and steel-wood hybrids filled with GLT and strands

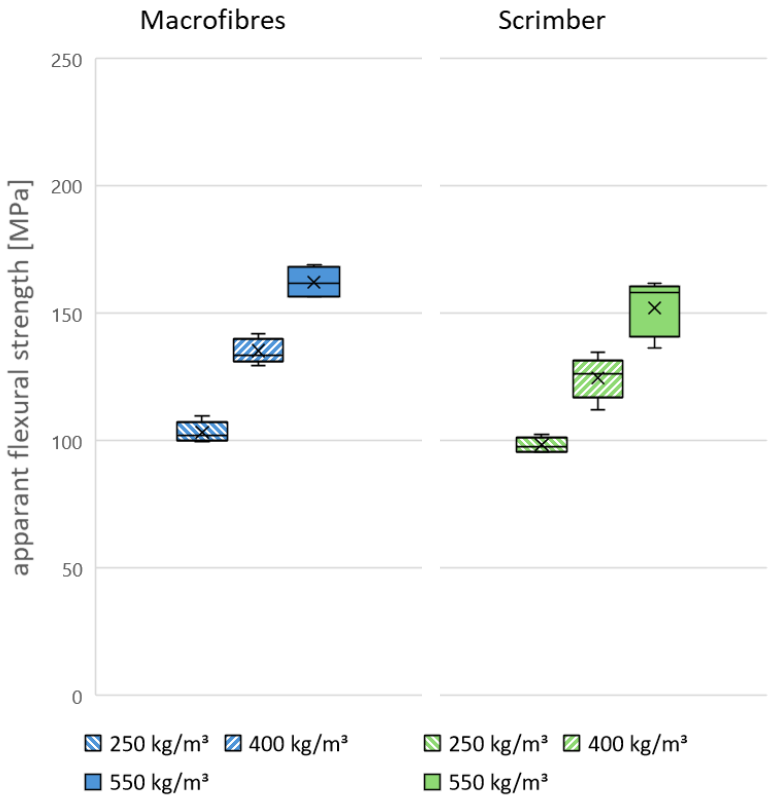

Figure 6: Apparent flexural strength of steel-wood hybrids filled with macrofibres and scrimber

CONCLUSIONS

This study demonstrates the feasibility of utilizing binder-free poplar fibre assortments derived from low-diameter timber for structural applications in steel–wood hybrid systems. The results show that both fibre morphology and densification significantly influence mechanical performance. In particular, macrofibres exhibited the highest apparent bending strength, followed by scrimber and strands, highlighting the importance of fibre alignment and processing method.

A clear density–performance relationship was observed across all fibre types. At a filling density of 550 kg/m³, the mechanical performance of fibre-based fillings approached that of the GLT-based reference system, although at a higher material density. This indicates that while fibre-based systems can achieve competitive strength, further optimization is required to improve material efficiency.

The findings confirm that crushing-roller-based defibration enables favourable fibre alignment and structural integrity, whereas strand production results in a higher proportion of fines and less controlled fibre orientation. This has direct implications for both processing optimization and mechanical performance.

Overall, the SMADBatt concept demonstrates that binder-free wood fibre materials can be successfully integrated into load-bearing hybrid structures while meeting key requirements for recyclability and resource efficiency. The approach opens new pathways for the valorisation of low-value deciduous wood assortments and supports the development of sustainable material solutions for the automotive industry.

ACKNOWLEDGMENTS

The authors gratefully acknowledge the financial support of the Austrian Research Promotion Agency (FFG) within the framework of the “Mobility 2023: Circular Economy” call (project no. FO999921894, SMADBatt).

The authors further thank René Chizzola for the production of macrofibres and scrimber, Tomáš Pipíška (Mendel University in Brno) for the production of strands and Alexander Schneider for characterisation of fibres.

REFERENCES

Balatinecz JJ, Kretschmann DE (2001) Properties and utilization of poplar wood. In: Dickmann DI, Isebrands JG, Eckenwalder JE, Richardson J. (eds) Poplar Culture in North America. Part A, Chapter 9. NRC Research Press, Ottawa, Canada. pp 277-291.

Pramreiter M, Nenning T, Huber C, Müller U, Kromoser B, Mayencourt P, Konnerth J (2023) A review of the resource efficiency and mechanical performance of commercial wood-based building materials. Sustain Mater Techno 38:e00728. https://doi.org/10.1016/j.susmat.2023.e00728

Wagenführ R, Wagenführ A (2021) Holzatlas, 7th ed. Carl Hanser Verlag, München, Germany

Wu GF, Shen YL, Fu F, Ren HQ, Qu W (2023) Mechanism of the super-large deformation behavior of poplar wood under transverse compression. Ind Crop Prod 205:117510. https://doi.org/10.1016/j.indcrop.2023.117510

12th Hardwood Conference

18-19 June 2026
Sopron, Hungary

WOOD KPLUS

FATE
FAIPARI TUDOMÁNYOS EGYESÜLET

UNIVERSITY of SOPRON